# Thermodynamic Optimization of Biomass Gasification

A Thesis
Submitted in Partial
Fulfillment of the Requirements for the Degree of

**DOCTOR OF PHILOSOPHY**

By


## Buljit Buragohain




**Center for Energy**
**Indian Institute of Technology Guwahati**
Guwahati – 781039, Assam, India


August 2011

Dedicated

to

My Parents

# CERTIFICATE

It is certified that the work contained in the thesis entitled "**THERMODYNAMIC OPTIMIZATION OF BIOMASS GASIFICATION**", by **Buljit Buragohain** (Roll No. 05615104), has been carried out under our supervision and that this work has not been submitted elsewhere for a degree.

**Date:26.08.2011**

**Dr. V.S. Moholkar**
Associate Professor
Department of Chemical Engineering

**Professor P. Mahanta**
Professor, Department of Mechanical Engineering and Head, Center for Energy

# CONTENTS

# List of Tables

# List of Figures

CHAPTER 1

# General Introduction and Motivation for the Thesis

For a developing country like India, meeting energy needs (mainly in the form of electricity and transportation fuels) in various sectors such as agriculture, industrial and transport is vital to achieve sustainable growth and economic development. The electricity generation in India is dominated by coal–thermal route [1]. Although the total installed capacity for electricity generation is 148 GW (as on February 2009), it is far insufficient to meet the needs of the population [2]. Moreover, supply of electricity to remote regions and hilly terrains (especially in the northeastern states) is difficult as extension of grid to these places is impractical. The transmission losses are as high as 30% and fluctuations in voltage are beyond acceptable limits [1,2]. Therefore, there is an urgent need to utilize and promote renewable energy sources in order to make these regions independent from grid supply [3]. Various options for decentralized electricity generation through renewable sources include biomass gasification, solar, wind and small hydro. However, from Indian perspective biomass gasification is the most feasible option among these for various reasons [4-9]: (1) biomass is

abundantly and evenly distributed in the country, (2) it is available throughout the year at cheap rates (3) the capital investment for gasifier, duel fuel or 100% producer gas generator, gas cleaning system and other accessories are quite low (4) technology is simple and unskilled/semi–skilled labor can handle operation and maintenance of the plant. Another critical energy need of India is in the form of liquid transportation fuels such as gasoline and diesel. Current demand of petroleum fuels in India is over 120 Million Metric Tons Per Annum (MMTPA) and oil reserves in the country are sufficient to meet only 1/3$^{rd}$ of this demand. Thus, the impact of crude oil puts heavy burden on national economy [10,11]. Fluctuating prices of oil in the international market makes situation even worse. Thus, there is also an urgent need of quest for alternative and renewable fuels. Biomass gasification integrated Fischer–Tropsch (BGIFT) synthesis is now being explored as an option for synthesis of liquid transport fuels [12-16]. Although Fischer–Tropsch (FT) reaction is more than a century old, interest of scientific /industrial community in it is renewed in past one and half decades [17-20] as it is possible to synthesize excellent quality fuel using producer gas from biomass gasification that contains carbon monoxide and hydrogen as main components. Conventionally, alkali promoted cobalt catalyst was used for the FT synthesis with producer gas feed in the molar ratio of $H_2/CO = 2$. However, extensive research has taken place in the past two decades to develop iron based catalysts that can handle gases, which do not have the required molar ratio (for example [21-24]). Another reason that also puts thrust on use of renewable energy sources is the fast depletion of fossil fuels environmental pollution and greenhouse gas emission that contributes to global warming. As far as electricity generation through thermal route is concerned, replacement of coal by biomass can help reduce emission of $CO_2$ (in the Indian context) at a rate 0.85 kg/kWh. On the other hand, replacement of 1 kg of petroleum–derived diesel by FT diesel reduces the $CO_2$ emission by 3.2 kg [25].

Taking into consideration the two possible outlets for producer gas obtained from biomass gasification, it is necessary to find optimum operating conditions in terms of temperature, air ratio (or equivalence ratio) and composition of gasifying medium. It must be noted, however, that the desired characteristics of producer gas for two applications, viz. power generation and FT synthesis are different. In the former case, we have to find conditions under which the producer gas has maximum Higher Heating Value (HHV), while in the latter situation, the $H_2$/CO ratio (along with actual content of hydrogen and carbon monoxide in terms of moles) is important. It is not necessary, however, that both of these conditions are met for same operating conditions. Therefore, a thorough study that scans the performance of gasifier for diverse range of biomass feedstock and combinations of operating conditions such as air ratio, temperature and gasification media is necessary for efficient design, optimization and scale-up of the gasifier for the applications of decentralized power generation and Fischer-Tropsch synthesis.

Several authors have addressed this matter with different approaches and a detailed literature review of modeling and optimization of biomass gasification is given in Chapter 3. However, a unified study that puts together different approaches and also gives a comprehensive account of the performance of gasifier under diverse range of operating conditions has not been reported yet. In this thesis, we have addressed the issue of optimization of biomass gasifier for the above two applications using thermodynamic equilibrium and semi-equilibrium models. We have also made a comparison of these models with the kinetic models. Given below is the broad outline and scope of the thesis.

## 1.1 OUTLINE AND SCOPE OF THE THESIS

The thesis comprises of 7 chapters. The summary of their contents is as follows:

- Chapter 2 gives an overview of biomass gasification from Indian and global perspectives. Starting with a brief history of renewable energy efforts in India, we have

discussed various biomass resources and utilization, potential of biomass as a coal substitute and various technical options for conversion of biomass to energy with relevant statistical data. Some details of technology of biomass gasification have also been included such as chemistry of gasification process, biomass pretreatment, fixed and fluidized bed gasification and post treatment of producer gas. Following this, the economic factors affecting decentralized power generation have been discussed. Next, review of biomass gasification efforts in Europe, USA, Latin America and other parts of the world is presented. Various major biomass gasification projects such as Ahlstrom Pyroflow, TPS-CFB, Batelle/FERCO have been discussed.

- Chapter 3 presents review of literature in the area of modeling of biomass gasification published in past one and half decades. More than 90 papers addressing the subject of modeling of gasification in downdraft and fluidized bed gasifiers, biomass pyrolysis and related processes such as catalytic tar cracking have been critically reviewed. Finally, an inference of the literature review has been presented with comparative analysis of the three approaches adopted in modeling, viz. equilibrium (both stoichiometric and non-stoichiometric), semi-equilibrium and kinetic modeling. Merits and demerits of these approaches have been discussed and the versatility of approach of non-stoichiometric equilibrium and semi-equilibrium models has been highlighted. Finally, the purpose of the present thesis has been justified.

- Chapter 4 presents a comprehensive study on thermodynamic optimization of biomass gasification for decentralized power generation and Fischer-Tropsch synthesis using the SOLGASMIX non-stoichiometric equilibrium model. The outcome of gasification process was assessed for different combinations of operating conditions. Four key parameters have

been used for optimization, viz. biomass type, gasification medium itself (air or air-steam mixture). Performance of gasification process has been assessed with four measures, viz. molar content of $H_2$ and CO in producer gas, $H_2$/CO molar ratio, LHV of producer gas, and overall efficiency of gasifier. Optimum set of operating condition have been found for gasification operation for decentralized power generation and Fischer-Tropsch synthesis.

- Chapter 5 addresses the issue of gasification of mixtures of biomasses using equilibrium and semi-equilibrium models. The semi-equilibrium models are essentially modified version of equilibrium models with restricted carbon conversion. This study is especially relevant for biomass gasifiers with power generation capacity exceeding 1 MW. Binary mixtures of common biomasses found in Northeastern India such as rice husk, bamboo dust and saw dust have been considered as basis. Potential for power generation has been evaluated on the basis of net yield and LHV of producer gas obtained from gasification. For all biomass mixtures, the optimum air ratio has been 0.3 with optimum gasification temperature of 800$^{o}$C. The least possible specific fuel consumption (under equilibrium condition) has been 0.8 kg/kW-h, while simulation of semi-equilibrium model estimate specific fuel consumption at 1.5 kg/kW-h under practical circumstances. Comparison of the simulation data with experimental data reported in literature show good agreement.

- In Chapter 6, an attempt is made to devise performance correlations for biomass gasifiers using simulations of semi-equilibrium non-stoichiometric models. Correlations have been devised for four principal parameters that benchmark the performance of gasifier, viz. lower heating value (LHV) and net yield (per unit biomass ) of producer gas, and volume fraction of CO and $CO_2$ in the gas resulting from biomass gasification. Three common biomass, viz. rice husk, saw dust and corn cobs have been chosen for analysis, with six

independent variables used in the correlations as air ratio, carbon conversion, gasification temperature and three elemental ratios in gasification mixture, viz. H/C, O/H and O/C. As many as 8 expressions (both linear and non-linear type) have been evaluated to best fit the data for each performance parameter. Best correlation has been chosen on the basis of statistical indicators. Comparison with experimental data has revealed that these correlations could predict the performance parameters within engineering accuracy of 10-20%. Moreover, these correlations are independent of the type of gasifier and are equally applicable to both fixed and fluidized bed systems.

- In Chapter 7, a comparative analysis is made of the three approaches in modeling of biomass gasifier system. These are equilibrium, semi-equilibrium (non-stoichiometric) and kinetic modeling. The SOLGASMIX algorithm forms the basis of equilibrium and non-equilibrium models, while a set of 13 simultaneous reactions forms the basis of kinetic model. A circulating fluidized bed reactor has been chosen as basis for comparison. The input to equilibrium and semi-equilibrium thermodynamic model is in terms of elemental vector, while input to kinetic model is the products that are formed out of pyrolysis of biomass entering the riser of the gasifier. Simulations of the kinetic model reveal that the products of gasification are far from equilibrium in the limited contact time available in the gasifier. Significant amount of biomass remains unconverted in the form of char and tar. Air ratio is revealed to be the most critical parameter, followed by temperature. The kinetic models also indicate that increasing the contact time, by raising the height of the riser (for given air ratio and temperature) does not help in improving quality of the producer gas. The comparative analysis of the three models also gives useful guideline for optimization of design of the gasifier.

- Chapter 8 presents an overview of all work done in the thesis and attempts to draw overall conclusions, which are useful not only for future research in the area but also for effective design and scale up of the gasifiers for applications of decentralized power generation and Fischer –Tropsch synthesis. Some suggestions for extending the research are also given.

## REFERENCES

[1] Ministry of Power, Government of India (web site: http://powermin.nic.in), accessed May 2009.

[2] Central Electricity Authority (CEA), Ministry of Power, Government of India (web site: http://www.cea.nic.in), accessed May 2009.

[3] Ministry of New and Renewable Energy (MNRE). 25 Years of Renewable Energy in India; New Delhi; 2007.

[4] Bharadwaj, A. Gasification and combustion technologies of agro–residues and their application to rural electric power systems in India. Ph.D. Dissertation, Carnegie Mellon University, Pittsburgh, PA (USA); 2002.

[5] Ghosh D, Sagar A, Kishore VVN. Scaling up biomass gasifier use: applications, barriers and interventions. Paper No. 103 (Climate Change Series), Washington: World Bank Environment Department; 2004.

[6] Dasappa S, Paul PJ, Mukunda HS, Rajan NKS, Sridhar G, Sridhar HV. Biomass gasification technology – A route to meet energy needs. Current Science India 2004;87(7):908–916.

[7] Meshram JR, Mohan S. Biomass power and its role in distributed power generation in India. In: 25 Years of Renewable Energy in India, New Delhi: Ministry of New and

Renewable Energy (MNRE); 2007. pp. 109–134.

[8] Tripathi, AK. Renewable energy development in India. In: Multiple Choice Questions on Renewable Energy; New Delhi: TERI Press; 2008. pp. 1–12.

[9] Nouni MR, Mullick SC, Kandpal TC. Providing electricity access to remote areas in rural India: An approach towards identifying potential areas for decentralized power supply. Renewable and Sustainable Energy Reviews 2008;12:1187–1220.

[10] Khan SA, Rashmi, Hussain MZ, Prasad S, Banerjee UC. Prospects of biodiesel production from microalgae in India. Reneweable and Sustainable Energy Reviews (2009), doi:10.1016/j.rser.2009.04.005.

[11] Ministry of Petroleum and Natural Gas, Annual Report 2007–08, New Delhi: Government of India, 2008 (available online on website: http://www.petroleum.nic.in).

[12] Tijmensen MJA, Faaij APC, Hamelinck CN, van Hardeveld MRM. Exploration of the possibilities for production of Fischer–Tropsch liquids and power via biomass gasification. Biomass and Bioenergy 2002;23:129–152.

[13] Boerrigter H, den Uil H, Calis HP. Green diesel from biomass via Fischer–Tropsch synthesis: new insights in gas cleaning and process design. In: AV Bridgwater, editor. Pyrolysis and Gasification of Biomass and Waste, Newbury:CPL Press; 2003, pp. 371–383.

[14] Hamelinck CN, Faaij APC, den Uil H, Boerrigter H. Production of FT transportation fuels from biomass: technical options, process analysis and optimization, and development potential. Energy 2004;29:1743–1771.

[15] Srinivas S, Malik RK, Mahajani SM. Fischer Tropsch synthesis using bio syngas and $CO_2$. In: Proc. of National Conference on Advances in Energy Research–2006, I.I.T. Bombay, Mumbai, 2006.

[16] Rohde D, Unruh D, Plas P, Lee K–W, Schaub G. Fischer–Tropsch synthesis from $CO_2$ containing syngas from biomass – Kinetic analysis of fixed bed reactor model

experiments. Studies in Surface Sciences and Catalysis 2004;153:97–102.

[17] Geerlings JJC, Wilson JH, Kramer GJ, Kuipers HPCE, Haek A, Huisman HM. Fischer-Tropsch technology – from active site to commercial process. Applied Catalysis A: General 1999;186:27-40.

[18] Sie ST, Krishna R. Fundamental and selection of advanced Fischer–Tropsch reactors. Applied Catalysis A: General 1999;186:55–70.

[19] Dry M. Present and future applications of the Fischer–Tropsch process. Appled Catalysis A: General 2004;276:1–3.

[20] Schulz H. Short history and present trends of Fischer–Tropsch synthesis. Applied Catalysis A: General 1999;186:3–12.

[21] Riedel T, Claeys M, Schulz H, Schaub G, Nam S-S, Jun K-W, Choi M-J, Kishan G, Lee K-W. Comparative study of Fischer-Tropsch synthesis with $H_2/CO$ and $H_2/CO_2$ syngas using Fe- and Co-based catalysts. Applied Catalysis A: General 1999;186:201-213.

[22] Wang Y-N, Ma W-P, Lu Y-J, Yang J, Xu Y-Y, Xiang H-W, Li Y-W, Zhao Y-L, Zhang B-J. Kinetics modeling of Fischer-Tropsch synthesis over an industrial Fe-Cu-K catalyst. Fuel 2003;82:195-213.

[23] Jun K-W, Roh H-S, Kim K-S, Ryu J-S, Lee K-W. Catalytic investigation for Fischer-Tropsch synthesis from biomass derived syngas. Applied Catalysis A: General 2004;259:221–228.

[24] Guo X, Liu Y, Chang J, Bai L, Xu Y, Xiang H, Li Y. Isothermal kinetics modeling of the Fischer-Tropsch synthesis over the spray dried Fe-Cu-K catalyst. Journal of Natural Gas Chemistry 2006;15:105-114.

[25] Purohit P. Economic potential of biomass gasification projects under clean development mechanism in India. Journal of Cleaner Production 2009;17:181–193.

भारतीय प्रौद्योगिकी संस्थान गुवाहाटी
Indian Institute of Technology Guwahati

CHAPTER 2

# Biomass Gasification: Indian and Global Perspective

## 2.1 INTRODUCTION

For a developing country like India, energy is the fundamental input for economic growth. The current target of economy growth rate is 10% and the energy demand in various sectors such as agriculture, industry, transport, commercial and domestic is fast rising. Electricity is perhaps the most vital form of energy input required for infrastructural development of the country in agriculture and industry, and it also plays a critical role in socio-economic development. The total installed capacity of power generation through various sources (as on February 2009) is about 147.72 GW with gross generation of more than 700 billion kWh [1]. The distribution of power generation through different sources, however, is uneven as shown in Figure 2.1. The thermal power contribution to this is ~ 63% followed by hydro power contributing ~ 25%. The share of nuclear power is the smallest with ~ 3%, and the power generation through renewable sources contributes the remaining ~ 9% [2,3]. The exact distribution of the power scenario in various states of India is given in Table

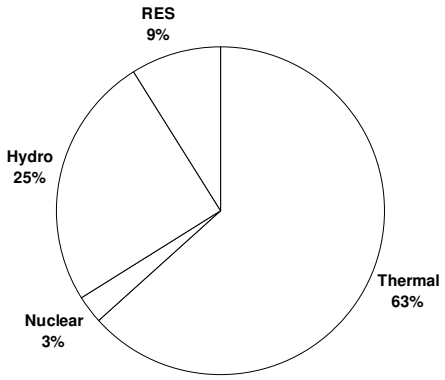


**Figure 2.1:** Contribution of various sources to total power generation in India

2.1. After grouping of the states into various regions, the distribution of power generation is shown in Figure 2.2. The reason behind this uneven distribution is that India has over 200 billions tons of coal deposits. Thus, the generation is mainly dominated by coal-based thermal power plants. However, the coal reserves are mainly concentrated in the north and northeastern states of India and not uniformly spread in the country (refer to Table 2.2 for distribution of coal deposits in various states). Presently the generation capacity is far insufficient to meet the demands. Although per capita electricity consumption in India during the past five years has risen from 566.7 to 704.2 kWh (refer to Figure 2.3), it is still far below the global average of 2000 kWh [4]. Currently, the estimated average gap between supply and demand of electricity (peak demand) is about 14%. The transmission and distribution losses are estimated between 26-32%. With rapid urbanization and industrialization, this gap is bound to rise fast. In addition, rural electrification has also posed a major challenge to India's growth. The major hurdles in rural electrification are extension of the grid to remote areas, large transmission losses and low peak loads due to small and isolated population [5-7]. Unlike urban areas, the primary electricity need of the rural population is for domestic lighting, running of irrigation pumps and small scale commercial activities such as floor mill and other rural industries. The National Electricity Policy (NEP) announced by Government

**Table 2.1:** Power Scenario in Various States of India
(Installed capacity in MW of power utilities including allocated shares in joint & central sector utilities)

| State | Mode wise breakup | | | | Nuclear | Hydro (Renewable) | Renewable Energy Sources | Grand Total |
|---|---|---|---|---|---|---|---|---|
| | Thermal | | | Total Thermal | | | | |
| | Coal | Gas | Diesel | | | | | |
| **States in Northern Region** | | | | | | | | |
| Delhi | 2240.50 | 804.70 | 0.00 | 3045.20 | 47.08 | 585.06 | 0.00 | 3677.34 |
| Haryana | 2518.07 | 532.04 | 3.92 | 3054.03 | 76.16 | 1331.40 | 68.70 | 4530.29 |
| Himachal | 95.41 | 60.89 | 0.13 | 156.43 | 14.08 | 1540.84 | 185.12 | 1896.47 |
| Jammu & Kashmir | 198.59 | 302.09 | 8.94 | 509.62 | 68.00 | 1469.50 | 111.83 | 2158.95 |
| Punjab | 3176.21 | 259.72 | 0.00 | 3435.93 | 151.04 | 3031.57 | 161.47 | 6780.01 |
| Rajasthan | 3112.49 | 661.54 | 0.00 | 3774.03 | 469.00 | 1456.82 | 726.30 | 6426.15 |
| Uttar Pradesh | 6493.31 | 541.16 | 0.00 | 7034.47 | 203.72 | 1605.49 | 402.98 | 9246.66 |
| Uttarakhand | 232.80 | 68.25 | 0.00 | 301.05 | 16.28 | 1955.73 | 109.97 | 2383.03 |
| Chandigarh | 26.51 | 15.07 | 0.00 | 41.58 | 4.84 | 47.04 | 0.00 | 93.46 |
| Central (Unallocated) | 713.61 | 285.73 | 0.00 | 999.34 | 129.80 | 401.70 | 0.00 | 1530.84 |
| **GRAND TOTAL FOR NORTHERN REGION** | **18807.50** | **3531.19** | **12.99** | **22351.68** | **1180.00** | **13425.15** | **1766.37** | **38723.20** |
| **States in Western Region** | | | | | | | | |
| Goa | 279.18 | 48.00 | 0.00 | 327.18 | 0.00 | 0.00 | 30.05 | 357.23 |
| Daman & Diu | 64.99 | 4.13 | 0.00 | 69.12 | 1.98 | 0.00 | 0.00 | 71.10 |
| Gujarat | 6349.79 | 2748.62 | 17.48 | 9115.89 | 825.00 | 772.00 | 1397.50 | 12110.39 |
| Madhya Pradesh | 4281.10 | 252.91 | 0.00 | 4534.01 | 92.88 | 3223.67 | 262.71 | 8113.27 |
| Chhattisgarh | 3312.90 | 0.00 | 0.00 | 3312.90 | 0.00 | 120.00 | 174.15 | 3607.05 |
| Maharashtra | 10112.00 | 3709.28 | 0.00 | 13821.28 | 852.06 | 3332.83 | 2159.21 | 20165.38 |
| Dadra & Nagar Haveli | 52.19 | 26.61 | 0.00 | 78.80 | 1.98 | 0.00 | 0.00 | 80.78 |
| Central (Unallocated) | 950.35 | 193.67 | 0.00 | 1144.02 | 66.10 | 0.00 | 0.00 | 1210.12 |
| **GRAND TOTAL FOR WESTERN REGION** | **25402.50** | **6600.72** | **17.48** | **32403.20** | **1840.00** | **7448.50** | **4023.62** | **45715.32** |

*Table 2.1 (continued……)*

| State | Mode wise breakup | | | | Nuclear | Hydro (Renewable) | Renewable Energy Sources | Grand Total |
|---|---|---|---|---|---|---|---|---|
| | Thermal | | | Total Thermal | | | | |
| | Coal | Gas | Diesel | | | | | |
| **States in Southern Region** | | | | | | | | |
| Andhra Pradesh | 5719.88 | 1603.40 | 36.80 | 7360.08 | 37.41 | 3572.93 | 668.66 | 11639.08 |
| Karnataka | 3302.67 | 220.00 | 234.42 | 3757.09 | 190.90 | 3518.20 | 1880.54 | 9346.73 |
| Kerala | 765.38 | 524.00 | 256.44 | 1545.82 | 80.09 | 1769.10 | 119.04 | 3514.05 |
| Tamil Nadu | 5519.81 | 1026.40 | 411.66 | 6957.87 | 657.39 | 2093.95 | 4379.64 | 14088.85 |
| NLC | 100.17 | 0.00 | 0.00 | 100.17 | 0.00 | 0.00 | 0.00 | 100.17 |
| Pondicherry | 207.01 | 32.50 | 0.00 | 239.51 | 17.09 | 0.00 | 0.02 | 256.62 |
| Central (Unallocated) | 1067.58 | 0.00 | 0.00 | 1067.58 | 117.12 | 0.00 | 0.00 | 1184.70 |
| **GRAND TOTAL FOR SOUTHERN REGION** | **16682.50** | **3646.10** | **939.32** | **21267.92** | **1100.00** | **10724.18** | **7047.90** | **40130.20** |
| **States in Eastern Region** | | | | | | | | |
| Bihar | 1846.59 | 0.00 | 0.00 | 1846.59 | 0.00 | 73.00 | 50.40 | 1969.99 |
| Jharkhand | 1972.52 | 0.00 | 0.00 | 1972.52 | 0.00 | 176.00 | 4.05 | 2152.57 |
| West Bengal | 6357.94 | 100.00 | 12.20 | 6470.14 | 0.00 | 1162.00 | 99.55 | 7731.69 |
| DVC | 3100.00 | 90.00 | 0.00 | 3190.00 | 0.00 | 196.00 | 0.00 | 3386.00 |
| Orissa | 1865.23 | 0.00 | 0.00 | 1865.23 | 0.00 | 2174.93 | 32.30 | 4072.46 |
| Sikkim | 1232.12 | 0.00 | 0.00 | 1232.12 | 0.00 | 77.00 | 0.00 | 1309.12 |
| Central (Unallocated) | 1232.12 | 0.00 | 0.00 | 1232.12 | 0.00 | 77.00 | 0.00 | 1309.12 |
| **GRAND TOTAL FOR EASTERN REGION** | **16446.38** | **190.00** | **17.20** | **16653.58** | **0.00** | **3933.93** | **227.41** | **20814.92** |

*Table 2.1 (continued……)*

| State | Mode wise breakup | | | | Nuclear | Hydro (Renewable) | Renewable Energy Sources | Grand Total |
|---|---|---|---|---|---|---|---|---|
| | Thermal | | | Total Thermal | | | | |
| | Coal | Gas | Diesel | | | | | |
| **States in Northeastern Region** | | | | | | | | |
| Assam | 60.00 | 441.50 | 20.69 | 522.19 | 0.00 | 431.00 | 27.11 | 980.30 |
| Arunachal Pradesh | 0.00 | 21.00 | 15.88 | 36.88 | 0.00 | 98.00 | 45.26 | 180.14 |
| Meghalaya | 0.00 | 26.00 | 2.05 | 28.05 | 0.00 | 229.00 | 31.03 | 288.08 |
| Tripura | 0.00 | 160.50 | 4.85 | 165.35 | 0.00 | 62.00 | 16.01 | 243.36 |
| Manipur | 0.00 | 26.00 | 45.41 | 71.41 | 0.00 | 81.00 | 5.45 | 157.86 |
| Nagaland | 0.00 | 19.00 | 2.00 | 21.00 | 0.00 | 53.00 | 28.67 | 102.67 |
| Mizoram | 0.00 | 16.00 | 51.86 | 67.86 | 0.00 | 34.00 | 17.47 | 119.33 |
| Central (Unallocated) | 0.00 | 56.00 | 0.00 | 56.00 | 0.00 | 128.00 | 0.00 | 184.00 |
| **GRAND TOTAL FOR NOREASTERN REGION** | **60.00** | **766.00** | **142.74** | **968.74** | **0.00** | **1116.00** | **171.00** | **2255.74** |
| **Islands** | | | | | | | | |
| Andaman & Nicobar | 0.00 | 0.00 | 60.05 | 60.05 | 0.00 | 0.00 | 5.35 | 65.40 |
| Lakshadweep | 0.00 | 0.00 | 9.97 | 9.97 | 0.00 | 0.00 | 0.76 | 10.73 |
| **GRAND TOTAL FOR ISLANDS** | **0.00** | **0.00** | **70.02** | **70.02** | **0.00** | **0.00** | **6.11** | **76.13** |

Source [1]

**Table 2.2:** Distribution of Coal Reserves in India

| Sr. No. | State | Total Reserves* (MMT) |
|---|---|---|
| 1. | Andhra Pradesh | 17715 |
| 2. | Arunachal Pradesh | 90 |
| 3. | Assam | 375 |
| 4. | Bihar | 160 |
| 5. | Chhattisgarh | 41450 |
| 6. | Jharkhand | 74392 |
| 7. | Madhya Pradesh | 20346 |
| 8. | Maharashtra | 9670 |
| 9. | Meghalaya | 460 |
| 10. | Nagaland | 20 |
| 11. | Orissa | 63223 |
| 12. | Sikkim | 73 |
| 13. | Uttar Pradesh | 1062 |
| 14. | West Bengal | 28335 |
| | **GRAND TOTAL** | **257381** |

Source [21]. * Total capacity including proven, indicated and inferred reserves.

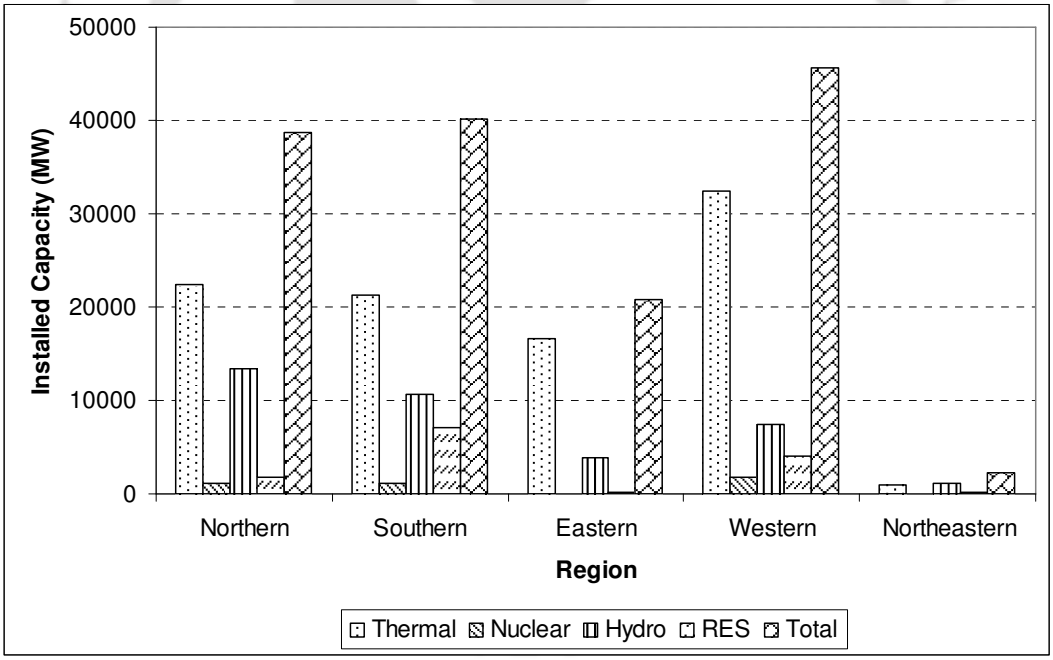


**Figure 2.2:** Distribution of power generation in different regions of India

of India along with other activities such as *Rajiv Gandhi Grameen Vidyutikaran Yojana* has given high priority to rural electrification. The primary aim of this is to achieve complete rural electrification by 2010. Table 2.3 gives a more detailed account of the status of rural electrification in various states of India. In order to present a realistic picture of rural

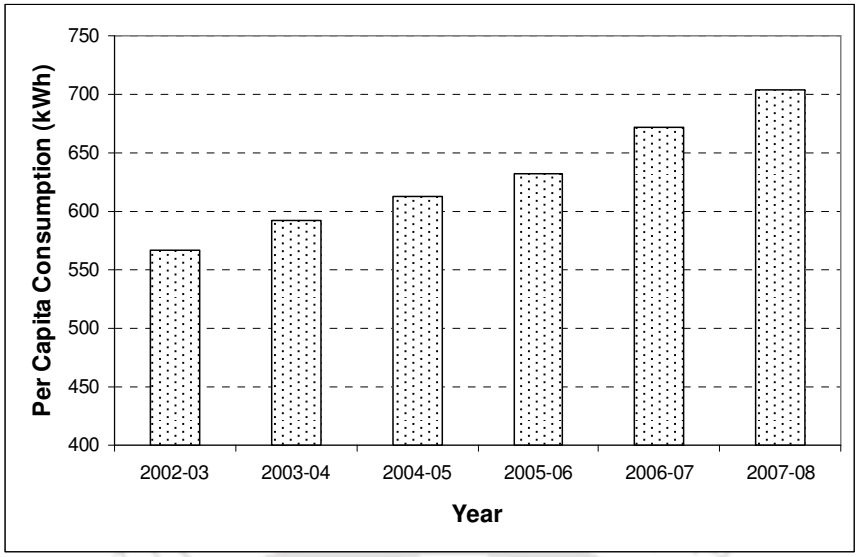


**Figure 2.3:** Per capita power consumption in India

electrification, Ministry of Power of Government of India has modified the definition of an "electrified village". Earlier definition of electrified village was "a village in which electricity is being used within its revenue area for any purpose whatsoever". In 2004-05, this definition was given four important criteria as follows [8,9]:

1. Provision of basic infrastructure such as distribution transformer and distribution lines in the inhabited locality.

2. Provision of electricity to public places like schools, *panchayat* offices, health centers etc.

3. Access of electricity to a minimum of 10% households in the village.

4. Compulsory certification from *Gram Panchayat* regarding completion of village electrification.

Although the overall rural electrification stands at an impressive figure of 82%, the actual number of households accessing the electricity is mere 44% [10]. Presently, the rural electrification is growing at a rate of 3-6% annually [9,11]. In very remote areas where extensive of grid is not feasible, decentralized power generation through renewable sources offers a viable solution for meeting the electricity needs of the local population [12-14]. In fact, the NEP insists on use of both conventional and renewable sources of electricity

**Table 2.3:** Current Status of Rural Electrification in India

| Sr. No. | State / Union Territory | Total Inhabited Villages* | Villages Electrified as on 31-01-2009 | Percentage of Village Electrification | Unelectrified Villages as on 31-01-2009 | No. of connections to rural households** |
|---|---|---|---|---|---|---|
| | | | **STATES** | | | |
| 1. | Andhra Pradesh | 26613 | 26613 | 100% | 0 | 3,954,128 |
| 2. | Arunachal Pradesh | 3863 | 2195 | 56.8% | 1668 | 76,407 |
| 3. | Assam | 25124 | 19741 | 78.6% | 5383 | 1,414,828 |
| 4. | Bihar | 39015 | 20620 | 52.9% | 18395 | 6,022,036 |
| 5. | Chhattisgarh | 19744 | 18877 | 95.6% | 867 | 1,285,545 |
| 6. | Delhi | 158 | 158 | 100% | 0 | N.A. |
| 7. | Jharkhand | 29354 | 9119 | 31.1% | 20235 | 2,926,260 |
| 8. | Goa | 347 | 347 | 100% | 0 | N.A. |
| 9. | Gujarat | 18066 | 18014 | 99.7% | 52 | 1,595,853 |
| 10. | Haryana | 6764 | 6764 | 100% | 0 | 569,686 |
| 11. | Himachal Pradesh | 17495 | 17183 | 98.2% | 312 | 36,479 |
| 12. | Jammu & Kashmir | 6417 | 6304 | 98.2% | 113 | 295,221 |
| 13. | Karnataka | 27481 | 27126 | 98.7% | 355 | 1,836,403 |
| 14. | Kerala | 1364 | 1364 | 100% | 0 | 23,799 |
| 15. | Madhya Pradesh | 52117 | 50255 | 96.3% | 1892 | 2,653,536 |
| 16. | Maharashtra | 41095 | 36296 | 88.3% | 4799 | 2,633,742 |
| 17. | Manipur | 2315 | 1982 | 333 | 85.5% | 76,267 |
| 18. | Meghalaya | 5782 | 3428 | 59.3% | 2354 | 188,648 |
| 19. | Mizoram | 707 | 570 | 80.6% | 137 | 44,334 |
| 20. | Nagaland | 1278 | 823 | 64.4% | 455 | 142,992 |
| 21. | Orissa | 47529 | 26535 | 55.8% | 20994 | 4,858,292 |
| 22. | Punjab | 12278 | 12278 | 100% | 0 | 405023 |
| 23. | Rajasthan | 39753 | 27286 | 68.3% | 12467 | 2230387 |
| 24. | Sikkim | 450 | 425 | 94.4% | 25 | 28166 |
| 25. | Tamil Nadu | 15400 | 15400 | 100% | 0 | 1692235 |
| 26. | Tripura | 858 | 491 | 57.2% | 367 | 228759 |
| 27. | Uttar Pradesh | 97942 | 86450 | 88.3% | 11492 | 1694075 |
| 28. | Uttaranchal (Uttarakhand) | 15761 | 15213 | 96.5% | 548 | 357309 |
| 29. | West Bengal | 37945 | 36462 | 96.1% | 1483 | 3974005 |
| | **Total (States)** | **593015** | **488289** | **82.3%** | **104726** | **41,244,415** |
| | | | **UNION TERRITORY*** ** | | | |
| 1. | Andaman and Nicobar Islands | 501 | 331 | 66.1% | 170 | N.A. |
| 2. | Chandigarh | 23 | 23 | 100% | 0 | N.A. |
| 3. | Dadra & Nagar Haveli | 70 | 70 | 100% | 0 | N.A. |
| 4. | Daman & Diu | 23 | 23 | 100% | 0 | N.A. |
| 5. | Lakshadweep | 8 | 8 | 100% | 0 | N.A. |
| 6. | Pondicherry | 92 | 92 | 100% | 0 | N.A. |
| **Total (Union Territories)** | | **717** | **547** | **76.3** | **170** | **--** |
| **TOTAL (ALL INDIA)** | | **593,732** | **488,836** | **82.3%** | **104,896** | **41,244,415** |

Source [1-2]

* - As per 2001 census.

** - Including the connections to households below poverty line (as on March 1, 2009) under *Rajiv Gandhi Gramin Vidyutikaran Yojana*.

*** - Union territories do not participate in the *Rajiv Gandhi Gramin Vidyutikaran Yojana*.

generation, as long as they are economically viable. In order to reduce load on grid and state electricity boards, NEP emphasizes use of renewable energy even in areas with access to grid, provided renewable sources are as economic as conventional ones. Options for decentralized generation through renewable sources for are wind energy systems, solar photovoltaics, biomass gasifiers and small hydro power systems etc. [10]. The most economic option depends on the location of area and natural resources available [15]. Another motive for exploration of renewable sources for power generation is the fluctuating economy of the conventional sources. The principal sources of energy are fossil fuels such as coal, oil and gas. However, the prices of oil and gas are highly fluctuating and there is also a fear of their acute shortage in the future. Moreover, emancipated use of fossil fuels also causes environmental pollution problems such as emission of greenhouse gases. Thus, there is an urgent need for harnessing the large potential of renewable energy sources in a planned and strategic manner to reduce the gap between demand and supply. Promotion of energy conservation and increased use of renewable energy are the twin planks of a sustainable energy supply [14,16]. In this chapter, we have attempted to review the feasibility of the decentralized power generation through biomass gasification and technical and economic aspects related to this. The estimated annual biomass production in India is 200 million tons, which (unlike coal) is distributed almost evenly in the country (greater details about this are given in section 2.3). This is equivalent of 20 GW of installed capacity. In addition, agroresidues and woody bio-residues from wastelands (estimated at 60 million hectares) could add another 100 – 300 millions tons, which amount to 45 GW of installed capacity. However, the total installed capacity of biomass based power generation (inclusive of bagasse & non-bagasse cogeneration and biomass gasifiers; as of September 2007) is 838 MW [17]. This capacity is mainly through cogeneration (692.3 MW through bagasse fired boilers), which is an inefficient method of utilization of the biomass energy. This indicates

that the vast potential of biomass power remains almost unused, and there is an urgent need of utilization of this resource through more efficient technologies such as biomass gasification.

## 2.2 BRIEF HISTORY OF RENEWABLE ENERGY EFFORTS IN INDIA

The main renewable sources are solar energy, wind energy, small hydropower, biomass, biogas and energy recovery from municipal and industrial wastes. India has tremendous natural resources that have potential of all of the above-mentioned renewable energy sources. The advantages of renewable energy are: (1) complete perpetuity; (2) local availability without needing major transport; (3) modularity, i.e. economy is independent of scale, and (4) non-polluting nature (carbon neutrality). Especially, for remote villages located in hilly and mountainous regions, where transmission of electricity through power grid is difficult, renewable energy is the only option for meeting energy requirements for cooking, heating and domestic and street lighting. Decentralized electricity generation through renewable sources even in urban areas gives a viable solution to the shortage and increasing cost of electricity. Ministry of New and Renewable Energy (MNRE) of Government of India has implemented comprehensive programs for the development and utilization of various renewable energy sources in the country.

The first ever endeavor in renewable energy in India dates back to 1897 in which a small hydro power project of 130 kW capacity was implemented at Sidrapong in Darjeeling [9,18]. This was followed by two more hydro projects of 40 and 50 kW capacity each at Chamba and Jubbal installed in 1902 ad 1911 respectively. The facility of transmission lines did not exit at that time, and hence, power generated through these projects was mainly utilized for meeting the local energy demands.

### 2.2.1 Ministry of New and Renewable Energy [19]

In the modern independent India, efforts in renewable energy began in 1981 during 6th five-year plan (1980–85) with establishment of Commission for Additional Sources of Energy (CASE) as a part of Department of Science and Technology (DST). This commission was in line with Atomic energy Commission and was bestowed the responsibility of developing renewable energy. In 1981, Government of India created Department of Non-conventional Energy Sources (DNES) for development, demonstration and application of renewable energy. CASE became a part of this department. In 1982, Ministry of Energy was expanded to include Department of Petroleum and DNES. In 1983, an advisory board on energy was set up to formulate an integrated energy policy covering commercial and noncommercial energy resources. Almost a decade later, DNES was transformed into a full-fledged ministry – Ministry of Non-Conventional Energy Sources (MNES). In October 2006, the MNES was renamed as Ministry of New and Renewable Energy (MNRE). MNRE is the nodal ministry of Government of India (and only of its kind in the world) that handles the matters related to development and promotion of renewable energy in India. In the 6th plan, Government encouraged research, design, development, indigenous fabrication and demonstration projects along with stand-alone systems on solar, wind, biomass and biogas (for decentralized power generation) through financial subsidy and incentives. During 7th plan (1985–90) as well priority was given to solar, thermal, biogas and solar photovoltaic systems for decentralized power generation. In the same period, Indian Renewable Energy Development Agency (IREDA, a financial arm of the MNES) was constituted for exclusive funding for natural renewable energy projects through soft loans. In the 8th plan (1992–97) Government emphasized on commercialization of the renewable energy technologies and new research & development policy was formulated that allowed industrial participation. Market-oriented approach was adopted for commercial / near-commercial technologies with

phasing out of subsidies. In some areas, capital subsidy regime was shifted to interest subsidy system. More fiscal incentives were provided during the 9th plan (1997–2002) such as customs and excise relief, income tax holiday, accelerated depreciation, provision of facilities by state electricity boards for wheeling, banking, buy-back and third-party sale at remunerative prices. Resources from external funding agencies such as World Bank, Asian Development Bank, UNDP (United Nations Development Program), GEF (Global Environment Facility) and DANIDA (Danish International Development Agency) were also utilized. The 10th plan emphasized on grid connected power, rural electrification and promotion of renewable energy systems and devices in urban areas. More incentive was given for the demand-driven rather than supply-driven programs and capital subsidies were replaced with subsidies linked with renewable energy generation that encouraged purchase of renewable energy. In the 11th plan (2007–11), which is being finalized, thrust will be on grid-interactive and distributed renewable power; rural, urban, industrial and commercial applications of renewable energy, R&D for new and emerging technologies through financial and fiscal incentives.

### 2.2.2 Important policies of Government of India for renewable energy

Some important policies and acts made by the Government regarding renewable energy are listed below [17]:

- *Renewable power purchase guideline (1993)*: Through these advisory guidelines, MNRE instructed states a buy back price of Rs. 2.25/kWh for power through renewable sources (5% annual increament) with 1993 as the base year.
- *Integrated coal policy (1996):* The committee on integrated coal policy recommended adoption of coal conservation measures, investment of private capital in the sector, deregulation of coal and coal product prices and setting up of a regulatory board.
- *Energy Conservation Act (2001)*: This act established comprehensive law that adopted

standards and procedures and prescribed measures for energy conservation.

- *Electricity Act (2003)*: This act identified the role of renewable energy technologies for supplying power to the utility grid as well as stand alone system. It stated that Central Government shall prepare a national electricity and tariff policy for optimal utilization of various resources including renewable sources in consultation with the state government along with quota for the renewables.
- *National Electricity Policy (2005):* This policy recognized the role of renewable electricity in the areas where grid connectivity was neither cost effective nor feasible.
- *National Tariff Policy (2006):* Through this policy the State Regulatory Commissions were authorized to decide upon a minimum percentage for purchase of energy from renewable sources taking into account local availability of such resources and its impact on retail tariffs.
- *Rural Electrification Policy (2006):* This policy had 3 principal aims, viz. (1) provision of access to electricity to all households by 2009, (2) quality and reliable power supply at a reasonable rate, (3) minimum consumption of 1 unit per household per day by 2012. It provided for decentralized distributed generation facilities together with local distribution network based on either conventional or renewable sources of electricity generation (whichever suitable and economical). The policy also encouraged utilization of renewable energy even where grid connectivity exists provided it is cost effective.

### 2.2.3 State-of-the-art on renewable energy front

In 2007, renewable energy endeavors in India completed 25 years. In these years, there has been a vigorous pursuit of activities relating to research, development, demonstration and fabrication of variety of new technologies suitable for different sectors. Several technologies and devices have been developed and commercialized such as biogas plants, improved *choolhas* (or woodstoves), various solar energy based devices (for example

solar cookers, solar lanterns, street lights, pumps etc), wind electricity generators, water pumping wind mills, biomass gasifiers and small hydroelectric devices. Approximately 11 GW of grid-interactive renewable power generating capacity has been produced with major contributions from wind (7660 MW), small hydropower (2015 MW), bio power (through agro residues and plantations, 560 MW), bagasse-based cogeneration (693 MW), urban & industrial wastes (55 MW) and solar (2.12 MW). The contribution by renewable sources to the total installed capacity (as of February 2009 [1]) stands at an impressive 9%, and is continuously growing. Government has been providing several financial and promotional incentives. During 2005–06 loan sanctions from IREDA stood at Rs. 505.83 crores, while in 2006–07 the sanctions totaled at Rs. 588 crores. Major sectors funded include wind, small hydropower, biomass power, energy efficiency and conservation, solar thermal and biofuels. IREDA has reintroduced the equipment financing scheme of biomass gasifiers for thermal applications (> 1000 kWh) for captive use in industry and small hydropower project exceeding station capacity of 25 MW. In 2006–07, the financing policy was reviewed and new scheme for financing industrial cogeneration was introduced. The target of IREDA for 11$^{th}$ plan is loan sanction of Rs. 5700 crore that would add capacity of 1.75 GW.

Estimated potential of various renewable energy sources and cumulative achievements throughout the country (as on September 30, 2007) have been given in Table 2.4 [3,17]. The global position of India in generation / utilization of renewable energy sources is notable, and it is likely to get higher in future. For biogas utilization, India ranks 2$^{nd}$ (after China), for wind energy India stands 4$^{th}$ (after Germany, Spain and USA), for small hydropower India ranks 5$^{th}$ while for solar photovoltaic India stands 7$^{th}$ in the world. The financial allocation for the renewable energy has grown from 0.1% in the 6$^{th}$ plan with 28.1% allocation to the energy sector as a whole to 0.48% in the 10$^{th}$ plan with 27.3% allocation to energy sector as a whole.

Table 2.4

**Renewable Energy in India at a Glance***

| Sl. No. | Source / System | Estimated Potential (MW) | Cumulative installed capacity (MW) / number |
|---|---|---|---|
| **I.** | **Power From Renewables** | | |
| *A* | *Grid interactive renewable power* | | |
| 1. | Bio power (agro residues and plantations) | 16 881 | 560.30 |
| 2. | Wind power | 45 195 | 7660.20 |
| 3. | Small hydropower (≤ 25 MW) | 15 000 | 2014.66 |
| 4. | Co-generation bagasse | 5000 | 692.33 |
| 5. | Urban waste to energy | 2700 | 55.20 |
| 6. | Solar power | -- | 2.12 |
| | **SUBTOTAL (MW)** | **84 776** | **10 984.81** |
| *B* | *Captive / Combined Heat and Power / Distributed Renewable Power* | | |
| 7. | Biomass / co-generation (bagasse) | -- | 59.00 |
| 8. | Biomass gasifier | -- | 86.53 |
| 9. | Energy recovery from waste | -- | 20.21 |
| | **SUBTOTAL (MW)** | **--** | **165.74** |
| | **TOTAL (A+B)** | | **11 150.55** |
| **II.** | **Remote Village Electrification** | | |
| 1. | Villages | -- | 3207 |
| 2. | Hamlets | -- | 830 |
| **III.** | **Decentralized Energy Systems** | | |
| 1. | Family type biogas plants | 12 million | 3.93 million |
| 2. | Solar photovoltaic programme | 20 MW / $km^2$ | |
| | (i) Street lighting systems (no.) | | 61 321 |
| | (ii) Home lighting systems (no.) | | 363 399 |
| | (iii) Solar lanterns (no.) | | 565 628 |
| | (iv) Solar power plants | | 2.18 MW |
| 3. | Wind pumps (no.) | -- | 1180 |
| 4. | Solar cookers (no.) | -- | 0.62 million |
| 5. | Solar water heating system ($m^2$ collector area) | 140 million | 2 million |
| 6. | Solar photovoltaic pumps (no.) | -- | 7068 |
| **IV** | **Other programs** | | |
| 1. | Energy parks (no.) | | 505 |
| 2. | Aditya solar shops (no.) | | 268 |
| 3. | Battery operated vehicles (no.) | | 262 |

* Data as of September 30, 2007

Source [3,17]

## 2.3 BIOMASS POWER IN INDIA

Per the Public Utility Regulatory Policies Act (PURPA, 1978) in USA, the word "Biomass" refers to any organic material not derived from fossil fuels. However, in the context of biomass based power generation, biomass refers to essentially all organic matter that originates from plants – including all land and water-based vegetation such as algae, trees and crop residues. Biomass has been a primary energy source for cooking and heating. It is estimated that if all biomass used in India was substituted by petroleum products, it would require import of 30 MMTPA of crude oil, creating a burden of Rs. 500 billion [20]. In the past few decades, interest in biomass based energy is increasing due to some distinct advantages it offers: it is renewable, widely available and uniformly distributed, carbon neutral and more economical than other renewable sources such as solar photovoltaics. By the year 2050, 15–30% of world's primary energy could come from biomass. As of now, about 11% of primary energy needs are being met with biomass. The estimates of MNRE [16] indicate that 32% of the total primary energy use in the country is derived from biomass and more than 70% of population is dependent on it for the energy needs. Biomass based power generation in India is attracting an investment of Rs. 1000 crore each year with generation of more than 700 billion units of electricity and an annual employment of 10 million man-days in rural areas [20].

### 2.3.1 Biomass as a coal substitute

As of April 2007, India has over 250 billion tons of coal reserves [21]. The distribution of these coal reserves in various states is given in Table 2.2.The consumption of coal by various industrial sectors was 492.5 MMT in 2007–08 (with 363.6 MMT utilized for power generation), while in 2008–09 consumption stood at 555 MMT (with 416 MMT utilized for power generation). With these consumption rates, the coal reserves are expected to last for the next 200 years [4]. As depicted in Figure 2.1, more than 60% of the current

**Table 2.5:** Analysis of Major Biomasses Available in Northeast Region of India

(A) Ultimate Analysis

| Composition in weight percent (Dry Basis) | | | | | |
|---|---|---|---|---|---|
| **Biomass** | **Carbon** | **Hydrogen** | **Nitrogen** | **Oxygen** | **Ash** |
| Bamboo dust | 39.88 | 5.5 | 0.89 | 47.92 | 5.81 |
| Rice husk | 37.03 | 5.25 | 0.09 | 40.94 | 16.69 |
| Bagasse | 47 | 6.5 | 0 | 42.5 | 4 |
| Coconut fiber | 45.68 | 5.89 | 0.99 | 44.63 | 2.81 |
| Saw dust | 52.28 | 5.2 | 0.47 | 40.85 | 1.2 |

(B) Proximate Analysis

| **Biomass** | **Fixed Carbon** | **Volatile matter** | **Ash** |
|---|---|---|---|
| Bamboo dust | 9.3 | 74.2 | 16.5 |
| Rice husk | 13.2 | 65.3 | 19.2 |
| Bagasse | 11.9 | 86.3 | 1.8 |
| Coconut fibre | 29.7 | 66.6 | 3.7 |
| Saw dust | 25.0 | 72.4 | 2.6 |

Source [77].

electricity generation is through coal-based thermal power plants. Therefore, we must compare the option of biomass-based power to the coal-based power so as to assess the feasibility of biomass route. The typical composition of biomass varies significantly (refer to Table 2.5 for composition of major biomasses in the northeastern region); however, typically all biomasses contain about 60–80% volatiles and 15–25% fixed carbon. On comparative basis, coal has only 20–30% volatiles and large (50–70%) fixed carbon. Ash and moisture content shows even wider range variation. Rice husk contains about 20% ash while wood has less than 1% ash, whereas moisture content of sugarcane bagasse could be as high as 50% against less than 20% moisture content in rice husk. As a result of this, the LHV of low ash coal (typically in the range 35–40 MJ/kg) is higher than that of biomass (16–18 MJ/kg). However, if the ash content of coal is high (~ 30% or so, typical of Indian coal), the LHV of coal (20–22 MJ/kg) is almost same as that of biomass (16–18 MJ/kg). This substantiates substitution of coal by biomass. Moreover, coal deposits are located only in the state of Bihar

and northeast. Thus, transportation costs play a major role in coal based thermal power projects. Biomass, on the other hand, is uniformly and widely distributed in the country.

### 2.3.2 Biomass resources and utilization

The major source of biomass in India is the waste and byproducts of agriculture. In 1985–86, National Productivity Council undertook a comprehensive survey of this massive resource. On the basis of survey of ratios of various crop residues and useful products, an estimate of state-wise and crop-wise residue generation was made. However, the "recoverable" residues showed significant variation as a function of geographical location and harvesting methods. This data has been updated regularly, and for the agricultural production for 2006–07 the net production of residue could be around 500 million tons, as described in greater detail in Table 2.6. More recently, Indian Institute of Science Bangalore has also completed MNRE-sponsored project of creating biomass atlas of India and results of this survey are given in Table 2.7. All of the residue cannot be available for power generation, as it has been utilized for other purposes such as cooking and cattle feed. Further studies indicated that about 15–20% of the agricultural residue can be made available for power generation without affecting the present usage. Survey of I.I.Sc. Bangalore indicates that about 125 MMTPA of biomass could be available for power generation with a potential of 16.23 GW. Moreover, technical improvement in the domestic usage of biomass could yield an additional surplus. For example, domestic cooking stoves (with efficiency ≤ 10%) use about 220 millions tons of biomass. Even a marginal improvement in this, with new stove models with efficiency of ~ 20%, can make available an additional surplus biomass of 100 million tons. Even conservative estimate indicate that availability of biomass through agro-residues would in the range 150–160 millions tons which is sufficient to sustain 16–18 GW of power generation with plant load factor of 60-80% [20].

The production of sugarcane in India was estimated at about 320 MMT in 2006–07.

**Table 2.6:** Estimation of Biomass Production in India (Crop-wise Data)

| Crop | Main Crop Production (MMTPA) | Type of Residue | Crop to residue ratio | Residue Quantity (MMTPA) | Conventional Use |
|---|---|---|---|---|---|
| Rice | 90 | Straw | 1.3 | 117 | Cattle feed |
| | | Husk | 0.3 | 27 | Fuel for small factories |
| Wheat | 80 | Straw | 1.5 | 120 | Cattle feed |
| Coarse cereals | 30 | Straws and husk | 1.8 | 54 | Cattle feed and fuel |
| Sugarcane | 320 | Bagasse | 0.3 | 96 | Captive fuel by sugar plants, raw material for paper manufacture |
| | | Tops | 0.05 | 16 | Cattle feed |
| | | Trash | 0.07 | 20 | Burnt in fields |
| Coconut | 14 billion nuts | Shell | 0.13 kg/nut | 0.2 | Domestic fuel, raw material for mattresses, carpets etc. |
| | | Fiber | 0.2 kg/nut | 2.8 | |
| | | Pith | 0.2 kg/nut | 2.8 | No specific use. Usually disposed off. |
| Cotton | 3.5 | Stalks | 3.0 | 10.5 | Domestic fuel |
| | | Gin waste | 0.1 | 0.35 | Fuel for brick factories |
| Oilseeds | 20 | Straws and husk | 1.1 | 22 | -- |
| Pulses | 14 | Straws | 1.3 | 18 | Domestic fuel |
| Jute | 2 | Stalks | 2.0 | 4 | Fuel for processing tobacco leaves and as domestic fuel |
| **GRAND TOTAL** | | | | **499** | |

Source [20]. * - *Agricultural production data is for the year 2006-07 (Ministry of Agriculture). The residue ratios and conventional uses from reports of Taluka level studies by MNRE (1998-2004).*

Out of this, about 200 MMT is consumed by 550 sugar factories in India. After crushing, this would generate about 60 MMT of wet bagasse (with about 50% moisture content). The total captive consumption of the factories to meet the steam and power demand is approx 50 MMT and rest is utilized for paper manufacture. Task force set by MNRE in 1993 indicated that an additional 3500 MW of electricity can be generated by adopting technically and economically

**Table 2.7:** Statewise Annual Biomass Production Data and Power Generation Potential (2002-04)

| Sr. No. | State | Area (kHa) | Crop Production (MMTPA) | Biomass Generation (MMTPA) | Biomass Surplus (MMTPA) | Power Potential (MWe) |
|---|---|---|---|---|---|---|
| 1. | Andhra Pradesh | 6021.5 | 28.345 | 21.569 | 3.948 | 481.3 |
| 2. | Assam | 2586.6 | 5.945 | 6625.1 | 1.362 | 163.1 |
| 3. | Bihar | 5833.1 | 13.818 | 20.442 | 4.286 | 530.3 |
| 4. | Chhattisgarh | 3815.5 | 6.143 | 10.124 | 1.908 | 220.9 |
| 5. | Goa | 156.3 | 0.555 | 0.929 | 0.181 | 22.7 |
| 6. | Gujarat | 6519.0 | 20.636 | 25.471 | 8.353 | 1131.1 |
| 7. | Haryana | 4890.2 | 13.520 | 26.581 | 10.106 | 1303.5 |
| 8. | Himachal Pradesh | 710.3 | 1.329 | 2.668 | 0.988 | 128.0 |
| 9. | Jammu and Kashmir | 368.7 | 0.649 | 1.199 | 0.238 | 31.8 |
| 10. | Jharkhand | 1299.8 | 1.509 | 2.191 | 0.568 | 66.8 |
| 11. | Karnataka | 7356.0 | 38.754 | 26.949 | 7.184 | 1041.3 |
| 12. | Kerala | 2058.4 | 9.773 | 13.073 | 7.529 | 1017.9 |
| 13. | Madhya Pradesh | 9937.0 | 14.167 | 28.349 | 9.284 | 1240.2 |
| 14. | Maharashtra | 15542.3 | 51.665 | 39.349 | 12.998 | 1751.1 |
| 15. | Manipur | 72.6 | 0.159 | 0.319 | 0.032 | 4.14 |
| 16. | Meghalaya | 0.80 | 0.014 | 0.042 | 0.008 | 1.09 |
| 17. | Nagaland | 27.1 | 0.088 | 0.149 | 0.027 | 3.12 |
| 18. | Orissa | 2436.6 | 3.633 | 5.350 | 1.163 | 147.3 |
| 19. | Punjab | 6776.6 | 31.731 | 49.988 | 24.544 | 3133.9 |
| 20. | Rajasthan | 10748.5 | 12.763 | 25.234 | 7.420 | 975.0 |
| 21. | Tamil Nadu | 2561.5 | 24.688 | 17.459 | 7.401 | 967.2 |
| 22. | Uttar Pradesh | 12672.5 | 46.842 | 50.622 | 11.870 | 1496.6 |
| 23. | Uttaranchal | 66.4 | 0.136 | 0.160 | 0.052 | 6.6 |
| 24. | West Bengal | 5575.6 | 21.063 | 23.333 | 2.968 | 369.5 |
| **GRAND TOTAL** | | **107763.0** | **347.926** | **398.175** | **125.046** | **16234.2** |

Source [78]

optimum levels of cogeneration. If all of the 320 MMT of sugarcane produced was crushed in large mills, the generated bagasse will have capacity of about 45 MMT of coal that would produce 6000–7000 MW of electricity.

### 2.3.3 Conversion of biomass to electricity: Technical options

There are essentially 6 possible technologies for converting biomass to electricity, as depicted in Table 2.8. Steam engines were considered robust for installation and operation in rural areas. However, this technology suffered major setback due to implementation of the regulations regarding certified operators for the boilers and non-availability of engines.

**Table 2.8:** Comparative Evaluation of Technical Options for Biomass Conversion to Electricity

| Technology | Efficiency | Relative capital cost per kW* | Merits | Limitations |
|---|---|---|---|---|
| 1. Gasifier with generator coupled to IC engine (with producer gas) | 15 – 22% | 1.0 | Low cost and simple construction | High maintenance for engine, fuel specificity, suitable for size up to 250 kW |
| 2. Biomass boiler – steam engine | < 10% | 1.5 – 2.0 | Robust design, biomass flexibility, low maintenance costs | Low efficiency, not suitable for installation and operation in rural and remote areas |
| 3. Biomass boiler – steam turbine | 15 – 24% | 1.1 – 1.3 | Relatively high efficiency, robust design, biomass flexibility | Economically feasible for capacity of about 5 MW or higher; thus, unsuitable for small to medium scale application for remote rural areas |
| 4. BIGCC (Biomass Integrated Gasification Combined Cycle) with either steam or gas turbine | 45 – 55% | 2.0 – 3.0 | High efficiency | Complex design, yet to be demonstrated for biomass (under R&D) |
| 5. Biomethanation followed by IC engine (with methane) | 20 – 25% | Under R&D | Low engine maintenance due to purer and cleaner gas, simple design, construction and operation | Yet to be demonstrated (under R&D) |
| 6. External combustion engines | 20 – 30% | 1.5 – 2.0 | Flexibility in biomass, high efficiency | Yet to be demonstrated (under R&D) |

Source [20]

BIGCC (Biomass Integrated Gasification Combined Cycle) with steam injected gas turbine was expected to have much higher conversion efficiency. But development of this technology was not marked. Most of the BIG projects aimed at linking producer gas to steam turbines could not proceed beyond gasifier design. The concept of bagasse gasification also did not show much potential for commercial implementation.

The only viable technologies for commercialization of electricity production from biomass are: (1) biomass gasification coupled with an IC engine operating on producer gas, and (2) boiler – steam turbine route (or cogeneration). The technology of biomass gasification is suitable for distributed and decentralized generation in remote villages. A single biomass gasification unit (with either updraft or downdraft design) can generate up to 500 kW power, while a gasification station (with fluidized bed design) could have capacity of about 5 MW. Typically, the costs of biomass gasifier based electricity generation ranges from Rs. 4 to 4.5 crore/$MW_e$ (Rs. 40 to 45 million/$MW_e$). Active and intense research in this area is going on all around the world in terms of better design and optimization of process parameters, which is aimed at improving energy efficiency of the gasifier that would bring down the cost of electricity generation in the near future.

Bagasse-based cogeneration has already been adopted by many sugar mills. In this route, high pressure steam is first utilized for generation of electricity and later for meeting the heat requirements of the process. Thus, the overall efficiency of fuel utilization is quite high, in the range of 60%. Typically, the cost of electricity produced through this route is somewhat cheaper than biomass gasification route; in the range of Rs. 3 to 4 crore/$MW_e$ (Rs.30 to 40 million/$MW_e$). Revenues earned from electricity cogeneration have improved economy of sugar mills. However, cogeneration units are preferred only for capacities > 5 MW, and these units could be installed and implemented in an industrial area. Thus, they are not suitable for applications in remote rural areas where grid connectivity is not possible. Secondly, the steam turbine based technology has already reached maturity. Any path-breaking efficiency improvement is, thus, not feasible. Thus, in terms of technology development and breakthrough for large capacity systems, gasification combined with IC engines may turn out a better option.

### 2.3.4 Biomass gasification efforts in India [22,23]

The biomass gasification program in India started mainly as a R&D effort with joint efforts of MNES, various academic institutions and private entrepreneurs. These efforts were initiated in the mid-eighties for development and subsequent commercialization of a efficient and economically viable technology for decentralized electricity generation from biomass, especially in remote and rural areas. The MNES set up five Gasifier Action Research Projects at I.I.T. Bombay, I.I.T. Delhi, I.I.Sc. Bangalore, M.K. University Madurai and SPRERI, V.V. Nagar. Research in these centers contributed immensely towards technology development, prototype fabrication and transfer of technology to commercial manufacturers. Combustion, Gasification and Propulsion Laboratory (CGPL) at I.I.Sc. Bangalore developed downdraft, atmospheric gasification technology for up to 500 kW systems along with effective gas cleaning systems. These gasifiers have been put to use for large scale power generation. Several commercial manufacturers have obtained license from I.I.Sc. Bangalore for manufacture of downdraft gasifiers based on I.I.Sc. technology. Some of these manufacturers are M/s Bioresidue Energy Technology Pvt. Ltd., M/s Energreen Power Ltd., M/s Arrya Hi-Tech Energy and M/s NetPro Renewable Energy (India) Pvt. Ltd. More than 25 gasifiers based on I.I.Sc. technology have been installed in India and abroad for diverse applications such as thermal, village electrification, water pumping applications, industrial applications (captive electricity generation) and research and educational purpose. Table 2.9(A) lists some of the gasifier installations based on I.I.Sc. Technology in India and aborad. SPRERI (V.V. Nagar, Gujarat) has also developed gasifiers for different energy requirements. These gasifiers are adopted for groundnut shells and installed in the ceramic industries for baking of raw items at about 900–1300 $^{o}$C. Due to these installations, the oil consumption of the industry has reduced by almost 70%. M.K. University at Madurai has also made vital contributions to development of gasifiers suitable for industrial applications. The major

**Table 2.9:** (A) List of Installation of Gasifiers (Based on I.I.Sc. Technology) for Various Applications

| Sl. No. | Location | Capacity (kWe) | Function | Biomass Employed |
|---|---|---|---|---|
| | | Industrial Applications | | |
| 1. | Sriguru Tea Estate, Coonoor, Tamil Nadu | 90 | Tea leaves drying | Wood |
| 2. | Agrobiochem Pvt. Ltd., Harihar, Karnataka | 250 (installed 1998)<br>450 (installed 2000) | Drying of marigold leaves | Juliflora prosopis |
| | | Agricultural applications | | |
| 1. | Bethamangala, Kolar district | 50 | Pumping water from bore-wells | Wood |
| 2. | Farm house, Chennarayapatna | 50 | Irrigation | Wood |
| | | Village electrification | | |
| 1. | Hosahalli, Karnataka | 50 | Domestic and street lighting, drinking water, grinding machines, water irrrigation | Pieces from different species of agro residues |
| 2. | Hanumanthanagara, Karnataka | 50 | | |
| | | Industrial Applications | | |
| 1. | Desi Power Orchcha Pvt. Ltd., Madhya Pradesh | 100 | Electricity for running paper industry | Ipomia wood |
| 2. | Senapathy Whiteley Pvt. Ltd., Ramanagaram, Karnataka | 500 | Electricity for varying load in industrial applications | Mulberry stalk and coconut shells |

Source [79]

achievement of this center is in terms of adoption of the gasifiers for high temperature applications typical of ceramic and aluminum industries.

Noteworthy R&D efforts of technology development have also taken place in industrial sector. Among the companies that have indigenously developed biomass gasification technologies in the country, remarkable contribution has been made by M/s Ankur Scientific Technologies Ltd. in Vadodara, Gujarat. This company has manufactured atmospheric downdraft gasifiers with wide range capacities – 5 to 500 kW. Various

(B) List (partial) of Installation of Gasifiers for Various Applications (based on Ankur Scientific Technology)

| Sl. No. | Location | Capacity (kWe) | Function | Biomass Employed |
|---|---|---|---|---|
| | | Captive Power Generation | | |
| 1. | M/s Sree Gopal Rice Hills, West Bengal | 120 (Dual Fuel) | Generation of power for meeting energy needs of the mill, reduction in diesel consumption | Rice husk |
| 2. | M/s Sree Brijuka Agro Products Pvt. Ltd. | 350 (Dual Fuel) | | |
| 3. | M/s Valli Chlorate, Kolvilpatti | 200 (100% producer gas) | | |
| 4. | M/s Meghaplast | 250 (100% producer gas) | | |
| | | Village electrification | | |
| 1. | Gosaba Islands, Sunderban | 100 (5 units) | Domestic and street lighting, drinking water, grinding machines, water irrigation | Pieces from different species of agro residues |
| 2. | Gasifier power plant, Kumarikanan, Purulia | 50 (2 units) | | |
| | | Industrial Applications | | |
| 1. | M/s Mahabhadra Industrial Gases Co. | 150 | Clean $CO_2$ generation (sulfur free) | Woody biomass |
| 2. | M/s Patson Industries Ltd. | 60 | Annealing of steel tubes | Woody biomass |

** - M/s AnkurScientific has installed more than 700 gasifiers worldwide using different kinds of biomasses as feedstock. More detailed information on these installations could be obtained from web site of the company. Source [80]

installations of Ankur Gasifiers have been listed in Table 2.9(B). To summarize, the biomass gasifier based thermal and electricity generation has tremendous growth potential in the country. MNRE has offered attractive financial support in terms of capital subsidies (Rs. 125,000 per 300 $kW_{th}$ for thermal application and Rs. 150,000 per 100 $kW_e$ for electrical applications in 2006) for gasifier installations in India. Table 2.10 gives information on state-wise gasifier installation (as of March 31, 2003).

**Table 2.10:** State-wise Biomass Gasifier Installations (as of 31.03.2003)

| State | Installed Capacity | | State | Installed Capacity | |
|---|---|---|---|---|---|
| | No. of units | Net Generation (kW) | | No. of units | Net Generation (kW) |
| Andhra Pradesh | 231 | 15384 | Maharashtra | 316 | 3823 |
| Arunachal Pradesh | 3 | 180 | Mizoram | 2 | 200 |
| Assam | 6 | 123 | Orissa | 16 | 72 |
| Bihar | 2 | 20 | Punjab | 27 | 700 |
| Chhattisgarh | 1 | 500 | Rajasthan | 21 | 218 |
| Goa | 3 | 22 | Tamil Nadu | 83 | 2652 |
| Gujarat | 237 | 11961 | Tripura | 4 | 1000 |
| Haryana | 25 | 964 | Uttar Pradesh | 50 | 2746 |
| Himachal Pradesh | 2 | 7 | West Bengal | 27 | 4100 |
| Jammu and Kashmir | 4 | 120 | Andaman and Nicobar Islands | 17 | 167 |
| Karnataka | 476 | 4499 | Delhi | 16 | 74 |
| Kerala | 13 | 725 | Others | 91 | 318 |
| Madhya Pradesh | 144 | 4529 | **TOTAL** | **1817** | **55104** |

**Source** [81]

## 2.4. TECHNOLOGY FOR BIOMASS GASIFICATION

Before we proceed to analysis of technical and economic feasibility of decentralized power generation through biomass gasification in the Indian context, we would like to discuss various technologies available for gasification of biomass and present a comparative analysis of the same. Depending on the mode of biomass-air (or oxygen) contact, biomass gasifiers are classified into two main types, viz. (i) fixed bed, and (ii) fluidized bed. The sub-categories for the fixed bed type gasifiers based on the relative directions of biomass and air flow are (a) updraft, (b) downdraft, and (c) cross draft gasifiers. The sub-categories for the fluidized bed gasifiers based on the mode of fluidization are (a) bubbling bed, and (b) circulating fluidized bed gasifiers. In addition to these, entrained bed gasifiers (as for coal gasification) were also developed for biomass, but they proved unsuitable for biomass material as biomass could not easily ground to the particle size range (100–400 microns) as required for these gasifiers.

Pretreatment of biomass and properties of biomass also influence the performance of gasifiers. In addition, proper cleaning and conditioning of gas is of utmost importance for proper functioning of the generator sets, in terms of both stability and efficiency. In this section we shall briefly touch upon these technical aspects. We begin with the basic chemistry involved in biomass gasification.

### 2.4.1 Chemistry of biomass gasification

The chemistry of biomass gasification is quite complex. However, on a broad basis, the following stages are involved in the gasification process [24-27].

*Drying*: In this stage, the moisture content of the biomass is reduced. Typically, the moisture content of biomass is in the range 5–35%. Drying occurs at about 100–200 $^{o}$C with reduction in moisture content of biomass to < 5%.

*Devolatilization (or pyrolysis)*: This is essentially thermal decomposition of biomass in absence of oxygen or air. As the name suggests, in this process the volatile matter in the biomass is reduced. This results in release of hydrocarbon gases from biomass due to which the biomass is reduced to solid charcoal. The hydrocarbon gases can condense at sufficiently low temperature to generate liquid tars.

*Oxidation*: This is reaction between solid carbonized biomass and oxygen in the air resulting in formation of $CO_2$. Hydrogen present in the biomass is also oxidized to generate water. Large amount of heat is released with the oxidation of carbon and hydrogen. If oxygen is present in substoichiometric quantities, partial oxidation of carbon may occur resulting in generation of carbon monoxide.

*Reduction:* In absence (or substoichiometric presence) of oxygen, several reduction reactions occur in the temperature range 800–1000 $^{o}$C. These reactions are mostly endothermic. The major reactions in this category are as follows:

Water - gas reaction: $C + H_2O \longrightarrow CO + H_2 - 131.4$ kJ/gmole

Boudard reaction: $C + CO_2 \rightleftharpoons 2CO - 172.6$ kJ/gmole

Shift reaction: $CO_2 + H_2 \rightleftharpoons CO + H_2O - 42$ kJ/gmole

Methane production: $C + 2H_2 \rightleftharpoons CH_4 + 75$ kJ/gmole

A comprehensive description of different zones in the gasifiers, their temperature ranges and the reactions occurring in these zones is given in Table 2.11. Depending on directions of air and biomass flow, the sequence of these zones in the gasifier varies. The extent of these reactions depends on two major factors, viz. temperature and equivalence ratio (ER), defined as: $ER = \dfrac{(\text{Weight of oxygen}/\text{Weight of dry fuel})_{\text{actual}}}{(\text{Weight of oxygen}/\text{Weight of dry fuel})_{\text{stoichiometric}}}$.

**Table 2.11:** Various Zones in the Gasifiers and the Reactions Occurring Therein

| Sr. No. | Zone | Temperature Range (°C) | Reactions |
|---|---|---|---|
| 1. | Drying zone | 30–65 | $H_2O\,(\text{moisture}) \longrightarrow H_2O\,(\text{steam})$ |
| 2. | Preheating zone | 100–200 | -- |
| 3. | Devolatilization (or pyrolysis) zone | 200–600 | $C_xH_yO_z \longrightarrow$ Volatile gases and tar |
| 4. | Oxidation zone | 1000–1200 | $C + 0.5\,O_2 \longrightarrow CO + 268$ kJ/gmole<br>$C + O_2 \longrightarrow CO_2 + 406$ kJ/gmole<br>$H_2 + 0.5\,O_2 \longrightarrow H_2O + 242$ kJ/gmole |
| 5. | Reduction zone (primary) | 800–1000 | $C + H_2O \longrightarrow CO + H_2 - 131.4$ kJ/gmole<br>$C + 2\,H_2O \longrightarrow CO_2 + 2\,H_2 - 78.7$ kJ/gmole<br>$C + CO_2 \rightleftharpoons 2\,CO - 172.6$ kJ/gmole<br>$CO + H_2O \rightleftharpoons CO_2 + H_2 + 42$ kJ/gmole<br>$CO + 3\,H_2 \rightleftharpoons CH_4 + H_2O + 88$ kJ/gmole |
| 6. | Reduction zone (secondary) | 800–1000 | $C + CO_2 \rightleftharpoons 2\,CO - 172.6$ kJ/gmole<br>$CO_2 + H_2 \longrightarrow CO + H_2O - 41.2$ kJ/gmole<br>$C + 2H_2 \longrightarrow CH_4 + 75$ kJ/gmole |
| 7. | Ash collection pit | < 500 | -- |

The denominator of the above expression is the amount of oxygen required for complete combustion of the fuel. This quantity depends on the composition of the fuel, i.e. C, H, N, O content of the fuel. The most important components of the producer gas resulting from biomass gasification are CO and $H_2$. Typically, an ER of 0.2–0.4 is considered to be optimum for gasification process. For ER < 0.2, pyrolysis dominates that results in generation of tars, while for ER > 0.4, combustion reactions dominate resulting in generation of $CO_2$.

Temperature is a critically important parameter in the gasification process. For high carbon conversion, temperature of 800 $^{o}$C or above is essential. The fraction of carbon monoxide in the producer gas increases with temperature. In addition, high temperature also helps in cracking of tar, which results in reduction in aromatic content of the tar. In addition, temperature also influences formation of nitrogen compounds such as ammonia and HCN.

### 2.4.2 Biomass pretreatment and properties

*Pretreatment*: The pretreatment biomass comprises mainly of two steps: (1) drying and (2) particle size reduction. Typical moisture content of the fresh wood is 50–60% w/w. The desired moisture content of biomass for gasification purpose is in the range of 10–15% w/w. The appropriate particle size of biomass for gasification depends on the design of gasifier. For fixed bed gasifier, particle size range is 20–80 mm, while for fluidized bed gasifier it is still lower – in the range of ~ 1 mm or smaller. Two additional treatments that can be applied to biomass are fractionation and leaching. These are aimed at reducing the nitrogen and alkali content of biomass so as to limit the impurities in the producer gas obtained from gasification.

*Influence of biomass properties*: Moisture content of the biomass is a parameter of critical importance. As noted earlier, appropriate moisture content of biomass is in the range 10-15%. Moisture content higher than 30% can make the ignition of the gasifier difficult and also reduces the calorific value of the producer gas [24]. Significant heat is required to evaporate

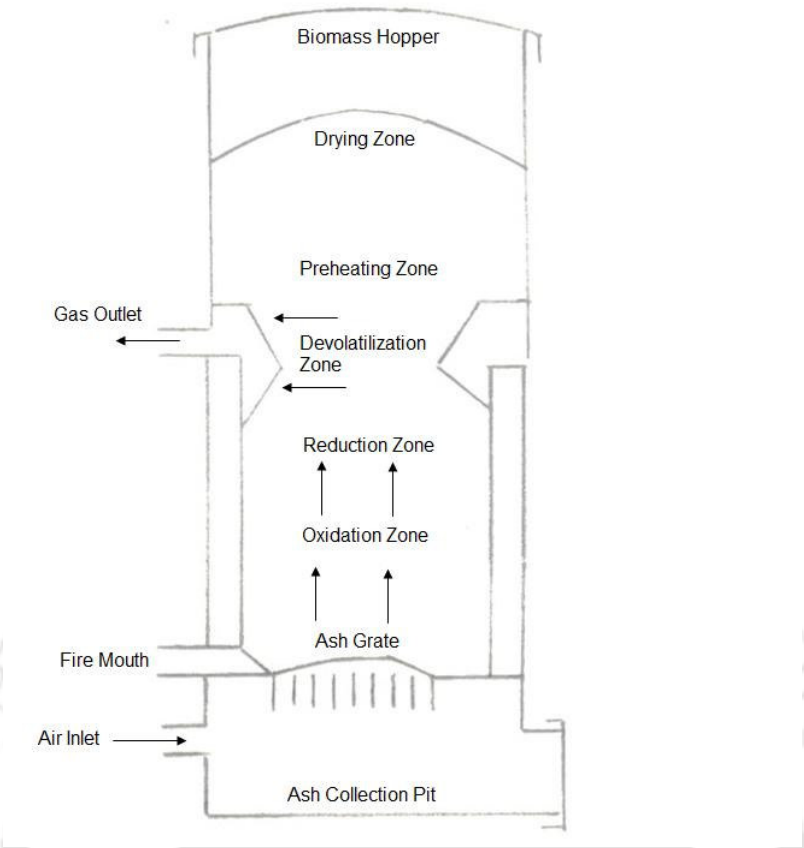


**Figure 2.4:** Schematic of an updraft biomass gasifier (adopted from [27])

the moisture prior to gasification or combustion. Higher moisture content also reduces the temperature of the combustion zone of the gasifier that has leads to incomplete cracking of hydrocarbons or tars released from pyrolysis zone. In addition, the extent of water gas shift reaction increases that result in production of more $H_2$. Thus, direct hydrogenation of carbon in biomass can occur resulting in production of methane. Consequently, the production of carbon monoxide reduces. As the combined heat of combustion of $H_2$ and $CH_4$ is lesser than the heat of combustion of CO, the net calorific value of the producer gas decreases.

### 2.4.3 Fixed bed gasification [25,28-29]

*Updraft gasifiers*: A schematic of the updraft gasifier is shown in Figure 2.4. In these gasifiers, the feed is introduced from the top and air is introduced from the bottom through grate. Feed

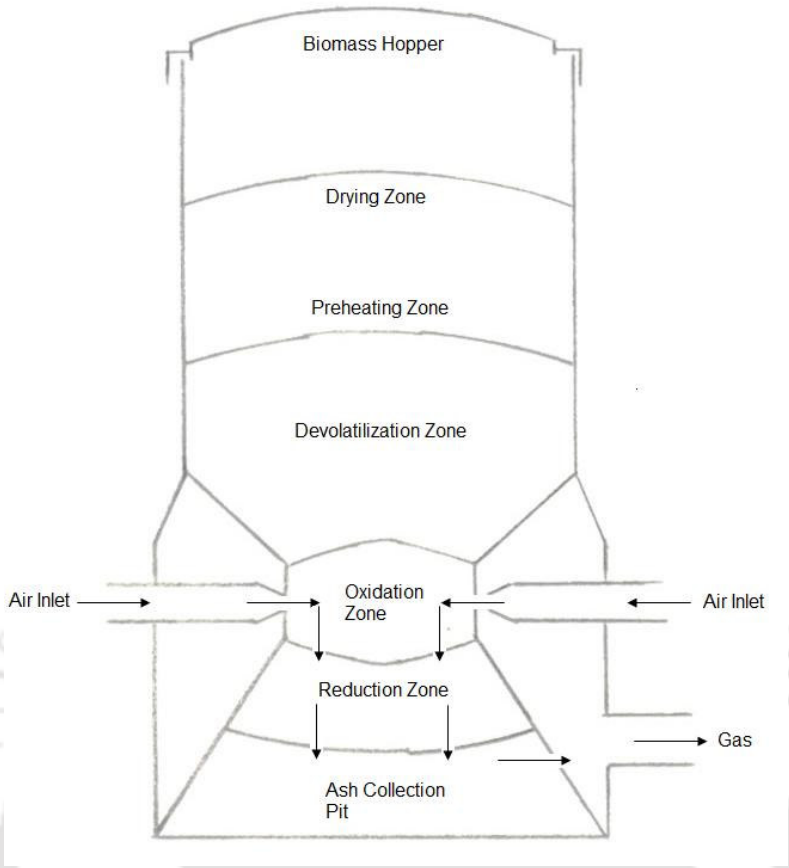


**Figure 2.5:** Schematic of a downdraft gasifier (adopted from [27])

and air move countercurrently in the gasifier. The lowest portion of the gasifier is essentially the "combustion" zone where the char formed due to drying and devolatilization of biomass is combusted. This helps in raising the temperature of the lower portion of the gasifier to about 1000 K. Hot gases passing upward through the bed of downflowing biomass are reduced in the portion immediately above the combustion zone. Further up the gasifier, the hot gases pyrolyse the biomass and dry it. These processes cool the gases to about 200–300$^{o}$C. Pyrolysis of biomass results in release of volatiles and formation of sizeable amount of tar. Some of this tar may leave with the outgoing gases. The overall efficiency of the process could be high due to low temperature of the gases leaving the gasifier. In addition, the gas flowing through the packed bed of biomass undergoes "filtration" as the particulate matter entrained with it is captured by the bed material. This helps in lowering of the

particulate content of the outgoing gas. The humidity of the gasifying air plays a major role in controlling the temperature of the gasification.

*Downdraft gasifier*: The downdraft design is essentially same as the updraft design except that both feed and air move concurrently from top to bottom of the gasifier. Figure 2.5 shows a schematic of the downdraft gasifier. Since the exit of the producer gas is close to the combustion zone of the gasifier with maximum temperature, the tar formed during devolatilization of biomass is thermally cracked to some extent. Thus, the tar content of the producer gas from downdraft design is lower than that in the updraft design. However, disadvantage of this type of design is that the gases leave at much higher temperature and amount to significant heat loss from the gasifier, thus lowering its thermal efficiency. In addition the particulate content of the gas is also high. Despite these demerits, downdraft design enjoys greater popularity due to its low tar content gas. Tar in the producer gas can condense over the shaft of the engine causing operational problems causing frequent shutdowns and cleanup. Thus, low tar content gas is always preferred for firing the gas engines and turbines.

*Cross draft gasifier*: In this design, the biomass feed is introduced from top and the air from the side of the gasifier. The biomass moves down as it gets dried, devolatilized, pyrolysed and finally gasified, while the air exits from opposite side of the unit. The exit for the gas is more-or-less at the same level as that of entrance. The combustion and gasification zone is located near the entrance of the air while the devolatilization and pyrolysis zones are at a higher level than the entrance and exit. Figure 2.6 shows a schematic of the cross draft gasifier. The producer gas leaves the gasifier at almost same temperature as gasification (~ 800–900 $^{o}$C). Thus, the heat loss from gasifier is high that reduces its thermal efficiency. Secondly, the overall residence time of the producer gas in the high temperature zone is small

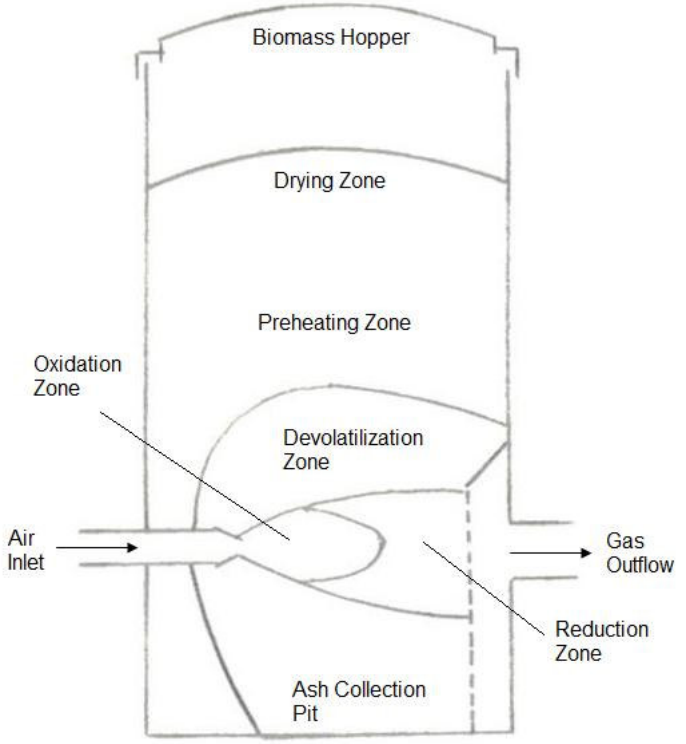


**Figure 2.6:** Schematic of a crossdraft biomass gasifier (adopted from [27])

(as the gas enters and exits from opposite ends), and hence, tar cracking is limited. This leaves significant amount of tar in the outgoing gas.

*Overview of fixed bed biomass gasification*: Typical composition of the producer gas from fixed bed gasifiers is: 40–50% $N_2$, 15–20% $H_2$, 10–15% CO, 10–15% $CO_2$ and 3–5% $CH_4$ [25-26,30-32]. Thus, the net calorific value of the gas is in the range 4–6 MJ/Nm$^3$. Nitrogen in the producer gas contributes considerably to the volume of the producer gas, which increases the size of the downstream equipment. The moisture content of the biomass is another parameter of paramount importance. Typically, the moisture content of biomass should be in the range 10–15%. Thus, considerable predrying of biomass is necessary. Many commercial fixed bed downdraft gasifiers have the facility of using waste heat from engine exhaust for predrying of the biomass. Typically, about 3/4$^{th}$ of the energy content of the biomass appears in the producer gas with radiation heat losses, sensible heat of producer gas

and heat content of ashes accounting for the rest 1/4$^{th}$ of energy. The principal products of the devolatilization process are volatiles and char. Volatiles exit with outgoing gas, while the char undergoes combustion. This char can be gasified further to improve the gas yield from the process. Typical yield of char varies from 20–40% w/w of dry biomass. However, reactivity of the char is a matter of question. The reactivity varies significantly with the composition of the char, especially the carbon and nitrogen content. McKendry [25] has proposed a two-stage gasification process, in which pyrolysis of the biomass occurs in the first stage at about 600 $^{o}$C using external heat. The gases from this stage may contain considerable amount of tar, which is cracked either catalytically or by reaction with steam. The second stage comprises of gasification of the char produced from first stage using the gases from first stage after tar removal.

### 2.4.4 Fluidized bed gasification [25-26]

Fluidized bed processes were first commercialized for coal gasification [33]. The first commercial fluidized bed process, Winkler gasifier, went into operation in Germany in 1941. Thereafter, fluidized bed processes have been extensively implemented by the petroleum refineries and petrochemical industries. In recent years, fluidized bed biomass gasification is becoming increasingly popular. The distinct merits of these processes over fixed bed biomass gasifiers are uniform temperature distribution in the reactor due to excellent gas-solid mixing, high carbon conversion with low tar production and flexibility in terms of fuel type, feed rate, particle size and moisture content. Typical capacity of the fixed bed gasifiers is 50–500 kW. However, due to above-mentioned features, scale-up and operation of the fluidized bed gasifiers for electricity generation in MW scale is much easier. There are two main types of fluidized bed gasification systems, viz. bubbling fluidized bed and circulating fluidized bed. Depending on scale of operation, the cyclone separators for capture and recycle of solid particles could be placed either internally or externally. It must be mentioned that internally

circulating fluidized bed reactors combine the design features possess of both bubbling and fluidized mode and thus have characteristics of both modes. In the past two decades significant experimental and theoretical research has taken place in design, development and scale up of fluidized bed gasifiers [34-43]. We describe below the design and operational features of these two kinds of fluidized systems.

*Bubbling bed systems (BFB)*: In these kind of systems, the bed material (which could be mixture of inert particles such as sand along with finely ground biomass) rests on a distributor plate (either perforated or porous type) through which the fluidizing medium, i.e. air is passed at velocity about 5 times that of minimum fluidization velocity. Typical temperature in the bed is about 700–900$^{o}$C. The feed, which is finely grained biomass, is introduced just above the distributor plate. The biomass first undergoes pyrolysis in the hot bed above distributor to form char and gaseous products due to devolatilization. The char particles are lifted along with fluidizing air and undergo gasification in relatively upper portions of the bed. Due to contact with high temperature bed, the high molecular weight tar compounds formed are cracked; thus reducing the net tar content of the producer gas to less than 1–3 g/Nm$^3$.

*Circulating fluidized beds*: Circulating fluidized beds (CFB) is an extension of the concept of bubbling bed fluidization. In this case the velocity of the fluidizing air is much higher than the terminal settling velocity of the bed material. Thus, the entire bed material (biomass + inert material such as sand) is lifted by the fluidizing air. The exhaust of the gasifier is a relatively lean mixture of solids and gas. This exhaust is admitted into a cyclone separator where solids get disengaged from the gas and are returned to the bed through a downcomer pipe. Depending upon the solids concentration and size distribution either single stage or multistage cyclones are employed. Circulation of the biomass particles is carried out till the particles are reduced in size due to combustion/gasification. An advantage that circulating

fluidized bed design offers is that gasifier can be operated at elevated pressures.

The summary of the salient features and comparative evaluation of fixed and fluidized bed type biomass gasifiers is presented in Table 2.12.

### 2.4.5 Post-treatment of producer gas

The producer gas obtained from fixed and fluidized bed gasifiers contains many impurities, with ash and tar being the main impurities. The cyclone separator are usually unable to remove particulate impurities below 10 µm. Removal of finer particles can be achieved using filter bags, sintered ceramic candles or metallic candles. However, depending on the operational load these devices may clog due to soot and/or tar adhering to ash particles. Wet scrubbing of gas is a common technique used for removal of particulate matter. Various wet scrubbing techniques include spray towers, centrifugal spray towers, packed bed column scrubbers, ejector venture scrubbers and free jet washers [27].

Effective removal of tar has been a principal problem in producer gas cleaning. Tar mainly comprises of condensable aromatics and polyaromatics. If the gas is to be used in engines or turbines, the tar removal is utmost essential as the condensation of tar on mechanical components moving with high speed can cause mechanical instability. The principal tar components are toluene, naphthalene and phenol with many other aromatics comprising of up to 7 benzene rings as secondary components [27]. Over past several decades extensive research has taken place on removal of tar from producer gas (for state-of-the-art review on tar elimination techniques has been given by Devi et al. [44]. The primary methods of tar removal includes (1) optimization of gasifier operating conditions in terms of air ratio, bed temperature and sufficient residence time; (2) use of bed additives or catalysts (such as nickel-based catalysts, calcined dolomites, magnesites, zeolites, olivine and iron catalysts) that act as tar reducers; (3) modification of gasifier design, i.e. splitting the gasifier into two stages – pyrolysis stage and reduction stage. The secondary methods of tar removal

**Table 2.12:** Salient Features and Comparative Evaluation of Different Designs of Biomass Gasifiers

| Gasifier Type | Salient Features | Gasifier Type | Salient Features |
|---|---|---|---|
| Downdraft | Simple and proven technology<br>Fuel specificity in terms of both type and size<br>Suitable for biomasses with low moisture<br>Producer gas with moderate calorific value and low tar and ash (or particulates) content<br>High exit gas temperature<br>Suitable for capacity of 20 – 200 kW<br>High residence time of solids<br>High overall carbon conversion<br>Limited scale-up potential with maximum capacity of 250 kW | Bubbling Fluidized Bed | High fuel flexibility in terms of both size and type<br>Flexibility of operation at lower loads than design load<br>Ease of operation<br>Low feedstock inventory<br>Good temperature control and high reaction rates<br>Good gas-solid contact and mixing<br>In-bed catalytic processing possible<br>Producer gas with moderate HHV but low tar levels and high particulates<br>Carbon loss with ash<br>High conversion efficiency<br>Suitable for large scale capacities (up to 1 MW or even higher)<br>Good scale-up potential |
| Updraft | Simple and proven technology<br>Low exit gas temperature<br>High thermal efficiency<br>Producer gas with moderate calorific value but high tar and ash (or particulates) content<br>High residence time of solids<br>High overall carbon conversion<br>Necessity of extensive gas cleanup before use in engines<br>Suitable for capacities up to 250 kW<br>Limited scale-up potential | Circulating Fluidized Bed | High fuel flexibility in terms of both size and type<br>Flexibility of operation at lower loads than design load<br>Ease of operation<br>Low feedstock inventory<br>Good temperature control and high reaction rates<br>In-bed catalytic processing possible<br>Producer gas with moderate tar levels but high particulates<br>High carbon conversion<br>Good gas-slid contact and mixing<br>Suitable for large scale capacities (up to 1 MW or even higher)<br>High conversion efficiency<br>Very good scale-up potential |

*Table 2.12 (Continued)….*

| Gasifier Type | Salient Features | Gasifier Type | Salient Features |
|---|---|---|---|
| Entrained Flow Bed | Relatively complex construction and operation<br>Fuel specificity in terms of particle sise (costly feed preparation)<br>Low feedstock inventory<br>High temperature give good gas quality<br>Materials of construction problems with high temperature<br>Good gas-solid contact and mixing<br>Producer gas with moderate HHV and low tar content<br>High conversion efficiency<br>Suitable for high capacities (> 1 MW)<br>Very good scale-up potential | Twin Fluidized Bed | Relatively complex construction and operation<br>Producer gas with moderate HHV and moderate tar levels<br>Cleaning of gas before firing into engines required<br>In-bed catalytic conversions possible<br>Good gas-solid contact and mixing<br>Relatively low efficiency<br>Suitable for high specific capacities (> 1 MW)<br>Good scale-up potential but relatively complex design |

Source [25,27,29,61]

consist of physical or chemical treatment such as (1) either thermal or catalytic cracking of tar downstream of the gasifier and (2) mechanical removal of tar using cyclone separator and baffle / ceramic / fabric / electrostatic filter. Some times a multi-stage process is used for secondary gas cleaning [45]. Although very effective in tar removal, the secondary methods have not been economically viable [46,47]. If the application of the producer gas is for purpose of direct combustion, tar removal prior to combustion is not necessary. If the burner is designed properly, all of the tar gets burnt.

## 2.5 ECONOMICS OF BIOMASS GASIFICATION

The principal components of the capital cost of biomass gasifier system (either updraft or downdraft) are biomass gasifier unit (which is essentially a combustion – gasification chamber made of stainless steel), a gas cooling and cleaning unit (comprising of scrubber and two or three stage filters for removal of particulate matter) and an engine – generator (which could be either of dual fuel type, employing diesel as pilot fuel or it could be operating on 100% producer gas). Other components of capital cost of gasifier system include civil construction (room shed and concrete supports various components of gasifier systems), biomass preparation and storage units, electrical wiring and piping , tar removal/cracking system, ash removal facility and distribution network for dissemination electricity to local consumers. The operating costs of the gasifier system include oil or fuel, i.e. biomass (including its preparation) and diesel (for duel fuel engine), labor charges, maintenance charges and replacement of spare parts on occasional basis.

The composition of the producer gas shows variation with gasifier type and design, fuel to air ratio, biomass type etc. Typical composition of producer gas was described in section 4.3. In a duel fuel engine generator, the producer gas can replace up to 80% of diesel. Most of the gasifiers fabricated prior to 2002–03 employed a dual fuel engine. However,

more recently 100% produced gas engines have appeared in market. As of 2004 end, more than 1800 gasifiers have been installed in India, amounting to more than 75 MW generating capacity .Ministry of New and Renewable Energy promotes the decentralized electricity generation by offering capital subsidy up to 90% for package of 50 KW project covering civil construction and local distribution network [9].

Analysis of the economics of the gasifier system has been done by several authors. We present herewith an overview of the same. The "measures" of the economic feasibility of the biomass gasifier for decentralized power generation are: 1. the levelized unit cost of electricity (LUCE) produced by the gasifier in comparison to diesel generator and 2. the breakeven analysis (i.e. comparison of the diesel price, for which gasifier is feasible with the prevalent market price of diesel). We first present the economic analysis of low to medium scale gasifiers (5–100 kW) with the two approaches mentioned above. This is followed by analysis of medium to large scale system (0.5–5 MW). We begin with discussion on cost facts involved in economic analysis.

### 2.5.1 Factors affecting cost of power generation

As noted earlier, the principal capital cost of biomass power projects includes cost of gasifier, engine generator, civil construction, biomass preparation unit, electricity distribution network and electrical and piping connections to the site of gasifier installation. In addition to this, several other factors influence the cost of power generation. These are: 1. specific fuel consumption (at full and part loads), 2. capacity utilization factors, 3.useful life of gasifier and generator, and lastly, 4. the unit price of biomass and supplementary fuel, i.e. diesel (in case of duel fuel system). The comprehensive list of factors and their typical values in the Indian context are given in Table 2.13. This data is adopted from work of Nouni et al. [48]. The contribution of various components to the total capital cost of the gasifier of different capacities and employing duel fuel or 100% producer gas engine is described in Figure 2.7.

**Table 2.13:** List of Parameters (along with their typical values) for Economic Model of Low to Medium Scale Biomass Gasifiers

| Parameter | Value |
|---|---|
| 1. Maintenance Costs of Gasifier System Components (as a fraction of their capital costs) | |
| a. Gasifier | 0.05 |
| b. Engine – Generator set | 0.10 |
| c. Electricity distribution network | 0.03 |
| d. Civil works related to gasifier installation | 0.02 |
| e. Auxiliary power consumption | 0.10 |
| 2. Capacity utilization factor | 25% |
| 3. Discount rate (for annualization of capital costs) | 10% |
| 4. Manpower | Rs. 15 per person per hour |
| 5. Manpower requirement | 1 no. for ≤ 20 kW system<br>2 nos. for > 20 kW system |
| 6. Fuel Costs | |
| a. Biomass (Main fuel) | Rs. 1.5 per kg |
| b. Diesel (Pilot fuel) | Rs. 30.45 per liter |
| 7. Sales tax | 4% |
| 8. Specific consumption of biomass (main fuel) in dual fuel engine | |
| a. At 100% rated capacity | 1.1 kg $kWh^{-1}$ |
| b. At 75% rated capacity | 1.21 kg $kWh^{-1}$ |
| c. At 50% rated capacity | 1.32 kg $kWh^{-1}$ |
| 9. Specific consumption of diesel (pilot fuel) in dual fuel engine | |
| a. At 100% rated capacity | 0.11 L $kWh^{-1}$ |
| b. At 75% rated capacity | 0.10 L $kWh^{-1}$ |
| c. At 50% rated capacity | 0.11 L $kWh^{-1}$ |
| 10. Specific consumption of biomass (main fuel) in 100% producer gas engine | |
| a. At 100% rated capacity | 1.4 kg $kWh^{-1}$ |
| b. At 75% rated capacity | 1.54 kg $kWh^{-1}$ |
| c. At 50% rated capacity | 1.68 kg $kWh^{-1}$ |
| 11. Specific consumption of diesel in diesel generator engine | |
| a. At 100% rated capacity | |
| b. At 75% rated capacity | 0.30 L $kWh^{-1}$ |
| c. At 50% rated capacity | 0.28 L $kWh^{-1}$<br>0.30 L $kWh^{-1}$ |
| 12. Unit cost of electricity distribution network | Rs. 1,25,000 $km^{-1}$ |
| 13. Useful life period of components | |
| a. Engine generator set (with diesel as main or pilot fuel) | 20,000 h |
| b. Biomass gasifier | 10,000 h |
| c. Electricity distribution network | 20 years |
| d. Civil works | 20 years |

Source [48]

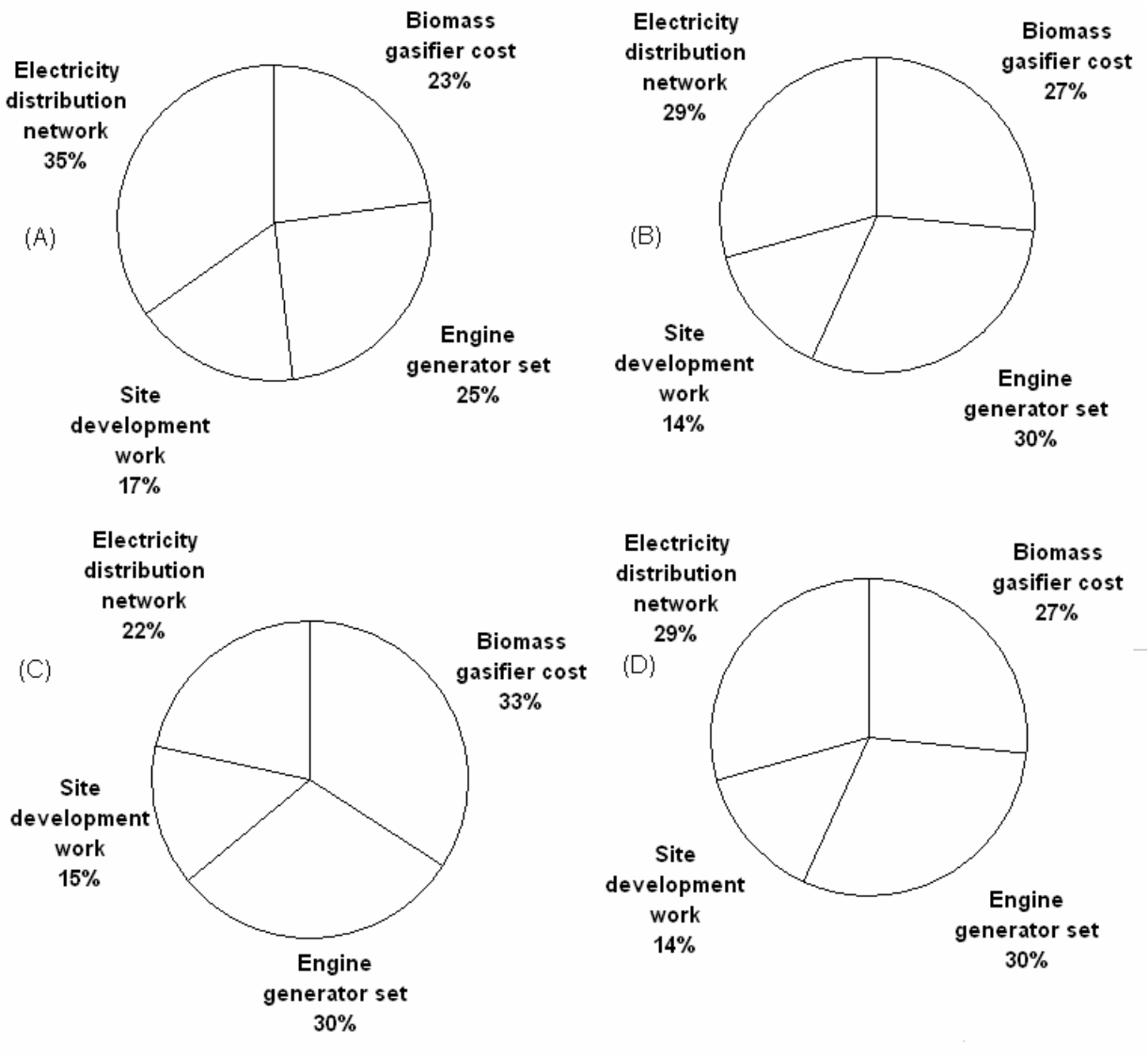


**Figure 2.7:** Capital cost distribution of biomass gasifier power projects. (A) 10 kW gasifier employing dual fuel generator. (B) 40 kW gasifier employing dual fuel generator. (C) 9 kW gasifier employing 100% producer gas generator. (D) 40 kW gasifier employing 100% producer gas generator.

The economy of scale (i.e. total capital cost per kW of installed capacity or unit capital cost) also shows an interesting variation with duel fuel or 100% producer gas engine, as depicted in Figure 2.8. Unit capital cost shows a sharp reduction with capacity for a dual fuel engine, while for gasifiers employing 100% producer gas capital cost reduces only marginally with capacity raising from 5 to 40 kW. We would like to specifically mention that other groups have also done the economic analysis for similar size of gasifiers [4,22,49-53], however,

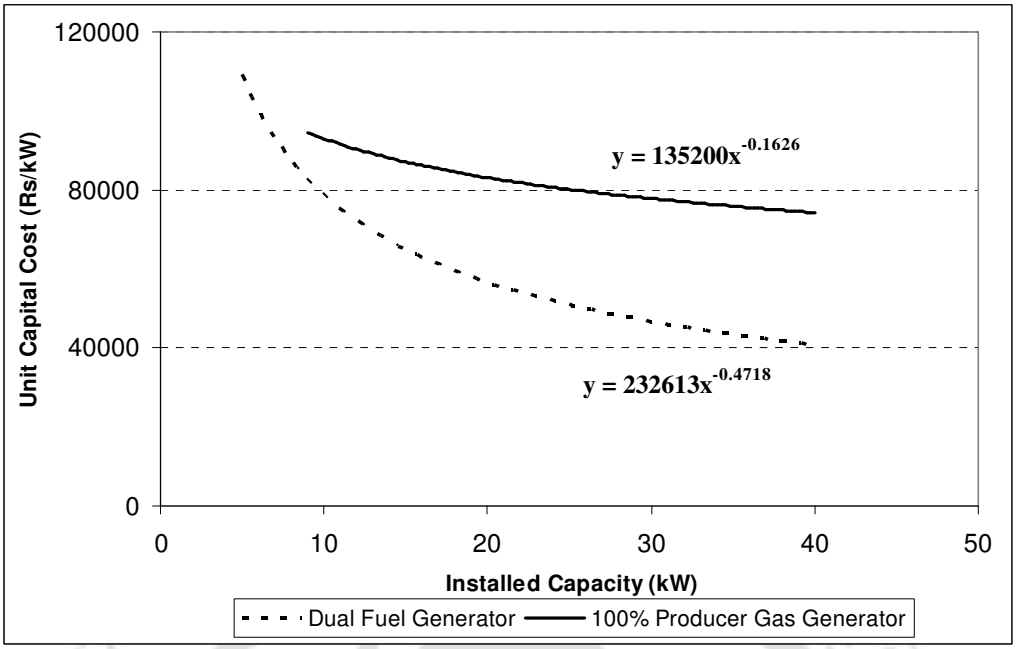


**Figure 2.8:** Economy of scale (variation of unit capital cost per installed capacity, in Rs/kW, with total installed capacity) for biomass gasifier power projects using either dual fuel generator or 100% producer gas generator.

using a different approach.

### 2.5.2 Feasibility of low to medium scale units (5–100 kW systems)

As noted earlier, there are two approaches, viz. LUCE and break even price of diesel for assessment of the economic feasibility of low to medium scale gasifiers. We present below description of these approaches and the results on economic viability of gasifier based power generation using these approaches:

*LUCE approach:* Kandpal and coworkers [9,18,48,54-56] have proposed the method of LUCE for assessment of economic feasibility of low to medium scale power projects with renewable energy. This method is applied for biomass gasifier based power projects as follows:

1. The net electricity produced from the project with installed capacity $P$ in a year (365 days of operation with 24 h production) is determined as follows: $E_O = 8760\,P$. Out of this production, a fraction is utilized for meeting the energy needs of the plants itself and some

power is lost through transmission and distribution. Moreover, the capital utilization factor is also an important factor. With this taken into account, the net production is:

$$E_O = 8760 \cdot (1-a) \cdot (1-l) \cdot CUF$$

2. The total capital cost for the project comprises of four components viz. gasifier, engine-generator, civil works and distribution network. This cost is annualized using capital recovery factor as follows: $AC_c = C_g R_g + C_{eg} R_{eg} + C_{cw} R_{cw} + C_{dn} R_{dn}$; where $R = \frac{d \cdot (1+d)^T}{(1+d)^T - 1}$ is the capital recovery factor for discount rate $d$ and life period of $T$ years. Various notations are as follows: $C_g$, $C_{eg}$, $C_{cw}$ and $C_{dn}$ are capital costs of gasifier, engine-generator unit and civil works related to gasifier installation and electricity distribution network, respectively.

3. The operating and maintenance cost is expressed as fraction of the capital cost as follows:

$$AC_{O\&M} = C_g m_g + C_{eg} m_{eg} + C_{cw} m_{cw} + C_{dn} m_{dn} + 8760 \cdot CUF \cdot m_l \cdot n$$

$m$ is the fraction of the total capital cost taken for maintenance and operation of the gasifier unit (with subscript denoting the fraction corresponding to the component). $m_l$ and $n$ are the wage rate of manpower and nos. of labor required for operation of the gasifier.

4. The cost of fuel consumption is: $AC_F = 8760 \cdot CUF \cdot (C_{pf} S_{spfc} P + C_{bm} S_{sbmc} P)$. Notation: $C_{pf}$ is the unit cost of pilot fuel (diesel), $C_{bm}$ is the unit cost of biomass fuel, while $S_{spfc}$ and $S_{sbmc}$ are the specific fuel consumption of pilot fuel and biomass per kWh of electricity generated.

5. The unit cost of electricity after substitution of all annualized costs is determined as:

$$LUCE = \frac{AC_C + AC_{O\&M} + AC_F}{E_O}$$

6. If a part of the capital cost (fraction $x$) is available to the investors on soft loan (with interest rate $d_1$), then the expression for LUCE is modified by multiplication of the soft loan

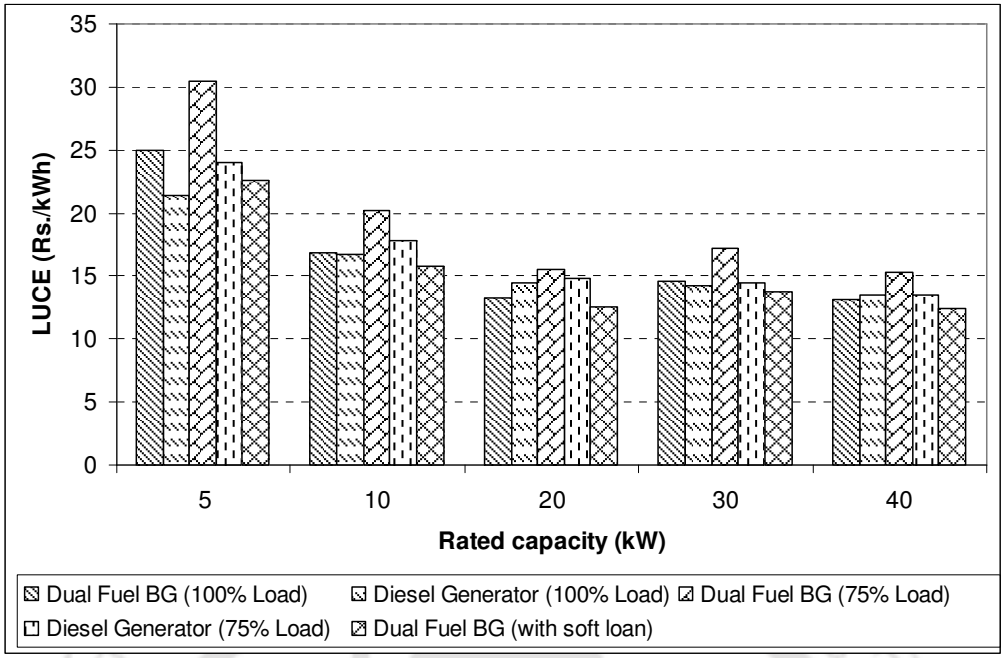


**Figure 2.9:** Variation in levelized unit cost of electricity (LUCE) with different factors (type of generator, plant load factor, soft loan availability). The LUCE for the diesel generator with 75% plant load factor is shown as base case for comparison.

fraction of all capital costs components and the operations and maintenance costs for these components with modified capital recovery factor calculated using interest rate $d_1$ as: $R_1 = \frac{d_1 \cdot (1+d_1)^T}{(1+d_1)^T - 1}$. The cost for manpower and fuel consumption, however, stays the same.

The overall variation in LUCE for biomass gasification projects with 5–40 kW rated capacity in comparison to diesel generator sets is shown in Figure 2.9. Also shown in Figure 2.9 is the influence of plant load factor and soft loan on the capital cost. Using above methodology, the following trends have been observed in the economic feasibility of biomass gasification based power generation:

1. Biomass gasification based electricity generation using duel fuel engine is found competitive with diesel generators only for capacities higher than 20 kW. However, 100% producer gas engines are not economically attractive even for 40 kW capacities.

2. The plant load factor is a crucially important parameter. Biomass gasification with

duel fuel engine is economically unfeasible for even 75% load in comparison to diesel generators.

3. If electricity distribution network already exits at the installation site, it reduces the LUCE by 20%, making biomass gasification even more attractive.

4. Splitting of gasifier capacities (in view of smaller day time loads and larger night time loads) helps in reduction of capital cost but not LUCE.

5. Capacity utilization factor is also a crucially important factor influencing the economy of power generation. Higher capacity utilization factor add to economy of biomass gasification.

Similar conclusions about biomass gasification based power generation have been drawn by other authors [22,50,52,57-59].

*Break even price approach:* Break even price of the pilot fuel used in dual fuel generator sets could be used as a measure of the financial viability of biomass gasifier. However, the results of this approach depend on the definition of the breakeven price used. We give below summary of the work of Siemons [53] and Nouni et al. [48] who have used this approach with different definitions of the breakeven price.

The formula used by Siemons [53] for calculation of the breakeven price of diesel is:

$$\text{Breakeven price} = \begin{pmatrix} \text{Prevailent market} \\ \text{price of diesel} \end{pmatrix} \times \left( 1 + \frac{\Delta AC + \Delta WC}{(\text{Total generation} \times \text{Unit price of diesel})} \right)$$

where ΔAC indicates difference in the total annualized capital cost of diesel generator and biomass gasifier, while ΔWC indicates difference in the total operating cost of diesel generator and biomass gasifier system for a given plant load factor and capacity utilization factor. In other words, the definition of breakeven price of diesel is the price for which the total production costs of biomass gasifier based generation and generation with 100% diesel are equal. The “unit price of diesel” appearing in the denominator of the second term in the

bracket is the price used for calculation of annualized capital cost and working capital. Thus, the formula of Siemons [53] is implicit.

On the other hand, Nouni et al. [48] have defined breakeven price of diesel as the price for which the levelized unit cost of electricity (LUCE) from a biomass gasifier employing dual fuel engine is equal to the unit cost from a biomass gasifier employing 100% producer gas engine. On the basis of this definition, the formula used by Nouni et al. [48] for calculation of the breakeven price of diesel is:

$$\text{Breakeven price} = \frac{\left( \frac{\text{LUCE}_{\text{hpg}} \times E_o^{DF} - AC_C^{DF} - AC_{O\&M}^{DF}}{8760 \times CUF} - C_{bm} S_{sbmc}^{DF} P^{DF} \right)}{S_{spfc}^{DF} \times P^{DF}}$$

Notations are as follows: $\text{LUCE}_{\text{hpg}}$ – levelized unit cost of electricity for biomass gasifier with 100% producer gas engine; $AC_C^{DF}$ - annualized capital cost for gasifier with dual fuel engine; $AC_{O\&M}^{DF}$ - annualized operating and maintenance cost for gasifier with dual fuel engine; $C_{bm}$ – unit cost (per kg) of biomass; $S_{sbmc}^{DF}$ - specific biomass consumption in a biomass gasifier with dual fuel engine; $P^{DF}$ – rated power of dual fuel engine-generator; CUF – capacity utilization factor.

Siemons [53] has determined the "*feasibility region*" of the gasifier on the basis of breakeven price for diesel for a given capacity factor and biomass price. Quite obviously, the gasifier based electricity generation is feasible in situation where the market price of diesel exceeds significantly the breakeven price. Although the economic feasibility for biomass gasifiers is lesser than charcoal gasifier (probably due to additional investments required for biomass preparation and storage), higher capacity system (> 150 kW) could be economic. Despite this, Siemons [53] has noted that biomass gasifier could be economically feasible in certain sites where sufficient biomass supply is available at low costs. Reduction in the capital investment required for biomass gasifier could play crucial role in improving economy. Nouni et al. [48]

**Table 2.14:** List of Parameters (along with their typical values) for Economic Model of Medium to Large Scale Biomass Gasifiers

| Parameter | Value |
|---|---|
| 1. Plant capacity | 500 kW – 5 MW |
| 2. Capital cost of the plant | Rs. 40 – 70 million per MW |
| 3. Debt ratio and interest | 0.8 and 15% |
| 4. Depreciation | 10% |
| 5. Biomass price | Rs. 1 – 3 per kg |
| 6. Village area | 200 – 400 hectares |
| 7. Process efficiency | 15 – 25% |
| 8. Biomass productivity | 8 – 10 MT per hectare |
| 9. Fraction of village biomass available for power production | 20 – 40% |
| 10. Concentration of villages | 1 per 5 $km^2$ |
| 11. Tractor capacity | 1 – 2 tons |
| 12. Discount rate for capital investment and cash earning | 15% |
| 13. Plant load factor | 68.5% |
| 14. Buy back price of electricity | Rs. 3.01 per kWh |

Source [4]

have determined the breakeven price for diesel for a 20 kW gasifier with CUF of 25% and plant load factor of 50% as Rs. 32.05 per liter. For a 40 kW gasifier with same CUF and plant load factor, the breakeven price of diesel is Rs. 37 per liter. If we apply formula of Siemons [53] using model data of Nouni et al. [48], the breakeven price of diesel comes out to be Rs. 35.60 per liter. This is fairly close to the breakeven prices determined by Nouni et al. [48]. Based on the approach and results of Siemons [53] and Nouni et al. [48], on a whole, one can conclude that biomass gasifier based generation becomes feasible for diesel costs above Rs. 35 per liter.

### 2.5.3 Economics of large scale units (500 kW–5 MW)

Gasifiers with capacity 500 kW or higher fall in this category. The technology as well as economics of these systems has distinct differences from the small scale stand alone system. Major factors contributing to this are use of more efficient technology due to large capacity and possibility of meeting the fuel needs of the plant by having short rotation coppice [4,60-62], better capacity utilization factors as these units can meet the power need of a group of

villages, higher plant load factor as these units can be connected to grid and possibility of selling power to the state government through power buy back policy. Commercial gasifiers available in the market are up to 500 kW only. Beyond this capacity, the fixed bed gasifiers (updraft and downdraft) suffer from limitations of oxygen channeling, high tar production, uneven temperature distribution that affect the overall stability of operation. Fluidized bed technology offers a viable solution for gasifier at capacities equal to or exceeding 5 MW. The fluidized bed technology is not commercialized in India. As noted earlier, the only option at these capacities is cogeneration projects with high pressure boilers and steam turbines. Bharadwaj [4] has reported a cost model for assessment of economic feasibility of biomass gasifiers at this scale of operation. The model parameters are listed in Table 2.14. In addition to annualized capital costs of gasifier and its operation, this model also accounts for transportation cost of biomass. At about some specific fuel consumption rate as low to medium scale gasifier, the 5 MW unit is expected consume 150–200 tons per day of biomass. Obviously, this quality of biomass may not be available in a single village. Therefore collection and transportation of biomass from adjacent village becomes an additional cost factor. For capacity utilization factor of about 68.5% (corresponding to 6000 h per annum of operation), the biomass collection area is located with radius of 10 km with the plant location taken as center. Obviously, the contribution of transportation cost factor to overall operational cost increases as the capacity of the plant increases. For example, for 5 MW capacity plant, the annual transportation costs amount to more than Rs. 1 crore (Rs. 10 million), if the overall plant efficiency is 20%. However, a marginal improvement in the efficiency to 25% can drastically reduced this cost to about Rs. 25 lakh (Rs.2.5 million). Typically, the share of transportation costs increases from 5% to 15% as the capacity increases from 500 kW to 10 MW. The levelized unit cost of electricity produced from these units is quite small ~ Rs. 2.75 per kWh (for 3 MW capacity), while power buy back is at Rs. 3 per kWh. Thus, the overall

annual profit from the operation is Rs. 50 lakh (Rs. 5 million). However, as the capacity of plant increases, the transportation cost becomes a major factor and can offset the economy of scale up making process unviable. Per calculation of Bharadwaj [4], the maximum profitable capacity of the biomass gasification plant is 5 MW, beyond which the process becomes unprofitable. Other factor that comes into picture is the availability of biomass at steady prices. This may not be feasible in reality. Due to interrupted supply of biomass, the operation of the plant can affected, which would hamper the economy.

## 2.6. CASE STUDIES

About 24500 villages in various states of India have been identified as remote villages where extension of grid electricity is not feasible. Therefore, all of these villages are proposed to be electrified with renewable energy options such as photovoltaics, micro-hydro, wind and biomass gasification. Among these options, biomass based electrification stands higher in the Indian context as the biomass is uniformly spread in the country and biomass based energy has a vital role in the rural life where agriculture is the principal activity [63-68]. Given below are some case studies of rural electrification by biomass gasification:

*Hosahalli and Hanumanthenagara in Karnataka [69-71]*: Indian Institute of Science Bangalore has installed 20 kW gasifier in the two villages of Hosahalli and Hanumanthenagara (in Karnataka) in 1987 and 1994 respectively. The population of these villages is rather small (220 and 300 respectively) and agriculture was primary business. The gasifier installed in these villages have duel fuel generator with efficiency of about 23% woody biomass obtained from social forestry is used as fuel in the gasifier. The typical specific consumption of these gasifiers is 1.25 kg/kWh and the tariff is fixed at Rs. 3.34/kWh. Electricity was mainly used for domestic and street lighting, irrigation, drinking water supply and flour mills. The gasifiers were operated by locally trained people and managed by village

committee. Electricity was generated and provided for 90% days in a year.

*Odanthurai and Nellithurai in Tamil Nadu [10,16,72]*: Village *Panchayat* (or village committee) of Odanthurai (Tamil Nadu) has installed 9 kW capacity Ankur Gasifier for electricity required for water pumps for drinking water supply. With usage of biomass gasified electricity, the load on grid electricity has been reduced by over 70%. The gasifier operates on waste wood obtained from a local saw mill purchased at Rs. 0.3/kg. The efficiency of gasifier is typically 1.5 kg of wood/kWh. The number of consumers of this facility is approximately 4000 and the tariff is fixed at Rs.30 per household per month. The installation at Nellithurai is similar as that in Odanthurai except that the village committee has decided to operate the street lights on gasifier electricity. The specific fuel consumption and tariff structure is same as that in Odanthurai but the cost of biomass purchase is much higher at Rs.800/ton dry wood.

*Installation at Sundarban in West Bengal* [10,49,73,74]: Two remote islands in Sundarbans, viz. Gosaba and Chottomollakhali have been electrified by West Bengal Renewable Energy Development Authority by installation of biomass gasifiers. The Gosaba island located in 24 Paraganas district (115 km from Kolkata) has five units of 100 kW capacity. To meet the fuel wood needs, energy plantation has been carried out on 100 ha waste land. The yield from this plantation is 10 tons of biomass per hectare per year. A cluster of five villages with total population of approximately 10000 has been provided electricity from this installation. The generators are of dual fuel type, which consume 70% producer gas and 30% diesel at full load. The specific biomass consumption is 0.8 kg of dry wood/kWh and units are operated for 16 h each day. The tariff structure is Rs.5.60/kWh for domestic users, Rs. 6.75/kWh for commercial users and Rs. 8/kWh for industrial users. The total capital cost of installation is Rs. 9.5 million, and this operation has provided direct and indirect employment to about 84 people.

Similar installations have been made in the village of Chottomollakhali at Sundarbans with population of 9219 (total 1726 households). In June 2001, four units of 125 kW capacity each have been set up in this village at a cost of Rs. 14 million. The capacity utilization factor is 80% and operation of the plant lasts for 5 h each day. To meet the fuel needs of the gasifiers, plantation has been carried out in 10 ha land at a cost of Rs. 500,000. The biomass yield from this plantation is estimated at 5 tons $ha^{-1}$ $year^{-1}$. The tariff structure is similar to the Gosaba island and total number of beneficiaries from this venture are 225 (1 industry, 74 commercial and 150 domestic households).

## 2.7 BIOMASS GASIFICATION: GLOBAL PERSPECTIVE

According to the review of gasifier manufactures and installations in Europe, USA and Canada presented by Knoef [82], there are 57 manufacturers and close to 100 installation. The gasifier market has been dominated by downdraft type gasifiers (75%) followed by fluidized bed systems (20%), updraft type gasifier (2.5%) and others (2.5%). Given below is a brief summary of the biomass gasification technology and commercialization in USA, Europe and Canada in the past two decades, based on reviews of Beenackers [83], Babu [84] and Maniatis [85].

### 2.7.1 Updraft Gasifiers

Since 1980s, the most successful implementation of this kind of gasifier was done by Bioneer for heating applications (with marketing rights with Foster Wheeler Energy Oy, Finland). This technology has been implemented at 10 locations in Finland. Initially, these gasifiers were designed for lime-kiln applications with peat as main fuel. However, later the gasifiers were adopted for locally available residues and wastes. Other manufacturers of updraft gasifier include Vøland (Denmark), which has installed 4 $MW_{th}$ plant in Harboøre and Krærner (Norway), which has developed slagging counter-current gasifier with biomass and

wastes as feed stock. Daneco SpA has built updraft gasification plant (600 $kW_e$) based on residue derived fuel (RDF). The gas is scrubbed and filtered before feeding into duel fuel engine. The gasifier can also gasify wood chips and briquettes of PET bottles as feedstock.

### 2.7.2 Downdraft Gasifiers

Due to low tar content, these designs have been preferred for smalls scale power generation in Europe. Some major commercial manufacturers of downdraft systems in Europe are Martezo & Chevet (France), Wamsler and Bio-Heizstoffwerk Berlin GmbH (Germany), Schelde (Netherland) and NIHPBS (Ireland). In 1994, Wamsler Ummelt technik GmbH successfully installed 3 units in capacities of 600 and 1500 $kW_{th}$. Martezo (France) implemented 135 kWe in Hogild (Denmark). However, this unit had start-up problems and the char burn out was lower than expected. Chevet (France) installed more than 10 systems with wood and agricultural waste as feedstock in developing countries. These systems are in the range of 25-40 $kW_e$, but economics has been reported to be poor.

In 1979, researchers at Twente University came up with a viable solution to the problem of tar content of producer gas. Identifying that proper design of the throat can alleviate tar problem by having tar cracking all over cross-section of throat, Groenveld [86] invented an annular throat by putting a rotating cone that would narrow down the flow area, ensuring high temperature prevalence everywhere in the throat, so as to have complete tar cracking. HTV-Juch gasifier adopted this concept for large-scale gasifier manufacture. NIHPBS in Ireland has successfully operated downdraft wood fuelled gasifier for combined heat (120 $kW_{th}$) and electricity (100 $kW_e$) supply to Agricultural College at Ennishillen. This design based on classical Imbert Gasifier with dual fuel engine.

### 2.7.3 Fluidized bed gasifiers

For capacities between few $MW_{th}$ to above 100 $MW_{th}$, circulating fluidized bed gasifiers operating at atmospheric pressure have been proved most efficient. It has been the

most preferred technology for large scale applications and has been implemented worldwide by leading companies, such as TPS, FOSTER WHEELER and LURGI. Fluidized bed gasifiers operating in bubbling mode have also been popular for medium scale operations. The principal advantage of fluidized bed gasifiers is fuel flexibility and ease of scale up. The companies marketing bubbling fluidized bed systems are Carbona and Dinamec. Fluidized bed systems operating at elevated pressure have also been marketed by leading companies such as FOSTER WHEELER. However, these systems have relative high cost than atmospheric systems due to high pressure. In addition, the operation of these gasifiers is also more complex. Nonetheless, pressurized systems have been found to suit well for the IGCC system, as the pressurized bed operation alleviates the need for the fuel compressor prior to turbine. In the next section, we give a brief overview of the major projects implemented world wide involving circulating fluidized bed technology. This is not a comprehensive account of the development and state-of-the-art in this area, but it definitely gives an idea of the status and feasibility of the CFB technology.

**2.7.3.1** ***Ahlstrom Pyrofow CFB Gasifier***

This gasifier was the first commercial application of CFB systems and commissioned in 1983 at Wisa Forest Pulp and Paper Mill at Pietarsaari in Finland. The capacity of this gasifier was 35 $MW_{th}$ with bark and saw dust as the primary fuel. The gasification temperature is about 900$^{o}$C and producer gas at 700$^{o}$C is fired directly into the lime kiln. After being coupled with gasifier system, the fuel oil consumption of the kiln reduced by about 85%, which is a significant saving on fuel cost. Following up successful installation and operation of this gasifier 3 more gasifiers were installed by Ahlstrom Inc in mid 80s for firing lime kiln: one each at Norrsuudet Bruks (Sweden, 25 $MW_{th}$), ASSI Karlsborg (Sweden, 27 $MW_{th}$) and Portucel Rodao mill (Portugal, 15 $MW_{th}$).

**2.7.3.2** ***TPS CFB Gasification Process***

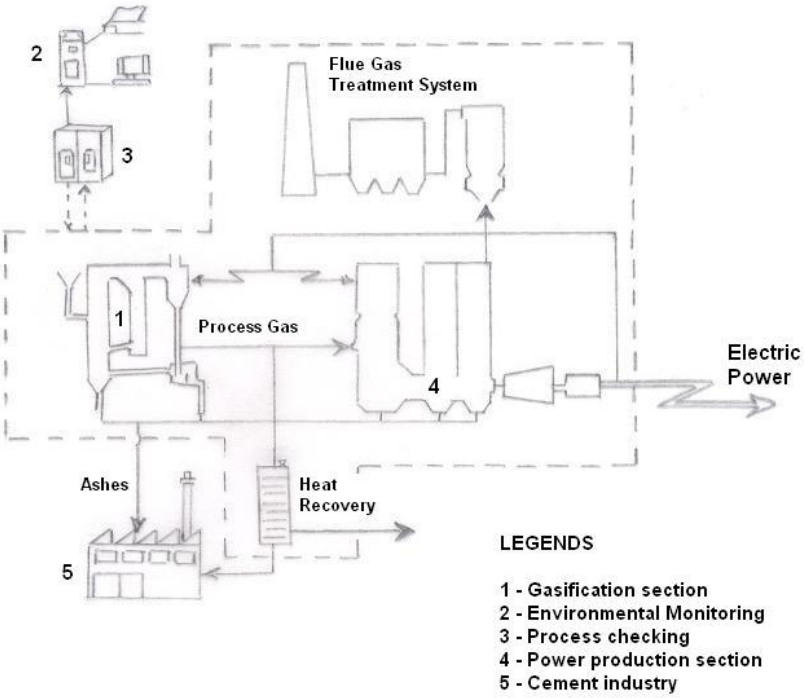


**Figure 2.10:** Schematic flow sheet of the Grieve-in-Chianti biomass gasification plant (adopted from [87])

The commercial operation of first ever TPS CFB process started at Greve-in-Chianti in 1993. The schematic of the process is shown in Figure 2.10 [87]. The fuel used was pellets of RDF (Refuse Derived Fuel). The feed rate of fuel was about 3 ton $h^{-1}$ and the capacity of gasifiers (2 no.) was 15 $MW_{th}$. The operating temperature was 875°C and the heating value of the gas was 8 $MJ/Nm^3$, one of the gasifiers was used for steam generation to run 2.3 $MW_e$ steam turbine, while gas from the second gasifier was supplied to cement factory (after solids removal and cooling to 450°C) for combustion in cement kiln. The operation has faced severe interruption due to irregularity of the RDF pellets supply.

#### 2.7.3.3 *Batelle/FERCO Project*

This project was built at McNeil power plant in Burlington, Vermont. The low pressure gasification process has a consumption of 200 tons per day of biomass and employs two reactors. Schematic flow sheet of the process is shown in Figure 2.11 [88]. The first reactor is used for gasification at 700–850°C and produces medium calorific value fuel gas along with

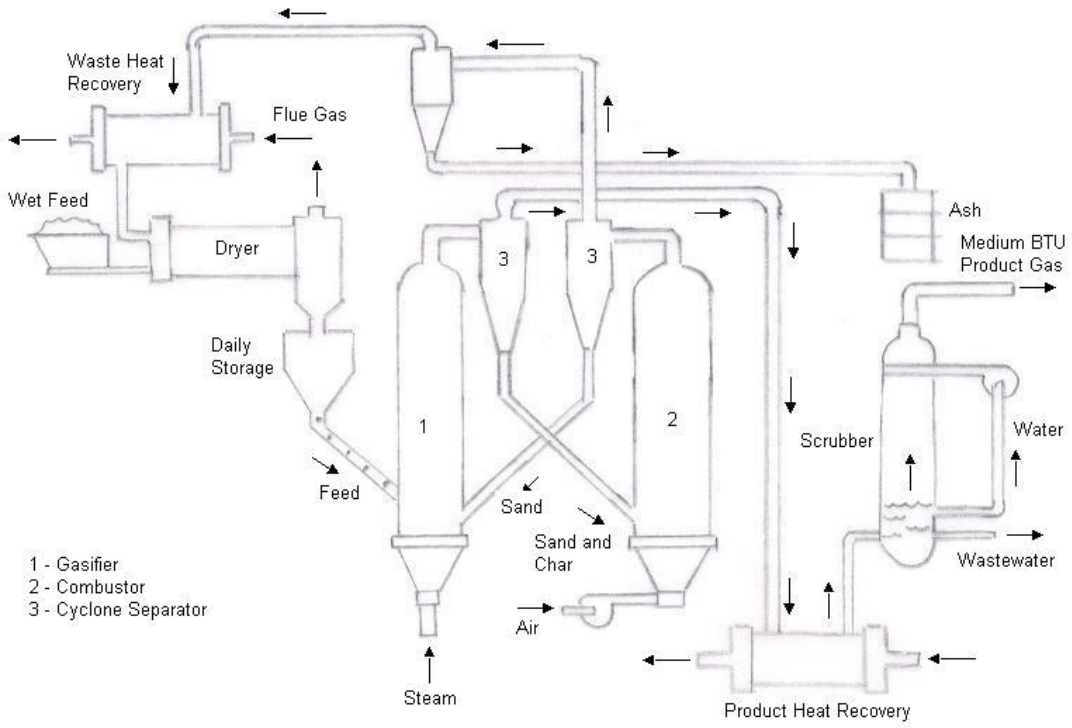


**Figure 2.11:** Schematic of the Batelle / Ferco gasification process (adopted from [88])

residual char. The second reactor is used as combustion chamber that uses the char for generation of heat for gasification. Circulating sand is used as the heat exchange medium between reactors. Wood chips were used as primary fuel and plant was fully functional in mid 2000. The gas is cooled for heat recovery, cleaned by scrubbing and compressed for use in 15 $MW_e$ gas turbine system. There are plan of converting this project to IGCC plant.

#### 2.7.3.4 *Brazilian BIG-GT Project*

This project was aimed at building 32 $MW_e$ power plant in Bahia (Northeastern Brazil). The plant was based on atmospheric pressure gasification process designed by TPS Termiska Processor AB. A circulating fluidized bed gasifier was used for gasification, and the gas cleaning system comprised of catalytic tar cracker, conventional cold filter and wet scrubbing technology. The process is shown schematically in Figure 2.12 [89]. The feedstock to plant was mainly eucalyptus wood from dedicated plantation harvested on 3 year cycle. The product gas was fired in modified GE LM 2500 gas turbine. The first phase of project

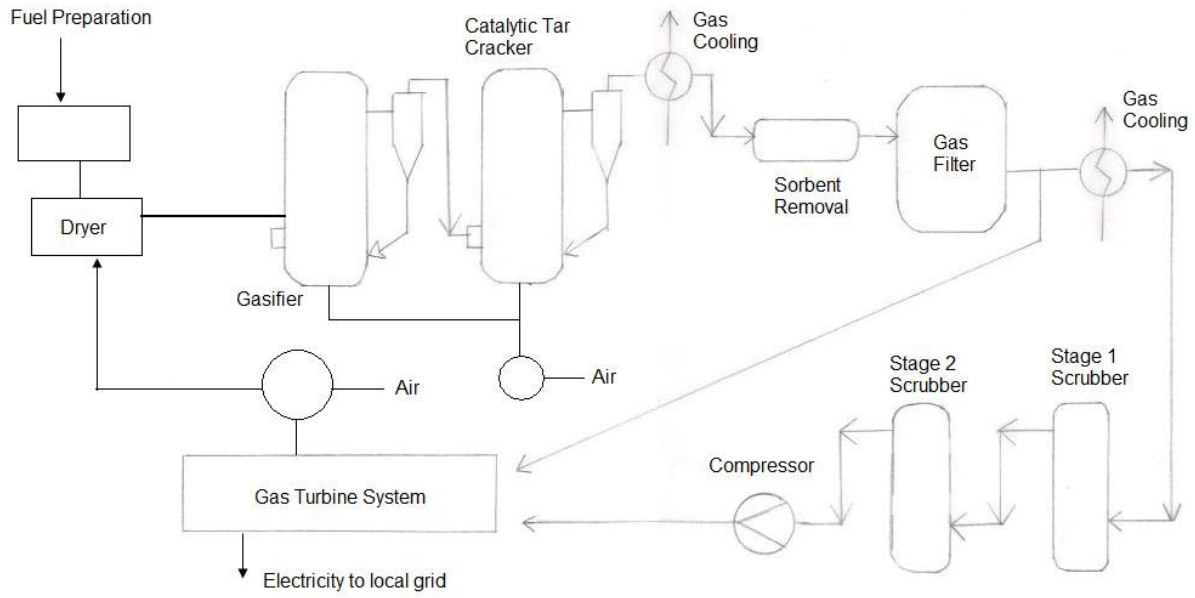


**Figure 2.12:** Schematic flow sheet of TPS atmospheric BIG – GT process (adopted from [89])

(experimental and engineering studies and basic engineering) was completed in 1997. The second phase of project (construction and commissioning of plant) received financial support from Global Environmental Facility (GEF), World Bank (WB) and United Nations Development Program (UNDP). The start up of plant was scheduled in 2000. The operational data of this project has not been available in the literature.

#### 2.7.3.5 *Biocycle Project*

The European Commission developed a plan to implement commercial biomass gasification projects under THERMIE program initiated in 1990. Denmark's BIOCYCLE project is one such project. This project used pressurized fluidized bed air blown gasification technology from Enviropower Inc. and employed tar cracking with dolomite and particulate removal by ceramic candle filters. The net output of gasifier is 7.2 $MW_e$ and 6.78 $MW_{th}$. Gas turbine employed was EGT/Typhom type. The fuel is wood chips supplied from 1325 ha of plantation of short rotation crops.

#### 2.7.3.6 *Hawaii Biomass Gasification Facility Project*

The major aim of this project, undertaken as a major USDOE initiative, was to scale up 2 $MW_{th}$ (10 TPD) IGT Renugas pressurized air blown fluidized bed gasification plant to 10 to 20 $MW_{th}$ (50–100 TDP) using bagasse and wood as fuel. This project was located on Maui island in Hawaii. Phase I of project was design, construction and preliminary operation of gasifier for generation of hot gas, which was flared. The second phase of project comprised of installation of gasifier with pressurized air or oxygen (2.07 MPa) at temperature 850–900$^{o}$C. This system was integrated with hot gas compression units and gas turbines for power generation the overall capacity of phase 2 unit was 20 $MW_{th}$ (90 TDP) with 5 $MW_e$ of electricity generation capacity.

**2.7.3.7** ***Vermont Biomass Gasification Project***

The Vermont project was also a DOE initiative, undertaken with objective of integration of Battelle "indirectly heated" gasifier with high efficiency turbine. The project was also funded by Future Resource Resources Company (FERCO) in addition to DOE. The detailed engineering design of the power plant was prepared by Zurn Nepco (Marine). The validation/ demonstration of the gasifier/ turbine system was undertaken at McNeil Power Generating Power Station, which is 50 $MW_e$ wood-fired/steam turbine facility at Burlington. The Battelle pilot plant gasifier was scaled up from 2 $MW_{th}$ (10 TPD) capacity to 40 $MW_{th}$ (200 TDP) capacity to provide producer gas to 15 $MW_e$ gas turbine.

**2.7.3.8** ***Varnamo Project***

This plant produces 6 $MW_e$ electricity along with 9 $MW_{th}$ of heat with total fuel input of 18 MW. The fuel feed was wood, bark, forest residues, willow grown on energy crops, straw and pellets of residue derived fuel. The plant underwent a test program on fuel flexibility and $NO_x$ emission problems. The $NO_x$ emission from plant was reduced (in collaboration with VTT Energy) by selective oxidation of $NH_3$ and HCN to $N_2$. Tests for reducing bed material feed were also conducted by feeding back the bottom ash from gasifier

into the process. The LHV of the producer gas was in the range 5.3–6.3 MJ/$Nm^3$. Tar production has not caused any operational problem, however the ceramic gas filter candles have been broken due to mechanical fatigue. To avoid this problem, sintered metal filter candles have been installed. The plant operation was remote controlled from a control room.

**2.7.3.9** ***ARBRE Plant***

This plant produces a net electrical output of 8 $MW_e$, sale of which has supported by NNFO Program in UK. The construction of plant started in 1998 at Selby, North Yorkshire, UK. The major fuel for the plant was coppice supplied by Yorkshire Environmental Ltd. using short rotation crops. Drying of the coppice wood chips to moisture content of 10–20% was done using low grade heat taken from warm dry air from air cooled condensers downstream of waste heat boiler. The gasifier system was TPS CFB gasifier operating is temperature range of 850–900$^oC$. The lock hopper system was used to feed the gasifier. The backflow and leakage of producer gas was prevented using seal gas. The tar cracking was accomplished in another CFB gasifier with similar dimensions .The tar cracking catalyst was dolomite at temperature of 900$^oC$. The gas was cooled to 100$^oC$, filtered using needle fiber bags and scrubbed to remove alkalis and ammonia. It is than compressed to 20 bar using ABB Alstrom Typhoon turbine the exhaust gas from turbine at 475$^oC$ is used to produce steam to generate additional 5.5 $MW_e$ in a steam turbine. Waste ash from both gasifier was recycled to coppice plantation as soil conditional and micronutrients source for improving soil fertility.

**2.7.3.10** ***FOSTER WHEELER Installation at Lahti***

A FOSTER-WHEELER CFB gasifier has been installed by Lahden Lämpövoima Oy in Lahti, Finland. The purpose of the gasifier is to supply alternate biofuel worth 50 MW to the steam boiler of power station of 550 MW capacity. The process is described schematically in Figure 2.13 [90]. The gasifier has fuel flexibility that 1/3$^{rd}$ of the fuel is

classified refuse from industry and households, and rest 2/3rd is made of different kinds of biomasses. The product gas from gasifier is sent to the burners that are located below the main coal burners of boiler.

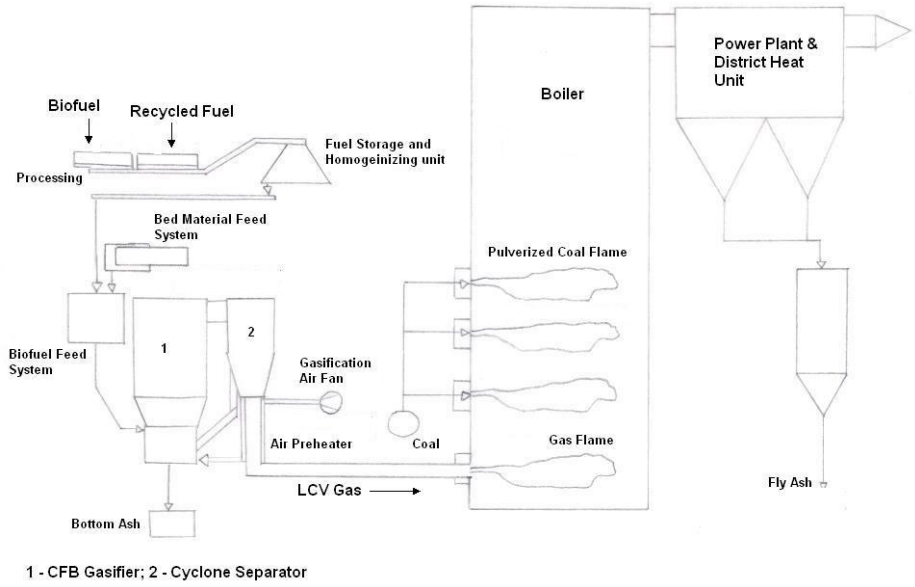


**Figure 2.13:** Schematic of the Lahden Lämpövomia Oy biofuel gasifier (adapted from [90])

If fuel is wet, the heating value of gas is as low as 2.2 MJ/Nm$^3$. The gasifier temperature is in the range 830–860 $^oC$ and overall capacity range is 35–55 MW, depending on gasifier fuel moisture content and required load on gasifier. The replacement of coal with producer gas has not caused any disturbance in operation of the main boiler steam cycle. Despite high moisture content of solid fuel and low HHV of product gas, combustion of gas has been stable. Moreover, stability of the main coal burners has not been affected by the presence of producer gas burners. The $CO_2$ emission from the plant reduced by 60000 to 80000 TPA due to replacement of coal by biofuel, while $SO_x$ and $NO_x$ emissions remained unchanged.

#### 2.7.3.11 *BioCoComb Project (Zeltweg, Austria)*

This plant has been installed at Zeltweg power plant. The Biocomb process prepares biofuels co-combustion by partial gasification in a CFB gasifier. The gasifier is integrated

with coal furnace in two ways: first, the product gas is fired in furnace of coal-fired power plant, and secondly, the char produced in gasifier is also fed into the furnace together with hot gas. The size reduction of the char particles is achieved in gasifier itself due to mechanical attrition and thermal stress. The cyclone separator is so designed that char particles, with size small enough to burn completely in the gasifier, pass through it. The fluidizing medium in gasifier is hot air – taken from preheat of power plant. The operating temperature of CFB gasifier is 750–850 $^{o}$C. Major fuel is spruce bark, chopped wood and sawdust. The power range of the gasifier is 5-20 $MW_{th}$, dominated by the moisture content of biofuel (spruce bark). Partial substitution of coal by biomass reduces $CO_2$ emission. The fuel gas can also be used as reducing gas in the re-burning zone of combustion chamber, thus avoiding the measures for controlling $NO_x$ emission. With this strategy, the biofuels can substitute to upto 10 $MW_{th}$ (3-5% of total capacity).

**2.7.3.12** ***Amer Project***

EPZ, an electricity producing company in the Netherlands has several coal fired power blocks. At one of these units, Amer 9, a gasifier for demolition wood will be added for producing gas that can be burnt in coal boiler – replacing some coal input. The aim of the project was to achieve saving of 70,000 tons of coal based on 150,000 tons of wood waste (basically construction and demolition waste) – equivalent to electricity capacity of 29 $MW_e$. This would also achieve a reduction in $CO_2$ emission of 170,000 TPA. Chipped demolition wood supplied to plant via trucks and ships is screened using a rotating disk separator by LURGI. The gasifier is CFB type operating at temperature of 800–950$^{o}$C. Limestone and dolomite are added to bed material as tar cracking agents. Since the demolition wood is contaminated with paint and metals. The product gas has to be cleaned before feeding to boilers. The gas is cooled to 200 $^{o}$C and de-dusted in bag house filter. Water scrubbing is applied to remove $NH_3$, and gas at about 100 $^{o}$C is fed to special burners in coal fired unit.

The plant has faced operational problems of slug formation. The fuel flexibility of the plant has been expanded to include RDF and grasses as additional fuel material.

#### 2.7.3.13 *BINAGAS Project*

BINAGAS project employs indirect firing of gas turbines for eliminating tar problem. In this process, the fuel gas is combusted directly in heat exchanger that heats up the clean air supplied by compressor of turbine to about 850–950 $^{o}$C. The hot air is then used to run gas turbine. BINGAS project is located on campus of Vrij Universitait Brussels, Belgium. The capacity of the plant is 500 kWe for production of heat and electricity for University campus district heating. The gasifier is atmospheric CFB type with operating temperature range of 725 to 850 $^{o}$C. The gas produced is fed to combustion chamber of heat exchanger through insulated lines and high temperature valve. The compressor of the Volvo gas turbine supplies air through heat exchanger where it is heated to 830 $^{o}$C. Water injection in air heater is included to enhance power output and allow flexible power to heat ratios. Overall performance efficiency is 24% electrical and 70% total. The main fuel fed to the CFB unit is wood pellets and saw dust.

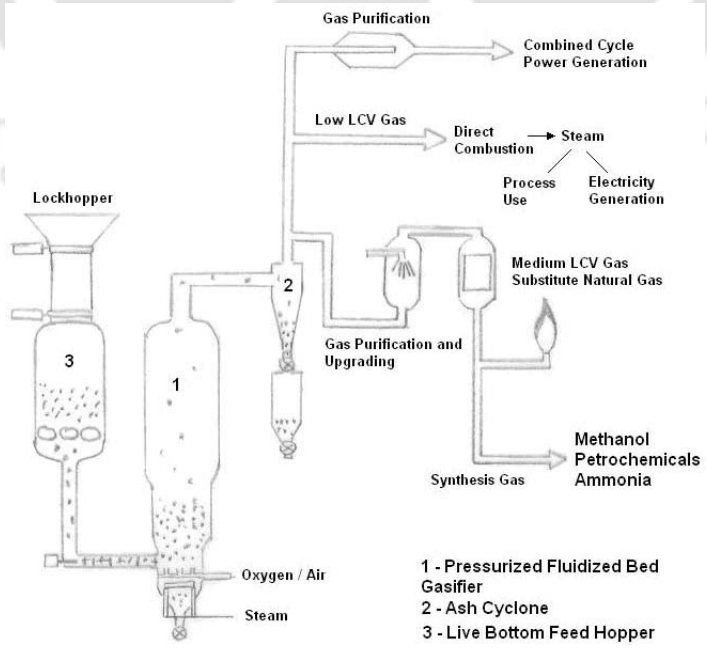


**Figure 2.14:** Schematic of the RENUGAS process (adopted from [91])

#### 2.7.3.14 *Other Installations*

A pressurized air-blown gasification plant with capacity of 15 $MW_{th}$ was built at Tampere, Finland. This plant was based on license granted by IGT for its IGT Renugas biomass gasification and the U-GAS coal gasification process (described schematically in Figure 2.14 [91]) to Enviro Power Inc. The operation of the plant was tested for about 650 h with 3000 tons of wood residue at IGCC conditions. Pilot plants also included tests on different types of biomass steam dryers, pressurized biomass feeder and hot gas clean up using ceramic filters. 98% carbon conversion was achieved with low tar content. Efficient dust and alkali removal was achieved with ceramic filter candles. The heating value of product gas was in the range 4–6 $MJ/Nm^3$ with low CO and $NO_x$ emissions.

Another RENUGAS pilot plant gasifier with 2 $MW_{th}$ (10 TPD) capacity has been installed and tested at IGT, Chicago. This gasifier is a pressurized air blown CFB type with bagasse as fuel. The tests included hot gas cleaning units and characterization of fuel gases for gas turbine applications. A bench-scale molten carbonate fuel cell (MCFC) was also successfully operated on the raw product gas stream.

## 2.8 OVERVIEW AND CONCLUSIONS FROM INDIAN PERSPECTIVE

In this chapter, we have discussed the technical and economic aspects of decentralized power generation through biomass gasification in the Indian context. Demand for electricity in rural areas is growing at a rate of 7%. Total peak hour shortage of electricity is around 20000 MW, while annual capacity addition is mere 3000 MW. India's power production potential is determined by coal based thermal plants. However, coal deposits in India are rather localized in the eastern and north eastern regions of India. Addition of further capacity through coal based thermal route would require transportation of coal to the plant site, which in turn would necessitate extension of railway network. During $11^{th}$ plan, capacity addition of

75000 MW is targeted, which is expected to fulfill the current gap between demand and supply of electricity in India. Despite this, extension of grid for accessing electricity is infeasible in some remote villages. In addition, high transmission and distribution losses add to difficulty of remote village electrification. Therefore, decentralized generation through locally available renewable energy sources is the only option for electrification of these villages.

There are strong arguments as how biomass gasification stands higher than other options for decentralized generation such as wind, photovoltaic and microhydro projects. The first argument is uniform and abundant distribution of biomass in the country; as well as availability at cheap rates throughout the year. Other arguments in favor of biomass gasification for decentralized generation are as follows [4,15,49,71,75]:

*Proven technology:* The technology for the downdraft gasifier design has been well developed and demonstrated. There are several commercial manufactures of biomass gasifiers, who provide various capacity gasifiers at competitive rates. These gasifiers are usually coupled to dual fuel engine generators and the overall efficiency of the system is around 20%. Engines working on 100% producer gas are under development. These engines are likely to reduce the cost of generation even further.

*Flexibility of installation and operation:* Biomass gasifiers can be installed at practically any village where sufficient biomass is available annually to ensure smooth operation. The duration of operation of gasifier is highly flexible. Low loads and low capacity utilization in rural areas is another hurdle in operation of ant renewable energy system. However, this problem can be overcome for biomass gasification based system as their operational hours are highly flexible. Moreover, the overall operation of biomass gasification system is very simple. It is quite possible to train villagers (with qualification of HSC/SSC/I.T.I. diploma) for operation of the plant. Maintenance and servicing spare part replacement is also relatively

easy than other options for renewable energy.

*Social and environmental benefits:* Biomass gasification based decentralized generation is likely to create employment opportunities in rural areas. These include the requirement of skilled/ semi-skilled labor for operation and maintenance of gasifier plants. In addition, plantation of energy crops in waste land is also going to prevent the rapid degradation. Another important benefit of biomass gasification based generation is reduction in $CO_2$ emission. It is estimated that replacement of each kilowatt hour of coal-based electricity by biomass gasification based electricity is likely to reduce $CO_2$ emission by 1 kg. Thus, biomass based gasification helps in mitigation of green house gas emissions and problems related to it (such as global warming).

Successful implementation of decentralized village electrification, program in Karnataka, Tamil Nadu and West Bengal has clearly demonstrated feasibility of this option. However, actual installed capacity is much lower than the estimated potential. Thus, the biomass energy potential remains mostly unexploited. Following actions plan is recommended for enhancing the effective utilization of this vast energy resource [22,23,49,52,75-76]:

1. Large production of gasifier at competitive rates with engines working on 100% producer gas with establishment of design guidelines, performance standards and testing and certification. Development of “energy system package”, which would enhance production, installation, operation and maintenance.

2. Enhancement of the load factor or capacity utilization factor by incorporating other commercial and industrial activities in the gasifier load, in addition to domestic and street lighting.

3. Encouragement of NGOs and other community based organizations to act as energy service companies. These companies will be responsible for operation and maintenance of

gasifier. Direct purchase of fuel biomass from individual villagers will provide them livelihood earning opportunity.

4. Subsidizing of the capital cost of gasifier will provide additional boost. Additional financing of working capital (as soft loans) for running the gasifier is also required. Regular information and awareness programs should be conducted to convince the rural population about the potential of gasifier based generation. This will increase the number of local consumers, and hence, the cash flow central regulation of the tariff structure is also required through an appropriate policy.

## REFERENCES

[1] Ministry of Power, Government of India (web site: http://powermin.nic.in).

[2] Central Electricity Authority, Ministry of Power, Government of India (web site: http://www.cea.nic.in).

[3] Tripathi, AK. Renewable energy development in India. In: Multiple Choice Questions on Renewable Energy; New Delhi: TERI Press; 2008. pp. 1-12.

[4] Bharadwaj, A. Gasification and combustion technologies of agro-residues and their application to rural electric power systems in India. Ph.D. Dissertation, Carnegie Mellon University, Pittsburgh, PA (USA); 2002.

[5] Sinha CS, Kanpal TC. Decentralized vs grid electricity for rural India. Energy Policy 1991;June:441-448.

[6] Chaurey A, Ranganathan M, Mohanty P. Electricity access for geographically disadvantaged rural communities – technology and policy insights. Energy Policy 2004;32:1693-1705.

[7] Bhattacharya SC. Energy access problem of the poor in India: is rural electrification a

remedy? Energy Policy 2006;34:3387-3397.

[8] Reddy AKN. Rural energy: goals, strategies and policies. Economic and Political Weekly 1999;34(49):3445-3455.

[9] Nouni MR, Mullick SC, Kandpal TC. Providing electricity access to remote areas in rural India: An approach towards identifying potential areas for decentralized power supply. Renewable and Sustainable Energy Reviews 2008;12:1187-1220.

[10] Hiremath RB, Kumar B, Balachandra P, Ravindranath NH, Raghunandan BN. Decentralized renewable energy: Scope, relevance and applications in the Indian context. Energy and Sustainable Development 2009;13:3-9.

[11] Chopra SK. Energy policy for India: Towards sustainable energy security in India in the 21st century. New Delhi: Oxford & IBH Publishing Co. Pvt. Ltd.; 2004.

[12] Reddy AKN, Subramanian DK. The design of rural energy centers. Indian Academy of Science Bangalore 1980:109-130.

[13] Ravindranath NH, Hall DO. Biomass energy and environment: a developing country perspective from India. Oxford: Oxford University Press (UK); 1995.

[14] Ravindranath NH, Rao U, Natarajan B, Monga P. Renewable energy and environment: A policy analysis for India. New Delhi: Tata McGraw Hill; 2000.

[15] Banerjee R. Comparison of options for distributed generation. Energy Policy 2006; 34:101-111.

[16] Biomass Booklet. Ministry of New and Renewable Energy, Government of India, New Delhi; 2005.

[17] Singh NP. Overview of renewable energy in India. In: 25 Years of Renewable Energy in India; New Delhi: Ministry of New and Renewable Energy; 2007. pp. 1-16.

[18] Nouni MR, Mullick SC, Kandpal TC. Techno-economics of micro-hydro projects for decentralized power generation in India. Energy Policy 2006;34:1161-1174.

[19] Ministry of New and Renewable Energy. 25 Years of Renewable Energy in India; New Delhi; 2007.

[20] Meshram JR, Mohan S. Biomass power and its role in distributed power generation in India. In: 25 Years of Renewable Energy in India, New Delhi: Ministry of New and Renewable Energy; 2007. pp. 109-134.

[21] Ministry of Coal (Annual Report, 2007-08. website: http://coal.nic.in), New Delhi; 2008.

[22] Ghosh D, Sagar A, Kishore VVN. Scaling up biomass gasifier use: applications, barriers and interventions. Paper No. 103 (Climate Change Series), Washington: World bank Environment Department; 2004.

[23] Jain BC. Commercialising biomass gasifiers: Indian experience. Energy for Sustainable Development 2000;IV (3):72-82.

[24] McKendry P. Energy production from biomass (part 1): overview of biomass. Bioresource Technology 2002;83:37-46.

[25] McKendry P. Energy production from biomass (part 3): gasification technologies. Bioresource Technology 2002;83:55-63.

[26] Li X. Biomass Gasification in Circulating Fluidized Bed, Ph.D. Dissertation, University of British Columbia, Vancouver, Canada, 2002.

[27] Kishore VVN (Ed.). Renewable Energy Engineering & Technology: A Knowledge Compendium. New Delhi: TERI Press; 2008.

[28] Beenackers AACM, Maniatis K. Gasification technologies for heat and power from biomass. In: Biomass Gasification and Pyrolysis: State-of-the-art and Future Prospects (Ed. Bridgwater AV), Newbury: CPL Press; 1997. pp. 24-52.

[29] Beenackers AACM. Biomass gasification in moving beds. A review of European technologies. Renewable Energy 1999;16:1180-1186.

[30] Kohli S, Ravi MR. Biomass gasification for rural electrification: prospects and challenges. SESI Journal 2003;13:83-101.

[31] Tijmensen MJA, Faaij APC, Hamelinck CN, van Hardeveld MRM. Exploration of the possibilities for production of Fischer-Tropsch liquids and power via biomass gasification. Biomass and Bioenergy 2002;23:129-152.

[32] Faaij A, van Ree R, Waldheim L, Olsson E, Oudhuis A, van Wijk A, Daey-Ouwens C, Turkenburg W. Gasification of biomass wastes and residues for electricity production. Biomass and Bioenergy 1997;12:387-407.

[33] Hebden D, Stroud HJF. Coal gasification processes. In: Chemistry of Coal Utilization (Ed. Elliott MA), New York:John Wiley and Sons; 1981.

[34] Liu P, Guo XF, Wu CZ, Chen Y, Arai N. Gasification characteristics of biomass wastes in fluidized bed gasifier. Journal of Propulsion Power 2000;16:606-608.

[35] Mansaray KG, Ghaly AE, Al-Taweel AM, Hamdullahpur F, Ugursal VI. Air gasification of rice husk in a dual distributor type fluidized bed gasifier. Biomass and Bioenergy 1999;17:315-332.

[36] Narvacz I, Orio A, Aznar MP, Corella J. Biomass gasification with air in an atmospheric bubbling fluidized bed. Effect of six operational variables on the quality of the produced raw gas. Industrial and Engineering Chemistry Research 1996;35:2110-2120.

[37] Ergudenler A, Ghaly AE, Hamdullahpur F, Al-Taweel AM. Mathematical modeling of a fluidized bed straw gasifier: Part I – Model development. Energy Sources 1997;19:1065-1084.

[38] Bilodeau J-F, Therien N, Proulx P, Czernik S, Chornet E. A mathematical modelof fluidized bed biomass gasification. Canadian Journal of Chemical Engineering 1993;71:549-557.

[39] Yin XL, Wu CZ, Zheng SP, Chen Y. Design and operation of a CFB gasification and

power generating system for rice husk. Biomass and Bioenergy 2002;23:181-187.

[40] Garcia-Ibanez P, Cabanillas A, Sanchez JM. Gasification of leached *orujillo* (olive oil waste) in a pilot plant circulating fluidized bed reactor – preliminary results. Biomass and Bioenergy 2004;27:183-194.

[41] Kersten SRA, Prins W, van der Drift A, van Swaaij WPM. Experimental fact finding in circulating fluidized bed biomass gasification for ECN's 500 $kW_{th}$ pilot plant. Industrial and Engineering Chemistry Research 2003;42:6755-6764.

[42] Corella J, Sanz A. Modeling circulating fluidized bed biomass gasifiers: A pseudo-rigorous model with stationary state. Fuel Processing Technology 2001;86:1021-1053.

[43] Liu H, Gibbs BM. Modeling $NH_3$ and HCN emissions from biomass circulating fluidized bed gasifiers. Fuel 2003;82(13):1591-1604.

[44] Devi L, Ptasinski KJ, Janssen FJJG. A review of the primary measures for tar elimination in biomass gasification processes. Biomass and Bioenergy 2003;24:125-140.

[45] Narvaez I, Corella J, Orio A. Fresh tar (from a biomass gasifier) elimination over a commercial steam-reforming catalyst. Kinetics and effect of different variables of operation. Industrial and Engineering Chemistry Research 1997;36:317-327.

[46] Milne TA, Evans RJ. Biomass gasification "tars": their nature, formation and conversion. Report No. NREL/TP-570-25357, Golden:NREL; 1998.

[47] Neeft JPA, Knoef HAM, Onaji P. Behavior of tars in biomass gasification systems. Tar related problems and their solutions. NOVEM Report No. 9199, EWAB:The Netherlands; 1999.

[48] Nouni MR, Mullick SC, Kandpal TC. Biomass gasifier projects for decentralized power generation in India: a financial evaluation. Energy Policy 2007;35:1373-1385.

[49] Ghosh D, Sagar AD, Kishore VVN. Scaling up biomass gasifier use: an application specific approach. Energy Policy 2006;34:1566-1582.

[50] Tripathi AK, Iyer PVR, Kandpal TC. A financial evaluation of biomass gasifier based power generation in India. Bioresource Technology 1997;61:53-59.

[51] Jorapur RM, Rajvanshi AK. Development of a low density biomass gasification system. In: Proceedings of 28th International Energy Conservation Engineering Conference, 1993;2:443-448.

[52] Kishore VVN, Bhandari PM, Gupta P. Biomass energy technologies for rural infrastructure and village power – opportunities and challenges in the context of global climate change concerns. Energy Policy 2004;32:801-810.

[53] Siemons RV. Identifying a role for biomass gasification in rural electrification in developing countries: the economic perspective. Biomass and Bioenergy 2001;20:271-285.

[54] Nouni MR, Mullick SC, Kandpal TC. Techno-economics of small wind electric generator projects for decentralized power supply in India. Energy Policy 2007;35:2491-2506.

[55] Nouni MR, Mullick SC, Kandpal TC. Photovoltaic projects for decentralized power supply in India: a financial evaluation. Energy Policy 2006;34:3727-3738.

[56] Kandpal TC, Garg HP. Financial Evaluation of Renewable Energy Technologies. New Delhi: McMillan India Ltd.; 2003.

[57] Jorapur RM, Rajvanshi AK. Operating experience and economics of a 15 KVA genset-gasifier system running on chopped sugarcane leaves. In: Recent Progresses in Biomass Gasification and Combustion (Ed. Paul PJ, Mukunda HS), Bangalore: Interline Publishing; 1993.

[58] Kapur T, Kandpal TC, Garg HP. Electricity generation from rice husk in Indian rice mills: potential and financial viability. Biomass and Bioenergy 1996;10:393-403.

[59] Ghosh S, Das TK, Jash T. Sustainability of decentralized woodfuel-based power plant: an experience with India. Energy 2004;29:155-166.

[60] Mitchell CP, Bridgwater AV, Sterens DJ, Toft AJ, Watters MP. Technoeconomic assessment of biomass to energy. Biomass and Bioenergy 1995;9(1-5):205-226.

[61] Bridgwater AV. The technical and economic feasibility of biomass gasification for power generation. Fuel 1995;74(5):631-653.

[62] Caputo AC, Palumbo M, Pelagagge PM, Scacchia F. Economics of biomass energy utilization in combustion and gasification plants: Effects of logistic variables. Biomass and Bioenergy 2005;28:35-51.

[63] Ramchandra TV, Joshi NV, Subramsnian DK. Present and prospective role of bioenergy in regional energy system. Renewable and Sustainable Energy Reviews 2000;4:375-430.

[64] Gupta CL. Role of renewable energy technologies in generating sustainable livelihood. Renewable and Sustainable Energy Reviews 2003;7:155-194.

[65] Demirbas AH, Demirbas I. Importance of rural bioenergy for developing countries. Energy Conversion and Management 2007;48:2386-2398.

[66] Varun, Singhal SK. Review of augmentation of energy needs as renewable energy sources in India. Renewable and Sustainable Energy Reviews 2007;11:1607-1615.

[67] Mukunda HS. 100% of energy from renewable –Is this an achievable goal or an important slogan? (http://cgpl.iisc.ernet.in).

[68] Ravindranath NH, Balachandra P. Sustainable bioenergy in India: Technical, economic and policy analysis. Energy (2009) doi:10.1016/j.energy.2008.12.012.

[69] Sridhar G, Sridhar HV, Basawaraj SMS, Somsekhar HI, Dasappa S, Paul PJ. Case studies on small scale biomass gasifier based decentralized energy generation system. (http://cgpl.ernet.in/site/portab0/publication/Nationalconf/caseStudiesOnSmall BiomassGasifier.pdf).

[70] Somashekhar HI, Dasappa S, Ravindranath NH. Rural bioenergy centers based on

biomass gasifiers for decentralized power generation: Case studies of two villages in Southern India. Energy for Sustainable Development 2000;4:55-63.

[71] Ravindranath NH, Somashekhar HI, Dasappa S, Reddy CNJ. Sustainable biomass power for rural India: case study of biomass gasifier for village electrification. Current Science 2004;87(7):932-941.

[72] Abe, H. Summary of biomas power generation in India (http://www.plants.uwa.edu.au/home/research/research_centres/ergo/students/hitofumi_abc), Crawley: Japan International Cooperation Agency; 2005.

[73] Mukhopadhyay K. An assessment of biomass gasification based power plants in sunderbans. Biomass and Bioenergy 2004;27:253-264.

[74] Mukhopadhyay K. A review of the socio-economic and environmental benefits of biomass gasification based plants: lessons from India. In: Progress in Biomass and Bioenergy Research (Ed. Warmer SF), New York:Nova Science Publishers; 2006.

[75] Mukunda HS. Low cost, high efficiency biofuel-to-electricity: past and future (http://cgpl.iisc.ernet.in).

[76] Mukunda HS, Dasappa S, Paul PJ, Rajan NKS, Sridhar G, Sridhar HV, Shrinivasa U. Thermo-chemical conversion of biomass- a retrospective and perspective. I.I.Sc. Bangalore (http://cgpl.iisc.ernet.in).

[77] Reference Material, International Training Program on Biomass Technologies; Combustion Gasification and Propulsion Laboratory, I.I.Sc. Bangalore, April 2001.

[78] Biomass Atlas of India, CGPL, Indian Institute of Science, Bangalore (http://cgpl.iisc.ernet.in).

[79] I.I.Sc. Gasifiers Installed in India and Overseas (PDF Document), International Training Program, Combustion Gasification and Propulsion Laboratory, I.I.Sc. Bangalore, April 2001 (http://cgpl.iisc.ernet.in).

[80] http://www.ankurscientific.com.

[81] Energy Development, In: Economic Review, Department of Planning and Economic Affairs, Government of Kerala, 2003.

[82] Knoef HAM. Inventory of Biomass Gasifier Manufacturers and Installations. Final Report to EC, Contract DIS/1734/98-NL; Biomass Technology Group B.V., University of Twente: Enschede (Netherlands), 2000.

[83] Beenackers AACM. Biomass gasification in moving beds: A review of European technologies. Renewable Energy 1999;16:1180-1186.

[84] Babu SP. Thermal gasification of biomass technology development: End of task report for 1992 to 1994. Biomass and Bioenergy 1995;1-5:271-285.

[85] Maniatis K. Progress in biomass gasification: An overview. In: Progress in Thermochemical Conversion of Biomass (Ed. Bridgwater AV), Blackwell Science Ltd.: Oxford (UK), 2001. pp. 1-31.

[86] Groenveld MJ. The Co-current Moving Bed Gasifier. Ph.D. Dissertation, Delft University of Technology, Delft (Netherlands), 1980.

[87] Morris M, Waldheim L. Energy recovery from solid waste fuels using advanced gasification technology. Waste Management 1998;18:557-564.

[88] Paisley MA, Anson D. Biomass gasification for gas turbine-based power generation. Transactions of the ASME: Journal of Engineering for Gas Turbines and Power 1998;120:284-288.

[89] Waldheim L, Carpentieri E. Update on the progress of the Brazilian wood BIG-GT demonstration project. Transactions of the ASME: Journal of Engineering for Gas Turbines and Power 2001;123:525-536.

[90] Nieminen J, Kivela M. Biomass CFB gasifier connected to a 300 $MW_{TH}$ steam boiler fired with coal and natural gas – Thermie demonstration project in Lahti in Finland. Biomass

and Bioenergy 1998;15(3):251-257.

[91] Lau FS. The Hawaiian project. Biomass and Bioenergy 1998;15(3):233-238.

भारतीय प्रौद्योगिकी संस्थान गुवाहाटी
Indian Institute of Technology Guwahati

CHAPTER 3

# Literature Review

## 3.1 INTRODUCTION

Modeling of biomass gasification with different approaches been active area of research for past 2 decades. Various approaches adopted by authors include thermodynamic (equilibrium and semi– or quasi–equilibrium using either stoichiometric or non–stoichiometric models), kinetic, combination of kinetic and thermodynamic, combination of kinetic and/or thermodynamic with hydrodynamics of the system etc. Majority of the literature has adopted thermodynamic approach (either exclusively or coupled with either kinetic and/or hydrodynamic). The cause leading to this is rather obvious: the chemistry of biomass gasification is rather complicated with numerous parallel or simultaneous reactions. Especially, oxidation of char and tar is rather complicated as exact composition of char is not known and varies from biomass to biomass. Tar as well comprises of thousand of hydrocarbons and all of these components of tar have different kinetic and chemistry of oxidation. The kinetic data for all reactions is, therefore, not available for wide range of temperature and pressure. This limitation puts a major constraint on application of kinetic models for assessing behavior of gasifiers under different condition and with wide range of feedstock. Thermodynamic models have advantage of application for gasification process

under wide range of operating conditions and feedstock. Especially, the non–stoichiometric models have merit of being able to handle feed streams with unknown species and molecular formulae. Predictions of semi–equilibrium version of thermodynamic models of gasification have a closer match with experimental results.

We present herewith a review of the literature published in the area of mathematical modeling of biomass gasification / gasifiers. The literature reviewed in this chapter also includes some experimental studies that also propose a suitable kinetic model (either empirical or semi–empirical) for the process. However, we would like to specify that literature review presented below is not an exhaustive one that covers all studies. Nonetheless, it gives an idea of the history as well as state–of–the–art of the subject of modeling of biomass gasification.

## 3.2 LITERATURE IN THE 1990S AND BEFORE

Earliest literature in the area of application of thermodynamic models for gasification process (with either coal or biomass as feedstock) includes work of Cousins [1], Denn et al. [2], Desrosiers [3] and Kosky and Floess [4]. Cousins [1] modified the thermodynamic theory of Gumz [5] and applied it for wood gasification with air and oxygen/steam mixture as medium in both cocurrent and countercurrent mode. Countercurrent process was found to have merits such as decreased oxygen consumption, predrying of biomass and production of gases with high flame temperature. Cocurrent process had merits of reduced air pollution and high gasification efficiency. Denn et al. [2] proposed detailed model of a moving–bed coal gasifier that provided temperature and composition profiles throughout the reactor, as well as effluent gas composition and temperature as a function of operating conditions, which were given as input for the model. The former parameters were sensitive to certain model inputs, but the latter were found to be insensitive to large variations in operating conditions. Based

on this analysis, Denn et al. [2] concluded that a kinetics–free model would be useful in prediction of reactor performance in regions of high C conversion due to insensitivity of overall model behavior to certain model parameters. Agreement between the kinetics–free calculations and the detailed model was found to be excellent for coals with negligible reactivity to H. Klosy and Floess [4] presented a model for coal gasification in fixed bed that assumed CO, $CO_2$, $H_2O$ and $H_2$ to be in thermodynamic shift equilibrium over a zone in which primary gasification reactions occur. Gas borne impurities were found to catalyze these reactions at temperatures > 550° C. Fresh coal is pyrolyzed in this gas stream and its gaseous products add to the shift gases. The composition and quantity of final raw product gases determined with the model, in addition to the heat effects of gasification, was found to be close to experimental data from oxygen and air–blown gasifiers. The model could correctly predict the effect of heat leak in establishing the composition of the raw coal gas from a fixed–bed gasifier. Shesh and Sunawala [5a] have studied the air–steam gasification of Bombay city municipal refuse at pressures ≤ 50 bar and temperature ≤ 1000 $^{o}$C using equilibrium models. They have also attempted to optimize the operating conditions based on calorific values and potential heat output of producer gas. Kovacik et al. [6] applied the F*A*C*T program developed by University of Montreal by prediction of coal gasifier operations at wide range of temperatures and pressures. This model is independent of design of the gasifier and thus is equally applicable for entrained–flow and fluidized bed designs. This model required coal composition, extent of conversion, and reactor operating conditions are required as input parameters. Kinoshita et al. [7] have tried to optimize the biomass gasification process as a precursor for methanol manufacture using equilibrium computations. The conditions for gasification, viz. temperature, pressure, biomass moisture content and equivalence ratio, have been optimized so as to make producer gas resulting from gasification suitable for methanol manufacture. Watkinson et al. [8] have performed simulations of

commercial coal gasifier to predict gas composition and yield. The basic approach of Watkinson et al. [8] is similar to that of Kosky and Floess [4], and the simulation results have compared with experimental results of 9 types of gasifiers. In a similar study, Garcia and Laborde [9] have examined production of hydrogen by steam reforming of ethanol using non–stoichiometric thermodynamic model. The range of reforming conditions were: pressure = 1–9 atm, temperature = 400–800 K, water:ethanol feed ratio 0.1–10:1. Maximum production of hydrogen was seen at temperature > 650 K, atmospheric pressure and excess water in feed. Least methane formation, with practically no formation of carbon was observed for these conditions. The behavior of this system was similar to methanol, except that temperature and water:alcohol feed ratio in case of ethanol was higher for maximum hydrogen production. Wang and Kinoshita [10] have developed a kinetic model for biomass gasification based on mechanism of surface reactions. The apparent rate constants were computed by minimizing the differences between the experimental data and theoretical results for different residence times and temperatures. Effect of various parameters such as type of oxidant, residence time, char particle size, temperature, pressure, equivalence ratio and moisture on outcome of gasification process was studied. Alderucci et al. [11] have tried to assess the technical feasibility of an integrated biomass catalytic gasifier – solid oxide fuel cell system for electricity production. The model feedstock was cellulose with water vapor or $CO_2$ as gasification agent. The electricity efficiencies of Solid Oxide Fuel Cell (SOFC) for gasification temperature of 700$^{o}$C were found to be 47% for steam as gasification medium and steam/biomass ratio of 1.12, and 51% for $CO_2$ as gasification agent and $CO_2$/biomass ratio of 1.3, respectively.

In the subsequent section, we have summarized the literature in the area of modeling of biomass gasification (and related processes such as tar cracking) published in past one and half decade.

## 3.3 LITERATURE IN THE PAST ONE AND HALF DECADE

- Kaushal et al. [12] have developed a comprehensive mathematical model for bubbling fluidized bed reactor. This model takes into account global reaction kinetics along with balances for mass and energy, and is capable of prediction of axial profiles of temperature; solid hold up and gas concentration. Simulation results with this model showed that gas release and mixing during pyrolysis step are critical parameters.
- Evans et al. [13] have modeled composition of syngas from a pressurized bubbling fluidized bed (PBFB) reactor using 1 dimensional kinetic calculation for combustion using Cantera. This model gives reasonable agreement with other combustion models such as MIT's soot model and Gas Research Institute GRI 3.0 mechanism, as well as experimental data from 5–TPD pilot scale gasifier operating at elevated pressure of 4.4 bar. The simulation results indicated that both product gas heating value and chemical energy efficiency increased with pressure of gasifier.
- Grana et al. [14] have developed a general mathematical model for fixed bed gasifier that addresses both transport phenomena and chemical kinetics of reactor at both macro– and micro (particle) scale. Pyrolysis of solid fuel is the first step in the reactor, followed by successive gas phase reactions.
- Sharma and Singh [15] have analyzed the energy and exergy of reduction zone in a downdraft biomass gasifier. The products leaving reduction zone have been modeled using equilibrium and kinetic models. The principal result of these simulations was identification of a critical char bed length for a given feedstock (in which all char generated during pyrolysis gets consumed). This bed length depends on residence time and reaction temperature in the reduction zone. For critical char bed length, the model would predict high calorific value gas indicating optimum reactor performance.

- Fermoso et al. [16] have investigated the thermal reactivity (under steam) of coal biomass blends. These blends showed gasification behavior similar to coal. The reactivity of chars during steam gasification was modeled using 3 $n^{th}$ order gas–solid models, viz. volumetric model, grain model and random pore model to determine the kinetic parameters of the model. Of these, the random pare model was the best fit for the data.
- Dong et al. [17] have done a CFD modeling of product gas (from biomass gasification) and coal co–firing in a 600MW boiler. Simulations results indicated that $NO_x$ emission reduced by ~ 50–70%, when the product gas was injected through the lowest layer burner. Simulation also indicated that convection heat transfer area should be increased or the co–firing ration of product gas should be decreased to keep boiler rated capacity.
- Dupont et al. [18] have analyzed the pyrolysis of biomass using dual approach of experiments coupled to kinetic modeling. The successive reactions between gas phase species have also been taken into account. The results of this study indicated that biomass particle size was a crucial parameter. For biomass particles of size < 0.4 mm, pyrolysis was finished with 30 cm of reaction length (with 75% gas release), while for particle of size > 1.1 mm, conversion was incomplete due to heat transfer limitation.
- Sheth and Babu [19] have used differential evolution approach for obtaining kinetics parameters in non–isothermal pyrolysis of biomass using two competing reactions giving gaseous volatiles and solid charcoal. They proposed four different models based on different possible relation of activity of biomass with normalized conversion. Among these models, the model in which rate of change of biomass reactivity (with normalized conversion) was considered as a function of activity itself gave the best agreement with experiment data.
- Simone et al. [20] have developed a procedure with both experimental and CFB modeling component to provide global kinetic parameters to large scale application of biomass fuels. The experiments in a drop tube reactor that simulates high heating rates and

low residence times at temperature range of 400–800°C have been coupled to CFD simulations. The kinetic parameters provided by this methodology are useful for modeling gasification process on macroscopic scale.

- Rodrigues et al. [21] have analyzed combined combustor gasifier unit processing solid waste of footware industries using kinetic and equilibrium models. Operational parameters of this unit was found to affect two major output parameters, viz. lower heating value of gas and cold gas efficiency.
- Pierucci and Ranzi [22] have analyzed the particle model for biomass gasifier using kinetic schemes for devolatilization and combustion, and also taking into basic heat and mass transfer aspects. A sensitivity analysis of inter and intraphase thermal resistance showed that overall external heat transfer coefficient was a crucial parameter affecting performance of gasifier.
- Roy et al. [23] have developed model for downdraft gasifier with two components, viz. chemical equilibrium in pyrolysis–oxidation zone and kinetics controlled chemical reactions in reduction zone. The char reactivity factor was taken as a manipulation parameter on the basis of experimental studies. Parametric study with equivalence ratio and moisture content of biomass indicated direct variation of the lower heating value (LHV) of producer gas with equivalence ratio (in the range 2–3.4) and indirect (inverse) variation of LHV with moisture content of biomass (in the range 0–40% w/w). Based on these simulations, Roy et al. have also identified an optimum divergence angle of the geometry of reduction of gasifier.
- Jaojaruek and Kumar [24] have developed a model for pyrolysis zone of a downdraft gasifier using finite computation method that takes into account heat and mass conservation. Kinetics of various chemical reactions were also taken into account. This model is capable of predicting the temperature profile, feedstock feed rate and composition of the pyrolysis gases generated for temperatures $\leq 800^0$C.

- Lu et al. [25] have developed an ODE – boundary value problem model for air–steam gasification of biomass in bubbling fluidized bed. The model has two phases, viz. bubble and emulsion, and chemical reactions occur in both of these. The model considers pyrolysis of biomass to be instantaneous. The kinetic component of model takes into account 8 chemical reactions among 5 species, viz. char, CO, $CO_2$, $H_2$, $H_2O$ and $CH_4$. With wood powder taken as the biomass feedstock, this model gives prediction of gasifier that is in reasonable agreement with experimental studies.
- Gao and Li [26] have modeled pyrolysis and reduction zone of a downdraft biomass gasifier using a combined model. Approach of Gao and Li (2008) is similar to other authors in that pyrolysis of biomass is assumed to be instantaneous and volatiles released in this section are assumed to crack into equivalent amount of CO, $CH_4$ and $H_2O$ .The coupled ODEs have been solved using Runga–Kutta method for pyrolysis zone and finite difference method for reduction zone. Two sets of simulations have been performed, one with a constant temperature of 1400 K at pyrolysis zone and the other with a heating rate of 25 K/min, yielded significantly different trends of species concentration.
- Sadhukhan et al. [27] have developed a kinetic model for co–pyrolysis of coal and biomass using thermo–gravimetric experiments. A parallel series kinetics model was proposed to predict the pyrolysis behavior of biomass, while pyrolysis of coal was described using a model similar to one reported in previous literature. The principal result of study of Sadhukhan et al. [27] was that no synergistic effect between coal and biomass was observed during gasification experiments.
- Gerun et al. [28] have performed 2–D simulations of oxidation zone in a 2–stage downdraft gasifier, which is crucial for cracking of tars. These simulations have brought out several crucial points of the tar cracking process as follows: 1. tertiary tars decompose by combustion; 2. the tar cracking process is influenced by pyrolysis gas composition; 3. the air

injector design is a crucial aspect of overall gasifier design as air velocity and air/fuel ratio affect the extent of tar decomposition. Authors have also indicated a critical air injection velocity of 34 m/s, which dramatically changes the flow pattern in the gasifier.

- Zhang et al. [29] have studied both experimental and theoretically the gasification reactivity of chars obtained from 14 different biomass. The experimental data was fitted with a semi–empirical model. The gasifier reactivity of char increased with increasing conversion. The random pore model was modified to fit the data. Potassium present in biomass char was found to have a catalytic effect on gasification kinetics and conversion.
- Nikoo and Mahipaney [30] have simulated an atmospheric fluidized bed gasifier using Aspen Plus. Four Aspen Plus reactor modules were coupled to external subroutine for hydrodynamics and reaction kinetics. Simulations indicated that rise in temperature increased both production of hydrogen and carbon conversion efficiency. Increase in steam–to–biomass ratio increased carbon monoxide production but reduced carbon conversion.
- Ratnadhariya and Channiwala [31] have proposed a 3–zone equilibrium and kinetic free model for biomass gasifier. The first zone considered in the model comprises of drying and pyrolysis. The second zone is the oxidation zone and third zone is the reduction zone. For each zone, the reaction stoichiometry, mass balance and heat (or energy) balance. The model can provide a range of optimum equivalence ratio and moisture content for woody biomass materials. In addition, the model also predicts maximum temperature in the oxidation zone of the gasifier, which is critically important parameters in gasifier design and operation. The principal merit of this model is that it is capable of handling wide operating range of equivalence ratio and moisture content in all 3 zones of gasifier.
- Sennecca [32] has compared and related the microstructure properties and intrinsic reactivities of 3 biomass, viz. pine seed shells, olive husk and wood chips under pyrolsis, combustion and gasification. These biomasses have quite different porosity structure, ash

structure and O/C, H/C elemental ratios. Of these biomass, olive husk turned out to be most reactive under pyrolysis, char gasification and combustion. This is followed by wood chips and pine seed shells. The high reactivity of olive husk was attributed to high mineral content in addition to accessible pore structure, which was also found to influence the change in reactivity of char with conversion. A single reaction kinetic model could describe the reactive processes for char combustion and gasification.

- Chaurasia and Kulkarni [33] have modeled pyrolysis of biomass particle with shrinking and non–shrinking approach. In this model biomass particle was assumed to have cylindrical geometry, the reaction kinetics is coupled to heat transfer using physically measurable parameters and thermal properties such as thermal conductivity, heat transfer coefficient, emissivity, reactor temperature and heat of reaction has been assessed. The most important variable was reaction temperature and exothermic reactions. The model is a useful tool for optimization of gasification and pyrolysis reactions.

- Radmanesh et al. [34] have developed a model for beech wood particle gasification in a bubbling fluidized bed gasifier and have validated it against experiments. This model comprises of hydrodynamics of solid and gas phases with reaction kinetics. The model also took into account freeboard and section of the gasifier, in which homogeneous reactions occur. The pyrolysis section of the gasifier was modeled using two kinetic models. The model gave good agreement with experimental results.

- Dupont et al. [35] have analyzed the relevance of the chemistry and physics of the steam gasification of biomass. Two independent reactions, viz. steam reforming of methane and water–gas shift reaction were taken into account. The former is kinetically controlled, while the latter is close to equilibrium under operating conditions 1073 K < T < 1273 K and 1 bar pressure. The size of biomass particle was a crucial parameter. For particles of size ≤ 500 µm, transformation had two successive steps, viz. biomass pyrolysis in which both chemistry

and heat transfer is relevant, and steam gasification of residue which is chemically controlled.

- Zhang et al. [36] have studied the kinetics of biomass pyrolysis with experiments and modeling. Thermal gravimetric analysis of different biomasses revealed pyrolysis data of biomass, which was fitted with a kinetic model. The kinetic parameters of biomass were related to biochemical constitution of biomass, and also the predominant pyrolysis mechanism.

- Rogel and Aguillon [37] have described a rigorous CFD model for gasification of pine wood pellets in a stratified downdraft gasifier, in which Eulerian conservation equation were solved for particle and gas phase components, velocities and specific enthalpies. This model accounts for diverse aspects of gasification process such as heating up of biomass, drying, primary pyrolysis of biomass, secondary pyrolysis of tar, homogeneous reaction and heterogeneous combustion / gasification reaction with particle size change. This CFD model can predict temperature profiles, gas composition, LHV of producer gas and carbon conversion efficiency as a function of operating parameters and feed properties.

- Jand et al. [38] have analyzed the thermodynamic limits and actual product yields and compositions in biomass gasification process. The method proposed by Jand et al. (2006) improves the predictive capability of equilibrium based calculation of fuel gas composition in high temperature gasification process. The two main steps of gasification process, viz. fast pyrolysis followed by slow (and non–equilibrium) conversion of char and methane have been taken into account, and input to the chemical equilibrium program is based on it. This new method can provide estimates of hydrogen and carbon monoxide yields, in addition to prediction of performance trends with operating parameters.

- Devi et al. [39] have developed a kinetic model for decomposition of naphthalene – a model tar in presence of product gas over pretreated olivine as a catalyst. The product gas composition was found to have strong influence on naphthalene decomposition kinetics. $H_2O$

and $CO_2$ have an enhancing effect, while $H_2$ has inhibitory effect. The kinetic parameters estimated with power law model revealed activation energy of 213 kJ/mol.

- Bain et al. [40] have studied kinetic deactivation of an alkali–promoted Ni–based/$Al_2O_3$ catalyst in temperature range of 775 to 875°C. The residual conversion of tar ranged from 96.6% at 875°C to 70.5% at 775°C, while conversion of methane (initially at 13% concentration) was 32%. The experimental results were correlated with first and second order catalytic deactivation models with residual activity. For reforming, the activation energies for first order models for various components were as follows: Ethane = 32 kJ/gmole, Tar + Benzene = 45 kJ/gmole, Benzene + Toluene = 8.9 kJ/gmole.
- Corella and Sanz [41] have developed a 1–D model for circulating fluidized bed biomass gasifier under steady state condition. This comprises of reaction network along with heat and mass balances and hydrodynamics. The model gives axial profile of tem different species of the producer gas along with temperatures.
- Corella et al. [42,43] have studied catalytic monolithic reactor for cleaning of hot biomass producer gas for tar elimination. The temperature range of the reactor was from 820°C – 956°C. Corella et al. [42] fitted a macro–kinetic model to determine kinetic constants used as indices of its activity. In the subsequent paper, Corella et al. [43] developed a model that has two zones, viz. gas–reheating and the monolith. The model took into account macro–kinetics of tar and $NH_3$ elimination, mass balances for tar and $NH_3$ and heat balances for monolith. Simulations of this model indicated external mass transfer (and not the temperature) in the channels of monolith reactor controls the overall process.
- Taralas and Kontominas [44] have developed kinetic models for catalytic steam cracking of toluene (model tar) in the temperature range of 923–1223 K. A commercial metal based catalyst NiMo/γ–$Al_2O_3$ was employed. The results with commercial catalyst were compared with pyrolysis in presence of basic non–metallic mineral additives such as

dolomitic magnesium oxide (MgO), low surface quicklime (CaO) and calcined dolomite ($CaMgO_2$). Swedish calcined Glanshammar dolomite significantly decreased the activation energy (E = 123 kJ/mol) of catalytic cracking of toluene as compared to the thermal cracking (E = 356 kJ/mol). Similarly, Norwegian dolomitic magnesium oxide showed higher catalytic decomposing activity than quicklime. Low surface quicklime (CaO) could be described by Langmuir–Hinshelwood type kinetic equation, in which single–site adsorption of toluene was the rate determining step.

- Liu and Gibbs [45] have developed a model for emission of ammonia ($NH_3$) and hydrogen cyanide (HCN) from a circulating fluidized bed biomass gasifier. The model has modules for devolatilization, tar cracking and a chemical reaction network (including nitrogen chemistry) with pine wood chips as model biomass. The solid concentration profile in the riser section was a manipulation or input parameter, and gaseous and solid phases were assumed to flow in plug flow manner. The predictions of this model on profiles of bed temperature, concentration of various species, and tar, $NH_3$ and HCN emissions during gasification generally agreed with the experimental data.
- Oliero et al. [46] have studied gasification of char generated from Orujillo (wood matter, which is residue from oil mill industry) and domestic biomass use at temperature range 800–950$^{o}$C and mixture of CO and $CO_2$ as gasification medium. The particle size of biomass was small so as to minimize heat and mass transfer resistances. CO had an inhibition effect on gasification of char with $CO_2$. Authors fitted the experimental data with two kinetic models, viz. $n^{th}$ order model and Langmuir–Hinshelwood model. The latter model was the best fit to the data.
- Correla et al. [47] have proposed two advanced kinetic models and reaction networks for catalytic decomposition of tar in a fluidized bed biomass gasifier. The first model provides evolution of mean and variance of molecular weight of tar with residence time of

gas. The second model comprises of six kinetics equations with 11 kinetic constants. This model allowed ranking of the species in tar accordingly to their reactivity.

- Corella et al. [48] have also proposed a simple micro–kinetic model for catalytic elimination of tar that considers tar components in the form of two lumps or groups depending on their reactivity. The decomposition of both lumps occurs by two mechanisms, viz. thermal and catalytic. 4 kinetic constants in the model are evaluated with experiments using two catalysts, viz. silica sand and a commercial nickel based steam reforming catalyst.
- Wurzenberger et al. [49] have presented a combined transient single particle and fuel–bed model for thermal conversion of biomass. Both fuel–bed and particle models are radially discretized (PDE) type models. Mass, momentum and energy balance are solved for the entire systems. The model comprise of two parts, viz. first part comprising of drying and pyrolysis and second part comprising of secondary tar cracking, homogeneous gas reactions and heterogeneous char reactions. The kinetic data for this model is borrowed from earlier/contemporary literature. Simulation results for single particle model were validated against experimental studies and good agreement was found.
- Fiaschi and Michelini [50] have developed a 1–D and biphasic mathematical model of biomass gasification kinetics in bubbling fluidized beds. The effect of mass transfer on reaction kinetics could be accounted for with this model –which has two phases, viz. bubble phase and dense phase. The model would predict temperature and concentration profile along reactor axis. Increase in reactor pressure, upto a limit determined by biomass composition, causes reduction in bubble diameter, as well as residence time in reactor. The reactor temperature was found to increase with pressure, but makes the reactions kinetically limited. Comparison between mass transfer and surface reactions kinetics effects show that former prevails at starting up of the gasification process, while second one dominates the process after stabilization of temperature.

- Schuster et al. [51] have studied decentralized combined heat and power station based on a dual fluidized bed steam gasifier, using thermodynamic equilibrium calculations. Wide parameter space, e.g. ultimate analysis and moisture content of fuel, temperature and steam/biomass ratio, was assessed. The influence of these parameters on quantity, composition and heating value of the producer gas was evaluated. The overall efficiency of the process was about ~ 20% (for a single process). The chemical efficiency of gasification was mainly a function of gasification temperature and fuel oxygen content.
- Pletka et al. [52] have developed mathematical model describing heat transfer and chemical reaction system for an indirectly heated biomass gasifier. This model is accurate within 13 K for both ballasted and un–ballasted case. The thermodynamic equilibrium model proved inadequate and under–predicted cooling time during pyrolysis phase by 50%. The model could be improved by substitution of measured product gas composition for calculated gas composition.
- Zainal et al. [53] have used equilibrium modeling to predict gasification process in a downdraft gasifier. The composition and calorific value of producer gas was determined using a stoichiometric model. Effect of factors such as moisture content of biomass and temperature of gasification on calorific value of producer gas was determined. An inverse variation of calorific value of producer gas with gasification temperature and moisture content of biomass was seen in the range of these parameters.
- Guo et al. [54] have developed an artificial neural network based model for simulation of gasification process. This model is applied for gasification of several types of biomass in a fluidized bed gasifier at atmospheric pressure, with steam as fluidizing medium. The gas compositions predicted by model are in consistence with experimental data. According to predictions of this model, gasification behavior of arboreal types of biomass is significantly different from that of herbaceous one.

- Groppi et al. [55] have done a mathematical modeling of the catalyst section of atmospheric pilot combustor fueled by gasified biomass. The 2–D model with circular channel geometry, accounting for axial conduction of heat in solid walls regarded as the most suitable model. Comparison of simulation data with experimental observation in 30 kW pilot facility revealed reasonable agreement. The role of kinetics of homogeneous as well as catalytic reaction in combustor performance was revealed by simulations. The palladium catalyst decomposed to PdO at high temperature, which reduced combustion of $CH_4$, providing a self–temperature control.
- Di Blasi [56] has formulated a mathematical model for biomass gasification in stratified co–current (downdraft) gasifier. The 1–D, unsteady state model combines several aspects of gasification such as heat and mass transfer across bed, moisture evaporation, biomass pyrolysis, char combustion & gasification and gas–phase combustion and thermal tar cracking. For high air to fuel ratio and pyrolysis rate, the gasification process is "top–stabilized" giving higher conversion and good gas quality. With reduction of air flow below critical value, the reaction front is grate stabilized. These two configurations were found to be influenced by gas phase combustion of volatile pyrolysis products. Thus, the model of Di Blasi is able to predict the effect of kinetic constants and operational variables on overall dynamics of gasification process, structure of reaction front and quality of producer gas.
- Coda Zabetta et al. [57] have studied reduction of nitrogen oxides in gas turbines combustor using chemical kinetic modeling under ideal flow conditions. The model system was gas turbines burning biomass–derived producer gas from an air–blown integrated gasification combined plant. The major results of this study are: (1) temperature in the range 900–1000$^{o}$C and high pressure of 10–20 bar favored $N_2$ formation, (2) for operation at atmospheric pressure, no of air addition stages increased conversion to $N_2$, (3) conversion of $NH_3$ to $N_2$ increased with inlet $NH_3$ concentration, (4) the main paths for fuel–$NH_3$ to $NO_x$

and $N_2$ conversion were through amino radicals or $H_2NO$ intermediate.

- Mansaray et al. [58,59] have reported mathematical modeling of fluidized bed rice husk gasifier in a series of two papers. Using ASPEN PLUS process simulator, two models (single compartment and 2–compartment) have been developed, which can simulate in a dual–distributor type fluidized bed rice husk gasifier for wide range of operating conditions. These models are based on material and energy balance, in addition to chemical equilibrium relations. The single compartment model does not take into account complex hydrodynamics of gasifier, and is based on overall carbon conversion only. The two compartment model takes into account both hydrodynamic and carbon conversion. In another study, Mansaray et al. [59] validated the model against experimental data with 3 values of parameters (bed height, fluidization velocity and equivalence ratio). The model could give reasonable prediction of temperature and product gas composition and heating value.
- Dong and Borgwardt [60] have used a thermobalance reactor to evaluate reactivity of poplar wood during gasification under conditions of 30 atm pressure and 800$^{o}$C temperature (typical of Hynol process). The gasification medium was hydrogen rich gas recycled from methanol synthesis. Gasification process involved rapid devolatilization and pyrolysis reaction of volatile matter in biomass, and slow reaction of residual carbon with process gas. Nearly 86% of 1/8" poplar particles and 90% of saw dust were converted to gas products by the gasification medium containing 66% of $H_2$ in 60 min. Gasification rate and biomass conversion was affected by reaction temperature and particle size of biomass. The conversion was proportional to partial pressure of $H_2$ and steam in the feed gas.
- The feasibility of gasification of coal–biomass mixtures, followed by combustion of resulting gas was assessed by Andries et al. [61] using 2–D model for gas turbine combustor. Standard k–ε model was used for describing the flow at combustor. The chemistry of the process was modeled by assumption of local chemical equilibrium. A probability distribution

function accounted for interaction of turbulence and chemistry. Predictions of this model of composition of producer gas resulting from gasification matched well with experimental observations.

- Aznar et al. [62] have proposed simple first order kinetic model for catalytic decomposition of tar using 8 different commercial catalysts. Main variables for the experiments underlying model were bed temperature, ($H_2O+O_2$)/biomass feed ratio, and time on stream. All catalysts meant for reforming of naphtha were active for tar removal and gas conditioning. 98% tar removal is easily obtained at space velocity of 14000 $h^{-1}$, and temperature range of 780–830$^{o}$C, with no deactivation of catalyst for 48–h on–stream.

In another paper, Delgado et al. [63] have reported use of calcined solids such as dolomite (MgO–CaO), pure calcite (CaO), pure magnesite (MgO) for upgrading of raw hot gas from bubbling fluidized bed reactor.

- Di Blasi [64] has constituted a detained transport model to predict the effects of various physical properties, viz. density, thermal conductivity, gas permeability and specific heat capacity of the biomass feedstock on the convective radiant pyrolysis of cellulosic fuels. In thermally thick regime, where intra particle heat transfer controls, variation in physical properties affects the activity of secondary reaction of tar vapors and conversion time. Most sensitive parameters are biomass density and char thermal conductivity. In thermal thin region, physical properties weakly affect the conversion time.

- Salaices et al. [65] have studied catalytic steam gasification of biomass with thermodynamic equilibrium models and experiments in a CREC riser simulator. This model is based on C, H, O elemental balances and various product species up to $C_6$ hydrocarbons. The model could assess the effects of biomass composition, temperature and steam on composition of producer gas. The most significant parameters affecting producer gas composition are temperature and steam/biomass ratio. The optimum values of these

parameters have been found to be 800°C and 0.5–0.7 g/g. Results of this study matched well with experimental data using Ni–$Al_2O_3$ catalyst. It is revealed that equilibration of chemical species in producer gas occurs for reaction times > 30 s. For reaction time < 10 s, non–equilibrium model was found to describe well performance of reactor.

- Coplan et al. [66] have modeled an integrated solid oxide fuel cell (SOFC) with biomass gasification. A heat transfer model is used for SOFC, and thermodynamic model is used for rest of the components. Effect of gasification agent, viz. air, enriched air and steam, is studied along with exergy balances for system components. Among the 3 gasification agents studied, steam provides highest electrical efficiency (41.8%), power–to–heat ratio (4.644), and exergetic efficiency (39.1%), but a rather low fuel utilization efficiency (50.8%). Exergy destruction was highest at gasifier for air and enriched oxygen as medium, and at heat exchanger (supplying heat to air entering SOFC) for steam as gasification medium.
- Li and Suzuki [67] have studied biomass pyrolysis process for producing $H_2$–rich producer gas using rigorous thermodynamic model. The proposed process comprises of a pyrolysis reactor connecting one oil cracking reactor, water gas reactor and gasifier. Effect of main operation parameter such as steam/biomass ratio and temperature (at pyrolysis reactor, oil thermal cracking and gasifier) on the composition of fuel gas and hydrogen yield. The results indicated that at optimal temperature of 800°C and steam to biomass ratio = 0.2, the hydrogen yield can reach 83 g/kg biomass with concentration of $H_2$ in the gas being 55 mol%.
- Roy et al. [68] have assessed feasibility of use of cow dung as supplementary fuel in a downdraft biomass gasifier. The pyrolysis (oxidation) zone is modeled with assumption of thermodynamic equilibrium, while the reduction zone modeled on the basis of kinetically controlled reduction reactions. Cow dung as a sole fuel was not feasible as the producer fuel gas resulting from it had very low heating value, with most of carbon leaving in char. Blends

of cow dung and saw dust could, however, be a feasible feedstock. For any equivalence ratio, overall yield as well as heating value of producer gas shows inverse relation with fraction of cow dung, resulting in net reduction in gasifier efficiency. Increase of cow dung fraction from 0 to 90% in blended fuel reduces heating value and conversion efficiency by 46.8% and 45% respectively. The optimal fraction of cow dung resulting in maximum fuel economy in blended fuel was found to be ~ 40–50% w/w.

- Mermelstein et al. [69] have reported experimental as well as simulation studies in assessment of impact of steam tars resulting in biomass gasification and nickel based SOFC anode material. Experiments were performed using 2 commercial Ni–based SOFC anode materials, viz. Ni/YSZ (yttria–stabilized zirconia, 60–40%) and Ni/CGO (Gd–droped ceria, 50–50%). The degree of carbon formation over these materials was assessed using steam reforming of 15 g/Nm$^3$ benzene as model tar. Addition of steam reduces carbon formation for both types of anode materials, with Ni/CGO showing slightly higher C–formation than Ni/YSZ. This could be a result of different Ni content of two materials, difference of activity of anode material towards tar reforming, and/or difference in surface area for each material. For steam to carbon (in biomass) ratio < 1, excessive carbon formation was seen. Tar conversion over Ni/YSZ material resulted in CO formation, while oxidation behavior of ceria in Ni/CGO material gave higher $CO_2$ concentration.

- Huang and Ramaswamy [70] have developed thermodynamic equilibrium models for biomass gasification, which could be applied to various types of gasifiers. These models could be used with or without incorporation of char as component. These models could be adjusted for internal fluid flow and heat & mass transfer characteristics, so as to simulate operation and performance of varying types of gasifiers.

- Spyrakis et al. [71] have done simulation studies of a process that combines an atmospheric and pressurized air blown gasifier with a Fischer–Tropsch reactor for

simultaneous generation of liquid transportation fuel as well as power. The process has 4 components, viz. gasifier, gas cleaning, gas conditioning and the FT reactor. The exergetic analysis of the process was assessed with or without recycle of tail gas. For 80% conversion of carbon monoxide in FT reactor without recycling of the unreacted or tail gas, the exergetic efficiency was 34.3% with atmospheric gasification and 30.64% for pressurized gasification. Recycling of the unreacted CO, $H_2$, in addition to light ends could enhance this efficiency to 48.1%.

- Lee et al. [72] have compared gasification driven direct carbon fuel cell with systems using separate gasification prior to fuel cell under auto–thermal condition using thermodynamic models. The latter system was found have lesser work output. For common solid fuels, both direct carbon fuel cells (DCFC) and indirect (or separate gasification) system gave conversion efficiency in the range of 51–58%. For direct systems, efficiency could be increased to 60% by increasing operating voltage and /or inclusion of bottoming cycle. The media of gasification, either steam or $CO_2$, yields producer gas that gives similar work output and thermal efficiency.

- Srinivas et al. [73] have done exergy analysis of a biomass gasifier for different biomass materials using a thermo–chemical model. A simplified numerical method is applied to solve thermo–chemical equilibrium reaction, so as to predict composition of producer gas. A pressurized circulating fluidized bed is considered as basis in the model. Effect of 3 parameters, viz. relative air fuel ratio, steam fuel ratio and gasifier pressure, was examined on gas composition, gasifier temperature, LHV of producer gas and exergy efficiency of biomass gasifier to obtain high yield from biomass. The LHV of producer gas as well as exergy efficiency of gasifier varied inversely with air fuel ratio and steam fuel ratio.

- Hau et al. [74] have analyzed gasification of solid waste for estimation of impurities in raw synthesis gas and the slag using thermodynamic equilibrium calculations and mass

balances. Several possible fates of the impurities in the feedstock were taken into account, i.e. impurity turning to oxide or chloride or remaining in its elemental form. The model can predict which impurities are formed and in which amounts as well as their distribution in raw synthesis gas and slag. This model is particularly useful for design of gas cleaning system and slag disposal method. The model could be applied to different waste materials including municipal solid waste mixed plastic waste, auto–shredder residue and biomass.

- Miccio Francesco et al. [75] have developed a model for a conceptual design of internal circulating fluidized bed (ICFB) biomass gasifier. This model is essentially combination of a thermodynamic sub–model with simplified lumped model for gasifier. For absolutely dry (water–free) gasification process, concentration of $H_2$ in the producer gas as high as 61% could be achieved. The major operational parameters affecting hydrogen yield were steam/fuel ratio and fuel moisture content.
- Proll and Hofbauer [76] have developed a steady state model for biomass gasification combining mass and energy balances with thermodynamic considerations. A dual fluidized bed biomass gasifier is considered as basis for model formulation. The model is used to simulate biomass gasification based plant for heat and power generation.
- Mahishi and Goswami [77] have studied optimization of biomass gasification process for hydrogen production using thermodynamic equilibrium model (Stanjan v3.932). Wood was used as model biomass. Effect of parameters such as temperature, pressure, steam biomass ratio and equivalence ratio on equilibrium production of biomass was studied along with energy consumption and thermodynamic efficiency. First–law thermodynamic analysis of gasifier revealed optimum condition for hydrogen production as: gasification temperature = 1000 K, steam/biomass ratio = 0.3 and equivalence ratio = 0.1. The simulation results matched with experimental data for high gas residence times and high gasification temperature.

- Melgar et al. [78] have developed a mathematical model for thermo–chemical process in a downdraft gasifier, which combines chemical and thermodynamic equilibrium of the global reactions in gasifier. This model can predict the final composition as well as temperature of the producer gas. The knowledge of composition of the producer gas enables calculations of range of parameters such as cold gas efficiency of gasifier, amount of dissociated water, lower heating value (LHV) and engine fuel quality of the producer gas. With different biomass types as fuel, Melgar et al. [78] have studied the effect of fuel/air ratio and moisture content of biomass on the producer gas. The maximum cold gas efficiency was obtained at relative fuel/air ratio between 2.5 and 5, and biomass moisture content less than 25%. At higher fuel/air ratio than these limits, the thermal sustainability of the process was lost. This model could be useful tool for optimization of design and operation of the process.
- Babu and Chaurasia [79] have proposed improved models for pyrolysis of biomass that include various facets of the pyrolysis process such as unsteady state 1–D heat conduction, convection and radiation, variable property model, volatiles and gas transport by diffusion and convection and momentum transport. Two submodels were added in a generalized reference model comprising of heat and momentum transfer equation and chemical kinetics model. A finite difference pure implicit scheme was employed for solution. Simulations were carried out for wide range of particle shape, size, temperature, conversion time and heat of reaction.
- Scott et al. [80] have employed a thermodynamic model based on Gibbs energy minimization to examine thermodynamic limits of performance of gasifier for biomass and other alternate fuels. Gibbs energy minimization allows assessment of large no of species (not available in kinetic models), and thus is useful for getting an insight into differences of behavior of coal and biomass in gasifier. Biomass differs from coal in terms of heating value, ash, volatile and carbon content and amount of elemental oxygen. Using dried sewage sludge

as model biomass, Scott et al. [80] have explored following aspects of co–gasification of coal and biomass: (1) product gas composition, (2) impact of process variables on heat balance, (3) effect of various gasification agents, and (4) optimization of the calorific value of hot and cold product gas. For low calorific value biomass fuels such as dried sewage sludge, co–gasification with support fuel such as coal is found to be a practical solution in this study.

- Khadase et al. [81] have performed equilibrium calculations for gasification of four Indian biomasses (viz. saw dust, bagasse, subabul and rice husk) using a stoichiometric equilibrium model and comparison of the calorific value of gas obtained at different gasifying conditions with different biomass feedstock was made. The calorific value of producer gas was found to increase with temperature till 1100 K and remain constant thereafter. The highest calorific value was obtained at air ratio of 0.1 and steam/air ratio of 0.8. The calorific value of gas resulting from bagasse was the highest and that from subabul was the lowest.
- Kersten [82] has developed "quasi" equilibrium model for biomass gasification based on introduction of equilibrium temperatures that are different than actual process temperatures in thermodynamic calculations. This model is an extension of earlier model by Gumz [5], in which a "quasi" equilibrium temperature in introduced for all reactions. Bacon [83] improved the model of Gumz [5] by allowing introduction of "quasi" equilibrium temperature independently for each reaction. Kersten's model is further extension of this model, which could be applied to both homogeneous and heterogeneous reactions. The model has been applied to 8 circulating fluidized bed reactors, 3 bubbling bed reactors and 3 downdraft reactors. It is revealed that for certain gasifier types, single set of quasi–equilibrium temperature is able to predict quantitative results of gasification. For other reactors, the equilibrium model needs to be coupled to empirical relation for the hydrocarbon fraction in the producer gas and carbon conversion.
- In another study, Kersten [82] has done simulations of flow in the riser section of

CFB gasifier with internal gas production. A 2–D continuum fluid dynamics model using kinetic theory of granular flow was applied to predict the flow structure in the riser. The increase in gas velocity was included in the model via a lumped gas production source term in the continuity equation of the gas phase, assuming that gas is produced only in the bottom part of the riser, and volumetric production rate of gas was uniform. The model can predict radial solids segregation and radial profiles of axial velocities. It is revealed that normalized radial distribution of axial velocity does not vary with axial position, even at the bottom zone of the riser where gas production occurs.

- Bharadwaj [84] has coupled the experimental studies on rice husk pyrolysis to the simulations of STANJAN program based on element potential method (Reynolds [85]) for prediction of composition of resulting gas. SEM observations of rice husk by Bharadwaj [84] revealed that structure of rice husk was similar to that of composite material with silica fiber constituting the strong phase and the matrix consisting of lignin. After exposure to high temperature in pyrolysis, the silica fiber remains unaffected, while large numbers of pores appear in the matrix. These are geometrically arranged and are indication of the preferential consumption of matrix material by gasification. These also indicate that char combustion is a sluggish process and some carbon in rice husk is always left as residue after gasification.
- Li et al. [86] have proposed an equilibrium model for circulating fluidized bed coal gasifier. This model employs RAND algorithm of Gibbs energy minimization (Smith and Missen [87]). They found that product gas composition and heating value varies mainly with temperature and relative abundance of the key elements in biomass, viz. C, H, N and O. Pressure of the system was found to influence the process only in limited temperature range. The model predicted onset of formation of solid carbon where the gas composition becomes insensitive to additional carbon. Li et al. [86] have also combined their equilibrium model with kinetic models, where the carbon conversion in equilibrium conversion would be fixed

according to the predictions of kinetic model. With this, the equilibrium model gives better prediction of the gas composition that matches closely with experimental data.

- Altafini et al. [88] have done simulations of wood waste (saw dust) gasifiers using equilibrium model based on Gibbs energy minimization. The model biomass feedstock was Pinus Elliotis saw dust and the influence of moisture content of feedstock on composition and heating value of producer gas was assessed. Altafini et al. [88] found that the equilibrium model do not account very well for reactions occurring at relatively high temperature (> 800$^{o}$C), although these models were useful to show the tendencies of gasifier performance with respect to working parameters of gasifier.
- Brown et al. [88a] have combined a stoichiometric equilibrium model for biomass gasification with artificial neural network (ANN) regressions. In this, the neural network relates temperature differences to fuel composition and gasifier operating conditions. The results of analysis for atmospheric air gasification of fluidized bed reactor indicate that temperature difference for reaction relating to equilibrium of major gas species could be constant. On the other hand, temperature differences for char, light hydrocarbon and tar formation reaction are more strongly correlated to changes in operating conditions.

## 3.4 INFERENCE AND JUSTIFICATION OF PRESENT THESIS

Literature review presented above shows that modeling of biomass gasification is an immensely active research area. We would like to refer the reader to several state–of–the–art reviews for greater details on literature (Shand and Bridgwater [89], Gururajan et al. [90], Nemtsov and Zabaniotou [91], Prakash and Karunanithi [92]; Puig–Aranavat et al. [93]). There are two approaches for the modeling and optimization of biomass gasifiers, viz. kinetic and equilibrium. Kinetic models take into account the rate expressions for various simultaneous and parallel reactions occurring in the gasifier. Although kinetic models are

physically more realistic, and several authors have given elaborate reaction schemes with rate constants for gasification process (for example Souza-Santos [94] and Corella and Sanz [41]), broad applicability of these models is limited due to several constraints. In the first place, the reaction schemes may not take into consideration all possible reactions occurring in gasification process. There is some discrepancy in the kinetic constants (for same reaction) reported by different authors. In addition, these models contain parameters related to the design of the gasifier. Any error in estimation/measurement of these parameters may lead to significant error in predictions of producer gas composition made by the model. Moreover, this feature often renders the kinetic model system specific. Moreover, not all possible chemical reaction might have been studied. The equilibrium models on the other hand, are more convenient as the input data required for them (Gibbs free energy, enthalpy of formation, heat capacity) is easily available. Moreover, these models predict the limiting (maximum) performance of the gasifier for given range of temperature, air or equivalence ratio and pressure. Due to these merits, it is always possible to find "parameters spaces" or "niche areas" in the practical operating range of the gasifier, where improvement can be made. The major limitation of these models is that actual performance of gasifier (in terms of composition and quality of producer gas) may deviate from that predicted by the model. But overall trend in results (such as molar composition of producer gas and its HHV) with respect to values of operating parameters stay essentially unchanged. Therefore, the equilibrium models form qualitative guidelines for the design, optimization and improvement of the gasification process.

### 3.4.1 Stoichiometric and non–stoichiometric models

The equilibrium models are sub–categorized as stoichiometric and non–stoichiometric models. The stoichiometric models take into consideration various reactions in the gasification process and their equilibrium constants. The non–stoichiometric models are

based on technique of Gibbs free energy minimization to predict the equilibrium composition of the species resulting from the reaction between gasifying medium and biomass. Comparing among the two approaches, we find that stoichiometric models suffer from some limitations as the kinetic models that equilibrium constant for all reactions may not be available. Secondly, the valid range of temperature and pressure for the equilibrium constant may be limited, which restricts scanning of extensive parameter space for operation of the gasifier. Non–stoichiometric models, on the other hand, have several distinct advantages such as ease in handling of feed streams with unknown molecular formula and unknown chemical species. The input to the mathematical model is given in terms of element vector, which could be determined from the ultimate analysis of biomass and given air or equivalence ratio.

Although the literature in area of modeling of biomass gasification modeling is rather voluminous, most of the published studies have employed either equilibrium stoichiometric models or kinetic models. Both equilibrium stoichiometric models and kinetic models suffer from several limitations, which strongly confine their use for design and optimization of gasifiers utilizing variety of biomasses. On the other hand, literature on non–stoichiometric models is quite limited. It is evident from the literature that overall performance of the gasifier is a strong function of several parameters such as biomass feedstock, air/fuel ratio, temperature of gasification and gasification media. In the present thesis, an attempt is made to give an extensive and in–depth analysis of the influence of these crucial parameters on gasifier performance using a rigorous non–stoichiometric equilibrium and semi–equilibrium thermodynamic model. In addition, we have also presented a comparative analysis of the three types models, viz. equilibrium, semi–equilibrium and kinetic, for biomass gasification. Moreover, most of the studies in literature attempt to optimize the gasifier for thermal applications (i.e. generation of heat or electricity or both). Little effort is dedicated to optimize the gasifier performance in view of downstream processing of the producer gas for

liquid fuel production. This thesis also attempts to address this issue and presents an analysis based on the results of equilibrium and semi–equilibrium non–stoichiometric model.

## REFERENCES

[1] Cousins WJ. A theoretical study of wood gasification processes. New Zealand Journal of Science 1978;21(2):175–183.

[2] Denn MM, Yu W–C, Wei J. Parameter sensitivity and kinetics–free modeling of moving bed coal gasifiers. Industrial and Engineering Chemistry Fundamentals 1979;18(3):286–288.

[3] Desrosiers R. Thermodynamics of gas–char reactions. In: A Survey of Biomass Gasification. SERI/TR–33–239, 1979.

[4] Kosky PG, Floess JK. Global model of countercurrent coal gasifiers. Industrial and Engineering Chemistry Process Design and Development 1980;19(4):586–592.

[5] Gumz W. Gas Producers and Blast Furnaces: Theory and Methods of Calculations. Wiley:New York, 1950.

[5a] Shesh KK, Sunawala PD. Thermodynamics of pressurized air–steam gasification of biomass. Indian Journal of Technology 1990;28(4):133–138.

[6] Kovacik G, Oguztoreli M, Chambers A, Ozum B. Equilibrium calculations in coal gasification. International Journal of Hydrogen Energy 1990;15(2):125–131.

[7] Kinoshita CM, Wang Y, Takahashi PK. Chemical equilibrium computations for gasification of biomass to produce methanol. Energy Sources 1991;13(3):361–368.

[8] Watkinson AP, Lucas JP, Lim CJ. A prediction of performance of commercial coal gasifiers. Fuel 1991;70:519–527.

[9] Garcia EY, Laborde MA. Hydrogen production by steam reforming of ethanol:

thermodynamic analysis. International Journal of Hydrogen Energy 1991;16(5):307–312.

[10] Wang Y, Kinoshita CM. Kinetic model of biomass gasification. Solar Energy 1993;51(1):19–25.

[11] Alderucci V. Thermodynamic analysis of SOFC fueled by biomass derived gas. International Journal of Hydrogen Energy 1994;19(4):369–376.

[12] Kaushal P, Abedi J, Mahinpey N. A comprehensive mathematical model for biomass gasification in a bubbling fluidized bed reactor. Fuel 2010;89(12):3650–3661.

[13]. Evans P, Paskach T, Reardon J. Detailed kinetic modeling to predict syngas composition from biomass gasification in a PBFB reactor. Environmental Progress & Sustainable Energy 2010;29(2):184–192.

[14]. Grana R, Sommariva S, Maffei T, Cuoci A, Faravelli T, Frassoldati A, Pierucci S, Ranzi E. Detailed kinetics in the mathematical model of fixed bed gasifiers. Computer–Aided Chemical Engineering 2010;28(20th Eur. Symp. Computer Aided Process Eng., 2010):829–834.

[15]. Sharma AK, Singh RK. Energy and exergy analysis of the teduction zone in a downdraft (biomass) gasifier. International Journal of Chemical Reactor Engineering 2010;8.

[16]. Fermoso J, Gil MV, Pevida C, Pis JJ, Rubiera F. Kinetic models comparison for non–isothermal steam gasification of coal–biomass blend chars. Chemical Engineering Journal (Amsterdam, Netherlands) 2010;161(1–2):276–284.

[17]. Dong C–Q, Yang Y–P, Yang R, Zhang J–J. Numerical modeling based of the gasification biomass co–firing in a 600 MW pulverized coal boiler. Applied Energy 2010;87(9):2834–2838.

[18]. Dupont C, Chen L, Cances J, Commandre J–M, Cuoci A, Pierucci S, Ranzi E. Biomass pyrolysis: Kinetic modelling and experimental validation under high temperature and flash heating rate conditions. Journal of Analytical and Applied Pyrolysis 2009;85(1–

2):260–267.

[19]. Sheth PN, Babu, BV. Differential evolution approach for obtaining kinetic parameters in nonisothermal pyrolysis of biomass. Materials and Manufacturing Processes 2009;24(1):47–52.

[20]. Simone M, Biagini E, Galletti C, Tognotti L. Evaluation of global biomass devolatilization kinetics in a drop tube reactor with CFD aided experiments. Fuel 2009;88(10):1818–1827.

[21]. Rodrigues R, Secchi AR, Marcilio NR, Godinho M. Modeling of biomass gasification applied to a combined gasifier–combustor unit: equilibrium and kinetic approaches. Computer–Aided Chemical Engineering 2009;27A (10th Int. Symp. Process Syst. Eng.): 657–662.

[22]. Pierucci S, Ranzi E. Modelling biomass gasifiers. Computer–Aided Chemical Engineering 2009;26(19th Eur. Symp. Comp. Aided Process Eng.):797–802.

[23]. Roy PC, Datta A, Chakraborty N. Modelling of a downdraft biomass gasifier with finite rate kinetics in the reduction zone. International Journal of Energy Research 2009;33(9):833–851.

[24]. Jaojaruek K, Kumar S. Numerical simulation of the pyrolysis zone in a downdraft gasification process. Bioresource Technology 2009;100(23):6052–6058.

[25]. Lu P, Kong X, Wu C, Yuan Z, Ma L, Chang J. Modeling and simulation of biomass air–steam gasification in a fluidized bed. Frontiers of Chemical Engineering in China 2008;2(2):209–213.

[26]. Gao N, Li A. Modeling and simulation of combined pyrolysis and reduction zone for a downdraft biomass gasifier. Energy Conversion and Management 2008;49(12):3483–3490.

[27]. Sadhukhan AK, Gupta P, Goyal T, Saha RK. Modelling of pyrolysis of coal–biomass blends using thermogravimetric analysis. Bioresource Technology 2008;99(17):8022–8026.

[28]. Gerun L, Paraschiv M, Vijeu R, Bellettre J, Tazerout M, Gobel B, Henriksen U. Numerical investigation of the partial oxidation in a two–stage downdraft gasifier. Fuel 2008;87(7):1383–1393.

[29]. Zhang Y, Ashizawa M, Kajitani S, Miura K. Proposal of a semi–empirical kinetic model to reconcile with gasification reactivity profiles of biomass chars. Fuel 2008;87(4–5):475–481.

[30]. Nikoo MB, Mahinpey N. Simulation of biomass gasification in fluidized bed reactor using ASPEN PLUS. Biomass and Bioenergy 2008;32(12):1245–1254.

[31]. Ratnadhariya JK, Channiwala SA. Three zone equilibrium and kinetic free modeling of biomass gasifier – a novel approach. Renewable Energy 2009;34(4):1050–1058.

[32]. Senneca O. Kinetics of pyrolysis, combustion and gasification of three biomass fuels. Fuel Processing Technology 2007;88(1),87–97.

[33]. Chaurasia AS, Kulkarni BD. Most sensitive parameters in pyrolysis of shrinking biomass particle. Energy Conversion and Management 2007;48(3):836–849.

[34]. Radmanesh R, Chaouki J, Guy C. Biomass gasification in a bubbling fluidized bed reactor: experiments and modeling. AIChE Journal 2006;52(12):4258–4272.

[35]. Dupont C, Boissonnet G, Seiler J–M, Gauthier P, Schweich D. Study about the kinetic processes of biomass steam gasification. Fuel 2007;86(1–2):32–40.

[36]. Zhang X, Xu M, Sun R, Sun L. Study on biomass pyrolysis kinetics. Journal of Engineering for Gas Turbines and Power 2006;128(3):493–496.

[37]. Rogel A, Aguillon J. The 2D Eulerian approach of entrained flow and temperature in a biomass stratified downdraft gasifier. American Journal of Applied Sciences 2006;3(10):2068–2075.

[38]. Jand N, Brandani V, Foscolo PU. Thermodynamic limits and actual product yields and compositions in biomass gasification processes. Industrial & Engineering Chemistry

Research 2006;45(2):834–843.

[39]. Devi L, Ptasinski KJ, Janssen FJJG.. Decomposition of naphthalene as a biomass tar over pretreated olivine: effect of gas composition, kinetic approach, and reaction scheme. Industrial & Engineering Chemistry Research 2005;44(24):9096–9104.

[40]. Bain RL, Dayton DC, Carpenter DL, Czernik SR, Feik CJ, French RJ, Magrini–Bair KA, Phillips SD. Evaluation of catalyst deactivation during catalytic steam reforming of biomass–derived syngas. Industrial & Engineering Chemistry Research 2005;44(21):7945–7956.

[41]. Corella J, Sanz A. Modeling circulating fluidized bed biomass gasifiers. A pseudo–rigorous model for stationary state. Fuel Processing Technology 2005;86(9):1021–1053.

[42]. Corella J, Toledo JM, Padilla R. Catalytic hot gas cleaning with monoliths in biomass gasification in fluidized beds. 1. Their effectiveness in tar elimination. Industrial and Engineering Chemistry Research 2004;43(10):2433–2445.

[43]. Corella J, Toledo JM, Padilla R. Catalytic hot gas cleaning with monoliths in biomass gasification in fluidized beds. 2. Modeling of the monolithic reactor. Industrial and Engineering Chemistry Research 2004;43(26):8207–8216.

[44]. Taralas G, Kontominas MG. Kinetic modelling of VOC catalytic steam pyrolysis for tar abatement phenomena in gasification/pyrolysis technologies. Fuel 2004;83(9):1235–1245.

[45]. Liu H, Gibbs BM. Modeling of $NH_3$ and HCN emissions from biomass CFB gasifiers. Proceedings of the 17$^{th}$ International Conference on Fluidized Bed Combustion 2003;547–561. (Liu H, Gibbs BM. Modeling $NH_3$ and HCN emissions from biomass circulating fluidized bed gasifiers. Fuel 2003;82:1591–1604)

[46]. Ollero P, Serrera A, Arjona R, Alcantarilla S. The $CO_2$ gasification kinetics of olive residue. Biomass and Bioenergy 2003;24(2):151–161.

[47]. Corella, J, Caballero MA, Aznar M–P, Brage C. Two advanced models for the

kinetics of the variation of the tar composition in its catalytic elimination in biomass gasification. Industrial & Engineering Chemistry Research 2003;42(13):3001–3011.

[48]. Corella J, Toledo JM, Aznar, M–P. Improving the modeling of the kinetics of the catalytic tar elimination in biomass gasification. Industrial & Engineering Chemistry Research 2002;41(14):3351–3356. (Corella J, Toledo JM, Aznar M–P. Improving the modelling of the kinetics of the catalytic tar elimination in biomass gasification. VTT Symposium 2002;222:313–332.)

[49]. Wurzenberger JC, Wallner S, Raupenstrauch H, Khinast JG. Thermal conversion of biomass: comprehensive reactor and particle modeling. AIChE Journal 2002;48(10):2398–2411.

[50]. Fiaschi D, Michelini M. A two–phase one–dimensional biomass gasification kinetics model. Biomass and Bioenergy 2001;21(2):121–132.

[51]. Schuster G, Loffler G, Weigl K, Hofbauer H. Biomass steam gasification – an extensive parametric modeling study. Bioresource Technology 2001;77(1):71–79.

[52]. Pletka R, Brown RC, Smeenk J. Indirectly heated biomass gasification using a latent heat ballast. Part 2: modeling. Biomass and Bioenergy 2001;20(4):307–315.

[53]. Zainal, ZA, Ali R, Lean CH, Seetharamu KN. Prediction of performance of a downdraft gasifier using equilibrium modeling for different biomass materials. Energy Conversion and Management 2001;42(12):1499–1515.

[54]. Guo B, Li D, Cheng C, Lu Z–A, Shen Y. Simulation of biomass gasification with a hybrid neural network model. Bioresource Technology 2001;76(2):77–83.

[55]. Groppi G, Tronconi E, Berg M, Forzatti Pio. Development and application of mathematical models of pilot–scale catalytic combustors fueled by gasified biomasses. Industrial & Engineering Chemistry Research 2000;39(11):4106–4113.

[56]. Blasi CD. Dynamic behavior of stratified downdraft gasifiers. Chemical Engineering

Science 2000;55(15):2931–2944.

[57]. Coda Zabetta E, Kilpinen P, Hupa M, Stahl K, Leppaelahti J, Cannon M, Nieminen J. Kinetic modeling study on the potential of staged combustion in gas turbines for the reduction of nitrogen oxide emissions from biomass IGCC plants. Energy & Fuels 2000;14(4):751–761.

[58]. Mansaray KG, Al–Taweel AM, Ghaly AE, Hamdullahpur F, Ugursal VI. Mathematical modeling of a fluidized bed rice husk gasifier: part I – model development. Energy Sources 2000;22(1):83–98.

[59]. Mansaray KG, Ghaly AE, Al–Taweel AM, Ugursal VI, Hamdullahpur F. Mathematical modeling of a fluidized bed rice husk gasifier: part II – model verification. Energy Sources 2000;22(3):281–296.

[60]. Dong Y, Borgwardt RH. Biomass reactivity in gasification by the hynol process. Energy & Fuels 1998;12(3):479–484.

[61]. Andries J, Hoppesteyn PDJ, Hein KRG. Combustion of biomass–derived, low calorific value, fuel gas in a gas turbine combustor. DGMK Tagungsbericht 1998;9802(Beitraege zur DGMK–Fachbereichstagung "Energetische und Stoffliche Nutzung von Abfaellen und Nachwachsenden Rohstoffen", 1998):21–28.

[62]. Aznar MP, Caballero MA, Gil J, Martin JA, Corella J. Commercial steam reforming catalysts to improve biomass gasification with steam–oxygen mixtures. 2. Catalytic tar removal. Industrial & Engineering Chemistry Research 1998;37(7):2668–2680.

[63]. Delgado J, Aznar MP, Corella J. Biomass gasification with steam in fluidized bed: Effectiveness of CaO, MgO, and CaO–MgO for hot raw gas cleaning. Industrial & Engineering Chemistry Research 1997;36(5):1535–1543.

[64]. Di Blasi, C. Influences of physical properties on biomass devolatilization characteristics. Fuel 1997;76(10):957–964.

[65]. Salaices E, Serrano B, de Lasa H. Biomass catalytic steam gasification thermodynamic analysis and reaction experiments in a riser simulator. Industrial and Engineering Chemistry Research 2010;49(15):6834–6844.

[66]. Colpan CO, Hamdullahpur F, Dincer I, Yoo Y. Effect of gasification agent on the performance of solid oxide fuel cell and biomass gasification systems. International Journal of Hydrogen Energy 2010;35(10):5001–5009.

[67]. Li C, Suzuki K. Process design and simulation of $H_2$–rich gases production from biomass pyrolysis process. Bioresource Technology 2010;101:S86–S90.

[68]. Roy PC, Datta A, Chakraborty N. Assessment of cow dung as a supplementary fuel in a downdraft biomass gasifier. Renewable Energy 2010;35(2):379–386.

[69]. Mermelstein J, Brandon N, Millan M. Impact of steam on the interaction between biomass gasification tars and nickel–based solid oxide fuel cell anode materials. Energy and Fuels 2009;23(10):5042–5048.

[70]. Huang H–J, Ramaswamy S. Modeling biomass gasification using thermodynamic equilibrium approach. Applied Biochemistry and Biotechnology 2009;154(1–3):193–204.

[71]. Spyrakis S, Panopoulos KD, Kakaras E. Synthesis, modeling and exergy analysis of atmospheric air blown biomass gasification for Fischer–Tropsch process. International Journal of Thermodynamics 2009;12(4):187–192.

[72]. Lee AC, Mitchell RE, Gur TM. Thermodynamic analysis of gasification–driven direct carbon fuel cells. Journal of Power Sources 2009;194(2):774–785.

[73]. Srinivas T, Gupta AVSSKS, Reddy BV. Thermodynamic Equilibrium Model and Exergy Analysis of a Biomass Gasifier. Journal of Energy Resources and Technology 2009;131(3):031801/1–031801/7.

[74]. Hau JL, Ray R, Thorpe RB, Azapagic A. A thermodynamic model of the outputs of gasification of solid waste. International Journal of Chemical Reactor Engineering 2008;6.

[75]. Miccio F, Svoboda K, Schosger J–P, Baxter D. Biomass gasification in internal circulating fluidized beds: a thermodynamic predictive tool. Korean Journal of Chemical Engineering 2008;25(4):721–726.

[76]. Proll T, Hofbauer H. Development and application of a simulation tool for biomass gasification based processes. International Journal of Chemical Reactor Engineering 2008;6.

[77]. Mahishi MR, Goswami DY. Thermodynamic optimization of biomass gasifier for hydrogen production. International Journal of Hydrogen Energy 2007;32(16):3831–3840.

[78]. Melgar A, Perez JF, Laget H, Horillo A. Thermochemical equilibrium modelling of a gasifying process. Energy Conversion and Management 2007;48(1):59–67.

[79]. Babu BV, Chaurasia AS. Pyrolysis of biomass: improved models for simultaneous kinetics and transport of heat, mass and momentum. Energy Conversion and Management 2004;45(9–10):1297–1327.

[80]. Scott SA, Harris AT, Dennis JS, Hayhurst AN, Davidson, JF. Gasification of biomass: the consequences of equilibrium. Proc. 17th Int. Conf. Fluidized Bed Combust. 2003, pp. 819–831.

[81]. Khadase A, Parulekar P, Aghalayam P, Ganesh A. Equilibrium model for biomass gasification. Proceedings of AER – 2006 (I.I.T. Bombay, Mumbai), pp. 106–112, 2006.

[82]. Kersten SRA. Biomass Gasification in Circulating Fluidized Beds. Ph.D. Dissertation, University of Twente, Twente University Press: Enschede, 2002.

[83]. Bacon DW, Downie T, Hsu TC, Peters J. Modeling of fluidized bed wood gasifiers. In: Fundamentals of Thermochemical Biomass Conversion (RP Overend, TA Milne, LK Mudge, Ed.), Elsevier Applied Science Publishers: Amsterdam, 1982.

[84]. Bharadwaj, A. Gasification and combustion technologies of agro–residues and their application to rural electric power systems in India. Ph.D. Dissertation, Carnegie Mellon University, Pittsburgh, PA (USA); 2002.

[85]. Reynolds WC. The element potential method for chemical equilibrium analysis: Implementation in the interactive program STANJAN. Technical Report, Stanford University, Stanford, 1986. 48 pp.

[86]. Li X, Grace JR, Watkinson AP, Lim CJ, Ergudenler A. Equilibrium modeling of gasification: a free energy minimization approach and its application to a circulating fluidized bed coal gasifier. Fuel 2001;80:195–207.

[87]. Smith WR, Missen RW. Chemical Reaction Equilibrium Analysis: Theory and Algorithms. New York: Wiley, 1982.

[88]. Altafini CR, Wander PR, Barreto RM. Prediction of working parameters of a wood waste gasifier through an equilibrium model. Energy Conversion and Management 2003;44:2763–2777.

[88a]. Brown DWM, Fuchino T, Marechal FMA. Stoichiometric equilibrium modeling of biomass gasification: Validation of artificial neural network temperature difference parameter regression. Journal of Chemical Engineering Japan 2007;40(3):244–254.

[89]. Shand RN, Bridgwater AV. Fuel gas from biomass: status and new modeling approaches. In: Thermochemical Processing of Biomass (Ed. AV Bridgwater), London: Butterworths; 1984, pp. 229–254.

[90]. Gururajan VS, Agrawal PK, Agnew JB. Mathematical modeling of fluidized bed coal gasifiers. Transactions of Institution of Chemical Engineers 1992;70:211–238.

[91]. Nemtsov DA, Zabaniotou. Mathematical modeling and simulation approaches of agricultural residues air gasification in a bubbling fluidized bed reactor. Chemical Engineering Journal 2008;143:10–31.

[92]. Prakash N, Karunanithi T. Advances in modeling and simulation of biomass pyrolysis. Asian Journal of Scientific Research 2009;2(1):1–27.

[93]. Puig–Arnavat M, Bruno JC, Coronas, A. Review and analysis of biomass gasification

models. Renewable and Sustainable Energy Reviews 2010;14(9):2841–2851.

[94]. de Souza-Santos ML. Solid Fuels Combustion and Gasification: Modeling, Simulations and Equipment Operation. New York: Marcel Dekker; 2004.

भारतीय प्रौद्योगिकी संस्थान गुवाहाटी
Indian Institute of Technology Guwahati

CHAPTER 4

# Thermodynamic Optimization of Biomass Gasification with Equilibrium Model

## 4.1 INTRODUCTION

As outlined in the previous chapters, two potential applications of producer gas resulting from biomass gasification are: (1) decentralized power generation through dual fuel or 100% producer gas engine-generator sets; (2) feedstock for Fischer-Tropsch synthesis for production of synthetic diesel / gasoline. Taking into consideration these two possible outlets for producer gas obtained from biomass gasification, it is necessary to find optimum operating conditions in terms of temperature, air ratio (or equivalence ratio) and composition of gasifying medium. It must be noted, however, that the desired characteristics of producer gas for two applications, viz. power generation and FT synthesis, is different. In the former case, we have to find conditions under which the producer gas has maximum HHV, while in the latter situation, the $H_2$/CO ratio (along with actual content of hydrogen and carbon monoxide in terms of moles) is important. It is not necessary, however, that both of these conditions are met for same operating conditions.

In this chapter, we have addressed the issue of optimization of biomass gasifier for the above two applications.

As mentioned in Chapter 3, there are two approaches for the modeling and optimization of biomass gasifiers, viz. kinetic and equilibrium. Although physically more realistic, the kinetic models suffer from several limitations that restrict their wide applicability. The equilibrium models on the other hand, are more convenient. Moreover, these models predict the limiting (maximum) performance of the gasifier for given range of temperature, air or equivalence ratio and pressure. Although actual performance of gasifier may deviate from that predicted by the model, overall trends in molar composition and HHV of the producer gas with respect to values of operating parameters are well captured by these models. The equilibrium models are sub–categorized as stoichiometric and non–stoichiometric models. The merits and limitations of these models have also been compared in Chapter 3. For a process such as biomass gasification, non-stoichiometric models are more appropriate choice (as compared to stoichiometric models) due to their versatility in handling of feed streams with unknown molecular formula and unknown chemical species. The input to the mathematical model is given in terms of element vector, which could be determined from the ultimate analysis of biomass and given air or equivalence ratio.

In the present study, we have adopted approach of determining the equilibrium composition of the producer gas resulting from gasification of three principal biomasses found in northeastern part of India, viz. rice husk, bamboo dust and saw dust. For this purpose, we have used the software FACTSAGE [1] that employs the non–stoichiometric model, SOLGASMIX, proposed by [2]. In subsequent section, we have given the essential equations and solution algorithm of the model.

## 4.2 THE THERMODYNAMIC MODEL

For determination of the optimum conditions for the gasification process, we have adopted the approach of determining the equilibrium composition of the producer gas using the software FACTSAGE (FactWeb, http://www. factsage.com). This software employs the model SOLGASMIX proposed by Eriksson in 1975. For the convenience of the reader, we describe in this section, the essential equations and algorithm of the SOLGASMIX model. For greater details, we refer the readers to the original paper (Eriksson [2]). Various notations used in the model have been explained at the end of this section.

SOLGASMIX adopts an iterative procedure for calculating an equilibrium composition, i.e. the non–negative set of mole numbers of the species at equilibrium that could result out of the reactant species (or set of elements with predetermined gatoms) at a specific temperature and pressure, which gives the lowest possible value of the total free energy of the system satisfying the mass balance constraints. The iteration starts with guess of number of moles of a particular species ($y_i^o$) comprising of reactant elements. The new (or improved) set of mole numbers can be calculated ($x_i$), which in turn are used for a new guess ($y_i^o$). This procedure continues until the equilibrium composition is obtained.

### 4.2.1 Basic Equations

The free energy G of the system comprised of mixture of *i* species is:

$$G = \sum_i x_i g_i \tag{4.1}$$

where $x_i$ denotes the mole number of a substance or species in the mixture, and $g_i$ is the chemical potential of that species written as:

$$g_i = g_i^o + RT \ln a_i \tag{4.2}$$

For the gaseous species, which are treated as ideal, the activities $a_i$ are equal to the partial pressure $p_i$:

$$a_i = p_i = (x_i / X)P \tag{4.3}$$

*X* and *P* denote the total number of moles in the gas phase and the total pressure, respectively. For the condensed substances, which are thought to pure, the activities are equal to unity. Using the definitions above, a dimensionless quantity (*G/RT*) can be obtained:

$$G/RT = \sum_{i=1}^{m} x_i^g [(g^o / RT)_i^g + \ln P + \ln(x_i^g / X)] + \sum_{i=1}^{s} x_i^c (g^o / RT)_i^c \tag{4.4}$$

The indices *g* and *c* indicate gas phase and condensed phase, respectively. The number of substances in the gas phase and condensed phase at equilibrium are denoted by *m* and *s* respectively. The value of ($g^o$/*RT*) for a certain substance is calculated using the expression:

$$(g^o / RT) = (1/R)[G^o - H_{298}^o)/T + \Delta_f H_{298}^o / RT \tag{4.5}$$

Alternatively, values of ($g^o$/*RT*) can be calculated according to the relation:

$$\Delta(g^o / RT) = -\ln 10 \log K_f \tag{4.6}$$

The mass balance relations can be written as:

$$\sum_{i=1}^{m} a_{ij}^g x_i^g + \sum_{i=1}^{s} a_{ij}^c x_i^c = b_j \, (j = 1, 2, .....l) \tag{4.7}$$

where $a_{ij}$ represents the number of atoms of the $j^{th}$ element in a molecule of the $i^{th}$ substance, $b_j$ is the total number of moles of the $j^{th}$ element, and *l* is the total number of elements. The method involves a search for a minimum value of the free energy *G* of a system (or equivalently *G/RT* as given in equation 4.1) subject to the mass balance relation as subsidiary conditions (as given in equation 4.3). For solution of this system of equations, Lagrange's methods of undetermined multipliers can be used as follows. We define equations 4.8 and 4.9 as below:

$$(g^o / RT)_i^g + \ln P + \ln(x_i^g / X) - \sum_{j=1}^{l} \pi_j a_{ij}^g = 0 \qquad (i = 1, 2, ...., m) \tag{4.8}$$

$$(g^o / RT)_i^c - \sum_{j=1}^{l} \pi_j a_{ij}^c = 0 \qquad (i = 1, 2, ...., s) \tag{4.9}$$

The factors $\pi_j$ are Lagrangian multipliers. Equations 4.3 and 4.4 are expanded in a Taylor series about an arbitrary point $(y_1^g, y_2^g, ....., y_m^g; y_1^c, y_2^c, ....., y_s^c)$, neglecting terms involving derivatives of second and higher orders:

$$\sum_{i=1}^{m} a_{ij}^g y_i^g + \sum_{i=1}^{s} a_{ij}^c y_i^c - b_j + \sum_{i=1}^{m} a_{ij}^g (x_i^g - y_i^g) + \sum_{i=1}^{s} a_{ij}^c (x_i^c - y_i^c) = 0 \qquad (j = 1,2,....,l) \qquad (4.10)$$

$$(g^o / RT)_i^g + \ln P + LN(y_i^g / Y) - \sum_{j=1}^{l} \pi_j a_{ij}^g + (x_i^g / y_i^g) - (X / Y) = 0 \qquad (i = 1,2,...,m) \qquad (4.11)$$

where $Y = \sum_{i=1}^{m} y_i^g$ . From equation 4.7, $x_i^g$ is calculated:

$$x_i^g = -f_i + y_i^g [(X / Y) + \sum_{j=1}^{l} \pi_i a_{ij}^g] \qquad (i = 1,2,....., m) \qquad (4.12)$$

where $f_i = y_i^g [(g^o / RT)_i^g + \ln P + \ln(y_i^g / Y)]$ $(i = 1,2,....., m)$. The summation of equation (4.8) over $i$ gives:

$$\sum_{j=1}^{l} \pi_j \sum_{i=1}^{m} y_i^g a_{ij}^g = \sum_{i=1}^{m} f_i \qquad (4.13)$$

The quantity $C_j$, which serves as a correction term in case where the initial guess of the mole numbers does not satisfy the mass balance relations, is defined as:

$$C_j = \sum_{i=1}^{m} a_{ij}^g y_i^g - b_j \quad (j = 1,2,..., l) \qquad (4.14)$$

Substitution of equations 4.8 and 4.10 into equation 4.6 gives:

$$\sum_{k=1}^{l} \pi_k r_{jk} + [(X / Y) - 1] \sum_{i=1}^{m} a_{ij}^g y_i^g + \sum_{i=1}^{s} a_{ij}^c x_i^c = \sum_{i=1}^{m} a_{ij}^g f_i - C_J \qquad (j = 1,2,....l) \qquad (4.15)$$

where: $r_{jk} = r_{ki} = \sum_{i=1}^{m} (a_{ij}^g a_{ik}^g) y_i^g$ $(j, k = 1,2,..., l)$. Now, the equations 4.11, 4.5, and 4.9 constitute a system of $l$+$s$+1 linear equations, consisting of $l$+$s$+1 unknown quantities $\pi_j$ ($j$ = 1,2,….,$l$), $x_i^c$ ($i$ = 1,2,….,$s$) and $[(X / Y) - 1]$, the latter, for sake of simplicity, hereafter called $\pi_{l+1}$. The

system of equations is solved using Gaussian elimination. The solution gives the $x^c$ values, while the $x^g$ values are obtained from equation 4.8, making use of the values for $\pi_j$ ($j$ = 1,2,….,$l$+1). A singular matrix will be obtained if a mixture of two or more elements reacts completely to one certain substance. It can be avoided in two ways: either by choosing the initial mixture so that it deviates minutely from the stoichiometric one, or by adding traces of a new element which reacts with the elements initially added.

### 4.2.2 Numerical Iterative Solution

If all $x$ values obtained are positive, they will be used as the new initial guess. If negative $x$ values appear, the difference between the initial and the calculated values is reduced in order to obtain positive values. For all substances with negative $x$ values, $y_i'$ is put equal to zero where $y_i' = y_i + \lambda(x_i - y_i)$, and $\lambda$ is calculated. Next, using the same equation, adjusted positive values of all mole numbers are calculated, using a value $\lambda = k\lambda_{\min}$, where $k < 1$ and $\lambda_{\min}$ is the smallest $\lambda$ value obtained. Usually, $k$ is chosen near unity, e.g. 0.99. The $y_i'$ values are then used as estimates in the subsequent iteration cycle. The limit on the accuracy of mixture composition is put by adopting a lowest $y$ value (e.g. $10^{-8}$ or $10^{-10}$ mol). If the mole number for a substance becomes less than this limit, $y_i$ is put equal to zero and that species is excluded from subsequent iterations.

The quantity $\pi_{l+1}$, which is a variable in the system of linear equations to be solved, is used to test if the free energy of the system has reached a minimum value. When $X$ approaches $Y$, i.e. when the improved and the guessed mole numbers are becoming equal, the value of $\pi_{l+1}$ approaches zero. To achieve a satisfactory accuracy for all mole numbers, it was found that a value of $\pi_{l+1}$ less than $10^{-8}$ was adequate. If the test is not satisfied, the calculated $y$ values are substituted into the equations 4.11, 4.5 and 4.9, and a new iteration starts.

### 4.2.3 Heat Calculations

Since the equilibrium composition has been obtained, the heat generation or the total heat of a process can be computed, using values of $\Delta_f H^o_{298}$, $C_p$, and $(H^o - H^o_{298})$ as follows:

The energy necessary for pre–heating the initial mixture (*HP*) from the initial temperature $T_1$ K to the reaction temperature *T* K, added to the heat of reaction $(HR)$, gives the total heat $(HT)$: $HT = HP + HR$. $HP$ and $HR$ are given by the following expressions:

$$HP = \sum_i x_i^* (H^o - H^o_{T1})_i \tag{4.16}$$

where $x^*$ denotes the number of moles in the initial mixture, and:

$$(H^o - H^o_{T1})_i = \int_{T_1}^{T} (C_p)_i \, dT \tag{4.17}$$

$$HR = \sum_i (\Delta_f H^o_T)_i (x_i - x_i^*) \tag{4.18}$$

where $(\Delta_f H^o_T)_i = (\Delta_f H^o_{298})_i + [(H^o - H^o_{298})_i - (H^o - H^o_{298})_{elements}]$.

***Notation:*** $G$ = Gibbs free energy; $g$ = chemical potential; $H$ = enthalpy (heat content); $K_f$ = equilibrium constant of formation; $P$ = total pressure; $p$ = partial pressure; $R$ = ideal gas constant; $T$ = absolute temperature; $x^*$ = number of moles in the initial mixture; $y^o$ = initial guess of the number of moles in the equilibrium mixture; $C_p$ = heat capacity at constant pressure as a function of temperature; $\Delta_f H^o_{298}$ = heat of formation at 298.15 K; $\left(G^o - H^o_{298}\right)/T$ = free energy function; $\left(H^o - H^o_{298}\right)$ = heat content function; superscript $^o$ refers to the thermodynamic standard state; subscript $_{298}$ refers to the reference temperature (25 $^o$C = 298.15 K); subscript $_f$ denotes the formation of a compound from the elopements in their standard states.

## 4.3 SIMULATION PARAMETERS AND PERFORMANCE YARDSTICKS

For the simulation of the gasification process, we need to choose operating conditions. The major parameters in this regard are: (1) biomass type; (2) gasification medium and (3)

temperature and pressure of gasification. These parameters have been decided upon as follows:

### 4.3.1 Biomass Type

The choice for this parameter is quite wide. In the Indian context, the potential biomasses for gasification (with estimated production of ~ 500 million tons per year) would be in terms of crop residues and byproducts, agro–residues and woody plantations in wasteland [3]. Of course, not all of these biomasses will be available for gasification due to other conventional applications such as cattle feed and domestic fuel. Nonetheless, an estimated 150–160 millions tons of biomass is available for power generation each year with potential of sustaining 16 to 18 GW of generation (Biomass Atlas [4]). As we are considering applications of biomass gasification in particularly the northeastern states, we choose three representative biomasses that are found in abundance throughout the year, viz. saw dust, rice husk and bamboo dust. The ultimate analyses of these biomasses are given in Table 4.1(A) (Reference material, I.I.Sc. Bangalore [5]). It could be inferred that saw dust has the highest carbon content while rice husk has high ash content. The approximate molecular formula for the biomasses (along with composition in terms of gatoms) is given in Table 4.1(B).

### 4.3.2 Gasification Medium

Gasification is essentially partial oxidation in presence of sub–stoichiometric quantities of oxygen – which is usually supplied through air. Thus, air is the most common gasification medium. Depending on application, air is often mixed with steam (in different proportions) prior to gasification. This is especially when the quantity of hydrogen in the producer gas resulting from biomass is to be enhanced. On the basis of above, we choose for simulations three gasification media: (1) dry air; (2) air–steam mixture, with steam content 10% mole/mole of dry air; (3) air–steam mixture with steam content 30% mole/mole of dry air. It needs to be mentioned that the average humidity of air throughout the year in the northeastern states of India is quite high ~ 70–80%. Thus, an air–steam mixture is a more realistic gasification medium that

absolute dry air.

### 4.3.3 Temperature and Pressure of Gasification

We choose 7 representative temperatures for simulation of gasification, viz. 400 to 1000 $^{o}$C. Most of the commercial gasifiers used for thermal applications operate at 800 $^{o}$C and above. Despite this, we choose a rather wide temperature range to assess the variation in composition of the producer gas with temperature, so as to get a closer insight into the influence of this parameter. Secondly, most of the commercial gasifiers operate at atmospheric pressure, although pressurized gasification has been investigated by institutions such as IGT [6,7]. We have chosen atmospheric pressure for gasification process in the simulations.

The summary of the simulation parameters is given in Table 4.1(C).

### 4.3.4 Performance Yardsticks

As noted earlier, the purpose of the present study is to optimize the operating conditions of gasification for two applications, viz. (1) decentralized power generation, and (2) Fischer–Tropsch synthesis for production liquid transportations fuels. As far as the first application is concerned, the measure of assessing suitability of the producer gas is LHV (lower heating value) or the net heat content in the gas that can be obtained from combustion in engines. For the second application, the important characteristic of producer gas is the molar content and ratio of hydrogen and carbon monoxide (which are the reactants for FT synthesis). Therefore, we have fixed the yardsticks of performance of gasifier as: (1) hydrogen content of producer gas; (2) carbon monoxide content of producer gas; (3) $H_2$/CO molar ratio; (4) LHV of the producer gas. In addition to these, we have also assessed the carbon and hydrogen distribution in the reactant mixture under different operating conditions among the (desired and undesired) product species. Finally, we have also determined the theoretical efficiency of the gasifier for different operating conditions.

## 4.4 RESULTS

Table 4.2 describes the elemental vector input (or the number of gatoms of the 4 major elements in the biomass gasification mixture, viz. C, H, N, O) under different gasification conditions for the three biomasses (with 100 g dry biomass as basis), viz. saw dust, rice husk and bamboo dust. Also given in Table 4.2 is the ratio of oxygen content–to–carbon content (O/C) and hydrogen content–to–carbon content (H/C) of the gasification mixture, significance of which will be brought out later in the discussion. The results of simulations are given in Tables 4.3 to 4.14 and Figures 4.1 to 4.9. Tables 4.3, 4.5 and 4.7 depict the hydrogen content, while Tables 4.4, 4.6 and 4.8 depict the carbon monoxide content of producer gas for different temperatures, air ratios and gasification media. The distribution of carbon in the gasification mixture among the four major carbon–containing species, viz. CO, $CO_2$, $CH_4$ and unconverted carbon, for different gasification media is described in Tables 4.9, 4.11 and 4.13, while distribution of hydrogen in the gasification mixture among the three hydrogen–containing species, viz. $H_2$, $H_2O$ and $CH_4$, is depicted in Tables 4.10, 4.12 and 4.14. The variation in $H_2$/CO molar ratio in the producer gas resulting from gasification of three biomasses with different media at various temperatures and air ratios is shown in Figures 4.1–4.3. Figures 4.4–4.6 depict the variation in the LHV of the producer gas obtained from gasification of three biomasses under different conditions of gasification media, temperature and air ratios, while Figures 4.7–4.9 describe the trends in the theoretical efficiency of the gasification process for different operating conditions for three biomasses. A sample calculation of the model is given in Appendix A.

**Table 4.1:** Biomass Data and Simulations Parameters

**(A) Ultimate Analysis of Biomass**

| Biomass | Composition in weight percent (Dry Basis) | | | | |
|---|---|---|---|---|---|
| | Carbon | Hydrogen | Nitrogen | Oxygen | Ash |
| Saw dust | 52.28 | 5.2 | 0.47 | 40.85 | 1.2 |
| Rice husk | 37.03 | 5.25 | 0.09 | 40.94 | 16.69 |
| Bamboo dust | 39.88 | 5.5 | 0.89 | 47.92 | 5.81 |

**(B) Composition of Biomass in gatoms and Molecular Formula**

| Biomass | Composition in gatom (per 100 g biomass) | | | | Molecular Formula |
|---|---|---|---|---|---|
| | Carbon (C) | Hydrogen (H) | Nitrogen (N) | Oxygen (O) | |
| Saw dust | 4.36 | 5.20 | 0.03 | 2.55 | $CH_{1.193}N_{0.007}O_{0.585}$ |
| Rice husk | 3.09 | 5.25 | 0.01 | 2.56 | $CH_{1.699}N_{0.003}O_{0.828}$ |
| Bamboo dust | 3.32 | 5.50 | 0.06 | 3.00 | $CH_{1.657}N_{0.018}O_{0.904}$ |

**(C) Parameters for Simulation**

| **Parameter** | **Name or Value** |
|---|---|
| Biomass Type | Saw Dust, Rice Husk, Bamboo Dust |
| Gasification medium | Air, Air-steam (10% mole /mole) mixture, Air-Steam (30% mole/mole) mixture |
| Gasification temperature ($^oC$) | 400, 500, 600, 700, 800, 900, 1000 |
| Air (or Equivalence) ratio | 0, 0.2, 0.4, 0.6, 0.8, 1.0 |

**Table 4.2:** Elemental Vector Input Under Different Operating Conditions

(A) Biomass: Saw Dust

| AR | C | H | O | N | H/C | O/C |
|---|---|---|---|---|---|---|
| Gasification with Air | | | | | | |
| 0 | 4.36 | 6.31 | 3.11 | 0.03 | 1.45 | 0.71 |
| 0.2 | 4.36 | 6.31 | 4.86 | 6.67 | 1.45 | 1.12 |
| 0.4 | 4.36 | 6.31 | 6.61 | 13.30 | 1.45 | 1.52 |
| 0.6 | 4.36 | 6.31 | 8.36 | 19.93 | 1.45 | 1.92 |
| 0.8 | 4.36 | 6.31 | 10.12 | 26.56 | 1.45 | 2.32 |
| 1 | 4.36 | 6.31 | 11.87 | 33.19 | 1.45 | 2.72 |
| Gasification with Steam (10% mole/mole) and Air | | | | | | |
| 0 | 4.36 | 6.31 | 3.11 | 0.03 | 1.45 | 0.71 |
| 0.2 | 4.36 | 7.15 | 5.28 | 6.67 | 1.64 | 1.21 |
| 0.4 | 4.36 | 7.99 | 7.45 | 13.30 | 1.83 | 1.71 |
| 0.6 | 4.36 | 8.83 | 9.62 | 19.93 | 2.03 | 2.21 |
| 0.8 | 4.36 | 9.66 | 11.79 | 26.56 | 2.22 | 2.71 |
| 1 | 4.36 | 10.50 | 13.96 | 33.19 | 2.41 | 3.21 |
| Gasification with Steam (30% mole/mole) and Air | | | | | | |
| 0 | 4.36 | 6.31 | 3.11 | 0.03 | 1.45 | 0.71 |
| 0.2 | 4.36 | 8.83 | 6.12 | 6.67 | 2.03 | 1.40 |
| 0.4 | 4.36 | 11.34 | 9.13 | 13.30 | 2.60 | 2.10 |
| 0.6 | 4.36 | 13.86 | 12.14 | 19.93 | 3.18 | 2.79 |
| 0.8 | 4.36 | 16.37 | 15.15 | 26.56 | 3.76 | 3.48 |
| 1 | 4.36 | 18.89 | 18.16 | 33.19 | 4.33 | 4.17 |

(B) Biomass: Rice Husk

| AR | C | H | O | N | H/C | O/C |
|---|---|---|---|---|---|---|
| Gasification with Air | | | | | | |
| 0 | 3.09 | 6.36 | 3.11 | 0.01 | 2.06 | 1.01 |
| 0.2 | 3.09 | 6.36 | 4.36 | 4.73 | 2.06 | 1.41 |
| 0.4 | 3.09 | 6.36 | 5.61 | 9.45 | 2.06 | 1.82 |
| 0.6 | 3.09 | 6.36 | 6.86 | 14.17 | 2.06 | 2.22 |
| 0.8 | 3.09 | 6.36 | 8.10 | 18.89 | 2.06 | 2.63 |
| 1 | 3.09 | 6.36 | 9.35 | 23.62 | 2.06 | 3.03 |
| Gasification with Steam (10% mole/mole) and Air | | | | | | |
| 0 | 3.09 | 6.36 | 3.11 | 0.01 | 2.06 | 1.01 |
| 0.2 | 3.09 | 6.96 | 4.66 | 4.73 | 2.25 | 1.51 |
| 0.4 | 3.09 | 7.55 | 6.21 | 9.45 | 2.45 | 2.01 |
| 0.6 | 3.09 | 8.15 | 7.75 | 14.17 | 2.64 | 2.51 |
| 0.8 | 3.09 | 8.75 | 9.30 | 18.89 | 2.84 | 3.01 |
| 1 | 3.09 | 9.35 | 10.84 | 23.62 | 3.03 | 3.51 |
| Gasification with Steam (30% mole/mole) and Air | | | | | | |
| 0 | 3.09 | 6.36 | 3.11 | 0.01 | 2.06 | 1.01 |
| 0.2 | 3.09 | 8.15 | 5.26 | 4.73 | 2.64 | 1.70 |
| 0.4 | 3.09 | 9.94 | 7.40 | 9.45 | 3.22 | 2.40 |
| 0.6 | 3.09 | 11.73 | 9.54 | 14.17 | 3.80 | 3.09 |
| 0.8 | 3.09 | 13.52 | 11.69 | 18.89 | 4.38 | 3.79 |
| 1 | 3.09 | 15.32 | 13.83 | 23.62 | 4.96 | 4.48 |

*Table 4.2 (continued……)*

(C) Biomass: Bamboo Dust

| AR | C | H | O | N | H/C | O/C |
|---|---|---|---|---|---|---|
| Gasification with Air | | | | | | |
| 0 | 3.32 | 6.61 | 3.55 | 0.06 | 1.99 | 1.07 |
| 0.2 | 3.32 | 6.61 | 4.83 | 4.91 | 1.99 | 1.45 |
| 0.4 | 3.32 | 6.61 | 6.11 | 9.76 | 1.99 | 1.84 |
| 0.6 | 3.32 | 6.61 | 7.39 | 14.60 | 1.99 | 2.22 |
| 0.8 | 3.32 | 6.61 | 8.67 | 19.45 | 1.99 | 2.61 |
| 1 | 3.32 | 6.61 | 9.95 | 24.29 | 1.99 | 2.99 |
| Gasification with Steam (10% mole/mole) and Air | | | | | | |
| 0 | 3.32 | 6.61 | 3.55 | 0.06 | 1.99 | 1.07 |
| 0.2 | 3.32 | 7.22 | 5.14 | 4.91 | 2.17 | 1.55 |
| 0.4 | 3.32 | 7.84 | 6.72 | 9.76 | 2.36 | 2.02 |
| 0.6 | 3.32 | 8.45 | 8.31 | 14.60 | 2.54 | 2.50 |
| 0.8 | 3.32 | 9.06 | 9.90 | 19.45 | 2.73 | 2.98 |
| 1 | 3.32 | 9.67 | 11.48 | 24.29 | 2.91 | 3.46 |
| Gasification with Steam (30% mole/mole) and Air | | | | | | |
| 0 | 3.32 | 6.61 | 3.55 | 0.06 | 1.99 | 1.07 |
| 0.2 | 3.32 | 8.45 | 5.75 | 4.91 | 2.54 | 1.73 |
| 0.4 | 3.32 | 10.29 | 7.95 | 9.76 | 3.10 | 2.39 |
| 0.6 | 3.32 | 12.12 | 10.15 | 14.60 | 3.65 | 3.05 |
| 0.8 | 3.32 | 13.96 | 12.35 | 19.45 | 4.20 | 3.72 |
| 1 | 3.32 | 15.80 | 14.55 | 24.29 | 4.75 | 4.38 |

**Table 4.3:** Production of Hydrogen During Gasification of Various Biomasses (Gasification with Air Alone)

| (A) Biomass: Saw Dust | | | | | | |
|---|---|---|---|---|---|---|
| Temp ($^oC$) | Air Ratio | | | | | |
| | 0 | 0.2 | 0.4 | 0.6 | 0.8 | 1 |
| 400 | 0.36 | 0.45 | 0.49 | 0.51 | 0.53 | 0.00 |
| 500 | 0.89 | 1.07 | 1.15 | 1.19 | 1.08 | 0.00 |
| 600 | 1.65 | 1.85 | 1.93 | 1.81 | 1.06 | 0.00 |
| 700 | 2.39 | 2.54 | 2.35 | 1.69 | 0.90 | 0.00 |
| 800 | 2.86 | 2.90 | 2.24 | 1.51 | 0.77 | 0.00 |
| 900 | 3.04 | 2.91 | 2.12 | 1.37 | 0.66 | 0.00 |
| 1000 | 3.11 | 2.89 | 2.02 | 1.25 | 0.58 | 0.00 |

| (B) Biomass: Rice Husk | | | | | | |
|---|---|---|---|---|---|---|
| Temp ($^oC$) | Air Ratio | | | | | |
| | 0 | 0.2 | 0.4 | 0.6 | 0.8 | 1 |
| 400 | 0.36 | 0.43 | 0.47 | 0.50 | 0.49 | 0.00 |
| 500 | 0.90 | 1.04 | 1.12 | 1.16 | 0.90 | 0.00 |
| 600 | 1.66 | 1.82 | 1.90 | 1.57 | 0.87 | 0.00 |
| 700 | 2.41 | 2.49 | 2.06 | 1.45 | 0.75 | 0.00 |
| 800 | 2.88 | 2.54 | 1.93 | 1.30 | 0.66 | 0.00 |
| 900 | 3.07 | 2.47 | 1.81 | 1.18 | 0.58 | 0.00 |
| 1000 | 3.13 | 2.41 | 1.72 | 1.08 | 0.51 | 0.00 |

| (C) Biomass: Bamboo Dust | | | | | | |
|---|---|---|---|---|---|---|
| Temp ($^oC$) | Air Ratio | | | | | |
| | 0 | 0.2 | 0.4 | 0.6 | 0.8 | 1 |
| 400 | 0.37 | 0.44 | 0.48 | 0.51 | 0.50 | 0.00 |
| 500 | 0.93 | 1.07 | 1.15 | 1.20 | 0.92 | 0.00 |
| 600 | 1.72 | 1.89 | 1.96 | 1.60 | 0.88 | 0.00 |
| 700 | 2.50 | 2.55 | 2.09 | 1.47 | 0.76 | 0.00 |
| 800 | 2.99 | 2.57 | 1.95 | 1.31 | 0.66 | 0.00 |
| 900 | 3.15 | 2.49 | 1.82 | 1.19 | 0.58 | 0.00 |
| 1000 | 3.16 | 2.41 | 1.72 | 1.09 | 0.51 | 0.00 |

**Table 4.4:** Production of Carbon Monoxide During Gasification of Various Biomasses (Gasification with Air Alone)

| (A) Biomass: Saw Dust | | | | | | |
|---|---|---|---|---|---|---|
| Temp ($^oC$) | Air Ratio | | | | | |
| | 0 | 0.2 | 0.4 | 0.6 | 0.8 | 1 |
| 400 | 0.01 | 0.03 | 0.04 | 0.06 | 0.08 | 0.00 |
| 500 | 0.11 | 0.23 | 0.34 | 0.46 | 0.41 | 0.00 |
| 600 | 0.55 | 1.04 | 1.53 | 1.50 | 0.69 | 0.00 |
| 700 | 1.60 | 2.80 | 2.83 | 1.81 | 0.85 | 0.00 |
| 800 | 2.61 | 4.01 | 3.01 | 1.99 | 0.99 | 0.00 |
| 900 | 2.97 | 4.09 | 3.14 | 2.14 | 1.09 | 0.00 |
| 1000 | 3.07 | 4.12 | 3.24 | 2.25 | 1.17 | 0.00 |

| (B) Biomass: Rice Husk | | | | | | |
|---|---|---|---|---|---|---|
| Temp ($^oC$) | Air Ratio | | | | | |
| | 0 | 0.2 | 0.4 | 0.6 | 0.8 | 1 |
| 400 | 0.01 | 0.02 | 0.04 | 0.05 | 0.05 | 0.00 |
| 500 | 0.11 | 0.19 | 0.27 | 0.36 | 0.22 | 0.00 |
| 600 | 0.55 | 0.90 | 1.23 | 0.83 | 0.38 | 0.00 |
| 700 | 1.61 | 2.22 | 1.64 | 1.04 | 0.49 | 0.00 |
| 800 | 2.61 | 2.43 | 1.81 | 1.19 | 0.59 | 0.00 |
| 900 | 2.98 | 2.51 | 1.93 | 1.31 | 0.67 | 0.00 |
| 1000 | 3.06 | 2.58 | 2.03 | 1.41 | 0.74 | 0.00 |

| (C) Biomass: Bamboo Dust | | | | | | |
|---|---|---|---|---|---|---|
| Temp ($^oC$) | Air Ratio | | | | | |
| | 0 | 0.2 | 0.4 | 0.6 | 0.8 | 1 |
| 400 | 0.02 | 0.03 | 0.04 | 0.05 | 0.05 | 0.00 |
| 500 | 0.12 | 0.21 | 0.30 | 0.38 | 0.23 | 0.00 |
| 600 | 0.62 | 0.98 | 1.30 | 0.87 | 0.39 | 0.00 |
| 700 | 1.82 | 2.32 | 1.71 | 1.09 | 0.52 | 0.00 |
| 800 | 2.97 | 2.53 | 1.89 | 1.25 | 0.62 | 0.00 |
| 900 | 3.20 | 2.63 | 2.02 | 1.37 | 0.70 | 0.00 |
| 1000 | 3.23 | 2.71 | 2.12 | 1.47 | 0.77 | 0.00 |

**Table 4.5:** Production of Hydrogen During Gasification of Various Biomasses (Gasification with Air + 10% mole/mole Steam Mixture)

| (A) Biomass: Saw Dust | | | | | | |
|---|---|---|---|---|---|---|
| Temp ($^oC$) | Air Ratio | | | | | |
| | 0 | 0.2 | 0.4 | 0.6 | 0.8 | 1 |
| 400 | 0.11 | 0.14 | 0.15 | 0.16 | 0.15 | 0.00 |
| 500 | 0.28 | 0.33 | 0.34 | 0.32 | 0.18 | 0.00 |
| 600 | 0.52 | 0.57 | 0.56 | 0.38 | 0.18 | 0.00 |
| 700 | 0.76 | 0.78 | 0.57 | 0.35 | 0.16 | 0.00 |
| 800 | 0.91 | 0.80 | 0.53 | 0.32 | 0.14 | 0.00 |
| 900 | 0.97 | 0.78 | 0.50 | 0.29 | 0.13 | 0.00 |
| 1000 | 0.99 | 0.76 | 0.47 | 0.27 | 0.12 | 0.00 |

| (B) Biomass: Rice Husk | | | | | | |
|---|---|---|---|---|---|---|
| Temp ($^oC$) | Air Ratio | | | | | |
| | 0 | 0.2 | 0.4 | 0.6 | 0.8 | 1 |
| 400 | 0.11 | 0.13 | 0.15 | 0.15 | 0.14 | 0.00 |
| 500 | 0.28 | 0.33 | 0.35 | 0.34 | 0.23 | 0.00 |
| 600 | 0.52 | 0.57 | 0.57 | 0.43 | 0.22 | 0.00 |
| 700 | 0.76 | 0.76 | 0.60 | 0.40 | 0.20 | 0.00 |
| 800 | 0.91 | 0.77 | 0.56 | 0.36 | 0.17 | 0.00 |
| 900 | 0.97 | 0.74 | 0.52 | 0.33 | 0.15 | 0.00 |
| 1000 | 0.99 | 0.72 | 0.49 | 0.30 | 0.14 | 0.00 |

| (C) Biomass: Bamboo Dust | | | | | | |
|---|---|---|---|---|---|---|
| Temp ($^oC$) | Air Ratio | | | | | |
| | 0 | 0.2 | 0.4 | 0.6 | 0.8 | 1 |
| 400 | 0.11 | 0.13 | 0.14 | 0.15 | 0.13 | 0.00 |
| 500 | 0.28 | 0.32 | 0.34 | 0.34 | 0.23 | 0.00 |
| 600 | 0.52 | 0.57 | 0.57 | 0.42 | 0.22 | 0.00 |
| 700 | 0.76 | 0.75 | 0.58 | 0.39 | 0.19 | 0.00 |
| 800 | 0.91 | 0.75 | 0.54 | 0.35 | 0.17 | 0.00 |
| 900 | 0.95 | 0.72 | 0.50 | 0.32 | 0.15 | 0.00 |
| 1000 | 0.96 | 0.69 | 0.48 | 0.29 | 0.13 | 0.00 |

**Table 4.6:** Production of Carbon Monoxide During Gasification of Various Biomasses (Gasification with Air + 10% mole/mole Steam Mixture)

(A) Biomass: Saw Dust

| Temp ($^{o}$C) | Air Ratio | | | | | |
|---|---|---|---|---|---|---|
| | 0 | 0.2 | 0.4 | 0.6 | 0.8 | 1 |
| 400 | 0.01 | 0.03 | 0.05 | 0.07 | 0.06 | 0.00 |
| 500 | 0.11 | 0.24 | 0.37 | 0.50 | 0.29 | 0.00 |
| 600 | 0.55 | 0.29 | 1.68 | 1.18 | 0.50 | 0.00 |
| 700 | 1.60 | 0.69 | 2.48 | 1.48 | 0.66 | 0.00 |
| 800 | 2.61 | 0.92 | 2.70 | 1.69 | 0.80 | 0.00 |
| 900 | 2.97 | 0.98 | 2.85 | 1.86 | 0.91 | 0.00 |
| 1000 | 3.07 | 3.95 | 2.98 | 2.00 | 1.00 | 0.00 |

(B) Biomass: Rice Husk

| Temp ($^{o}$C) | Air Ratio | | | | | |
|---|---|---|---|---|---|---|
| | 0 | 0.2 | 0.4 | 0.6 | 0.8 | 1 |
| 400 | 0.01 | 0.03 | 0.04 | 0.05 | 0.04 | 0.00 |
| 500 | 0.11 | 0.20 | 0.29 | 0.30 | 0.17 | 0.00 |
| 600 | 0.55 | 0.95 | 1.09 | 0.68 | 0.29 | 0.00 |
| 700 | 1.61 | 2.10 | 1.47 | 0.88 | 0.40 | 0.00 |
| 800 | 2.61 | 2.31 | 1.64 | 1.04 | 0.49 | 0.00 |
| 900 | 2.98 | 2.41 | 1.78 | 1.17 | 0.57 | 0.00 |
| 1000 | 3.06 | 2.49 | 1.89 | 1.27 | 0.64 | 0.00 |

(C) Biomass: Bamboo Dust

| Temp ($^{o}$C) | Air Ratio | | | | | |
|---|---|---|---|---|---|---|
| | 0 | 0.2 | 0.4 | 0.6 | 0.8 | 1 |
| 400 | 0.02 | 0.03 | 0.04 | 0.05 | 0.04 | 0.00 |
| 500 | 0.13 | 0.22 | 0.32 | 0.32 | 0.18 | 0.00 |
| 600 | 0.62 | 1.04 | 1.15 | 0.71 | 0.31 | 0.00 |
| 700 | 1.82 | 2.20 | 1.53 | 0.92 | 0.42 | 0.00 |
| 800 | 2.97 | 2.42 | 1.72 | 1.09 | 0.52 | 0.00 |
| 900 | 3.20 | 2.53 | 1.86 | 1.22 | 0.60 | 0.00 |
| 1000 | 3.23 | 2.62 | 1.98 | 1.33 | 0.67 | 0.00 |

Table 4.7

**Production of Hydrogen During Gasification of Various Biomasses (Gasification with Air + 30% mole/mole Steam Mixture)**

(A) Biomass: Saw Dust

| Temp (°C) | Air Ratio | | | | | |
|---|---|---|---|---|---|---|
| | 0 | 0.2 | 0.4 | 0.6 | 0.8 | 1 |
| 400 | 0.36 | 0.60 | 0.81 | 1.01 | 0.98 | 0.00 |
| 500 | 0.89 | 1.45 | 1.94 | 2.20 | 1.51 | 0.00 |
| 600 | 1.65 | 2.53 | 3.16 | 2.63 | 1.43 | 0.00 |
| 700 | 2.39 | 3.46 | 3.25 | 2.42 | 1.30 | 0.00 |
| 800 | 2.86 | 3.54 | 3.03 | 2.20 | 1.18 | 0.00 |
| 900 | 3.04 | 3.45 | 2.83 | 2.02 | 1.06 | 0.00 |
| 1000 | 3.11 | 3.36 | 2.67 | 1.87 | 0.97 | 0.00 |

(B) Biomass: Rice Husk

| Temp (°C) | Air Ratio | | | | | |
|---|---|---|---|---|---|---|
| | 0 | 0.2 | 0.4 | 0.6 | 0.8 | 1 |
| 400 | 0.36 | 0.58 | 0.69 | 0.82 | 0.76 | 0.00 |
| 500 | 0.90 | 1.38 | 1.66 | 1.73 | 1.10 | 0.00 |
| 600 | 1.66 | 2.39 | 2.54 | 1.98 | 1.05 | 0.00 |
| 700 | 2.41 | 2.94 | 2.53 | 1.83 | 0.96 | 0.00 |
| 800 | 2.88 | 2.87 | 2.35 | 1.67 | 0.88 | 0.00 |
| 900 | 3.07 | 2.76 | 2.20 | 1.54 | 0.80 | 0.00 |
| 1000 | 3.13 | 2.66 | 2.08 | 1.43 | 0.74 | 0.00 |

(C) Biomass: Bamboo Dust

| Temp (°C) | Air Ratio | | | | | |
|---|---|---|---|---|---|---|
| | 0 | 0.2 | 0.4 | 0.6 | 0.8 | 1 |
| 400 | 0.37 | 0.55 | 0.71 | 0.84 | 0.78 | 0.00 |
| 500 | 0.93 | 1.34 | 1.71 | 1.77 | 1.13 | 0.00 |
| 600 | 1.72 | 2.38 | 2.60 | 2.01 | 1.07 | 0.00 |
| 700 | 2.50 | 2.97 | 2.57 | 1.85 | 0.98 | 0.00 |
| 800 | 2.99 | 2.90 | 2.38 | 1.69 | 0.89 | 0.00 |
| 900 | 3.15 | 2.77 | 2.22 | 1.56 | 0.81 | 0.00 |
| 1000 | 3.16 | 2.67 | 2.09 | 1.44 | 0.74 | 0.00 |

Table 4.8

**Production of Carbon Monoxide During Gasification of Various Biomasses (Gasification with Air + 30% mole/mole Steam Mixture)**

(A) Biomass: Saw Dust

| Temp ($^oC$) | Air Ratio | | | | | |
|---|---|---|---|---|---|---|
| | 0 | 0.2 | 0.4 | 0.6 | 0.8 | 1 |
| 400 | 0.01 | 0.03 | 0.05 | 0.06 | 0.05 | 0.00 |
| 500 | 0.11 | 0.27 | 0.43 | 0.37 | 0.18 | 0.00 |
| 600 | 0.55 | 1.26 | 1.46 | 0.81 | 0.32 | 0.00 |
| 700 | 1.60 | 3.14 | 1.97 | 1.08 | 0.45 | 0.00 |
| 800 | 2.61 | 3.44 | 2.23 | 1.30 | 0.58 | 0.00 |
| 900 | 2.97 | 3.56 | 2.42 | 1.48 | 0.69 | 0.00 |
| 1000 | 3.07 | 3.65 | 2.58 | 1.64 | 0.78 | 0.00 |

(B) Biomass: Rice Husk

| Temp ($^oC$) | Air Ratio | | | | | |
|---|---|---|---|---|---|---|
| | 0 | 0.2 | 0.4 | 0.6 | 0.8 | 1 |
| 400 | 0.01 | 0.03 | 0.04 | 0.04 | 0.03 | 0.00 |
| 500 | 0.11 | 0.24 | 0.31 | 0.23 | 0.11 | 0.00 |
| 600 | 0.55 | 1.13 | 0.88 | 0.49 | 0.20 | 0.00 |
| 700 | 1.61 | 1.92 | 1.20 | 0.67 | 0.28 | 0.00 |
| 800 | 2.61 | 2.11 | 1.39 | 0.82 | 0.37 | 0.00 |
| 900 | 2.98 | 2.23 | 1.54 | 0.95 | 0.45 | 0.00 |
| 1000 | 3.06 | 2.33 | 1.67 | 1.06 | 0.51 | 0.00 |

(C) Biomass: Bamboo Dust

| Temp ($^oC$) | Air Ratio | | | | | |
|---|---|---|---|---|---|---|
| | 0 | 0.2 | 0.4 | 0.6 | 0.8 | 1 |
| 400 | 0.02 | 0.03 | 0.05 | 0.04 | 0.03 | 0.00 |
| 500 | 0.13 | 0.24 | 0.33 | 0.25 | 0.12 | 0.00 |
| 600 | 0.62 | 1.15 | 0.93 | 0.52 | 0.21 | 0.00 |
| 700 | 1.82 | 2.00 | 1.26 | 0.71 | 0.30 | 0.00 |
| 800 | 2.97 | 2.21 | 1.46 | 0.87 | 0.39 | 0.00 |
| 900 | 3.20 | 2.35 | 1.62 | 1.00 | 0.47 | 0.00 |
| 1000 | 3.23 | 2.45 | 1.75 | 1.12 | 0.54 | 0.00 |

Table 4.9

**Distribution of Carbon in the Gasification Mixture Among Various Chemical Species (Gasification with Air Alone)**

| | Biomass: Saw Dust | | | | | | Biomass: Rice Husk | | | | | | Biomass: Bamboo Dust | | | | | |
|---|---|---|---|---|---|---|---|---|---|---|---|---|---|---|---|---|---|---|
| | (A) Temp = 400 $^{o}$C | | | | | | (A) Temp = 400 $^{o}$C | | | | | | (A) Temp = 400 $^{o}$C | | | | | |
| AR | 0 | 0.2 | 0.4 | 0.6 | 0.8 | 1 | 0 | 0.2 | 0.4 | 0.6 | 0.8 | 1 | 0 | 0.2 | 0.4 | 0.6 | 0.8 | 1 |
| CO | 0.00 | 0.01 | 0.01 | 0.01 | 0.02 | 0.00 | 0.00 | 0.01 | 0.01 | 0.77 | 0.02 | 0.00 | 0.01 | 0.01 | 0.01 | 0.02 | 0.02 | 0.00 |
| $CO_2$ | 0.17 | 0.34 | 0.52 | 0.71 | 0.90 | 1.00 | 0.24 | 0.41 | 0.59 | 0.02 | 0.93 | 1.00 | 0.27 | 0.43 | 0.60 | 0.78 | 0.93 | 1.00 |
| $CH_4$ | 0.14 | 0.10 | 0.08 | 0.06 | 0.05 | 0.00 | 0.20 | 0.15 | 0.12 | 0.10 | 0.06 | 0.00 | 0.18 | 0.14 | 0.11 | 0.10 | 0.06 | 0.00 |
| C | 0.69 | 0.56 | 0.39 | 0.22 | 0.03 | 0.00 | 0.55 | 0.43 | 0.28 | 0.11 | 0.00 | 0.00 | 0.54 | 0.42 | 0.27 | 0.11 | 0.00 | 0.00 |
| | (B) Temp = 500 $^{o}$C | | | | | | (B) Temp = 500 $^{o}$C | | | | | | (B) Temp = 500 $^{o}$C | | | | | |
| CO | 0.03 | 0.05 | 0.08 | 0.11 | 0.10 | 0.00 | 0.04 | 0.06 | 0.09 | 0.12 | 0.07 | 0.00 | 0.04 | 0.06 | 0.09 | 0.11 | 0.07 | 0.00 |
| $CO_2$ | 0.19 | 0.37 | 0.54 | 0.73 | 0.89 | 1.00 | 0.27 | 0.44 | 0.62 | 0.80 | 0.92 | 1.00 | 0.30 | 0.47 | 0.64 | 0.81 | 0.92 | 1.00 |
| $CH_4$ | 0.11 | 0.07 | 0.05 | 0.04 | 0.02 | 0.00 | 0.16 | 0.11 | 0.09 | 0.08 | 0.01 | 0.00 | 0.14 | 0.11 | 0.09 | 0.07 | 0.01 | 0.00 |
| C | 0.67 | 0.51 | 0.32 | 0.13 | 0.00 | 0.00 | 0.53 | 0.38 | 0.20 | 0.01 | 0.00 | 0.00 | 0.52 | 0.36 | 0.19 | 0.01 | 0.00 | 0.00 |
| | (C) Temp = 600 $^{o}$C | | | | | | (C) Temp = 600 $^{o}$C | | | | | | (C) Temp = 600 $^{o}$C | | | | | |
| CO | 0.13 | 0.24 | 0.35 | 0.35 | 0.16 | 0.00 | 0.18 | 0.29 | 0.40 | 0.27 | 0.12 | 0.00 | 0.19 | 0.30 | 0.39 | 0.26 | 0.12 | 0.00 |
| $CO_2$ | 0.19 | 0.33 | 0.47 | 0.64 | 0.84 | 1.00 | 0.27 | 0.41 | 0.55 | 0.72 | 0.88 | 1.00 | 0.29 | 0.43 | 0.57 | 0.73 | 0.88 | 1.00 |
| $CH_4$ | 0.07 | 0.04 | 0.03 | 0.01 | 0.00 | 0.00 | 0.10 | 0.07 | 0.05 | 0.01 | 0.00 | 0.00 | 0.09 | 0.06 | 0.04 | 0.01 | 0.00 | 0.00 |
| C | 0.62 | 0.39 | 0.15 | 0.00 | 0.00 | 0.00 | 0.46 | 0.23 | 0.00 | 0.00 | 0.00 | 0.00 | 0.43 | 0.22 | 0.00 | 0.00 | 0.00 | 0.00 |
| | (D) Temp = 700 $^{o}$C | | | | | | (D) Temp = 700 $^{o}$C | | | | | | (D) Temp = 700 $^{o}$C | | | | | |
| CO | 0.37 | 0.24 | 0.65 | 0.42 | 0.20 | 0.00 | 0.52 | 0.72 | 0.53 | 0.34 | 0.16 | 0.00 | 0.55 | 0.70 | 0.52 | 0.33 | 0.16 | 0.00 |
| $CO_2$ | 0.12 | 0.33 | 0.35 | 0.59 | 0.80 | 1.00 | 0.17 | 0.26 | 0.46 | 0.66 | 0.84 | 1.00 | 0.18 | 0.28 | 0.48 | 0.67 | 0.85 | 1.00 |
| $CH_4$ | 0.04 | 0.04 | 0.01 | 0.00 | 0.00 | 0.00 | 0.05 | 0.02 | 0.00 | 0.00 | 0.00 | 0.00 | 0.04 | 0.02 | 0.00 | 0.00 | 0.00 | 0.00 |
| C | 0.48 | 0.39 | 0.00 | 0.00 | 0.00 | 0.00 | 0.26 | 0.00 | 0.00 | 0.00 | 0.00 | 0.00 | 0.23 | 0.00 | 0.00 | 0.00 | 0.00 | 0.00 |
| | (E) Temp = 800 $^{o}$C | | | | | | (E) Temp = 800 $^{o}$C | | | | | | (E) Temp = 800 $^{o}$C | | | | | |
| CO | 0.60 | 0.93 | 0.69 | 0.46 | 0.23 | 0.00 | 0.85 | 0.79 | 0.59 | 0.39 | 0.19 | 0.00 | 0.89 | 0.76 | 0.57 | 0.38 | 0.19 | 0.00 |
| $CO_2$ | 0.04 | 0.07 | 0.31 | 0.54 | 0.77 | 1.00 | 0.05 | 0.21 | 0.41 | 0.61 | 0.81 | 1.00 | 0.06 | 0.24 | 0.43 | 0.63 | 0.81 | 1.00 |
| $CH_4$ | 0.02 | 0.01 | 0.00 | 0.00 | 0.00 | 0.00 | 0.02 | 0.00 | 0.00 | 0.00 | 0.00 | 0.00 | 0.02 | 0.00 | 0.00 | 0.00 | 0.00 | 0.00 |
| C | 0.35 | 0.00 | 0.00 | 0.00 | 0.00 | 0.00 | 0.08 | 0.00 | 0.00 | 0.00 | 0.00 | 0.00 | 0.03 | 0.00 | 0.00 | 0.00 | 0.00 | 0.00 |
| | (F) Temp = 900 $^{o}$C | | | | | | (F) Temp = 900 $^{o}$C | | | | | | (F) Temp = 900 $^{o}$C | | | | | |
| CO | 0.68 | 0.94 | 0.72 | 0.49 | 0.25 | 0.00 | 0.97 | 0.82 | 0.63 | 0.43 | 0.22 | 0.00 | 0.96 | 0.79 | 0.61 | 0.41 | 0.21 | 0.00 |
| $CO_2$ | 0.01 | 0.06 | 0.28 | 0.51 | 0.75 | 1.00 | 0.01 | 0.19 | 0.38 | 0.57 | 0.78 | 1.00 | 0.03 | 0.21 | 0.39 | 0.59 | 0.79 | 1.00 |
| $CH_4$ | 0.01 | 0.00 | 0.00 | 0.00 | 0.00 | 0.00 | 0.01 | 0.00 | 0.00 | 0.00 | 0.00 | 0.00 | 0.00 | 0.00 | 0.00 | 0.00 | 0.00 | 0.00 |
| C | 0.30 | 0.00 | 0.00 | 0.00 | 0.00 | 0.00 | 0.01 | 0.00 | 0.00 | 0.00 | 0.00 | 0.00 | 0.00 | 0.00 | 0.00 | 0.00 | 0.00 | 0.00 |
| | (G) Temp = 1000 $^{o}$C | | | | | | (G) Temp = 1000 $^{o}$C | | | | | | (G) Temp = 1000 $^{o}$C | | | | | |
| CO | 0.70 | 0.95 | 0.74 | 0.52 | 0.27 | 0.00 | 0.99 | 0.84 | 0.66 | 0.46 | 0.24 | 0.00 | 0.97 | 0.82 | 0.64 | 0.44 | 0.23 | 0.00 |
| $CO_2$ | 0.00 | 0.05 | 0.26 | 0.48 | 0.73 | 1.00 | 0.01 | 0.16 | 0.34 | 0.54 | 0.76 | 1.00 | 0.03 | 0.19 | 0.36 | 0.56 | 0.77 | 1.00 |
| $CH_4$ | 0.00 | 0.00 | 0.00 | 0.00 | 0.00 | 0.00 | 0.00 | 0.00 | 0.00 | 0.00 | 0.00 | 0.00 | 0.00 | 0.00 | 0.00 | 0.00 | 0.00 | 0.00 |
| C | 0.29 | 0.00 | 0.00 | 0.00 | 0.00 | 0.00 | 0.00 | 0.00 | 0.00 | 0.00 | 0.00 | 0.00 | 0.00 | 0.00 | 0.00 | 0.00 | 0.00 | 0.00 |

Table 4.10

**Distribution of Hydrogen in the Gasification Mixture Among Various Chemical Species (Gasification with Air Alone)**

| | Biomass: Saw Dust | | | | | | Biomass: Rice Husk | | | | | | Biomass: Bamboo Dust | | | | | |
|---|---|---|---|---|---|---|---|---|---|---|---|---|---|---|---|---|---|---|
| | (A) Temp = 400 °C | | | | | | (A) Temp = 400 °C | | | | | | (A) Temp = 400 °C | | | | | |
| AR | 0 | 0.2 | 0.4 | 0.6 | 0.8 | 1 | 0 | 0.2 | 0.4 | 0.6 | 0.8 | 1 | 0 | 0.2 | 0.4 | 0.6 | 0.8 | 1 |
| $H_2$ | 0.11 | 0.14 | 0.16 | 0.16 | 0.17 | 0.00 | 0.11 | 0.14 | 0.15 | 0.16 | 0.15 | 0.00 | 0.11 | 0.13 | 0.15 | 0.15 | 0.15 | 0.00 |
| $H_2O$ | 0.50 | 0.59 | 0.64 | 0.67 | 0.69 | 1.00 | 0.50 | 0.57 | 0.61 | 0.64 | 0.74 | 1.00 | 0.53 | 0.58 | 0.62 | 0.65 | 0.74 | 1.00 |
| $CH_4$ | 0.38 | 0.27 | 0.21 | 0.17 | 0.14 | 0.00 | 0.39 | 0.29 | 0.24 | 0.20 | 0.11 | 0.00 | 0.36 | 0.28 | 0.23 | 0.19 | 0.11 | 0.00 |
| | (B) Temp = 500 °C | | | | | | (B) Temp = 500 °C | | | | | | (B) Temp = 500 °C | | | | | |
| $H_2$ | 0.28 | 0.34 | 0.36 | 0.38 | 0.34 | 0.00 | 0.28 | 0.33 | 0.35 | 0.37 | 0.28 | 0.00 | 0.28 | 0.33 | 0.35 | 0.36 | 0.28 | 0.00 |
| $H_2O$ | 0.42 | 0.46 | 0.49 | 0.50 | 0.62 | 1.00 | 0.41 | 0.45 | 0.47 | 0.49 | 0.70 | 1.00 | 0.44 | 0.46 | 0.48 | 0.50 | 0.70 | 1.00 |
| $CH_4$ | 0.30 | 0.20 | 0.15 | 0.12 | 0.04 | 0.00 | 0.30 | 0.22 | 0.18 | 0.15 | 0.02 | 0.00 | 0.28 | 0.21 | 0.17 | 0.14 | 0.02 | 0.00 |
| | (C) Temp = 600 °C | | | | | | (C) Temp = 600 °C | | | | | | (C) Temp = 600 °C | | | | | |
| $H_2$ | 0.52 | 0.59 | 0.61 | 0.57 | 0.34 | 0.00 | 0.52 | 0.57 | 0.60 | 0.49 | 0.27 | 0.00 | 0.52 | 0.57 | 0.59 | 0.48 | 0.27 | 0.00 |
| $H_2O$ | 0.29 | 0.30 | 0.31 | 0.40 | 0.66 | 1.00 | 0.29 | 0.30 | 0.31 | 0.49 | 0.73 | 1.00 | 0.30 | 0.30 | 0.32 | 0.50 | 0.73 | 1.00 |
| $CH_4$ | 0.19 | 0.11 | 0.08 | 0.03 | 0.00 | 0.00 | 0.19 | 0.13 | 0.10 | 0.02 | 0.00 | 0.00 | 0.18 | 0.13 | 0.09 | 0.01 | 0.00 | 0.00 |
| | (D) Temp = 700 °C | | | | | | (D) Temp = 700 °C | | | | | | (D) Temp = 700 °C | | | | | |
| $H_2$ | 0.76 | 0.80 | 0.74 | 0.54 | 0.29 | 0.00 | 0.76 | 0.78 | 0.65 | 0.46 | 0.24 | 0.00 | 0.76 | 0.77 | 0.63 | 0.44 | 0.23 | 0.00 |
| $H_2O$ | 0.15 | 0.14 | 0.24 | 0.46 | 0.72 | 1.00 | 0.15 | 0.17 | 0.35 | 0.54 | 0.76 | 1.00 | 0.16 | 0.19 | 0.36 | 0.56 | 0.77 | 1.00 |
| $CH_4$ | 0.09 | 0.05 | 0.01 | 0.00 | 0.00 | 0.00 | 0.09 | 0.05 | 0.01 | 0.00 | 0.00 | 0.00 | 0.09 | 0.04 | 0.01 | 0.00 | 0.00 | 0.00 |
| | (E) Temp = 800 °C | | | | | | (E) Temp = 800 °C | | | | | | (E) Temp = 800 °C | | | | | |
| $H_2$ | 0.91 | 0.92 | 0.71 | 0.48 | 0.24 | 0.00 | 0.91 | 0.80 | 0.61 | 0.41 | 0.21 | 0.00 | 0.91 | 0.78 | 0.59 | 0.40 | 0.20 | 0.00 |
| $H_2O$ | 0.05 | 0.07 | 0.29 | 0.52 | 0.76 | 1.00 | 0.05 | 0.20 | 0.39 | 0.59 | 0.79 | 1.00 | 0.06 | 0.22 | 0.41 | 0.60 | 0.80 | 1.00 |
| $CH_4$ | 0.04 | 0.02 | 0.00 | 0.00 | 0.00 | 0.00 | 0.04 | 0.00 | 0.00 | 0.00 | 0.00 | 0.00 | 0.04 | 0.00 | 0.00 | 0.00 | 0.00 | 0.00 |
| | (F) Temp = 900 °C | | | | | | (F) Temp = 900 °C | | | | | | (F) Temp = 900 °C | | | | | |
| $H_2$ | 0.97 | 0.92 | 0.67 | 0.43 | 0.21 | 0.00 | 0.97 | 0.78 | 0.57 | 0.37 | 0.18 | 0.00 | 0.95 | 0.75 | 0.55 | 0.36 | 0.18 | 0.00 |
| $H_2O$ | 0.02 | 0.08 | 0.33 | 0.57 | 0.79 | 1.00 | 0.02 | 0.22 | 0.43 | 0.63 | 0.82 | 1.00 | 0.04 | 0.25 | 0.45 | 0.64 | 0.83 | 1.00 |
| $CH_4$ | 0.02 | 0.00 | 0.00 | 0.00 | 0.00 | 0.00 | 0.02 | 0.00 | 0.00 | 0.00 | 0.00 | 0.00 | 0.01 | 0.00 | 0.00 | 0.00 | 0.00 | 0.00 |
| | (G) Temp = 1000 °C | | | | | | (G) Temp = 1000 °C | | | | | | (G) Temp = 1000 °C | | | | | |
| $H_2$ | 0.99 | 0.91 | 0.64 | 0.40 | 0.18 | 0.00 | 0.99 | 0.76 | 0.54 | 0.34 | 0.17 | 0.00 | 0.96 | 0.73 | 0.52 | 0.33 | 0.16 | 0.00 |
| $H_2O$ | 0.01 | 0.09 | 0.36 | 0.60 | 0.82 | 1.00 | 0.01 | 0.24 | 0.46 | 0.66 | 0.84 | 1.00 | 0.04 | 0.27 | 0.48 | 0.67 | 0.85 | 1.00 |
| $CH_4$ | 0.01 | 0.00 | 0.00 | 0.00 | 0.00 | 0.00 | 0.01 | 0.00 | 0.00 | 0.00 | 0.00 | 0.00 | 0.00 | 0.00 | 0.00 | 0.00 | 0.00 | 0.00 |

Table 4.11

**Distribution of Carbon in the Gasification Mixture Among Various Chemical Species (Gasification with Air + 10% mole/mole Steam Mixture)**

| | Biomass: Saw Dust | | | | | | Biomass: Rice Husk | | | | | | Biomass: Bamboo Dust | | | | | |
|---|---|---|---|---|---|---|---|---|---|---|---|---|---|---|---|---|---|---|
| | (A) Temp = 400 °C | | | | | | (A) Temp = 400 °C | | | | | | (A) Temp = 400 °C | | | | | |
| AR | 0 | 0.2 | 0.4 | 0.6 | 0.8 | 0 | 0 | 0.2 | 0.4 | 0.6 | 0.8 | 1 | 0 | 0.2 | 0.4 | 0.6 | 0.8 | 1 |
| CO | 0.00 | 0.01 | 0.01 | 0.02 | 0.02 | 0.00 | 0.00 | 0.01 | 0.01 | 0.02 | 0.01 | 0.00 | 0.01 | 0.01 | 0.01 | 0.02 | 0.01 | 0.00 |
| $CO_2$ | 0.17 | 0.36 | 0.56 | 0.77 | 0.93 | 1.00 | 0.24 | 0.43 | 0.63 | 0.84 | 0.94 | 1.00 | 0.27 | 0.45 | 0.65 | 0.84 | 0.94 | 1.00 |
| $CH_4$ | 0.14 | 0.11 | 0.10 | 0.10 | 0.06 | 0.00 | 0.20 | 0.17 | 0.16 | 0.15 | 0.05 | 0.00 | 0.18 | 0.16 | 0.14 | 0.14 | 0.05 | 0.00 |
| C | 0.69 | 0.52 | 0.32 | 0.12 | 0.00 | 0.00 | 0.55 | 0.39 | 0.20 | 0.00 | 0.00 | 0.00 | 0.54 | 0.38 | 0.20 | 0.01 | 0.00 | 0.00 |
| | (B) Temp = 500 °C | | | | | | (B) Temp = 500 °C | | | | | | (B) Temp = 500 °C | | | | | |
| CO | 0.03 | 0.06 | 0.09 | 0.12 | 0.07 | 0.00 | 0.04 | 0.07 | 0.10 | 0.10 | 0.05 | 0.00 | 0.04 | 0.07 | 0.10 | 0.10 | 0.05 | 0.00 |
| $CO_2$ | 0.19 | 0.39 | 0.59 | 0.80 | 0.92 | 1.00 | 0.27 | 0.47 | 0.67 | 0.84 | 0.94 | 1.00 | 0.30 | 0.49 | 0.68 | 0.84 | 0.94 | 1.00 |
| $CH_4$ | 0.11 | 0.09 | 0.08 | 0.07 | 0.01 | 0.00 | 0.16 | 0.13 | 0.12 | 0.07 | 0.01 | 0.00 | 0.14 | 0.12 | 0.11 | 0.06 | 0.01 | 0.00 |
| C | 0.67 | 0.47 | 0.25 | 0.01 | 0.00 | 0.00 | 0.53 | 0.34 | 0.12 | 0.01 | 0.00 | 0.00 | 0.52 | 0.32 | 0.11 | 0.00 | 0.00 | 0.00 |
| | (C) Temp = 600 °C | | | | | | (C) Temp = 600 °C | | | | | | (C) Temp = 600 °C | | | | | |
| CO | 0.13 | 0.07 | 0.39 | 0.27 | 0.14 | 0.00 | 0.18 | 0.31 | 0.35 | 0.22 | 0.09 | 0.00 | 0.19 | 0.31 | 0.35 | 0.21 | 0.09 | 0.00 |
| $CO_2$ | 0.19 | 0.03 | 0.52 | 0.72 | 0.89 | 1.00 | 0.27 | 0.43 | 0.61 | 0.78 | 0.91 | 1.00 | 0.29 | 0.45 | 0.62 | 0.78 | 0.91 | 1.00 |
| $CH_4$ | 0.07 | 0.09 | 0.04 | 0.01 | 0.00 | 0.00 | 0.10 | 0.08 | 0.04 | 0.01 | 0.00 | 0.00 | 0.09 | 0.07 | 0.04 | 0.01 | 0.00 | 0.00 |
| C | 0.62 | 0.82 | 0.05 | 0.00 | 0.00 | 0.00 | 0.46 | 0.18 | 0.00 | 0.00 | 0.00 | 0.00 | 0.43 | 0.17 | 0.00 | 0.00 | 0.00 | 0.00 |
| | (D) Temp = 700 °C | | | | | | (D) Temp = 700 °C | | | | | | (D) Temp = 700 °C | | | | | |
| CO | 0.37 | 0.16 | 0.57 | 0.34 | 0.15 | 0.00 | 0.52 | 0.68 | 0.48 | 0.29 | 0.13 | 0.00 | 0.55 | 0.66 | 0.46 | 0.28 | 0.13 | 0.00 |
| $CO_2$ | 0.12 | 0.02 | 0.43 | 0.66 | 0.85 | 1.00 | 0.17 | 0.30 | 0.52 | 0.71 | 0.82 | 1.00 | 0.18 | 0.32 | 0.54 | 0.72 | 0.87 | 1.00 |
| $CH_4$ | 0.03 | 0.04 | 0.00 | 0.00 | 0.00 | 0.00 | 0.05 | 0.02 | 0.00 | 0.00 | 0.00 | 0.00 | 0.04 | 0.02 | 0.00 | 0.00 | 0.00 | 0.00 |
| C | 0.48 | 0.79 | 0.00 | 0.00 | 0.00 | 0.00 | 0.26 | 0.00 | 0.00 | 0.00 | 0.00 | 0.00 | 0.23 | 0.00 | 0.00 | 0.00 | 0.00 | 0.00 |
| | (E) Temp = 800 °C | | | | | | (E) Temp = 800 °C | | | | | | (E) Temp = 800 °C | | | | | |
| CO | 0.60 | 0.21 | 0.62 | 0.39 | 0.18 | 0.00 | 0.85 | 0.75 | 0.53 | 0.34 | 0.16 | 0.00 | 0.89 | 0.73 | 0.52 | 0.33 | 0.16 | 0.00 |
| $CO_2$ | 0.04 | 0.00 | 0.38 | 0.61 | 0.82 | 1.00 | 0.05 | 0.25 | 0.47 | 0.66 | 0.84 | 1.00 | 0.06 | 0.27 | 0.48 | 0.67 | 0.84 | 1.00 |
| $CH_4$ | 0.02 | 0.02 | 0.00 | 0.00 | 0.00 | 0.00 | 0.02 | 0.00 | 0.00 | 0.00 | 0.00 | 0.00 | 0.02 | 0.00 | 0.00 | 0.00 | 0.00 | 0.00 |
| C | 0.35 | 0.77 | 0.00 | 0.00 | 0.00 | 0.00 | 0.08 | 0.00 | 0.00 | 0.00 | 0.00 | 0.00 | 0.03 | 0.00 | 0.00 | 0.00 | 0.00 | 0.00 |
| | (F) Temp = 900 °C | | | | | | (F) Temp = 900 °C | | | | | | (F) Temp = 900 °C | | | | | |
| CO | 0.68 | 0.22 | 0.66 | 0.43 | 0.21 | 0.00 | 0.97 | 0.78 | 0.58 | 0.38 | 0.19 | 0.00 | 0.96 | 0.76 | 0.56 | 0.37 | 0.18 | 0.00 |
| $CO_2$ | 0.01 | 0.00 | 0.35 | 0.57 | 0.79 | 1.00 | 0.01 | 0.22 | 0.42 | 0.62 | 0.81 | 1.00 | 0.03 | 0.24 | 0.44 | 0.63 | 0.82 | 1.00 |
| $CH_4$ | 0.01 | 0.01 | 0.00 | 0.00 | 0.00 | 0.00 | 0.01 | 0.00 | 0.00 | 0.00 | 0.00 | 0.00 | 0.00 | 0.00 | 0.00 | 0.00 | 0.00 | 0.00 |
| C | 0.30 | 0.77 | 0.00 | 0.00 | 0.00 | 0.00 | 0.01 | 0.00 | 0.00 | 0.00 | 0.00 | 0.00 | 0.00 | 0.00 | 0.00 | 0.00 | 0.00 | 0.00 |
| | (G) Temp = 1000 °C | | | | | | (G) Temp = 1000 °C | | | | | | (G) Temp = 1000 °C | | | | | |
| CO | 0.70 | 0.91 | 0.65 | 0.46 | 0.23 | 0.00 | 0.99 | 0.81 | 0.61 | 0.41 | 0.21 | 0.00 | 0.97 | 0.79 | 0.60 | 0.40 | 0.20 | 0.00 |
| $CO_2$ | 0.00 | 0.09 | 0.32 | 0.54 | 0.77 | 1.00 | 0.01 | 0.19 | 0.39 | 0.59 | 0.79 | 1.00 | 0.03 | 0.21 | 0.40 | 0.60 | 0.80 | 1.00 |
| $CH_4$ | 0.00 | 0.00 | 0.00 | 0.00 | 0.00 | 0.00 | 0.00 | 0.00 | 0.00 | 0.00 | 0.00 | 0.00 | 0.00 | 0.00 | 0.00 | 0.00 | 0.00 | 0.00 |
| C | 0.29 | 0.00 | 0.00 | 0.00 | 0.00 | 0.00 | 0.00 | 0.00 | 0.00 | 0.00 | 0.00 | 0.00 | 0.00 | 0.00 | 0.00 | 0.00 | 0.00 | 0.00 |

Table 4.12

**Distribution of Hydrogen in the Gasification Mixture Among Various Chemical Species (Gasification with Air + 10% mole/mole Steam Mixture)**

| | Biomass: Saw Dust | | | | | | Biomass: Rice Husk | | | | | | Biomass: Bamboo Dust | | | | | |
|---|---|---|---|---|---|---|---|---|---|---|---|---|---|---|---|---|---|---|
| | (A) Temp = 400 °C | | | | | | (A) Temp = 400 °C | | | | | | (A) Temp = 400 °C | | | | | |
| AR | 0 | 0.2 | 0.4 | 0.6 | 0.8 | 1 | 0 | 0.2 | 0.4 | 0.6 | 0.8 | 1 | 0 | 0.2 | 0.4 | 0.6 | 0.8 | 1 |
| $H_2$ | 0.11 | 0.14 | 0.15 | 0.16 | 0.15 | 0.00 | 0.11 | 0.13 | 0.15 | 0.15 | 0.14 | 0.00 | 0.11 | 0.13 | 0.14 | 0.15 | 0.13 | 0.00 |
| $H_2O$ | 0.50 | 0.58 | 0.62 | 0.65 | 0.75 | 1.00 | 0.50 | 0.57 | 0.60 | 0.63 | 0.79 | 1.00 | 0.53 | 0.58 | 0.61 | 0.63 | 0.80 | 1.00 |
| $CH_4$ | 0.38 | 0.28 | 0.23 | 0.20 | 0.10 | 0.00 | 0.39 | 0.30 | 0.25 | 0.22 | 0.07 | 0.00 | 0.36 | 0.29 | 0.25 | 0.22 | 0.07 | 0.00 |
| | (B) Temp = 500 °C | | | | | | (B) Temp = 500 °C | | | | | | (B) Temp = 500 °C | | | | | |
| $H_2$ | 0.28 | 0.33 | 0.34 | 0.32 | 0.18 | 0.00 | 0.28 | 0.33 | 0.35 | 0.34 | 0.23 | 0.00 | 0.28 | 0.32 | 0.34 | 0.34 | 0.23 | 0.00 |
| $H_2O$ | 0.42 | 0.45 | 0.47 | 0.62 | 0.81 | 1.00 | 0.41 | 0.45 | 0.47 | 0.56 | 0.76 | 1.00 | 0.43 | 0.46 | 0.47 | 0.57 | 0.77 | 1.00 |
| $CH_4$ | 0.30 | 0.22 | 0.19 | 0.07 | 0.00 | *0.00* | 0.30 | 0.23 | 0.19 | 0.10 | 0.01 | 0.00 | 0.29 | 0.29 | 0.18 | 0.10 | 0.01 | 0.00 |
| | (C) Temp = 600 °C | | | | | | (C) Temp = 600 °C | | | | | | (C) Temp = 600 °C | | | | | |
| $H_2$ | 0.52 | 0.57 | 0.56 | 0.38 | 0.18 | 0.00 | 0.52 | 0.57 | 0.57 | 0.43 | 0.29 | 0.00 | 0.52 | 0.57 | 0.57 | 0.42 | 0.22 | 0.00 |
| $H_2O$ | 0.29 | 0.30 | 0.39 | 0.62 | 0.83 | 1.00 | 0.29 | 0.30 | 0.36 | 0.56 | 0.78 | 1.00 | 0.30 | 0.30 | 0.37 | 0.57 | 0.79 | 1.00 |
| $CH_4$ | 0.19 | 0.13 | 0.06 | 0.00 | 0.00 | 0.00 | 0.19 | 0.13 | 0.07 | 0.01 | 0.00 | 0.00 | 0.18 | 0.13 | 0.06 | 0.01 | 0.00 | 0.00 |
| | (D) Temp = 700 °C | | | | | | (D) Temp = 700 °C | | | | | | (D) Temp = 700 °C | | | | | |
| $H_2$ | 0.76 | 0.78 | 0.57 | 0.35 | 0.16 | 0.00 | 0.76 | 0.76 | 0.60 | 0.40 | 0.20 | 0.00 | 0.76 | 0.75 | 0.58 | 0.39 | 0.19 | 0.00 |
| $H_2O$ | 0.15 | 0.17 | 0.42 | 0.65 | 0.84 | 1.00 | 0.15 | 0.20 | 0.40 | 0.60 | 0.81 | 1.00 | 0.16 | 0.22 | 0.41 | 0.61 | 0.81 | 1.00 |
| $CH_4$ | 0.09 | 0.05 | 0.00 | 0.00 | 0.00 | 0.00 | 0.09 | 0.03 | 0.00 | 0.00 | 0.00 | 0.00 | 0.09 | 0.03 | 0.00 | 0.00 | 0.00 | 0.00 |
| | (E) Temp = 800 °C | | | | | | (E) Temp = 800 °C | | | | | | (E) Temp = 800 °C | | | | | |
| $H_2$ | 0.91 | 0.80 | 0.53 | 0.32 | 0.14 | 0.00 | 0.91 | 0.77 | 0.56 | 0.36 | 0.17 | 0.00 | 0.91 | 0.75 | 0.54 | 0.35 | 0.17 | 0.00 |
| $H_2O$ | 0.05 | 0.19 | 0.47 | 0.68 | 0.86 | 1.00 | 0.05 | 0.23 | 0.44 | 0.64 | 0.83 | 1.00 | 0.06 | 0.25 | 0.46 | 0.65 | 0.83 | 1.00 |
| $CH_4$ | 0.04 | 0.00 | 0.00 | 0.00 | 0.00 | 0.00 | 0.04 | 0.00 | 0.00 | 0.00 | 0.00 | 0.00 | 0.04 | 0.00 | 0.00 | 0.00 | 0.00 | 0.00 |
| | (F) Temp = 900 °C | | | | | | (F) Temp = 900 °C | | | | | | (F) Temp = 900 °C | | | | | |
| $H_2$ | 0.97 | 0.78 | 0.50 | 0.29 | 0.13 | 0.00 | 0.91 | 0.77 | 0.56 | 0.36 | 0.17 | 0.00 | 0.95 | 0.72 | 0.50 | 0.32 | 0.15 | 0.00 |
| $H_2O$ | 0.02 | 0.22 | 0.50 | 0.71 | 0.87 | 1.00 | 0.05 | 0.23 | 0.44 | 0.64 | 0.83 | 1.00 | 0.04 | 0.28 | 0.50 | 0.68 | 0.85 | 1.00 |
| $CH_4$ | 0.02 | 0.00 | 0.00 | 0.00 | 0.00 | 0.00 | 0.04 | 0.00 | 0.00 | 0.00 | 0.00 | 0.00 | 0.01 | 0.00 | 0.00 | 0.00 | 0.00 | 0.00 |
| | (G) Temp = 1000 °C | | | | | | (G) Temp = 1000 °C | | | | | | (G) Temp = 1000 °C | | | | | |
| $H_2$ | 0.99 | 0.76 | 0.47 | 0.27 | 0.12 | 0.00 | 0.99 | 0.72 | 0.49 | 300.00 | 0.14 | 0.00 | 0.96 | 0.69 | 0.48 | 0.29 | 0.13 | 0.00 |
| $H_2O$ | 0.01 | 0.24 | 0.53 | 0.73 | 0.88 | 1.00 | 0.01 | 0.28 | 0.51 | 0.70 | 0.86 | 1.00 | 0.04 | 0.30 | 0.53 | 0.71 | 0.87 | 1.00 |
| $CH_4$ | 0.01 | 0.00 | 0.00 | 0.00 | 0.00 | 0.00 | 0.01 | 0.00 | 0.00 | 0.00 | 0.00 | 0.00 | 0.00 | 0.00 | 0.00 | 0.00 | 0.00 | 0.00 |

Table 4.13

**Distribution of Carbon in the Gasification Mixture Among Various Chemical Species (Gasification with Air + 30% mole/mole Steam Mixture)**

| | Biomass: Saw Dust | | | | | | Biomass: Rice Husk | | | | | | Biomass: Bamboo Dust | | | | | |
|---|---|---|---|---|---|---|---|---|---|---|---|---|---|---|---|---|---|---|
| | (A) Temp = 400 °C | | | | | | (A) Temp = 400 °C | | | | | | (A) Temp = 400 °C | | | | | |
| AR | 0 | 0.2 | 0.4 | 0.6 | 0.8 | 1 | 0 | 0.2 | 0.4 | 0.6 | 0.8 | 1 | 0 | 0.2 | 0.4 | 0.6 | 0.8 | 1 |
| CO | 0.00 | 0.01 | 0.01 | 0.02 | 0.01 | 0.00 | 0.00 | 0.01 | 0.01 | 0.01 | 0.01 | 0.00 | 0.01 | 0.01 | 0.01 | 0.01 | 0.01 | 0.00 |
| $CO_2$ | 0.17 | 0.41 | 0.65 | 0.85 | 0.95 | 1.00 | 0.24 | 0.48 | 0.72 | 0.85 | 0.95 | 1.00 | 0.27 | 0.50 | 0.73 | 0.86 | 0.96 | 1.00 |
| $CH_4$ | 0.14 | 0.15 | 0.17 | 0.14 | 0.04 | 0.00 | 0.20 | 0.20 | 0.22 | 0.13 | 0.04 | 0.00 | 0.18 | 0.19 | 0.21 | 0.13 | 0.04 | 0.00 |
| C | 0.69 | 0.44 | 0.17 | 0.00 | 0.00 | 0.00 | 0.55 | 0.31 | 0.04 | 0.00 | 0.00 | 0.00 | 0.54 | 0.30 | 0.05 | 0.00 | 0.00 | 0.00 |
| | (B) Temp = 500 °C | | | | | | (B) Temp = 500 °C | | | | | | (B) Temp = 500 °C | | | | | |
| CO | 0.03 | 0.06 | 0.10 | 0.09 | 0.04 | 0.00 | 0.04 | 0.08 | 0.10 | 0.08 | 0.04 | 0.00 | 0.04 | 0.07 | 0.10 | 0.08 | 0.04 | 0.00 |
| $CO_2$ | 0.19 | 0.44 | 0.70 | 0.86 | 0.96 | 1.00 | 0.27 | 0.53 | 0.76 | 0.88 | 0.96 | 1.00 | 0.30 | 0.54 | 0.77 | 0.88 | 0.96 | 1.00 |
| $CH_4$ | 0.11 | 0.11 | 0.13 | 0.05 | 0.00 | *0.00* | 0.16 | 0.15 | 0.14 | 0.04 | 0.00 | 0.00 | 0.14 | 0.15 | 0.14 | 0.04 | 0.00 | 0.00 |
| C | 0.67 | 0.38 | 0.08 | 0.00 | 0.00 | 0.00 | 0.53 | 0.25 | 0.00 | 0.00 | 0.00 | 0.00 | 0.52 | 0.24 | 0.00 | 0.00 | 0.00 | 0.00 |
| | (C) Temp = 600 °C | | | | | | (C) Temp = 600 °C | | | | | | (C) Temp = 600 °C | | | | | |
| CO | 0.13 | 0.29 | 0.34 | 0.19 | 0.07 | 0.00 | 0.18 | 0.37 | 0.29 | 0.16 | 0.06 | 0.00 | 0.19 | 0.35 | 0.28 | 0.16 | 0.06 | 0.00 |
| $CO_2$ | 0.19 | 0.41 | 0.63 | 0.81 | 0.93 | 1.00 | 0.27 | 0.48 | 0.69 | 0.84 | 0.94 | 1.00 | 0.29 | 0.50 | 0.70 | 0.84 | 0.94 | 1.00 |
| $CH_4$ | 0.07 | 0.07 | 0.04 | 0.00 | 0.00 | 0.00 | 0.10 | 0.09 | 0.03 | 0.00 | 0.00 | 0.00 | 0.09 | 0.09 | 0.02 | 0.00 | 0.00 | 0.00 |
| C | 0.62 | 0.24 | 0.00 | 0.00 | 0.00 | 0.00 | 0.46 | 0.07 | 0.00 | 0.00 | 0.00 | 0.00 | 0.43 | 0.07 | 0.00 | 0.00 | 0.00 | 0.00 |
| | (D) Temp = 700 °C | | | | | | (D) Temp = 700 °C | | | | | | (D) Temp = 700 °C | | | | | |
| CO | 0.37 | 0.72 | 0.45 | 0.25 | 0.10 | 0.00 | 0.52 | 0.62 | 0.39 | 0.22 | 0.09 | 0.00 | 0.55 | 0.60 | 0.38 | 0.21 | 0.09 | 0.00 |
| $CO_2$ | 0.12 | 0.26 | 0.55 | 0.75 | 0.90 | 1.00 | 0.17 | 0.37 | 0.61 | 0.78 | 0.91 | 1.00 | 0.18 | 0.39 | 0.62 | 0.79 | 0.91 | 1.00 |
| $CH_4$ | 0.03 | 0.02 | 0.00 | 0.00 | 0.00 | 0.00 | 0.05 | 0.01 | 0.00 | 0.00 | 0.00 | 0.00 | 0.04 | 0.01 | 0.00 | 0.00 | 0.00 | 0.00 |
| C | 0.48 | 0.00 | 0.00 | 0.00 | 0.00 | 0.00 | 0.26 | 0.00 | 0.00 | 0.00 | 0.00 | 0.00 | 0.23 | 0.00 | 0.00 | 0.00 | 0.00 | 0.00 |
| | (E) Temp = 800 °C | | | | | | (E) Temp = 800 °C | | | | | | (E) Temp = 800 °C | | | | | |
| CO | 0.60 | 0.79 | 0.51 | 0.30 | 0.13 | 0.00 | 0.85 | 0.68 | 0.45 | 0.27 | 0.12 | 0.00 | 0.89 | 0.67 | 0.44 | 0.26 | 0.12 | 0.00 |
| $CO_2$ | 0.04 | 0.21 | 0.49 | 0.70 | 0.87 | 1.00 | 0.05 | 0.32 | 0.55 | 0.73 | 0.88 | 1.00 | 0.06 | 0.33 | 0.56 | 0.74 | 0.88 | 1.00 |
| $CH_4$ | 0.02 | 0.00 | 0.00 | 0.00 | 0.00 | 0.00 | 0.02 | 0.00 | 0.00 | 0.00 | 0.00 | 0.00 | 0.02 | 0.00 | 0.00 | 0.00 | 0.00 | 0.00 |
| C | 0.35 | 0.00 | 0.00 | 0.00 | 0.00 | 0.00 | 0.08 | 0.00 | 0.00 | 0.00 | 0.00 | 0.00 | 0.03 | 0.00 | 0.00 | 0.00 | 0.00 | 0.00 |
| | (F) Temp = 900 °C | | | | | | (F) Temp = 900 °C | | | | | | (F) Temp = 900 °C | | | | | |
| CO | 0.68 | 0.82 | 0.56 | 0.34 | 0.16 | 0.00 | 0.97 | 0.72 | 0.50 | 0.31 | 0.14 | 0.00 | 0.96 | 0.71 | 0.49 | 0.30 | 0.14 | 0.00 |
| $CO_2$ | 0.01 | 0.18 | 0.44 | 0.66 | 0.84 | 1.00 | 0.01 | 0.28 | 0.50 | 0.69 | 0.86 | 1.00 | 0.03 | 0.29 | 0.51 | 0.70 | 0.86 | 1.00 |
| $CH_4$ | 0.01 | 0.00 | 0.00 | 0.00 | 0.00 | 0.00 | 0.01 | 0.00 | 0.00 | 0.00 | 0.00 | 0.00 | 0.00 | 0.00 | 0.00 | 0.00 | 0.00 | 0.00 |
| C | 0.30 | 0.00 | 0.00 | 0.00 | 0.00 | 0.00 | 0.01 | 0.00 | 0.00 | 0.00 | 0.00 | 0.00 | 0.00 | 0.00 | 0.00 | 0.00 | 0.00 | 0.00 |
| | (G) Temp = 1000 °C | | | | | | (G) Temp = 1000 °C | | | | | | (G) Temp = 1000 °C | | | | | |
| CO | 0.70 | 0.84 | 0.59 | 0.38 | 0.18 | 0.00 | 0.99 | 0.76 | 0.54 | 0.35 | 0.17 | 0.00 | 0.97 | 0.74 | 0.53 | 0.34 | 0.16 | 0.00 |
| $CO_2$ | 0.00 | 0.16 | 0.41 | 0.62 | 0.82 | 1.00 | 0.01 | 0.25 | 0.46 | 0.66 | 0.83 | 1.00 | 0.03 | 0.26 | 0.47 | 0.66 | 0.84 | 1.00 |
| $CH_4$ | 0.00 | 0.00 | 0.00 | 0.00 | 0.00 | 0.00 | 0.00 | 0.00 | 0.00 | 0.00 | 0.00 | 0.00 | 0.00 | 0.00 | 0.00 | 0.00 | 0.00 | 0.00 |
| C | 0.29 | 0.00 | 0.00 | 0.00 | 0.00 | 0.00 | 0.00 | 0.00 | 0.00 | 0.00 | 0.00 | 0.00 | 0.00 | 0.00 | 0.00 | 0.00 | 0.00 | 0.00 |

Table 4.14

**Distribution of Hydrogen in the Gasification Mixture Among Various Chemical Species (Gasification with Air + 30% mole/mole Steam Mixture)**

| | Biomass: Saw Dust | | | | | | Biomass: Rice Husk | | | | | | Biomass: Bamboo Dust | | | | | |
|---|---|---|---|---|---|---|---|---|---|---|---|---|---|---|---|---|---|---|
| | (A) Temp = 400 °C | | | | | | (A) Temp = 400 °C | | | | | | (A) Temp = 400 °C | | | | | |
| AR | 0 | 0.2 | 0.4 | 0.6 | 0.8 | 1 | 0 | 0.2 | 0.4 | 0.6 | 0.8 | 1 | 0 | 0.2 | 0.4 | 0.6 | 0.8 | 1 |
| $H_2$ | 0.11 | 0.14 | 0.14 | 0.15 | 0.12 | 0.00 | 0.11 | 0.14 | 0.14 | 0.14 | 0.11 | 0.00 | 0.11 | 0.13 | 0.14 | 0.14 | 0.11 | 0.00 |
| $H_2O$ | 0.50 | 0.57 | 0.60 | 0.68 | 0.84 | 1.00 | 0.50 | 0.55 | 0.59 | 0.72 | 0.85 | 1.00 | 0.53 | 0.57 | 0.59 | 0.72 | 0.86 | 1.00 |
| $CH_4$ | 0.38 | 0.29 | 0.26 | 0.18 | 0.04 | 0.00 | 0.39 | 0.30 | 0.28 | 0.14 | 0.03 | 0.00 | 0.36 | 0.30 | 0.27 | 0.14 | 0.03 | 0.00 |
| | (B) Temp = 500 °C | | | | | | (B) Temp = 500 °C | | | | | | (B) Temp = 500 °C | | | | | |
| $H_2$ | 0.28 | 0.33 | 0.34 | 0.32 | 0.18 | 0.00 | 0.28 | 0.34 | 0.34 | 0.30 | 0.16 | 0.00 | 0.28 | 0.32 | 0.33 | 0.29 | 0.16 | 0.00 |
| $H_2O$ | 0.42 | 0.45 | 0.47 | 0.62 | 0.81 | 1.00 | 0.41 | 0.44 | 0.49 | 0.66 | 0.83 | 1.00 | 0.43 | 0.45 | 0.49 | 0.66 | 0.84 | 1.00 |
| $CH_4$ | 0.30 | 0.22 | 0.19 | 0.07 | 0.00 | 0.00 | 0.30 | 0.23 | 0.18 | 0.05 | 0.00 | 0.00 | 0.29 | 0.23 | 0.18 | 0.05 | 0.00 | 0.00 |
| | (C) Temp = 600 °C | | | | | | (C) Temp = 600 °C | | | | | | (C) Temp = 600 °C | | | | | |
| $H_2$ | 0.52 | 0.57 | 0.59 | 0.38 | 0.18 | 0.00 | 0.52 | 0.59 | 0.51 | 0.34 | 0.16 | 0.00 | 0.52 | 0.56 | 0.51 | 0.33 | 0.15 | 0.00 |
| $H_2O$ | 0.29 | 0.30 | 0.39 | 0.62 | 0.83 | 1.00 | 0.29 | 0.28 | 0.46 | 0.66 | 0.85 | 1.00 | 0.30 | 0.30 | 0.47 | 0.67 | 0.85 | 1.00 |
| $CH_4$ | 0.19 | 0.13 | 0.06 | 0.00 | 0.00 | 0.00 | 0.19 | 0.13 | 0.03 | 0.00 | 0.00 | 0.00 | 0.18 | 0.13 | 0.03 | 0.00 | 0.00 | 0.00 |
| | (D) Temp = 700 °C | | | | | | (D) Temp = 700 °C | | | | | | (D) Temp = 700 °C | | | | | |
| $H_2$ | 0.76 | 0.78 | 0.57 | 0.35 | 0.16 | 0.00 | 0.76 | 0.70 | 0.47 | 0.29 | 0.13 | 0.00 | 0.76 | 0.70 | 0.50 | 0.31 | 0.14 | 0.00 |
| $H_2O$ | 0.15 | 0.17 | 0.42 | 0.65 | 0.84 | 1.00 | 0.15 | 0.30 | 0.53 | 0.73 | 0.87 | 1.00 | 0.16 | 0.28 | 0.50 | 0.69 | 0.86 | 1.00 |
| $CH_4$ | 0.09 | 0.05 | 0.00 | 0.00 | 0.00 | 0.00 | 0.09 | 0.00 | 0.00 | 0.00 | 0.00 | 0.00 | 0.09 | 0.02 | 0.00 | 0.00 | 0.00 | 0.00 |
| | (E) Temp = 800 °C | | | | | | (E) Temp = 800 °C | | | | | | (E) Temp = 800 °C | | | | | |
| $H_2$ | 0.91 | 0.80 | 0.53 | 0.32 | 0.14 | 0.00 | 0.91 | 0.70 | 0.47 | 0.29 | 0.13 | 0.00 | 0.91 | 0.69 | 0.46 | 0.28 | 0.13 | 0.00 |
| $H_2O$ | 0.05 | 0.19 | 0.47 | 0.68 | 0.86 | 1.00 | 0.05 | 0.30 | 0.53 | 0.72 | 0.87 | 1.00 | 0.06 | 0.31 | 0.54 | 0.72 | 0.87 | 1.00 |
| $CH_4$ | 0.04 | 0.00 | 0.00 | 0.00 | 0.00 | 0.00 | 0.04 | 0.00 | 0.00 | 0.00 | 0.00 | 0.00 | 0.04 | 0.00 | 0.00 | 0.00 | 0.00 | 0.00 |
| | (F) Temp = 900 °C | | | | | | (F) Temp = 900 °C | | | | | | (F) Temp = 900 °C | | | | | |
| $H_2$ | 0.97 | 0.78 | 0.50 | 0.29 | 0.13 | 0.00 | 0.97 | 0.68 | 0.44 | 0.26 | 0.12 | 0.00 | 0.95 | 0.68 | 0.43 | 0.26 | 0.26 | 0.00 |
| $H_2O$ | 0.02 | 0.29 | 0.50 | 0.71 | 0.87 | 1.00 | 0.02 | 0.32 | 0.56 | 0.74 | 0.88 | 1.00 | 0.04 | 0.34 | 0.57 | 0.74 | 0.74 | 1.00 |
| $CH_4$ | 0.02 | 0.00 | 0.00 | 0.00 | 0.00 | 0.00 | 0.02 | 0.00 | 0.00 | 0.00 | 0.00 | 0.00 | 0.01 | 0.00 | 0.00 | 0.00 | 0.00 | 0.00 |
| | (G) Temp = 1000 °C | | | | | | (G) Temp = 1000 °C | | | | | | (G) Temp = 1000 °C | | | | | |
| $H_2$ | 0.99 | 0.76 | 0.47 | 0.27 | 0.12 | 0.00 | 0.99 | 0.65 | 0.42 | 0.24 | 0.11 | 0.00 | 0.96 | 0.63 | 0.41 | 0.24 | 0.11 | 0.00 |
| $H_2O$ | 0.01 | 0.24 | 0.53 | 0.73 | 0.88 | 1.00 | 0.01 | 0.35 | 0.58 | 0.76 | 0.89 | 1.00 | 0.04 | 0.37 | 0.59 | 0.76 | 0.89 | 1.00 |
| $CH_4$ | 0.01 | 0.00 | 0.00 | 0.00 | 0.00 | 0.00 | 0.01 | 0.00 | 0.00 | 0.00 | 0.00 | 0.00 | 0.00 | 0.00 | 0.00 | 0.00 | 0.00 | 0.00 |

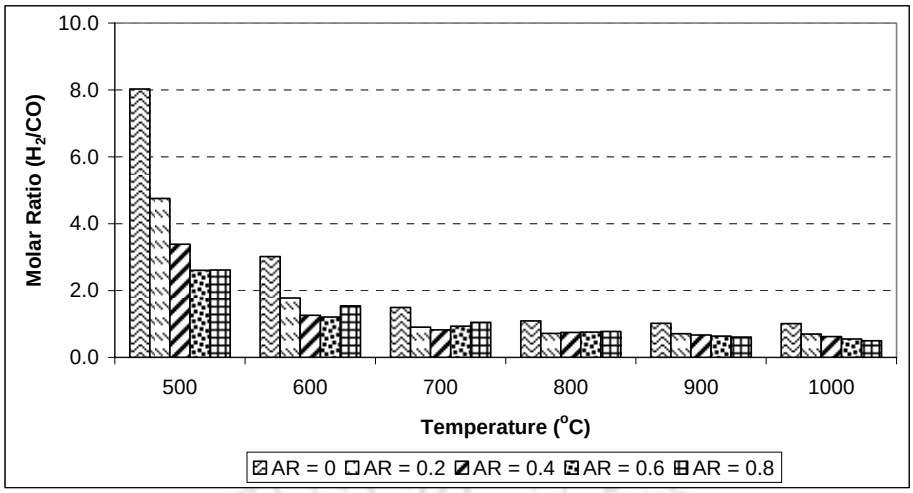


(A)

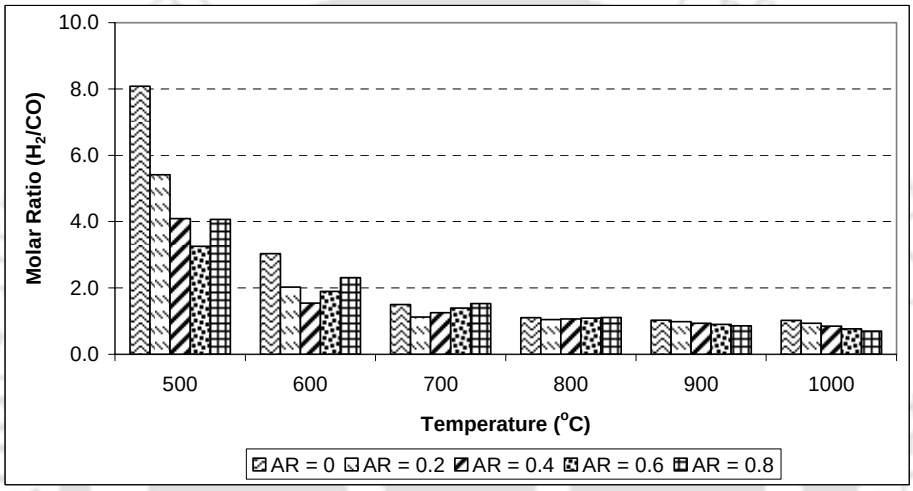


(B)

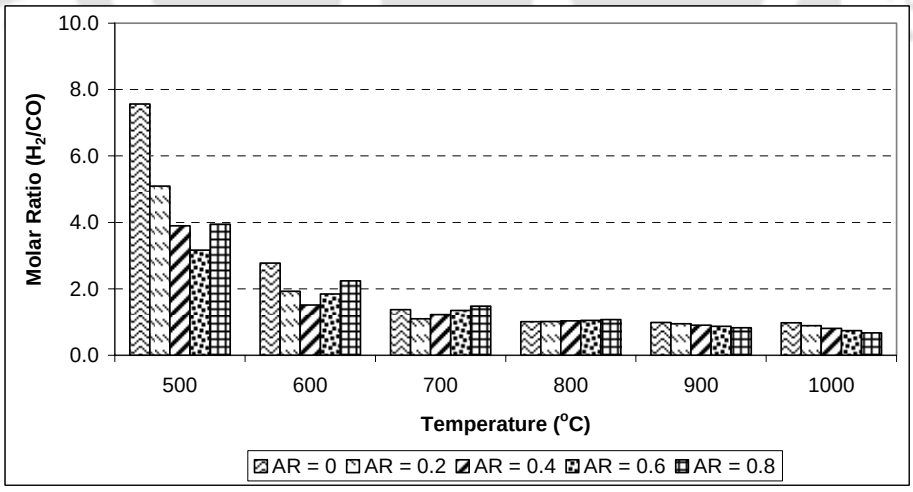


(C)

**Figure 4.1:** Variation in $H_2$/CO ratio in producer gas resulting from gasification of different biomasses (with air alone) at various temperatures and air ratios. (A) Biomass: Saw Dust; (B) Biomass: Rice Husk; (C) Biomass: Bamboo Dust

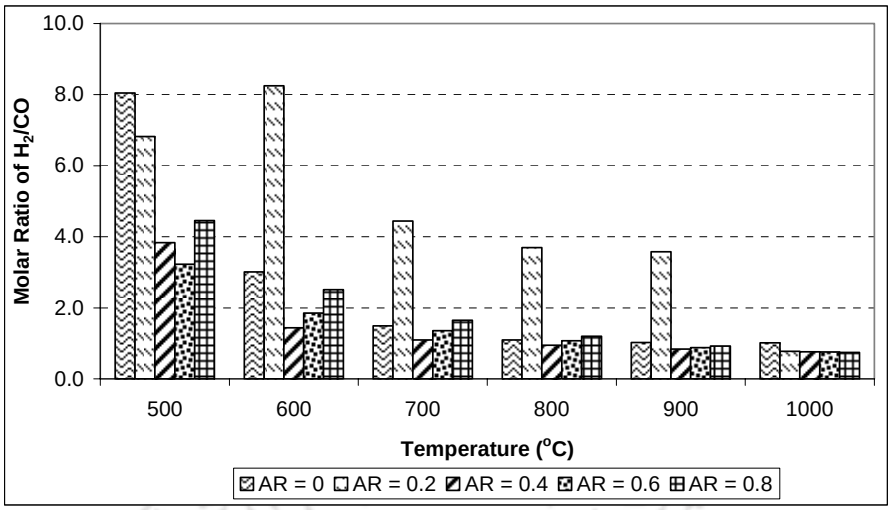


(A)

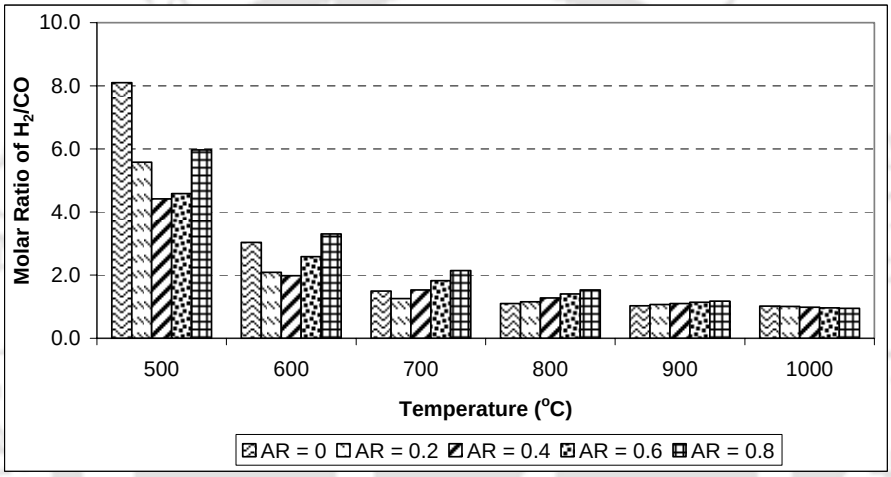


(B)

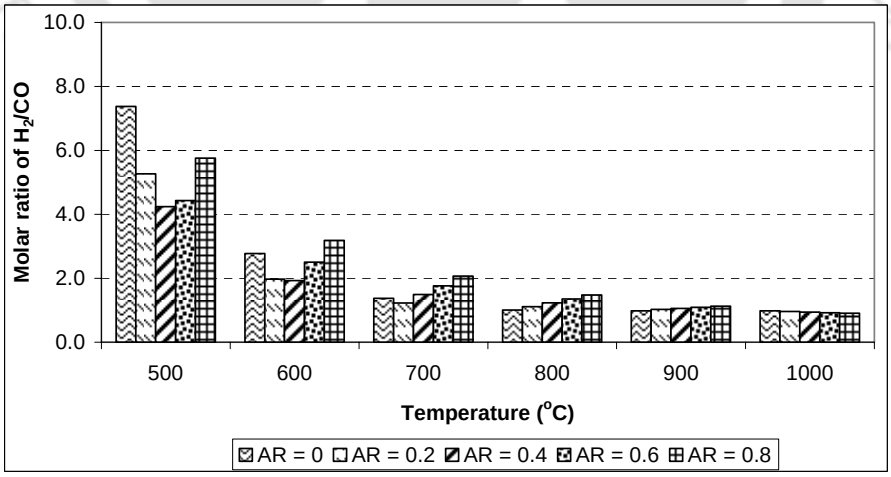


(C)

**Figure 4.2:** Variation in $H_2$/CO ratio in producer gas resulting from gasification of different biomasses (with air + 10% mole/mole steam mixture) at various temperatures and air ratios. (A) Biomass: Saw Dust; (B) Biomass: Rice Husk; (C) Biomass: Bamboo Dust

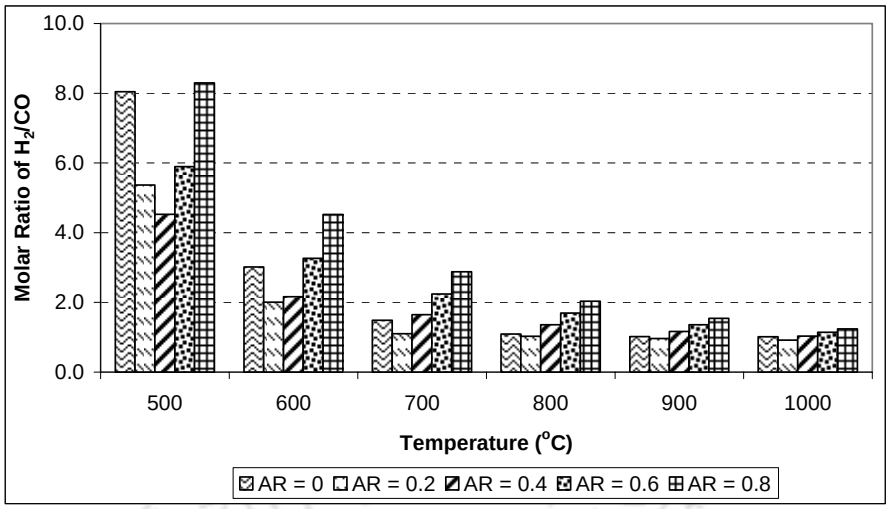


(A)

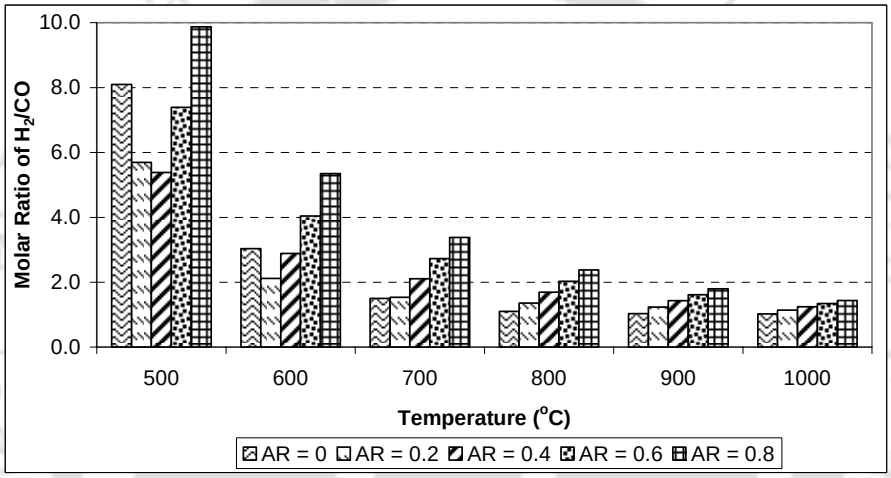


(B)

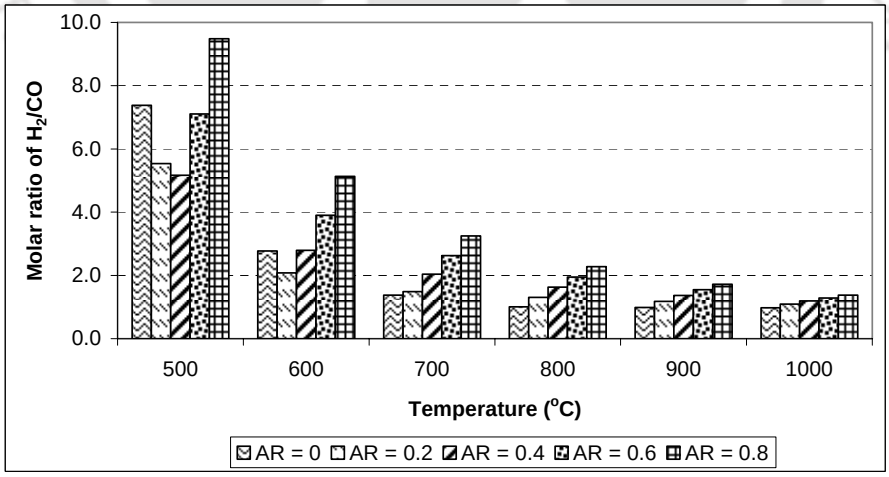


(C)

**Figure 4.3:** Variation in $H_2$/CO ratio in producer gas resulting from gasification of different biomasses (with air + 30% mole/mole steam mixture) at various temperatures and air ratios. (A) Biomass: Saw Dust; (B) Biomass: Rice Husk; (C) Biomass: Bamboo Dust

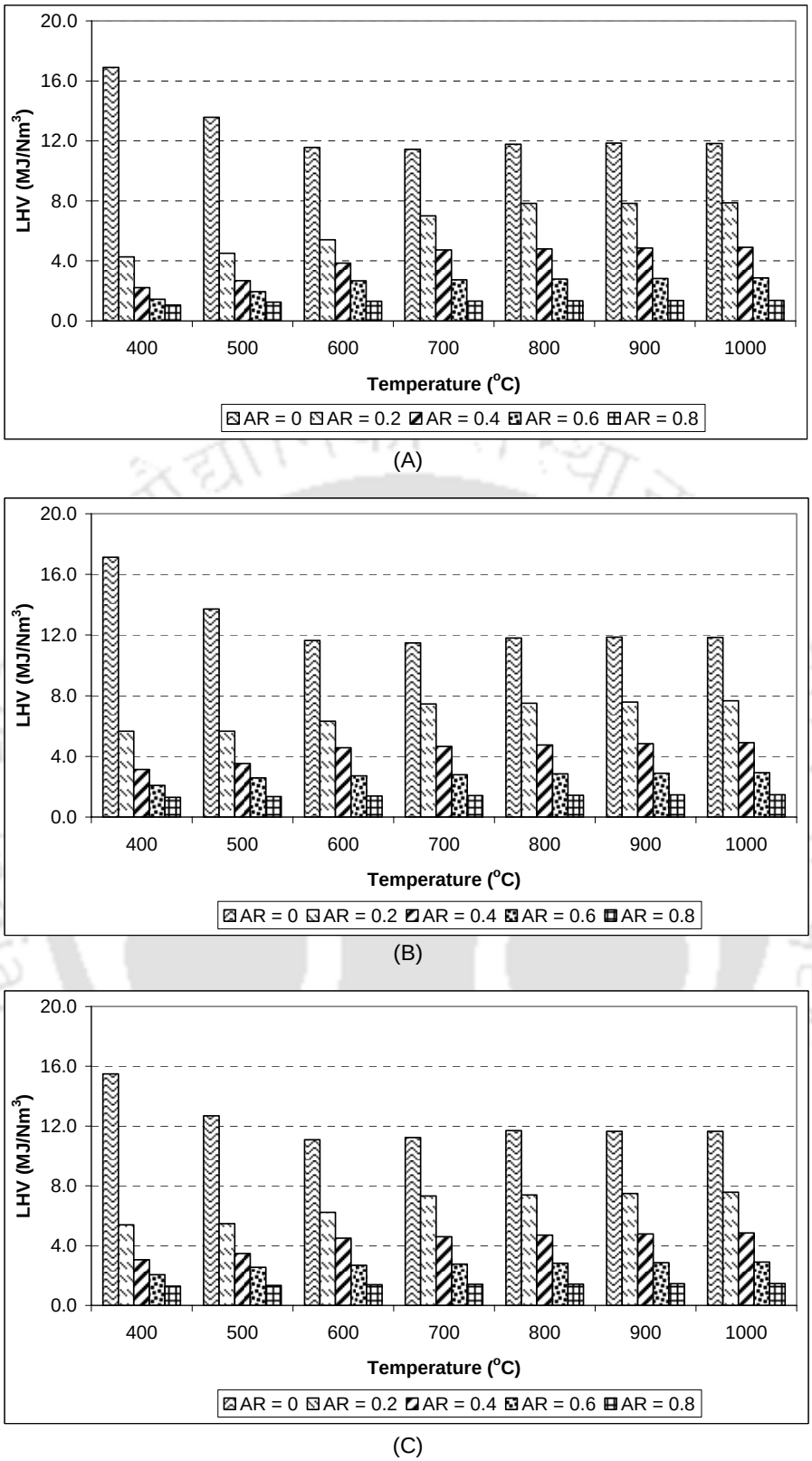


**Figure 4.4:** Variation in the LHV of producer gas obtained from gasification of different biomasses with air alone at various temperatures and air ratios. (A) Biomass: Saw Dust; (B) Biomass: Rice Husk; (C) Biomass: Bamboo Dust

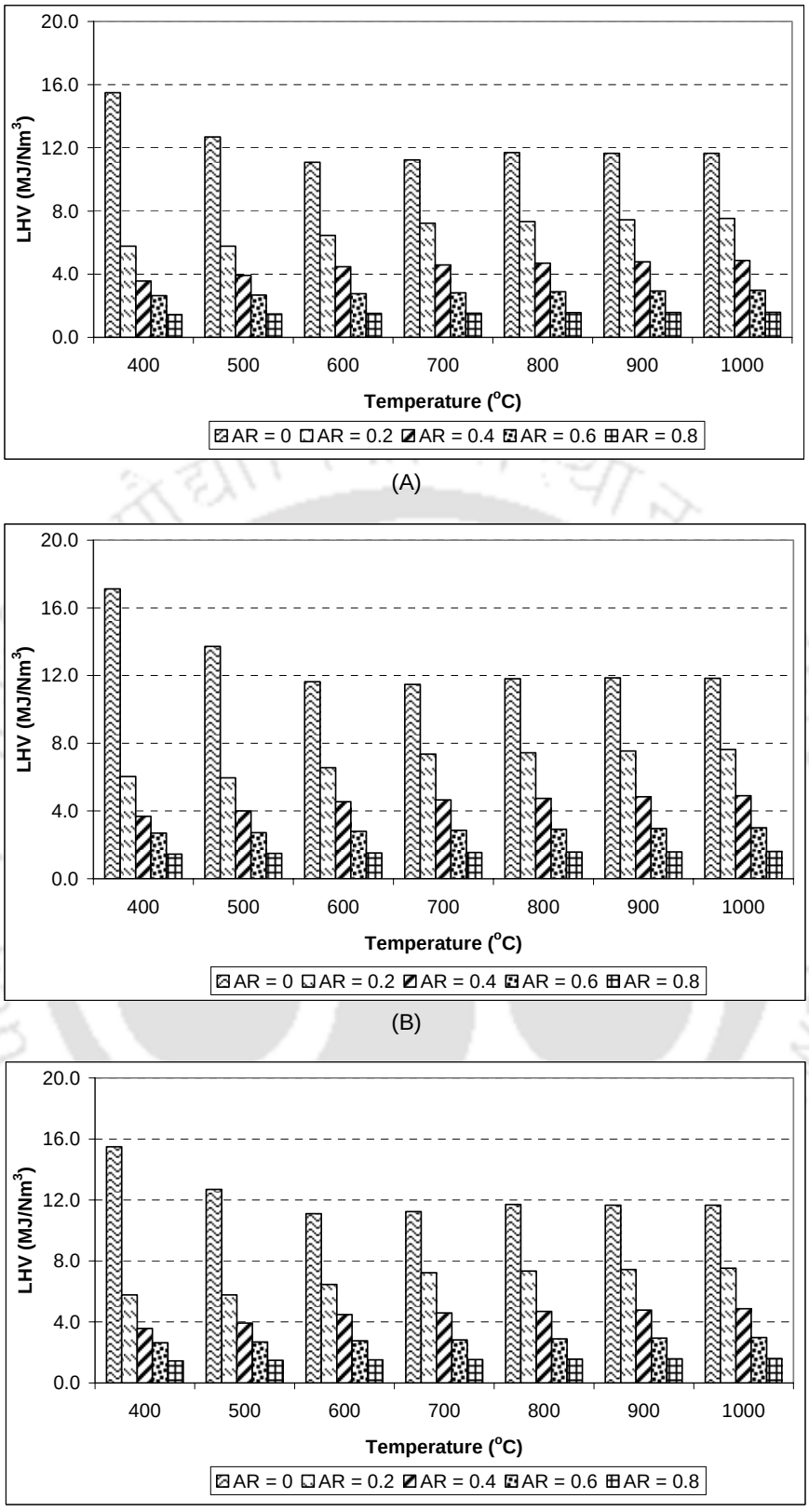


**Figure 4.5:** Variation in the LHV of producer gas obtained from gasification of different biomasses with air + 10% mole/mole steam at various temperatures and air ratios. (A) Biomass: Saw Dust; (B) Biomass: Rice Husk; (C) Biomass: Bamboo Dust

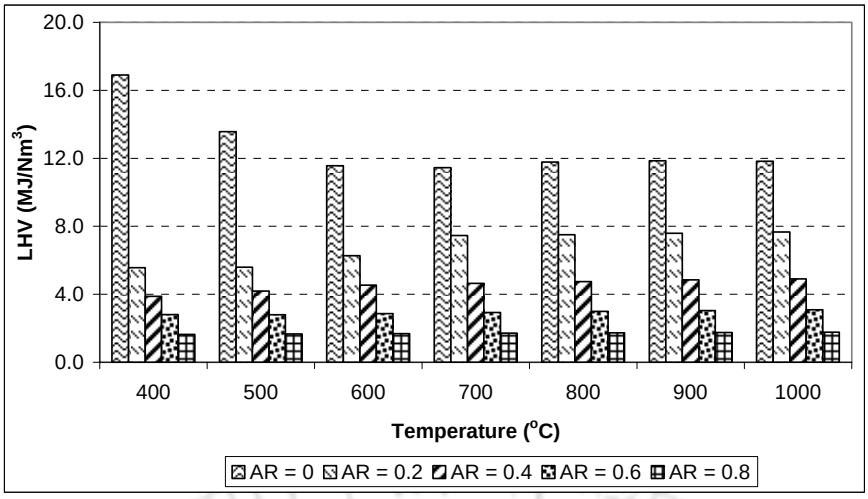


(A)

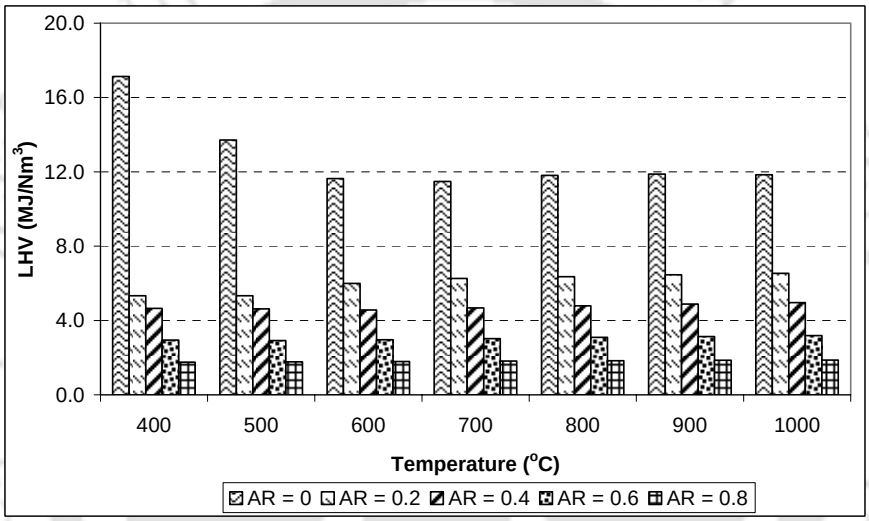


(B)

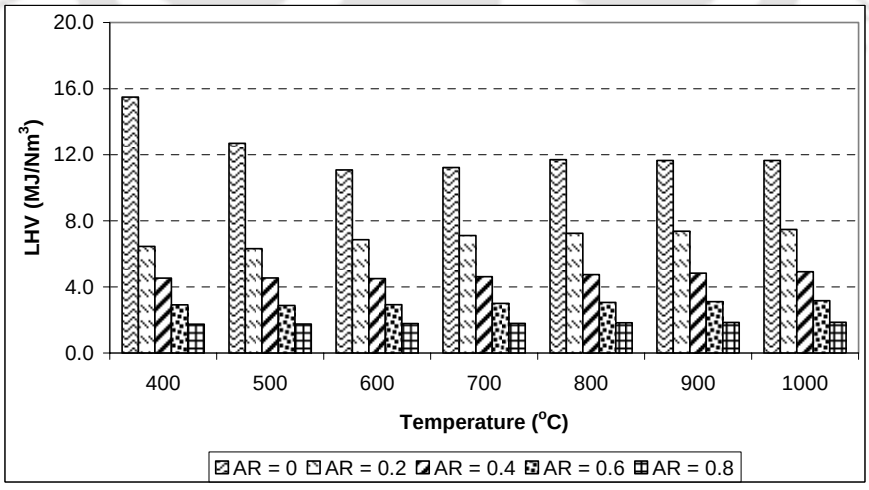


(C)

**Figure 4.6:** Variation in the LHV of producer gas obtained from gasification of different biomasses with air + 30% mole/mole steam at various temperatures and air ratios. (A) Biomass: Saw Dust; (B) Biomass: Rice Husk; (C) Biomass: Bamboo Dust

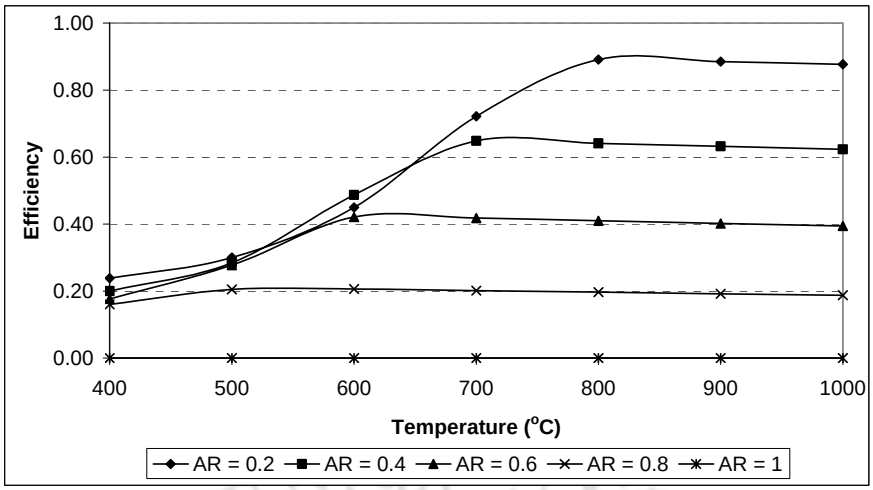


(A)

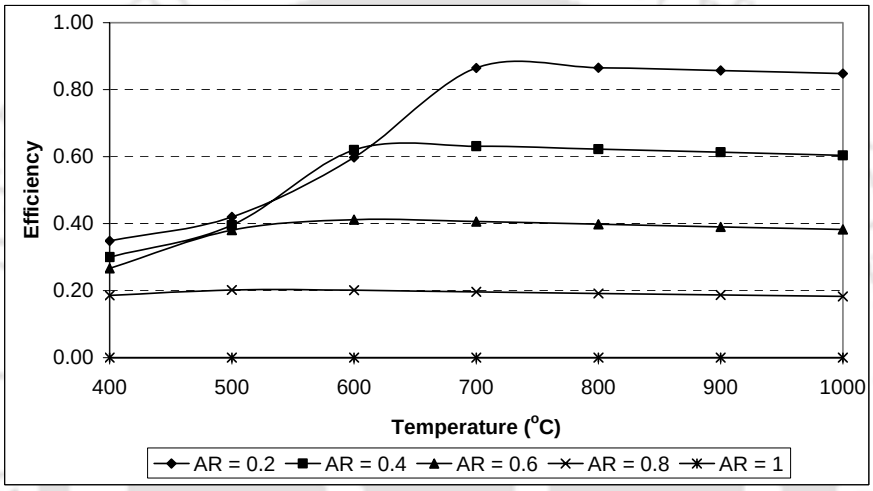


(B)

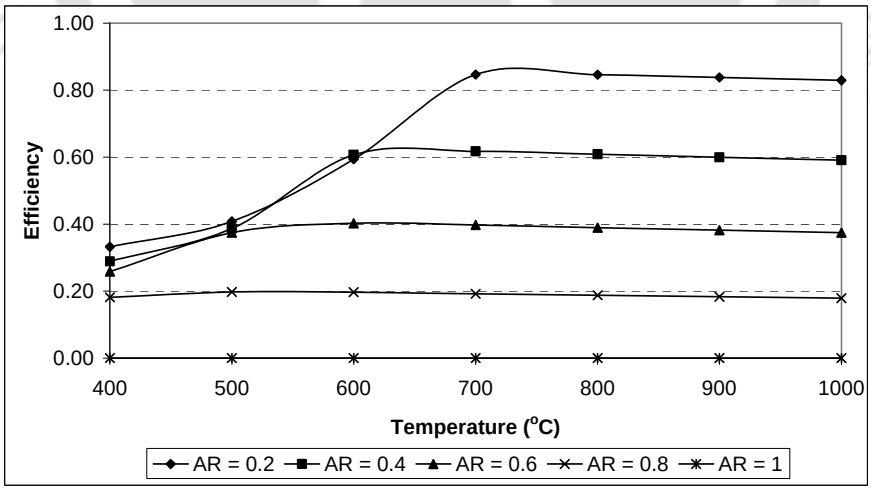


(C)

**Figure 4.7:** Theoretical efficiency of the gasification process with air as the gasification medium using different biomasses. (A) Biomass: Saw Dust; (B) Biomass: Rice Husk; (C) Biomass: Bamboo dust.

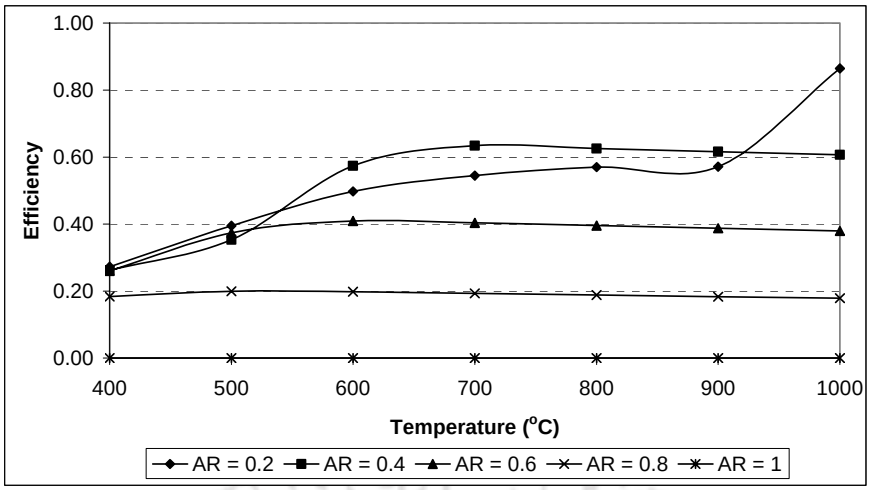


(A)

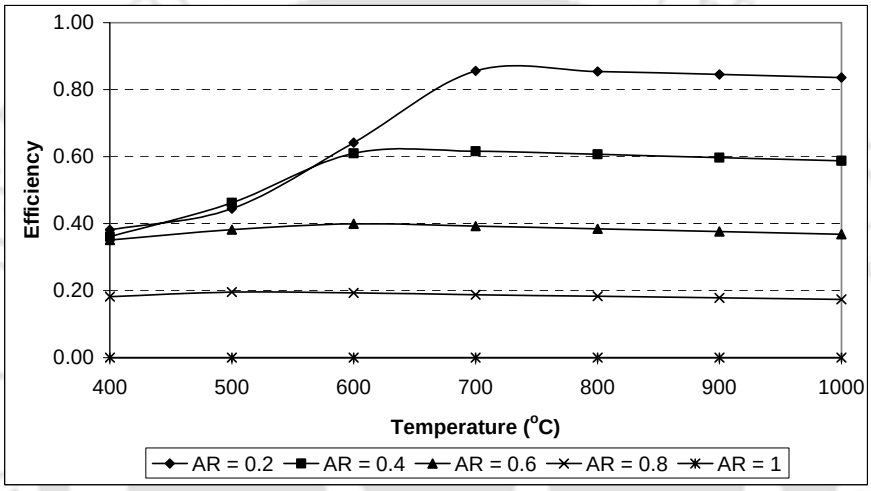


(B)

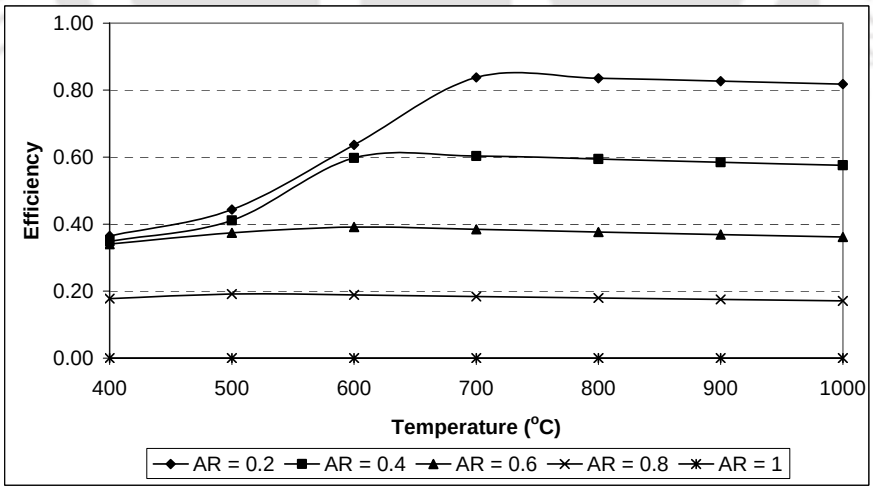


(C)

**Figure 4.8:** Theoretical efficiency of the gasification process with air + 10% mole/mole steam as the gasification medium using different biomasses. (A) Biomass: Saw Dust; (B) Biomass: Rice Husk; (C) Biomass: Bamboo dust.

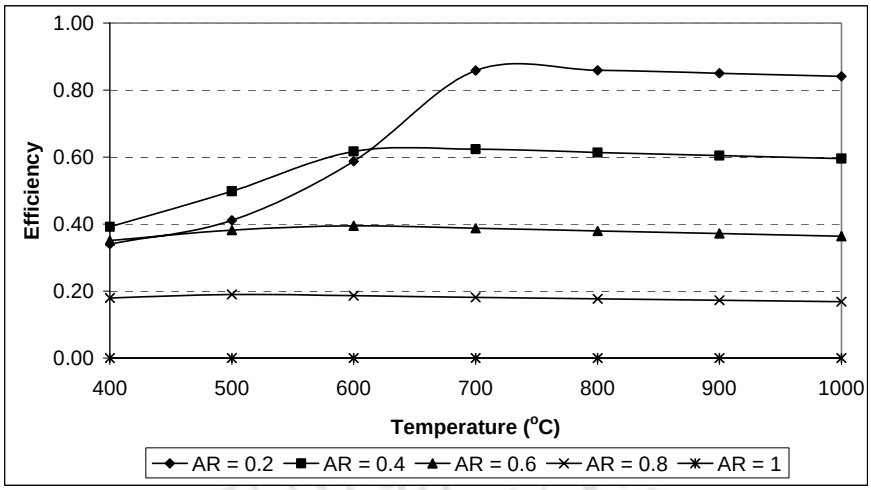


(A)

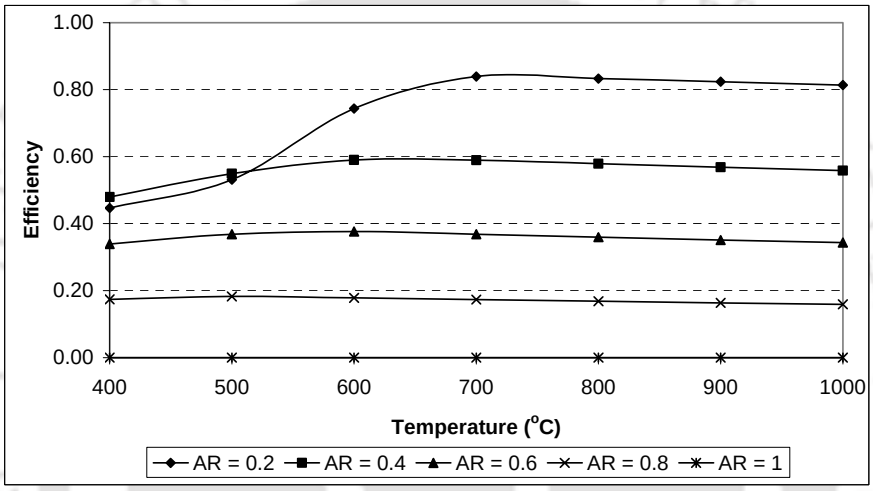


(B)

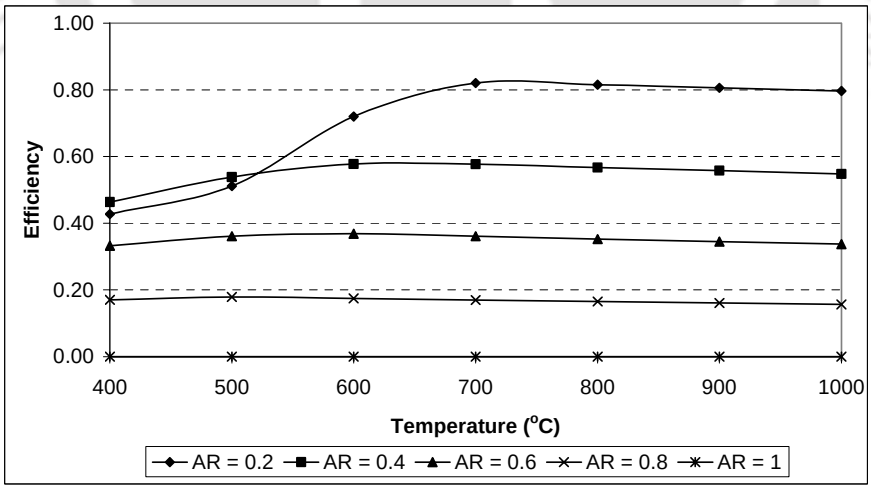


(C)

**Figure 4.9:** Theoretical efficiency of the gasification process with air + 30% mole/mole steam as the gasification medium using different biomasses. (A) Biomass: Saw Dust; (B) Biomass: Rice Husk; (C) Biomass: Bamboo dust.

### 4.4.1 Trends in $H_2$ and CO Formation with Different Gasifying Conditions

From the data given in Tables 4.3–4.8, we can observe following trends in the hydrogen and carbon monoxide content of producer gas obtained at different operating conditions:

***4.4.1.1 Gasification with air alone***: (1) For low air (or equivalence) ratios, the hydrogen production increases with gasification temperatures. However, at higher air ratios (0.4–0.8), the hydrogen production shows an optimum with temperature (at around 500–600 $^{o}$C). (2) At low to medium gasification temperatures (400–600 °C), the extent of hydrogen production increases with air ratio; however, at high temperatures (800–1000 °C), the hydrogen production drops with increasing air ratio. (3) The extent of carbon monoxide production shows continuous rise with gasification temperature at any air ratio. The highest production of CO is seen in absence of air (AR = 0) at 1000 °C, while least production of CO is obtained at AR = 0.8. Obviously, for AR = 1 (when air in stoichiometric production is provided to achieve complete oxidation), no production of CO (which is a result of partial oxidation) is seen. (4) For a given temperature, production of CO shows a maxima with air ratio. For low to moderate temperatures (400–600 °C), maximum CO production is seen for AR = 0.6–0.8. However for higher temperature (800–1000 °C), the highest production of CO is obtained in absence of air (equivalent to pyrolysis condition) at AR = 0.

***4.4.1.2 Gasification with air–steam (10% mole/mole) mixture:*** (1) The hydrogen production for any air ratio and temperature increases (by ~ 10–15%) with mixing of steam with gasification air. (2) For any air ratio, the hydrogen production shows a mixture at a particular temperature. However, this temperature reduces with increasing air ratio. For example, for saw dust, for air ratio of 0.2, maximum $H_2$ production is seen at 900 $^{o}$C, while for air ratio of 0.8, optimum temperature for $H_2$ production is 500 $^{o}$C. This trend is consistent for other two biomasses, viz. bamboo dust and rice husk – although the optimum temperature for any air ratio varies slightly. (3) For a given gasification temperature, the hydrogen production with increasing air ratio.

However, this trend is seen for moderate to high temperatures (600–1000 °C). For low gasification temperatures (400–500 °C), an optimum is seen with respect to the air ratio that $H_2$ production reaches maximum for AR = 0.4–0.6, and thereafter reduces as AR increases. (4) Carbon monoxide production shows a peculiar trend with respect to gasification to pressure for given air ratio. After a certain temperature, there is a sudden rise in production of CO. The temperature at which this transition occurs depends on air ratio. For AR = 0.2, the transition in CO production occur at 1000 °C, while for AR = 0.4 to 0.6, the transition temperature is 600 °C. (5) For a particular gasification temperature, the CO production shows an optimum with respect to air ratio. As the gasification temperature increases the air ratio, for which maximum production of CO is seen, reduces. For example, for rice husk gasification, maximum production of CO is seen for AR = 0.6 at low temperatures (400–500 °C), while for high temperature (800–1000 $^{o}$C), maximum CO production is seen for air ratios of 0, 0.2 and 0.4.

***4.4.1.3 Gasification with air–steam (30 % mole/mole) mixture:*** (1) The extent of hydrogen production for any combination of air ratio and gasification temperature further increases with vise in fraction of steam in gasification air. (2) The trend in hydrogen production with temperature at a given air ratio is essentially same as gasification with 10% mole/mole steam–air mixture. However, the temperature at which maximum production of $H_2$ is obtained reduces for lower AR. For example, for saw dust and rice husk at AR = 0.2, maxima in hydrogen production is seen at 900 and 800 °C, respectively at 10% steam–air mixture as gasification medium. As steam fraction in air increases to 30% these temperatures for max $H_2$ production reduce to 700 °C. (3) On the other hand, for a particular gasification temperature, the hydrogen production shows an optimum with respect to air ratio. For low to moderate temperature (400–600 $^{o}$C), maximum hydrogen production is seen for relatively high air ratios of 0.4–0.6. However, at high gasification temperature (800–1000 °C), maximum $H_2$ production occurs at AR = 0.2. (4) On a whole, the extent CO production reduces with steam ratio increasing to 30% mole/mole. The

exceptions to this trend are combinations of low air ratios and temperatures, where slight increase is seen in CO production for all biomasses. Typically, this exception is more marked for AR = 0.2 in case of saw dust, where sharp rise in CO production is seen for temperatures of 400–900 °C. (5) For any air ratio, the CO production increases with gasification temperatures and the highest CO production is seen at 1000 °C. (6) For a given gasification temperature, however, the CO production shows a maxima with air ratio. For low to moderate gasification temperatures of 400–600 °C, the air ratio for maximum CO production is 0.4–0.6, while for higher temperatures (700–1000 °C), maximum CO production is seen for AR = 0.2.

### 4.4.2 Trends in Carbon Distribution

The biomass mainly comprises of 4 elements, viz. C, H, N and O. Out of these elements, C, H, and N undergo partial / total oxidation during gasification process. The major components of the producer gas resulting from gasification of biomass are CO, $CO_2$, $CH_4$, $H_2$ and $N_2$ along with water vapor ($H_2O$). Moreover, depending on the supply of oxygen through gasification medium, not all of the carbon gets oxidized to CO or $CO_2$ and some carbon may remain unconverted at certain conditions of air ratio and temperature. Among C, H and N, carbon and hydrogen undergo oxidation in preference to nitrogen, which relatively inert element. It would be worthwhile to see as how these elements get distributed among various products. In Tables 4.9 to 4.14, we give distribution of carbon and hydrogen in terms of mole fraction in various products.

***4.4.2.1 Gasification with air alone:*** Table 4.9 gives the distribution of carbon in the gasification mixture among four product species, viz. CO, $CO_2$, $CH_4$ and unconverted carbon, for gasification with air alone. Some peculiar trends are as follows: (1) For low gasification temperatures and low air ratios, significant fraction of carbon remains unconverted. For any gasification temperature, the fraction of unconverted carbon reduces with increasing air ratio. For AR = 0.2 and higher, no unconverted carbon is seen for gasification temperatures above 800

°C. For rice husk and bamboo dust, complete conversion of carbon is found to occur at even lower temperature of 700 °C. (2) As far as relative distribution of carbon among two oxides, viz. CO and $CO_2$, is concerned, an interesting trend is seen. For low air ratios (0.2–0.4), the fraction of carbon undergoing partial oxidation increases rapidly as the gasification temperature rises, with proportionate reduction in fraction in total carbon undergoing complete oxidation to $CO_2$. On the other hand, as air ratio rises for any gasification temperature, the fraction of carbon getting converted to $CO_2$ increases. Obviously, at AR = 1, when stoichiometric air is supplied for complete oxidation, entire carbon is converted to $CO_2$. (3) Fraction of carbon getting converted to $CH_4$ is relatively small. The highest production of $CH_4$ is seen for truly pyrolytic conditions, i.e. AR = 0. With increasing air ratio any gasification temperature, the fraction of carbon getting unconverted to $CH_4$ reduces. Same trend is seen with rising gasification temperature at any given air ratio. For high gasification temperature (800–1000 °C), total carbon is distributed only among CO and $CO_2$, with other two products, viz. $CH_4$ and unconverted carbon, reducing to zero.

***4.4.2.2 Gasification with air–steam (10% mole/mole) mixture:*** Table 4.11 gives the distribution of carbon in the gasification mixture among four product species, viz. CO, $CO_2$, $CH_4$ and unconverted carbon, for gasification with air–steam (10% mole/mole) mixture. The overall trend in distribution of carbon among the four products is same as in case of gasification with air alone. However, some deviations occur as follows: (1) For saw dust, significant amount of carbon is seen unconverted even at high gasification temperature of 700–900 °C at air ratio of 0.2. As noted earlier, CO production shows sudden rise at 1000 °C. For other two biomasses, viz. bamboo dust and rice husk, significant reduction in unconverted carbon is seen to occur for all temperature and air ratios, as compared to gasification with air alone. (2) For higher gasification temperature of 800–1000 °C, the distribution of carbon towards $CO_2$ increases slightly. This change is seen for all air ratios. (3) The fraction of carbon getting converted to

$CH_4$ also increases slightly for all air ratios at low gasification temperature. For higher gasification temperature, however, no change is seen in production of $CH_4$.

***4.4.2.3 Gasification with air–steam (30% mole/mole) mixture:*** Table 4.13 gives the distribution of carbon in the gasification mixture among product species for gasification with air–steam (30% mole/mole) mixture. Once again, the overall trend is same as that for gasification with 10% mole/mole steam–air mixture. However, some aberrations are seen as follows: (1) The fraction of unconverted carbon shows marginal reduction at all temperatures and air ratios. Typically, for all biomasses no unconverted carbon is seen at and above AR = 0.6 for all gasification temperatures. (2) The fraction carbon converted to $CH_4$ increases slightly for low gasification temperatures (400–500 °C) at all air ratios. However, for higher gasification temperatures, (800–1000 °C), fractional conversion of carbon to $CH_4$ reduces. (3) The fractional conversion of carbon to $CO_2$ increases further, as compared to gasification with air alone or 10% mole/mole steam–air mixture. This is, of course, accompanied by proportionate reduction in carbon conversion to CO – especially at high gasification temperatures of 800–1000 °C, where distribution of carbon to other two products, viz. $CH_4$ and unconverted carbon, drops to zero.

***4.4.2.4 The effect of O/C and H/C ratio on carbon distribution*:** It could be seen from Table 4.2 that O/C ratio in the gasification increases with AR (due to oxygen supplied by air), and it further increases with presence of steam (due to oxygen contribution by water molecules). On the other hand, H/C ratio does not change with AR for gasification with air alone (as air does not contribute any hydrogen), but it does increase with presence of steam in gasification medium. The oxygen and hydrogen in gasification mixture compete for reaction with carbon. The products of the reaction between C and O are CO and $CO_2$, while reaction between H and C gives $CH_4$. It is interesting to note the trend in production of CO, $CO_2$ and $CH_4$ and correlate them with O/C and H/C ratios in gasification mixture. If we assess the H/C and O/C ratios for three biomasses, we see that for any gasification medium, temperature and air ratio, O/C and

H/C ratios show the following trend: Rice husk > Bamboo dust > Saw dust. We now examine the variation in carbon distribution among CO, $CO_2$ and $CH_4$ for various gasification conditions and try to justify it in terms O/C and H/C ratios for these conditions.

(1) Higher H/C (than O/C) ratio for AR = 0 makes $CH_4$ dominant product for carbon in gasification mixture for any biomass, especially at lower temperatures. At higher temperatures, however, CO and $CO_2$ dominate the product distribution and we attribute this to higher energy of C–O bond (–1096.38 kJ/mole) than C–O bond (–338.4 kJ/mole), due to which compound having C–O bond are favored at higher temperature.

(2) As AR increases, O/C ratio increases for all three gasification media. However, H/C ratio shows increase only for air–steam mixtures. As a result, fraction of carbon getting converted to $CH_4$ drops rapidly with increasing air ratio for air gasification than gasification with air–steam mixtures.

(3) Comparison of variation in carbon distribution for any biomass with different gasification media (for same air ratio and temperature) reveals that fraction of C converting to $CH_4$ increases with increasing steam content. This is clearly attributed to higher H/C ratio at higher steam content of gasification media. O/C ratio also increases with steam content of the gasification medium. As a result rise in both H/C and O/C ratios, the fraction of unconverted carbon seen for certain combinations of AR and temperature reduces.

(4) Comparison of carbon distribution among different biomasses for a given gasification medium, AR and temperature reveals interesting features. For any AR and gasification medium, both O/C and H/C ratios for rice husk are much higher than saw dust. On the other hand, the O/C and H/C ratios for rice husk and bamboo dust are the similar. This difference is reflected in terms of unconverted carbon. We see that fraction of unconverted carbon seen for certain combination of AR, temperature and gasification medium is much higher for saw dust than rice husk and bamboo dust.

### 4.4.3 Trends in Hydrogen Distribution

There are two sources of hydrogen in feed gasification: (1) the hydrogen in the biomass itself, and (2) the hydrogen in steam in case of gasification with air– steam mixtures. As stated earlier, this hydrogen gets distributed into three principal products, viz. $H_2$, $H_2O$ and $CH_4$. Tables 4.10, 4.12 and 4.14 depict the distribution of hydrogen among these products in terms of mole fraction. Given below are the typical trends seen in distribution of hydrogen under different conditions of gasification.

***4.4.3.1 Gasification with air alone (Table 4.10):*** The trends observed in distribution of hydrogen among product species are as follows: (1) The fraction of hydrogen getting converted to $H_2$ shows an increasing trend with gasification temperature at a given air ratio. On the other hand, fraction of hydrogen converted to $H_2O$ increases with air ratio at a given gasification temperature .The exact distribution of hydrogen among $H_2$ and $H_2O$ also depends on oxygen content of biomass itself. This is evident from the fact that at high temperatures (900–1000 °C) and low air ratio (AR = 0.2), saw dust gasification shows very high conversion of hydrogen to $H_2$ (> 90%), with correspondingly small fraction of $H_2O$ (< 10%). However, gasification of rice husk and bamboo dust at the same conditions shows significant fractions of total hydrogen converted to $H_2O$ (~ 22–27%). However, for all three biomasses the fraction of hydrogen converted to $H_2O$ shows marked rise as air ratio changes from 0 to 0.2 (9 to 20 fold increase). However, there after this rise is slowed down (for example, increasing air ratio from 0.2 to 0.8 shows ~ 2–4 fold rise in fraction of hydrogen converted to $H_2O$). (2) The fraction of hydrogen appearing in $CH_4$ is relatively low. Only at truly pyrolytic conditions (AR = 0), this fraction is significant. With rise in air ratio, at any gasification temperature, it rapidly decreases. For high gasification temperatures (800–1000 °C), no hydrogen is converted to $CH_4$ for AR = 0.2–1, and the dominant products are $H_2$ and $H_2O$. Similar trend is also seen with increasing gasification

temperature at given air ratio.

***4.4.3.2 Gasification with air–steam mixture (10% mole/mole):*** Referring to Table 4.12, we can identify following trends in the distribution of hydrogen in the gasification mixture among various product species in producer gas: (1) With mixing of steam in gasification air, the fraction of $H_2$ converted to $H_2O$ increases. This effect is more marked at low air ratios for all gasification temperatures. Therefore, the jump in hydrogen distribution to $H_2O$ with air ratio changing from 0 to 0.2, and from 0.2 to 0.4 is not as marked as seen for gasification with air. (2) Fraction of hydrogen in $CH_4$ shows a marginal rise for low gasification temperatures (400–700 °C) and low air ratios. However, for higher air ratios (AR = 0.6–0.8), reduction is seen in fraction of hydrogen appearing in $CH_4$.

***4.4.3.3 Gasification with 30% mole/mole steam–air mixture:*** With reference to Table 4.14, we can identify following trends in hydrogen distribution among product species for gasification with steam (30% mole/mole)–air mixture: (1) With steam content of air increasing to 30%, the fractional conversion of hydrogen to $H_2O$ rises, but this effect is more marked for high air ratios (AR = 0.6–0.8), and low–to–moderate gasification temperatures (400–600 °C). For lower air ratios and high temperatures, the distribution of hydrogen among the three products remains unaltered. (2) A noteworthy change is also seen in hydrogen fraction appearing in $CH_4$ for high air ratios and low–to–moderate gasification temperatures (400–500 °C). For high gasification temperature (800–1000°C), no change is seen in $CH_4$ (which is already zero) for all air ratios.

### 4.4.4 Trends in LHV

The LHV of the producer gas obtained with biomass gasification depends on the quantity of combustible components CO, $H_2$ and $CH_4$, present in it. It is, therefore, obvious that variation in LHV would follow essentially same trend as carbon monoxide and hydrogen production.

***4.4.4.1 Gasification with air alone:*** For all the three biomass variation in LHV with respect to

air ratio (for a given gasification temperature), and with respect to gasification temperature (at a given air ratio), shows similar trends. For a particular air ratio, LHV shows an increasing trend with gasification temperature. This clearly attributed to increasing amount of carbon monoxide and hydrogen in the producer gas. Moreover, for any gasification temperature, LHV reduces with increasing air ratio. This reduction is due to reducing quantity of $H_2$ and CO in the producer gas due to increasing distribution of carbon and hydrogen towards $CO_2$ and $H_2O$ respectively. At AR = 1, LHV is essentially zero as all carbon and hydrogen in the gasification mixture is converted to $CO_2$ and $H_2O$, respectively. Significantly high values of LHV (for all three biomasses) for AR = 0 are attributed to complete absence of external oxygen in the gasification mixture, due to which relatively larger production of $CH_4$ (at low–to–moderate temperatures) and $H_2$ (at high temperatures) is seen. As air ratio rises from 0 to 0.2 for any particular gasification temperature, the LHV falls sharply. Thereafter, the reduction in LHV is almost linear with air ratio. At higher gasification temperatures (800–1000 $^oC$), the LHV stays practically constant for any air ratio.

***4.4.4.2 Gasification with 10% mole/mole steam–air mixture:*** Although the overall trends in LHV with air ratio and gasification temperature are essentially same as found in case of gasification with air alone, although a slight rise in LHV (~ 10–15%) is seen for all air ratios at all gasification temperatures.

***4.4.4.3 Gasification with 30% mole/mole steam–air mixture:*** Once again, the overall trends in LHV with air ratio and gasification temperature are essentially same as found in case of gasification with air and 10% mole/mole steam–air mixture. However, LHV for all air ratios and temperatures rise further by ~ 10–15%.

### 4.4.5 Trends in $H_2$/CO Molar Ratio

The molar ratio of $H_2$/CO depends on the relative content of carbon monoxide and hydrogen in the producer gas. As outlined in the previous section, some trends in CO and $H_2$

production with respect to air ratio and temperature are similar. Therefore, trends $H_2$/CO molar ratio are along same lines. Nonetheless, we must realize that high $H_2$/CO molar ratio does not necessarily mean high molar content of CO and $H_2$ (it is only the ratio of molar content). It could well be possible that absolute production of CO and $H_2$ (in moles) is lesser for high $H_2$/CO molar ratio and vice versa. We now describe the trends in this parameter under different gasification conditions.

***4.4.5.1 Gasification with air alone:*** For all three biomasses, higher $H_2$/CO molar ratios are seen for low gasification temperature of 500 $^oC$ for all air ratios. But thereafter the ratio falls quite rapidly. Large $H_2$/CO ratios at low temperatures are attributed to very low production of CO. As temperature rises, the production of CO increases more rapidly than hydrogen, and hence, the molar ratio falls. At high temperatures (900–1000 $^oC$), this ratio falls below 1, which means that CO production supersedes the hydrogen production. Especially, for saw dust, $H_2$/CO ratios below 1 are seen at even moderate temperature of 700–800 $^oC$. For any gasification temperature, the molar ratio shows a minima with respect to air ratio. For all three biomasses, the minima is found to occur at AR = 0.6.

***4.4.5.2 Gasification with steam (10% mole/mole)–air mixture:*** The overall trend in $H_2$/CO molar ratio stays unchanged with 10% mole/mole steam–air mixture. For any air ratio, the H2/CO molar ratio falls with rising temperatures. However, as compared to gasification with air alone, these molar ratios are higher. This increase is marginal (~ 5%) at low air ratios (AR = 0.2–0.4), while for higher air ratio (AR = 0.6–0.8), higher rise (of about ~ 40–50%) is observed. Moreover, similar to air gasification $H_2$/CO molar ratio shows a minima at AR = 0.6 for any gasification temperature. Quite interestingly, for rice husk and bamboo dust, the $H_2$/CO ratio stays above or very close to 1 at high gasification temperatures (800–1000 $^oC$). However, for rice husk molar ratio still falls below 1 at 1000 $^oC$.

***4.4.5.3 Gasification with steam (30% mole/mole)–air mixture:*** With steam content of gasifying

air increasing to 30% mole/mole, the trends in $H_2$/CO molar ratio are similar to those observed with air gasification and 10% mole/mole steam–air mixture, although some quantitative changes are seen as follows: (1) For all combination of gasification temperatures and air ratios, molar ratio of $H_2$/CO rises further. (2) The rise in molar ratio is marginal (~ 5%) for low air ratios (AR = 0.2–0.4), while for higher air ratios (AR = 0.6–0.8) the rise is ~ 30–50%. (3) The molar ratio for all three biomass stays above or close to 1 for all air ratios at high gasification temperatures (800–1000 $^{o}$C). (4) Similar to gasification with air and 10% mole/mole steam air mixture, the molar ratio shows a minima with air ratio at any gasification temperature. However, the minima is observed at AR = 0.4 (instead of AR = 0.6 as in case of air gasification or gasification with 10% mole/mole steam–air mixture).

### 4.4.6 Trends in Efficiency

The efficiency of the gasifier has been calculated using the LHV value of the producer gas at NTP conditions, which is the net energy output from gasifier and the sum total of HHV of biomass, energy input through gasification medium (either air or air–steam mixture) and heat required to raise the temperature biomass and accompanying moisture to gasification temperature. A detailed calculation of the efficiency of the gasifier is explained in Appendix A. It should be noted, however, that the gasification process itself is an overall exothermic process. The net heat released form the process is absorbed by the reactants (biomass + air) and products (the producer gas). Most of this heat is carried out by the producer gas, in the form of its sensible heat. This heat may be recovered by various means such as preheating and drying of biomass and/or preheating of the air entering the gasifier. Therefore, other than HHV of the biomass, the two additional components of input energy (viz. energy input through gasification medium and energy required to heat biomass and accompanying moisture) in the equation A.12 in appendix A are irrelevant at steady state operation. The energy in the biomass feed appears in two forms, first the “chemical energy” – which the heat of combustion of the producer gas, and secondly,

the thermal energy, which the net energy released from the gasification process. Obviously, in accordance with principle conservation of energy, these two energies vary inversely. Given below are the $\Delta H_C$ (heat of combustion of producer gas) and $\Delta H_T$ (thermal energy released from the process) for saw dust at 900 $^oC$ for various AR: (1) AR = 0.2, $\Delta H_C$ = –1990.32 kJ, $\Delta H_T$ = –316.7 kJ; (2) AR = 0.4, $\Delta H_C$ = –1493.1 kJ, $\Delta H_T$ = –668.3 kJ; (3) AR = 0.6, $\Delta H_C$ = –995.32 kJ, $\Delta H_T$ = –1022 kJ; (4) AR = 0.8, $\Delta H_C$ = –995.32 kJ, $\Delta H_T$ = –1377 kJ.

As far as application of biomass gasification for decentralized power generation is concerned, it is the chemical energy of biomass which is relevance (and not the thermal energy). Therefore, an apt definition of efficiency of gasifier would be: LHV of the producer gas/HHV of biomass. With this preamble, we present the results of the efficiency calculation. The trends in the efficiency of the gasification process with different gasification media are presented in Figures 4.7, 4.8 and 4.9 respectively, from which we can identify following trends:

(1) For lower ARs (0.2–0.4), the efficiency shows rise with gasification temperature for low to moderate range (400–700 $^oC$). However, beyond 700 $^oC$, the efficiency levels off. We attribute the initial rise in efficiency to increasing carbon conversion with rising temperature. However, beyond 700 $^oC$ complete carbon conversion is achieved and LHV of producer gas stays the same, as a result of which the efficiency also stays unaltered. This trend is consistent among three biomasses for a given gasification medium (air or air–steam mixture).

(2) The efficiency falls sharply with rising AR at any particular temperature. This is obviously due to greater conversion of carbon and hydrogen to $CO_2$ and $H_2O$, due to which LHV of the producer gas falls.

(3) With increasing steam content of gasification medium, the efficiency rises marginally for ARs between 0–0.6 and temperature 400–700 $^oC$, and this is attributed to higher production of $H_2$ and $CH_4$ at these conditions. However, at high temperature, the efficiency of the gasification process for any biomass with all three gasification media is essentially the same.

## 4.5 DISCUSSION

The results in preceding section give a comprehensive account of variation of important characteristics of the producer gas and gasification process as a whole with four operating conditions or parameters viz. AR, temperature of gasification, gasification media, and type of biomass. An analysis of these results helps as identify optimum combinations or sets of operating conditions for gasifier for purpose of decentralized power generation and Fisher–Tropsch synthesis.

### 4.5.1 Optimum Parameters for FT Synthesis

The principal chemical reactions for the FT Synthesis are:

(1) Synthesis of paraffin: $(2n+1)\ H_2 + n\ CO \longrightarrow C_nH_{2n+2} + n\ H_2O$

(2) Synthesis of olefins: $2n\ H_2 + n\ CO \longrightarrow C_nH_{2n} + n\ H_2O$

It is evident from these reactions that the two components of the synthesis gas, $H_2$ and CO, need to be in the ratio 2:1 or higher. If we analyze variation in the $H_2$/CO ratio with different operating parameters we may arrive at conclusion that low gasification temperature and low ARs would be best choice. However, we must also see the absolute number of moles (or molar composition) of the gas at various conditions. For low ARs and gasification temperature, the net molar content of $H_2$ and CO in producer gas is quite low, so the net "useful' fraction of gas is small. On the other hand, for high temperatures (800–1000 $^oC$) at AR = 0.2 or 0.4, we have $H_2$/CO ratio less than 1 for all three biomasses, but net molar content of $H_2$ and CO in the producer gas is higher. Moreover, the net molar content of the $H_2$ and CO in producer gas is essentially same in the temperature range of 800–1000 $^oC$. With use of iron–based catalyst that have higher activity for water–gas shift reaction ($CO + H_2 \rightleftharpoons CO_2 + H_2$), which releases hydrogen by selectively consuming CO, producer gas with $H_2$/CO ratio less than 1 can be used

for FT synthesis. Mixing gasification air with steam can help enhance hydrogen content but only marginally (~ 10% or less). Taking into consideration, the additional costs associated with air–steam mixtures, it appears that air is the most suited gasification medium. On a whole, the optimum combinations or sets of operational parameters for gasifier operation for FT synthesis are: AR = 0.2 to 0.4, temperatures = 800–1000 $^{o}$C, gasification medium: air.

### 4.5.2 Optimum Parameters for Decentralized Power Generation

The key characteristic of the producer gas from viewpoint of power generation is the lower heating value (LHV). It is evident from the trends in LHV that low ARs and high temperatures would be preferred for gasification operations. However, for any biomass and gasification medium, LHV stays essentially constant after 700 $^{o}$C. Therefore, gasifier operation above 700 $^{o}$C would mean excessive energy input that does not pay off. Secondly, too low ARs (i.e. AR = 0 or 0.2) would result in significant unconverted carbon, while too high ARs (i.e. AR ≥ 0.6) give more carbon dioxide than carbon monoxide, which is undesired. As far as gasification media is concerned, no significant rise in LHV is seen by replacing air by air + steam mixture. Therefore, as in case of FT synthesis, gasification with air–steam mixtures is uneconomic. On a whole, the optimum set of parameters for gasifier operation for decentralized power generation are: temperature ~ 700–800 $^{o}$C, AR = 0.3–0.4 and gasification medium: air.

## 4.6 CONCLUSIONS

This study presents comprehensive thermodynamic equilibrium analysis of biomass gasification process using the non–stoichiometic SOLGASMIX model for Gibbs energy minimization. This analysis is aimed at finding the optimum combination of values of key parameters for biomass gasifier operation for two potential uses, viz. decentralized power generation and producing synthesis gas for Fischer–Tropsch process. These parameters are: (1) type of biomass, (2) temperature of gasification, (3) air or equivalence ratio, and (4) gasification

medium. Using combinations of different values for these parameters, variation in three important characteristics of producer gas has been assessed, viz. net molar content of $H_2$ and CO in the producer gas, $H_2$/CO molar ratio and LHV. The first and second characteristics are of relevance for the FT synthesis, while the third parameter is a measure of utility of producer gas for decentralized power generation (with gas engine–generator sets that use producer gas). The optimum values of parameters for gasifier operation for FT synthesis have been found to be: AR = 0.2–0.4, temperature = 800–1000 $^{o}$C, gasification medium: air. Similarly, the optimum combinations of values of operating parameters for decentralized power generation are: AR = 0.3–0.4, temperature = 700–800 $^{o}$C, with gasification medium being air. In addition to this analysis, our study also bring to light some important features of gasification such as effect of O/C and H/C ratio in the gasification mixture on distribution of carbon and hydrogen among different product species and the analysis of overall efficiency of the process (along with distribution of HHV of biomass among chemical and thermal energy during the gasification process).

Quite interestingly, the optimum set of parameters for gasifier operation for both FT synthesis and decentralized power generation overlap closely. Therefore, the producer gas generated from operation these parameters could be used for both applications. Nonetheless, the major difference in operating conditions of FT process and an IC engine (connected to generator set) is the pressure of operation. FT synthesis occurs at highly elevated pressures (15–20 bar), while IC engines operate at atmospheric pressure. On the basis of similar operating condition for gasifiers, one can propose a combined process in which producer gas from biomass gasifier will first be compressed and treated in the FT reactor on “once through” basis. The unreacted producer gas will be separated from the FT products (which are essentially higher, i.e. $C_5$+, hydrocarbons) and will be fired into the IC engine, which would generated electricity – some of which could be used for running the compressor for the producer gas prior to FT reactor.

Summarizing, the present study has put forth a rigorous frame work for optimization of biomass gasification with four operating parameters for two potential uses. Nonetheless, this frame work can be extended for optimization of gasifier (with additional parameters) for other potential applications than considered in this study, such as generation of hydrogen for fuel cells and thermal operation such as in ceramic industry.

## REFERENCES

[1] Bale CW, Chartrand P, Degterov SA, Eriksson G, Hack K, Mahfoud RB, Melancon J, Pelton AD, Petersen S. FACTSAGE thermochemical software and databases. Calphad 2002;26(2): 189–228.

[2] Eriksson G. Thermodynamic studies of high temperature equilibria – XII: SOLGAMIX, A computer program for calculation of equilibrium composition in multiphase systems. Chemica Scripta 1975;8:100–103.

[3] Meshram JR, Mohan S. Biomass power and its role in distributed power generation in India. In: 25 Years of Renewable Energy in India, New Delhi: Ministry of New and Renewable Energy; 2007. pp. 109–134.

[4] Biomass Atlas of India, Combustion Gasification and Propulsion Laboratory, Bangalore: Indian Institute of Science. (website: http://cgpl.iisc.ernet.in), 2007.

[5] Reference Material, International Training Program on Biomass Technologies; Combustion Gasification and Propulsion Laboratory, Bangalore: Indian Institute of Science, April 2001.

[6] Lau FS. The Hawaiian project. Biomass and Bioenergy 1998;15:233–238.

[7] Maniatis K. Progress in Biomass Gasification: An Overview. In: AV Bridgwater, editor. Progress in Thermochemical Conversion of Biomass. Oxford:Blackwell Science Ltd; 2001, pp.

1–31.

[8] Tijmensen MJA, Faaij APC, Hamelinck CN, van Hardeveld MRM. Exploration of the possibilities for production of Fischer–Tropsch liquids and power via biomass gasification. Biomass and Bioenergy 2002;23:129–152.

[9] Li X, Grace JR, Watkinson AP, Lim CJ, Ergudenler A. Equilibrium modeling of gasification: a free energy minimization approach and its application to a circulating fluidized bed coal gasifier. Fuel 2001;80:195–207.

[10] Channiwala SA, Parikh PP. A unified correlation for estimating HHV of solid, liquid and gaseous fuels. Fuel 2002;81:1051–1063.

[11] Specific Heat Capacity. In: Wikipedia – the free encyclopedia. (website: http://en.wikipedia.org/wiki/Specific_Heat_Capacity; accessed September 2009).

APPENDIX A

# SAMPLE CALCULATION FOR EQUILIBRIUM MODEL

We present herewith the complete sample calculation for the equilibrium model for biomass gasification for rice husk. The calculation described in this section can be easily extended to other two biomasses viz bamboo dust and saw dust. The starting point of calculation, of course, is the ultimate analysis of the biomass. Referring to data given in Table 4.1, the ultimate analysis of rice husk in weight percent (dry basis) is:

C = 37.03%, H = 5.25 %, N = 0.09%, O = 40.94%, Ash = 16.69%.

The next step would be to calculate stoichiometric air required for complete oxidation of various elements (C to $CO_2$, N to $NO_2$ and H to $H_2O$). We ignore the role of ash content in the oxidation process, although we do account for the influence of ash content on HHV, as explained later in this appendix.

## A.1 Stoichiometric Air Requirement

We take 100 g of biomass (dry basis) as the basis for calculations. The elemental content of it in gmole or gatom is as follows:

$$\text{Carbon (C)} = \frac{37.03}{12} = 3.086 \text{ gatom} \qquad \text{(A.1)}$$

Hydrogen (H) = $\frac{5.25}{1}$ =5.25 gatom = 2.625 gmole (A.2)

Nitrogen (N) = $\frac{0.09}{14}$ = 0.006 gatom = 0.003 gmole (A.3)

Oxygen (O) = $\frac{40.94}{16}$ = 2.559 gatom =1.279 gmole (A.4)

The molecular formula for the biomass can be determined on the basis of per gatom of carbon is:

$C\ H_{5.25/3.086}\ N_{0.003/3.086}\ O_{1.279/3.086} = CH_{1.699}N_{0.003}O_{0.828}$.

***A.1.1 Oxygen requirement:*** The oxygen ($O_2$) required for complete oxidation of these elements (not including nitrogen as it is present in small amount) is: $= \left(3.086 \times 1 + \frac{2.625}{2}\right) = 4.3985$ gmole. However, oxygen available in biomass itself fulfills same of this demand. The external oxygen required (from gasification air) is then 4.3985 – 1.279 = 3.119 gmole. This oxygen is provided by air, the amount of nitrogen in the air stream is: $\frac{3.119}{0.21} \times 0.79 = 11.804$ gmole. The total air moles are: 3.119 + 11.804 = 14.923.

***A.1.2 Equivalence or air ratio (AR)***: This is the ratio of actual moles of oxygen supplied for gasification to the number of moles required for complete oxidation. We have varied the air ratio from zero (pyrolysis) to 1 (complete oxidation). For sample calculation we choose two air ratios, viz. 0.2 and 0.4. With this, the amount of oxygen and air for two air ratios are:

**AR = 0.2**: $O_2 = 3.119 \times 0.2 = 0.0624$ moles; Air = $\frac{0.624}{0.209} = 2.985$ moles. (A.5)

**AR = 0.4**: $O_2 = 3.119 \times 0.4 = 1.248$ moles; Air = $\frac{1.248}{0.209} = 5.969$ moles. (A.6)

***A.1.3 Moisture content:*** We assume that biomass contains about 10% moisture. Thus, the gatoms of Hydrogen (H) and oxygen (O) contributed by moisture per 100 g of biomass are:

H: $\frac{0.1 \times 100}{18} \times 2 = 1.111$ (A.7)

O: $\frac{0.1\times100}{18}\times1=0.555$ (A.8)

***A.1.4 Steam ratio:*** This is the amount of steam present in the gasifying air. We assume that mixture of air-steam is made by spraying water in the gasifying air till the required steam ratio (moles of steam/moles of air) is obtained. As explained in greater details in subsequent section, the temperature of gasification is the equilibrium temperature reached by the steam-air mixture after evaporation of water and superheating of the steam. For sample calculations we take two cases, viz . no steam injection (gasification with air alone) and 10% mole/mole steam. The net moles of steam for the latter case are:

**AR = 0.2:** Steam moles = $2.985\times0.1=0.298$ moles

**AR = 0.4:** Steam moles = $5.969\times0.1=0.597$ moles

***A.1.5 Element vector input:*** With contribution of biomass itself, gasifying medium (air or air-steam mixture) and moisture content of biomass, the total element vector input (or gatoms of each of C, H, N and O element) is determined as follows:

*A.1.5.1 Gasification with air*

| C | H | | N | | O | |
|---|---|---|---|---|---|---|
| | AR = 0.2 | AR = 0.4 | AR = 0.2 | AR = 0.4 | AR = 0.2 | AR = 0.4 |
| 3.086 | 6.361 | 6.361 | 4.728 | 9.45 | 4.362 | 5.609 |

*A.1.5.2 Gasification with air-steam (10% mole/mole) mixture*

| C | H | | N | | O | |
|---|---|---|---|---|---|---|
| | AR = 0.2 | AR = 0.4 | AR = 0.2 | AR = 0.4 | AR = 0.2 | AR = 0.4 |
| 3.086 | 6.958 | 7.555 | 4.728 | 9.45 | 4.66 | 6.206 |

***A.1.6 Gasification conditions:*** The next step in the equilibrium calculation is the selection of gasification conditions in terms of pressure and temperature. We give here with calculation for two temperatures, viz. 500 $^{o}$C (in the range of low to moderate temperature) and 900 $^{o}$C (in the range of high temperature). The pressure of gasification mixture is assumed to be atmospheric or

1 bar.

## A.2 Equilibrium Calculations

After feeding the element vector and gasification conditions to the FACTSAGE software, which has the inbuilt database of the thermodynamic properties (such as ΔH, ΔG and $C_p$ vs. T relationship) for more than 5500 chemical species, the product or output composition of the gasification process is obtained as follows:

### *A.2.1 Gasification with air (AR = 0.2)*

| Component | Equilibrium Amount (moles) | | Equilibrium Mole Fraction (-) | |
|---|---|---|---|---|
| | Temp = 500 °C | Temp = 900 °C | Temp = 500 °C | Temp = 900 °C |
| CO | 1.91870E–01 | 2.5143E+00 | 2.8418E–02 | 2.9136E–01 |
| $H_2$ | 1.04180E+00 | 2.4739E+00 | 1.5430E–01 | 2.8669E–01 |
| $CO_2$ | 1.36920E+00 | 5.7121E–01 | 2.0279E–01 | 6.6194E–02 |
| $H_2O$ | 1.43170E+00 | 7.0531E–01 | 2.1205E–01 | 8.1734E–02 |
| $N_2$ | 2.36350E+00 | 2.3639E+00 | 3.5005E–01 | 2.7394E–01 |
| $CH_4$ | 3.52750E–01 | 5.0922E–04 | 5.2245E–02 | 5.9010E–05 |
| $NH_3$ | 9.69670E–04 | 1.5344E–04 | 1.4361E–04 | 1.7781E–05 |
| C | 1.17220E+00 | - | - | - |

### *A.2.2 Gasification with air (AR = 0.4)*

| Component | Equilibrium Amount (moles) | | Equilibrium Mole Fraction (-) | |
|---|---|---|---|---|
| | Temp = 500 °C | Temp = 900 °C | Temp = 500 °C | Temp = 900 °C |
| CO | 2.7359E–01 | 1.9288E+00 | 2.7876E–02 | 1.7549E–01 |
| $H_2$ | 1.1165E+00 | 1.8143E+00 | 1.1376E–01 | 1.6507E–01 |
| $CO_2$ | 1.9152E+00 | 1.1571E+00 | 1.9514E–01 | a1.0528E–01 |
| $H_2O$ | 1.5051E+00 | 1.3659E+00 | 1.5335E–01 | 1.2427E–01 |
| $N_2$ | 4.7245E+00 | 4.7249E+00 | 4.8138E–01 | 4.2988E–01 |
| $CH_4$ | 2.7869E–01 | 4.9042E–05 | 2.8396E–02 | 4.4619E–06 |
| $NH_3$ | 1.0463E–03 | 1.0697E–04 | 1.0661E–04 | 9.7318E–06 |
| C | 6.1854E–01 | - | - | - |

### *A.2.3 Gasification with 10% mole/mole steam-air mixture (AR = 0.2)*

| Component | Equilibrium Amount (moles) | | Equilibrium Mole Fraction (-) | |
|---|---|---|---|---|
| | Temp = 500 °C | Temp = 900 °C | Temp = 500 °C | Temp = 900 °C |
| CO | 2.0245E–01 | 2.4128E+00 | 2.8516E–02 | 2.7025E–01 |
| $H_2$ | 1.1300E+00 | 2.5764E+00 | 1.5916E–01 | 2.8857E–01 |
| $CO_2$ | 1.4497E+00 | 6.7282E–01 | 2.0420E–01 | 7.5361E–02 |
| $H_2O$ | 1.5582E+00 | 9.0158E–01 | 2.1948E–01 | 1.0098E–01 |
| $N_2$ | 2.3635E+00 | 2.3639E+00 | 3.3291E–01 | 2.6477E–01 |
| $CH_4$ | 3.9464E–01 | 4.0335E–04 | 5.5587E–02 | 4.5178E–05 |
| $NH_3$ | 1.0416E–03 | 1.5761E–04 | 1.4672E–04 | 1.7654E–05 |
| C | 1.0392E+00 | - | - | - |

### *A.2.4 Gasification with 10% mole/mole steam-air mixture (AR = 0.4)*

| Component | Equilibrium Amount (moles) | | Equilibrium Mole Fraction (-) | |
|---|---|---|---|---|
| | Temp = 500 °C | Temp = 900 °C | Temp = 500 °C | Temp = 900 °C |
| CO | 2.9464E–01 | 1.7785E+00 | 2.8021E–02 | 1.5347E–01 |
| $H_2$ | 1.3026E+00 | 1.9647E+00 | 1.2388E–01 | 1.6954E–01 |
| $CO_2$ | 2.0732E+00 | 1.3075E+00 | 1.9716E–01 | 1.1283E–01 |
| $H_2O$ | 1.7650E+00 | 1.8126E+00 | 1.6785E–01 | 1.5641E–01 |
| $N_2$ | 4.7244E+00 | 4.7249E+00 | 4.4930E–01 | 4.0773E–01 |
| $CH_4$ | 3.5406E–01 | 3.8927E–05 | 3.3671E–02 | 3.3592E–06 |
| $NH_3$ | 1.2306E–03 | 1.1432E–04 | 1.1703E–04 | 9.8655E–06 |
| C | 3.6411E–01 | - | - | - |

We would like to specifically note that compositions of producer gas depicted in sections A.2.1 to A.2.4 match fairly closely with the compositions of producer gas reported in literature (for example [8, 9])

## A.3 Characterization of the Producer Gas

We characterize the producer gas for three properties: (1) $H_2$/CO molar ratio, (2) Higher Heating Value (HHV), and (3) Distribution of carbon and hydrogen elements among various chemical species.

***A.3.1 $H_2$/CO molar ratio:*** Calculation of this parameter is rather straightforward. Taking ratio of equilibrium amounts (in moles) of $H_2$ and CO in Tables A.2.1 to A.2.4, we obtain following values:

| | |
|---|---|
| Air gasification (500 $^{o}$C) | AR = 0.2; $H_2$/CO Ratio = $\frac{1.0418}{0.1919} = 5.4$<br>AR = 0.4, $H_2$/CO ratio = 4.1 |
| Air gasification (900 $^{o}$C) | AR = 0.2, $H_2$/CO ratio = 1.0<br>AR = 0.4, $H_2$/CO ratio = 0.9 |
| Gasification with air + 10% mole/mole steam mixture (500 $^{o}$C) | AR = 0.2, $H_2$/CO ratio = 5.6<br>AR = 0.4, $H_2$/CO ratio = 4.4 |
| Gasification with air + 10% mole/mole steam mixture (900 $^{o}$C) | AR= 0.2, $H_2$/CO ratio = 1.1<br>AR= 0.4, $H_2$/CO ratio = 1.1 |

***A.3.2 Determination of LHV and HHV:*** Among various chemical species in the producer gas, those which contribute to combustion are: $H_2$, CO and $CH_4$. The producer gas is cooled to ambient temperature before firing into the engine (or combustion chamber) or admitting into the reactor. Due to this, the water vapor in the gas condenses and the numbers of gas phase moles reduce accordingly. Moreover, the water vapor gives up latent heat (40.608 kJ/gmole) to the gas, which is added to the total heat of combustion of the species mentioned earlier. Therefore, we calculate the LHV of the gas on the basis of total heat of combustion $(\Delta H_C)$ of the species mentioned above and the volume of the producer gas at NTP conditions. Heat of combustion are: (1) $H_2$: 285.63 kJ/mole; (2) CO: 282.9 kJ/mole; (3) $CH_4$: 890.3 kJ/mole

**Gasification with air at 500 $^{o}$C; AR = 0.2:**

1. Heat of combustion of producer gas:

$$\Delta H_C = 1.04 \times 285.63 + 0.192 \times 282.99 + 0.353 \times 890.3 = 665.92 \text{ kJ} = 0.666 \text{ MJ}$$

2. Latent heat of water molecules: 1.4317 × 40.608 = 58.138 kJ

3. Total moles of gasification products (in gas phase): 5.32

4. Volume of the gaseous products at NTP conditions: 0.13 $m^3$

5. HHV of the producer gas $= (0.666 + 0.0581)/0.13 = 5.66$ MJ/$Nm^3$

6. LHV $= 0.666/0.13 = 5.12$ MJ/$Nm^3$

**Gasification with air at 500 $^{o}$C; AR = 0.4:**

1. Heat of combustion of producer gas:

$$\Delta H_C = 1.12 \times 285.63 + 0.274 \times 282.99 + 0.279 \times 890.3 = 644.45 \text{ kJ} = 0.644 \text{ MJ}$$

2. Latent heat of water molecules: $1.5051 \times 40.608 = 61.12$ kJ

3. Total moles of gasification products (in gas phase): 8.31

4. Volume of the gaseous products at NTP: 0.20 $m^3$

5. HHV of the producer gas $= (0.644 + 0.0611)/0.2 = 3.53$ MJ/$Nm^3$

6. LHV of the producer gas $= (0.644)/0.2 = 3.22$ MJ/$Nm^3$

**Gasification with air at 900 $^oC$; AR = 0.2:**

1. Heat of combustion of producer gas:

$$\Delta H_C = 2.47 \times 285.63 + 2.51 \times 282.99 + 5.09 \times 10^{-4} \times 890.3 = 1418.6 \text{ kJ} = 1.419 \text{ MJ}$$

2. Latent heat of water molecules: $0.7053 \times 40.608 = 28.641$ kJ

3. Total moles of gasification products (in gas phase): 7.92

4. Volume of the gaseous products at NTP: 0.19 $m^3$

5. HHV of the producer gas $= (1.419 + 28.641 \times 10^{-3})/0.19 = 7.59$ MJ/$Nm^3$

6. LHV of the producer gas $= (1.419)/0.19 = 7.47$ MJ/$Nm^3$

**Gasification with air at 900 $^oC$; AR = 0.4:**

1. Heat of combustion of producer gas:

$$\Delta H_C = 1.81 \times 285.63 + 1.93 \times 282.99 + 4.9 \times 10^{-5} \times 890.3 = 1064.1 \text{ kJ} = 1.064 \text{ MJ}$$

2. Latent heat of water molecules: $1.37 \times 40.608 = 55.63$ kJ

3. Total moles of gasification products (in gas phase): 9.63

4. Volume of the gaseous products at NTP: 0.23 $m^3$

5. HHV of the producer gas $= (1.064 + 55.63 \times 10^{-3})/0.23 = 4.84$ MJ/$Nm^3$

6. LHV of the producer gas $= (1.064)/0.23 = 4.63$ MJ/$Nm^3$

**Gasification with air + steam (10% mole/mole) mixture at 500 $^{o}$C; AR = 0.2:**

1. Heat of combustion of producer gas:

$$\Delta H_C = 1.13 \times 285.63 + 0.202 \times 282.99 + 0.395 \times 890.3 = 731.6 \text{ kJ} = 0.732 \text{ MJ}$$

2. Latent heat of water molecules: $1.56 \times 40.608 = 63.35$ kJ

3. Total moles of gasification products (in gas phase): 5.54

4. Volume of the gaseous products at NTP: 0.13 $m^3$

5. HHV of the producer gas $= \left(0.732 + 63.35 \times 10^{-3}\right) / 0.13 = 5.96$ MJ/$Nm^3$

6. LHV of the producer gas $= \left(0.732\right) / 0.13 = 5.63$ MJ/$Nm^3$

**Gasification with air + steam (10% mole/mole) mixture at 500 $^{o}$C; AR = 0.4:**

1. Heat of combustion of producer gas:

$$\Delta H_C = 1.3 \times 285.63 + 0.295 \times 282.99 + 0.354 \times 890.3 = 769.96 \text{ kJ} = 0.77 \text{ MJ}$$

2. Latent heat of water molecules: $1.765 \times 40.608 = 71.67$ kJ

3. Total moles of gasification products (in gas phase): 8.75

4. Volume of the gaseous products at NTP: 0.21 $m^3$

5. HHV of the producer gas $= \left(0.77 + 71.67 \times 10^{-3}\right) / 0.21 = 4$ MJ/$Nm^3$

6. LHV of the producer gas $= \left(0.77\right) / 0.21 = 3.67$ MJ/$Nm^3$

**Gasification with air + steam (10% mole/mole) mixture at 900 $^{o}$C; AR = 0.2:**

1. Heat of combustion of producer gas:

$$\Delta H_C = 2.58 \times 285.63 + 2.41 \times 282.99 + 4.03 \times 10^{-4} \times 890.3 = 1419.3 \text{ kJ} = 1.419 \text{ MJ}$$

2. Latent heat of water molecules: $0.9016 \times 40.608 = 36.61$ kJ

3. Total moles of gasification products (in gas phase): 8.03

4. Volume of the gaseous products at NTP: 0.19 $m^3$

5. HHV of the producer gas $= \left(1.419 + 36.61 \times 10^{-3}\right) / 0.19 = 7.54$ MJ/$Nm^3$

6. LHV of the producer gas $= (1.419)/0.19 = 7.47$ MJ/Nm$^3$

**Gasification with air + 10% mole/mole steam mixture at 900 $^o$C with AR = 0.4**

1. Heat of combustion of producer gas:

$\Delta H_C = 1.96 \times 285.63 + 1.78 \times 282.99 + 3.89 \times 10^{-5} \times 890.3 = 1063.6$ kJ $= 1.064$ MJ

2. Latent heat of water molecules: $1.8126 \times 40.608 = 73.61$ kJ

3. Total moles of gasification products (in gas phase): 9.78

4. Volume of the gaseous products at NTP: 0.24 m$^3$

5. HHV of the producer gas $= \left(1.064 + 73.61 \times 10^{-3}\right)/0.24 = 4.84$ MJ/Nm$^3$

6. LHV of the producer gas $= (1.064)/0.24 = 4.43$ MJ/Nm$^3$

***A.3.3 Distribution of carbon and hydrogen among species:*** In section A.1.5, we determined the element vector input or the exact elemental composition of the gasification reaction mixture. We now determine as how the key elements carbon and hydrogen get distributed among various chemical species produced during gasification process. The principal species forming out of gasification of carbon are CO, $CO_2$, $CH_4$ and unconverted carbon (under certain conditions). On the other hand, the hydrogen in the gasification mixture gets distributed among 3 species, viz. $H_2$, $H_2O$ and $CH_4$.

The net carbon content of 4 carbonaceous species mentioned above (in gatoms per gmole) is 1 gatoms of C per mole of species. The net hydrogen content of various species, however, differs; both $H_2$ and $H_2O$ contain 2 gatoms of H per molecule, while $CH_4$ contains 4 gatoms of H per molecule. Therefore, on the basis of total elemental input and C and H content of various species, the fractional distribution of C and H is calculated as follows:

**Air gasification (Carbon distribution at 500 $^{o}$C)**

| Species | Total C = 3.09 gatoms; AR = 0.2 | | | Total C = 3.09 gatom; AR = 0.4 | | |
|---|---|---|---|---|---|---|
| | Moles | C content (gatom) | Fractional Carbon | Moles | C content (gatom) | Fractional Carbon |
| CO | 0.192 | 0.192 | 0.06 | 0.274 | 0.274 | 0.09 |
| $CO_2$ | 1.37 | 1.37 | 0.44 | 0.192 | 1.92 | 0.62 |
| $CH_4$ | 0.353 | 0.353 | 0.11 | 0.279 | 0.279 | 0.09 |
| C | 1.17 | 1.17 | 0.38 | 0.619 | 0.619 | 0.20 |

**Air gasification (Carbon distribution at 900 $^{o}$C)**

| Species | Total C = 3.09 gatom; AR = 0.2 | | | Total C = 3.09 gatom; AR = 0.4 | | |
|---|---|---|---|---|---|---|
| | Moles | C content (gatom) | Fractional Carbon | Moles | C content (gatom) | Fractional Carbon |
| CO | 2.51 | 2.51 | 0.82 | 1.93 | 1.93 | 0.63 |
| $CO_2$ | 0.571 | 0.571 | 0.19 | 1.16 | 1.16 | 0.38 |
| $CH_4$ | 0.00 | 0.00 | 0.00 | 0.00 | 0.00 | 0.00 |
| C | 0.00 | 0.00 | 0.00 | 0.00 | 0.00 | 0.00 |

**Air gasification (Hydrogen distribution at 500 $^{o}$C)**

| Species | Total H = 5.25 gatom; AR = 0.2 | | | Total C = 5.2 gatom; AR = 0.4 | | |
|---|---|---|---|---|---|---|
| | Moles | H content (gatom) | Fractional Hydrogen | Moles | H content (gatom) | Fractional Hydrogen |
| $H_2$ | 1.04 | 1.04 | 0.33 | 1.12 | 1.12 | 0.35 |
| $H_2O$ | 1.43 | 1.43 | 0.45 | 1.51 | 1.51 | 0.47 |
| $CH_4$ | 0.353 | 0.353 | 0.22 | 0.279 | 0.279 | 0.18 |

**Air gasification (Hydrogen distribution at 900 $^{o}$C)**

| Species | Total H = 5.25 gatom; AR = 0.2 | | | Total H = 5.25 gatom; AR = 0.4 | | |
|---|---|---|---|---|---|---|
| | Moles | H content (gatom) | Fractional Hydrogen | Moles | H content (gatom) | Fractional Hydrogen |
| $H_2$ | 2.47 | 2.47 | 0.78 | 1.81 | 1.81 | 0.57 |
| $H_2O$ | 0.705 | 0.705 | 0.22 | 1.37 | 1.37 | 0.43 |
| $CH_4$ | 0.00 | 0.00 | 0.00 | 0.00 | 0.00 | 0.00 |

The fractional distribution of elements for gasification with steam-air mixture can be calculated along similar lines.

## A.4 Determination of Efficiency of Gasification

In this section, we attempt to determine the theoretical efficiency of the gasification process. According to first principle, the definition of efficiency is: Energy output/Energy input. We first identify the components of energy input and output of the gasification system:

### A.4.1 Energy input and output

Various components of the energy input are (1) Energy of the gasification medium; (2) Energy content (HHV) of the biomass (dry basis); (3) Energy required for raising temperature of biomass to gasification temperature. The energy output from gasifier is essentially the heat of combustion of the producer gas (we do not include in this the latent heat of the water vapor content in the producer gas for reasons explained later). We describe calculation of each of this component and finally calculate the efficiency of the gasification process.

### A.4.2 Gasification with air (Temp = 900 $^{o}$C, AR = 0.2)

(1) *Energy of gasification medium:* This is the energy required to heat the medium to the required temperature and it is determined as: $H_{air} = C_{P_{air}} n_{air} (T_{final} - T_{ambient})$ (A.9)

Notation: $H_{air}$ = energy content of air; $C_{p,air}$ = heat capacity of air; $T_{final}$ = gasification temperature (to which air has to be heated); $T_{ambient}$ = ambient or atmospheric temperature.

In section A.1.1 & A.1.2, calculation of number of moles of air was explained. Per this calculation, the number of moles of air for gasification of 100 g of rice husk at AR = 0.2 are $n_{air}$ = 2.985 moles , Heat capacity of air is: $C_{p_{air}}$ = 30.24 J/gmole K . Substituting values, we get: $H_{air}$ = 81240 J or 81.2 kJ.

The biomass is assumed to contain 10% w/w moisture, which is 10 g for 100 g biomass under consideration. The energy required for vaporization of this moisture and superheating of the vapor to the gasification temperature is also supplied by air. This energy required is calculated as follows:

$$H_{moisture} = n_{moisture}\left[C_{p_{water}}\left(100 - T_{ambient}\right) + \lambda_{f_g} + C_{p_{steam}}\left(T_{final} - 100\right)\right] \qquad \text{(A.10)}$$

where $n_{moisture}$ are the number of moles of moisture in the biomass, $\lambda_{fg}$ is the latent heat of vaporization and $C_{P,steam}$ is the heat capacity of steam. Values of these parameters are: $n_{moisture}$ = 10/18 = 0.5556 gmoles; $C_{p_{water}}$ = 75.24 J/gmole K ; $C_{p_{,steam}}$ = 37.44 J/gmole K ; $\lambda_{f_g}$ = 40.608 kJ/gmole and $T_{ambient}$ = 30°C . The total energy content of the gasification medium is: 42130 + 81240 = 123370 J or 123.37 kJ.

(2) *Energy content (HHV) of biomass*: For estimation of the energy content of biomass, we use the correlation of Channiwala and Parikh [10]:

$$\text{HHV (MJ/kg)} = 0.3491\ C + 1.1783\ H + 0.10055\ S - 0.1034\ O - 0.151\ N - 0.0211\ A \qquad \text{(A.11)}$$

where C, H, S, O, N and A represent carbon, hydrogen, oxygen, nitrogen, sulfur and ash contents of the biomass expressed in mass percentages on dry basis. The values of these parameters for rice husk are: C = 37.03%, H = 5.25%, N = 0.09%, O = 40.94%, A = 16.69%. Substituting values we get the HHV of rice husk is 14.528 MJ/kg. We consider 100 g of biomass for calculation, and hence, the net energy content of biomass is: 14.528 × 0.1 = 1.4528 MJ or 1452.8 kJ.

(3) *Energy required for raising temperature of biomass*: The heat capacity of biomass (dry basis) can be taken to be 0.42 J/g K (Wikipedia [11]). Energy required for raising temperature of 100 g rice husk (assume to be at an initial temperature of 30 °C) to 900 °C is then: 100 × 0.42 × (900 – 30) = 36540 J (or 36.54 kJ).

(4) *Energy output from the gasifier:* This is essentially the heat of combustion of the producer gas resulting from gasification. It must be noted that heat of combustion of different than the HHV of the producer gas calculated earlier. Since we are considering producer gas for purpose of firing the internal combustion engines or for chemical synthesis, the energy content (or the

latent heat) of vapor is not useful. The net energy content of gas relevant for applications in the present context is essentially the heat of combustion, i.e. energy obtained after burning of components such as CO, $H_2$ and $CH_4$. As already calculated in section A.3.2, the producer gas resulting from gasification of rice husk at 900°C and AR = 0.2 has heat of combustion of 1418.6 kJ or 1.419 MJ.

(5) *Efficiency of gasification:* As mentioned earlier, the efficiency of gasification is the net energy output divided by the total energy input. After identifying various components of energy input and output from gasifier, we defined efficiency as follows:

$$\lambda = \frac{\text{Energy output from gasifier}}{\left\{\begin{array}{l}\text{Energy input through gasification medium (either air or air-steam mixture)} \\ + \text{HHV of biomass} \\ + \text{Energy required to heat biomass with accompanying moisture to gasification temperature}\end{array}\right\}} \quad \text{(A.12)}$$

Substituting values of various components, we get the efficiency as:

$$\eta = \frac{1418.6}{(1452.8 + 36.54 + 123.37)} = 0.8796 \text{ or } 87.96\% \quad \text{(A.13)}$$

### A.4.3 Gasification with air + 10% mole/mole steam mixture (Temp = 900 °C, AR = 0.2)

(1) *Energy of the gasification medium:* For gasification with steam-air mixture, we assume that this mixture is made by spraying water in hot air. The heat required for vaporization of water and superheating of the vapor to the gasification temperature is supplied by air itself. As mentioned earlier, the number of air moles required for gasification of rice husk at AR = 0.2 are 2.985. The numbers of steam moles are: $0.1 \times 2.985 = 0.2985$ moles. The energy required for vaporization of 0.2985 moles of water sprayed in hot air and superheating of the vapor to gasification temperature is calculated as follows:

$$H_{steam} = n_{steam}\left[C_{p_{steam}}(100 - T_{ambient}) + \lambda_{f_g} + C_{p_{steam}}(T_{final} - 100)\right] \quad \text{(A.14)}$$

Values of various parameters are: $n_{steam} = 0.2985$ moles , $C_{P_{water}} = 75.24$ J/gmole K , $C_{P_{steam}} = 37.44$ J/gmole K , $\lambda_{f_g} = 40608$ J/gmole , $T_{ambient} = 30\ ^{o}\text{C}$ . Substituting these we get: $H_{steam}$ = 22630 J or 22.63 kJ. The energy required for heating of air to gasification temperature evaporation and superheating of moisture content of biomass, however, remains same as before. Thus, the net energy input through gasification medium is: $H_{steam} + H_{air} + H_{moisture}$ = 22630 + 81240 + 42310 = 146 kJ.

(2) *Energy content (HHV) of biomass*: This is same as calculated in previous section, viz. 1452.8 kJ.

(3) *Energy required for raising temperature of biomass to gasification temperature:* This value is again same as previous case, viz. 36.54 kJ.

(4) *Energy output from gasifier*: this is essentially the heat of combustion of producer gas resulting from gasification. As calculated in section A.3.2, this value is 1.4193 MJ.

(5) *Efficiency of gasification*: This parameter is calculated in the same manner as described in previous section:

$$\eta = \frac{1419.3}{(146 + 1452.8 + 36.54)} = 0.8678 \text{ or } 86.78\% \qquad \text{(A.15)}$$

### A.4.4 Steady state efficiency

The gasification process as a whole is an exothermic process and the heat released is carried out by the producer gas. At steady state, the energy requirement for heating the gasification medium (either air or air-steam mixtures) and biomass (with accompanying moisture) to the required temperature could be met by having heat recovery from the producer gas itself (or the energy integration of the process). In this case, the efficiency of the gasification would be simply: η = Heat of combustion of producer gas/HHV of biomass. With this modified definition, the gasification efficiency for conditions in section A.4.2 would be η = 1418.6/1452.8 = 0.9764 or 97.64%, and that for section A.4.3 would be η = 1419.3/1452.8 =

0.9769 or 97.69%. It should, however, be noted that these are theoretical efficiencies. The efficiencies observed experimentally are smaller than these due to the thermal losses in the gasifier system.

CHAPTER 5

# Investigations in Gasification of Biomass Mixtures

## 5.1 INTRODUCTION

In recent years, biomass gasification has emerged as the most viable option for decentralized power generation in India. The most popular gasifiers are atmospheric and downdraft type with either dual fuel or 100% producer gas engine–generator sets. Most of these gasifiers mainly use wood chips as fuel, although several new designs have been developed that can use alternative fuels such as coconut shells and briquettes. Typical capacity of these gasifiers ranges from 5 to 250 kW [1,2]. For capacities higher than 1 MW, fluidized bed gasifier is the most feasible design [3]. These gasifiers have the merits of fuel flexibility, uniformity of temperature over reactor volume, low tar content of producer gas and high overall carbon conversion. Typical specific consumption of biomass fuel in these gasifiers is 1 to 1.2 kg/kWh [4]. Thus, the annual biomass requirement of a typical 5 MW gasifier plant (with capacity utilization factor of 70%) is more than 35,000 tons. It is rather unlikely, in any region of the country, that a single biomass would be available through out the year in such large quantities for meeting the fuel demands of the plant, and thus, mixtures of different biomasses that are available in different seasons would have to be used. This

necessitates a thorough study of the performance of gasifier in terms of fuel flexibility, i.e. variation in the quality and quantity of the producer gas resulting from gasification of biomass mixtures of different compositions. Such a study would provide important guidelines for design and scale–up of fluidized bed gasifiers with biomass mixtures as fuel input.

In this chapter, we have addressed this issue with equilibrium thermodynamic models. We assess gasification characteristics of mixtures three representative biomasses, which are available in abundance in the northeastern states of India [5], viz. rice husk, saw dust and bamboo dust. In addition, we also evaluate the gasification process with semi–equilibrium models, in which we take into consideration partial conversion of carbon in the biomass. In the next section, we have described the aim and approach of this study in greater detail.

## 5.2 AIM & APPROACH

In the context of the present study, where we are concerned with biomass gasification for decentralized power generation, the principal outcome would be the LHV of the producer gas resulting from biomass gasification. The ultimate analyses of the individual biomasses considered in this study are given in Table 5.1(A). In addition to biomass fuel, we must consider other important parameters that influence the content and quality of the producer gas resulting from gasification. These are: (1) temperature of gasification and (2) air or equivalence ratio, which is the ratio of actual oxygen supplied for gasification to the oxygen required for complete combustion of biomass [6,7]. From the analysis presented in previous chapter on gasification of individual biomasses (viz. rice husk, bamboo dust and saw dust), we have established that the most suitable ranges of these parameters are: temperature = 700–1000$^{o}$C and air ratio = 0.2–0.4. We, therefore, choose four representative temperatures, viz. 700, 800, 900 and 1000$^{o}$C and three air ratios, viz. 0.2, 0.3 and 0.4 for the simulations. Although we vary the air ratio and temperature of gasification independently in simulations

with permutation–combinations of the values mentioned, it should be noted that under practical situation, the air ratio and temperature of gasification are related or interdependent parameters. Most of the gasifiers operate adiabatically and higher air ratio would result in greater biomass conversion and would lead to higher gasification temperature.

Moreover, we consider binary biomass mixtures for analysis (i.e. biomass mixtures comprised of any two of the three biomasses mentioned above). We combine these two individual biomasses in three proportions in weight percent as 25%–75%, 50%–50% and 75%–25%. Thus, we have 9 combinations of biomass mixtures. The elemental analysis of these mixtures of biomasses along with a representative molecular formula for the biomass mixture is given in Table 5.1(B).

### 5.2.1 Determination of the Energy Content of Biomass Mixture

Prior to simulations of the gasification of the biomass mixtures, it is essential to estimate the energy content of these mixtures. It is basically this energy that appears in two forms after gasification, viz. the "chemical" energy which is the LHV of the producer gas resulting from gasification process and the "physical" energy, which is the net enthalpy change or heat release from the gasification process. For this purpose, we have chosen two correlations as follows:

(1) A general correlation for all solid fuels such as coal, biomass etc. [8]:

$$\text{HHV (MJ/kg or kJ/g)} = 0.3491\,C + 1.1783\,H + 0.10055\,S - 0.1034\,O - 0.151\,N - 0.0211\,A \quad (5.1)$$

(2) A specific correlation for HHV of biomasses only [9]:

$$\text{HHV (kJ/kg)} = 3.55\,C^2 - 232\,C - 2230\,H + 51.2\,C{\times}H + 131\,N + 20{,}600 \quad (5.2)$$

where C, H, S, O, N and A represent carbon, hydrogen, oxygen, nitrogen, sulfur and ash content of the biomass expressed in mass percentages on dry basis. The values of these parameters for the three biomasses are given in Table 5.1(A). To estimate the energy content

of the biomass mixture, we first determine the HHV per gram of the individual biomasses with above correlation and add up the values of HHV in kJ as per the mixture composition. Table 5.1(B) lists the energy content of the 9 biomass mixtures considered in this study. It could be inferred from Table 5.1(B) that HHV predicted by specific correlation of Friedl et al. [9] are somewhat higher than those predicted by general correlation of Channiwala and Parikh [8]. Sheng and Azevedo [10] have also reported a similar correlation for HHV of biomass as that of Friedl et al. [9].

**Table 5.1**: Elemental compositions
(A) Individual biomasses (ultimate analysis)

| Biomass | Composition in weight percent (Dry Basis) | | | | | Molecular Formula |
|---|---|---|---|---|---|---|
| | Carbon | Hydrogen | Nitrogen | Oxygen | Ash | |
| Saw dust | 52.28 | 5.2 | 0.47 | 40.85 | 1.2 | $CH_{1.193}N_{0.007}O_{0.585}$ |
| Rice husk | 37.03 | 5.25 | 0.09 | 40.94 | 16.69 | $CH_{1.699}N_{0.003}O_{0.828}$ |
| Bamboo dust | 39.88 | 5.5 | 0.89 | 47.92 | 5.81 | $CH_{1.657}N_{0.018}O_{0.904}$ |

(B) Biomass mixtures (Basis: 100 g of total biomass mixture)

| Biomass Components | Mixture Composition | Elemental Composition (gatoms) | | | | Molecular Formula** | Net Energy Content (kJ per 100 g) | |
|---|---|---|---|---|---|---|---|---|
| | | C | H | N | O | | Ref. [8] | Ref. [9] |
| Rice Husk **(RH)** Saw Dust **(SD)** | RH = 25%, SD = 75% | 4.039 | 5.213 | 0.027 | 2.555 | $CH_{1.291}N_{0.007}O_{0.633}$ | 1867 | 1920 |
| | RH = 50%, SD = 50% | 3.721 | 5.225 | 0.02 | 2.556 | $CH_{1.404}N_{0.005}O_{0.687}$ | 1729 | 1785 |
| | RH = 75%, SD = 25% | 3.404 | 5.238 | 0.013 | 2.557 | $CH_{1.539}N_{0.004}O_{0.751}$ | 1590 | 1649 |
| Bamboo Dust **(BD)** Rice Husk **(RH)** | BD = 25%, RH = 75% | 3.145 | 5.313 | 0.021 | 2.668 | $CH_{1.689}N_{0.007}O_{0.848}$ | 1468 | 1537 |
| | BD = 50%, RH = 50% | 3.205 | 5.375 | 0.035 | 2.777 | $CH_{1.677}N_{0.011}O_{0.866}$ | 1485 | 1560 |
| | BD = 75%, RH = 25% | 3.264 | 5.438 | 0.049 | 2.886 | $CH_{1.666}N_{0.015}O_{0.884}$ | 1502 | 1584 |
| Bamboo Dust **(BD)** Saw Dust **(SD)** | BD = 25%, SD = 75% | 4.098 | 5.275 | 0.041 | 2.664 | $CH_{1.287}N_{0.010}O_{0.650}$ | 1884 | 1944 |
| | BD = 50%, SD = 50% | 3.84 | 5.35 | 0.049 | 2.774 | $CH_{1.393}N_{0.013}O_{0.722}$ | 1762 | 1832 |
| | BD = 75%, SD = 25% | 3.582 | 5.425 | 0.056 | 2.885 | $CH_{1.515}N_{0.016}O_{0.805}$ | 1641 | 1720 |

** *The molecular formula represents the mixture of two biomasses as a single entity. All biomasses are assumed to contain 10% w/w moisture.*

These nine combinations of biomass mixtures coupled with three air ratios and four temperatures mentioned above constitute 108 conditions for which we do simulations with thermodynamic equilibrium model. The elemental compositions (or elemental vector input)

for the 27 mixtures for gasification process (i.e. 9 combinations of biomass mixtures, along with gasification medium, i.e. air, for 3 different air ratios) are given in Table 5.2 (please note that this elemental input also includes moisture content of biomass, assumed to be 10% w/w).

**Table 5.2:** Elemental vector input (in gatom) for simulations
(Basis: 100 g of total biomass mixture + air for gasification)

| **Biomass: RH (25%) + SD (75%)** | | | |
|---|---|---|---|
| Element / | AR | | |
| Elemental Ratio | 0.2 | 0.3 | 0.4 |
| C | 4.039 | 4.039 | 4.039 |
| H | 6.324 | 6.324 | 6.324 |
| N | 6.180 | 9.257 | 12.334 |
| O | 4.736 | 5.549 | 6.362 |
| H/C | 1.566 | 1.566 | 1.566 |
| O/C | 1.173 | 1.374 | 1.575 |

| **Biomass: RH (50%) + SD (50%)** | | | |
|---|---|---|---|
| Element / | AR | | |
| Elemental Ratio | 0.2 | 0.3 | 0.4 |
| C | 3.721 | 3.721 | 3.721 |
| H | 6.336 | 6.336 | 6.336 |
| N | 5.696 | 8.534 | 11.373 |
| O | 4.611 | 5.361 | 6.111 |
| H/C | 1.703 | 1.703 | 1.703 |
| O/C | 1.239 | 1.441 | 1.642 |

| **Biomass: RH (75%) + SD (25%)** | | | |
|---|---|---|---|
| Element / | AR | | |
| Elemental Ratio | 0.2 | 0.3 | 0.4 |
| C | 3.404 | 3.404 | 3.404 |
| H | 6.349 | 6.349 | 6.349 |
| N | 5.212 | 7.812 | 10.411 |
| O | 4.487 | 5.173 | 5.860 |
| H/C | 1.865 | 1.865 | 1.865 |
| O/C | 1.318 | 1.520 | 1.722 |

| **Biomass: BD (25%) + RH (75%)** | | | |
|---|---|---|---|
| Element / | AR | | |
| Elemental Ratio | 0.2 | 0.3 | 0.4 |
| C | 3.145 | 3.145 | 3.145 |
| H | 6.424 | 6.424 | 6.424 |
| N | 4.773 | 7.150 | 9.526 |
| O | 4.479 | 5.107 | 5.735 |
| H/C | 2.043 | 2.043 | 2.043 |
| O/C | 1.424 | 1.624 | 1.824 |

| **Biomass: BD (50%) + RH (50%)** | | | |
|---|---|---|---|
| Element / | AR | | |
| Elemental Ratio | 0.2 | 0.3 | 0.4 |
| C | 3.205 | 3.205 | 3.205 |
| H | 6.486 | 6.486 | 6.486 |
| N | 4.819 | 7.211 | 9.602 |
| O | 4.596 | 5.228 | 5.860 |
| H/C | 2.024 | 2.024 | 2.024 |
| O/C | 1.434 | 1.631 | 1.828 |

| **Biomass: BD (75%) + RH (25%)** | | | |
|---|---|---|---|
| Element / | AR | | |
| Elemental Ratio | 0.2 | 0.3 | 0.4 |
| C | 3.264 | 3.264 | 3.264 |
| H | 6.549 | 6.549 | 6.549 |
| N | 4.864 | 7.271 | 9.679 |
| O | 4.714 | 5.350 | 5.986 |
| H/C | 2.006 | 2.006 | 2.006 |
| O/C | 1.444 | 1.639 | 1.834 |

| **Biomass: BD (25%) + SD (75%)** | | | |
|---|---|---|---|
| Element / | AR | | |
| Elemental Ratio | 0.2 | 0.3 | 0.4 |
| C | 4.098 | 4.098 | 4.098 |
| H | 6.386 | 6.386 | 6.386 |
| N | 6.226 | 9.318 | 12.410 |
| O | 4.863 | 5.670 | 6.487 |
| H/C | 1.558 | 1.558 | 1.558 |
| O/C | 1.187 | 1.384 | 1.583 |

| **Biomass: BD (50%) + SD (50%)** | | | |
|---|---|---|---|
| Element / | AR | | |
| Elemental Ratio | 0.2 | 0.3 | 0.4 |
| C | 3.840 | 3.840 | 3.840 |
| H | 6.461 | 6.461 | 6.461 |
| N | 5.787 | 8.656 | 11.525 |
| O | 4.846 | 5.604 | 6.362 |
| H/C | 1.683 | 1.683 | 1.683 |
| O/C | 1.262 | 1.459 | 1.657 |

| **Biomass: BD (75%) + SD (25%)** | | | |
|---|---|---|---|
| Element / | AR | | |
| Elemental Ratio | 0.2 | 0.3 | 0.4 |
| C | 3.582 | 3.582 | 3.582 |
| H | 6.536 | 6.536 | 6.536 |
| N | 5.348 | 7.994 | 10.640 |
| O | 4.838 | 5.537 | 6.237 |
| H/C | 1.825 | 1.825 | 1.825 |
| O/C | 1.351 | 1.546 | 1.741 |

***Note:*** *All biomasses are assumed to contain 10% w/w moisture. The elements C, H, N and O are given in gatom while the elemental ratio is dimensionless.*

### 5.2.2 Incomplete Carbon Conversion

In a fluidized bed biomass gasifier, the residence time of the biomass mixture is small as it is carried out of the riser section with the gasification air. Therefore, kinetics of various chemical reactions in the gasification process comes into the picture. The major result of short residence time of biomass is incomplete conversion of carbon in it. Several authors have established that biomass gets devolatilized and pyrolysed almost instantly as it enters the riser section near the bottom [11–15], where the temperatures are quite high (~ 900–1100 K). The major products of pyrolysis process are char, tar (or heavy hydrocarbons), CO, $CO_2$, $H_2$, $H_2O$, $CH_4$ and $C_2H_6$+$C_2H_4$ [11,14]. Char essentially comprises of carbon, which is then

oxidized by the oxygen present in gasification medium [7]. However, the oxidation may not complete till the biomass leaves the riser section of fluidized bed gasifier. This incomplete conversion of carbon leads to reduction in the quality as well as quantity of producer gas. In this chapter, we have also tried to assess this effect with approach of semi–equilibrium model. In this approach, we reduce the moles of carbon in the elemental vector input (given in Table 5.2). The number of input moles of other three elements, viz. H, N and O are kept unchanged, or in other words, conversion of these elements is assumed to be complete. This approach is known as semi (or quasi)–equilibrium model [16–18]. In this category, however, we have considered binary biomass mixtures with even composition only (i.e. 50%–50% w/w fraction of two biomasses in the mixture). Moreover, we have considered only one air ratio (= 0.3) and temperature of gasification (800$^{o}$C or 1073 K). These parameters have been chosen in view of practical values of carbon conversions observed in fluidized bed gasification, as explained in the next paragraph.

Lv et al. [19] have given experimental values of carbon conversion in a fluidized bed using pine saw dust (particle size 0.3–0.45 mm, feed rate = 0.512 kg/h) as feed–stock. For an air ratio range of 0.19–0.27, and gasification temperature of 800$^{o}$C, the carbon conversion efficiency of the gasifier varied between 70.6–90.6%. On the basis of these experimental observations, we have chosen 3 representative values for carbon conversion in our simulations, viz. 60%, 70% and 80% (or 0.6, 0.7 and 0.8). This range is slightly on lower side than that reported by Lv et al. [19], and thus, our simulations give a rather “conservative” estimate of the performance of the biomass gasification process.

In view of this, we have chosen three representative values for carbon conversion ($x_C$), viz. 0.6, 0.7 and 0.8. The gatom of carbon in the elemental vector input in the semi–equilibrium model are $x_C \times$ C, where C are gatom of carbon in the biomass mixtures as given in Table 5.2 (i.e. elemental vector input in the equilibrium model). The balance carbon, i.e.

$(1–x_C) \times C$, is assumed to remain unconverted, and appears as elemental carbon (C) species in the products of biomass gasification.

## 5.3 THE MATHEMATICAL MODEL

For the simulations, we have used the software FACTSAGE (Fact Web [20], Bale et al. [21]). This software employs the algorithm SOLGASMIX proposed by Eriksson [22] for calculation of thermodynamic equilibrium. The SOLGASMIX model was described in detail in previous chapter. However, for the convenience of the reader, we give below the main equations of this model.

### 5.3.1 Equations for Gibbs energy minimization

For a system comprising of mixture of *i* species, the total Gibbs free energy (*G*) is:

$$G = \sum_i x_i g_i \tag{5.3}$$

$x_i$ is the mole number of a substance or species in the mixture, and $g_i$ is the chemical potential written as:

$$g_i = g_i^0 + RT \ln a_i \tag{5.4}$$

We assume ideal behavior for the gaseous species, and hence, the activities $a_i$ are equal to the partial pressure $p_i$:

$$a_i = p_i = (x_i / X)P \tag{5.5}$$

*X* represents total number of moles in the gas phase and *P* is the total pressure of the system, respectively. The condensed substances are assumed to be pure, and hence, their activities are equal to unity. With these quantities, we define a new dimensionless quantity (*G/RT*) as:

$$G/RT = \sum_{i=1}^{m} x_i^g [(g^0/RT)_i^g + \ln P + \ln(x_i^g / X)] + \sum_{i=1}^{s} x_i^c (g^0/RT)_i^c \tag{5.6}$$

Superscripts *g* and *c* represent gas phase and condensed phase, respectively, while *m* and *s*

represent the total number of substances in the gas phase and condensed phase, respectively, at equilibrium. $R$ is the ideal gas constant. The value of ($g^o/RT$) for a certain substance is calculated using the expression:

$$(g^o / RT) = (1/R)[G^o - H^o_{298})/T + \Delta_f H^o_{298} / RT \qquad (5.7)$$

Superscript $^o$ refers to the thermodynamic standard state; subscript $_{298}$ refers to the reference temperature (25$^o$C = 298.15 K); subscript $_f$ denotes the formation of a compound from the elements in their standard states. The mass balance among various species can be written as:

$$\sum_{i=1}^{m} a_{ij}^g x_i^g + \sum_{i=1}^{s} a_{ij}^c x_i^c = b_j \, (j = 1,2,.....l) \qquad (5.8)$$

where $a_{ij}$ represents the number of atoms of the $j^{th}$ element in a molecule of the $i^{th}$ substance, $b_j$ is the total number of moles of the $j^{th}$ element, and $l$ is the total number of elements. The method involves a search for a minimum value of the free energy $G$ of a system (or equivalently $G/RT$ as given in equation 5.6) subject to the mass balance relation as subsidiary conditions. For solution of this system of equations, Lagrange's methods of undetermined multipliers can be used.

Since the equilibrium composition has been obtained, the heat generation or the total heat of a process can be computed, using values of $\Delta_f H^o_{298}$, $C_p$ and $(H^o - H^o_{298})$ as follows:

The energy necessary for pre–heating the initial mixture ($HP$) from the initial temperature $T_1$ K to the reaction temperature T K, added to the heat of reaction $(HR)$, gives the total heat $(HT)$: $HT = HP + HR$. $HP$ and $HR$ are given by the following expressions:

$$HP = \sum_i x_i^* (H^o - H^o_{T1})_i \qquad (5.9)$$

where $x^*$ denotes the number of moles in the initial mixture, and:

$$(H^o - H^o_{T1})_i = \int_{T_1}^{T} (C_p)_i \, dT \qquad (5.10)$$

$$HR = \sum_i (\Delta_f H_T^o)_i (x_i - x_i^*) \qquad (5.11)$$

where $(\Delta_f H_T^o)_i = (\Delta_f H_{298}^o)_i + [(H^o - H_{298}^o)_i - (H^o - H_{298}^o)_{elements}]$. Other notations in equations 5.9–5.11 are: $H$ = enthalpy (heat content); $T$ = absolute temperature of the system; $x^*$ = number of moles in the initial mixture; $C_p$ = heat capacity at constant pressure as a function of temperature; $\Delta_f H_{298}^o$ = heat of formation at 298.15 K; $\left(G^o - H_{298}^o\right)/T$ = free energy function; $\left(H^o - H_{298}^o\right)$ = heat content function.

## 5.4 RESULTS OF SIMULATION

We have presented the results of gasification of biomass mixtures in two parts: (1) simulations with equilibrium models and (2) simulations with semi–equilibrium models. In both of these parts, we have first assessed the principal characteristics of the producer gas (viz. net yield of producer gas in $Nm^3$ per 100 g of biomass mixture, hydrogen and carbon monoxide content of the gas in gmoles and the LHV of the gas in $MJ/Nm^3$) resulting from gasification of biomass, followed by net thermal energy available for power generation (in kJ per 100 g of biomass mixture) and net enthalpy change (or heat of reaction in kJ per 100 g of biomass mixture) in the gasification process. Next, we have presented the fractional distribution of carbon and hydrogen in the gasification mixture (biomass mixture + air) among various species in the producer gas such as CO, $CO_2$, $H_2$, $H_2O$, $CH_4$ and C (i.e. unconverted carbon). Figures 5.1–5.10 and Table 5.3 depict the simulation results of gasification of biomass mixtures with equilibrium models, while Table 5.4 and Figure 5.11 summarizes simulation results of gasification of biomass mixtures with semi–equilibrium models.

### 5.4.1 Trends in Simulation Results (Equilibrium Model)

From the data presented in Figures 5.1–5.10 and Table 5.3, we identify following

trends in various characteristics of producer gas obtained from gasification of biomass mixtures at different conditions.

**Net gas yield (Figure 5.1):** For all biomass mixtures, the net gas yield increases with air ratio; however, the temperature rise from 700–1000$^{o}$C does not affect the gas yield. For biomass mixtures containing saw dust (which has higher carbon content than other two biomasses), the gas yield slightly reduces as the proportion of the saw dust in the mixture reduces. However, for mixtures of rice husk and bamboo dust, the gas yield is practically independent of the mixture composition.

**Hydrogen content of producer gas (Figure 5.2):** For a given gasification temperature, the hydrogen content of the producer gas decreases with air ratio for all biomass mixtures. On the other hand, for a given air ratio, the hydrogen content does not show a common trend with gasification temperature. For AR = 0.2, the hydrogen content rises till 900$^{o}$C and thereafter decreases, whereas for AR = 0.3 and 0.4, the hydrogen content reduces continuously with rising gasification temperature. No particular trend can be seen for hydrogen with constituents of the biomass mixture. For a given combination of temperature and air ratio, the hydrogen content of producer gas varies by less than ±10% with composition of the mixtures. Even among mixtures of different biomasses (RH+SD; SD+BD or RH+BD), the hydrogen content of producer gas shows insignificant variation.

**Carbon monoxide content of producer gas (Figure 5.3):** For a given gasification temperature, the CO content of the producer gas reduces with air ratio. This trend is consistent for all 9 mixtures of biomasses. Similarly, for all 9 mixtures, the CO content of producer gas increases with temperature at a constant air ratio. For biomass mixtures constituting saw dust, at any combination of air ratio and gasification temperature, the CO content is significantly higher (by about 25–40%) than the corresponding value for mixtures of rice husk and bamboo dust. Moreover, for biomass mixtures comprising saw dust, the CO

content reduces with the proportion of saw dust in the mixture. This effect is clearly attributed to higher carbon content of saw dust than rice husk and bamboo dust.

**LHV of producer gas (Figure 5.4):** The major combustible components of the producer gas are CO and $H_2$. It is thus obvious that the trend in the LHV of the producer gas is similar to that of hydrogen and carbon monoxide. For a given gasification temperature, the LHV reduces with increasing air ratio; whereas, for a given air ratio, the LHV increases with gasification temperature. For biomass mixtures comprising saw dust, the LHV values for any combination of air ratio and gasification temperature are higher than the corresponding values for mixtures of rice husk and bamboo dust. Moreover, for mixtures of saw dust, the LHV at any air ratio and temperature reduces with proportion of saw dust in the mixture. These trends are essentially same as that of CO content.

**Net thermal energy content of producer gas (Table 5.3A):** The thermal energy content of producer gas resulting from gasification of 100 g of biomass mixture can be obtained by product of net yield of the gas (in $Nm^3$) and the LHV of the gas (in $MJ/Nm^3$). This energy is essentially the potential of the producer gas for generation of power (through engine–generator sets operating on dual fuel or 100% producer gas). This parameter shows same trends as the LHV. It reduces with increasing air ratio for a particular gasification temperature, and increases with gasification temperature for a particular air ratio. Moreover, thermal energy content of producer gas is higher for mixtures containing saw dust and varies directly with the proportion of the saw dust in the mixture.

**Net enthalpy change in gasification (Table 5.3B):** This is the net energy released by the gasification reaction system in the process of attaining equilibrium (and hence, this parameter is similar to the heat of reaction). One can infer from Table 5.3(B) that for a given air ratio, net enthalpy change reduces with gasification temperature while for a particular gasification temperature it increases with air ratio. Enthalpy change for any combination of temperature

and air ratio is lower for biomass mixtures comprising saw dust (as compared to the mixtures of bamboo dust and rice husk). Moreover, for mixtures of saw dust, the enthalpy change shows inverse variation with the proportion of saw dust in the mixture for any particular air ratio and gasification temperature. Interestingly, these trends are exactly opposite to the trends in LHV of the producer gas – reasons for which are explained in section 5.5.

**Table 5.3:** Simulation results for the gasification of biomass mixtures
(Basis: 100 g of total biomass mixture)
(A) Net thermal energy ($\Delta H_{th,P}$, kJ) content of producer gas

| (A) Biomass: RH (25%) + SD (75%) | | | | (A) Biomass: BD (25%) + SD (75%) | | | | (A) Biomass: BD (25%) + RH (75%) | | | |
|---|---|---|---|---|---|---|---|---|---|---|---|
| Temp (°C) | Air Ratio | | | Temp (°C) | Air Ratio | | | Temp (°C) | Air Ratio | | |
| | 0.2 | 0.3 | 0.4 | | 0.2 | 0.3 | 0.4 | | 0.2 | 0.3 | 0.4 |
| 700 | 1570 | 1604 | 1382 | 700 | 1594 | 1612 | 1389 | 700 | 1411 | 1244 | 1069 |
| 800 | 1844 | 1616 | 1386 | 800 | 1853 | 1624 | 1393 | 800 | 1427 | 1249 | 1071 |
| 900 | 1848 | 1617 | 1386 | 900 | 1857 | 1625 | 1393 | 900 | 1428 | 1249 | 1071 |
| 1000 | 1848 | 1617 | 1386 | 1000 | 1857 | 1625 | 1392 | 1000 | 1428 | 1249 | 1071 |
| (B) Biomass: RH (50%) + SD (50%) | | | | (B) Biomass: BD (50%) + SD (50%) | | | | (B) Biomass: BD (50%) + RH (50%) | | | |
| Temp (°C) | Air Ratio | | | Temp (°C) | Air Ratio | | | Temp (°C) | Air Ratio | | |
| | 0.2 | 0.3 | 0.4 | | 0.2 | 0.3 | 0.4 | | 0.2 | 0.3 | 0.4 |
| 700 | 1548 | 1481 | 1275 | 700 | 1596 | 1498 | 1290 | 700 | 1421 | 1252 | 1077 |
| 800 | 1702 | 1491 | 1278 | 800 | 1721 | 1507 | 1292 | 800 | 1437 | 1258 | 1078 |
| 900 | 1704 | 1491 | 1278 | 900 | 1723 | 1508 | 1292 | 900 | 1437 | 1258 | 1078 |
| 1000 | 1705 | 1491 | 1278 | 1000 | 1723 | 1508 | 1292 | 1000 | 1437 | 1258 | 1078 |
| (C) Biomass: RH (75%) + SD (25%) | | | | (C) Biomass: BD (75%) + SD (25%) | | | | (C) Biomass: BD (75%) + RH (25%) | | | |
| Temp (°C) | Air Ratio | | | Temp (°C) | Air Ratio | | | Temp (°C) | Air Ratio | | |
| | 0.2 | 0.3 | 0.4 | | 0.2 | 0.3 | 0.4 | | 0.2 | 0.3 | 0.4 |
| 700 | 1527 | 1359 | 1169 | 700 | 1569 | 1384 | 1190 | 700 | 1431 | 1260 | 1083 |
| 800 | 1560 | 1367 | 1172 | 800 | 1588 | 1391 | 1192 | 800 | 1446 | 1266 | 1085 |
| 900 | 1562 | 1367 | 1172 | 900 | 1590 | 1391 | 1192 | 900 | 1446 | 1266 | 1085 |
| 1000 | 1562 | 1367 | 1171 | 1000 | 1590 | 1391 | 1192 | 1000 | 1446 | 1265 | 1085 |

(B) Net enthalpy change ($\Delta H$, kJ) in the gasification process

| (A) Biomass: RH (25%) + SD (75%) | | | | (A) Biomass: BD (25%) + SD (75%) | | | | (A) Biomass: BD (25%) + RH (75%) | | | |
|---|---|---|---|---|---|---|---|---|---|---|---|
| Temp (°C) | Air Ratio | | | Temp (°C) | Air Ratio | | | Temp (°C) | Air Ratio | | |
| | 0.2 | 0.3 | 0.4 | | 0.2 | 0.3 | 0.4 | | 0.2 | 0.3 | 0.4 |
| 700 | -5.10E+02 | -6.10E+02 | -7.79E+02 | 700 | -5.25E+02 | -6.30E+02 | -8.00E+02 | 700 | -5.30E+02 | -6.55E+02 | -7.87E+02 |
| 800 | -3.85E+02 | -5.53E+02 | -7.23E+02 | 800 | -4.03E+02 | -5.72E+02 | -7.43E+02 | 800 | -4.80E+02 | -6.10E+02 | -7.40E+02 |
| 900 | -3.45E+02 | -5.07E+02 | -6.70E+02 | 900 | -3.63E+02 | -5.26E+02 | -6.90E+02 | 900 | -4.46E+02 | -5.70E+02 | -6.95E+02 |
| 1000 | -3.08E+02 | -4.63E+02 | -6.18E+02 | 1000 | -3.25E+02 | -4.81E+02 | -6.38E+02 | 1000 | -4.12E+02 | -5.31E+02 | -6.50E+02 |
| (B) Biomass: RH (50%) + SD (50%) | | | | (B) Biomass: BD (50%) + SD (50%) | | | | (B) Biomass: BD (50%) + RH (50%) | | | |
| Temp (°C) | Air Ratio | | | Temp (°C) | Air Ratio | | | Temp (°C) | Air Ratio | | |
| | 0.2 | 0.3 | 0.4 | | 0.2 | 0.3 | 0.4 | | 0.2 | 0.3 | 0.4 |
| 700 | -5.02E+02 | -6.19E+02 | -7.75E+02 | 700 | -5.33E+02 | -6.58E+02 | -8.17E+02 | 700 | -5.48E+02 | -6.75E+02 | -8.08E+02 |
| 800 | -4.10E+02 | -5.65E+02 | -7.22E+02 | 800 | -4.48E+02 | -6.05E+02 | -7.63E+02 | 800 | -4.99E+02 | -6.29E+02 | -7.60E+02 |
| 900 | -3.73E+02 | -5.22E+02 | -6.72E+02 | 900 | -4.09E+02 | -5.60E+02 | -7.12E+02 | 900 | -4.63E+02 | -5.89E+02 | -7.15E+02 |
| 1000 | -3.37E+02 | -4.80E+02 | -6.23E+02 | 1000 | -3.72E+02 | -5.16E+02 | -6.61E+02 | 1000 | -4.29E+02 | -5.49E+02 | -6.69E+02 |
| (C) Biomass: RH (75%) + SD (25%) | | | | (C) Biomass: BD (75%) + SD (25%) | | | | (C) Biomass: BD (75%) + RH (25%) | | | |
| Temp (°C) | Air Ratio | | | Temp (°C) | Air Ratio | | | Temp (°C) | Air Ratio | | |
| | 0.2 | 0.3 | 0.4 | | 0.2 | 0.3 | 0.4 | | 0.2 | 0.3 | 0.4 |
| 700 | -4.95E+02 | -6.27E+02 | -7.71E+02 | 700 | -5.48E+02 | -6.87E+02 | -8.34E+02 | 700 | -5.67E+02 | -6.95E+02 | -8.29E+02 |
| 800 | -4.36E+02 | -5.78E+02 | -7.21E+02 | 800 | -4.92E+02 | -6.36E+02 | -7.82E+02 | 800 | -5.17E+02 | -6.49E+02 | -7.81E+02 |
| 900 | -4.00E+02 | -5.37E+02 | -6.74E+02 | 900 | -4.54E+02 | -5.93E+02 | -7.33E+02 | 900 | -4.82E+02 | -6.08E+02 | -7.35E+02 |
| 1000 | -3.66E+02 | -4.96E+02 | -6.27E+02 | 1000 | -4.18E+02 | -5.51E+02 | -6.85E+02 | 1000 | -4.47E+02 | -5.68E+02 | -6.89E+02 |

### 5.4.2 Trends in Carbon and Hydrogen Distribution (Equilibrium Models)

The fractional distribution of carbon in the gasification reaction mixture (biomasses + air) among various carbonaceous species present in the producer gas is given in Figures 5.5–5.7. As noted earlier, the principal carbonaceous species in the producer gas are CO, $CO_2$, $CH_4$ and unconverted carbon. From Figures 5.5–5.7, we can identify following trends in the fractional distribution among these species:

(1) For all 9 biomass mixtures gasified at air ratios of 0.2–0.4 and temperatures of 700–1000$^o$C, conversion of carbon is complete at equilibrium except for two cases, viz. mixture of rice husk (25%) & saw dust (75%) and mixture of bamboo dust (25%) & saw dust (75%) at air ratio of 0.2 and temperature of 700$^o$C. We attribute this effect to three causes: (i) relatively high carbon content of saw dust, (ii) less availability of oxygen at air ratio of 0.2 and (iii) lower temperature of gasification.

(2) The fraction of carbon ending up as carbon monoxide shows inverse variation with air ratio at any given gasification temperature, and shows direct variation with gasification temperature at any given air ratio. The fraction of carbon appearing in the form of $CO_2$ shows exactly opposite trend.

(3) The fraction of carbon appearing in the form of methane is quite small for all biomass mixtures. This is basically a consequence of low moisture content (~ 10% w/w) of biomass. At high temperatures (≥ 800$^o$C) and high air ratios, the amount of carbon forming methane is practically zero.

Distribution of hydrogen in the gasification mixture among three major species in the producer gas, viz. $H_2$, $H_2O$ and $CH_4$, is given in Figures 5.8–5.10. The trends in fractional distribution of hydrogen can be summarized as follows:

(1) For air ratios of 0.2 and temperature 700–800$^o$C, most of hydrogen in biomass ends up as $H_2$ in the producer gas, with small fractions forming $H_2O$ and $CH_4$.

(2) As the temperature of gasification rises, the fraction of hydrogen appearing in the form of

water vapor in producer gas increases with proportionate reduction in hydrogen in methane.

(3) As air ratio increases, the fraction of hydrogen ending up in water vapor increases with proportionate reduction in the fraction of hydrogen ending up as $H_2$. This effect is obviously attributed to greater presence of oxygen in the gasification mixture with increasing air ratio.

### 5.4.3 Trends in Simulation Results with Semi–equilibrium Model

As discussed in section 5.2.1, we restricted the conversion of carbon in the biomass mixture by certain percentage, which was determined on the basis of experimental results of Lv et al. [19]. The results of simulations are presented in Table 5.4 and Figure 5.11. Two major deviations from the equilibrium model are evident as follows:

(1) The net yield and LHV of the producer gas reduces as compared to the total equilibrium conditions. Obviously, these two parameters vary directly with extent of carbon conversion.

(2) Hydrogen and carbon monoxide content of the producer gas also reduces as compared to the equilibrium conditions, and again, these two parameters show direct variation with the extent of carbon conversion.

In addition, the net enthalpy change of gasification reduces, while the net thermal energy content of producer gas increases with increasing carbon conversion.

**Table 5.4:** Simulation results for gasification of biomass mixtures with semi–equilibrium model (incomplete carbon conversion; basis: 100 g of biomass mixture)

| $x_C$ | $H_2$ moles | CO moles | ΔH (kJ) | Gas yield ($Nm^3$) | LHV ($MJ/Nm^3$) | $\Delta H_P$ (kJ) |
|---|---|---|---|---|---|---|
| **(A) Biomass mixture: RH (50%) + SD (50%)** | | | | | | |
| 60% | 1.36 | 0.91 | -800.83 | 0.19 | 3.42 | 647 |
| 70% | 1.69 | 1.33 | -743.78 | 0.21 | 4.17 | 858 |
| 80% | 1.97 | 1.79 | -685.35 | 0.22 | 4.82 | 1069 |
| **(B) Biomass mixture: BD (50%) + RH (50%)** | | | | | | |
| 60% | 1.19 | 0.67 | -814.70 | 0.16 | 3.28 | 530 |
| 70% | 1.51 | 0.99 | -767.87 | 0.18 | 4.02 | 712 |
| 80% | 1.79 | 1.35 | -730.35 | 0.19 | 4.67 | 894 |
| **(C) Biomass mixture: BD (50%) + SD (50%)** | | | | | | |
| 60% | 1.33 | 0.90 | -832.36 | 0.19 | 3.32 | 636 |
| 70% | 1.67 | 1.33 | -775.67 | 0.21 | 4.09 | 854 |
| 80% | 1.97 | 1.80 | -728.28 | 0.23 | 4.76 | 1072 |

**Abbreviations:** $x_C$ – carbon conversion; LHV – Lower heating value; ΔH – net enthalpy change of the biomass gasification process; $\Delta H_{th,P}$ – net available thermal energy for power generation.

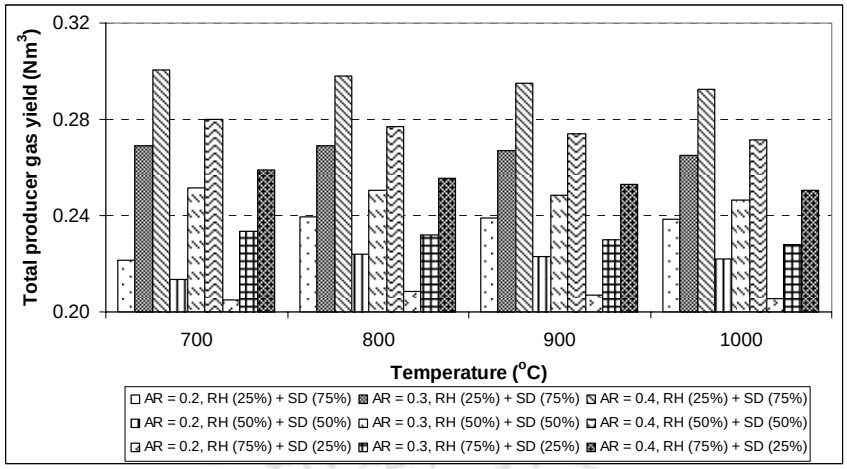


(A)

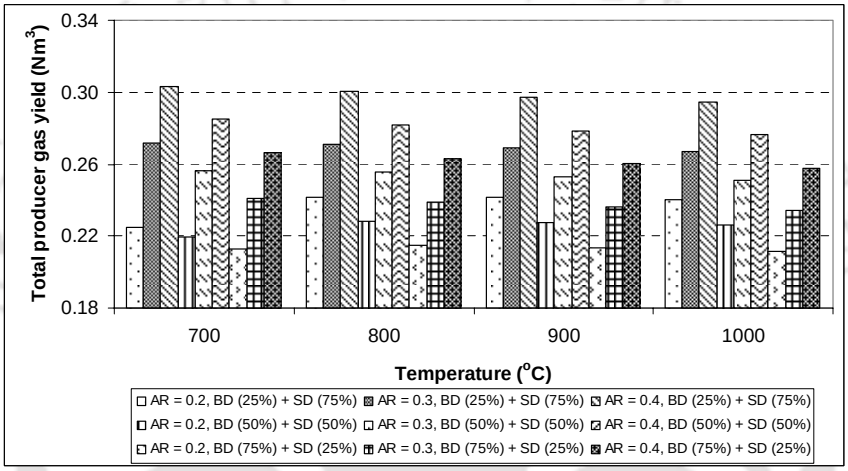


(B)

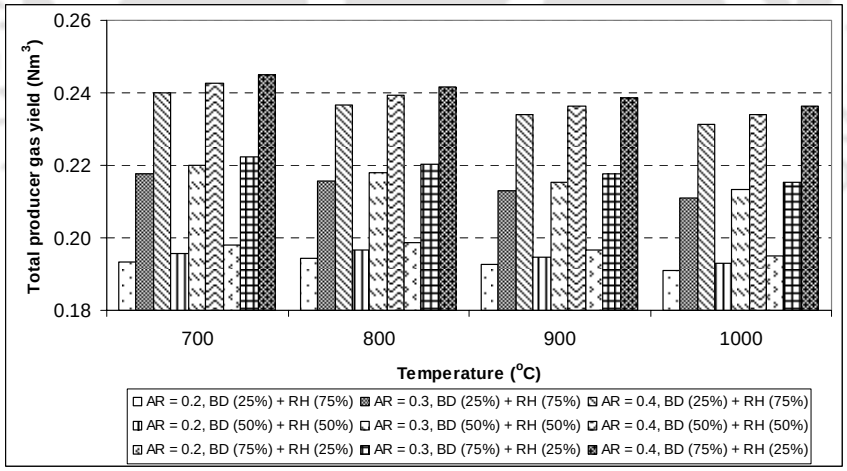


(C)

**Figure 5.1:** Simulations results for the gasification of biomass mixtures (Basis: 100g of total biomass mixture). Variation in total producer gas yield for different biomass mixtures with air ratio and temperature. (A) Mixtures of rice husk and saw dust. (B) Mixtures of bamboo dust and saw dust. (C) Mixtures of bamboo dust and rice husk.

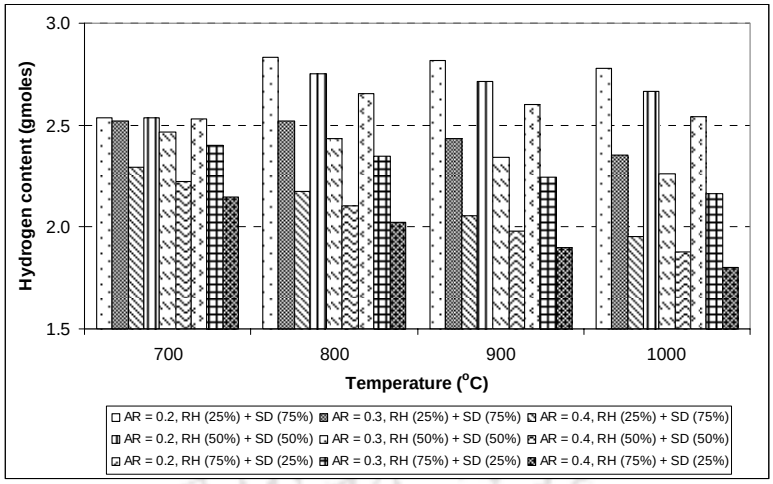


(A)

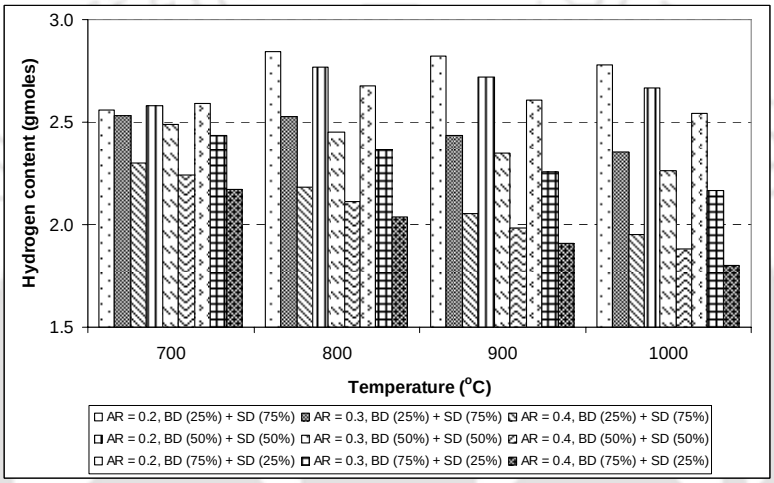


(B)

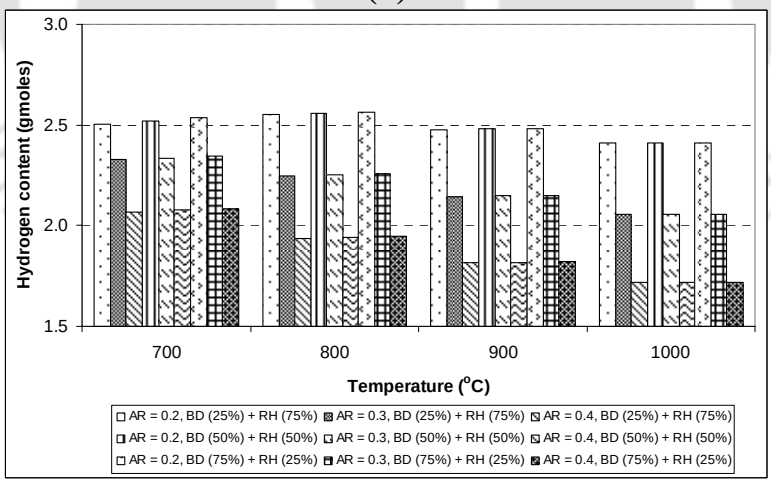


(C)

**Figure 5.2:** Simulations results for the gasification of biomass mixtures (Basis: 100g of total biomass mixture). Variation in hydrogen content in producer gas for different biomass mixtures with air ratio and temperature. (A) Mixture of rice husk and saw dust. (B) Mixture of bamboo dust and saw dust. (C) Mixture of bamboo dust and rice husk.

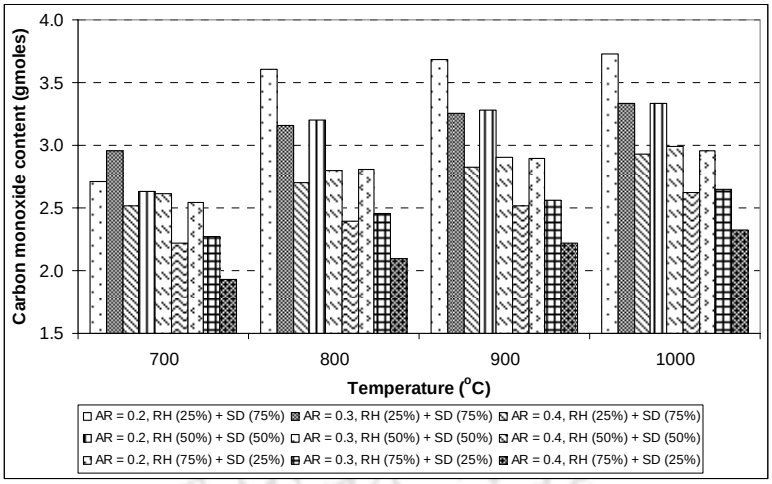


(A)

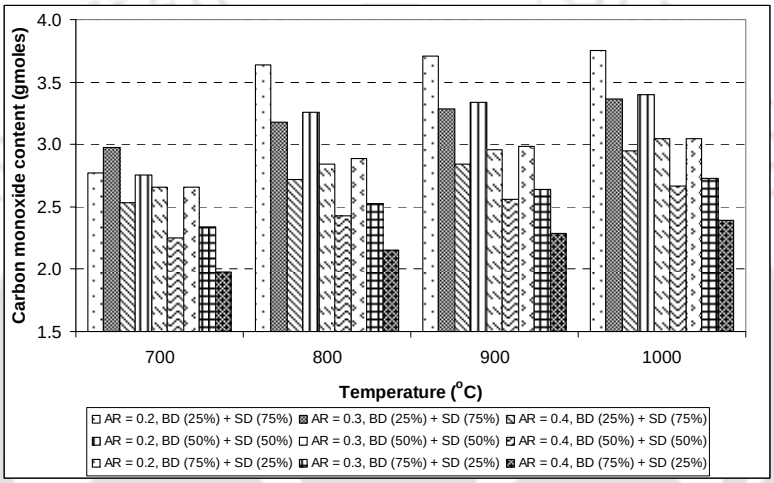


(B)

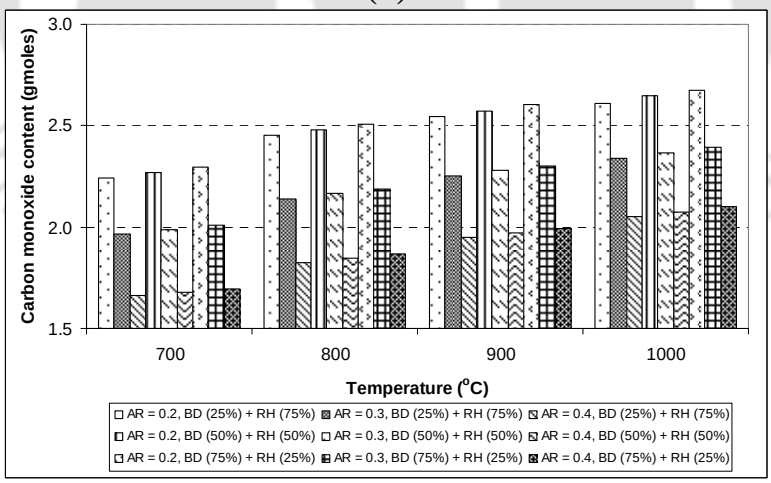


(C)

**Figure 5.3:** Simulations results for the gasification of biomass mixtures (Basis: 100g of total biomass mixture). Variation in carbon monoxide content in producer gas for different biomass mixtures with air ratio and temperature. (A) Mixtures of rice husk and saw dust. (B) Mixtures of bamboo dust and saw dust. (C) Mixtures of bamboo dust and rice husk.

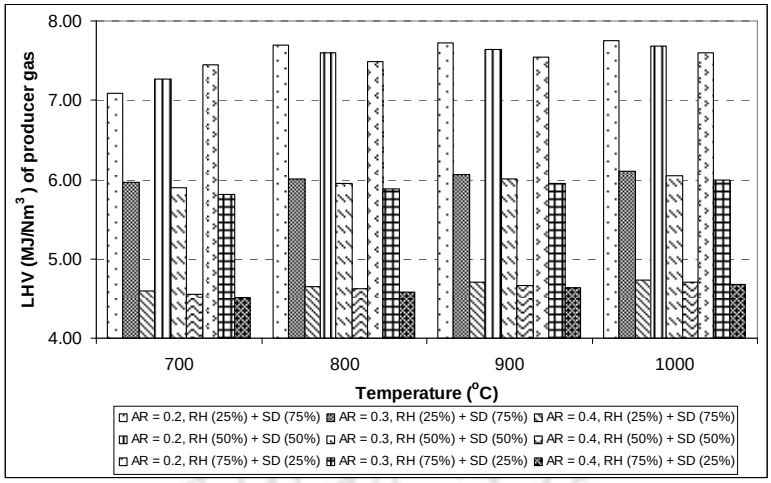


(A)

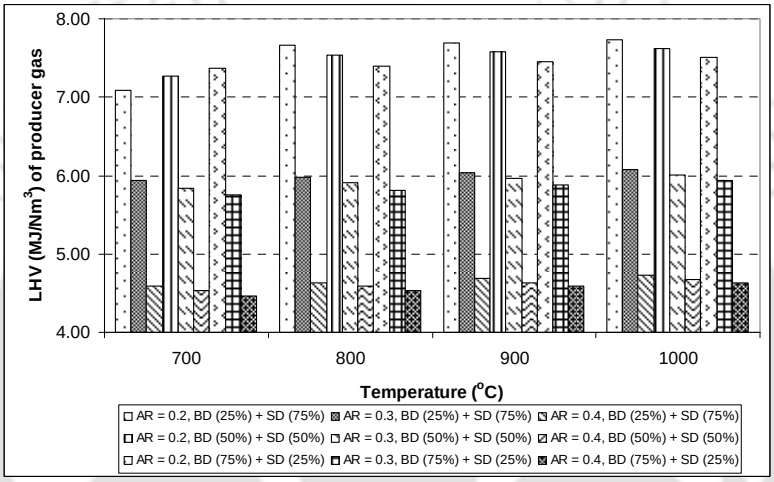


(B)

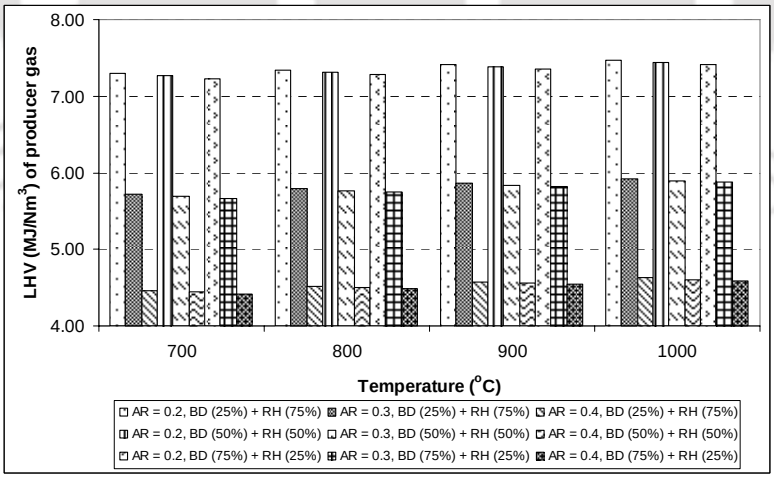


(C)

**Figure 5.4:** Simulations results for the gasification of biomass mixtures (Basis: 100g of total biomass mixture). Variation in LHV of producer gas for different biomass mixtures with air ratio and temperature. (A) Mixtures of rice husk and saw dust. (B) Mixtures of bamboo dust and saw dust. (C) Mixtures of bamboo dust and rice husk.

### 5.4.4 Trends in distribution of carbon and hydrogen

As the carbon conversion increases, greater fraction of carbon in the biomass mixture ends up as CO in the producer gas. Quite interestingly, the fraction of carbon appearing in the form of $CO_2$ shows insignificant variation with carbon conversion. This trend is consistent for all biomass mixtures. Among the three biomass mixtures, those containing saw dust show greater fractional carbon distribution towards CO than $CO_2$.

The fractional distribution of hydrogen towards $H_2$ shows direct variation with extent of carbon conversion, with proportionate reduction in distribution towards $H_2O$. This effect is attributed to competitive consumption of oxygen in the gasification mixture by carbon undergoing oxidation to CO and $CO_2$. The fraction of hydrogen appearing in the form of $CH_4$ is practically zero for the conditions considered for present simulation.

### 5.4.5 Comparative Assessment with Previous Literature

In this section, we compare our simulation results with previous literature. Our comparative assessment is two fold in that we first contrast our results with those reported in theoretical (or simulation) studies in biomass gasification, followed by comparison with results of experimental studies. The basis for comparison is three parameters is variation in three parameters, viz. (1) variation in product gas composition, (2) LHV of product gas, and (3) net product gas yield per unit biomass, with temperature and air (or equivalence) ratio. We would like to specifically state that a quantitative match between our results and the data reported previous theoretical as well as experimental literature is unlikely due to differences between the biomass type and gasification medium used these papers and the present study. Nonetheless, the trends observed in parameters mentioned above with gasification temperature and air ratio can be considered for comparison.

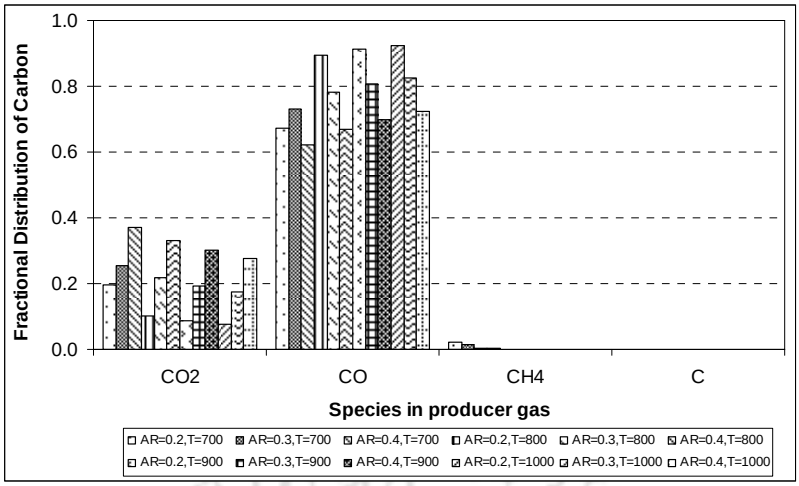


(A)

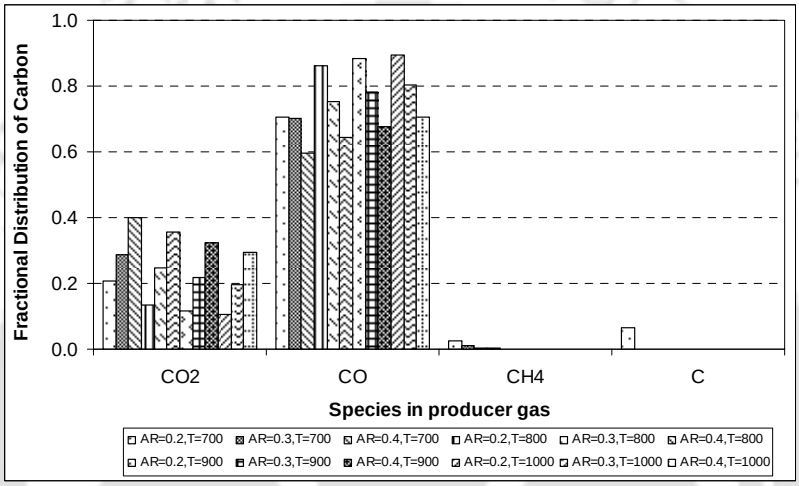


(B)

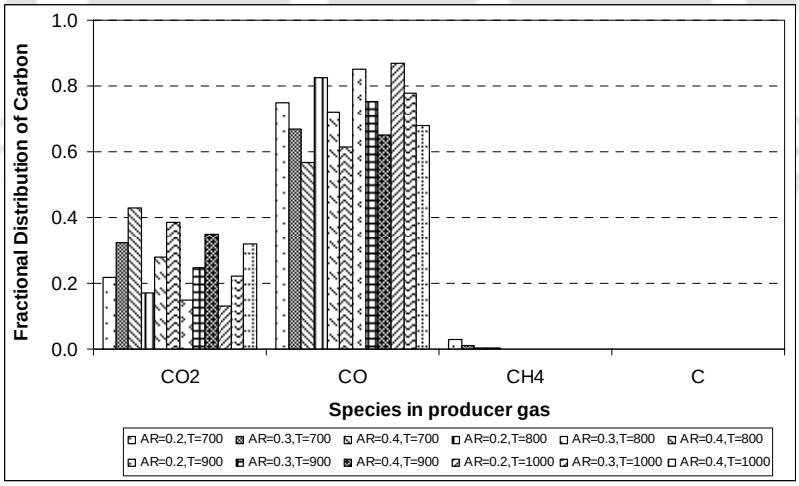


(C)

**Figure 5.5:** Simulations results for the gasification of biomass mixtures (Basis: 100g of total biomass mixture). Fractional distribution of carbon in the gasification mixture among various species in the producer gas for mixture of rice husk and saw dust. Compositions: (A) RH (25%) + SD (75%) (B) RH (50%) + SD (50%) (C) RH (75%) + SD (25%).

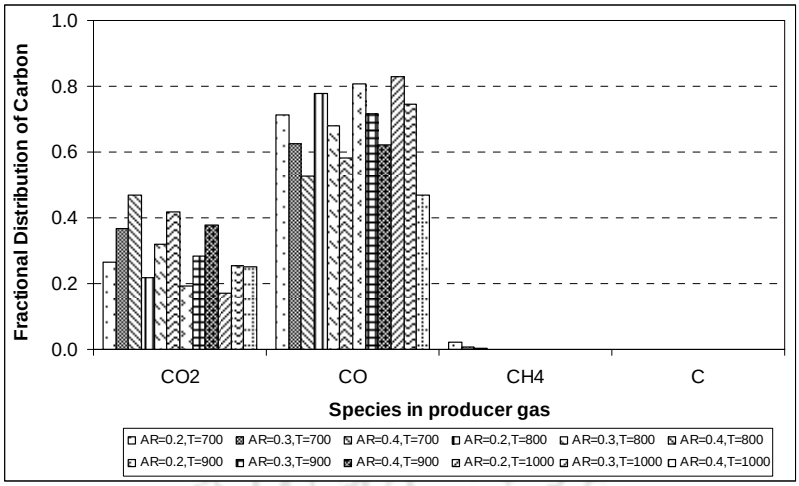


(A)

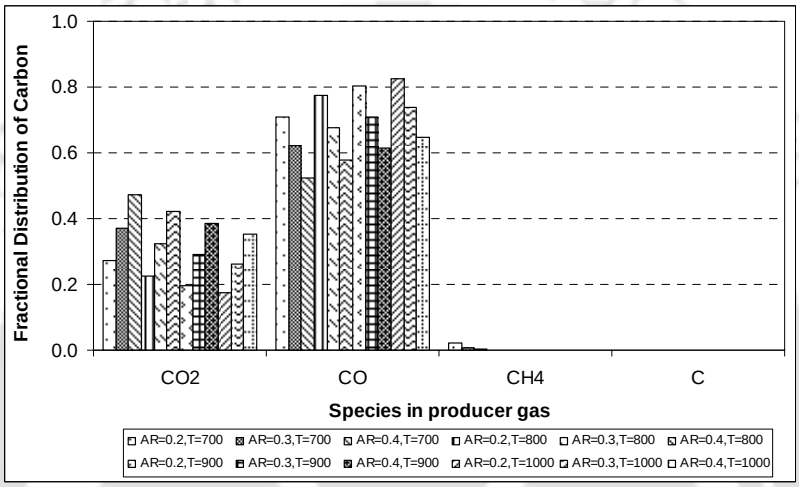


(B)

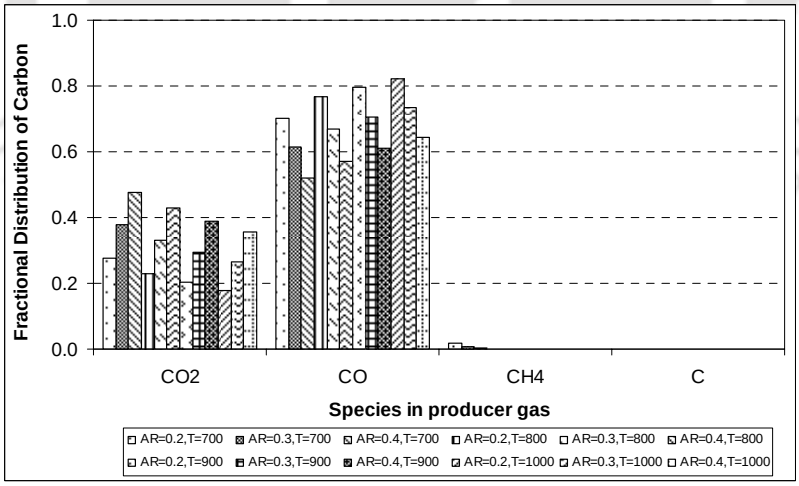


(C)

**Figure 5.6:** Simulations results for the gasification of biomass mixtures (Basis: 100g of total biomass mixture). Fractional distribution of carbon in the gasification mixture among various species in the producer gas for mixture of bamboo dust and rice husk. Compositions: (A) BD (25%) + RH (75%) (B) BD (50%) + RH (50%) (C) BD (75%) + RH (25%).

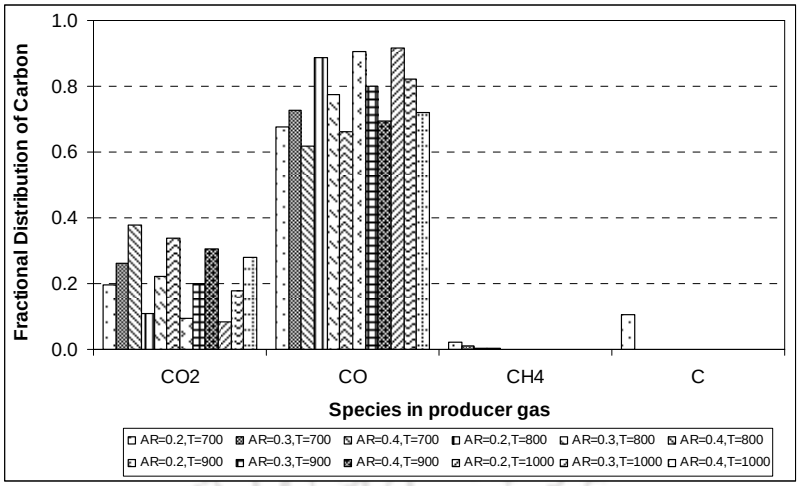


(A)

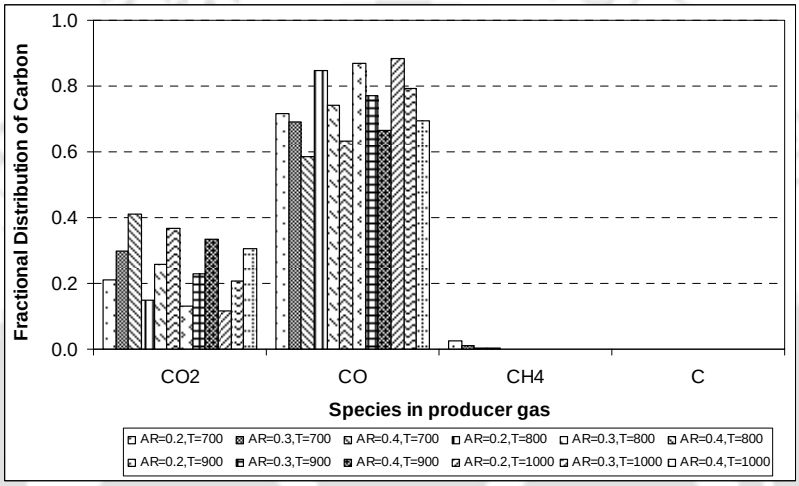


(B)

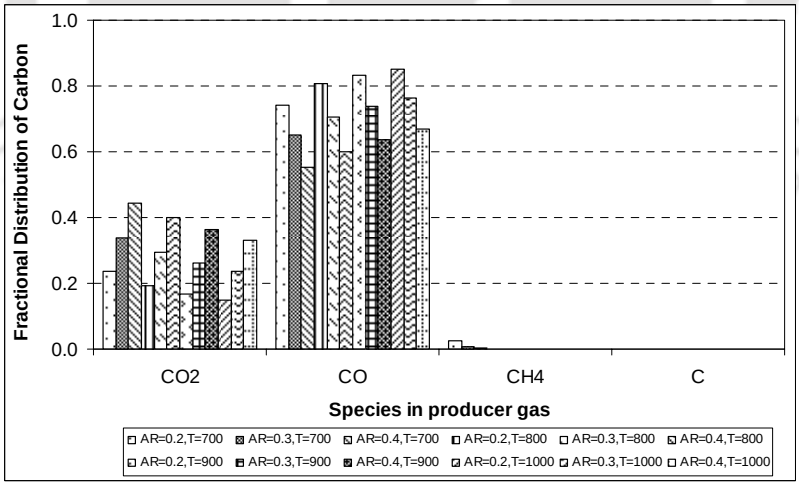


(C)

**Figure 5.7:** Simulations results for the gasification of biomass mixtures (Basis: 100g of total biomass mixture). Fractional distribution of carbon in the gasification mixture among various species in the producer gas for mixture of bamboo dust and saw dust. Compositions: (A) BD (25%) + SD (75%) (B) BD (50%) + SD (50%) (C) BD (75%) + SD (25%).

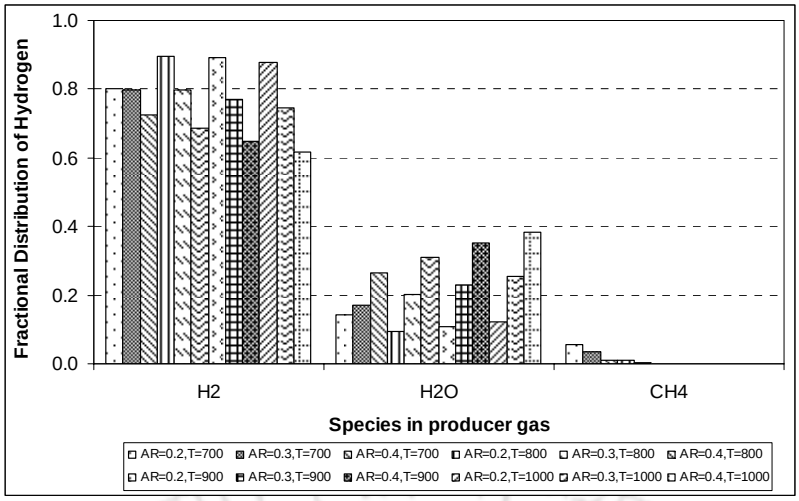


(A)

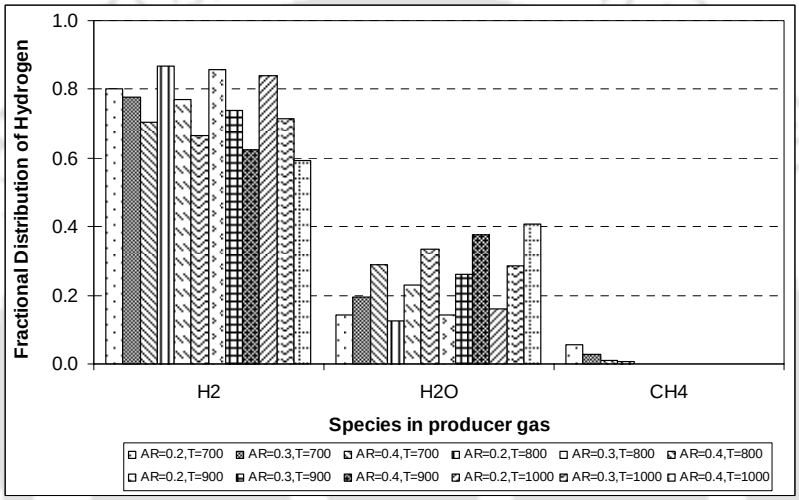


(B)

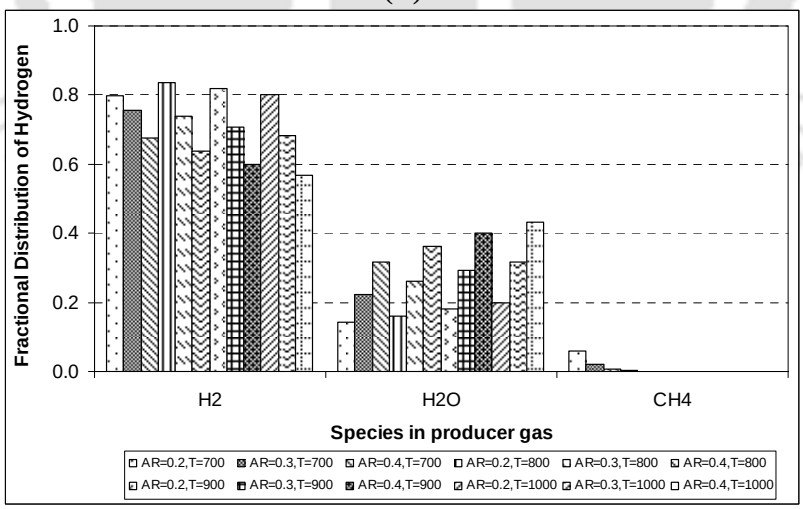


(C)

**Figure 5.8:** Simulations results for the gasification of biomass mixtures (Basis: 100g of total biomass mixture). Fractional distribution of hydrogen in the gasification mixture among various species in the producer gas for mixture of rice husk and saw dust. Compositions: (A) RH (25%) + SD (75%) (B) RH (50%) + SD (50%) (C) RH (75%) + SD (25%).

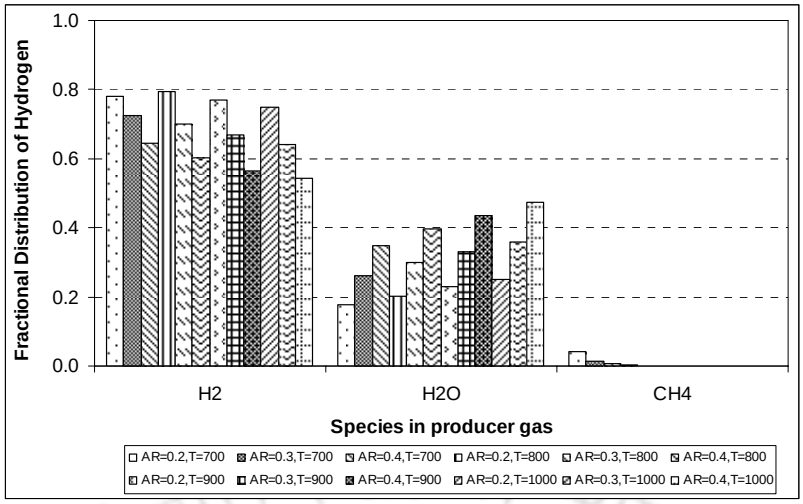


(A)

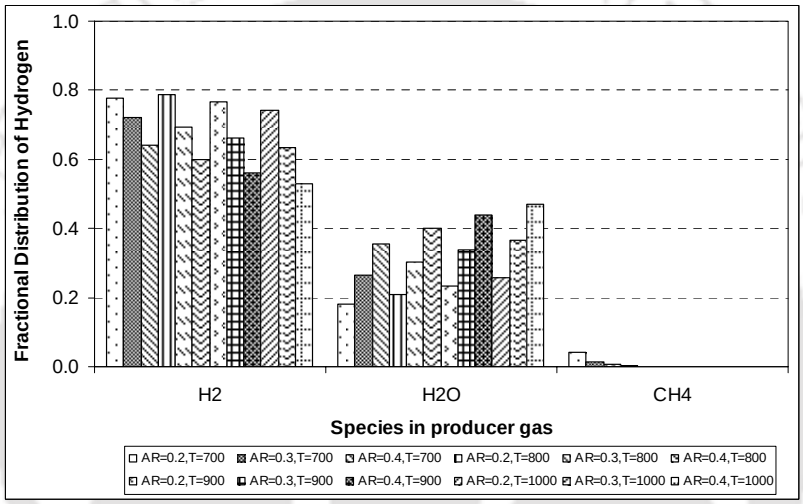


(B)

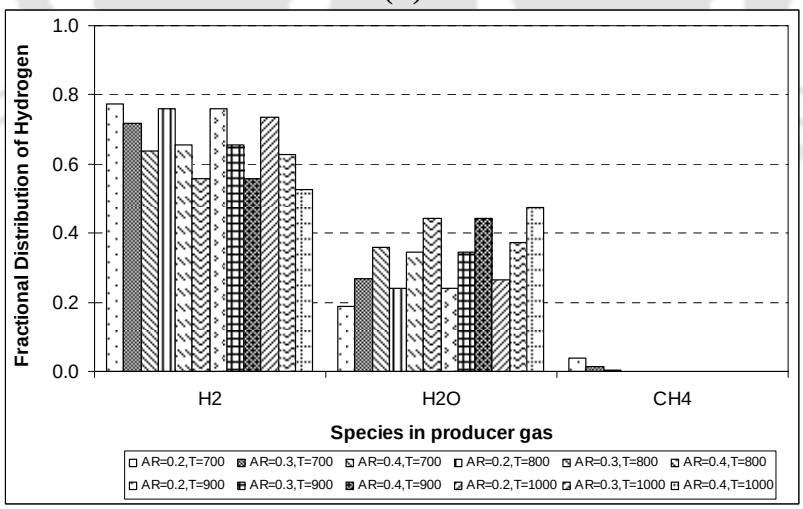


(C)

**Figure 5.9:** Simulations results for the gasification of biomass mixtures (Basis: 100g of total biomass mixture). Fractional distribution of hydrogen in the gasification mixture among various species in the producer gas for mixture of bamboo dust and rice husk. Compositions: (A) BD (25%) + RH (75%) (B) BD (50%) + RH (50%) (C) BD (75%) + RH (25%).

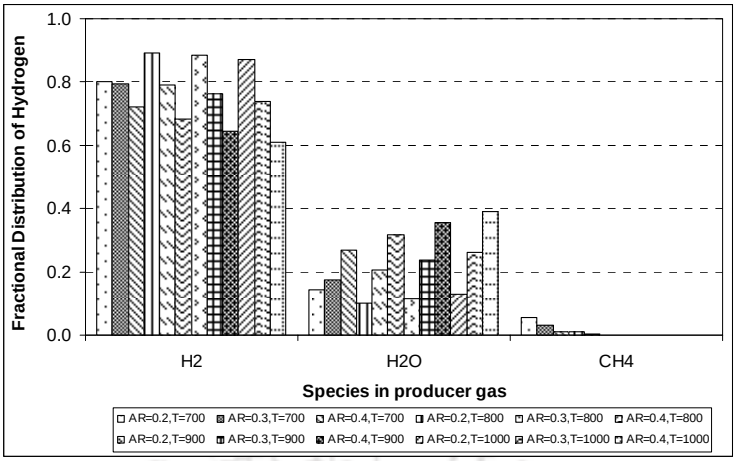


(A)

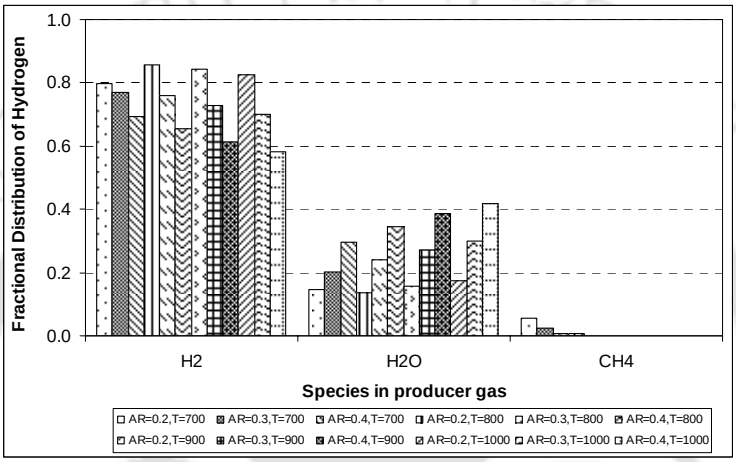


(B)

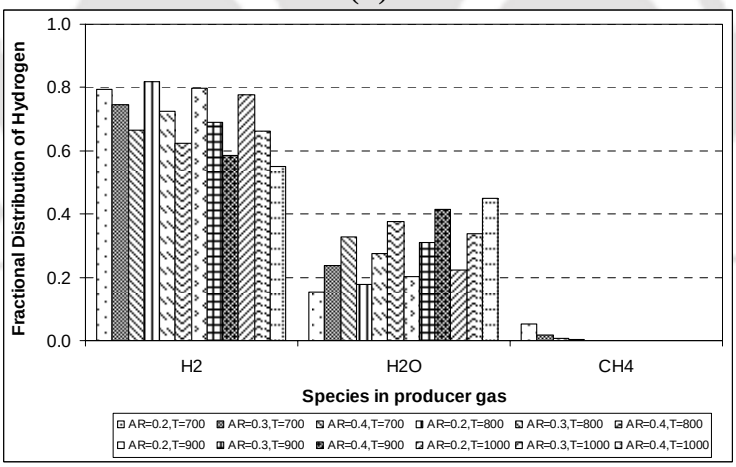


(C)

**Figure 5.10:** Simulations results for the gasification of biomass mixtures (Basis: 100g of total biomass mixture). Fractional distribution of hydrogen in the gasification mixture among various species in the producer gas for mixture of bamboo dust and saw dust. Compositions: (A) BD (25%) + SD (75%) (B) BD (50%) + SD (50%) (C) BD (75%) + SD (25%).

*5.4.5.1 Comparison with theoretical or simulations studies*

Table 5.5 gives composition and LHV of the product gas reported in six previous studies on gasification of different biomass materials. The temperature of gasification in these studies is in the range 700 – 900$^{o}$C with an equivalence ratio of 0.2 to 0.4. Also given in the table are our simulation results for gasification of mixtures of saw dust (which is a widely employed biomass for gasification in previous literature) with rice husk and bamboo dust. It could be inferred from Table 5.5 that both LHV and composition of product gas in our simulations is quite similar to that reported in previous literature. It could also be perceived that use of air–steam mixture as gasification medium [23] results in product gas with higher hydrogen content (and as a consequence has higher LHV) than gas obtained with air gasification (as considered in our study). In addition to the data presented in Table 5.5, we would like to cite following trends observed in previous studies that are in concurrence with our results:

1. Melgar et al. [24] have reported increasing CO content in the product gas with reduction in air ratio, and increasing $CO_2$ content at higher air ratios. Moreover, Melgar et al. [24] have also reported higher $CH_4$ content in product gas at low air ratios and low temperatures.

2. Schuster et al. [23] have reported leveling off of LHV of producer gas at gasification temperatures above 800$^{o}$C. They have also reported no presence of methane in the product gas at temperatures higher than 800$^{o}$C.

All of these findings coincide with the results of simulations in this study.

*5.4.5.2 Comparison with experimental results*

Several authors have studied gasification of single biomasses and mixtures of coal and biomass in fixed and/or fluidized bed gasifiers. In this section, we make comprehensive comparison of results of our simulations with the experimental data reported in previous papers. Tables 5.6–5.8 present the data for the three parameters considered for comparison.

Although quantitative match between the mole fractions of different species in product gas with those observed and the predictions of the equilibrium model is not possible for the reasons stated earlier, one can perceive that experimental trends in gas composition is in concurrence with the results of simulations. From Tables 5.6–5.8, we can identify following matching trends between experimental and simulations results:

1. For a fixed gasification temperature, increasing ER reduces mole fractions of $H_2$ and CO, with simultaneous rise in $CO_2$.

2. The fraction of $CH_4$ in product gas obtained above 700$^oC$ is very small (< 1%).

3. For a given air ratio, the hydrogen content of product gas shows little variation with temperature (in the range 700–900$^oC$), while CO content decreases.

4. The LHV of product gas shows inverse relation with air ratio at fixed gasification temperature. On the other hand, for a given air ratio, LHV increases with gasification temperature.

5. The net yield of the product gas increases with air ratio as well as temperature of gasification. Quite notably, the experimentally observed values of LHV and net product gas yield for single biomasses matches with calculated values for biomass mixtures in this study within an experimental variation of ± 15–20%.

The quantitative discrepancies between experimental and simulations results are as follows:

(1) Jiang et al. [25] have reported very low $H_2$ content in product gas as compared to Narvaez et al. [26] and Lv et al. [19]. This could be a consequence of low (per pass) biomass conversion in the gasifier.

(2) The $CH_4$ content of gas in all studies is somewhat higher than our simulation. In our opinion, this is an indication of non–equilibrium conditions in the gasification system – in that not all methane formed in the initial pyrolysis stage of gasification is converted to equilibrium quantities of CO, $CO_2$ and $H_2O$ prior to exit from gasifier.

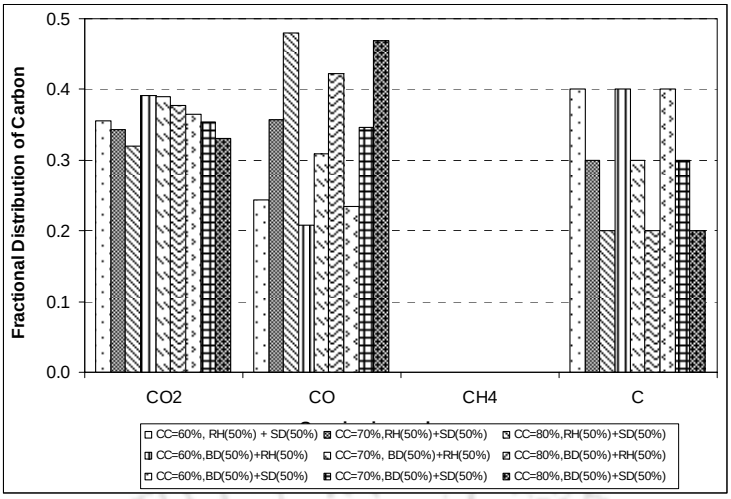


(A)

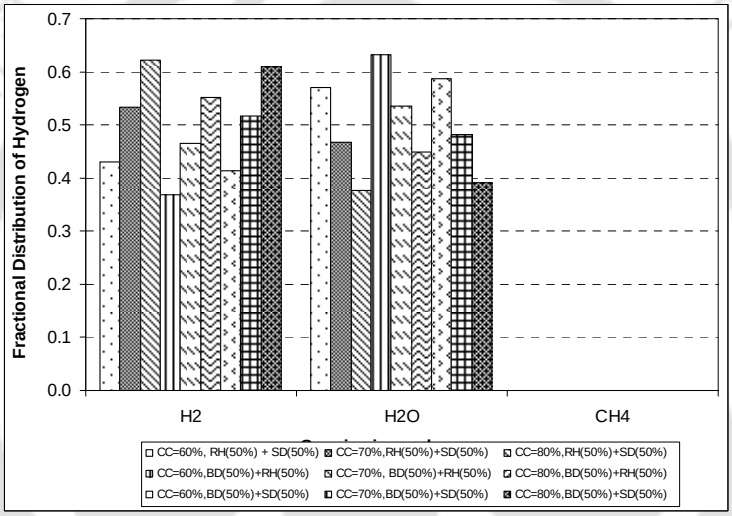


(B)

**Figure 5.11:** Simulations results for the gasification of biomass mixtures for incomplete carbon conversion (Basis: 100g of total biomass mixture) at AR = 0.3 and temperature = 800$^{o}$C. The exact biomass compositions and extent of carbon conversions are given in the legends. (A) Fractional distribution of carbon in the gasification mixture among various species in the producer gas. (B) Fractional distribution of hydrogen in the gasification mixture among various species in the producer gas.

**Table 5.5:** Comparison with simulations data

| Reference | Biomass | LHV ($MJ/Nm^3$) | $CH_4$ | $H_2$ | $CO_2$ | CO |
|---|---|---|---|---|---|---|
| | | | Volume (or mole) fraction | | | |
| Ruggerio and Manfrida [28] | Saw Dust | 5.109 | 0.009 | 0.194 | 0.114 | 0.220 |
| Zainal et al. [29] | Wood chips | 4.72 | 0.006 | 0.216 | 0.120 | 0.196 |
| Melgar et al. [24] | Pine Wood | N.A. | 0.002 | 0.166 | 0.110 | 0.192 |
| Schuster et al. [23] | Beech Chips (Air-steam gasification) | 8.316 | 0.001 | 0.466 | 0.103 | 0.258 |
| Jayah et al. [30] | Rubber Wood | N.A. | 0.001 | 0.164 | 0.111 | 0.183 |
| **Present Study (Saw dust rich mixtures)** | **SD - 75%, RH - 25%** | **6.01** | **0** | **0.225** | **0.078** | **0.282** |
| | **SD - 75%, BD - 25%** | **5.99** | **0** | **0.224** | **0.081** | **0.282** |
| **Present Study (Saw dust mixtures with 80% carbon conversion)** | **SD - 50%, RH - 50%** | **4.67** | **0** | **0.225** | **0.152** | **0.170** |
| | **SD - 50%, BD - 50%** | **4.76** | **0** | **0.210** | **0.136** | **0.192** |

Note: Temperature of gasification: 700 – 900 $^oC$; Air (or equivalence) ratio: 0.2 – 0.4.

**Table 5.6:** Comparison with experimental data on product gas composition

(A) Effect of air (or equivalence) ratio

| Reference | Biomass | Temp ($^oC$) | ER | $CH_4$ | $H_2$ | $CO_2$ | CO |
|---|---|---|---|---|---|---|---|
| | | | | Volume (or mole) fraction | | | |
| Jiang et al. [25] | Rice husk | 770 | 0.16 | 0.005 | 0.009 | 0.162 | 0.036 |
| | | | 0.22 | 0.005 | 0.001 | 0.136 | 0.027 |
| **Present Study (Rice husk rich mixtures)** | **RH - 75%, SD - 25%** | **800** | **0.20** | **0.001** | **0.306** | **0.068** | **0.324** |
| | **RH - 75%, BD - 25%** | | | **0.001** | **0.316** | **0.085** | **0.303** |
| **Present Study (Rice husk mixtures with 80% carbon conversion)** | **SD - 50%, RH - 50%** | **800** | **0.30** | **0** | **0.214** | **0.129** | **0.194** |
| | **BD - 50%, RH - 50%** | | | **0** | **0.225** | **0.152** | **0.170** |
| Lv et al. [19] | Pine Sawdust | 800 | 0.19 | 0.078 | 0.323 | 0.179 | 0.379 |
| | | | 0.23 | 0.076 | 0.315 | 0.169 | 0.401 |
| | | | 0.27 | 0.067 | 0.318 | 0.199 | 0.384 |
| Ergudenler and Ghaly [31] | Wheat Straw | 800 | 0.25 | 0.049 | 0.074 | 0.136 | 0.170 |
| Narvaez et al. [26] | Pine sawdust | 800 | 0.26 | 0.027 | 0.095 | 0.150 | 0.130 |
| **Present Study (Saw dust rich mixtures)** | **SD - 75%, RH - 25%** | **800** | **0.20** | **0.002** | **0.284** | **0.042** | **0.362** |
| | **SD - 75%, BD - 25%** | | | **0.001** | **0.283** | **0.045** | **0.361** |
| Maniatis et al. [32] | Pine Wood | 800 | 0.30 | 0.051 | 0.105 | 0.166 | 0.131 |
| van der Aarsen et al. [33] | Wood chips | 800 | 0.31 | 0.045 | 0.111 | 0.159 | 0.134 |
| Narvaez et al. [26] | Pine sawdust | 800 | 0.32 | 0.030 | 0.070 | 0.135 | 0.140 |
| **Present Study (Saw dust rich mixtures)** | **SD - 75%, RH - 25%** | **800** | **0.30** | **0** | **0.225** | **0.078** | **0.282** |
| | **SD - 75%, BD - 25%** | | | **0** | **0.224** | **0.081** | **0.282** |
| **Present Study (Saw dust mixtures with 80% carbon conversion)** | **SD - 50%, RH - 50%** | **800** | **0.30** | **0** | **0.214** | **0.129** | **0.194** |
| | **SD - 50%, BD - 50%** | | | **0** | **0.210** | **0.136** | **0.192** |
| Jiang and Morey [34] | Corn Cobs | 800 | 0.42 | 0.021 | 0.109 | 0.129 | 0.147 |
| Narvaez et al. [26] | Pine sawdust | 800 | 0.44 | 0.032 | 0.095 | 0.151 | 0.137 |
| **Present Study (Saw dust rich mixtures)** | **SD - 75%, RH - 25%** | **800** | **0.40** | **0** | **0.176** | **0.108** | **0.218** |
| | **SD - 75%, BD - 25%** | | | **0** | **0.175** | **0.111** | **0.218** |

## 5.5 DISCUSSION

Simulations of gasification of biomass mixtures with equilibrium and semi–equilibrium models give us an insight into the technicalities of the process and the relative influence of different operational parameters. An immediate conclusion that one can draw from simulation results is that the quality and quantity of producer gas resulting from

gasification of biomass mixtures has high potential for power generation through dual fuel or 100% producer gas engines. This potential can be quantified as follows: if a gasifier consumes 100 g of 50%–50% w/w mixture of rice husk and saw dust per second (corresponding to 360 kg/h of gross consumption of mixture) for air ratio of 0.3 and gasification temperature of 800°C, the maximum thermal energy available (as seen from Table 5.3A) in the producer gas after attainment of total equilibrium in the gasification system is 1491 kJ/s or kWth. Typical efficiency of dual fuel engine–generator sets available in the market is ~ 30%. Thus, maximum electrical power generated with the producer gas is 1491 × 0.3 = 450 $kW_e$. Under practical situation, the conversion of biomass in gasifier is not complete. As inferred from Table 5.4, the net thermal energy in the producer gas for 60%, 70% and 80% conversion (as same biomass consumption rate of 100 g/s) is 647, 858 and 1069 $kW_{th}$.

**Table 5.6(B):** Effect of gasification temperature

| Reference | Biomass | ER | Temp (°C) | $CH_4$ | $H_2$ | $CO_2$ | CO |
|---|---|---|---|---|---|---|---|
| | | | | Volume (or mole) fraction | | | |
| Jiang et al. [25] | Rice husk | 0.22 | 700 | 0.013 | 0.012 | 0.143 | 0.048 |
| | | | 750 | 0.005 | 0.010 | 0.119 | 0.026 |
| **Present Study (Rice husk rich mixtures)** | **RH - 75%, SD - 25%** | **0.20** | **700** | **0.011** | **0.297** | **0.087** | **0.299** |
| | | | **900** | **0** | **0.302** | **0.059** | **0.336** |
| | **RH - 75%, BD - 25%** | **0.20** | **700** | **0.009** | **0.312** | **0.104** | **0.279** |
| | | | **900** | **0** | **0.309** | **0.075** | **0.318** |
| Lv et al. [19] | Pine saw dust | 0.19 | 700 | 0.092 | 0.215 | 0.206 | 0.428 |
| | | | 800 | 0.075 | 0.322 | 0.186 | 0.376 |
| | | | 900 | 0.062 | 0.392 | 0.194 | 0.334 |
| Narvaez et al. [26] | Pine saw dust | 0.30 | 700 | 0.040 | 0.046 | 0.153 | 0.124 |
| | | | 750 | 0.039 | 0.078 | 0.141 | 0.138 |
| | | | 820 | 0.032 | 0.100 | 0.131 | 0.165 |
| **Present Study (Saw dust rich mixtures)** | **SD - 75%, RH - 25%** | **0.30** | **700** | **0.005** | **0.225** | **0.092** | **0.264** |
| | | | **900** | **0** | **0.219** | **0.070** | **0.294** |
| | **SD - 75%, BD - 25%** | **0.30** | **700** | **0.005** | **0.224** | **0.095** | **0.264** |
| | | | **900** | **0** | **0.218** | **0.073** | **0.293** |

Under presumption that efficiency of engine–generator system stays unchanged, the net power generation through this producer gas is 190, 255 and 320 $kW_e$. From these figures one can also calculate the specific biomass consumption for electricity generation. For example, for 50%–50% w/w mixture of rice husk and saw dust, the minimum possible specific fuel

consumption (for total equilibrium conditions) is 360/450 = 0.8 kg/kW–h. This consumption varies inversely with carbon conversion.

**Table 5.7:** Comparison with experimental data on LHV of producer gas

(A) Effect of air (or equivalence) ratio

| Reference | Biomass | Temp (°C) | ER | LHV (MJ/Nm$^3$) |
|---|---|---|---|---|
| Mansaray et al. [27] | Rice Husk | 750 | 0.25<br>0.35 | 4.38<br>3.15 |
| Narvaez et al. [26] | Pine Sawdust | 800 | 0.32<br>0.44 | 6.28<br>4.59 |
| Maniatis et al. [35] | Woodwaste | 800 | 0.23<br>0.30<br>0.40 | 6.42<br>5.59<br>4.48 |
| Ergudenler and Ghaly [31] | Wheat Straw | 800 | 0.25<br>0.40 | 1.61<br>2.40 |
| Lv et al. [19] | Pine Sawdust | 800 | 0.19<br>0.27 | 8.82<br>7.28 |
| Gulyurtlu et al. [36] | Pine Wood | 800 | 0.21<br>0.35 | 5.60<br>3.80 |
| **Present Study (Saw dust rich mixtures)** | **SD - 75%, RH - 25%** | **800** | **0.20<br>0.30** | **7.70<br>6.01** |
| | **SD - 75%, BD - 25%** | **800** | **0.20<br>0.30** | **7.67<br>5.99** |

For 60%, 70% and 80% carbon conversion, the typical consumption of biomass mixture (not including the recycled unconverted biomass) is 360/190, 360/255 and 360/320, i.e. 1.89, 1.41 and 1.13 kg/kW–h, respectively. The value of specific fuels consumption reported in literature are higher than the calculated values in the present study by ± 5–20%. For gasification of rice husk alone, Lv et al. [19] have reported carbon conversion in the range of 0.7 to 0.9, while Mansaray et al. [27] have reported slightly lower values of 0.6 to 0.8. Yin et al. [37] have reported specific fuel consumption of 1.7–1.9 kg/kWh for rice husk gasification for electricity generation capacity of 800 kW or higher. However, for low capacity (~ 200 kW), the specific fuel consumption is reported to be as high as 3.5 kg/kW–h. Values of specific fuel consumption reported by Mansaray et al. [27] are in the same range (1.91 kg/kW–h). It should be noted that in addition to overall carbon conversion in the gasifier, the specific fuel consumption also depends overall efficiencies of gasifier, duel fuel or 100% producer gas engine and the generator set. Typical values of these are 55%, 33% and 88%

[38].

**Table 5.7(B):** Effect of gasification temperature

| Reference | Biomass | ER | Temp (°C) | LHV (MJ/Nm$^3$) |
|---|---|---|---|---|
| Narvaez et al. [26] | Pine Sawdust | 0.30 | 700<br>800 | 4.00<br>5.50 |
| Lv et al. [19] | Pine Sawdust | 0.22 | 700<br>900 | 7.95<br>7.36 |
| Maniatis et al. [32] | Pine Wood | 0.32 | 700<br>800 | 5.83<br>6.23 |
| **Present Study (Saw dust rich mixtures)** | **SD - 75%, RH - 25%** | **0.20** | **700<br>800<br>900** | **7.09<br>7.70<br>7.72** |
| | **SD - 75%, BD - 25%** | **0.30** | **700<br>800<br>900** | **5.94<br>5.99<br>6.04** |

**Table 5.8:** Comparison with experimental data on net producer gas yield: Effect of gasification temperature and air (or equivalence) ratio

| Reference | Biomass | ER | Temp (°C) | Yield (Nm$^3$/100 g biomass) |
|---|---|---|---|---|
| Narvaez et al. [26] | Pine Sawdust | 0.28<br>0.44 | 800 | 0.25<br>0.29 |
| Maniatis et al. [35] | Woodwaste | 0.23<br>0.40 | 800 | 0.18<br>0.27 |
| Ergudenler and Ghaly [31] | Wheat Straw | 0.25<br>0.40 | 800 | 0.16<br>0.24 |
| Mansaray et al. [27] | Rice Husk | 0.25<br>0.35 | 750 | 0.15<br>0.19 |
| Yin et al. [37] | Rice Husk | 0.25 | 800 | 0.22 |
| **Present Study (Rice husk rich mixtures)** | **RH - 75%, SD - 25%** | **0.20<br>0.30** | **800** | **0.21<br>0.23** |
| | **RH - 75%, BD - 25%** | **0.30** | **700<br>900** | **0.22<br>0.21** |
| Lv et al. [19] | Pine Sawdust | 0.21<br>0.27 | 800 | 0.23<br>0.19 |
| | | 0.22 | 700<br>900 | 0.14<br>0.25 |
| **Present Study (Saw dust rich mixtures)** | **SD - 75%, RH - 25%** | **0.20<br>0.30** | **800** | **0.24<br>0.27** |
| | **SD - 75%, BD - 25%** | **0.30** | **700<br>900** | **0.27<br>0.27** |

Kapur et al. [38] have given following formula for estimation of specific fuel consumption for electricity generation through rice husk gasification using duel fuel engine with generator set:

$$Q_h = \left[ \frac{1/DF - (1 - RF)}{\eta_g \times CV_h \times \eta_d \times \eta_a} \right] \times 3.6 \qquad (12)$$

where *DF* – derating factor; *RF* – diesel replacement factor; $CV_h$ – calorific value of rice husk; $\eta_d$ – efficiency of diesel engine; $\eta_a$ – efficiency of the duel–fuel generator; $\eta_g$ – efficiency of gasification. With representative values (as given by Kapur et al. [38]) of *DF* = 0.75, *RF* = 0.7, $CV_h$ = 13.4 MJ/kg, $\eta_g$ = 0.55, $\eta_d$ = 0.33 and $\eta_a$ = 0.875, $Q_h$ is calculated as 1.74 kg/kW–h. Nouni et al. [4] have reported specific fuel consumption in the range 1.1 to 1.68 kg/kWh for fixed bed downdraft gasifier of capacity 20–40 kWe employing either dual fuel or producer gas engine, and plant load factor ranging between 50 to 75%. It should be noted that "economy of scale" is another dominant aspect determining specific fuel consumption, in addition to various factors mention above. For large scale gasifiers in the range of 30 MWe or higher, the specific fuel consumption (either demolition wood or clean wood) could be as low as 0.9 kg/kW–h [39].

Another important factor is the net enthalpy change of gasification process (or the energy released in gasification). Part of this energy is absorbed by the gasification system itself and part is carried out of the gasifier by the producer gas. The absorbed heat helps maintaining the temperature of the gasifier. Moreover, the heat in the producer gas can be recovered through various means such as preheating of gasification air or drying of the biomass feed.

It can be seen from Table 5.3(A) that thermal energy content of producer gas essentially stays constant after 800$^{o}$C. Therefore, at first impression it appears that operation of gasifier at higher temperatures (900 or 1000$^{o}$C) may not fetch additional advantage. However, for a fluidized bed system where residence time of biomass is limited, higher gasification temperature can enhance single–pass conversion of biomass. Air ratio, on the other hand, has high influence on the process. For all biomass mixtures, rise of air ratio from 0.2 to 0.4 has been found to reduce the thermal energy content of producer gas by 30–40%. This result points out that low air ratios favor better performance of gasifier, but one must

also take into consideration incomplete conversion of carbon even under total equilibrium conditions for air ratio of 0.2. This effect is more pronounced for biomass mixtures containing saw dust, which has higher carbon content than rice husk or bamboo dust.

The power generation capacity of gasifier is higher for biomass mixtures containing saw dust. Among all 9 biomass mixtures, the least power generation is seen for biomass mixtures containing higher proportions of rice husk. This effect is clearly attributed to high ash content of rice husk.

## 5.6 CONCLUSION

This study as assessed the feasibility of use of biomass mixtures as fuel in biomass gasifiers for decentralized power generation equilibrium and semi–equilibrium (with limited carbon conversion) models employing Gibbs energy minimization. Binary mixtures of common biomasses found in northeastern states of India such as rice husk, bamboo dust and saw dust have been taken for analysis. The potential for power generation from gasifier has been evaluated on the basis of net yield (in $Nm^3$) and LHV (in $MJ/Nm^3$) of the producer gas obtained from gasification of 100 g of biomass mixture. The results of simulations have revealed interesting trends in performance of gasifiers with operating parameters such as air ratio, temperature of gasification and composition of the biomass mixture. For all biomass mixtures, the optimum air ratio is ~ 0.3 with gasification temperature of 800$^oC$. Under total equilibrium conditions, and for engine–generator efficiency of 30%, the least possible fuel consumption is found to be 0.8 kg/kW–h. This parameter shows an inverse variation with the extent of carbon conversion (or oxidation) achieved in the gasifier, which in turn depends on parameters such as air ratio, temperature of gasification and residence time of biomass in the gasifier. For low carbon conversions (~ 60% or so), the specific fuel consumption could be as high as 1.5 kg/kW–h. Comparative analysis of net yield (per unit biomass) and LHV of the

product gas calculated in our simulations with experimental results published in previous literature confirms that performance of gasification process for decentralized electricity generation stays essentially same after replacement of single biomass (either saw dust or rice husk) by mixtures of these biomasses with bamboo dust in different proportions. This feature, obviously, adds to the flexibility of operations of gasifiers in different locations under different operating conditions.

On a whole, this chapter has tried to get an insight into performance of gasifier employing biomass mixtures as fuel. The results of this study could form useful guidelines for design and optimization of medium to large scale biomass gasifiers employing biomass mixtures as feedstocks. Moreover, methodology presented in this chapter can be easily extended for the analysis of gasification of mixtures of other biomasses than considered in this study.

## REFERENCES

[1] McKendry P. Energy production from biomass (part 3): gasification technologies. Bioresource Technology 2002;83:55–63.

[2] Ghosh D, Sagar A, Kishore VVN. Scaling up biomass gasifier use: applications, barriers and interventions. Paper No. 103 (Climate Change Series), World Bank Environment Department, Washington, 2004.

[3] Bharadwaj A. Gasification and combustion technologies of agro–residues and their application to rural electric power systems in India. Ph.D. Dissertation, Carnegie Mellon University (Pittsburgh, USA), 2002.

[4] Nouni M.R., Mullick S.C., Kandpal T.C. Biomass gasifier projects for decentralized power generation in India: a financial evaluation. Energy Policy 2007;35:373–1385.

[5] Biomass Atlas of India, Combustion Gasification and Propulsion Laboratory, Bangalore: Indian Institute of Science. Homepage: http://cgpl.iisc.ernet.in (accessed November 2009).

[6] Gumz W. Gas producers and blast furnaces: Theory and methods of calculations. Wiley, 1950.

[7] Desrosiers R. Thermodynamics of gas-char reactions. In: Biomass gasification – Principles and technology (Ed. Reed T.B.), Noyes Data Corporation, 1981.

[8] Channiwala SA, Parikh PP. A unified correlation for estimating HHV of solid, liquid and gaseous fuels. Fuel 2002;81:1051–1063.

[9] Friedl A, Padouvas E, Rotter H, Varmuza K. Prediction of heating values of biomass fuel from elemental composition. Analytica Chimica Acta 2005;544:191-198.

[10] Sheng C, Azevedo JLT. Estimating higher heating value of biomass fuels from basic analysis data. Biomass and Bioenergy 2005;28:499-507.

[11] Jiang H–M, Morey RV. Pyrolysis of corncobs at fluidization. Biomass and Bioenergy 1992;3(2):81–85.

[12] Raveendran K, Ganesh A, Khilar KC. Pyrolysis characteristics of biomass and biomass components. Fuel 1996;75(8):987–998.

[13] Janse AMC, de Jonge HG, Prins W, van Swaaij WPM. Combustion kinetics of char obtained by flash pyrolysis of pine wood. Industrial and Engineering Chemistry Research 1998;37(10):3909–3918.

[14] Di Blasi C, Signorelli G, Di Russo C, Rea G. Product distribution from pyrolysis of wood and agricultural residues. Industrial and Engineering Chemistry Research 1999;38:2216–2224.

[15] Corella J, Sanz A. Modeling circulating fluidized bed biomass gasifiers: A pseudo–rigorous model with stationary state. Fuel Processing Technology 2005;86:1021–1053.

[16] Li X, Grace JR, Watkinson AP, Lim CJ, Ergudenler A. Equilibrium modeling of gasification: a free energy minimization approach and its application to a circulating fluidized bed coal gasifier. Fuel 2001;80:195–207.

[17] Li X. Biomass gasification in circulating fluidized bed, Ph.D. Dissertation, University of British Columbia (Vancouver, Canada), 2002.

[18] Kersten SRA. Biomass gasification in circulating fluidized beds. Ph.D. Dissertation, Twente University Press (Enschede, Netherlands), 2002.

[19] Lv PM, Xiong ZH, Chang J, Wu CZ, Chen Y, Zhu JX. An experimental study on biomass air–steam gasification in a fluidized bed. Bioresource Technology 2004;95:95–101.

[20] FactWeb. Homepage: http://www.factsage.com (accessed November 2009).

[21] Bale CW, Chartrand P, Degterov SA, Eriksson G, Hack K, Mahfoud K, Melancon J, Pelton AD, Petersen S. FACTSAGE thermochemical software and databases. Calphad 2002;26(2):189–228.

[22] Eriksson G. Thermodynamic studies of high temperature equilibria – XII: SOLGAMIX, A computer program for calculation of equilibrium composition in multiphase systems. Chemica Scripta 1975;8:100–103.

[23] Schuster G, Loffler G, Weigl K, Hofbauer H. Biomass steam gasification – an extensive parametric modeling study. Bioresource Technology 2001;77:71–79.

[24] Melgar A, Perez JF, Laget H, Horillo A. Thermochemical equilibrium modeling of a gasifying process. Energy Conversion and Management 2007;48:59-67.

[25] Jiang H, Zhu X, Guo Q, Zhu Q. Gasification of rice husk in a fluidized bed gasifier without inert additives. Industrial and Engineering Chemistry Research 2003;42:5745–5750.

[26] Narvaez I, Orio A, Aznar MP, Corella J. Biomass gasification with air in an atmospheric bubbling fluidized bed. Effect of six operational variables on the quality of the produced raw gas. Industrial and Engineering Chemistry Research 1996;35:2110–2120.

[27] Mansaray KG, Ghaly AE, Al–Taweel AM, Hamdullahpur F, Ugursal VI. Air gasification of rice husk in a dual distributor type fluidized bed reactor. Biomass and Bioenergy 1999;17:315–332.

[28] Ruggiero M, Manfrida G. An equilibrium model for biomass gasification process. Renewable Energy 1999;16:106–1109.

[29] Zainal ZA, Ali R, Dean CH, Seetharamu K. Prediction of performance of a downdraft gasifier using equilibrium modeling for different biomass materials. Energy Conversion and Management 2001;42:1499-1515.

[30] Jayah TH, Aye L, Fuller RJ, Stewart DF. Computer simulation of a downdraft wood gasifier for tea drying. Biomass and Bioenergy 2003;25:456–469.

[31] Ergudenler E, Ghaly AE. Quality of gas produced from wheat straw in a dual distributor type fluidized bed gasifier. Biomass and Bioenergy 1992;3:419–430.

[32] Maniatis K, Bridgwater AV, Buekens A. Fluidized bed gasification of wood. In: Research in Thermochemical Biomass Conversion (Ed. Bridgwater AV, Kuester JL), pp. 1094–1105, Elsevier Applied Science, 1988.

[33] van der Aarsen FG, Beenackers AACM, van Swaaij WPM. Thermochemical gasification in a pilot plant fluidized bed wood gasifier. Communications of European Communities 1983;8245:425–429.

[34] Jiang H, Morey RV. Air gasification of corncobs at fluidization. Biomass and Bioenergy 1992;3:87–92.

[35] Maniatis K, Vassilatos V, Kyritsis S. Design of pilot plant fluidized bed gasifier. In: Advances in thermo-chemical biomass conversion Vol. 1 (Ed. Bridgwater AV), pp. 403–410, Blakie Academic and Professional, 1994.

[36] Gulyurtlu I, Franco C, Mascarenhas F, Cabrita I. Steam gasification versus fast pyrolysis to produce medium calorific value gaseous fuel. In: Advances in thermo-chemical

biomass conversion Vol. 1 (Ed. Bridgwater AV), pp. 1187–1196, Blakie Academic and Professional, 1994.

[37] Yin XL, Wu CZ, Zheng SP, Chen Y. Design and operation of a CFB gasification and power generation system for rice husk. Biomass and Bioenergy 2002;23:181–187.

[38] Kapur T, Kandpal TC, Garg HP. Electricity generation from rice husk in Indian rice mills: Potential and financial viability. Biomass and Bioenergy 1998;14:573–583.

[39] Faaij A, van Ree R, Waldheim L, Olsson E, Oudhuis A, van Wijk A, Daey–Ouwens C, Turkenburg W. Gasification of biomass wastes and residues for electricity production. Biomass and Bioenergy 1997;12:387–407.

भारतीय प्रौद्योगिकी संस्थान गुवाहाटी
Indian Institute of Technology Guwahati

CHAPTER 6

# Performance Correlations for Biomass Gasifiers

## 6.1 INTRODUCTION

Major components of producer gas generated from biomass gasification (on dry basis) are CO, $CO_2$, $H_2$, $CH_4$ and $N_2$. The relative proportions of these species in the producer gas and the net yield of gas (per unit biomass) depends on several process and design parameters such as air ratio, temperature of gasification, dimensions of the gasifier, residence time of fuel and fuel quality (elemental composition, moisture content, particle size, HHV) etc. Gasification process is aimed at partial oxidation of the biomass. Carbon forms a significant fraction of any biomass. Thus, selective conversion of carbon in biomass to carbon monoxide is the basis of efficient utilization of biomass energy through gasification process. Complete oxidation of carbon to $CO_2$, however, is a loss of biomass energy. The extent of conversion of carbon in the biomass during gasification process depends on operating conditions as well as design features of the gasifier. Practically complete conversion of carbon is not achieved, and some fraction of the carbon in biomass remains unconverted in the form of char and tar. This

is also a loss of efficiency. The net quantity of the producer gas resulting from the gasification process depends on level of carbon conversion achieved in the gasifier.

From viewpoint of chemistry of the process, the elemental composition of C, H and O in the gasification mixture determines the composition of the producer gas. The elemental composition, in turn, is decided by the biomass type, moisture content of biomass and air ratio. Elemental ratios that influence relative proportions of different species in producer gas are: H/C, O/C and O/H. The H/C ratio governs the extent of $CH_4$ production relative to $H_2$ while O/H ratio determines the $H_2/H_2O$ ratio. Distribution of carbon in the biomass among CO and $CO_2$ (or in other words the $CO/CO_2$ ratio) is controlled by O/C ratio.

In this chapter, we have attempted to devise correlations for four major characteristics or features of the producer gas resulting from gasification process. These features are: (1) Lower Heating Value (LHV, $MJ/Nm^3$); (2) Net gas yield per unit biomass (Y, $Nm^3/100g$); (3) volume fraction of CO ($X_{CO}$) and (4) volume fraction of $CO_2$ ($X_{CO2}$). The independent variables used in these correlations are: (1) Air or equivalence ratio (AR); (2) temperature of gasification (Temp); (3) three elemental ratios, viz. H/C, O/H and O/C. These correlations are, however, independent of the design of the gasifier. The data for devising these correlations is generated through simulations of semi–equilibrium thermodynamic model for different combinations of air ratio, temperature and biomass type. Simulations of gasification of 3 common biomasses, 4 different gasification temperatures, 3 air ratios and 4 levels of carbon conversion have been carried out. Permutation–combination of these parameters gives a comprehensive set of 144 simulations. A peculiar feature of the semi–equilibrium model is that extent of carbon conversion in biomass is taken as basis, and has been used as an independent parameter in the model. It should be noted that extent of carbon conversion is a function of other parameters used in the model such as temperature and air ratio. Thus, in principle, it cannot be an independent parameter. However, for a given temperature and air

ratio, the carbon conversion also depends on the residence time of biomass in the reactor, which is an independent factor decided by the reactor design. Thus, for similar conditions of temperature and air ratio, carbon conversion in the reactor will vary (inversely) with residence time. It is in this spirit that we have considered carbon conversion as an independent parameter in our simulations.

From these simulations, we have determined the volume fraction of CO and $CO_2$ in the gas along with net yield (Y) and LHV of the producer gas. Further, we have attempted to fit different linear and non–linear correlations to the data for these parameters and have compared the predictions of these correlations with experimental data reported in literature. We have screened a total of 8 correlations of linear and non–linear type for fitting the data generated by simulations of thermodynamic model. We have also validated these correlations against experimental data reported in literature. The best correlation for each of the four parameters listed above is chosen on the basis of correlation coefficient, root mean square deviation, variance (as compared to the simulations data) and average absolute error (as compared to experimental data). To the best knowledge of the authors of present study, this is the first ever attempt to devise correlations for parameters that benchmark performance of gasifier in terms of operating conditions and elemental ratios.

## 6.2 MATHEMATICAL MODEL

Simulations have been carried out with software FACTSAGE [1, 2] that employs the algorithm SOLGASMIX proposed by Eriksson [3] for calculation composition of reaction system at thermodynamic equilibrium through Gibbs energy minimization of the system. For convenience of the reader, we give below only the main equations of this model (for greater details we refer the reader to Chapter 4).

### 6.2.1 Equations for Gibbs Energy Minimization

Total Gibbs free energy (G) of a system comprising of mixture of *i* species is:

$$G = \sum_i x_i g_i \tag{6.1}$$

$x_i$ is the mole number of a substance or species in the mixture. Chemical potential of a species *i* ( $g_i$ ) is:

$$g_i = g_i^0 + RT \ln a_i \tag{6.2}$$

$a_i$ represents activity coefficient of a species and it is equal to the partial pressure $p_i$ for a gaseous species assuming ideal behavior:

$$a_i = p_i = (x_i / X)P \tag{6.3}$$

*X* represents total number of moles in the gas phase and *P* is the total pressure of the system, respectively. The condensed substances are assumed to be pure, and hence, their activities are equal to unity. With these assumptions, a new dimensionless quantity (*G/RT*) is defined as:

$$G/RT = \sum_{i=1}^{m} x_i^g [(g^0/RT)_i^g + \ln P + \ln(x_i^g / X)] + \sum_{i=1}^{s} x_i^c (g^0/RT)_i^c \tag{6.4}$$

Superscripts *g* and *c* represent gas phase and condensed phase, respectively, while *m* and *s* represent the total number of substances in the gas phase and condensed phase, respectively, at equilibrium. *R* is the ideal gas constant. The quantity ($g^o$/*RT*) for a certain substance is calculated as with reference to standard state at 298 K:

$$(g^o/RT) = (1/R)[G^o - H_{298}^o)/T + \Delta_f H_{298}^o / RT \tag{6.5}$$

Superscript $^o$ refers to the thermodynamic standard state; subscript $_{298}$ refers to the reference temperature; subscript $_f$ denotes the formation of a compound from the elements in their standard states. Overall mass balance in the system among various species can be written as:

$$\sum_{i=1}^{m} a_{ij}^g x_i^g + \sum_{i=1}^{s} a_{ij}^c x_i^c = b_j \, (j = 1, 2, .....l) \tag{6.6}$$

Various notations are as follows: $a_{ij}$ – number of atoms of the $j^{th}$ element in a molecule of the $i^{th}$ substance, $b_j$ – total number of moles of the $j^{th}$ element, $l$ – total number of elements. The method involves a. For solution of this system of equations, Lagrange's method of undetermined multipliers is used. The solution essentially involves minimization of the free energy $G$ of a system (or equivalently $G/RT$ as given in equation 6.4) subject to the mass balance constraints.

Total heat of the process for attainment of equilibrium is determined as follows: The energy necessary for pre–heating the initial mixture ($HP$) from the initial temperature $T_1$ K to the reaction temperature $T$ K, added to the heat of reaction $(HR)$, gives the total heat $(HT)$: $HT = HP + HR$. $HP$ and $HR$ are determined as follows:

$$HP = \sum_i x_i^* (H^o - H_{T1}^o)_i \tag{6.7}$$

where $x^*$ denotes the number of moles in the initial mixture, and:

$$(H^o - H_{T1}^o)_i = \int_{T_1}^{T} (C_p)_i \, dT \tag{6.8}$$

$$HR = \sum_i (\Delta_f H_T^o)_i (x_i - x_i^*) \tag{6.9}$$

where $(\Delta_f H_T^o)_i = (\Delta_f H_{298}^o)_i + [(H^o - H_{298}^o)_i - (H^o - H_{298}^o)_{elements}]$. Various notations in equations 6.7–6.9 are: $H$ = enthalpy (heat content); $T$ = absolute temperature of the system; $x^*$ = number of moles in the initial mixture; $C_p$ = heat capacity at constant pressure as a function of temperature; $\Delta_f H_{298}^o$ = heat of formation at 298.15 K; $\left(G^o - H_{298}^o\right)/T$ = free energy function; $\left(H^o - H_{298}^o\right)$ = heat content function.

### 6.2.2 Simulation Parameters

Simulations of the gasification process requires 3 major parameters: (1) the elemental

vector or elemental composition of the gasification mixture; (2) temperature of gasification and (3) pressure of gasification. The elemental vector input is determined by 3 factors: (1) type of biomass; (2) gasification medium and (3) molar ratio of biomass to the gasification medium. In most commercial gasifiers, air is used as the gasification medium. Therefore, the same has been selected for our simulations of gasification. The amount of air supplied for gasification is characterized by air or equivalence ratio, which is defined as: AR = (moles of air actually supplied for gasification)/(stoichiometric amount of air required for complete combustion of biomass). In Chapter 4 (and also ref [4]), we have shown that the most optimum set of operating conditions for gasifier operation are: AR = 0.2–0.4, Temp = 700–1000$^{o}$C. In view of this, we have selected 3 air ratios, viz. 0.2, 0.3 and 0.4 and four gasification temperatures, viz. 700, 800, 900 and 1000$^{o}$C for the simulations. The pressure of the gasifier is taken to be atmospheric, which is again typical of most commercial gasifiers.

As far as biomass type is concerned, one has a wide choice. We have chosen 3 typical biomasses, viz. saw dust, rice husk and corn cob as the representative biomasses. These biomasses are among the most common feedstock for gasifiers. The ultimate analyses of these biomasses are given in Table 6.1(A), while Table 6.1(B) gives elemental composition of biomass along with molecular formula for the same. It could be perceived from Table 6.1(B) that three biomasses differ significantly in terms of elemental composition. The carbon content per unit mass varies as: saw dust > corn cob > rice husk. Corn cob has the highest oxygen content, while saw dust and rice husk have almost similar oxygen content. On the other hand, rice husk has high ash content than other two biomasses for which ash content is almost similar.

### 6.2.3 Extent of Carbon Conversion

As noted earlier, this parameter depends on many factors such as temperature of

**Table 6.1:** Data on biomasses

(A) Ultimate analysis of biomass

| Biomass | Composition in weight percent (Dry Basis) | | | | |
|---|---|---|---|---|---|
| | Carbon | Hydrogen | Nitrogen | Oxygen | Ash |
| Saw dust | 52.28 | 5.2 | 0.47 | 40.85 | 1.2 |
| Rice husk | 37.03 | 5.25 | 0.09 | 40.94 | 16.69 |
| Corn Cob | 41.44 | 5.96 | 0.14 | 51.26 | 1.2 |

(B) Composition of biomass (in gatoms) and molecular formulae

| Biomass | Composition in gatom (per 100 g biomass) | | | | Molecular Formula |
|---|---|---|---|---|---|
| | Carbon (C) | Hydrogen (H) | Nitrogen (N) | Oxygen (O) | |
| Saw dust | 4.36 | 5.20 | 0.03 | 2.55 | $CH_{1.193}N_{0.007}O_{0.585}$ |
| Rice husk | 3.09 | 5.25 | 0.01 | 2.56 | $CH_{1.699}N_{0.003}O_{0.828}$ |
| Corn Cob | 3.45 | 5.96 | 0.01 | 3.20 | $CH_{1.728}N_{0.003}O_{0.928}$ |

gasification, air ratio, particle size of biomass and residence time in the reactor. We have shown in our previous study that for low air ratios (≤ 0.2) and temperature (< 600°C), even under equilibrium conditions, some of the carbon in biomass remains unconverted [4]. For gasification temperatures > 700°C and AR > 2, the carbon conversion is essentially complete under equilibrium conditions. However, under practical situations, the residence time of biomass in the gasifier is limited and equilibrium conditions are not achieved, due to which some carbon in the biomass stays unreacted. In our simulations, we have chosen representative values of carbon conversion based on the experimental data reported in literature. Lv et al. [5] have reported extent of carbon conversion for gasification of pine saw dust in the range of 70–90%, while Mansaray et al. [6] have reported somewhat lower range of carbon conversion (60–80%) for gasification of rice husk. Similar range of extent of carbon conversion in gasification of rice husk has also been reported by Zhao et al. [7]. Cao et al. [8] have reported carbon conversion in the range of 72–87% for air gasification of saw dust. In view of these studies, we have chosen four levels of carbon conversion, viz. 70%,

**Table 6.2:** Elemental vector input for the simulation and the elemental ratios for various operating conditions

| Biomass: Rice Husk | | | | Biomass: Saw Dust | | | | Biomass: Corn Cob | | | |
|---|---|---|---|---|---|---|---|---|---|---|---|
| **Carbon Conversion: 70%** | | | | **Carbon Conversion: 70%** | | | | **Carbon Conversion: 70%** | | | |
| Element / | AR | | | Element / | AR | | | Element / | AR | | |
| Elemental Ratio | 0.2 | 0.3 | 0.4 | Elemental Ratio | 0.2 | 0.3 | 0.4 | Elemental Ratio | 0.2 | 0.3 | 0.4 |
| C | 2.160 | 2.160 | 2.160 | C | 3.050 | 3.050 | 3.050 | C | 2.417 | 2.417 | 2.417 |
| H | 6.361 | 6.361 | 6.361 | H | 6.311 | 6.311 | 6.311 | H | 7.071 | 7.071 | 7.071 |
| N | 4.720 | 7.080 | 9.440 | N | 6.660 | 9.980 | 13.300 | N | 5.060 | 7.600 | 10.120 |
| O | 4.362 | 4.986 | 5.609 | O | 4.861 | 5.737 | 6.613 | O | 5.096 | 5.764 | 6.432 |
| H/C | 2.061 | 2.061 | 2.061 | H/C | 1.448 | 1.448 | 1.448 | H/C | 2.048 | 2.048 | 2.048 |
| O/H | 0.686 | 0.784 | 0.882 | O/H | 0.770 | 0.909 | 1.048 | O/H | 0.721 | 0.815 | 0.910 |
| O/C | 1.413 | 1.616 | 1.818 | O/C | 1.116 | 1.317 | 1.518 | O/C | 1.476 | 1.669 | 1.863 |
| **Carbon Conversion: 80%** | | | | **Carbon Conversion: 80%** | | | | **Carbon Conversion: 80%** | | | |
| Element / | AR | | | Element / | AR | | | Element / | AR | | |
| Elemental Ratio | 0.2 | 0.3 | 0.4 | Elemental Ratio | 0.2 | 0.3 | 0.4 | Elemental Ratio | 0.2 | 0.3 | 0.4 |
| C | 2.469 | 2.469 | 2.469 | C | 3.486 | 3.486 | 3.486 | C | 2.762 | 2.762 | 2.762 |
| H | 6.361 | 6.361 | 6.361 | H | 6.311 | 6.311 | 6.311 | H | 7.071 | 7.071 | 7.071 |
| N | 4.720 | 7.080 | 9.440 | N | 6.660 | 9.980 | 13.300 | N | 5.060 | 6.160 | 10.120 |
| O | 4.362 | 4.986 | 5.609 | O | 4.861 | 5.737 | 6.613 | O | 5.096 | 5.764 | 6.432 |
| H/C | 2.061 | 2.061 | 2.061 | H/C | 1.448 | 1.448 | 1.448 | H/C | 2.048 | 2.048 | 2.048 |
| O/H | 0.686 | 0.784 | 0.882 | O/H | 0.770 | 0.909 | 1.048 | O/H | 0.721 | 0.815 | 0.910 |
| O/C | 1.413 | 1.616 | 1.818 | O/C | 1.116 | 1.317 | 1.518 | O/C | 1.476 | 1.669 | 1.863 |
| **Carbon Conversion: 90%** | | | | **Carbon Conversion: 90%** | | | | **Carbon Conversion: 90%** | | | |
| Element / | AR | | | Element / | AR | | | Element / | AR | | |
| Elemental Ratio | 0.2 | 0.3 | 0.4 | Elemental Ratio | 0.2 | 0.3 | 0.4 | Elemental Ratio | 0.2 | 0.3 | 0.4 |
| C | 2.774 | 2.774 | 2.774 | C | 3.921 | 3.921 | 3.921 | C | 3.108 | 3.108 | 3.108 |
| H | 6.361 | 6.361 | 6.361 | H | 6.311 | 6.311 | 6.311 | H | 7.071 | 7.071 | 7.071 |
| N | 4.720 | 7.080 | 9.440 | N | 6.660 | 9.980 | 13.300 | N | 5.060 | 6.160 | 10.120 |
| O | 4.362 | 4.986 | 5.609 | O | 4.861 | 5.737 | 6.613 | O | 5.096 | 5.764 | 6.432 |
| H/C | 2.061 | 2.061 | 2.061 | H/C | 1.448 | 1.448 | 1.448 | H/C | 2.048 | 2.048 | 2.048 |
| O/H | 0.686 | 0.784 | 0.882 | O/H | 0.770 | 0.909 | 1.048 | O/H | 0.721 | 0.815 | 0.910 |
| O/C | 1.413 | 1.616 | 1.818 | O/C | 1.116 | 1.317 | 1.518 | O/C | 1.476 | 1.669 | 1.863 |
| **Carbon Conversion: 100%** | | | | **Carbon Conversion: 100%** | | | | **Carbon Conversion: 100%** | | | |
| Element / | AR | | | Element / | AR | | | Element / | AR | | |
| Elemental Ratio | 0.2 | 0.3 | 0.4 | Elemental Ratio | 0.2 | 0.3 | 0.4 | Elemental Ratio | 0.2 | 0.3 | 0.4 |
| C | 3.086 | 3.086 | 3.086 | C | 4.357 | 4.357 | 4.357 | C | 3.453 | 3.453 | 3.453 |
| H | 6.361 | 6.361 | 6.361 | H | 6.311 | 6.311 | 6.311 | H | 7.071 | 7.071 | 7.071 |
| N | 4.720 | 7.080 | 9.440 | N | 6.660 | 9.980 | 13.300 | N | 5.060 | 6.160 | 10.120 |
| O | 4.362 | 4.986 | 5.609 | O | 4.861 | 5.737 | 6.613 | O | 5.096 | 5.764 | 6.432 |
| H/C | 2.061 | 2.061 | 2.061 | H/C | 1.448 | 1.448 | 1.448 | H/C | 2.048 | 2.048 | 2.048 |
| O/H | 0.686 | 0.784 | 0.882 | O/H | 0.770 | 0.909 | 1.048 | O/H | 0.721 | 0.815 | 0.910 |
| O/C | 1.413 | 1.616 | 1.818 | O/C | 1.116 | 1.317 | 1.518 | O/C | 1.476 | 1.669 | 1.863 |

Note: The elemental ratios H/C and O/C have been calculated on the basis of total carbon content of the biomass (and *not* the converted fraction).

80%, 90% and 100% for the simulations.

### 6.2.4 Elemental Vector Input

The elemental vector is generated by taking 100 g of biomass as basis. The elemental content of 100 g of each of biomass considered in this study is given in Table 6.1(B). For simulations with incomplete carbon conversion, the gatoms of carbon in 100 g biomass ($C_c$) are reduced by a factor $(1 - x_c)$, where $x_c$ is the extent of carbon conversion. Thus, the number of gatoms of carbon included in elemental vector input to the simulations are $x_c \cdot C_c$. The

unconverted carbon mainly appears in the form of char and tar. Table 6.2 gives the complete elemental vector input for the 3 biomasses under different conditions of air ratio and carbon conversion.

### 6.2.5 Fitting of Suitable Correlation to Simulations Data

We choose 8 different correlations of linear and non–linear form for fitting the data generated through simulations. The independent parameters used in these correlations are: (1) air ratio; (2) temperature of gasification, and 3 elemental ratios in gasification mixture, viz. H/C, O/H and O/C. The exact equations of the correlations for a performance parameter P (LHV, Y, $X_{CO}$, $X_{CO2}$) in linear and non–linear category are as follows:

**Linear Category:**

1. $P = \mathbf{a_1} \times Temp + \mathbf{a_2} \times (H/C) + \mathbf{a_3} \times (O/C)$ (6.10)
2. $P = \mathbf{a_1} \times Temp + \mathbf{a_2} \times (H/C) + \mathbf{a_3} \times (O/H)$ (6.11)
3. $P = \mathbf{a_1} \times Temp + \mathbf{a_2} \times (AR) + \mathbf{a_3} \times (H/C)$ (6.12)

**Non–linear Category:**

4. $P = \mathbf{a_1} \times (Temp)^{\mathbf{b1}} + \mathbf{a_2} \times (H/C)^{\mathbf{b2}} + \mathbf{a_3} \times (O/C)^{\mathbf{b3}}$ (6.13)
5. $P = \mathbf{a_1} \times (Temp)^{\mathbf{b1}} + \mathbf{a_2} \times (H/C)^{\mathbf{b2}} + \mathbf{a_3} \times (O/H)^{\mathbf{b3}}$ (6.14)
6. $P = \mathbf{a_1} \times (Temp)^{\mathbf{b1}} + \mathbf{a_2} \times (AR)^{\mathbf{b2}} + \mathbf{a_3} \times (H/C)^{\mathbf{b3}}$ (6.15)
7. $P = \mathbf{a_1} \times (Temp)^{\mathbf{b1}} \times (AR)^{\mathbf{b2}} \times (H/C)^{\mathbf{b3}}$ (6.16)
8. $P = \mathbf{a_1} \times (Temp)^{\mathbf{b1}} \times (H/C)^{\mathbf{b2}} \times (O/C)^{\mathbf{b3}} \times (O/H)^{\mathbf{b4}}$ (6.17)

These forms of correlations have been chosen by assumption of either linear or non–linear effect of the independent variable on the parameter P. The constant for each of these correlations were computed using software Polymath (Ver 6.0), which uses Levenberg–Marquardt algorithm [9]. For evaluation of constants 144 data points generated from simulations of gasification process under different combinations of operating conditions

(biomass type, air ratio, temperature) and extent of carbon conversion described earlier.

### 6.2.6 Comparison and Selection of Best Correlation

The best correlation among the 8 linear and nonlinear expressions given above for a particular performance parameter was found using a 3 step procedure as follows:

(1) The precision of the correlation generated using 144 data points was evaluated on the basis of 3 statistical indicators: Correlation coefficient (or regression coefficient, $R^2$); Root mean square deviation ($R_{msd}$); and Variance ($s^2$). These indicators are given as:

$$R^2 = 1 - \sum_{i=1}^{n} \left( y_{i,calc} - y_{i,pred} \right)^2 \tag{6.18}$$

$$R_{msd} = \frac{1}{n} \left[ \sum_{i=1}^{n} \left( y_{i,calc} - y_{i,pred} \right)^2 \right]^{0.5} \tag{6.19}$$

$$s^2 = \sum_{i=1}^{n} \left( y_{i,pred} - \overline{y} \right)^2 \text{ where } \overline{y} = \frac{1}{n} \left( \sum_{i=1}^{n} y_{i,calc} \right) \tag{6.20}$$

Notation: y is the value of performance parameter. Subscript “calc” represents value of a parameter calculated with simulations, while notation “pred” represents value predicted by the correlation for the given input set of independent parameters.

(2) The value of any parameter predicted by the correlation (obtained using all 144 points) is compared against the model value for any single biomass for a given set of independent parameters. This step assesses the compatibility of the correlation with the model data.

(3) Finally, the correlations are evaluated against experimental data reported in the literature. Using temperature, air ratio and the 3 elemental ratios reported experimental studies, values of the LHV, Y, $X_{CO}$ and $X_{CO2}$ predicted by different correlations are compared with the experimentally observed values. The disparity between experimental and correlations data is adjudged using average absolute error (AAE) calculated as:

$$AAE = \frac{1}{n}\sum_{i=1}^{n}\left|\frac{y_{corr} - y_{exptl}}{y_{exptl}}\right| \times 100 \qquad (6.21)$$

The best correlation for a performance parameter is chosen on the basis of lowest values $s^2$, $R_{msd}$ and AAE, and highest value of $R^2$.

## 6.3 RESULTS AND DISCUSSION

Tables 6.3, 6.4 and 6.5 give the summary of simulations results for rice husk, saw dust and corn cob respectively. An analysis of simulations results is presented in Table 6.6 and 6.7, which describe fractional distribution of carbon in the biomass among 4 major species, viz. CO, $CO_2$, $CH_4$ and unconverted C; and fractional distribution of hydrogen among 3 major species, viz. $H_2$, $H_2O$ and $CH_4$. Table 6.8 gives the list of 8 correlations for the four performance parameters along with the corresponding statistical indicators. Figures 6.1 – 6.4 show the parity plots for compatibility of the correlations with data for any single biomass calculated using thermodynamic model (given in Tables 6.3–6.5). In tables 6.9, 6.10, 6.11 and 6.12 we evaluate the predictions of 8 correlations for the performance parameter against experimental data reported in literature. For this evaluation, we have used experimental data from 3 papers that report air gasification of biomasses considered in the simulations, viz. Narvaez et al. [10] for pine saw dust, Mansaray et al. [6] for rice husk and Jiang and Morey [11] for corn cob. We would like to specifically mention that in addition to these papers, we have also evaluated our correlations against other experimental studies that use different types of biomasses such as wood chips, wheat straw, pine wood, wood–waste or demolition wood etc. than considered in this study [8, 12-15]. However, for brevity, we have given results only for the 3 papers mentioned above. Parity plots for the experimental data and model predictions for different performance parameters are shown in Figures 6.5–6.8.

**Table 6.3:** Simulations results for rice husk gasification (Basis: 100 g of rice husk)

| Temp | Fraction of Carbon Converted | $CO_2$ vol fraction | CO vol fraction | $CO/CO_2$ Ratio | Gas yield ($Nm^3$) | LHV ($MJ/Nm^3$) |
|---|---|---|---|---|---|---|
| | **(A) AR = 0.2, H/C = 2.061, O/C = 1.413** | | | | | |
| 700°C | 0.7 | 0.16 | 0.17 | 1.05 | 0.16 | 5.68 |
| | 0.8 | 0.14 | 0.21 | 1.46 | 0.17 | 6.27 |
| | 0.9 | 0.12 | 0.24 | 2.01 | 0.18 | 6.82 |
| | 1.0 | 0.10 | 0.28 | 2.76 | 0.19 | 7.34 |
| 800°C | 0.7 | 0.14 | 0.19 | 1.35 | 0.15 | 5.78 |
| | 0.8 | 0.12 | 0.23 | 1.88 | 0.17 | 6.37 |
| | 0.9 | 0.10 | 0.27 | 2.59 | 0.18 | 6.89 |
| | 1.0 | 0.08 | 0.30 | 3.70 | 0.19 | 7.37 |
| 900°C | 0.7 | 0.13 | 0.21 | 1.63 | 0.15 | 5.87 |
| | 0.8 | 0.11 | 0.25 | 2.26 | 0.17 | 6.46 |
| | 0.9 | 0.09 | 0.28 | 3.12 | 0.18 | 6.97 |
| | 1.0 | 0.07 | 0.32 | 4.40 | 0.19 | 7.44 |
| 1000°C | 0.7 | 0.12 | 0.23 | 1.91 | 0.15 | 5.95 |
| | 0.8 | 0.10 | 0.26 | 2.63 | 0.14 | 6.53 |
| | 0.9 | 0.08 | 0.30 | 3.62 | 0.18 | 7.04 |
| | 1.0 | 0.06 | 0.33 | 5.13 | 0.19 | 7.50 |
| | **(B) AR = 0.3, H/C = 2.061, O/C = 1.616** | | | | | |
| 700°C | 0.7 | 0.18 | 0.12 | 0.66 | 0.18 | 4.05 |
| | 0.8 | 0.16 | 0.15 | 0.93 | 0.19 | 4.66 |
| | 0.9 | 0.14 | 0.18 | 1.29 | 0.20 | 5.22 |
| | 1.0 | 0.13 | 0.22 | 1.74 | 0.22 | 5.74 |
| 800°C | 0.7 | 0.16 | 0.14 | 0.84 | 0.17 | 4.12 |
| | 0.8 | 0.15 | 0.17 | 1.18 | 0.19 | 4.74 |
| | 0.9 | 0.13 | 0.21 | 1.61 | 0.20 | 5.30 |
| | 1.0 | 0.11 | 0.24 | 2.19 | 0.21 | 5.82 |
| 900°C | 0.7 | 0.15 | 0.15 | 1.02 | 0.17 | 4.17 |
| | 0.8 | 0.13 | 0.19 | 1.41 | 0.19 | 4.81 |
| | 0.9 | 0.12 | 0.22 | 1.91 | 0.20 | 5.37 |
| | 1.0 | 0.10 | 0.25 | 2.59 | 0.21 | 5.88 |
| 1000°C | 0.7 | 0.14 | 0.17 | 1.19 | 0.17 | 4.22 |
| | 0.8 | 0.12 | 0.20 | 1.64 | 0.18 | 4.86 |
| | 0.9 | 0.11 | 0.24 | 2.22 | 0.20 | 5.43 |
| | 1.0 | 0.09 | 0.27 | 2.99 | 0.21 | 5.94 |
| | **(C) AR = 0.4, H/C = 2.061, O/C = 1.818** | | | | | |
| 700°C | 0.7 | 0.19 | 0.08 | 0.40 | 0.20 | 2.75 |
| | 0.8 | 0.18 | 0.11 | 0.60 | 0.21 | 3.38 |
| | 0.9 | 0.16 | 0.14 | 0.84 | 0.23 | 3.95 |
| | 1.0 | 0.15 | 0.17 | 1.15 | 0.27 | 4.47 |
| 800°C | 0.7 | 0.18 | 0.09 | 0.52 | 0.19 | 2.79 |
| | 0.8 | 0.16 | 0.12 | 0.75 | 0.21 | 3.44 |
| | 0.9 | 0.15 | 0.15 | 1.05 | 0.22 | 4.01 |
| | 1.0 | 0.13 | 0.19 | 1.41 | 0.23 | 4.51 |
| 900°C | 0.7 | 0.17 | 0.11 | 0.63 | 0.19 | 2.82 |
| | 0.8 | 0.15 | 0.14 | 0.91 | 0.21 | 3.48 |
| | 0.9 | 0.14 | 0.17 | 1.24 | 0.22 | 4.06 |
| | 1.0 | 0.12 | 0.20 | 1.67 | 0.23 | 4.60 |
| 1000°C | 0.7 | 0.16 | 0.12 | 0.73 | 0.19 | 2.84 |
| | 0.8 | 0.14 | 0.15 | 1.05 | 0.20 | 3.52 |
| | 0.9 | 0.13 | 0.18 | 1.43 | 0.22 | 4.10 |
| | 1.0 | 0.11 | 0.21 | 1.92 | 0.23 | 4.64 |

**Table 6.4:** Simulations results for saw dust gasification (Basis: 100 g of saw dust)

| Temp | Fraction of Carbon Converted | $CO_2$ vol fraction | CO vol fraction | $CO/CO_2$ Ratio | Gas yield ($Nm^3$) | LHV ($MJ/Nm^3$) |
|---|---|---|---|---|---|---|
| | **(A) AR = 0.2, H/C = 1.449, O/C = 1.116** | | | | | |
| 700°C | 0.7 | 0.12 | 0.23 | 1.84 | 0.21 | 5.94 |
| | 0.8 | 0.10 | 0.27 | 2.82 | 0.22 | 6.62 |
| | 0.9 | 0.08 | 0.29 | 3.49 | 0.23 | 6.92 |
| | 1.0 | 0.08 | 0.29 | 3.49 | 0.23 | 6.92 |
| 800°C | 0.7 | 0.11 | 0.25 | 2.30 | 0.21 | 6.01 |
| | 0.8 | 0.08 | 0.29 | 3.66 | 0.23 | 6.66 |
| | 0.9 | 0.06 | 0.34 | 6.13 | 0.24 | 7.25 |
| | 1.0 | 0.03 | 0.38 | 12.63 | 0.26 | 7.80 |
| 900°C | 0.7 | 0.10 | 0.26 | 2.72 | 0.21 | 6.08 |
| | 0.8 | 0.07 | 0.31 | 4.30 | 0.22 | 6.72 |
| | 0.9 | 0.05 | 0.35 | 7.23 | 0.24 | 7.29 |
| | 1.0 | 0.03 | 0.39 | 15.44 | 0.26 | 7.81 |
| 1000°C | 0.7 | 0.09 | 0.27 | 3.15 | 0.20 | 6.14 |
| | 0.8 | 0.06 | 0.32 | 4.92 | 0.22 | 6.77 |
| | 0.9 | 0.04 | 0.35 | 8.23 | 0.24 | 7.33 |
| | 1.0 | 0.02 | 0.39 | 17.73 | 0.25 | 7.83 |
| | **(B) AR = 0.3, H/C = 1.449, O/C = 1.317** | | | | | |
| 700°C | 0.7 | 0.15 | 0.15 | 1.01 | 0.24 | 4.15 |
| | 0.8 | 0.13 | 0.20 | 1.53 | 0.26 | 4.83 |
| | 0.9 | 0.11 | 0.24 | 2.27 | 0.27 | 5.45 |
| | 1.0 | 0.08 | 0.28 | 3.39 | 0.29 | 6.03 |
| 800°C | 0.7 | 0.14 | 0.17 | 1.25 | 0.27 | 4.22 |
| | 0.8 | 0.12 | 0.21 | 1.86 | 0.26 | 4.90 |
| | 0.9 | 0.09 | 0.26 | 2.77 | 0.27 | 5.51 |
| | 1.0 | 0.07 | 0.30 | 4.28 | 0.29 | 6.06 |
| 900°C | 0.7 | 0.13 | 0.19 | 1.46 | 0.23 | 4.27 |
| | 0.8 | 0.11 | 0.23 | 2.17 | 0.25 | 4.95 |
| | 0.9 | 0.08 | 0.27 | 3.23 | 0.27 | 5.56 |
| | 1.0 | 0.06 | 0.31 | 4.92 | 0.29 | 6.11 |
| 1000°C | 0.7 | 0.12 | 0.20 | 1.69 | 0.23 | 4.31 |
| | 0.8 | 0.10 | 0.24 | 2.49 | 0.25 | 5.00 |
| | 0.9 | 0.08 | 0.28 | 3.66 | 0.27 | 5.60 |
| | 1.0 | 0.06 | 0.31 | 5.59 | 0.28 | 6.15 |
| | **(C) AR = 0.4, H/C = 1.449, O/C = 1.518** | | | | | |
| 700°C | 0.7 | 0.17 | 0.10 | 0.57 | 0.27 | 2.78 |
| | 0.8 | 0.15 | 0.14 | 0.88 | 0.29 | 3.46 |
| | 0.9 | 0.13 | 0.17 | 1.30 | 0.31 | 4.07 |
| | 1.0 | 0.11 | 0.21 | 1.88 | 0.32 | 4.64 |
| 800°C | 0.7 | 0.16 | 0.11 | 0.71 | 0.27 | 2.82 |
| | 0.8 | 0.14 | 0.15 | 1.07 | 0.29 | 3.51 |
| | 0.9 | 0.12 | 0.19 | 1.56 | 0.30 | 4.12 |
| | 1.0 | 0.10 | 0.23 | 2.23 | 0.32 | 4.69 |
| 900°C | 0.7 | 0.15 | 0.13 | 0.83 | 0.26 | 2.85 |
| | 0.8 | 0.13 | 0.17 | 1.25 | 0.28 | 3.55 |
| | 0.9 | 0.11 | 0.20 | 1.81 | 0.30 | 4.17 |
| | 1.0 | 0.09 | 0.24 | 2.57 | 0.32 | 4.73 |
| 1000°C | 0.7 | 0.14 | 0.14 | 0.95 | 0.26 | 2.88 |
| | 0.8 | 0.12 | 0.18 | 1.42 | 0.28 | 3.58 |
| | 0.9 | 0.11 | 0.21 | 2.04 | 0.30 | 4.20 |
| | 1.0 | 0.09 | 0.25 | 2.90 | 0.31 | 4.77 |

**Table 6.5:** Simulations results for corn cob gasification (Basis: 100 g of corn cob)

| Temp | Fraction of Carbon Converted | $CO_2$ vol fraction | CO vol fraction | $CO/CO_2$ Ratio | Gas yield ($Nm^3$) | LHV ($MJ/Nm^3$) |
|---|---|---|---|---|---|---|
| | **(A) AR = 0.2, H/C = 2.048, O/C = 1.476** | | | | | |
| 700°C | 0.7 | 0.16 | 0.16 | 1.01 | 0.17 | 5.49 |
| | 0.8 | 0.14 | 0.20 | 1.42 | 0.18 | 6.10 |
| | 0.9 | 0.12 | 0.24 | 1.97 | 0.20 | 6.67 |
| | 1.0 | 0.10 | 0.25 | 2.50 | 0.21 | 6.66 |
| 800°C | 0.7 | 0.14 | 0.19 | 1.31 | 0.17 | 5.59 |
| | 0.8 | 0.12 | 0.23 | 1.83 | 0.18 | 6.21 |
| | 0.9 | 0.10 | 0.26 | 2.55 | 0.20 | 6.75 |
| | 1.0 | 0.08 | 0.28 | 3.39 | 0.20 | 6.75 |
| 900°C | 0.7 | 0.13 | 0.21 | 1.59 | 0.16 | 5.68 |
| | 0.8 | 0.11 | 0.25 | 2.23 | 0.18 | 6.30 |
| | 0.9 | 0.09 | 0.28 | 3.09 | 0.19 | 6.84 |
| | 1.0 | 0.07 | 0.30 | 4.11 | 0.20 | 6.84 |
| 1000°C | 0.7 | 0.12 | 0.22 | 1.87 | 0.16 | 5.76 |
| | 0.8 | 0.10 | 0.26 | 2.60 | 0.18 | 6.38 |
| | 0.9 | 0.08 | 0.30 | 3.60 | 0.19 | 6.92 |
| | 1.0 | 0.06 | 0.31 | 4.86 | 0.20 | 6.92 |
| | **(B) AR = 0.3, H/C = 2.048, O/C = 1.669** | | | | | |
| 700°C | 0.7 | 0.18 | 0.11 | 0.63 | 0.19 | 3.89 |
| | 0.8 | 0.16 | 0.15 | 0.90 | 0.21 | 4.54 |
| | 0.9 | 0.14 | 0.18 | 1.26 | 0.22 | 5.12 |
| | 1.0 | 0.13 | 0.21 | 1.71 | 0.24 | 5.65 |
| 800°C | 0.7 | 0.16 | 0.13 | 0.81 | 0.19 | 3.95 |
| | 0.8 | 0.15 | 0.17 | 1.15 | 0.20 | 4.62 |
| | 0.9 | 0.13 | 0.20 | 1.59 | 0.22 | 5.20 |
| | 1.0 | 0.11 | 0.24 | 2.16 | 0.23 | 5.73 |
| 900°C | 0.7 | 0.15 | 0.15 | 0.99 | 0.19 | 4.01 |
| | 0.8 | 0.13 | 0.18 | 1.38 | 0.20 | 4.68 |
| | 0.9 | 0.12 | 0.22 | 1.89 | 0.22 | 5.27 |
| | 1.0 | 0.10 | 0.25 | 2.57 | 0.23 | 5.80 |
| 1000°C | 0.7 | 0.14 | 0.16 | 1.16 | 0.18 | 4.06 |
| | 0.8 | 0.12 | 0.20 | 1.62 | 0.20 | 4.74 |
| | 0.9 | 0.11 | 0.23 | 2.20 | 0.21 | 5.33 |
| | 1.0 | 0.09 | 0.27 | 2.98 | 0.23 | 5.86 |
| | **(C) AR = 0.4, H/C = 2.048, O/C = 1.862** | | | | | |
| 700°C | 0.7 | 0.19 | 0.07 | 0.38 | 0.21 | 2.61 |
| | 0.8 | 0.18 | 0.10 | 0.58 | 0.23 | 3.28 |
| | 0.9 | 0.16 | 0.13 | 0.83 | 0.24 | 3.87 |
| | 1.0 | 0.15 | 0.16 | 1.13 | 0.26 | 4.41 |
| 800°C | 0.7 | 0.18 | 0.09 | 0.49 | 0.21 | 2.65 |
| | 0.8 | 0.16 | 0.12 | 0.74 | 0.23 | 3.33 |
| | 0.9 | 0.15 | 0.15 | 1.03 | 0.24 | 3.93 |
| | 1.0 | 0.13 | 0.18 | 1.40 | 0.26 | 4.48 |
| 900°C | 0.7 | 0.17 | 0.10 | 0.60 | 0.21 | 2.68 |
| | 0.8 | 0.15 | 0.13 | 0.88 | 0.22 | 3.37 |
| | 0.9 | 0.14 | 0.17 | 1.23 | 0.24 | 3.99 |
| | 1.0 | 0.12 | 0.20 | 1.66 | 0.25 | 4.54 |
| 1000°C | 0.7 | 0.16 | 0.11 | 0.70 | 0.20 | 2.70 |
| | 0.8 | 0.14 | 0.15 | 1.03 | 0.22 | 3.41 |
| | 0.9 | 0.13 | 0.18 | 1.42 | 0.23 | 4.03 |
| | 1.0 | 0.11 | 0.21 | 1.91 | 0.25 | 4.58 |

We present the analysis in 2 sections. In the first section, we discuss the trends in simulations results and distribution of C and H among product species. In the second section, we present and analyze different correlations for the performance parameters.

### 6.3.1 Trends in LHV, Y, $X_{CO}$ and $X_{CO2}$

The trends in four performance parameters with variables in the simulations are identified as follows: (1) For a given level of carbon conversion and temperature of gasification, the fraction of CO in the producer gas decreases (with concomitant increase in $CO_2$) with rising air ratio. (2) For a given air ratio and gasification temperature, fraction of CO in the producer gas increases with level of carbon conversion. (3) Rise in gasification temperature (at a fixed air ration and carbon conversion) increases the fraction of CO in producer gas.

Comparison of the simulation results for the 3 biomasses yields interesting trends in volume fractions of CO and $CO_2$, which is attributed to the elemental compositions of the biomasses. For similar gasification conditions (AR, temperature and fractional carbon conversion), the fraction of CO in the producer gas from saw dust is much higher than the other two biomasses. This disparity is more marked for low air ratio of 0.2. On the other hand, the values of $X_{CO}$ and $X_{CO2}$ for rice husk and corn cob are almost similar for a given set of gasifying conditions. However, a closer look into these values reveals that $X_{CO2}$ for corn cob is slightly higher than rice husk.

Trends in LHV and Y fall in line with the trends in $X_{CO}$ and $X_{CO2}$. For a given AR and gasification temperature, LHV and Y increase with increasing carbon conversion, for obvious reasons. For a given AR and carbon conversion, LHV and Y are practically constant in the temperature range of 700 – 1000$^{o}$C. Comparing among the 3 biomasses, we see that LHV and Y for a given set of gasifying conditions is higher for saw dust than rice husk or corn cob.

Although the producer gas yield is practically same for rice husk and corn cob for a given set of gasifying conditions, the LHV for rice husk is somewhat higher. We analyze these results in the next section.

### 6.3.2 Trends in carbon and hydrogen distribution in producer gas

As noted earlier, saw dust has the highest carbon content while corn cob has the highest oxygen content among the 3 biomasses considered in this study. From data presented in Table 6.6(A), (B) and (C), we discern following trends: (1) For all 3 biomasses, the converted fraction of carbon is mainly distributed among two oxides, CO and $CO_2$. Fraction of carbon appearing in the form of methane is very low, and for temperatures $\geq 800^oC$, it practically reduces to zero. (2) Fraction of carbon appearing in the form of CO is higher for saw dust than for rice husk and corn cob. This result is attributed to higher carbon content of saw dust. (3) Comparing among rice husk and corn cob, we see higher fraction of carbon ending up in $CO_2$ for corn cob for any given AR, gasification temperature and carbon conversion. This is a result of higher oxygen content of corn cob.

Similar trends are also seen for hydrogen distribution: (1) For low temperatures and air ratios, major fraction of hydrogen in gasification mixture ends up in $H_2$. (2) Fraction of hydrogen appearing in the form of $H_2O$ increases rapidly with temperature of gasification for a given level of carbon conversion and air ratio. (3) Fraction of hydrogen in $H_2O$ also increases with rising air ratio for a given gasification temperature and level of carbon conversion, due to higher oxygen content of gasification mixture. (4) Fraction of hydrogen appearing in the form of $H_2$ is significantly higher for saw dust than rice husk and corn cob for any set of gasifying conditions. This is clearly attributed to high carbon content of saw dust, due to which the oxygen in the gasification mixture is competitively consumed by carbon as compared to hydrogen. (5) Fraction of hydrogen ending up in $H_2O$ in higher for

**Table 6.6:** Fractional Distribution of Carbon Among Various Species in Producer Gas

(A) Biomass: Rice Husk

| Species | AIR RATIO = 0.2 % Carbon Conversion | | | | Species | AIR RATIO = 0.3 % Carbon Conversion | | | | Species | AIR RATIO = 0.4 % Carbon Conversion | | | |
|---|---|---|---|---|---|---|---|---|---|---|---|---|---|---|
| | 70% | 80% | 90% | 100% | | 70% | 80% | 90% | 100% | | 70% | 80% | 90% | 100% |
| | Temp = 700°C | | | | | Temp = 700°C | | | | | Temp = 700°C | | | |
| $CO_2$ | 0.34 | 0.322 | 0.294 | 0.259 | $CO_2$ | 0.421 | 0.412 | 0.392 | 0.361 | $CO_2$ | 0.498 | 0.499 | 0.487 | 0.464 |
| CO | 0.357 | 0.471 | 0.592 | 0.718 | CO | 0.278 | 0.385 | 0.503 | 0.63 | CO | 0.202 | 0.3 | 0.41 | 0.533 |
| $CH_4$ | 0.005 | 0.009 | 0.015 | 0.023 | $CH_4$ | 0.001 | 0.003 | 0.005 | 0.008 | $CH_4$ | 0 | 0.001 | 0.002 | 0.003 |
| C | 0.3 | 0.2 | 0.101 | 0 | C | 0.3 | 0.2 | 0.101 | 0 | C | 0.3 | 0.2 | 0.101 | 0 |
| | Temp = 800°C | | | | | Temp = 800°C | | | | | Temp = 800°C | | | |
| $CO_2$ | 0.298 | 0.278 | 0.249 | 0.212 | $CO_2$ | 0.38 | 0.367 | 0.345 | 0.314 | $CO_2$ | 0.461 | 0.455 | 0.439 | 0.414 |
| CO | 0.402 | 0.521 | 0.649 | 0.786 | CO | 0.32 | 0.432 | 0.554 | 0.686 | CO | 0.239 | 0.345 | 0.46 | 0.586 |
| $CH_4$ | 0 | 0.001 | 0.001 | 0.002 | $CH_4$ | 0 | 0 | 0 | 0.001 | $CH_4$ | 0 | 0 | 0 | 0 |
| C | 0.3 | 0.2 | 0.101 | 0 | C | 0.3 | 0.2 | 0.101 | 0 | C | 0.3 | 0.2 | 0.101 | 0 |
| | Temp = 900°C | | | | | Temp = 900°C | | | | | Temp = 900°C | | | |
| $CO_2$ | 0.266 | 0.246 | 0.219 | 0.185 | $CO_2$ | 0.347 | 0.331 | 0.309 | 0.279 | $CO_2$ | 0.43 | 0.419 | 0.401 | 0.375 |
| CO | 0.434 | 0.554 | 0.680 | 0.815 | CO | 0.353 | 0.468 | 0.59 | 0.721 | CO | 0.27 | 0.381 | 0.498 | 0.625 |
| $CH_4$ | 0 | 0 | 0 | 0 | $CH_4$ | 0 | 0 | 0 | 0 | $CH_4$ | 0 | 0 | 0 | 0 |
| C | 0.3 | 0.2 | 0.101 | 0 | C | 0.3 | 0.2 | 0.101 | 0 | C | 0.3 | 0.2 | 0.101 | 0 |
| | Temp = 1000°C | | | | | Temp = 1000°C | | | | | Temp = 1000°C | | | |
| $CO_2$ | 0.24 | 0.22 | 0.194 | 0.164 | $CO_2$ | 0.32 | 0.303 | 0.280 | 0.251 | $CO_2$ | 0.405 | 0.390 | 0.370 | 0.343 |
| CO | 0.46 | 0.579 | 0.705 | 0.836 | CO | 0.38 | 0.497 | 0.619 | 0.749 | CO | 0.295 | 0.41 | 0.529 | 0.657 |
| $CH_4$ | 0 | 0 | 0 | 0 | $CH_4$ | 0 | 0 | 0 | 0 | $CH_4$ | 0 | 0 | 0 | 0 |
| C | 0.3 | 0.2 | 0.101 | 0 | C | 0.3 | 0.2 | 0.101 | 0 | C | 0.3 | 0.2 | 0.101 | 0 |

(B) Biomass: Saw Dust

| Species | AIR RATIO = 0.2 % Carbon Conversion | | | | Species | AIR RATIO = 0.3 % Carbon Conversion | | | | Species | AIR RATIO = 0.4 % Carbon Conversion | | | |
|---|---|---|---|---|---|---|---|---|---|---|---|---|---|---|
| | 70% | 80% | 90% | 100% | | 70% | 80% | 90% | 100% | | 70% | 80% | 90% | 100% |
| | Temp = 700°C | | | | | Temp = 700°C | | | | | Temp = 700°C | | | |
| $CO_2$ | 0.245 | 0.206 | 0.185 | 0.185 | $CO_2$ | 0.347 | 0.315 | 0.274 | 0.225 | $CO_2$ | 0.445 | 0.424 | 0.390 | 0.346 |
| CO | 0.449 | 0.580 | 0.642 | 0.642 | CO | 0.352 | 0.481 | 0.619 | 0.76 | CO | 0.255 | 0.375 | 0.508 | 0.649 |
| $CH_4$ | 0.01 | 0.018 | 0.021 | 0.019 | $CH_4$ | 0.002 | 0.005 | 0.009 | 0.015 | $CH_4$ | 0 | 0.001 | 0.002 | 0.005 |
| C | 0.3 | 0.2 | 0.1 | 0 | C | 0.3 | 0.2 | 0.1 | 0 | C | 0.3 | 0.2 | 0.1 | 0 |
| | Temp = 800°C | | | | | Temp = 800°C | | | | | Temp = 800°C | | | |
| $CO_2$ | 0.211 | 0.172 | 0.125 | 0.073 | $CO_2$ | 0.311 | 0.279 | 0.238 | 0.19 | $CO_2$ | 0.410 | 0.386 | 0.351 | 0.309 |
| CO | 0.488 | 0.627 | 0.773 | 0.921 | CO | 0.389 | 0.52 | 0.661 | 0.809 | CO | 0.29 | 0.414 | 0.549 | 0.691 |
| $CH_4$ | 0.001 | 0.001 | 0.002 | 0.006 | $CH_4$ | 0 | 0 | 0.001 | 0.001 | $CH_4$ | 0 | 0 | 0 | 0 |
| C | 0.3 | 0.2 | 0.1 | 0 | C | 0.3 | 0.2 | 0.1 | 0 | C | 0.3 | 0.2 | 0.1 | 0 |
| | Temp = 900°C | | | | | Temp = 900°C | | | | | Temp = 900°C | | | |
| $CO_2$ | 0.188 | 0.152 | 0.109 | 0.061 | $CO_2$ | 0.283 | 0.252 | 0.214 | 0.169 | $CO_2$ | 0.382 | 0.355 | 0.321 | 0.28 |
| CO | 0.512 | 0.648 | 0.791 | 0.938 | CO | 0.417 | 0.548 | 0.686 | 0.831 | CO | 0.318 | 0.445 | 0.579 | 0.72 |
| $CH_4$ | 0 | 0 | 0 | 0.001 | $CH_4$ | 0 | 0 | 0 | 0 | $CH_4$ | 0 | 0 | 0 | 0 |
| C | 0.3 | 0.2 | 0.1 | 0 | C | 0.3 | 0.2 | 0.1 | 0 | C | 0.3 | 0.2 | 0.1 | 0 |
| | Temp = 1000°C | | | | | Temp = 1000°C | | | | | Temp = 1000°C | | | |
| $CO_2$ | 0.169 | 0.135 | 0.097 | 0.054 | $CO_2$ | 0.261 | 0.230 | 0.193 | 0.152 | $CO_2$ | 0.360 | 0.331 | 0.296 | 0.257 |
| CO | 0.531 | 0.665 | 0.803 | 0.946 | CO | 0.439 | 0.570 | 0.707 | 0.848 | CO | 0.340 | 0.469 | 0.604 | 0.743 |
| $CH_4$ | 0 | 0 | 0 | 0 | $CH_4$ | 0 | 0 | 0 | 0 | $CH_4$ | 0 | 0 | 0 | 0 |
| C | 0.3 | 0.2 | 0.1 | 0 | C | 0.3 | 0.2 | 0.1 | 0 | C | 0.3 | 0.2 | 0.1 | 0 |

corn cob than rice husk for similar gasifying conditions. This result is attributed to higher oxygen content of corn cob, in addition to almost similar carbon content of rice husk and corn cob. Greater amount of oxygen available in corn cob increases the fraction of hydrogen appearing in the form of $H_2O$.

(C) Biomass: Corn Cob

| Species | AIR RATIO = 0.2 | | | | Species | AIR RATIO = 0.3 | | | | Species | AIR RATIO = 0.4 | | | |
|---|---|---|---|---|---|---|---|---|---|---|---|---|---|---|
| | % Carbon Conversion | | | | | % Carbon Conversion | | | | | % Carbon Conversion | | | |
| | 70% | 80% | 90% | 100% | | 70% | 80% | 90% | 100% | | 70% | 80% | 90% | 100% |
| | Temp = 700°C | | | | | Temp = 700°C | | | | | Temp = 700°C | | | |
| $CO_2$ | 0.367 | 0.351 | 0.325 | 0.368 | $CO_2$ | 0.444 | 0.437 | 0.418 | 0.39 | $CO_2$ | 0.516 | 0.519 | 0.51 | 0.488 |
| CO | 0.331 | 0.444 | 0.564 | 0.622 | CO | 0.256 | 0.361 | 0.478 | 0.603 | CO | 0.184 | 0.28 | 0.389 | 0.509 |
| $CH_4$ | 0.004 | 0.007 | 0.012 | 0.01 | $CH_4$ | 0.001 | 0.002 | 0.004 | 0.007 | $CH_4$ | 0 | 0.001 | 0.001 | 0.002 |
| C | 0.3 | 0.2 | 0.1 | 0 | C | 0.3 | 0.2 | 0.1 | 0 | C | 0.3 | 0.2 | 0.1 | 0 |
| | Temp = 800°C | | | | | Temp = 800°C | | | | | Temp = 800°C | | | |
| $CO_2$ | 0.325 | 0.306 | 0.279 | 0.319 | $CO_2$ | 0.403 | 0.392 | 0.371 | 0.341 | $CO_2$ | 0.481 | 0.476 | 0.462 | 0.438 |
| CO | 0.375 | 0.493 | 0.62 | 0.68 | CO | 0.297 | 0.408 | 0.529 | 0.658 | CO | 0.219 | 0.324 | 0.438 | 0.562 |
| $CH_4$ | 0 | 0 | 0.001 | 0.001 | $CH_4$ | 0 | 0 | 0 | 0 | $CH_4$ | 0 | 0 | 0 | 0 |
| C | 0.3 | 0.2 | 0.1 | 0 | C | 0.3 | 0.2 | 0.1 | 0 | C | 0.3 | 0.2 | 0.1 | 0 |
| | Temp = 900°C | | | | | Temp = 900°C | | | | | Temp = 900°C | | | |
| $CO_2$ | 0.292 | 0.273 | 0.247 | 0.284 | $CO_2$ | 0.370 | 0.356 | 0.334 | 0.305 | $CO_2$ | 0.451 | 0.441 | 0.423 | 0.398 |
| CO | 0.408 | 0.527 | 0.653 | 0.716 | CO | 0.330 | 0.444 | 0.566 | 0.695 | CO | 0.249 | 0.359 | 0.477 | 0.602 |
| $CH_4$ | 0 | 0 | 0 | 0 | $CH_4$ | 0 | 0 | 0 | 0 | $CH_4$ | 0 | 0 | 0 | 0 |
| C | 0.3 | 0.2 | 0.1 | 0 | C | 0.3 | 0.2 | 0.1 | 0 | C | 0.3 | 0.2 | 0.1 | 0 |
| | Temp = 1000°C | | | | | Temp = 1000°C | | | | | Temp = 1000°C | | | |
| $CO_2$ | 0.265 | 0.246 | 0.221 | 0.256 | $CO_2$ | 0.343 | 0.327 | 0.304 | 0.276 | $CO_2$ | 0.427 | 0.413 | 0.392 | 0.366 |
| CO | 0.435 | 0.554 | 0.679 | 0.744 | CO | 0.357 | 0.473 | 0.596 | 0.724 | CO | 0.273 | 0.387 | 0.508 | 0.634 |
| $CH_4$ | 0 | 0 | 0 | 0 | $CH_4$ | 0 | 0 | 0 | 0 | $CH_4$ | 0 | 0 | 0 | 0 |
| C | 0.3 | 0.2 | 0.1 | 0 | C | 0.3 | 0.2 | 0.1 | 0 | C | 0.3 | 0.2 | 0.1 | 0 |

### 6.3.3 Formulation and Comparison of Correlations

The constants in the 8 correlations for performance parameters were evaluated using software Polymath (Ver 6.0), and the expressions for the correlations are given in Table 6.8. Also listed in Table 6.8 are the values of statistical indicators $R^2$, $R_{msd}$ and $s^2$ for each correlation. A comparison of statistical indicators of various linear and non–linear correlations for any performance parameter reveals that linear correlations are not best fit for LHV, Y and $X_{CO}$. The non–linear correlations have much higher $R^2$ and low $s^2$ and $R_{msd}$. On the other hand, for $X_{CO2}$, even linear correlations 2 and 3 have $R^2$ values comparable to the non–linear models. To corroborate this analysis further, we have shown parity plots between model data for single biomass and prediction of 8 correlations in Figures 6.1 to 6.4.

Next, we have compared the predictions of correlations with experimental data. The results of this analysis are given in Tables 6.9, 6.10, 6.11 and 6.12, for LHV, Y, $X_{CO}$ and $X_{CO2}$ respectively. Also given in these tables are values of AAE and $R^2$ for each correlation. The parity plots between experimental data and predictions of correlations for LHV, Y, $X_{CO}$

**Table 6.7:** Fractional distribution of hydrogen among various species in producer gas

(A) Biomass: Rice Husk

| Species | AIR RATIO = 0.2 | | | | Species | AIR RATIO = 0.3 | | | | Species | AIR RATIO = 0.4 | | | |
|---|---|---|---|---|---|---|---|---|---|---|---|---|---|---|
| | % Carbon Conversion | | | | | % Carbon Conversion | | | | | % Carbon Conversion | | | |
| | 70% | 80% | 90% | 100% | | 70% | 80% | 90% | 100% | | 70% | 80% | 90% | 100% |
| | Temp = 700°C | | | | | Temp = 700°C | | | | | Temp = 700°C | | | |
| $H_2$ | 0.627 | 0.695 | 0.747 | 0.782 | $H_2$ | 0.518 | 0.602 | 0.671 | 0.728 | $H_2$ | 0.398 | 0.495 | 0.577 | 0.649 |
| $H_2O$ | 0.366 | 0.291 | 0.227 | 0.173 | $H_2O$ | 0.48 | 0.394 | 0.32 | 0.255 | $H_2O$ | 0.601 | 0.504 | 0.42 | 0.346 |
| $CH_4$ | 0.007 | 0.014 | 0.026 | 0.045 | $CH_4$ | 0.002 | 0.004 | 0.009 | 0.016 | $CH_4$ | 0 | 0.001 | 0.003 | 0.006 |
| | Temp = 800°C | | | | | Temp = 800°C | | | | | Temp = 800°C | | | |
| $H_2$ | 0.596 | 0.672 | 0.74 | 0.8 | $H_2$ | 0.480 | 0.564 | 0.638 | 0.705 | $H_2$ | 0.363 | 0.454 | 0.535 | 0.608 |
| $H_2O$ | 0.403 | 0.327 | 0.258 | 0.197 | $H_2O$ | 0.520 | 0.436 | 0.361 | 0.294 | $H_2O$ | 0.637 | 0.546 | 0.465 | 0.392 |
| $CH_4$ | 0 | 0.001 | 0.002 | 0.003 | $CH_4$ | 0 | 0 | 0.001 | 0.001 | $CH_4$ | 0 | 0 | 0 | 0 |
| | Temp = 900°C | | | | | Temp = 900°C | | | | | Temp = 900°C | | | |
| $H_2$ | 0.566 | 0.642 | 0.713 | 0.778 | $H_2$ | 0.448 | 0.529 | 0.604 | 0.673 | $H_2$ | 0.333 | 0.42 | 0.498 | 0.57 |
| $H_2O$ | 0.434 | 0.358 | 0.287 | 0.222 | $H_2O$ | 0.552 | 0.471 | 0.396 | 0.327 | $H_2O$ | 0.667 | 0.58 | 0.502 | 0.429 |
| $CH_4$ | 0 | 0 | 0 | 0 | $CH_4$ | 0 | 0 | 0 | 0 | $CH_4$ | 0 | 0 | 0 | 0 |
| | Temp = 1000°C | | | | | Temp = 1000°C | | | | | Temp = 1000°C | | | |
| $H_2$ | 0.54 | 0.617 | 0.689 | 0.758 | $H_2$ | 0.422 | 0.501 | 0.576 | 0.646 | $H_2$ | 0.309 | 0.391 | 0.467 | 0.54 |
| $H_2O$ | 0.46 | 0.382 | 0.311 | 0.242 | $H_2O$ | 0.578 | 0.498 | 0.424 | 0.354 | $H_2O$ | 0.691 | 0.609 | 0.533 | 0.46 |
| $CH_4$ | 0 | 0 | 0 | 0 | $CH_4$ | 0 | 0 | 0 | 0 | $CH_4$ | 0 | 0 | 0 | 0 |

(B) Biomass: Saw Dust

| Species | AIR RATIO = 0.2 | | | | Species | AIR RATIO = 0.3 | | | | Species | AIR RATIO = 0.4 | | | |
|---|---|---|---|---|---|---|---|---|---|---|---|---|---|---|
| | % Carbon Conversion | | | | | % Carbon Conversion | | | | | % Carbon Conversion | | | |
| | 70% | 80% | 90% | 100% | | 70% | 80% | 90% | 100% | | 70% | 80% | 90% | 100% |
| | Temp = 700°C | | | | | Temp = 700°C | | | | | Temp = 700°C | | | |
| $H_2$ | 0.736 | 0.789 | 0.804 | 0.804 | $H_2$ | 0.621 | 0.706 | 0.77 | 0.812 | $H_2$ | 0.484 | 0.59 | 0.676 | 0.744 |
| $H_2O$ | 0.245 | 0.171 | 0.142 | 0.142 | $H_2O$ | 0.375 | 0.283 | 0.208 | 0.147 | $H_2O$ | 0.516 | 0.407 | 0.318 | 0.243 |
| $CH_4$ | 0.018 | 0.039 | 0.053 | 0.053 | $CH_4$ | 0.004 | 0.01 | 0.021 | 0.041 | $CH_4$ | 0.001 | 0.002 | 0.006 | 0.013 |
| | Temp = 800°C | | | | | Temp = 800°C | | | | | Temp = 800°C | | | |
| $H_2$ | 0.716 | 0.798 | 0.866 | 0.918 | $H_2$ | 0.578 | 0.671 | 0.752 | 0.821 | $H_2$ | 0.437 | 0.541 | 0.631 | 0.71 |
| $H_2O$ | 0.283 | 0.2 | 0.128 | 0.066 | $H_2O$ | 0.422 | 0.328 | 0.247 | 0.176 | $H_2O$ | 0.563 | 0.459 | 0.368 | 0.289 |
| $CH_4$ | 0.001 | 0.003 | 0.006 | 0.016 | $CH_4$ | 0 | 0.001 | 0.001 | 0.003 | $CH_4$ | 0 | 0 | 0 | 0.001 |
| | Temp = 900°C | | | | | Temp = 900°C | | | | | Temp = 900°C | | | |
| $H_2$ | 0.685 | 0.773 | 0.852 | 0.923 | $H_2$ | 0.540 | 0.634 | 0.719 | 0.796 | $H_2$ | 0.399 | 0.499 | 0.59 | 0.672 |
| $H_2O$ | 0.315 | 0.227 | 0.147 | 0.076 | $H_2O$ | 0.460 | 0.366 | 0.281 | 0.204 | $H_2O$ | 0.601 | 0.501 | 0.41 | 0.328 |
| $CH_4$ | 0 | 0 | 0.001 | 0.002 | $CH_4$ | 0 | 0 | 0 | 0 | $CH_4$ | 0 | 0 | 0 | 0 |
| | Temp = 1000°C | | | | | Temp = 1000°C | | | | | Temp = 1000°C | | | |
| $H_2$ | 0.659 | 0.751 | 0.836 | 0.914 | $H_2$ | 0.508 | 0.604 | 0.691 | 0.773 | $H_2$ | 0.367 | 0.465 | 0.556 | 0.639 |
| $H_2O$ | 0.341 | 0.249 | 0.164 | 0.085 | $H_2O$ | 0.492 | 0.396 | 0.309 | 0.227 | $H_2O$ | 0.633 | 0.535 | 0.444 | 0.36 |
| $CH_4$ | 0 | 0 | 0 | 0 | $CH_4$ | 0 | 0 | 0 | 0 | $CH_4$ | 0 | 0 | 0 | 0 |

and $X_{CO2}$ are given in Figures 6.5, 6.6, 6.7 and 6.8 respectively. For convenience of the reader the values of AAE and $R^2$ for each plot is also given in Figure caption. The best correlation for any parameter is with the highest (absolute) $R^2$ value and least AAE. It should be noted that least value of AAE and highest (absolute) value of $R^2$ may not occur for same correlation. In such cases, we have preferred the correlation with least AAE that gives best prediction than one with the highest $R^2$ that gives best fit. On the basis of this criteria, we

(C) Biomass: Corn Cob

| Species | AIR RATIO = 0.2 | | | | Species | AIR RATIO = 0.3 | | | | Species | AIR RATIO = 0.4 | | | |
|---|---|---|---|---|---|---|---|---|---|---|---|---|---|---|
| | % Carbon Conversion | | | | | % Carbon Conversion | | | | | % Carbon Conversion | | | |
| | 70% | 80% | 90% | 100% | | 70% | 80% | 90% | 100% | | 70% | 80% | 90% | 100% |
| | Temp = 700°C | | | | | Temp = 700°C | | | | | Temp = 700°C | | | |
| $H_2$ | 0.593 | 0.667 | 0.724 | 0.719 | $H_2$ | 0.485 | 0.573 | 0.647 | 0.707 | $H_2$ | 0.368 | 0.468 | 0.554 | 0.627 |
| $H_2O$ | 0.402 | 0.323 | 0.255 | 0.26 | $H_2O$ | 0.514 | 0.424 | 0.346 | 0.279 | $H_2O$ | 0.632 | 0.531 | 0.444 | 0.368 |
| $CH_4$ | 0.005 | 0.011 | 0.02 | 0.02 | $CH_4$ | 0.001 | 0.003 | 0.007 | 0.013 | $CH_4$ | 0 | 0.001 | 0.002 | 0.005 |
| | Temp = 800°C | | | | | Temp = 800°C | | | | | Temp = 800°C | | | |
| $H_2$ | 0.559 | 0.638 | 0.708 | 0.7 | $H_2$ | 0.447 | 0.533 | 0.61 | 0.678 | $H_2$ | 0.334 | 0.427 | 0.51 | 0.585 |
| $H_2O$ | 0.441 | 0.361 | 0.29 | 0.299 | $H_2O$ | 0.553 | 0.466 | 0.389 | 0.321 | $H_2O$ | 0.666 | 0.573 | 0.489 | 0.415 |
| $CH_4$ | 0 | 0.001 | 0.001 | 0.001 | $CH_4$ | 0 | 0 | 0 | 0.001 | $CH_4$ | 0 | 0 | 0 | 0 |
| | Temp = 900°C | | | | | Temp = 900°C | | | | | Temp = 900°C | | | |
| $H_2$ | 0.527 | 0.606 | 0.678 | 0.667 | $H_2$ | 0.415 | 0.499 | 0.575 | 0.644 | $H_2$ | 0.305 | 0.393 | 0.473 | 0.546 |
| $H_2O$ | 0.473 | 0.394 | 0.321 | 0.332 | $H_2O$ | 0.585 | 0.501 | 0.425 | 0.355 | $H_2O$ | 0.695 | 0.607 | 0.527 | 0.454 |
| $CH_4$ | 0 | 0 | 0 | 0 | $CH_4$ | 0 | 0 | 0 | 0 | $CH_4$ | 0 | 0 | 0 | 0 |
| | Temp = 1000°C | | | | | Temp = 1000°C | | | | | Temp = 1000°C | | | |
| $H_2$ | 0.501 | 0.58 | 0.653 | 0.64 | $H_2$ | 0.389 | 0.47 | 0.546 | 0.616 | $H_2$ | 0.281 | 0.365 | 0.443 | 0.515 |
| $H_2O$ | 0.499 | 0.42 | 0.347 | 0.36 | $H_2O$ | 0.611 | 0.53 | 0.454 | 0.384 | $H_2O$ | 0.719 | 0.635 | 0.557 | 0.485 |
| $CH_4$ | 0 | 0 | 0 | 0 | $CH_4$ | 0 | 0 | 0 | 0 | $CH_4$ | 0 | 0 | 0 | 0 |

select correlation 7 for LHV, correlation 4 for Y, correlation 7 for $X_{CO}$ and correlation 3 for $X_{CO2}$. These correlations are listed below:

$$\mathrm{LHV} = 0.936(\mathrm{Temp})^{0.114}(\mathrm{AR})^{-0.796}(\mathrm{H/C})^{-0.142} \tag{6.22}$$

$$\mathrm{Y} = -8.585\times10^{-10}(\mathrm{Temp})^{2.413} - 0.263(\mathrm{H/C})^{0.753} + 0.571(\mathrm{O/C})^{0.306} \tag{6.23}$$

$$X_{CO} = 1.56\times10^{-3}(\mathrm{Temp})^{0.636}(\mathrm{AR})^{-0.768}(\mathrm{H/C})^{-0.611} \tag{6.24}$$

$$X_{CO2} = -1.917\times10^{-6}(\mathrm{Temp}) + 0.316(\mathrm{AR}) + 0.0137(\mathrm{H/C}) \tag{6.25}$$

These correlations are able to predict the values of performance parameters within engineering accuracy of ±10–20%. An examination of the coefficients and exponents of variables in each correlation gives relative impact of the variables on the performance parameter. In the temperature range considered in our simulations, the net yield of producer gas and volume fraction of $CO_2$ in the producer gas are practically independent of temperature. This is evident from very low coefficient for temperature in the correlation for Y and $X_{CO2}$. The exponent for temperature in the correlation for LHV is also quite low, which indicates relative independence of LHV on the temperature of gasification. The principal variable affecting all performance parameters seems to be the air ratio. H/C ratio of fuel also

has marginal effect on all four parameters.

**Table 6.8:** Correlations for Performance of Biomass Gasifier

(A) Correlations for the LHV of producer gas

| Correlation Type | $R^2$ | $R_{msd}$ | $s^2$ |
|---|---|---|---|
| 1. $LHV = 6.289 \times 10^{-3} \times Temp + 4.463 \times (H/C) - 5.588 \times (O/C)$ | 0.362 | 0.0907 | 1.211 |
| 2. $LHV = 5.946 \times 10^{-3} \times Temp + 0.966 \times (H/C) - 2.147 \times (O/H)$ | –0.0848 | 0.118 | 2.06 |
| 3. $LHV = 6.432 \times 10^{-3} \times Temp - 10.793 \times (AR) + 1.518 \times (H/C)$ | 0.334 | 0.0927 | 1.264 |
| 4. $LHV = 0.255 \times Temp^{0.299} + 20.571 \times (H/C)^{0.259} - 16.689 \times (O/C)^{0.528}$ | 0.774 | 0.054 | 0.438 |
| 5. $LHV = 1.6 \times Temp^{0.14} + 66.788 \times (H/C)^{-0.072} - 64.965 \times (O/H)^{0.172}$ | 0.770 | 0.0544 | 0.445 |
| 6. $LHV = 0.306 \times Temp^{0.281} - 16.08 \times (AR)^{0.476} + 12.506 \times (H/C)^{-0.058}$ | 0.777 | 0.0536 | 0.432 |
| 7. $LHV = 0.936 \times (Temp)^{0.114} \times (AR)^{-0.796} \times (H/C)^{-0.142}$ | 0.767 | 0.0548 | 0.445 |
| 8. $LHV = 2.588 \times (Temp)^{0.114} \times (H/C)^{-15.281} \times (O/C)^{14.451} \times (O/H)^{-16.498}$ | 0.765 | 0.055 | 0.452 |

(B) Correlations for the producer gas yield per 100 g biomass

| Correlation Type | $R^2$ | $R_{msd}$ | $s^2$ |
|---|---|---|---|
| 1. $Y = 1.914 \times 10^{-4} \times Temp - 0.132 \times (H/C) + 0.196 \times (O/C)$ | 0.081 | 0.00322 | 0.00152 |
| 2. $Y = 1.241 \times 10^{-5} \times Temp - 2.949 \times 10^{-2} \times (H/C) + 0.317 \times (O/H)$ | 0.748 | 0.00168 | 0.000416 |
| 3. $Y = 1.83 \times 10^{-4} \times Temp + 0.395 \times (AR) - 0.03 \times (H/C)$ | 0.103 | 0.00318 | 0.00149 |
| 4. $Y = -8.585 \times 10^{-10} \times Temp^{2.413} - 0.263 \times (H/C)^{0.753} + 0.571 \times (O/C)^{0.306}$ | 0.806 | 0.00148 | 0.000328 |
| 5. $Y = -4.245 \times 10^{-6} \times Temp^{1.249} - 2.792 \times 10^{-12} \times (H/C)^{32.319} + 0.302 \times (O/H)^{0.73}$ | 0.813 | 0.00145 | 0.000317 |
| 6. $Y = 0.429 \times Temp^{-0.153} + 0.253 \times (AR)^{0.693} - 3.352 \times 10^{-13} \times (H/C)^{35.999}$ | 0.805 | 0.00148 | 0.00033 |
| 7. $Y = 1.06 \times (Temp)^{-0.104} \times (AR)^{0.337} \times (H/C)^{-0.759}$ | 0.79 | 0.00154 | 0.00035 |
| 8. $Y = 0.678 \times (Temp)^{-0.104} \times (H/C)^{16.498} \times (O/C)^{-16.933} \times (O/H)^{17.789}$ | 0.805 | 0.00148 | 0.000328 |

(C) Correlations for the volume fraction of carbon monoxide in the producer gas

| Correlation Type | $R^2$ | $R_{msd}$ | $s^2$ |
|---|---|---|---|
| 1. $X_{CO} = 3.889 \times 10^{-4} \times Temp + 0.117 \times (H/C) - 0.222 \times (O/C)$ | 0.394 | 0.00443 | 0.00289 |
| 2. $X_{CO} = 3.763 \times 10^{-4} \times Temp - 0.0217 \times (H/C) - 0.0865 \times (O/H)$ | 0.114 | 0.00535 | 0.00422 |
| 3. $X_{CO} = 3.945 \times 10^{-4} \times Temp - 0.428 \times (AR) + 9.76 \times 10^{-5} \times (H/C)$ | 0.376 | 0.0045 | 0.00297 |
| 4. $X_{CO} = 8.397 \times 10^{-2} \times Temp^{0.269} + 2.107 \times (H/C)^{0.065} - 2.322 \times (O/C)^{0.175}$ | 0.663 | 0.0033 | 0.00164 |
| 5. $X_{CO} = 0.416 \times Temp^{0.135} - 7.562 \times 10^{-7} \times (H/C)^{16.414} - 0.840 \times (O/H)^{0.576}$ | 0.666 | 0.0033 | 0.00162 |
| 6. $X_{CO} = 1.521 \times 10^{-3} \times Temp^{0.719} - 0.6 \times (AR)^{0.6} + 0.404 \times (H/C)^{-0.413}$ | 0.659 | 0.0033 | 0.00166 |
| 7. $X_{CO} = 1.56 \times 10^{-3} \times (Temp)^{0.636} \times (AR)^{-0.768} \times (H/C)^{-0.611}$ | 0.656 | 0.0033 | 0.00165 |
| 8. $X_{CO} = 4.17 \times 10^{-3} \times (Temp)^{0.636} \times (H/C)^{-15.117} \times (O/C)^{13.851} \times (O/H)^{-15.794}$ | 0.655 | 0.0033 | 0.00169 |

(D) Correlations for the volume fraction of carbon dioxide in the producer gas

| Correlation Type | $R^2$ | $R_{msd}$ | $s^2$ |
|---|---|---|---|
| 1. $X_{CO2} = 9.686\times10^{-6} \times \text{Temp} - 0.0591 \times (\text{H/C}) + 0.143 \times (\text{O/C})$ | 0.109 | 0.00276 | 0.00112 |
| 2. $X_{CO2} = -1.048\times10^{-4} \times \text{Temp} + 0.0176 \times (\text{H/C}) + 0.211 \times (\text{O/H})$ | 0.414 | 0.00224 | 0.000738 |
| 3. $X_{CO2} = -1.917\times10^{-6} \times \text{Temp} + 0.316 \times (\text{AR}) + 0.0137 \times (\text{H/C})$ | 0.224 | 0.00258 | 0.000977 |
| 4. $X_{CO2} = -5.538\times10^{-6}\times\text{Temp}^{-3.863} - 0.0471\times(\text{H/C})^{1.314} + 0.167\times(\text{O/C})^{0.734}$ | 0.274 | 0.0249 | 0.000935 |
| 5. $X_{CO2} = -1.678\times10^{-4}\times\text{Temp}^{0.954} + 7.7\times10^{-32}\times(\text{H/C})^{94} + 0.248\times(\text{O/H})^{0.886}$ | 0.488 | 0.0021 | 0.000659 |
| 6. $X_{CO2} = -6.315\times10^{-6}\times\text{Temp}^{1.384} + 0.296\times(\text{AR})^{0.374} + 2.379\times(\text{H/C})^{-13.549}$ | 0.494 | 0.00208 | 0.000652 |
| 7. $X_{CO2} = 1.158\times(\text{Temp})^{-0.205}\times(\text{AR})^{0.567}\times(\text{H/C})^{-0.321}$ | 0.41 | 0.00225 | 0.000748 |
| 8. $X_{CO2} = 1.421\times(\text{Temp})^{-0.347}\times(\text{H/C})^{-14.758}\times(\text{O/C})^{14.92}\times(\text{O/H})^{-13.612}$ | 0.368 | 0.00233 | 0.000806 |

### 6.3.4 Limitation of Our Correlations

With air being considered to be the gasification medium, the range of H/C ratio for the gasification mixture in our simulations is 1.4 – 2.1. Use of mixture of air–steam as gasification medium gives much higher H/C ratios (> 5) for which our correlations may not give good predictions with reasonable accuracy. Moreover, if gasifying air is mixed with some other gas (e.g. $CO_2$), one needs to make proper calculations of the elemental ratios in the biomass mixture to account for the additional species. The correlations may also give larger error for values of other two variables beyond the range considered in this study, i.e. AR > 0.4 and temperature < 700°C. However, these operating conditions are not typical of normal gasification process. Most of the commercial gasifiers are designed and operated in the range of air ratio and temperature considered in this study. Therefore, we do not anticipate this to be a serious limitation of our correlations. Finally, our correlations may not hold good for gasification operations at elevated pressures, as we have considered atmospheric conditions for the thermodynamic simulations.

**Table 6.9:** Comparative analysis of the predicted values of LHV of producer gas using different correlations with experimental data reported in literature

| Reference | Temp (°C) | AR | H/C | O/C | O/H | LHV (exp) MJ/Nm$^3$ | LHV (calc) MJ/Nm$^3$ | | | | | | | |
|---|---|---|---|---|---|---|---|---|---|---|---|---|---|---|
| | | | | | | | CR - 1 | CR - 2 | CR - 3 | CR - 4 | CR - 5 | CR - 6 | CR - 7 | CR - 8 |
| **Narvaez et al. [10] Biomass: Pine saw dust** | 670 | 0.32 | 2.2 | 1.6 | 0.7 | 4.30 | 5.09 | 4.54 | 4.20 | 5.63 | 5.53 | 4.50 | **4.35** | 5.10 |
| | 800 | 0.37 | 2.1 | 1.6 | 0.8 | 4.60 | 5.46 | 5.15 | 4.34 | 5.42 | 5.42 | 3.97 | **3.98** | 5.45 |
| | 810 | 0.47 | 2.2 | 1.9 | 0.9 | 3.70 | 4.30 | 5.10 | 3.48 | 3.70 | 3.88 | 2.73 | **3.28** | 4.18 |
| | 800 | 0.26 | 2.1 | 1.5 | 0.7 | 4.60 | 6.02 | 5.26 | 5.53 | 6.14 | 6.14 | 5.51 | **5.28** | 6.59 |
| | 790 | 0.36 | 2.3 | 1.7 | 0.7 | 4.60 | 5.73 | 5.33 | 4.69 | 5.31 | 5.28 | 4.03 | **4.01** | 5.05 |
| | 800 | 0.32 | 2 | 1.5 | 0.8 | 6.30 | 5.58 | 5.08 | 4.73 | 5.82 | 5.78 | 4.67 | **4.50** | 5.62 |
| **Mansaray et al. [6] Biomass: Rice husk** | 665 | 0.25 | 2.08 | 1.4 | 0.7 | 5.03 | 5.44 | 4.48 | 4.74 | 6.43 | 6.35 | 5.57 | **5.34** | 6.29 |
| | 742 | 0.3 | 2.08 | 1.5 | 0.7 | 3.83 | 5.32 | 4.83 | 4.70 | 5.71 | 5.66 | 4.88 | **4.67** | 5.54 |
| | 810 | 0.35 | 2.08 | 1.7 | 0.8 | 3.28 | 5.15 | 5.12 | 4.60 | 5.00 | 4.99 | 4.24 | **4.17** | 4.81 |
| | 669 | 0.25 | 2.08 | 1.4 | 0.7 | 4.38 | 5.46 | 4.51 | 4.77 | 6.43 | 6.36 | 5.58 | **5.34** | 6.29 |
| | 750 | 0.3 | 2.08 | 1.5 | 0.7 | 3.54 | 5.37 | 4.88 | 4.75 | 5.71 | 5.67 | 4.89 | **4.68** | 5.55 |
| | 821 | 0.35 | 2.08 | 1.7 | 0.8 | 3.15 | 5.22 | 5.19 | 4.67 | 5.01 | 5.00 | 4.25 | **4.18** | 4.82 |
| | 700 | 0.25 | 2.08 | 1.4 | 0.7 | 3.75 | 5.66 | 4.69 | 4.97 | 6.45 | 6.38 | 5.60 | **5.37** | 6.32 |
| | 766 | 0.3 | 2.08 | 1.5 | 0.7 | 3.26 | 5.47 | 4.97 | 4.85 | 5.72 | 5.68 | 4.90 | **4.69** | 5.56 |
| | 827 | 0.35 | 2.08 | 1.7 | 0.8 | 3.09 | 5.26 | 5.23 | 4.70 | 5.01 | 5.00 | 4.25 | **4.18** | 4.82 |
| **Jiang and Morey [11] Biomass: Corn cob** | 648 | 0.29 | 2.05 | 1.7 | 0.8 | 4.95 | 3.96 | 4.09 | 4.11 | 4.75 | 4.74 | 4.92 | **4.70** | 4.57 |
| | 649 | 0.29 | 2.05 | 1.7 | 0.8 | 5.03 | 3.97 | 4.10 | 4.11 | 4.75 | 4.75 | 4.91 | **4.69** | 4.58 |
| | 776 | 0.43 | 2.05 | 1.9 | 0.9 | 3.97 | 3.25 | 4.57 | 3.42 | 3.03 | 3.18 | 3.18 | **3.51** | 3.41 |
| | 778 | 0.44 | 2.05 | 1.9 | 0.9 | 4.01 | 3.23 | 4.58 | 3.40 | 2.99 | 3.15 | 3.14 | **3.49** | 3.39 |
| | 779 | 0.42 | 2.05 | 1.9 | 0.9 | 4.02 | 3.43 | 4.62 | 3.60 | 3.22 | 3.35 | 3.36 | **3.61** | 3.51 |
| | | | | | **AAE (%)** | | 32.46 | 26.52 | 21.47 | 34.49 | 33.63 | 23.46 | **19.66** | 31.86 |
| | | | | | **Correlation Coeff ($R^2$)** | | 0.203 | 0.203 | 0.248 | 0.0354 | -0.301 | 0.0364 | **0.248** | 0.21 |

**Table 6.10:** Comparative analysis of the predicted values of producer gas yield using different correlations with experimental data reported in literature

| Reference | Temp (°C) | AR | H/C | O/C | O/H | Y (exp) $Nm^3/100g$ biomass | Y (calc) $Nm^3/100g$ biomass | | | | | | | |
|---|---|---|---|---|---|---|---|---|---|---|---|---|---|---|
| | | | | | | | CR - 1 | CR - 2 | CR - 3 | CR - 4 | CR - 5 | CR - 6 | CR - 7 | CR - 8 |
| Narvaez et al. [10] Biomass: Pine saw dust | 670 | 0.32 | 2.2 | 1.6 | 0.7 | 0.23 | 0.18 | -0.10 | -0.44 | **0.15** | 0.17 | 0.18 | 0.20 | 0.20 |
| | 800 | 0.37 | 2.1 | 1.6 | 0.8 | 0.25 | 0.19 | 0.16 | 0.15 | **0.19** | 0.19 | 0.23 | 0.22 | 0.19 |
| | 810 | 0.47 | 2.2 | 1.9 | 0.9 | 0.25 | 0.21 | -0.07 | -0.41 | **0.24** | 0.22 | 0.27 | 0.23 | 0.20 |
| | 800 | 0.26 | 2.1 | 1.5 | 0.7 | 0.21 | 0.18 | 0.14 | 0.12 | **0.17** | 0.17 | 0.19 | 0.19 | 0.16 |
| | 790 | 0.36 | 2.3 | 1.7 | 0.7 | 0.24 | 0.17 | -1.14 | -3.25 | **0.18** | 0.18 | 0.22 | 0.20 | 0.19 |
| | 800 | 0.32 | 2 | 1.5 | 0.8 | 0.21 | 0.19 | 0.21 | 0.25 | **0.18** | 0.19 | 0.21 | 0.21 | 0.20 |
| Mansaray et al. [6] Biomass: Rice husk | 665 | 0.25 | 2.08 | 1.4 | 0.7 | 0.15 | 0.18 | 0.16 | 0.15 | **0.13** | 0.17 | 0.16 | 0.19 | 0.18 |
| | 742 | 0.3 | 2.08 | 1.5 | 0.7 | 0.17 | 0.19 | 0.17 | 0.16 | **0.17** | 0.18 | 0.19 | 0.20 | 0.19 |
| | 810 | 0.35 | 2.08 | 1.7 | 0.8 | 0.20 | 0.20 | 0.18 | 0.18 | **0.20** | 0.20 | 0.22 | 0.21 | 0.20 |
| | 669 | 0.25 | 2.08 | 1.4 | 0.7 | 0.15 | 0.18 | 0.16 | 0.15 | **0.13** | 0.17 | 0.16 | 0.19 | 0.18 |
| | 750 | 0.3 | 2.08 | 1.5 | 0.7 | 0.17 | 0.19 | 0.17 | 0.16 | **0.17** | 0.18 | 0.19 | 0.20 | 0.19 |
| | 821 | 0.35 | 2.08 | 1.7 | 0.8 | 0.20 | 0.20 | 0.18 | 0.17 | **0.21** | 0.20 | 0.23 | 0.21 | 0.20 |
| | 700 | 0.25 | 2.08 | 1.4 | 0.7 | 0.13 | 0.17 | 0.16 | 0.15 | **0.14** | 0.17 | 0.16 | 0.19 | 0.18 |
| | 766 | 0.3 | 2.08 | 1.5 | 0.7 | 0.15 | 0.19 | 0.17 | 0.16 | **0.17** | 0.18 | 0.20 | 0.20 | 0.19 |
| | 827 | 0.35 | 2.08 | 1.7 | 0.8 | 0.17 | 0.20 | 0.18 | 0.17 | **0.21** | 0.20 | 0.23 | 0.21 | 0.20 |
| Jiang and Morey [11] Biomass: Corn cob | 648 | 0.29 | 2.05 | 1.7 | 0.8 | 0.19 | 0.21 | 0.21 | 0.21 | **0.18** | 0.20 | 0.17 | 0.21 | 0.21 |
| | 649 | 0.29 | 2.05 | 1.7 | 0.8 | 0.19 | 0.21 | 0.21 | 0.21 | **0.18** | 0.20 | 0.17 | 0.21 | 0.21 |
| | 776 | 0.43 | 2.05 | 1.9 | 0.9 | 0.26 | 0.24 | 0.24 | 0.24 | **0.26** | 0.25 | 0.25 | 0.23 | 0.24 |
| | 778 | 0.44 | 2.05 | 1.9 | 0.9 | 0.26 | 0.24 | 0.24 | 0.24 | **0.26** | 0.25 | 0.25 | 0.23 | 0.24 |
| | 779 | 0.42 | 2.05 | 1.9 | 0.9 | 0.25 | 0.24 | 0.24 | 0.24 | **0.25** | 0.24 | 0.25 | 0.23 | 0.24 |
| | | | | | **AAE (%)** | | 14.77 | 52.20 | 111.09 | **10.51** | 12.66 | 11.75 | 16.74 | 15.96 |
| | | | | | **Correlation Coeff ($R^2$)** | | 0.583 | -0.243 | -0.266 | **0.746** | 0.674 | 0.78 | 0.74 | 0.531 |

**Table 6.11:** Comparative analysis of the predicted values of fraction of CO in producer gas using different correlations with experimental data reported in literature

| Reference | Temp (°C) | AR | H/C | O/C | O/H | $X_{CO}$ (exp) vol fraction | $X_{CO}$ (exp) vol fraction | | | | | | | |
|---|---|---|---|---|---|---|---|---|---|---|---|---|---|---|
| | | | | | | | CR - 1 | CR - 2 | CR - 3 | CR - 4 | CR - 5 | CR - 6 | CR - 7 | CR - 8 |
| Narvaez et al. [10] Biomass: Pine saw dust | 670 | 0.32 | 2.2 | 1.6 | 0.7 | 0.14 | 0.18 | -0.01 | 0.14 | 0.16 | 0.14 | 0.13 | **0.15** | 0.17 |
| | 800 | 0.37 | 2.1 | 1.6 | 0.8 | 0.13 | 0.20 | 0.16 | 0.14 | 0.20 | 0.19 | 0.16 | **0.15** | 0.20 |
| | 810 | 0.47 | 2.2 | 1.9 | 0.9 | 0.10 | 0.13 | -0.06 | 0.09 | 0.15 | 0.18 | 0.12 | **0.12** | 0.15 |
| | 800 | 0.26 | 2.1 | 1.5 | 0.7 | 0.13 | 0.23 | 0.19 | 0.21 | 0.22 | 0.19 | 0.20 | **0.20** | 0.24 |
| | 790 | 0.36 | 2.3 | 1.7 | 0.7 | 0.13 | 0.18 | -0.33 | 0.14 | 0.20 | 0.18 | 0.16 | **0.14** | 0.18 |
| | 800 | 0.32 | 2 | 1.5 | 0.8 | 0.18 | 0.22 | 0.25 | 0.18 | 0.21 | 0.19 | 0.18 | **0.17** | 0.21 |
| Mansaray et al. [6] Biomass: Rice husk | 665 | 0.25 | 2.08 | 1.4 | 0.7 | 0.20 | 0.22 | 0.19 | 0.19 | 0.18 | 0.15 | 0.16 | **0.18** | 0.21 |
| | 742 | 0.3 | 2.08 | 1.5 | 0.7 | 0.15 | 0.20 | 0.18 | 0.17 | 0.19 | 0.17 | 0.16 | **0.17** | 0.20 |
| | 810 | 0.35 | 2.08 | 1.7 | 0.8 | 0.13 | 0.18 | 0.16 | 0.16 | 0.19 | 0.19 | 0.17 | **0.16** | 0.18 |
| | 669 | 0.25 | 2.08 | 1.4 | 0.7 | 0.18 | 0.22 | 0.19 | 0.19 | 0.18 | 0.15 | 0.16 | **0.18** | 0.21 |
| | 750 | 0.3 | 2.08 | 1.5 | 0.7 | 0.14 | 0.20 | 0.18 | 0.17 | 0.19 | 0.17 | 0.17 | **0.17** | 0.20 |
| | 821 | 0.35 | 2.08 | 1.7 | 0.8 | 0.13 | 0.19 | 0.17 | 0.16 | 0.20 | 0.20 | 0.17 | **0.16** | 0.18 |
| | 700 | 0.25 | 2.08 | 1.4 | 0.7 | 0.15 | 0.23 | 0.20 | 0.20 | 0.20 | 0.16 | 0.17 | **0.19** | 0.22 |
| | 766 | 0.3 | 2.08 | 1.5 | 0.7 | 0.13 | 0.21 | 0.18 | 0.18 | 0.20 | 0.18 | 0.17 | **0.17** | 0.20 |
| | 827 | 0.35 | 2.08 | 1.7 | 0.8 | 0.12 | 0.19 | 0.17 | 0.16 | 0.20 | 0.20 | 0.18 | **0.16** | 0.18 |
| Jiang and Morey [11] Biomass: Corn cob | 648 | 0.29 | 2.05 | 1.7 | 0.8 | 0.14 | 0.15 | 0.16 | 0.16 | 0.12 | 0.13 | 0.13 | **0.16** | 0.16 |
| | 649 | 0.29 | 2.05 | 1.7 | 0.8 | 0.13 | 0.15 | 0.16 | 0.16 | 0.12 | 0.13 | 0.13 | **0.16** | 0.16 |
| | 776 | 0.43 | 2.05 | 1.9 | 0.9 | 0.14 | 0.11 | 0.11 | 0.11 | 0.11 | 0.17 | 0.12 | **0.13** | 0.13 |
| | 778 | 0.44 | 2.05 | 1.9 | 0.9 | 0.15 | 0.11 | 0.11 | 0.11 | 0.11 | 0.17 | 0.12 | **0.13** | 0.13 |
| | 779 | 0.42 | 2.05 | 1.9 | 0.9 | 0.15 | 0.11 | 0.12 | 0.12 | 0.12 | 0.17 | 0.13 | **0.14** | 0.13 |
| | | | | | **AAE (%)** | | 35.35 | 52.81 | 19.12 | 33.55 | 28.36 | 20.66 | **17.24** | 33.32 |
| | | | | | **Correlation Coeff ($R^2$)** | | 0.325 | 0.387 | 0.442 | 0.0329 | -0.404 | 0.0616 | **0.44** | 0.274 |

**Table 6.12:** Comparative analysis of the predicted values of fraction of $CO_2$ in producer gas using different correlations with experimental data reported in literature

| Reference | Temp (°C) | AR | H/C | O/C | O/H | $X_{CO2}$ (exp) vol fraction | $X_{CO2}$ (exp) vol fraction | | | | | | | |
|---|---|---|---|---|---|---|---|---|---|---|---|---|---|---|
| | | | | | | | CR - 1 | CR - 2 | CR - 3 | CR - 4 | CR - 5 | CR - 6 | CR - 7 | CR - 8 |
| Narvaez et al. [10] Biomass: Pine saw dust | 670 | 0.32 | 2.2 | 1.6 | 0.7 | 0.14 | 0.10 | 11.94 | **0.14** | 0.11 | 0.12 | 0.13 | 0.12 | 0.11 |
| | 800 | 0.37 | 2.1 | 1.6 | 0.8 | 0.15 | 0.11 | 0.24 | **0.14** | 0.11 | 0.11 | 0.14 | 0.13 | 0.11 |
| | 810 | 0.47 | 2.2 | 1.9 | 0.9 | 0.12 | 0.14 | 11.96 | **0.16** | 0.15 | 0.14 | 0.18 | 0.15 | 0.14 |
| | 800 | 0.26 | 2.1 | 1.5 | 0.7 | 0.15 | 0.10 | 0.23 | **0.11** | 0.10 | 0.10 | 0.11 | 0.11 | 0.11 |
| | 790 | 0.36 | 2.3 | 1.7 | 0.7 | 0.15 | 0.11 | 772.71 | **0.14** | 0.11 | 0.11 | 0.14 | 0.13 | 0.11 |
| | 800 | 0.32 | 2 | 1.5 | 0.8 | 0.14 | 0.11 | 0.09 | **0.13** | 0.10 | 0.11 | 0.13 | 0.12 | 0.11 |
| Mansaray et al. [6] Biomass: Rice husk | 665 | 0.25 | 2.08 | 1.4 | 0.7 | 0.14 | 0.10 | 0.17 | **0.13** | 0.09 | 0.11 | 0.11 | 0.11 | 0.10 |
| | 742 | 0.3 | 2.08 | 1.5 | 0.7 | 0.16 | 0.11 | 0.17 | **0.13** | 0.11 | 0.12 | 0.12 | 0.12 | 0.11 |
| | 810 | 0.35 | 2.08 | 1.7 | 0.8 | 0.17 | 0.12 | 0.17 | **0.13** | 0.12 | 0.12 | 0.14 | 0.13 | 0.12 |
| | 669 | 0.25 | 2.08 | 1.4 | 0.7 | 0.15 | 0.10 | 0.17 | **0.12** | 0.09 | 0.11 | 0.11 | 0.11 | 0.10 |
| | 750 | 0.3 | 2.08 | 1.5 | 0.7 | 0.16 | 0.11 | 0.17 | **0.13** | 0.11 | 0.11 | 0.12 | 0.12 | 0.11 |
| | 821 | 0.35 | 2.08 | 1.7 | 0.8 | 0.17 | 0.12 | 0.17 | **0.13** | 0.12 | 0.12 | 0.14 | 0.13 | 0.11 |
| | 700 | 0.25 | 2.08 | 1.4 | 0.7 | 0.15 | 0.10 | 0.16 | **0.12** | 0.09 | 0.11 | 0.11 | 0.11 | 0.10 |
| | 766 | 0.3 | 2.08 | 1.5 | 0.7 | 0.17 | 0.11 | 0.17 | **0.13** | 0.11 | 0.11 | 0.12 | 0.12 | 0.11 |
| | 827 | 0.35 | 2.08 | 1.7 | 0.8 | 0.17 | 0.12 | 0.17 | **0.13** | 0.12 | 0.12 | 0.14 | 0.13 | 0.11 |
| Jiang and Morey [11] Biomass: Corn cob | 648 | 0.29 | 2.05 | 1.7 | 0.8 | 0.17 | 0.12 | 0.14 | **0.14** | 0.12 | 0.14 | 0.12 | 0.12 | 0.13 |
| | 649 | 0.29 | 2.05 | 1.7 | 0.8 | 0.16 | 0.12 | 0.14 | **0.14** | 0.12 | 0.14 | 0.12 | 0.12 | 0.13 |
| | 776 | 0.43 | 2.05 | 1.9 | 0.9 | 0.12 | 0.15 | 0.15 | **0.15** | 0.16 | 0.15 | 0.16 | 0.15 | 0.15 |
| | 778 | 0.44 | 2.05 | 1.9 | 0.9 | 0.12 | 0.15 | 0.15 | **0.15** | 0.16 | 0.15 | 0.16 | 0.15 | 0.15 |
| | 779 | 0.42 | 2.05 | 1.9 | 0.9 | 0.13 | 0.15 | 0.15 | **0.15** | 0.16 | 0.15 | 0.16 | 0.14 | 0.14 |
| | | | | | **AAE (%)** | | 28.23 | 2.67E+04 | **18.48** | 30.54 | 24.03 | 23.26 | 21.95 | 26.25 |
| | | | | | **Correlation Coeff ($R^2$)** | | -0.468 | 0.002 | **-0.6** | -0.493 | -0.503 | -0.532 | -0.543 | -0.519 |

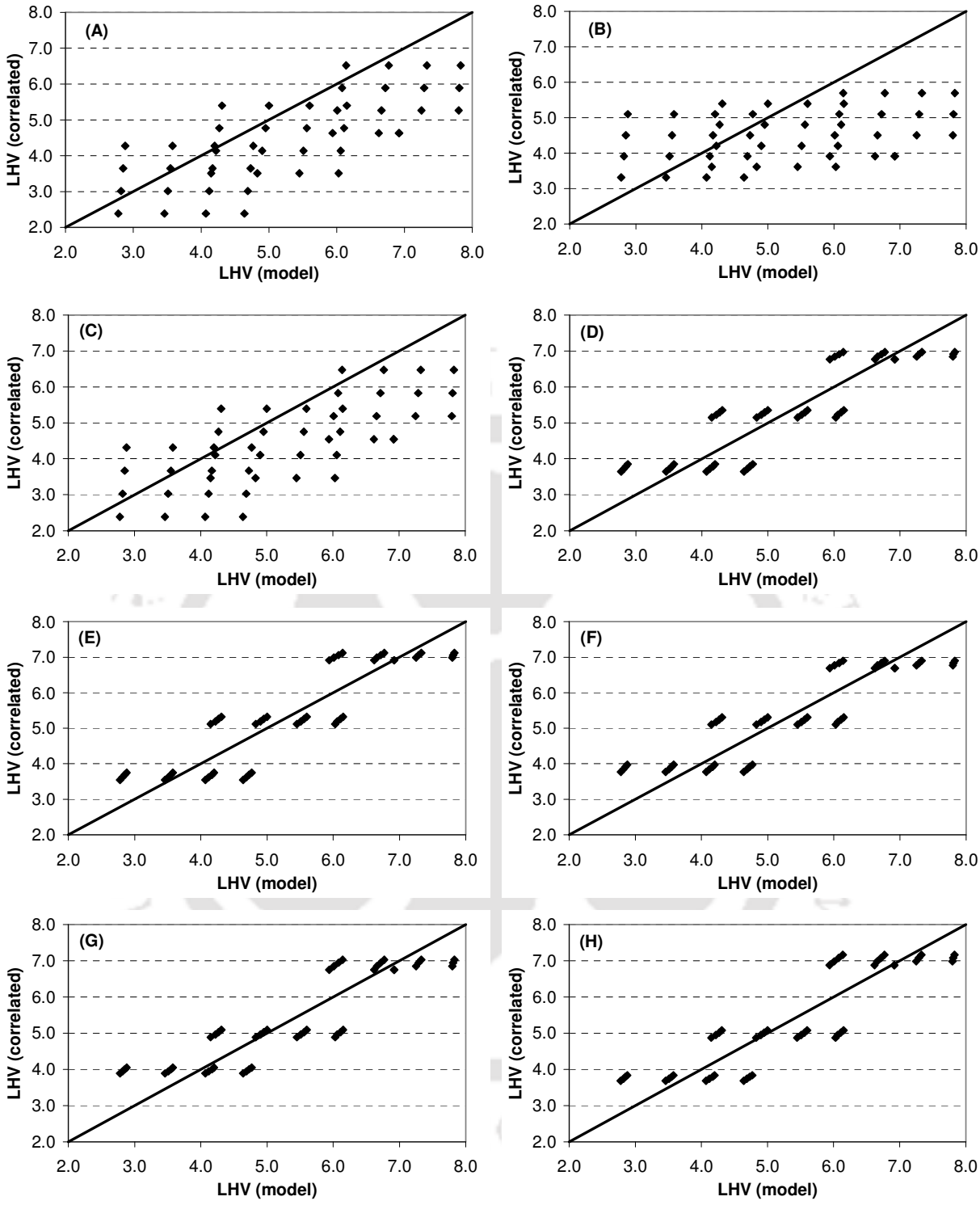


**Figure 6.1:** Comparative evaluation of linear and non–linear correlations for LHV (MJ/Nm$^3$) of producer gas. Parity plot of values predicted by the correlation and the values calculated with semi–equilibrium models (for saw dust as biomass). (A) Correlation 1; (B) Correlation 2; (C) Correlation 3; (D) Correlation 4; (E) Correlation 5; (F) Correlation 6; (G) Correlation 7; (H) Correlation 8. For details on correlations, refer to Table 6.8.

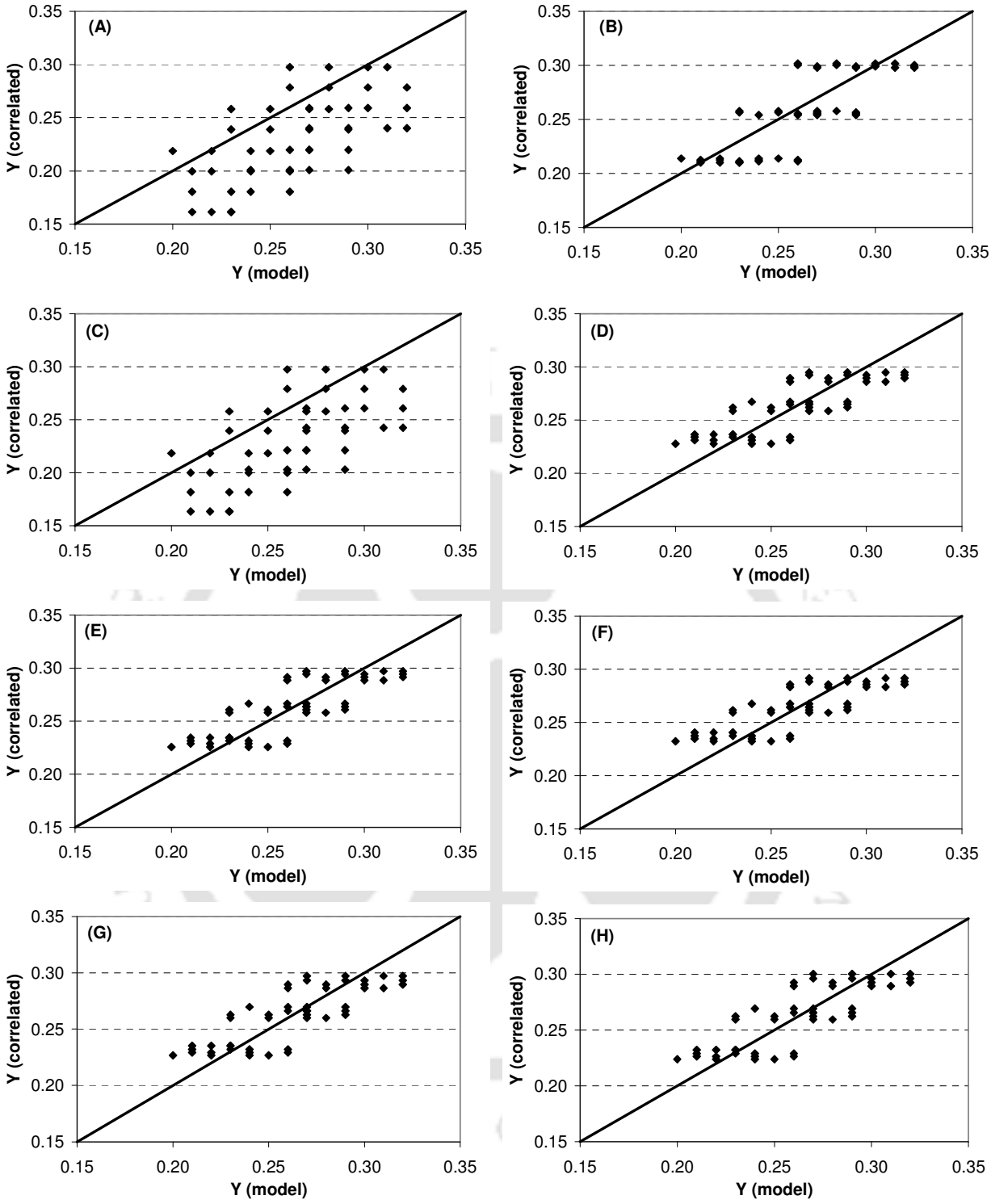


**Figure 6.2:** Comparative evaluation of linear and non–linear correlations for producer gas yield ($Nm^3$ per 100g biomass) of producer gas. Parity plot of values predicted by the correlation and the values calculated with semi–equilibrium models (for saw dust as biomass). (A) Correlation 1; (B) Correlation 2; (C) Correlation 3; (D) Correlation 4; (E) Correlation 5; (F) Correlation 6; (G) Correlation 7; (H) Correlation 8. For details on correlations, refer to Table 6.8.

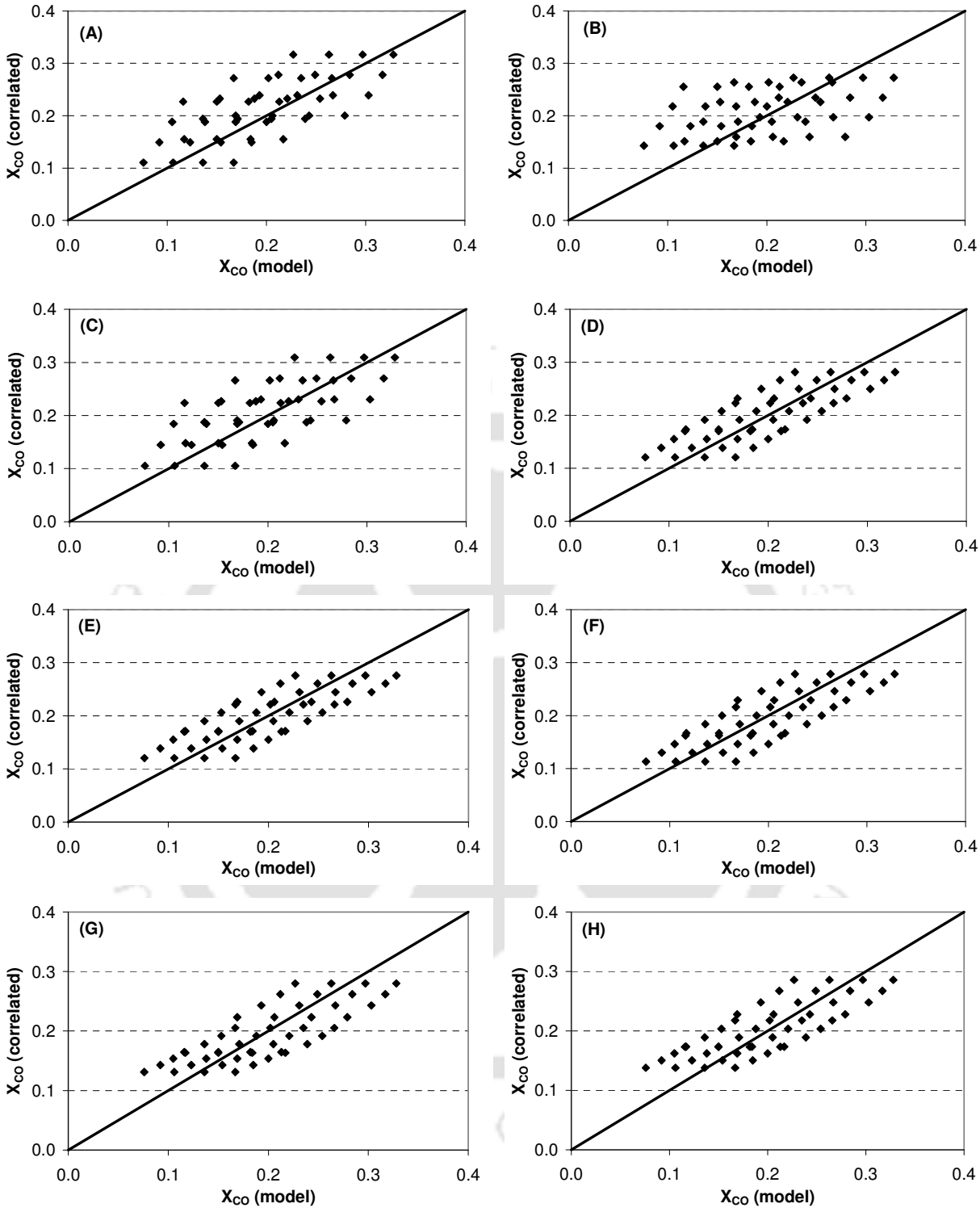


**Figure 6.3:** Comparative evaluation of linear and non–linear correlations for volume fraction of carbon monoxide in producer gas. Parity plot of values predicted by the correlation and the values calculated with semi–equilibrium models (for rice husk as biomass). (A) Correlation 1; (B) Correlation 2; (C) Correlation 3; (D) Correlation 4; (E) Correlation 5; (F) Correlation 6; (G) Correlation 7; (H) Correlation 8. For details on correlations, refer to Table 6.8.

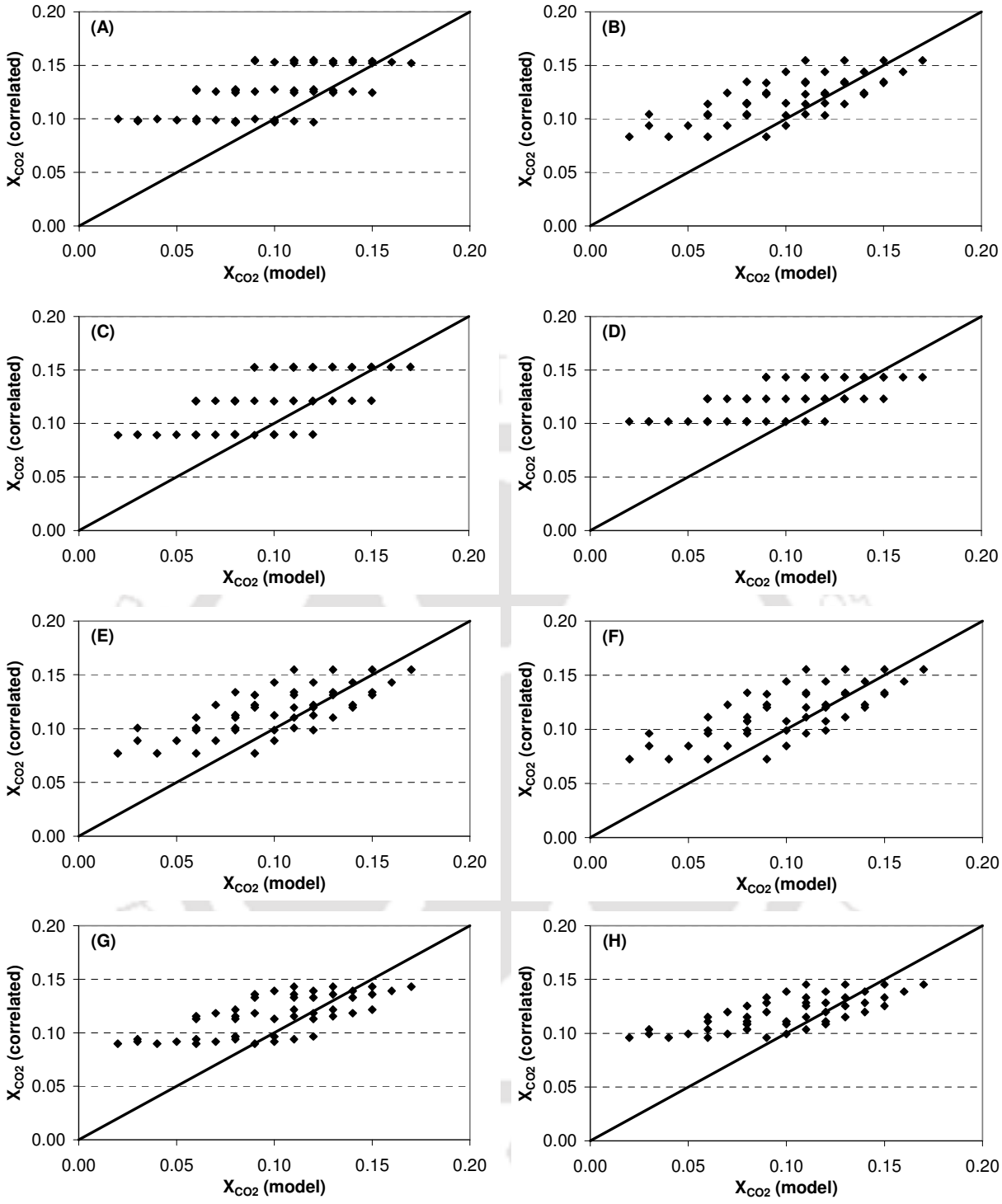


**Figure 6.4:** Comparative evaluation of linear and non–linear correlations for volume fraction of carbon dioxide in producer gas. Parity plot of values predicted by the correlation and the values calculated with semi–equilibrium models (for corn cob as biomass). (A) Correlation 1; (B) Correlation 2; (C) Correlation 3; (D) Correlation 4; (E) Correlation 5; (F) Correlation 6; (G) Correlation 7; (H) Correlation 8. For details on correlations, refer to Table 6.8.

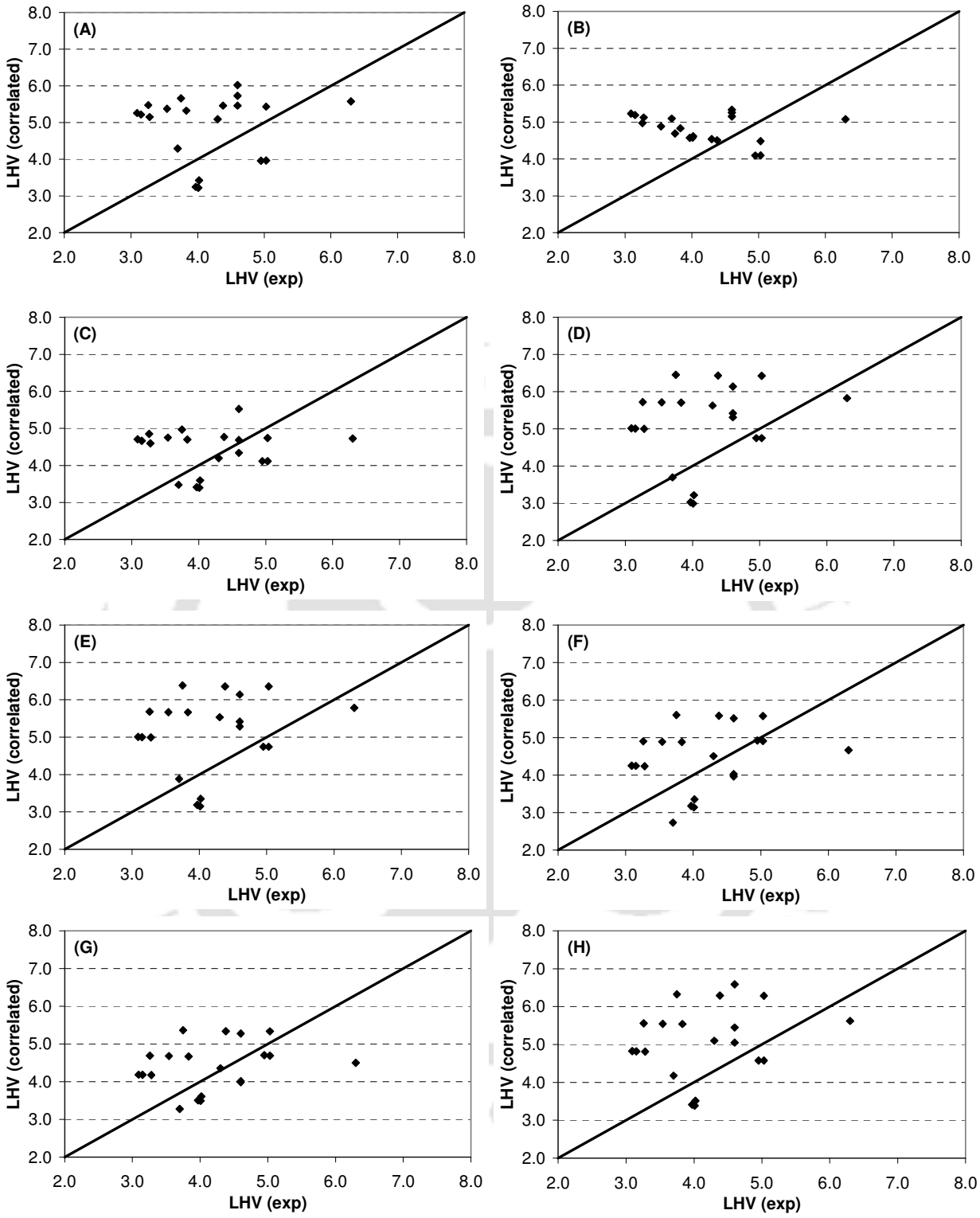


**Figure 6.5:** Parity plots between values predicted by different correlations and experimental data reported in literature for LHV of producer gas. (A) Correlation 1; (B) Correlation 2; (C) Correlation 3; (D) Correlation 4; (E) Correlation 5; (F) Correlation 6; (G) Correlation 7; (H) Correlation 8. For details on correlations, refer to Table 6.8. Experimental data given in Table 6.9.

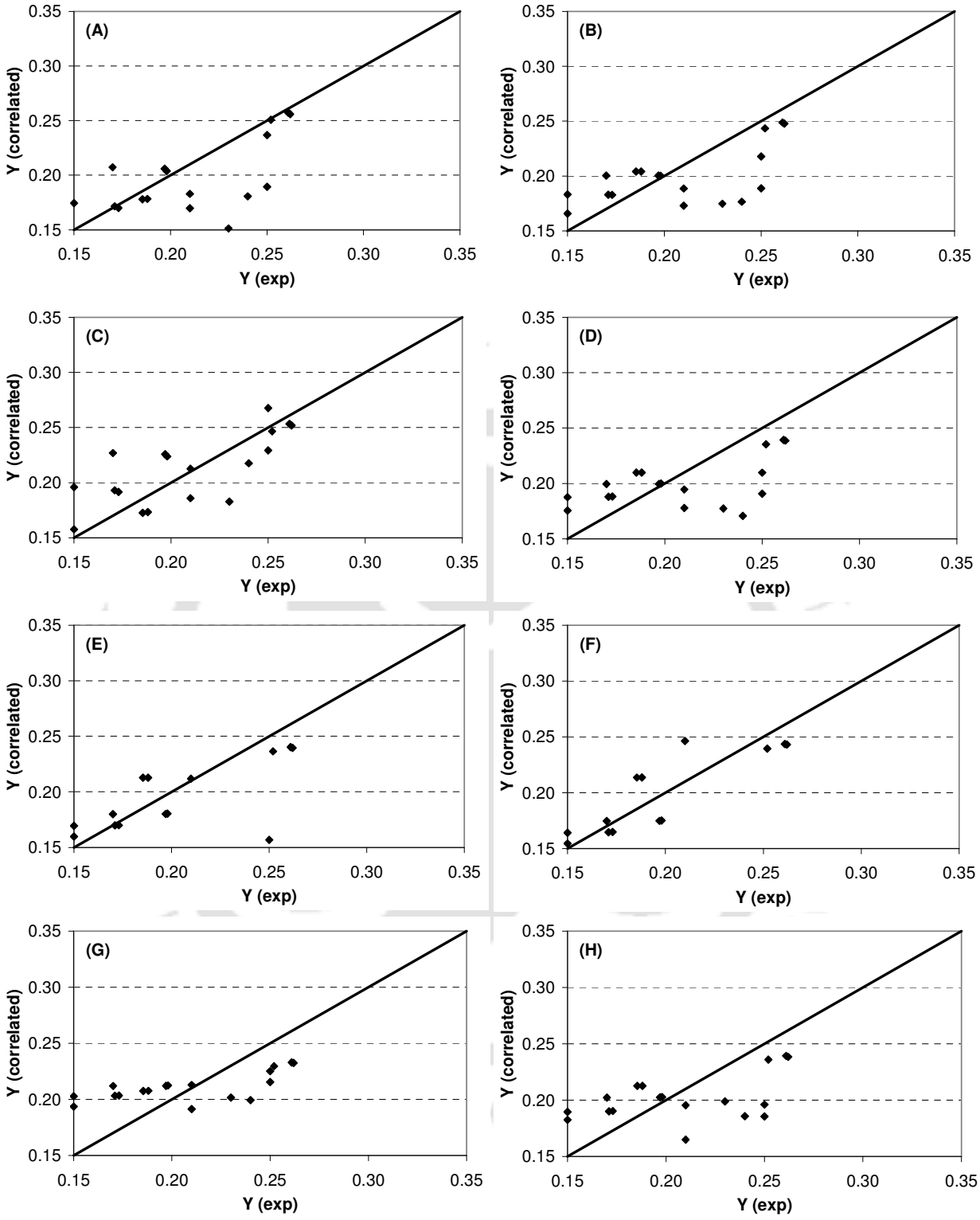


**Figure 6.6:** Parity plots between values predicted by different correlations and experimental data reported in literature for producer gas yield (per 100 g biomass). (A) Correlation 1; (B) Correlation 2; (C) Correlation 3; (D) Correlation 4; (E) Correlation 5; (F) Correlation 6; (G) Correlation 7; (H) Correlation 8. For details on correlations, refer to Table 6.8. Experimental data given in Table 6.10.

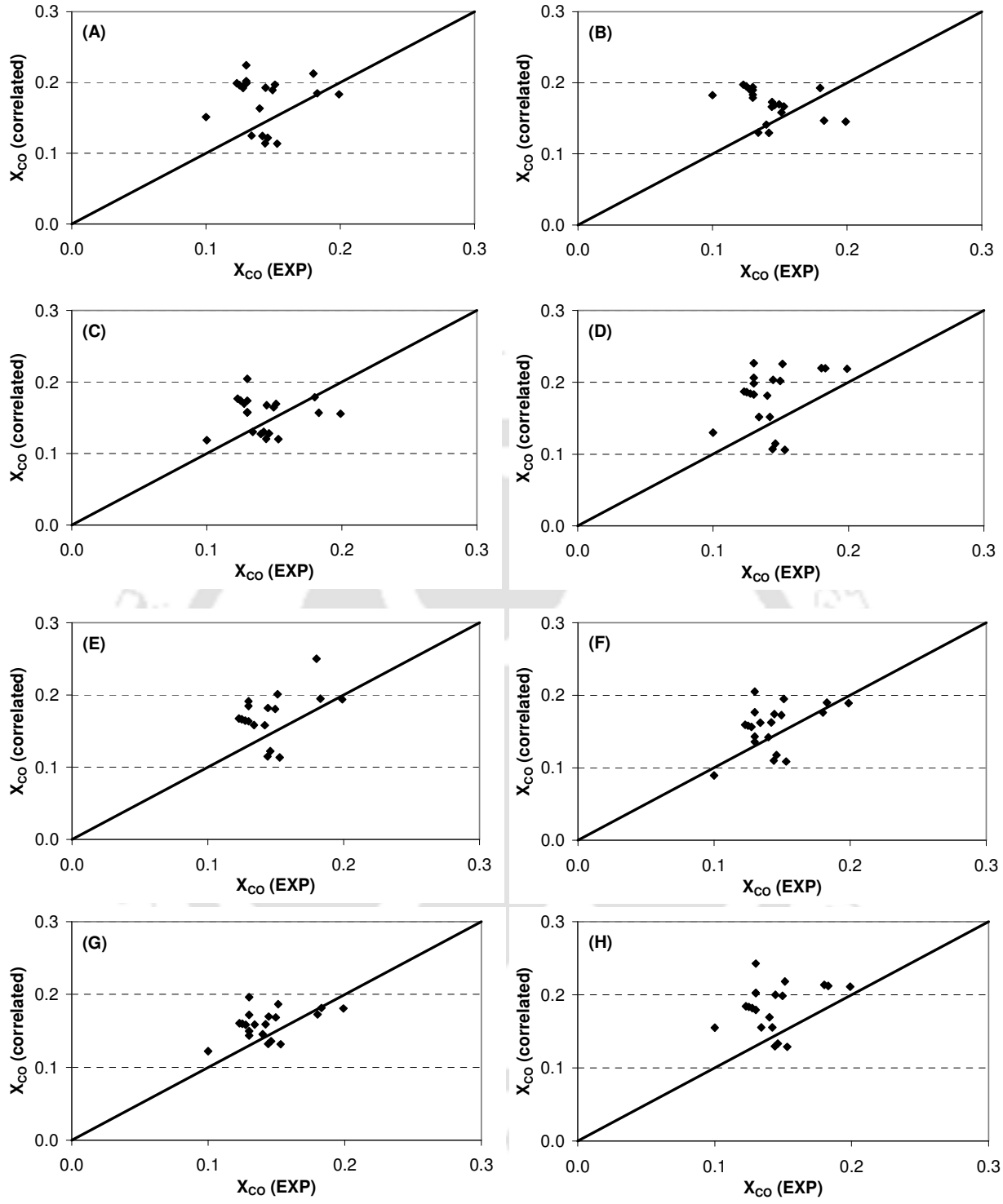


**Figure 6.7:** Parity plots between values predicted by different correlations and experimental data reported in literature for volume fraction of carbon monoxide in producer gas. (A) Correlation 1; (B) Correlation 2; (C) Correlation 3; (D) Correlation 4; (E) Correlation 5; (F) Correlation 6; (G) Correlation 7; (H) Correlation 8. For details on correlations, refer to Table 6.8. Experimental data given in Table 6.11.

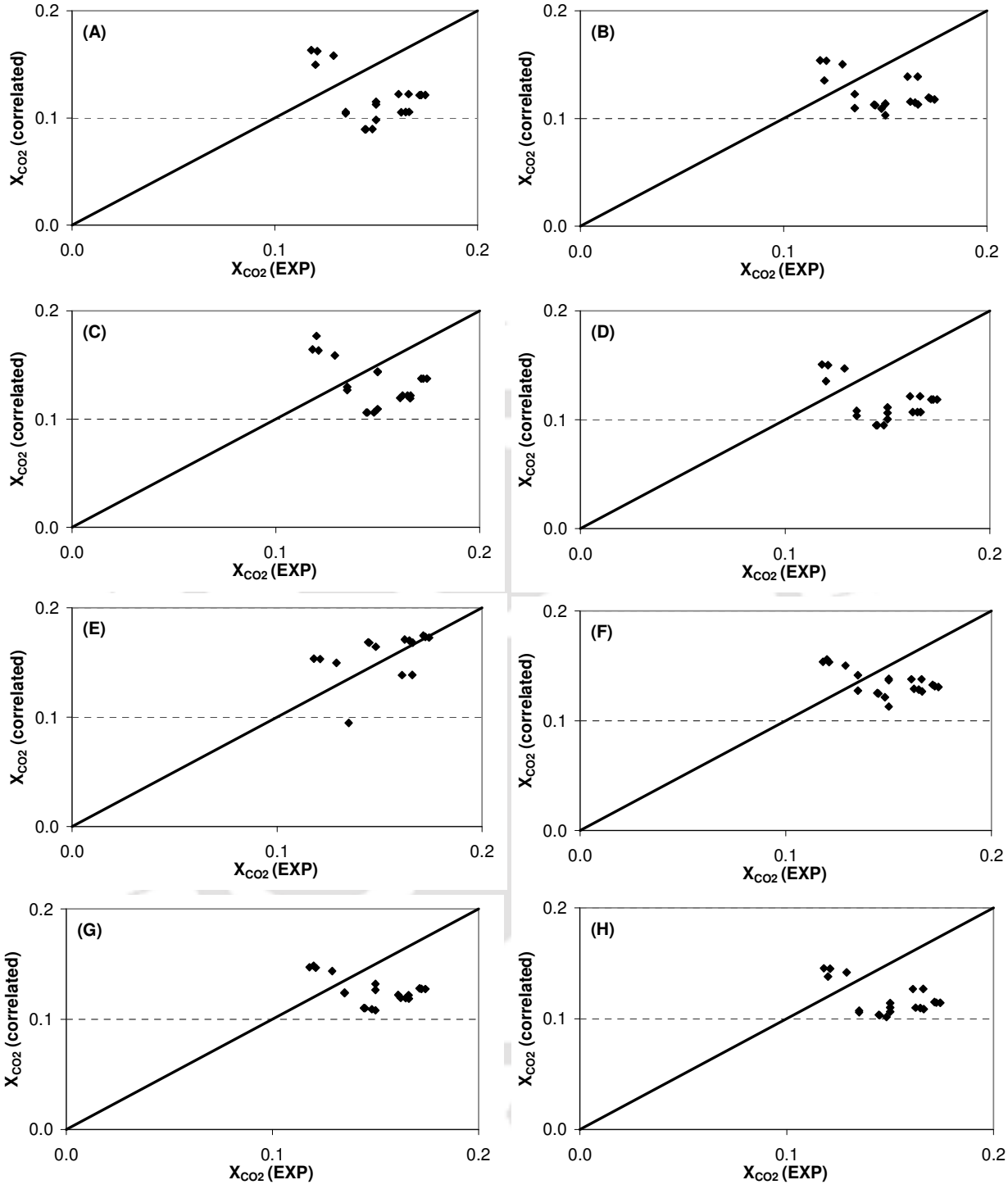


**Figure 6.8:** Parity plots between values predicted by different correlations and experimental data reported in literature for volume fraction of carbon dioxide in producer gas. (A) Correlation 1; (B) Correlation 2; (C) Correlation 3; (D) Correlation 4; (E) Correlation 5; (F) Correlation 6; (G) Correlation 7; (H) Correlation 8. For details on correlations, refer to Table 6.8. Experimental data given in Table 6.12.

## 6.4 CONCLUSIONS

This study makes an attempt to devise generalized correlations for the performance of a biomass gasifier for decentralized power generation using simulations of biomass gasification process with semi–equilibrium non–stoichiometric thermodynamic models. Variables used in the correlations are air ratio, temperature of gasification and elemental ratios (i.e. H/C, O/C and O/H) in the gasification mixture. These correlations have been found to give estimates of LHV, yield and composition of producer gas (in terms of volume fraction of two principal components, viz. CO and $CO_2$) with an engineering accuracy of ±10–20%. The strength of these correlations is that they are completely independent of the design of the gasifier, and are only a function of biomass type and operating conditions. Thus, these are applicable for gasifiers of both fixed bed and fluidized bed design. We believe that these correlations will be helpful in selection of operating conditions for a biomass gasifier depending on the quality of the feedstock. Moreover, these correlations can also be a handy tool for optimization of biomass gasifiers.

## REFERENCES

[1] FactWeb. Homepage: http://www.factsage.com (accessed November 2009).

[2] Bale CW, Chartrand P, Degterov SA, Eriksson G, Hack K, Mahfoud RB, Melancon J, Pelton AD, Petersen S. FACTSAGE thermochemical software and databases. Calphad 2002;26(2):189–228.

[3] Eriksson G. Thermodynamic studies of high temperature equilibria – XII: SOLGAMIX, A computer program for calculation of equilibrium composition in multiphase systems. Chemica Scripta 1975;8:100–103.

[4] Buragohain B, Mahanta P, Moholkar VS. Thermodynamic optimization of biomass

gasification for decentralized power generation and Fischer–Tropsch synthesis. Energy 2010;35:2557–2579.

[5] Lv PM, Xiong ZH, Chang J, Wu CZ, Chen Y, Zhu JX. An experimental study on biomass air–steam gasification in a fluidized bed. Bioresource Technology 2004;95:95–101.

[6] Mansaray KG, Ghaly AE, Al–Taweel AM, Hamdullahpur F, Ugursal VI. Air gasification of rice husk in a dual distributor type fluidized bed reactor. Biomass and Bioenergy 1999;17:315–332.

[7] Zhao Y, Sun S, Tian H-M, Qian J, Su F-M, Ling F. Characteristics of rice husk gasification in an entrained flow reactor. Bioresource Technology 2009;100:6040-6044.

[8] Cao Y, Wang Y, Riley JT, Pan W–P. A novel biomass air gasification process for producing tar–free higher heating value fuel gas. Fuel Processing Technology 2006;87:343–353.

[9] Press WH, Teukolsky SA, Flannery BP, Vetterling WT. Numerical recipes. New York: Cambridge University Press, 1992.

[10] Narvaez I, Orio A, Aznar MP, Corella J. Biomass gasification with air in an atmospheric bubbling fluidized bed. Effect of six operational variables on the quality of the produced raw gas. Industrial & Engineering Chemistry Research 1996;35:2110–2120.

[11] Jiang H, Morey RV. Air gasification of corncobs at fluidization. Biomass and Bioenergy 1992;3:87–92.

[12] Maniatis K, Vassilatos V, Kyritsis S. Design of pilot plant fluidized bed gasifier. In: Bridgwater AV, editor. Advances in thermo–chemical biomass conversion (Vol. 1), Glasgow:Blakie Academic and Professional, 1994. pp. 403–410.

[13] Ergudenler E, Ghaly AE. Quality of gas produced from wheat straw in a dual distributor type fluidized bed gasifier. Biomass and Bioenergy 1992;3:419–430.

[14] Kersten SRA, Prins W, van der Drift B, van Swaaij WPM. Principles of a novel multistage circulating bed reactor for biomass gasification. Chemical Engineering Science 2003;58:725-731.

[15] van der Aarsen FG, Beenackers AACM, van Swaaij WPM. Thermochemical gasification in a pilot plant fluidized bed wood gasifier. Communications of European Communities 1983;8245:425–429.

भारतीय प्रौद्योगिकी संस्थान गुवाहाटी
Indian Institute of Technology Guwahati

CHAPTER 7

# Comparative Assessment of Kinetic, Equilibrium and Semi-Equilibrium Models

## 7.1 INTRODUCTION

Basic chemistry of biomass gasification closely resembles that of coal gasification, and hence, mathematical models for biomass gasification have been derived from coal gasification. However, these are several differences in the composition of biomass and coal. In addition to lignin (as in coal), biomass also contains significant amount of hemi–cellulose and cellulose. The reactivity of biomass is usually much higher than that of coal, which is mainly attributed to very low ash content of biomass. Another important difference is in term of relative contents of volatiles and fixed carbon. The fixed carbon content of coal is much higher than biomass, while volatiles content of biomass is significantly higher than coal. The volatiles released during the pyrolysis of biomass (which occurs at much faster rate than coal) can condense in the form of tar, if the gasification temperature is below ~ 1000$^{o}$C. Tar content in the producer gas resulting from biomass gasification can create significant operational problems in the equipment (for example, furnace, dual fuel or 100% producer gas

engines etc.), in which the gas is used. There have been mainly two approaches adopted by researcher in modeling of biomass gasification. First is that of equilibrium modeling, in which the Gibbs free energy of the gasification system is minimized to determine the composition of the species resulting from gasification of biomass. These models are further classified on the basis of algorithm used for Gibbs energy minimization as stoichiometric and non–stoichiometric models. The stoichiometric models take into account specific chemical reactions and the equilibrium constants of these reactions at gasification temperature. The non–stoichiometric models are based on elemental balance technique, in which the composition of the reaction mixture is determined using Gibbs energy minimization using numerical methods such as Langrangian multipliers. The second approach for modeling of gasifier is kinetic modeling, in which the scheme of reactions occurring during gasification is coupled to hydrodynamics of the gasifier. Among the three approaches, physically most realistic approach is the kinetic modeling. However, many limitations of these models restrict their wide applicability. The first limitation is that of availability of precise kinetic constants over a wide range of temperature and pressure. Second limitation is in terms of coupling of hydrodynamics of the gasifiers and kinetics of reaction scheme by identification and quantification of proper linkages between the two. These models involve various physical aspects of the gasification system such as gas solid and solid–solid (heat and mass) transport coefficients, velocities of various phases and residence time distribution. These features make the model system specific and more error prone. Equilibrium models are on the contrary, independent of design of gasifier. Thus, these can be applied to both moving and fluidized bed gasifiers. In addition, thermodynamic models predict the “limiting” or maximum possible performance of the gasifier under a given set of operating conditions. Thus, predictions of these models form useful basis for optimization of gasifier in terms of operating conditions.

## 7.2 AIM AND APPROACH

In this chapter, we have attempted to compare the equilibrium, semi–equilibrium and kinetic models of biomass gasification using a circulation fluidized bed gasifier as basis. We have selected two biomass, viz. wood particles (or dust) and rice husk, with gasification medium being air as the model system. The equilibrium model used in our study is based on well known algorithm SOLGASMIX (Eriksson [1]). The elemental vector input to this model is determined from ultimate composition of biomass and the air ratio. This model has also been used to determine semi–equilibrium conditions by using extent of carbon conversion as a manipulation parameter. The kinetic model comprises of scheme of 13 known chemical reactions (both homogeneous and heterogeneous) among various species resulting from pyrolysis of biomass. The kinetic constants for these reactions have been obtained from literature. Section 7.4 gives greater details the physical picture of the gasification process in the CFB gasifier. Extent of carbon conversion achieved in the gasifier depends mainly on the temperature and air ratio. It should be noted, however, that temperature of the gasifier itself depends on extent of carbon conversion due to simultaneous endothermic /exothermic reactions during gasification. Thus, in principle carbon conversion can not be considered as an "independent" or manipulation parameter. But, for a CFB gasifier, the extent of carbon conversion also depends on the residence time of biomass particles, which is governed by velocity of these particles. For no slip condition, velocity of the biomass particles is equal to air velocity in the riser section of gasifier. On the basis of these arguments, the semi–equilibrium model uses carbon conversion as independent parameter.

## 7.3 LITERATURE REVIEW

A detailed review of literature in modeling of biomass gasification has been presented in Chapter 3. However, for convenience of reader we briefly reproduce it here. The literature

review given in this section also includes some additional papers in kinetic modeling which have not been included in Chapter 3. Kinetic models are mostly associated with fluidized bed gasifiers, in which the process of gasification is kinetically limited. As far as modeling of fluidized bed gasifiers is concerned, coal gasification has been extensively studied. Some notable contribution to coal gasification are from Rhinehart et al. [2], Ciesielczyk and Gawdzik [3], Sotudeh–Gharebaagh [4], Srinivasan [5], Yan et al. [6], Wang [7], Huilin et al. [8], Kim et al. [9], Chen et al. [10,11], Chejne and Hernandez [12]. The models for coal gasification /combustion in fluidized bed systems have formed basis for development of models for biomass gasification. Literature on kinetic modeling of biomass gasification in various types of gasifiers has also seen numerous contributions in last two decades.

Contribution in 1980s are from Belleville and Capart [13], who developed a model to predict outlet gas concentration from wood gasifier, and Chang et al. [14], who developed a model for biomass gasification in fluidized bed. In another notable contribution, van der Aarsen [15] modeled a fluidized bed wood gasifier. Literature published in 1990s includes contribution from Corella et al. [16], who addressed the issue of non–stationary states in a commercial fluidized bed air–biomass gasifier. Jiang and Morey [17,18] have developed a numerical model for fluidized bed biomass gasifier, which was based on their own experiments. Experiments were conducted in lab–scale gasifier–combustion system, with gas samples analyzed using online gas chromatograph.

The numerical model of Jiang and Morey was 1–D, steady state comprising of 4 sub–models, viz. fuel pyrolysis model, oxidation model, gasification model and freeboard model. The model could assess major mechanisms of gasification such as fuel pyrolysis and chemical/physical rate processes. Wang and Kinoshita [19] have also developed kinetic model of biomass gasification based on mechanism of surface reaction, in which the approach rate constants were computed by minimizing differences between experimental data

and theoretical results. Mansaray et al. [20,21] have developed two models (single and double compartment) using ASPEN PLUS process simulator that could predict steady state performance of a dual distributor type fluidized bed rice husk gasifier under wide range of operating conditions. Sadaka et al. [22-24] developed a model for bubbling fluidized bed gasifier on the basis of two–phase theory of fluidization. In this model, the fluidized bed was divided in 3 zones and transport co–efficient (heat and mass) were calculated in each zone for both bubble and combustion phase. Other models include those from Hamel and Krumm [25], Jennen et al. [26], Kersten et al. [27], Corella and Sanz [28], Liu and Gibbs [29,30], Dupont et al. [31], Radmanesh [32], Nikoo and Mahinpey [33], Rodrigues et al. [34], Roy et al. [35], Kaushal et al. [36] and Evans et al. [37].

Numerous authors have applied both stoichiometric and non–stoichoimetric models for biomass gasification. The notable contributions include: Cousins [38], Denn et al. [39], Kosky and Floess [40], Kovacik et al. [41], Shesh and Sunawala [42], Watkinson et al. [43], and Garcia and Laborde [44]. In addition to these, Schuster et al. [45] have assessed performance of biomass gasification system for decentralized heat and power generation with equilibrium models, and Zainal et al. [46] have studied effect of gasification temperature and moisture content of biomass on producer gas composition. Similarly, Alderucci [47] has studied gasification of biomass with steam and $CO_2$ as gasification medium. Ruggerio and Manfrida [48] have also attempted to predict performance of downdraft gasifier (in terms of product gas composition and overall efficiency) using thermodynamic model. Some other studies using equilibrium (or semi–equlibrium) models are from Altafini et al. [49], Melgar et al. [50], Brown et al. [51], Vera et al. [52], Saxena and Thomas [53].

Literature involving application of non–stoichiometric model is relatively less. Researchers have applied different algorithms for Gibbs energy minimization. These algorithms include STANJAN (Reynolds [54]), RAND (Smith and Missen [55]) and

SOLGASMIX (Eriksson [1]). The major contributions in this area are from Bharadwaj [56], Mahishi et al. [57], Li et al. [58] and Kersten [59].

For greater details on both equilibrium and kinetic modeling of biomass gasification we refer the reader to state of the art reviews Shand and Bridgwater [60], Nemtsov and Zabaniotou [61], Puig–Aranavat et al. [62] and Prakash and Karunanithi [63].

### 7.3.1 Inference and Justification of Present Study

Voluminous literature has been published in the area of modeling of biomass gasification using both kinetic and equilibrium approach. As noted earlier, kinetic models have advantage of being physically more realistic, while equilibrium model have merit of wide applicability and being independent of gasifier design. A comparative study is, thus, necessary to compare the predictions of the two models under same gasification conditions. Such comparison will give quantitative account of the discrepancy in the predictions of the two models. This will help identify suitability of the models under a particular situation. It will also help identify conditions for which and under which the gasification system deviates from equilibrium. Such an analysis will help identify process/design parameters, which play vital role in achieving equilibrium in the system (i.e. conditions for which the output of gasification process will be at its maximum).

## 7.4 PHYSICAL PICTURE OF GASIFICATION IN A CFB BIOMASS GASIFIER

We take a typical pilot scale circulating fluidized bed biomass gasifier as basis for comparison of kinetic and equilibrium models. This gasifier unit comprises of: (1) riser, (2) cyclone separator, (3) burner–blower system for hot gas generation, (4) biomass hopper and screw feeder, (5) gas cooling system, (6) particulate filter system (either single or double stage), and (7) dual fuel generator. We briefly describe here the physics or mechanics of the

process. Biomass enters the riser section of the gasifier near (just above) the perforated plate distributor. The gasifier medium is hot air at about 700–900$^{o}$C, and enters from the below the distributor plate. A bed of sand (stagnant height ~ 30 cm) is used as inert material in the riser (ID = 4 in.). Initially, hot air–sand mixture is circulated in the gasifier riser section to establish (almost) uniform temperature in the riser. The velocity of air through riser is so adjusted as to give turbulent or vigorous bubbling mode of fluidization for sand, while pneumatic conveyance regime for biomass particles. Under these fluidization conditions, the bed of sand expands about 50–60% of its initial height. Biomass entering the riser has medium particle size of ~ 0.5 – 1 mm, and gets mixed with hot sand in turbulent motion. Both gas–particle and particle–particle heat transfer rates are high, and hence, biomass particles reach the temperature of sand bed and get pyrolyzed almost instantly. Liu and Gibbs [30] have given following expression for the devolatilization time (in seconds) of biomass particles: $t_d = \frac{27.443\, d_p^{1.662}}{(T-613)^{0.508}}$, where $d_p$ is the biomass particle size in mm, and T is the temperature in K. It should be noted that biomass particles may also get ruptured or sintered during mixing with hot sand. We, therefore, have considered a range of particle sizes, viz. 0.5 – 1 mm for our analysis. The pyrolysis time for these particles is ~ 0.13 s and 1.38 s, respectively. This is sufficiently small to justify assumption of instantaneous devolatilization of biomass particles. Pyrolysis of biomass results in fractionation of biomass into three components: char (which is carbon rich solid fraction), tar (which is essentially heavy hydrocarbons) and light gases such as CO, $CO_2$, $H_2$, $CH_4$, $C_2H_4$ and $C_2H_6$.

The products of pyrolysis, viz. char, tar and gases disengage and emerge out of the turbulent sand bed, and flow along the riser with gasification medium; finally exiting at the top to enter a cyclone separator. Various species in the gas undergo reactions during their flow through the riser. These reactions are both heterogeneous (between char and gases) and

homogeneous (among gas species) type. The cyclone separator separates the solid from exhaust gas, i.e. char particles and also some sand particles that get elutriated, and return them to the riser bottom. The gas exiting from cyclone separator has fine dust particles (of a size smaller than the critical particle size captured by cyclone separator). This gas in initially cooled by spraying water in it. With cooling of gas at room temperature, the tar component condenses and gets carried in the form of droplets in the gas. The gas is then filtered to remove both solid particles and tar droplets, and also passed through moisture absorber beds (such as saw dust). It is then fired into the producer gas engine coupled to a generator.

## 7.5 MODEL FORMULATION

### 7.5.1 Kinetic Model

The kinetic model takes into account 13 simultaneous reactions among various species resulting out of pyrolysis. These reactions and their kinetic constants are given in Table 7.1. The reaction scheme comprises of 4 heterogeneous reactions of char gasification with $O_2$, $H_2O$, $CO_2$ and $H_2$. In addition, 9 homogeneous reactions have been considered among 9 species, viz. $O_2$, CO, $CO_2$, $H_2O$, $H_2$, $CH_4$, $C_2H_6$, $C_2H_4$ and tar. The mole / mass balance for various species is written as:

$$\text{Carbon: } \frac{dF_{Char}}{dV}\left(\frac{kg}{m^3 - s}\right) = -\frac{1}{uA}\left(r_1 + r_2 + r_3 + r_4\right) \qquad (7.1)$$

**Table 7.1:** Scheme of reactions in the kinetic model along with rate expressions

| Sr. No. | Reaction | Rate Expression (either kg/s or kmol/m$^3$-s, as applicable) | Reference |
|---|---|---|---|
| | | Heterogeneous Reactions of Char Gasification | |
| 1. | $(1+\beta_c)\ C + \left(1+\frac{\beta_c}{2}\right) O_2 \longrightarrow \beta_c\ CO + CO_2$<br>$C + 0.85O_2 \longrightarrow 0.3CO + 0.7CO_2$ | $r_1 = -\frac{dW}{dt} = 2.268\times10^7 \times \exp\left(\frac{-8559}{T}\right) W_p [O_2]$ (kg/s)<br>($\beta_c = 0.43$) | Liu and Gibbs [29], Luo et al. [64], Saito et al. [65], Yan et al. [66] |
| 2. | $C + H_2O \longrightarrow CO + H_2$ | $r_2 = -\frac{dW}{dt} = \frac{6692\times\exp\left(\frac{-15516}{T}\right)\times W_p \times [H_2O]}{1+3.16\times10^{-2}\exp\left(\frac{3620}{T}\right)[H_2O]+5.36\times10^{-3}\exp\left(\frac{7193}{T}\right)\times[H_2]+8.25\times10^{-5}\exp\left(\frac{11559}{T}\right)[CO]}$ (kg/s) | Luo et al. [64] |
| 3. | $C + CO_2 \longrightarrow 2\ CO$ | $r_3 = -\frac{dW}{dt} = \frac{1.3692\times10^9\left(\frac{-32235}{T}\right)\times W_p \times [CO_2]}{1+6.6\times10^{-2}[CO_2]+0.12\exp\left(\frac{3067}{T}\right)\times[CO]}$ (kg/s) | Luo et al. [64] |
| 4. | $C + 2\ H_2 \longrightarrow CH_4$ | $r_4 = -\frac{dW}{dt} = \frac{66.92\times\exp\left(\frac{-15516}{T}\right)\times[H_2]\times W_p}{1+3.16\times10^{-2}\exp\left(\frac{3620}{T}\right)[H_2O]+5.36\times10^{-3}\exp\left(\frac{7193}{T}\right)\times[H_2]+8.25\times10^{-5}\exp\left(\frac{11559}{T}\right)[CO]}$ (kg/s) | Liu and Gibbs [30] |
| | | Homogeneous Reaction among Gaseous Species | |
| 5. | $CO + H_2O \rightleftharpoons CO_2 + H_2$ | $r_5 = \frac{-d[CO]}{dt} = 2.78\times10^3 \times \exp\left(\frac{-1510.7}{T}\right)\left[[CO][H_2O] - \frac{[CO_2][H_2]}{0.0265\exp\left(\frac{3958.5}{T}\right)}\right]$ (kmol/m$^3$·s) | Biba et al. [67], Gururajan et al. [68] |
| 6. | $CO + 0.5\ O_2 \longrightarrow CO_2$ | $r_6 = \frac{-d[CO]}{dt} = 3.25\times10^{10}\exp\left(\frac{-15098}{T}\right)\left[[CO][O_2]^{1/2}[H_2O]^{1/2}\right]$ (kmol/m$^3$·s) | Jensen et al. [69] |

*Table 7.1 continued….*

| Sr. No. | Reaction | Rate Expression (either kg/s or kmol/m$^3$-s, as applicable) | Reference |
|---|---|---|---|
| 7. | $CH_4 + \frac{3}{2} O_2 \longrightarrow CO + 2 H_2O$ | $r_7 = \frac{-d[CH_4]}{dt} = 5\times10^{11} \exp\left(\frac{-24157}{T}\right)[CH_4]^{0.7}[O_2]^{0.8}$ (kmol/m$^3$·s) | Jensen et al. [69] |
| 8. | $CH_4 + \frac{1}{2} O_2 \longrightarrow CO + 2 H_2$ | $r_8 = \frac{-d[CH_4]}{dt} = 4.4\times10^{11} \exp\left(\frac{-15098}{T}\right)[CH_4]^{1/2}[O_2]^{5/4}$ (kmol/m$^3$·s) | Jones and Lindstedt [70] |
| 9. | $CH_4 + H_2O \longrightarrow CO + 3 H_2$ | $r_9 = \frac{-d[CH_4]}{dt} = 3\times10^{8} \times \exp\left(\frac{-15098}{T}\right)[CH_4][H_2O]$ kmol/m$^3$·s | Jones and Lindstedt [70], Fletcher et al. [71] |
| 10. | $H_2 + \frac{1}{2}O_2 \longrightarrow H_2O$ | $r_{10} = \frac{-d[H_2]}{dt} = 5.183\times10^{13} T^{3/2} \exp\left(\frac{-3420}{T}\right)[H_2]^{3/2}[O_2]$ | Jones and Lindstedt [70] |
| 11. | $C_2H_6 + \frac{5}{2} O_2 \longrightarrow 2 CO + 3 H_2O$ | $r_{11} = \frac{-d[O_2]}{dt} = 2.281\times10^{11} \exp\left(\frac{-20131}{T}\right) T^{0.5}[C_nH_m][O_2]$ | Zimont and Trushin [72] |
| 12. | $C_2H_4 + 3 O_2 \longrightarrow 2 CO_2 + 2 H_2O$ | $r_{12} = \frac{-d[C_2H_4]}{dt} = 4\times10^{11} \exp\left(\frac{-24200}{T}\right)[C_2H_4]^{0.7}[O_2]^{0.8}$ | Corella and Sanz [28] |
| 13. | $CH_{0.85}O_{0.17}$ (Tar) + 0.68 $O_2 \longrightarrow$ 0.75 CO + 0.25 $CO_2$ + 0.28 $H_2O$ | $r_{13} = \frac{-d[Tar]}{dt} = 1.264\times10^{13} \exp\left(\frac{-24200}{T}\right)[Tar][O_2]$ | Corella and Sanz [28] |

Oxygen: $\frac{dF_{O2}}{dV}\left(\frac{kmol}{m^3-s}\right)=-\left(\frac{0.85}{12}\right)\frac{r_1}{uA}-0.5r_6-1.5r_7-0.5r_8-0.5r_{10}-r_{11}-3r_{12}-0.68r_{13}$ (7.2)

Carbon monoxide (CO):

$$\frac{dF_{CO}}{dV}\left(\frac{kmol}{m^3-s}\right)=\left(\frac{0.3}{12}\right)\frac{r_1}{uA}+\frac{1}{12}\frac{r_2}{uA}+\left(\frac{2}{12}\right)\frac{r_3}{uA}-r_5-r_6+r_7+r_8+r_9+0.8r_{11}+0.75r_{13} \quad (7.3)$$

Carbon Dioxide ($CO_2$): $\frac{dF_{CO2}}{dV}\left(\frac{kmol}{m^3-s}\right)=\left(\frac{0.7}{12}\right)\frac{r_1}{uA}-\frac{r_3}{12uA}+r_5+r_6+2r_{12}+0.25r_{13}$ (7.4)

Water ($H_2O$): $\frac{dF_{H2O}}{dV}\left(\frac{kmol}{m^3-s}\right)=-r_5+2r_7-r_9+r_{10}+1.2r_{11}+2r_{12}+0.28r_{13}$ (7.5)

Hydrogen ($H_2$): $\frac{dF_{H2}}{dV}\left(\frac{kmol}{m^3-s}\right)=\frac{r_{12}}{12uA}-\left(\frac{2}{12}\right)\frac{r_4}{uA}+r_5+2r_8-3r_9-r_{10}$ (7.6)

Methane ($CH_4$): $\frac{dF_{CH4}}{dV}\left(\frac{kmol}{m^3-s}\right)=\frac{r_4}{12uA}-r_7-r_8-r_9$ (7.7)

Ethane ($C_2H_6$): $\frac{dF_{C2H6}}{dV}\left(\frac{kmol}{m^3-s}\right)=-.04r_{11}$ (7.8)

Ethylene ($C_2H_4$): $\frac{dF_{C2H4}}{dV}\left(\frac{kmol}{m^3-s}\right)=-r_{12}$ (7.9)

Tar: $\frac{dF_{Tar}}{dV}\left(\frac{kmol}{m^3-s}\right)=-r_{13}$ (7.10)

The term ($uA$) is the instantaneous volume of the reaction mixture and a factor that converts the original rate expression for char gasification in kg/s to kg/$m^3$–s. It has been derived with simple chain rule as follows:

$$\frac{dW}{dV}\left(\frac{kg}{m^3-s}\right)=\frac{dW}{dt}\times\frac{dt}{dV}=\frac{r_1}{A}\times\left(\frac{dt}{dx}\right)=\frac{r_1}{uA} \quad (7.11)$$

$dV$ is the differential volume of the gasification mixture. Since the gasification mixture flows axially through the riser, we can represent the differential volume of thickness $dx$ as $A \times dx$, where $A$ is the area of cross–section. $dx/dt$ is the axial velocity ($u$) of the gasification mixture (char + tar + gaseous species). Assuming no slip condition in the gasification mixture, i.e. the solid char particles move with same velocity as the gasification mixture, the velocity can be calculated by dividing the volume of the gaseous species in the mixture by the cross–

sectional area of riser. The above reaction scheme is integrated with volume as an independent variable with Runge–Kutta 4$^{th}$ order – 5$^{th}$ order adaptive step size method. We consider two heights for the riser section, viz. 6 and 10 m. The corresponding volumes of the riser (for 4 in. ID) are 0.0486 and 0.081 m$^3$, respectively.

### 7.5.2 Equilibrium Model

The equilibrium model is based on algorithm SOLGASMIX proposed by Eriksson [1] for calculation composition of reaction system at thermodynamic equilibrium through Gibbs energy minimization of the system. Simulations have been carried out with software FACTSAGE [73,74]. For convenience of reader, we give below only the main equations of this model. For greater details on the model, please refer to Chapter 4. Solution to this model is obtained using an iterative procedure (method of Lagrangian multipliers with constraint of mass balance equations) in terms of mole numbers and fractions of gas / condensed phase species at equilibrium that could result from reactant species at a specific temperature and pressure, for which the total free energy of the system is at its minimum.

Total Gibbs free energy (G) of a system comprising of mixture of *i* species is:

$$G = \sum_i x_i g_i \tag{7.12}$$

$x_i$ is the mole number of a substance or species in the mixture. Chemical potential of a species *i* ( $g_i$ ) is:

$$g_i = g_i^0 + RT \ln a_i \tag{7.13}$$

$a_i$ represents activity coefficient of a species and it is equal to the partial pressure $p_i$ for a gaseous species assuming ideal behavior:

$$a_i = p_i = (x_i / X)P \tag{7.14}$$

*X* represents total number of moles in the gas phase and *P* is the total pressure of the system, respectively. The condensed substances are assumed to be pure, and hence, their activities are

equal to unity. With these assumptions, a new dimensionless quantity (*G/RT*) is defined as:

$$G/RT = \sum_{i=1}^{m} x_i^g [(g^0/RT)_i^g + \ln P + \ln(x_i^g / X)] + \sum_{i=1}^{s} x_i^c (g^0/RT)_i^c \qquad (7.15)$$

Superscripts *g* and *c* represent gas phase and condensed phase, respectively, while *m* and *s* represent the total number of substances in the gas phase and condensed phase, respectively, at equilibrium. *R* is the ideal gas constant. The quantity ($g^o/RT$) for a certain substance is calculated as with reference to standard state at 298 K:

$$(g^o/RT) = (1/R)[G^o - H_{298}^o)/T + \Delta_f H_{298}^o / RT \qquad (7.16)$$

Superscript $^o$ refers to the thermodynamic standard state; subscript $_{298}$ refers to the reference temperature; subscript $_f$ denotes the formation of a compound from the elements in their standard states. Overall mass balance in the system among various species can be written as:

$$\sum_{i=1}^{m} a_{ij}^g x_i^g + \sum_{i=1}^{s} a_{ij}^c x_i^c = b_j \, (j = 1, 2, .... l) \qquad (7.17)$$

Various notations are as follows: $a_{ij}$ – number of atoms of the $j^{th}$ element in a molecule of the $i^{th}$ substance, $b_j$ – total number of moles of the $j^{th}$ element, $l$ – total number of elements. The method involves a. For solution of this system of equations, Lagrange's method of undetermined multipliers is used. The solution essentially involves minimization of the free energy *G* of a system (or equivalently *G/RT* as given in equation 15) subject to the mass balance constraints.

Total heat of the process for attainment of equilibrium is determined as follows:

The energy necessary for pre–heating the initial mixture (*HP*) from the initial temperature $T_1$ K to the reaction temperature *T* K, added to the heat of reaction $(HR)$, gives the total heat $(HT)$: $HT = HP + HR$. $HP$ and $HR$ are determined as follows:

$$HP = \sum_i x_i^* (H^o - H_{T1}^o)_i \qquad (7.18)$$

where $x^*$ denotes the number of moles in the initial mixture, and:

$$(H^o - H^o_{T1})_i = \int_{T_1}^{T} (C_p)_i \, dT \tag{7.19}$$

$$HR = \sum_i (\Delta_f H^o_T)_i (x_i - x^*_i) \tag{7.20}$$

where $(\Delta_f H^o_T)_i = (\Delta_f H^o_{298})_i + [(H^o - H^o_{298})_i - (H^o - H^o_{298})_{elements}]$. Various notations are: $H$ = enthalpy (heat content); $T$ = absolute temperature of the system; $x^*$ = number of moles in the initial mixture; $C_p$ = heat capacity at constant pressure as a function of temperature; $\Delta_f H^o_{298}$ = heat of formation at 298.15 K; $\left(G^o - H^o_{298}\right)/T$ = free energy function; $\left(H^o - H^o_{298}\right)$ = heat content function.

### 7.5.3 Simulation Parameters for Kinetic and Equilibrium Model

The simulation of gasification using either kinetic or equilibrium model requires 3 important parameters. These are: (i) temperature of gasification, (ii) pressure of gasification, and (iii) type of biomass. We have chosen values of these parameters on the basis of results of our previous studies, experimental studies published in literature and specifications of commercial gasifiers available in market. For the biomass type, our choice is rice husk and wood particles (or dust). These are most common feedstock used in commercial gasifiers. As far as gasification medium is concerned, we have chosen air for our analysis.

*Temperature Profile*: The axial profile of temperature in the riser section is a critical parameter influencing gasification process. The axial profile of temperature, in turn, is affected by several factors such as temperature of incoming gasification medium (air or air–steam mixture), the heat released during gasification, the heat capacity of gasification mixture (sand, char particles and producer gas) and the losses of heat occurring from the riser. The temperature is the highest near the distributor, where the biomass entering the riser mixes with hot and turbulent sand bed and undergoes pyrolysis. The temperature shows a decreasing profile with height of the riser. The kinetic constants of various oxidation /

**Table 7.2:** Hydrodynamic properties of sand and biomass particles in the fluidized bed

| Property | Sand | Biomass Particles | | |
|---|---|---|---|---|
| $d_p$ (μm) | 271 | 250 | 500 | 1000 |
| $\varphi_s$ (–) | 0.8 | 0.8 | 0.8 | 0.8 |
| ρ (kg $m^{-3}$) | 2600 | 120 | 120 | 120 |
| $u_{mf}$ (m $s^{-1}$) | 0.028 | $1.08 \times 10^{-3}$ | $4.32 \times 10^{-3}$ | 0.017 |
| $Re_{p,mf}$ (–) | 0.254 | $9.13 \times 10^{-3}$ | 0.073 | 0.584 |
| $d_p^*$ (–) | 7.85 | 2.59 | 5.18 | 10.36 |
| $u_t^*$ (–) | 1.69 | 0.31 | 0.96 | 2.34 |
| $u_t$ (m/s) | 1.45 | 0.096 | 0.29 | 0.72 |
| $u^*$ (range)# | 2 – 10 | 2 – 11 | 3 – 12 | 4 – 30 |
| u (range, m $s^{-1}$) | 1.71 – 8.56 | 0.61 – 3.37 | 0.92 – 3.67 | 1.23 – 9.18 |

Properties of fluidizing medium: $\rho_{air} = 1.2$ kg $m^{-3}$, $\mu_{air} = 3.546 \times 10^{-5}$ Pa-s, $\varepsilon_{mf} = 0.4$.
# - The range of $u^*$ values is for fast fluidization regime in case of sand particles, and for pneumatic conveying regime for biomass particles.

reduction occurring in the riser depend on temperature. As an approximation, we have considered in our analysis an average of typical temperatures at the distributor plate of the riser and exit point of the gasification mixture (Narvaez et al. [75], Mansaray et al. [76]). We choose two temperatures, viz. 700 and 800°C for our simulations. Another basis for the choice of these temperatures are the results of Chapter 4, in which we have determined optimum operating conditions for gasification of different biomass. A more rigorous approach in the report would be a step–by–step iterative calculation in which the extent of reaction, heat released /absorbed during reaction, and temperature of the gasifier are calculated in discrete manner.

*Velocity of air:* The superficial velocity of hot air (gasification medium) entering the riser was chosen on the basis of hydrodynamic behavior of sand and biomass particles. We have considered that smooth sand as inert bed material. The particle size of sand is uniformly 270 μm. The minimum fluidization velocity and terminal settling velocity for these particles are

0.028 m/s and 1.45 m/s, respectively. The biomass, on the other hand, undergoes significant particle size reduction after getting pyrolyzed. The char particles emerging out of sand bed have a broad range of size and shape. We have considered 3 sizes of char particles for deciding the superficial velocity of air through the riser. The minimum fluidization velocities and terminal settling velocities of these particles are listed in Table 7.2. As noted earlier, the desired fluidization regime for hot sand bed is turbulent (or fast fluidization), while fluidized regime for biomass particles is pneumatic conveying. Kunii and Levenspiel [77] have given a comprehensive charts of fluidization regimes in terms of non–dimensional velocity ($u^*$) and non–dimensional particle size ($d_p^*$) for solid particles in different categories (A, B, C and D based on their physical properties). The range of actual gas velocities required for having sand particles in turbulent (fast fluidization) mode and biomass particles in pneumatic conveying mode is given in Table 7.2. On the basis of above analysis, we decided the superficial air velocity through the riser as 3.5 m/s, which corresponds correspond to volumetric flow rate of 100 $Nm^3/h$ for cross–sectional area of 0.0081 $m^2$ of the riser. For this air velocity, sand particles will always be in the turbulent or fast fluidization regime, while biomass particles will be in pneumatic conveyance regime.

The pyrolysis products emerging from the turbulent sand bed have different velocities. The larger the diameter of riser, the larger is the spatial velocity distribution in the gasification mixture passing through the riser. However, for small diameter (ID 4 in.) riser as considered in this study, one can assume a uniform velocity profile across the cross–section, without any back–mixing. Thus, the gasification mixture essentially passes in a plug flow manner through the riser.

*Air Ratio and Biomass Feed Rate*: Another important factor is the air or equivalence ratio (the ratio of actual moles of air supplied to the stoichiometric moles of air required for complete oxidation of biomass). In a previous study, we have shown that for gasification

**Table 7.3:** Data on Biomass

(A) Ultimate analysis

| Biomass | Composition in weight percent (Dry Basis) | | | | |
|---|---|---|---|---|---|
| | Carbon | Hydrogen | Nitrogen | Oxygen | Ash |
| Wood chips | 40.3 | 5.7 | 0.3 | 38.4 | 15.3 |
| Rice husk | 46.4 | 5.9 | 0.09 | 47.17 | 0.45 |

(B) Elemental composition and molecular formula for biomasses

| Biomass | Composition in gatom (per 100 g biomass) | | | | Molecular Formula |
|---|---|---|---|---|---|
| | Carbon (C) | Hydrogen (H) | Nitrogen (N) | Oxygen (O) | |
| Wood chips | 3.36 | 5.70 | 0.30 | 2.40 | $CH_{1.696}N_{0.09}O_{0.714}$ |
| Rice husk | 3.87 | 5.90 | 0.01 | 2.95 | $CH_{1.525}N_{0.002}O_{0.762}$ |

(C) Air and biomass flow rate in the CFB gasifier

| Biomass | Air Ratio (AR) | Air requirement (in gmoles) for 100 g biomass | Biomass Flow Rate* ($g\ s^{-1}$) |
|---|---|---|---|
| Rice Husk | 0.2 | 2.985 | 38.06 |
| | 0.3 | 4.477 | 25.37 |
| | 0.4 | 5.969 | 19.03 |
| Wood Particles | 0.2 | 3.701 | 30.69 |
| | 0.3 | 5.552 | 20.46 |
| | 0.4 | 7.402 | 15.34 |

* - This value is calculated on the basis of 100 $Nm^3/h$ of air flow rate to the riser of the gasifier.

temperature range of 700 – 1000°C, the optimum range of air ratio is 0.2–0.4. On the basis of this result, we have chosen three air ratios for our analysis, viz. 0.2. 0.3 and 0.4. At the NTP conditions, 100 $m^3/h$ air would correspond to 4089 mol/h or 1.136 mol/s. This would essentially mean $O_2$ flow rate of $2.3856 \times 10^{-3}$ kmol/s and $N_2$ flow rate of $8.9744 \times 10^{-3}$ kmol/s. The actual air requirement for biomass gasification depends on elemental composition or ultimate analysis of biomass. We have considered rice husk and wood particles (or dust) as biomass in this study and the ultimate analysis and elemental composition of the same is given in Table 7.3(A) and (B), respectively. On the basis of ultimate analysis of biomass, the actual air requirement in moles for 100 g of biomass at different air ratios (0.2, 0.3 and 0.4) is given in Table 7.3(C). On the basis of this, the biomass

feed rate required for achieving these air ratios (corresponding to fixed air flow of 100 $Nm^3/h$) at the inlet of the gasifier is calculated, and given in Table 7.3(C).

### 7.5.4 Input for the Equilibrium Model

Input to the equilibrium model is in the form of an elemental vector, which is determined from the moles of air and the elemental composition of amount of biomass fed to the gasifier (which in turn is determined from the ultimate analysis of biomass). As noted earlier, the moles of air fed to the riser of the gasifier are 1.136 mol/s (or 4089 mol/h corresponding to volumetric flow rate of 100 $m^3/h$). The biomass feed rate required for having air ratio of 0.2, 0.3 or 0.4 is given in Table 7.3(C). The elemental vector in the present simulations is calculated using these values. For the equilibrium model, we consider complete conversion of carbon present in the biomass, while for the semi–equilibrium model we put restriction on the extent of carbon conversion. Thus, the g atoms of carbon in the elemental vector input are reduced by $(1 - x_c)$, where $x_c$ is the extent of carbon conversion. The carbon conversion achieved in gasification through a circulating fluidized bed gasifier depends on several parameters. Main among these are: (1) temperature, (2) biomass particle size, (3) air ratio, and (4) residence time of particles in the riser. Some of these factors are inter–dependent, i.e. heat released with conversion of carbon raises the temperature of gasification mixture, which further boosts the kinetics of carbon gasification. However, due to limited residence time of biomass in gasifier, conversion of carbon in biomass in a single pass through riser is not complete, and unconverted carbon appears in the form of char. On the basis of values of carbon conversions in experimental studies using CFB gasifiers (either lab or pilot scale) by Lv et al. [78], Mansaray et al. [76], Cao et al. [79], Zhao et al. [80], we have selected two levels of carbon conversion for our simulation with semi–equilibrium model, viz. 60% and 80%. The complete elemental vector for different sets of simulations is depicted in Table 7.4.

**Table 7.4:** Elemental Vector Input for Equilibrium and Semi-Equilibrium Models

| **Biomass: Rice Husk** | | | | **Biomass: Wood Chips** | | | |
|---|---|---|---|---|---|---|---|
| **Carbon Conversion: 60%** | | | | **Carbon Conversion: 60%** | | | |
| Element / | AR | | | Element / | AR | | |
| Elemental Ratio | 0.2 | 0.3 | 0.4 | Elemental Ratio | 0.2 | 0.3 | 0.4 |
| C | 0.767 | 0.511 | 0.383 | C | 0.712 | 0.475 | 0.356 |
| H | 3.281 | 2.557 | 2.196 | H | 2.922 | 2.318 | 2.016 |
| N | 2.073 | 2.070 | 2.069 | N | 1.799 | 1.798 | 1.797 |
| O | 2.015 | 1.710 | 1.558 | O | 1.935 | 1.633 | 1.482 |
| H/C | 2.567 | 3.001 | 3.437 | H/C | 2.462 | 2.930 | 3.400 |
| O/H | 0.614 | 0.669 | 0.709 | O/H | 0.662 | 0.704 | 0.735 |
| O/C | 1.577 | 2.007 | 2.438 | O/C | 1.630 | 2.064 | 2.499 |
| **Carbon Conversion: 80%** | | | | **Carbon Conversion: 80%** | | | |
| Element / | AR | | | Element / | AR | | |
| Elemental Ratio | 0.2 | 0.3 | 0.4 | Elemental Ratio | 0.2 | 0.3 | 0.4 |
| C | 1.022 | 0.682 | 0.511 | C | 0.950 | 0.633 | 0.474 |
| H | 3.281 | 2.557 | 2.196 | H | 2.922 | 2.318 | 2.016 |
| N | 2.073 | 2.070 | 2.069 | N | 1.799 | 1.798 | 1.797 |
| O | 2.015 | 1.710 | 1.558 | O | 1.935 | 1.633 | 1.482 |
| H/C | 1.063 | 0.829 | 0.712 | H/C | 2.462 | 2.930 | 3.400 |
| O/H | 0.614 | 0.669 | 0.709 | O/H | 0.662 | 0.704 | 0.735 |
| O/C | 0.653 | 0.554 | 0.505 | O/C | 1.630 | 2.064 | 2.499 |
| **Carbon Conversion: 100%** | | | | **Carbon Conversion: 100%** | | | |
| Element / | AR | | | Element / | AR | | |
| Elemental Ratio | 0.2 | 0.3 | 0.4 | Elemental Ratio | 0.2 | 0.3 | 0.4 |
| C | 1.278 | 0.852 | 0.639 | C | 1.187 | 0.791 | 0.593 |
| H | 3.281 | 2.557 | 2.196 | H | 2.922 | 2.318 | 2.016 |
| N | 2.073 | 2.070 | 2.069 | N | 1.799 | 1.798 | 1.797 |
| O | 2.015 | 1.710 | 1.558 | O | 1.935 | 1.633 | 1.482 |
| H/C | 1.063 | 0.829 | 0.712 | H/C | 2.462 | 2.930 | 3.400 |
| O/H | 0.614 | 0.669 | 0.709 | O/H | 0.662 | 0.704 | 0.735 |
| O/C | 0.653 | 0.554 | 0.505 | O/C | 1.630 | 2.064 | 2.499 |

### 7.5.5 Input for Kinetic Model

Input to the kinetic model is in terms of the molar flow rates of species forming out of pyrolysis of biomass entering the gasifier. The composition of the pyrolysis products depend on several factors such as biomass particle size, temperature, gasification medium etc. Several authors have studied the product distribution from fast pyrolysis of biomass particles, in which the biomass particles are suddenly expressed to high temperature environment (for example, Scott and Piskorz [81,82], Scott et al. [83], Beaumont and Schwob [84], Gray et al.

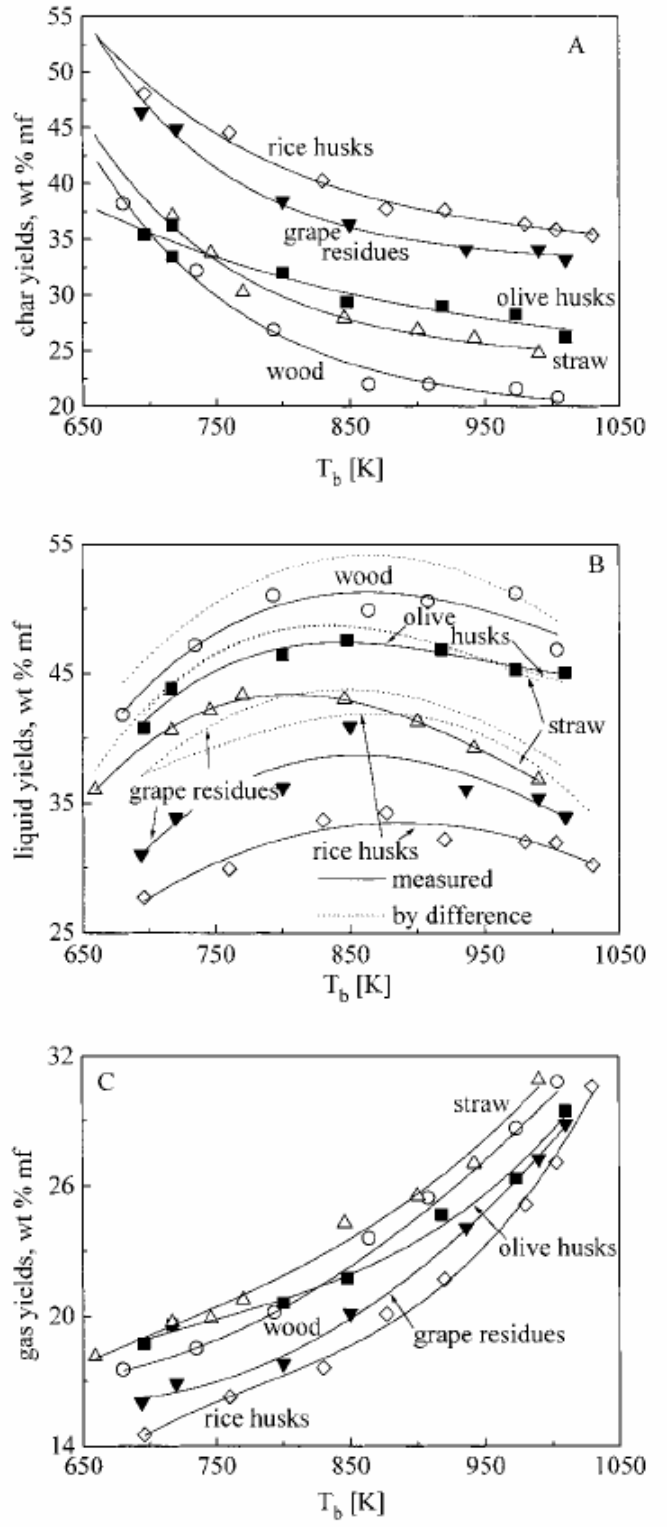


**Figure 7.1:** Yield of different pyrolysis products (as wt% of moisture free biomass): (A) char, (B) liquid or tar and (C) gas from various biomass, as a function of temperature of pyrolysis (reproduced from Di Blasi et al., 1999 with permission of ACS).

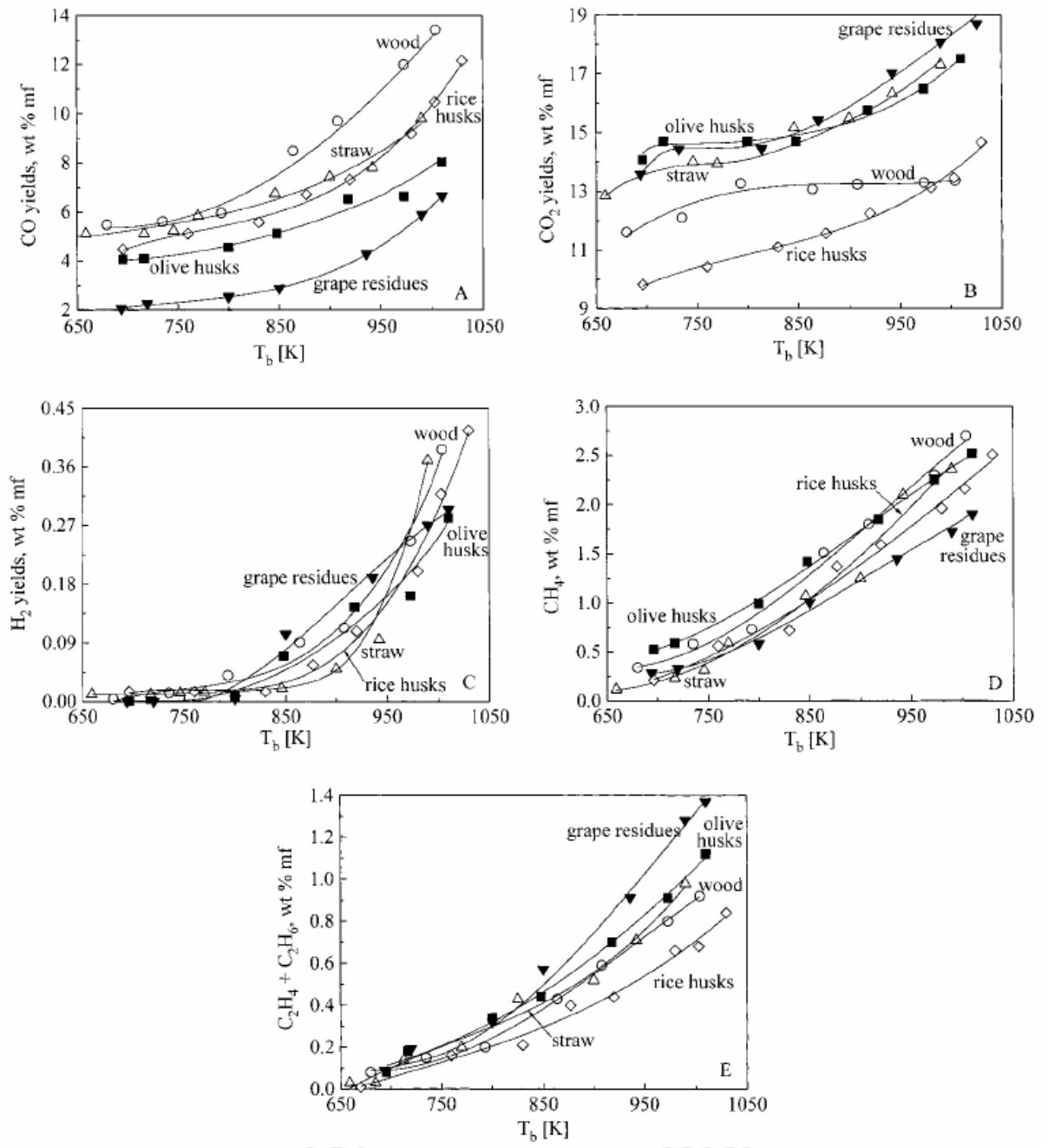


**Figure 7.2:** Yield of different gas species from pyrolysis of various biomass (as wt% of moisture free biomass): (A) CO, (B) $CO_2$, (C) $H_2$, (D) $CH_4$, (E) $C_2H_4 + C_2H_6$, as a function of temperature of pyrolysis (reproduced from Di Blasi et al., 1999 with permission of ACS).

[85], Nunn et al. [86], Kashiwagi et al. [87], Chan et al. [88], Bilbao et al. [89], Figueiredo et al. [90], Scott et al. [91], William and Besler [92], Jiang and Morey [18], Janse et al. [93], Di Blasi et al. [94]. The product distribution from pyrolysis is mainly a function of temperature.

**Table 7.5:** Pyrolysis Correlations

(A) Correlations for yield of various components resulting from rice husk pyrolysis

| Sr. No. | Component | Correlation |
|---|---|---|
| 1. | Char | $y_{char} = 1.055\times10^{-4}T^2 - 0.22016T + 150.4764$ |
| 2. | Tar | $y_{tar} = 1.582\times10^{-4}T^2 + 0.28218T - 92.1972$ |
| 3. | Gas (total) | $y_{gas} = 1.154\times10^{-4}T^2 - 0.15576T + 67.5489$ |
| | Individual gas Components | |
| 4. | CO | $y_{CO} = 7.261\times10^{-5}T^2 - 0.10416T + 42.0829$ |
| 5. | $CO_2$ | $y_{CO_2} = 2.534\times10^{-5}T^2 - 0.03036T + 18.7576$ |
| 6. | $H_2$ | $y_{H_2} = 6.198\times10^{-6}T^2 - 9.6545T + 3.75195$ |
| 7. | $CH_4$ | $y_{CH_4} = 7.954\times10^{-6}T^2 - 6.9416\times10^{-3}T + 1.2026$ |
| 8. | $C_2H_4$+$C_2H_6$ | $y_{C_2H_4+C_2H_6} = 3.568\times10^{-6}T^2 - 3.8788\times10^{-3}T + 1.01864$ |

(B) Correlations for yield of various components resulting from wood particles pyrolysis

| Sr. No. | Component | Correlation |
|---|---|---|
| 1. | Char | $y_{char} = -5.694\times10^{-9}T^2 + 1.897\times10^{-5}T^3 - 0.0233T^2 + 12.4438T - 2395.73$ |
| 2. | Tar | $y_{tar} = -1.114\times10^{-8}T^4 + 3.787\times10^{-5}T^3 - 0.04821T^2 + 27.247T - 5719.65$ |
| 3. | Gas (total) | $y_{gas} = 1.793\times10^{-9}T^4 - 6.198\times10^{-6}T^3 + 8.039\times10^{-3}T^2 - 4.5927T + 988.76$ |
| | Individual gas Components | |
| 4. | CO | $y_{CO} = 6.675\times10^{-10}T^4 - 2.437\times10^{-6}T^3 + 3.369\times10^{-3}T^2 - 2.05453T + 468.25$ |
| 5. | $CO_2$ | $y_{CO_2} = 1.342\times10^{-9}T^4 - 4.414\times10^{-6}T^3 + 5.373\times10^{-3}T^2 - 2.8624T + 574.28$ |
| 6. | $H_2$ | $y_{H_2} = 1.852\times10^{-10}T^4 - 5.478\times10^{-7}T^3 + 7.221\times10^{-4}T^2 - 0.38626T + 77.131$ |
| 7. | $CH_4$ | $y_{CH_4} = 2.338\times10^{-10}T^4 - 8.289\times10^{-7}T^3 + 1.1029\times10^{-3}T^2 - 0.64438T + 139.2$ |
| 8. | $C_2H_4$+$C_2H_6$ | $y_{C_2H_4+C_2H_6} = -1.133\times10^{-10}T^4 + 3.625\times10^{-7}T^3 - 4.25\times10^{-4}T^2 + 0.21849T - 41.686$ |

For our study, we take the results of Di Blasi et al. [94] on pyrolysis characteristics of agro–residues as basis.

Di Blasi et al. [94] have studied the pyrolysis of rice husk and wood particles, and have reported the distribution of pyrolysis products, viz. char, tar and gaseous species, viz. CO, $CO_2$, $H_2$, $CH_4$, $C_2H_4$ and $C_2H_6$ (on the basis of moisture free biomass) as a function of temperature of pyrolysis. We have reproduced the results of Di Blasi et al. in Figure 7.1 and 7.2. We have fitted polynomial expressions to the results of Di Blasi et al. [94]. The best fit

**Table 7.6:** Distribution of Products of Pyrolysis of Rice Husk at Different Temperatures and Air Ratio

(A) Temperature = 700°C

| Component | AR = 0.2 | | AR = 0.3 | | AR = 0.4 | |
|---|---|---|---|---|---|---|
| | Yield (kmol/s) | Concentration (kmol/m$^3$) | Yield (kmol/s) | Concentration (kmol/m$^3$) | Yield (kmol/s) | Concentration (kmol/m$^3$) |
| Char (kg/s) | 1.373E–02 | – | 9.179E–03 | – | 6.866E–03 | – |
| Tar | 7.741E–04 | 0.15663 | 5.174E–04 | 0.10469 | 1.704E–04 | 0.03447 |
| CO | 1.286E–04 | 0.02602 | 8.596E–05 | 0.01739 | 6.43E–05 | 0.01301 |
| $CO_2$ | 1.141E–04 | 0.02308 | 7.624E–05 | 0.01543 | 5.703E–05 | 0.01154 |
| $H_2$ | 4.293E–05 | 0.00869 | 2.87E–05 | 0.00581 | 2.147E–05 | 0.00434 |
| $CH_4$ | 4.7E–05 | 0.00951 | 3.141E–05 | 0.00636 | 2.35E–05 | 0.00475 |
| $C_2H_4$ | 4.224E–06 | 0.00085 | 2.823E–06 | 0.00057 | 2.112E–06 | 0.00043 |
| $C_2H_6$ | 3.942E–06 | 0.0008 | 2.635E–06 | 0.00053 | 1.971E–06 | 0.0004 |
| $H_2O$ | 2.111E–04 | 0.04272 | 1.411E–04 | 0.02855 | 1.056E–04 | 0.02136 |

(B) Temperature = 800°C

| Component | AR = 0.2 | | AR = 0.3 | | AR = 0.4 | |
|---|---|---|---|---|---|---|
| | Yield (kmol/s) | Concentration (kmol/m$^3$) | Yield (kmol/s) | Concentration (kmol/m$^3$) | Yield (kmol/s) | Concentration (kmol/m$^3$) |
| Char (kg/s) | 1.357E–02 | – | 8.927E–03 | – | 6.784E–03 | – |
| Tar | 6.755E–04 | 0.13669 | 4.444E–04 | 0.08993 | 3.378E–04 | 0.06834 |
| CO | 1.889E–04 | 0.03821 | 1.242E–04 | 0.02514 | 9.443E–05 | 0.01911 |
| $CO_2$ | 1.326E–04 | 0.02683 | 8.725E–05 | 0.01765 | 6.631E–05 | 0.01342 |
| $H_2$ | 1.004E–04 | 0.02032 | 6.608E–05 | 0.01337 | 5.022E–05 | 0.01016 |
| $CH_4$ | 6.916E–04 | 0.01399 | 4.550E–05 | 0.00921 | 3.458E–05 | 0.00700 |
| $C_2H_4$ | 6.546E–06 | 0.00132 | 4.306E–06 | 0.00087 | 3.273E–06 | 0.00066 |
| $C_2H_6$ | 6.109E–06 | 0.00124 | 4.019E–06 | 0.00081 | 3.055E–06 | 0.00062 |
| $H_2O$ | 2.111E–04 | 0.04272 | 1.389E–04 | 0.02810 | 1.056E–04 | 0.02136 |

**Table 7.7:** Distribution of products of pyrolysis of wood particles at different temperatures and air ratios

(A) Temperature = 700°C

| Component | AR = 0.2 | | AR = 0.3 | | AR = 0.4 | |
|---|---|---|---|---|---|---|
| | Yield (kmol/s) | Concentration (kmol/m$^3$) | Yield (kmol/s) | Concentration (kmol/m$^3$) | Yield (kmol/s) | Concentration (kmol/m$^3$) |
| Char (kg/s) | 6.964E–03 | – | 4.718E–03 | – | 3.594E–03 | – |
| Tar | 9.474E–04 | 0.1917 | 6.418E–04 | 0.12986 | 4.89E–04 | 0.09894 |
| CO | 1.351E–04 | 0.02734 | 9.154E–05 | 0.01852 | 6.974E–05 | 0.01411 |
| $CO_2$ | 8.981E–05 | 0.01817 | 6.084E–05 | 0.01231 | 4.636E–05 | 0.00938 |
| $H_2$ | 3.92E–05 | 0.00793 | 2.655E–05 | 0.00537 | 2.023E–05 | 0.00409 |
| $CH_4$ | 4.591E–05 | 0.00929 | 3.11E–05 | 0.00629 | 2.369E–05 | 0.00479 |
| $C_2H_4$ | 5.07E–06 | 0.00103 | 3.435E–06 | 0.00069 | 2.617E–06 | 0.00053 |
| $C_2H_6$ | 4.732E–06 | 0.00096 | 3.206E–06 | 0.00065 | 2.442E–06 | 0.00049 |
| $H_2O$ | 1.722E–04 | 0.03485 | 1.167E–04 | 0.02361 | 8.889E–05 | 0.01799 |

(B) Temperature = 800°C

| Component | AR = 0.2 | | AR = 0.3 | | AR = 0.4 | |
|---|---|---|---|---|---|---|
| | Yield (kmol/s) | Concentration (kmol/m$^3$) | Yield (kmol/s) | Concentration (kmol/m$^3$) | Yield (kmol/s) | Concentration (kmol/m$^3$) |
| Char (kg/s) | 4.781E–03 | – | 3.177E–03 | – | 2.336E–03 | – |
| Tar | 5.132E–04 | 0.10384 | 3.410E–04 | 0.06900 | 2.507E–04 | 0.05074 |
| CO | 1.850E–04 | 0.03744 | 1.230E–04 | 0.02488 | 9.041E–05 | 0.01829 |
| $CO_2$ | 1.045E–04 | 0.02114 | 6.944E–05 | 0.01405 | 5.106E–05 | 0.01033 |
| $H_2$ | 1.587E–04 | 0.03212 | 1.055E–04 | 0.02134 | 7.755E–05 | 0.01569 |
| $CH_4$ | 6.714E–05 | 0.01358 | 4.461E–05 | 0.00903 | 3.280E–05 | 0.00664 |
| $C_2H_4$ | 5.893E–06 | 0.00119 | 3.916E–06 | 0.00079 | 2.879E–06 | 0.00058 |
| $C_2H_6$ | 5.500E–06 | 0.00111 | 3.655E–06 | 0.00074 | 2.687E–06 | 0.00054 |
| $H_2O$ | 1.706E–04 | 0.03451 | 1.133E–04 | 0.02293 | 8.333E–05 | 0.01686 |

expressions for yields of various species are listed in Table 7.5(A) and (B) for rice husk and wood particles, respectively. The actual yield of these species (in either kg/s or kmol/s) at gasification temperature of 973 and 1073 K (700 and 800 $^{o}$C) and air ratios of 0.2, 0.3 and 0.4 is given in Tables 7.6 and 7.7 for rice husk and wood particles, respectively. These values form input to the kinetic model.

The extent of carbon conversion for kinetic model is determined by residence time of gasification mixture in the riser section. This factor is determined by the velocity of the gasification mixture and the length of the riser. We have considered two lengths of the riser, viz. 6 m and 10 m above the turbulent sand bed from which the pyrolysis products emerge. This would essentially give reaction volumes of 0.0486 and 0.081 m$^3$, respectively.

### 7.5.6 Simulation Sets

With permutation–combination of 3 air ratios (0.2, 0.3 and 0.4), 2 gasification temperatures (700 and 800$^{o}$C), and 3 levels of carbon conversions (viz. 100% for equilibrium model and 60 and 80% for semi–equilibrium model), we get 18 simulation sets with thermodynamic equilibrium and semi–equilibrium models for each biomass, viz. rice husk and wood particles. For the kinetic model, we have essentially 12 simulation sets for each biomass with permutation combination of 3 air ratios, 2 gasification temperatures and two reaction volumes.

## 7.6 Results and Discussion

We have presented the results of simulations in three parts. We begin with presentation of the results with kinetic model, followed by results with equilibrium and semi–equilibrium models. Finally, we present a comparative analysis of the results with all three models. The simulation results for all three models comprise of: (1) the molar composition of the gas, (2) net yield (Nm$^3$) of the gas, and (3) the LHV (MJ/Nm$^3$) of the gas. In case of

kinetic model, we have also presented the profiles of char formation and char gasification /combustion under different sets of operating conditions. Figures 7.3 and 7.4 depict the molar composition of producer gas calculated for rice husk using kinetic model for different air ratios at 700 and 800$^{o}$C respectively, while Figures 7.5 and 7.6 present the molar composition of producer gas for wood particles gasification at 700 and 800$^{o}$C. Figure 7.7 shows the trends in formation of char (as wt% of initial moisture free biomass) for rice husk and wood particles, while Figure 7.8 shows the extent of gasification of char (wt% of initial char ) in the riser at different gasification of char (wt% of initial char) in the riser at different air ratios and temperature. Figures 7.9 and 7.10 show molar composition of producer gas resulting from gasification of rice husk at 700$^{o}$C and 800$^{o}$C using equilibrium and semi–equilibrium models. Figures 7.11 and 7.12 depict the molar composition of producer gas for wood particle gasification calculated using equilibrium and semi–equilibrium models at 700$^{o}$C and 800$^{o}$C respectively. Figures 7.13 and 7.14 describe the trends in net producer gas yield and LHV of the producer gas resulting from gasification of wood particles and rice husk, respectively, calculated using kinetic model under different gasifying conditions. Figures 7.15 and 7.16 show the trends of producer gas yield and LHV of the gas for wood particles and rice husk gasification under different conditions calculated using equilibrium and semi–equilibrium models. For convenience of the readers, we have also added data tables in Figures 7.3–7.5 and 7.9–7.16. In our analysis, we initially identify the (qualitative) trends in the molar of gas, producer gas yield, LHV of the gas and the composition of gas and char formation/gasification (in case of kinetic model only) for the two models. Subsequently, we attempt to do quantitative comparison of the simulation results with various models.

### 7.6.1 Analysis of Results of Kinetic Model

*Trends in Molar Composition of producer Gas:* The composition of products resulting from pyrolysis of biomass emanating from the hot sand bed (or the pyrolysis zone) is given in

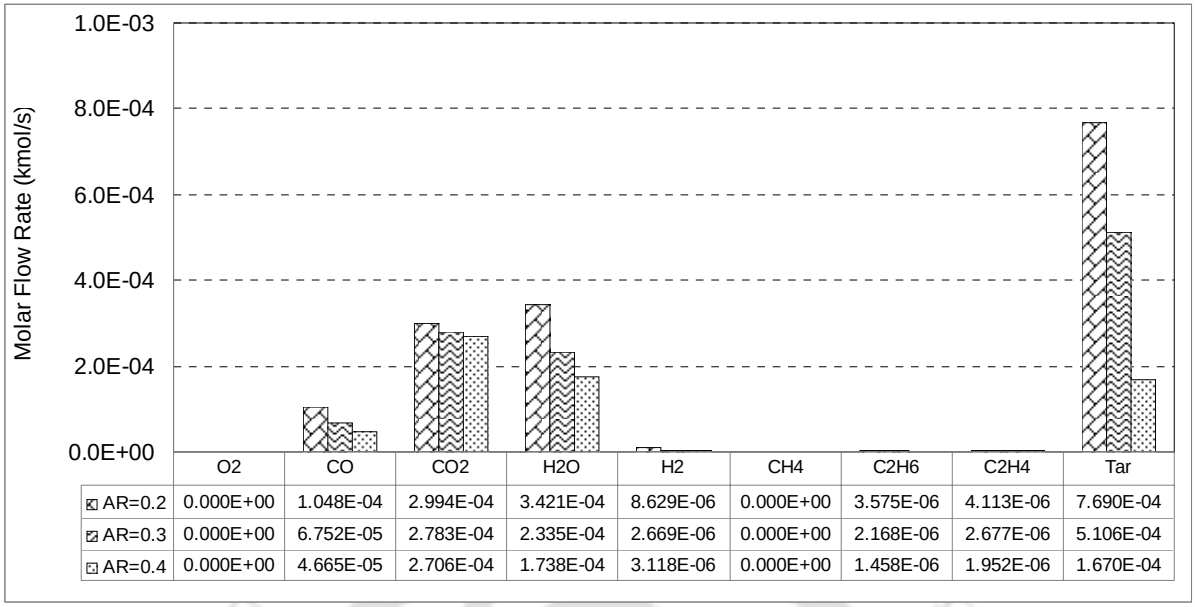


| | O2 | CO | CO2 | H2O | H2 | CH4 | C2H6 | C2H4 | Tar |
|---|---|---|---|---|---|---|---|---|---|
| AR=0.2 | 0.000E+00 | 1.048E-04 | 2.994E-04 | 3.421E-04 | 8.629E-06 | 0.000E+00 | 3.575E-06 | 4.113E-06 | 7.690E-04 |
| AR=0.3 | 0.000E+00 | 6.752E-05 | 2.783E-04 | 2.335E-04 | 2.669E-06 | 0.000E+00 | 2.168E-06 | 2.677E-06 | 5.106E-04 |
| AR=0.4 | 0.000E+00 | 4.665E-05 | 2.706E-04 | 1.738E-04 | 3.118E-06 | 0.000E+00 | 1.458E-06 | 1.952E-06 | 1.670E-04 |

(A)

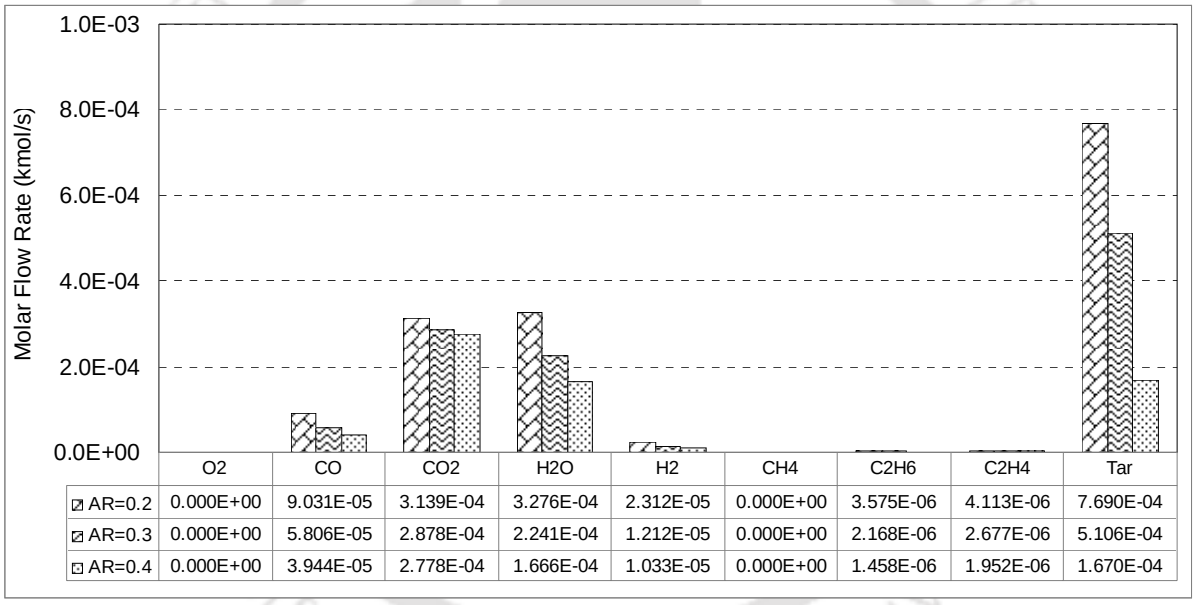


| | O2 | CO | CO2 | H2O | H2 | CH4 | C2H6 | C2H4 | Tar |
|---|---|---|---|---|---|---|---|---|---|
| AR=0.2 | 0.000E+00 | 9.031E-05 | 3.139E-04 | 3.276E-04 | 2.312E-05 | 0.000E+00 | 3.575E-06 | 4.113E-06 | 7.690E-04 |
| AR=0.3 | 0.000E+00 | 5.806E-05 | 2.878E-04 | 2.241E-04 | 1.212E-05 | 0.000E+00 | 2.168E-06 | 2.677E-06 | 5.106E-04 |
| AR=0.4 | 0.000E+00 | 3.944E-05 | 2.778E-04 | 1.666E-04 | 1.033E-05 | 0.000E+00 | 1.458E-06 | 1.952E-06 | 1.670E-04 |

(B)

**Figure 7.3:** Results of simulations with kinetic model for rice husk for different gasifying conditions. (A) Temperature = 973 K, Volume = 0.0486 $m^3$. (B) Temperature = 973 K, Volume = 0.08105 $m^3$.

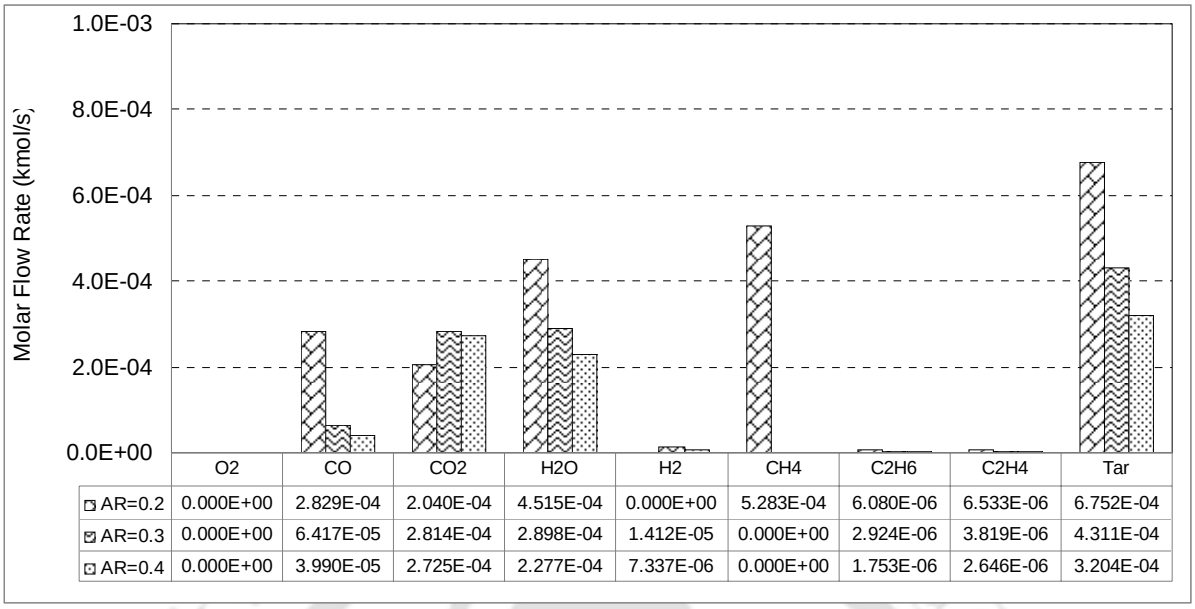


| | O2 | CO | CO2 | H2O | H2 | CH4 | C2H6 | C2H4 | Tar |
|---|---|---|---|---|---|---|---|---|---|
| AR=0.2 | 0.000E+00 | 2.829E-04 | 2.040E-04 | 4.515E-04 | 0.000E+00 | 5.283E-04 | 6.080E-06 | 6.533E-06 | 6.752E-04 |
| AR=0.3 | 0.000E+00 | 6.417E-05 | 2.814E-04 | 2.898E-04 | 1.412E-05 | 0.000E+00 | 2.924E-06 | 3.819E-06 | 4.311E-04 |
| AR=0.4 | 0.000E+00 | 3.990E-05 | 2.725E-04 | 2.277E-04 | 7.337E-06 | 0.000E+00 | 1.753E-06 | 2.646E-06 | 3.204E-04 |

(A)

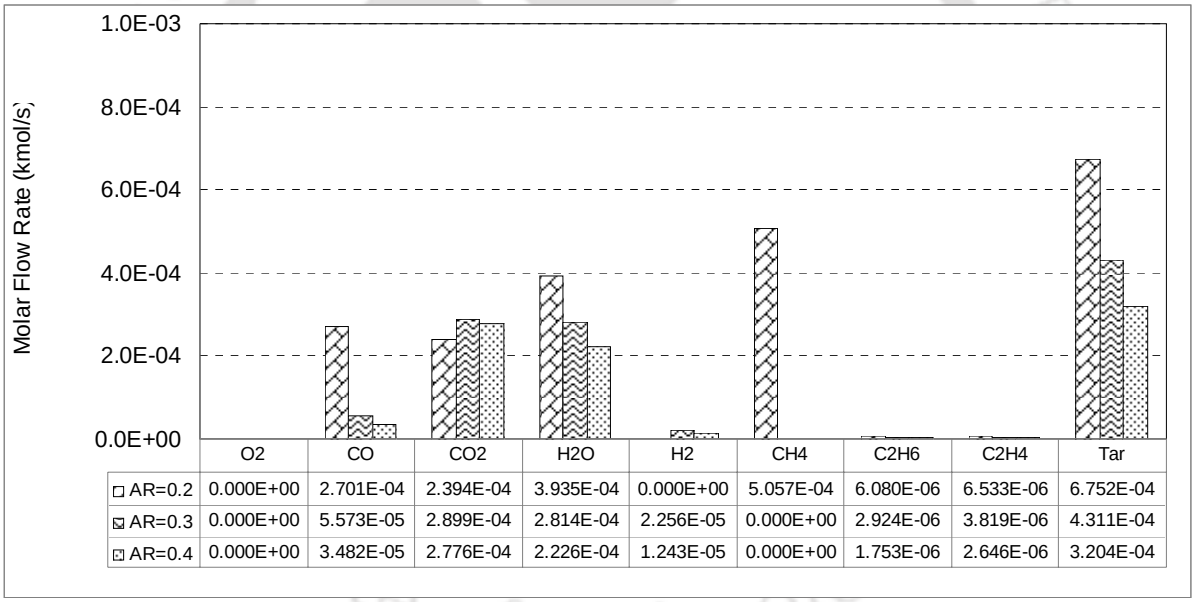


| | O2 | CO | CO2 | H2O | H2 | CH4 | C2H6 | C2H4 | Tar |
|---|---|---|---|---|---|---|---|---|---|
| AR=0.2 | 0.000E+00 | 2.701E-04 | 2.394E-04 | 3.935E-04 | 0.000E+00 | 5.057E-04 | 6.080E-06 | 6.533E-06 | 6.752E-04 |
| AR=0.3 | 0.000E+00 | 5.573E-05 | 2.899E-04 | 2.814E-04 | 2.256E-05 | 0.000E+00 | 2.924E-06 | 3.819E-06 | 4.311E-04 |
| AR=0.4 | 0.000E+00 | 3.482E-05 | 2.776E-04 | 2.226E-04 | 1.243E-05 | 0.000E+00 | 1.753E-06 | 2.646E-06 | 3.204E-04 |

(B)

**Figure 7.4:** Results of simulations with kinetic model for rice husk for different gasifying conditions. (A) Temperature = 1073 K, Volume = 0.0486 $m^3$. (B) Temperature = 1073 K, Volume = 0.08105 $m^3$.

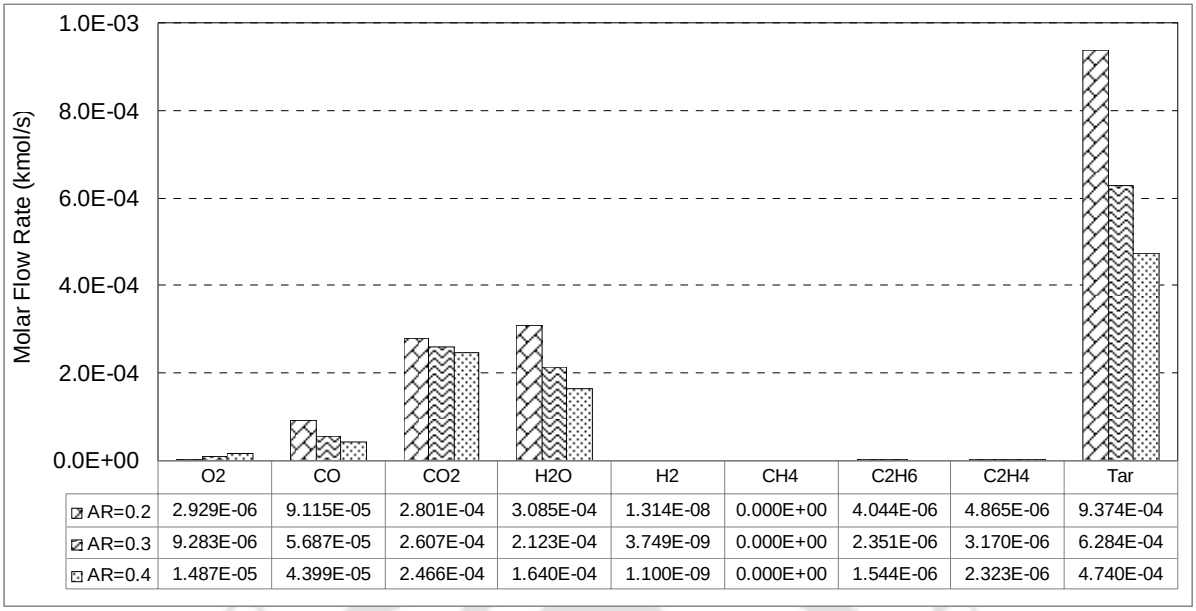


| | O2 | CO | CO2 | H2O | H2 | CH4 | C2H6 | C2H4 | Tar |
|---|---|---|---|---|---|---|---|---|---|
| AR=0.2 | 2.929E-06 | 9.115E-05 | 2.801E-04 | 3.085E-04 | 1.314E-08 | 0.000E+00 | 4.044E-06 | 4.865E-06 | 9.374E-04 |
| AR=0.3 | 9.283E-06 | 5.687E-05 | 2.607E-04 | 2.123E-04 | 3.749E-09 | 0.000E+00 | 2.351E-06 | 3.170E-06 | 6.284E-04 |
| AR=0.4 | 1.487E-05 | 4.399E-05 | 2.466E-04 | 1.640E-04 | 1.100E-09 | 0.000E+00 | 1.544E-06 | 2.323E-06 | 4.740E-04 |

(A)

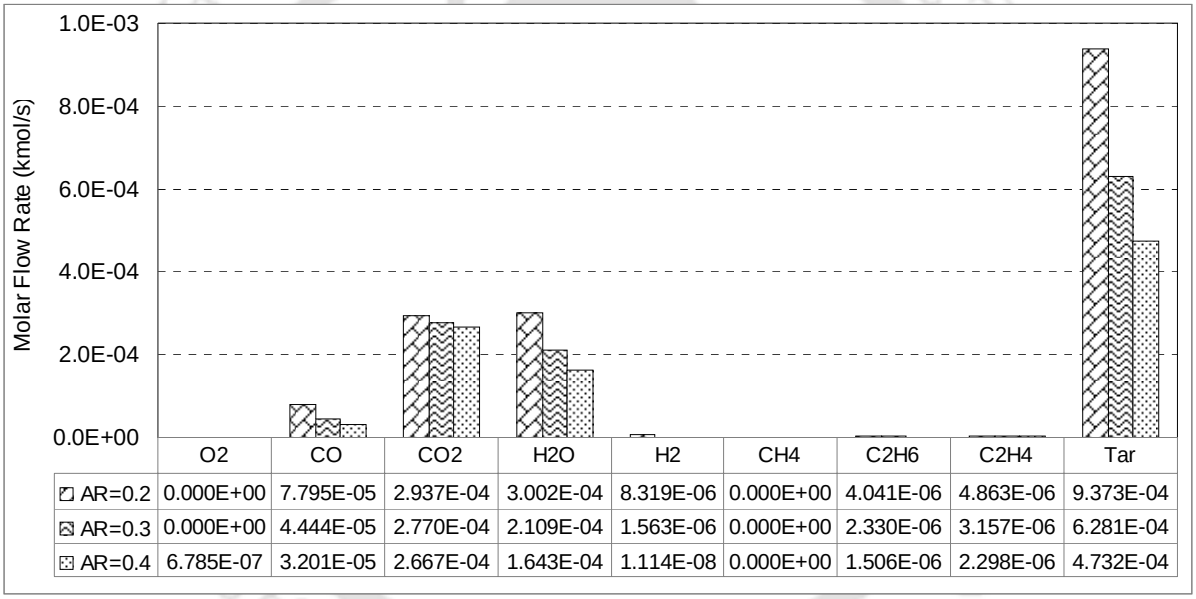


| | O2 | CO | CO2 | H2O | H2 | CH4 | C2H6 | C2H4 | Tar |
|---|---|---|---|---|---|---|---|---|---|
| AR=0.2 | 0.000E+00 | 7.795E-05 | 2.937E-04 | 3.002E-04 | 8.319E-06 | 0.000E+00 | 4.041E-06 | 4.863E-06 | 9.373E-04 |
| AR=0.3 | 0.000E+00 | 4.444E-05 | 2.770E-04 | 2.109E-04 | 1.563E-06 | 0.000E+00 | 2.330E-06 | 3.157E-06 | 6.281E-04 |
| AR=0.4 | 6.785E-07 | 3.201E-05 | 2.667E-04 | 1.643E-04 | 1.114E-08 | 0.000E+00 | 1.506E-06 | 2.298E-06 | 4.732E-04 |

(B)

**Figure 7.5:** Results of simulations with kinetic model for wood particles for different gasifying conditions. (A) Temperature = 973 K, Volume = 0.0486 $m^3$. (B) Temperature = 973 K, Volume = 0.08105 $m^3$.

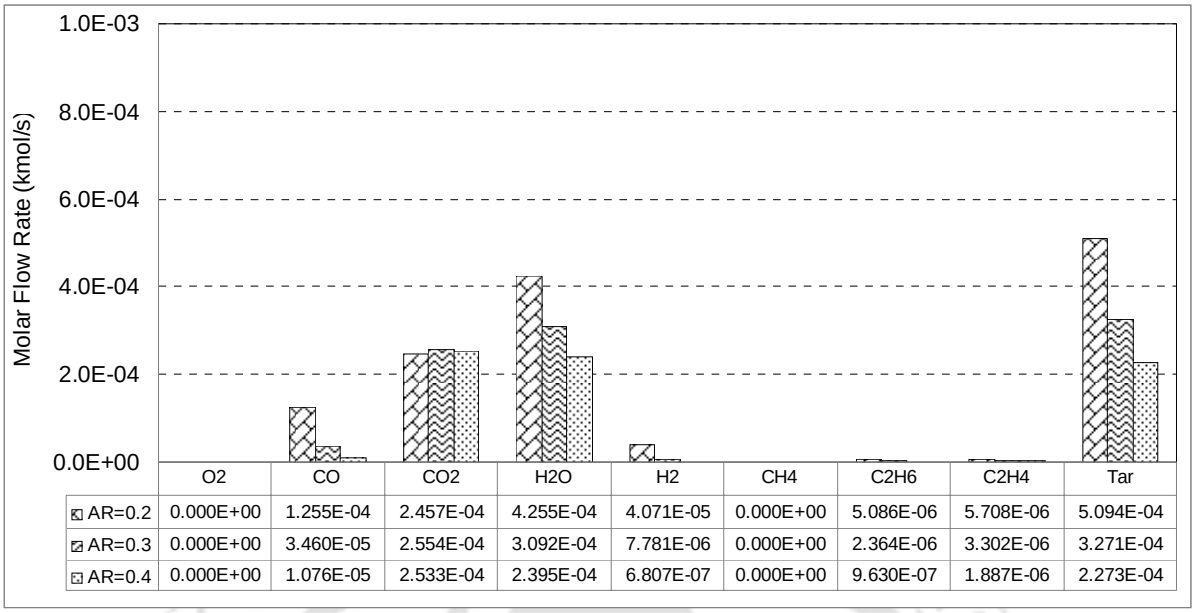


| | O2 | CO | CO2 | H2O | H2 | CH4 | C2H6 | C2H4 | Tar |
|---|---|---|---|---|---|---|---|---|---|
| AR=0.2 | 0.000E+00 | 1.255E-04 | 2.457E-04 | 4.255E-04 | 4.071E-05 | 0.000E+00 | 5.086E-06 | 5.708E-06 | 5.094E-04 |
| AR=0.3 | 0.000E+00 | 3.460E-05 | 2.554E-04 | 3.092E-04 | 7.781E-06 | 0.000E+00 | 2.364E-06 | 3.302E-06 | 3.271E-04 |
| AR=0.4 | 0.000E+00 | 1.076E-05 | 2.533E-04 | 2.395E-04 | 6.807E-07 | 0.000E+00 | 9.630E-07 | 1.887E-06 | 2.273E-04 |

(A)

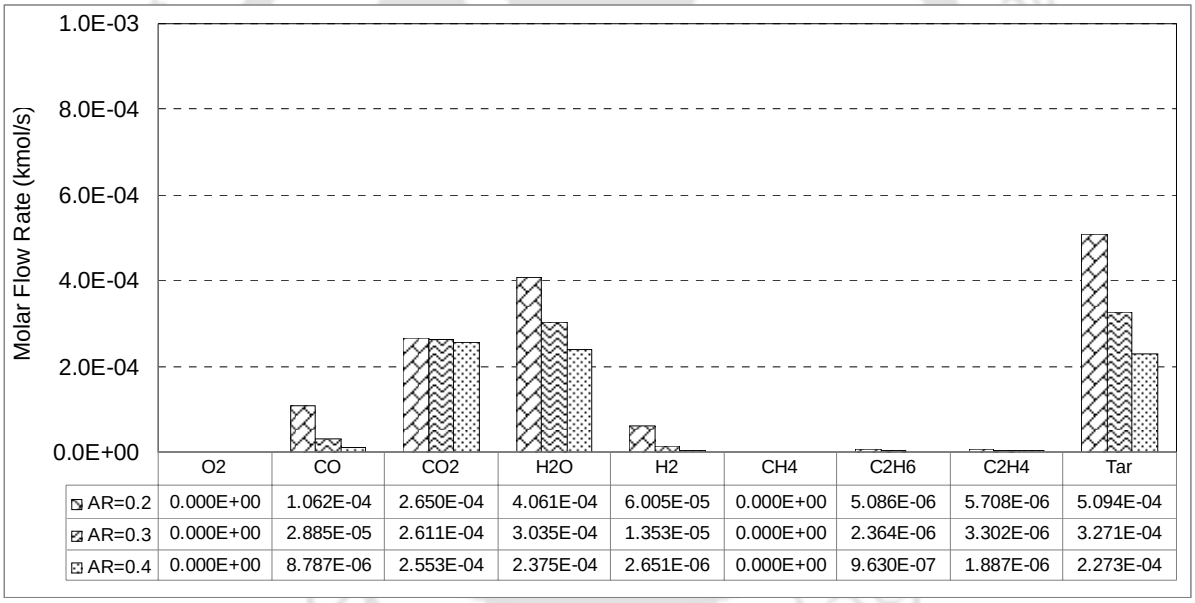


| | O2 | CO | CO2 | H2O | H2 | CH4 | C2H6 | C2H4 | Tar |
|---|---|---|---|---|---|---|---|---|---|
| AR=0.2 | 0.000E+00 | 1.062E-04 | 2.650E-04 | 4.061E-04 | 6.005E-05 | 0.000E+00 | 5.086E-06 | 5.708E-06 | 5.094E-04 |
| AR=0.3 | 0.000E+00 | 2.885E-05 | 2.611E-04 | 3.035E-04 | 1.353E-05 | 0.000E+00 | 2.364E-06 | 3.302E-06 | 3.271E-04 |
| AR=0.4 | 0.000E+00 | 8.787E-06 | 2.553E-04 | 2.375E-04 | 2.651E-06 | 0.000E+00 | 9.630E-07 | 1.887E-06 | 2.273E-04 |

(B)

**Figure 7.6:** Results of simulations with kinetic model for wood particles for different gasifying conditions. (A) Temperature = 1073 K, Volume = 0.0486 $m^3$. (B) Temperature = 1073 K, Volume = 0.08105 $m^3$.

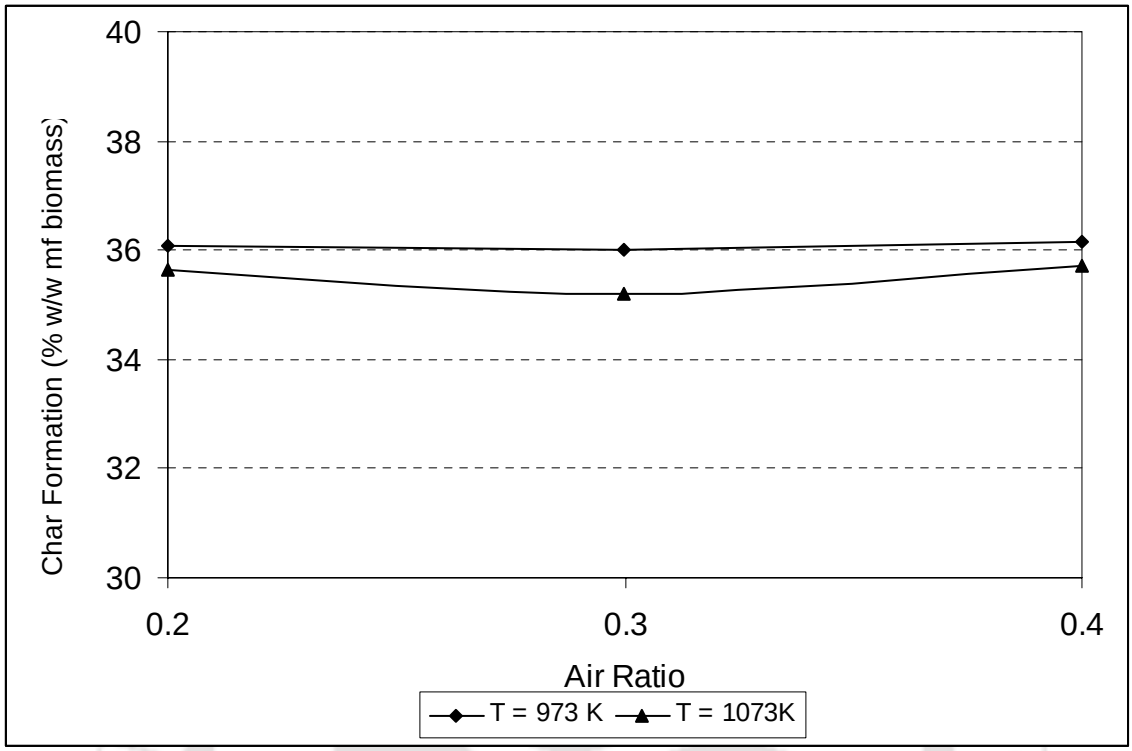


(A)

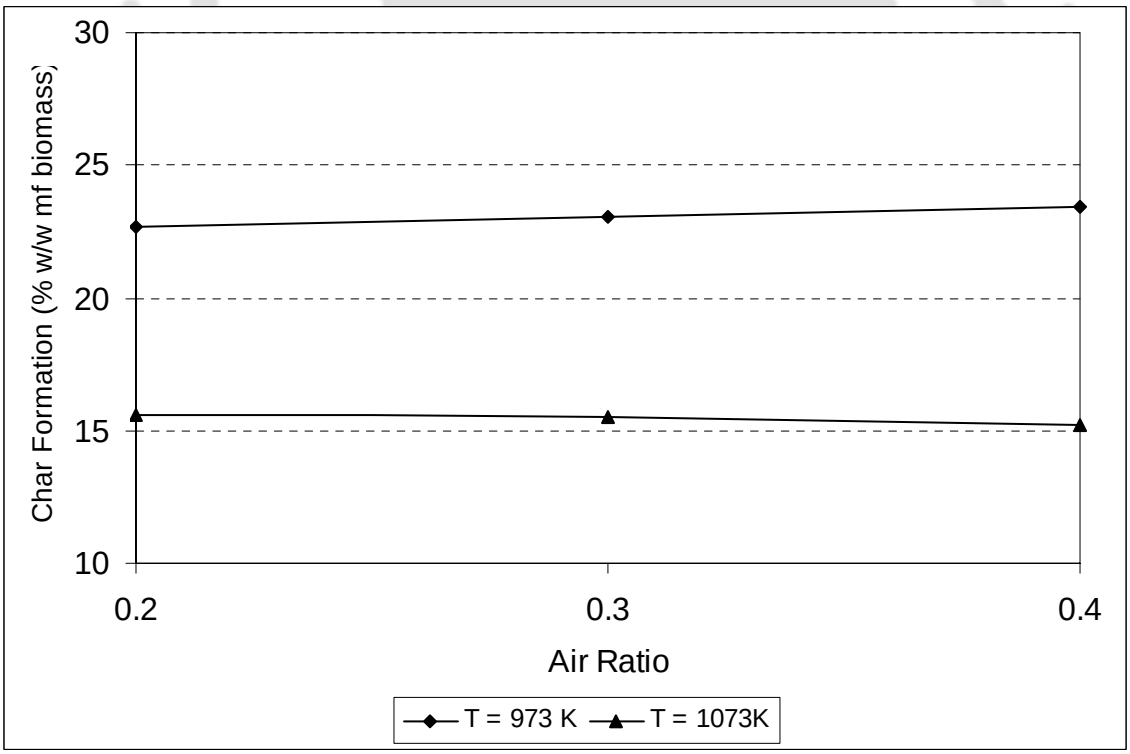


(B)

**Figure 7.7:** Trends in char formation (as wt % of initial moisture free biomass in the pyrolysis zone at the entry of the gasifier. (A) Biomass: Rice husk, (B) Biomass: Wood particles

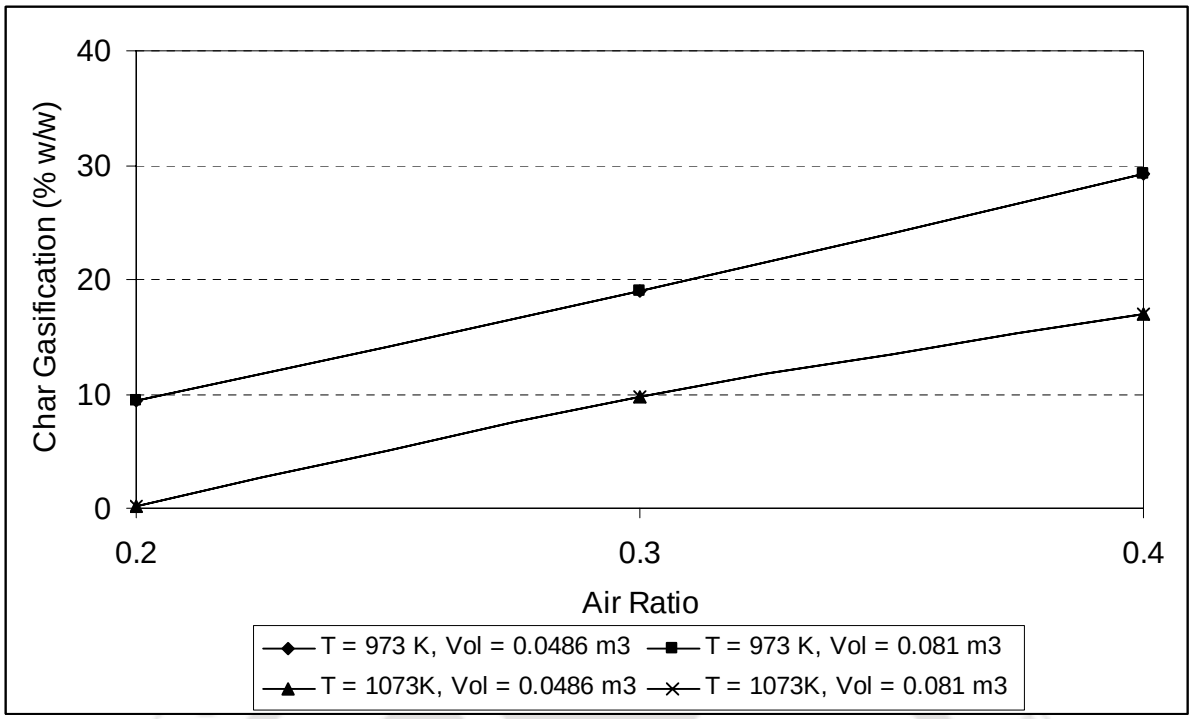


(A)

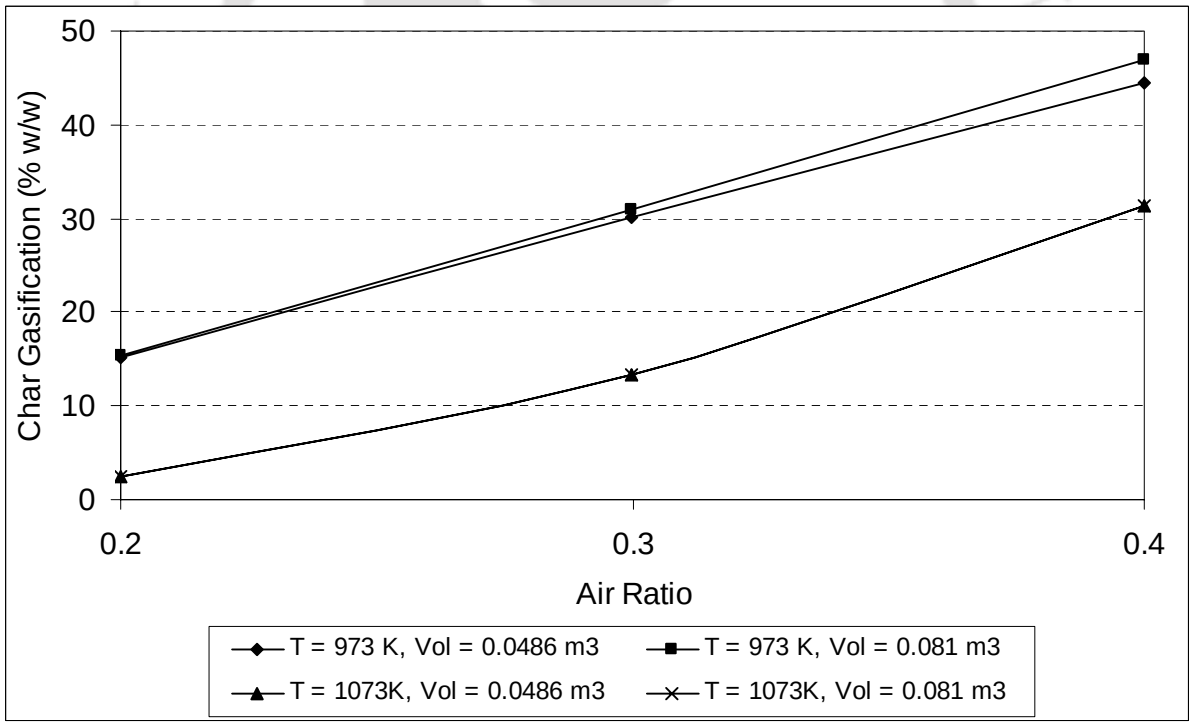


(B)

**Figure 7.8:** Results of char gasification (wt % of initial char gasified) in the riser section above pyrolysis. (A) Biomass: Rice husk, (B) Biomass: Wood particles

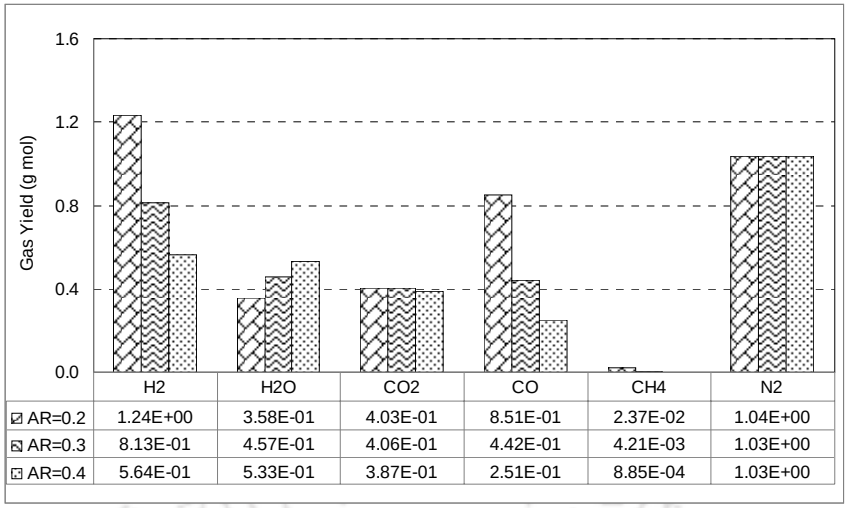


| | H2 | H2O | CO2 | CO | CH4 | N2 |
|---|---|---|---|---|---|---|
| AR=0.2 | 1.24E+00 | 3.58E-01 | 4.03E-01 | 8.51E-01 | 2.37E-02 | 1.04E+00 |
| AR=0.3 | 8.13E-01 | 4.57E-01 | 4.06E-01 | 4.42E-01 | 4.21E-03 | 1.03E+00 |
| AR=0.4 | 5.64E-01 | 5.33E-01 | 3.87E-01 | 2.51E-01 | 8.85E-04 | 1.03E+00 |

(A)

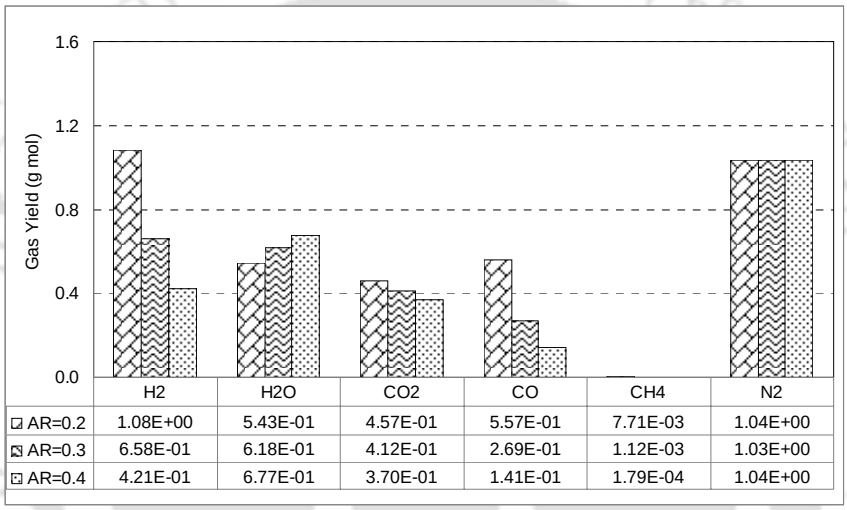


| | H2 | H2O | CO2 | CO | CH4 | N2 |
|---|---|---|---|---|---|---|
| AR=0.2 | 1.08E+00 | 5.43E-01 | 4.57E-01 | 5.57E-01 | 7.71E-03 | 1.04E+00 |
| AR=0.3 | 6.58E-01 | 6.18E-01 | 4.12E-01 | 2.69E-01 | 1.12E-03 | 1.03E+00 |
| AR=0.4 | 4.21E-01 | 6.77E-01 | 3.70E-01 | 1.41E-01 | 1.79E-04 | 1.04E+00 |

(B)

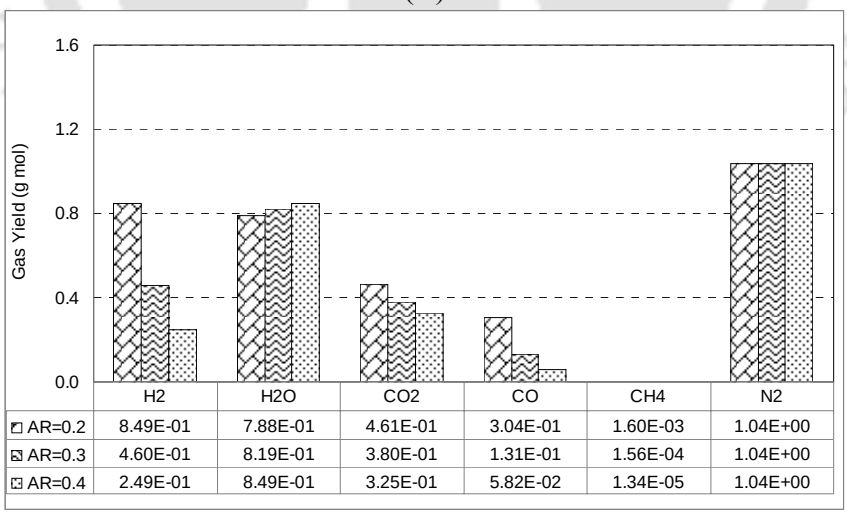


| | H2 | H2O | CO2 | CO | CH4 | N2 |
|---|---|---|---|---|---|---|
| AR=0.2 | 8.49E-01 | 7.88E-01 | 4.61E-01 | 3.04E-01 | 1.60E-03 | 1.04E+00 |
| AR=0.3 | 4.60E-01 | 8.19E-01 | 3.80E-01 | 1.31E-01 | 1.56E-04 | 1.04E+00 |
| AR=0.4 | 2.49E-01 | 8.49E-01 | 3.25E-01 | 5.82E-02 | 1.34E-05 | 1.04E+00 |

(C)

**Figure 7.9:** Results of simulations of biomass gasification with equilibrium and semi-equilibrium models for rice husk under different gasifying conditions. (A) Temperature = 973 K, Carbon conversion = 100%. (B) Temperature = 973 K, Carbon conversion = 80%. (C) Temperature = 973 K, Carbon conversion = 60%.

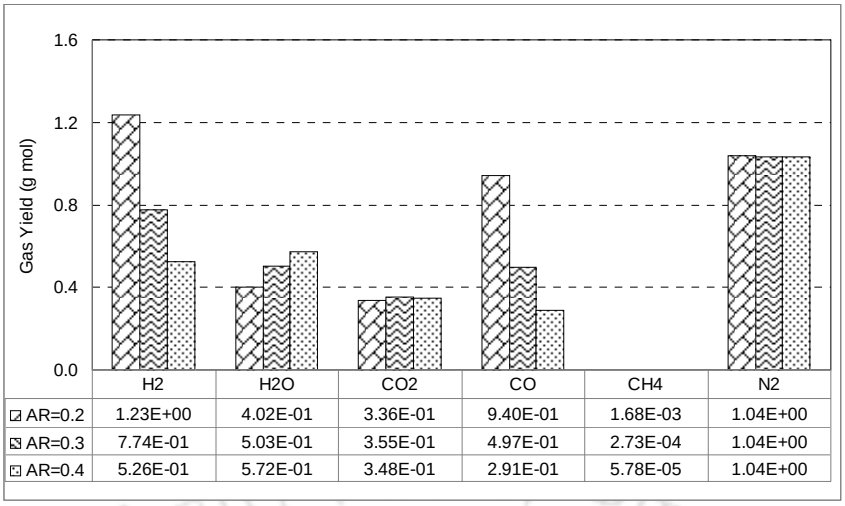


| | H2 | H2O | CO2 | CO | CH4 | N2 |
|---|---|---|---|---|---|---|
| AR=0.2 | 1.23E+00 | 4.02E-01 | 3.36E-01 | 9.40E-01 | 1.68E-03 | 1.04E+00 |
| AR=0.3 | 7.74E-01 | 5.03E-01 | 3.55E-01 | 4.97E-01 | 2.73E-04 | 1.04E+00 |
| AR=0.4 | 5.26E-01 | 5.72E-01 | 3.48E-01 | 2.91E-01 | 5.78E-05 | 1.04E+00 |

(A)

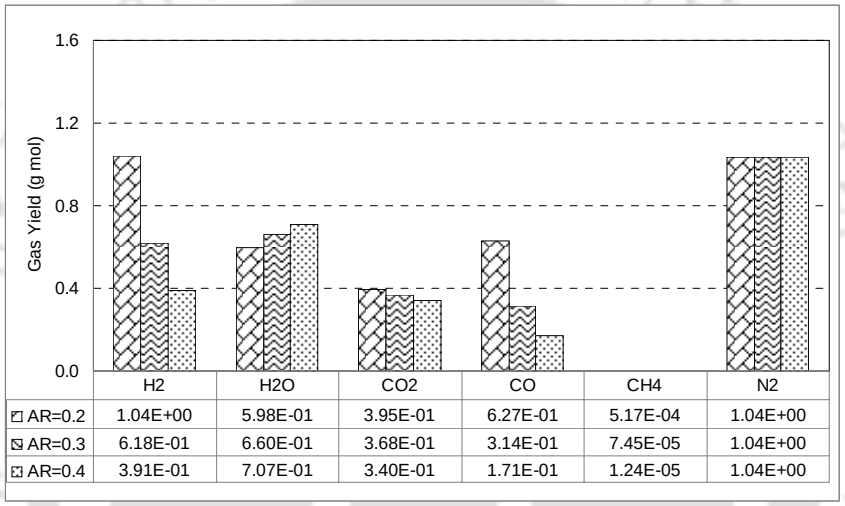


| | H2 | H2O | CO2 | CO | CH4 | N2 |
|---|---|---|---|---|---|---|
| AR=0.2 | 1.04E+00 | 5.98E-01 | 3.95E-01 | 6.27E-01 | 5.17E-04 | 1.04E+00 |
| AR=0.3 | 6.18E-01 | 6.60E-01 | 3.68E-01 | 3.14E-01 | 7.45E-05 | 1.04E+00 |
| AR=0.4 | 3.91E-01 | 7.07E-01 | 3.40E-01 | 1.71E-01 | 1.24E-05 | 1.04E+00 |

(B)

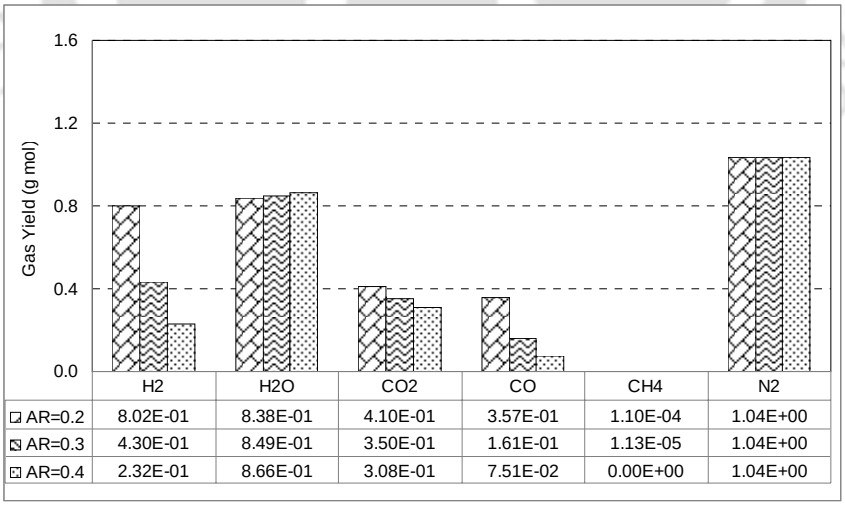


| | H2 | H2O | CO2 | CO | CH4 | N2 |
|---|---|---|---|---|---|---|
| AR=0.2 | 8.02E-01 | 8.38E-01 | 4.10E-01 | 3.57E-01 | 1.10E-04 | 1.04E+00 |
| AR=0.3 | 4.30E-01 | 8.49E-01 | 3.50E-01 | 1.61E-01 | 1.13E-05 | 1.04E+00 |
| AR=0.4 | 2.32E-01 | 8.66E-01 | 3.08E-01 | 7.51E-02 | 0.00E+00 | 1.04E+00 |

(C)

**Figure 7.10:** Results of simulations of biomass gasification with equilibrium and semi-equilibrium models for rice husk under different gasifying conditions. (A) Temperature = 1073 K, Carbon conversion = 100%. (B) Temperature = 1073 K, Carbon conversion = 80%. (C) Temperature = 1073 K, Carbon conversion = 60%.

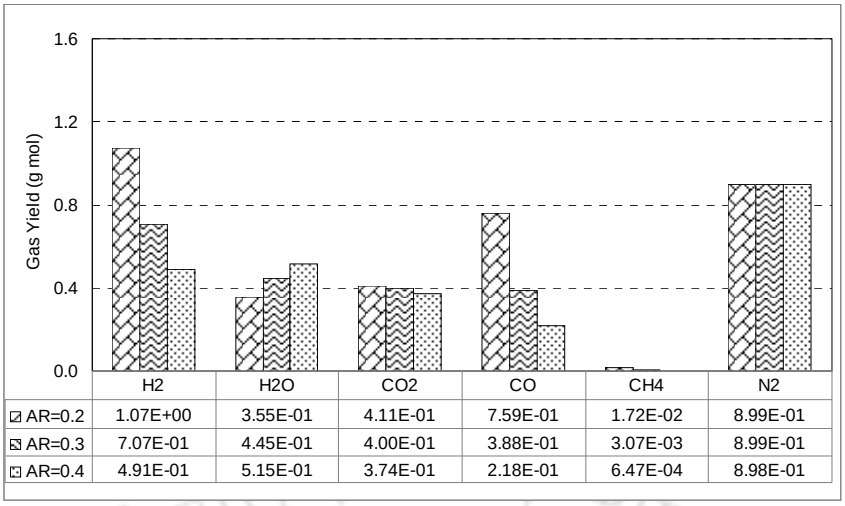


| | H2 | H2O | CO2 | CO | CH4 | N2 |
|---|---|---|---|---|---|---|
| AR=0.2 | 1.07E+00 | 3.55E-01 | 4.11E-01 | 7.59E-01 | 1.72E-02 | 8.99E-01 |
| AR=0.3 | 7.07E-01 | 4.45E-01 | 4.00E-01 | 3.88E-01 | 3.07E-03 | 8.99E-01 |
| AR=0.4 | 4.91E-01 | 5.15E-01 | 3.74E-01 | 2.18E-01 | 6.47E-04 | 8.98E-01 |

(A)

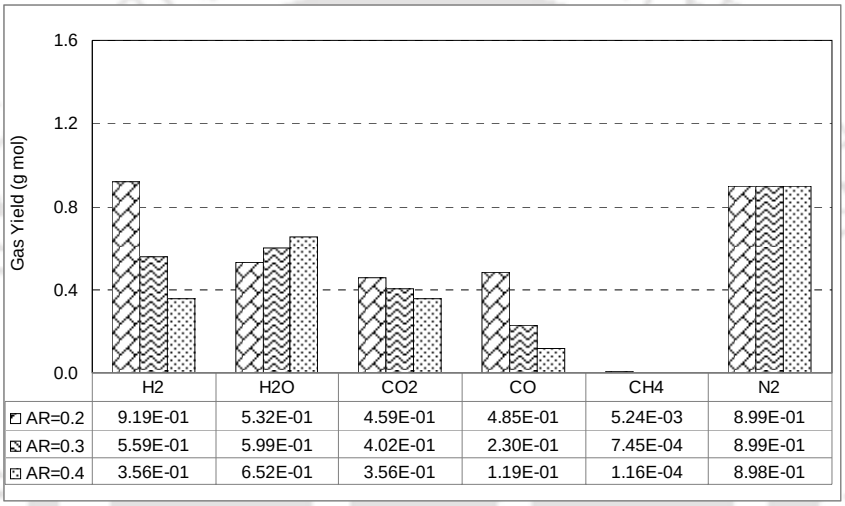


| | H2 | H2O | CO2 | CO | CH4 | N2 |
|---|---|---|---|---|---|---|
| AR=0.2 | 9.19E-01 | 5.32E-01 | 4.59E-01 | 4.85E-01 | 5.24E-03 | 8.99E-01 |
| AR=0.3 | 5.59E-01 | 5.99E-01 | 4.02E-01 | 2.30E-01 | 7.45E-04 | 8.99E-01 |
| AR=0.4 | 3.56E-01 | 6.52E-01 | 3.56E-01 | 1.19E-01 | 1.16E-04 | 8.98E-01 |

(B)

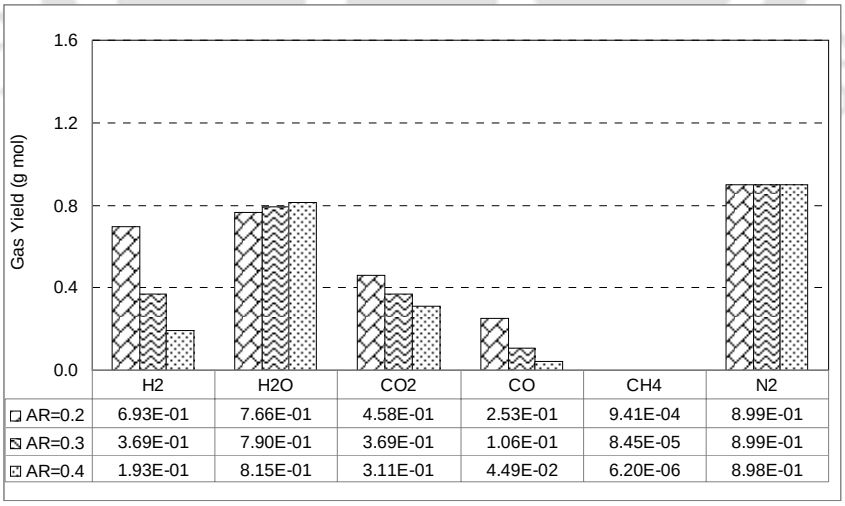


| | H2 | H2O | CO2 | CO | CH4 | N2 |
|---|---|---|---|---|---|---|
| AR=0.2 | 6.93E-01 | 7.66E-01 | 4.58E-01 | 2.53E-01 | 9.41E-04 | 8.99E-01 |
| AR=0.3 | 3.69E-01 | 7.90E-01 | 3.69E-01 | 1.06E-01 | 8.45E-05 | 8.99E-01 |
| AR=0.4 | 1.93E-01 | 8.15E-01 | 3.11E-01 | 4.49E-02 | 6.20E-06 | 8.98E-01 |

(C)

**Figure 7.11:** Results of simulations of biomass gasification with equilibrium and semi-equilibrium models for wood particles under different gasifying conditions. (A) Temperature = 973 K, Carbon conversion = 100%. (B) Temperature = 973 K, Carbon conversion = 80%. (C) Temperature = 973 K, Carbon conversion = 60%.

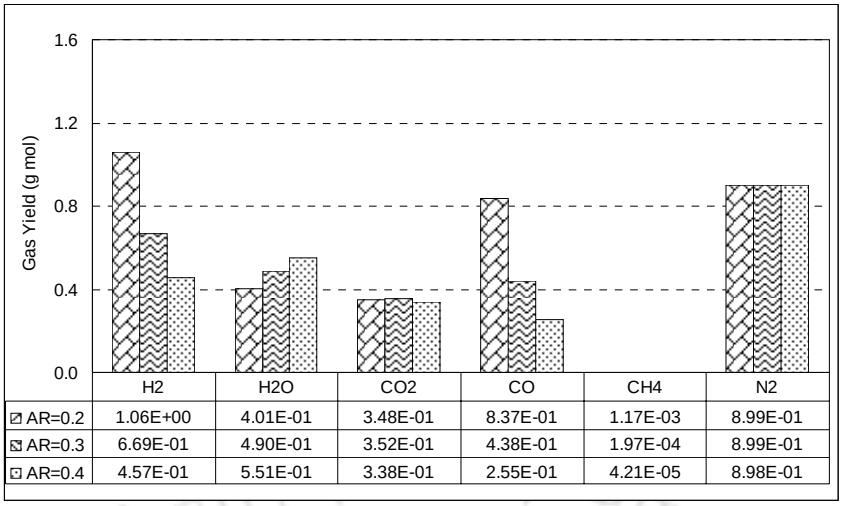


| | H2 | H2O | CO2 | CO | CH4 | N2 |
|---|---|---|---|---|---|---|
| AR=0.2 | 1.06E+00 | 4.01E-01 | 3.48E-01 | 8.37E-01 | 1.17E-03 | 8.99E-01 |
| AR=0.3 | 6.69E-01 | 4.90E-01 | 3.52E-01 | 4.38E-01 | 1.97E-04 | 8.99E-01 |
| AR=0.4 | 4.57E-01 | 5.51E-01 | 3.38E-01 | 2.55E-01 | 4.21E-05 | 8.98E-01 |

(A)

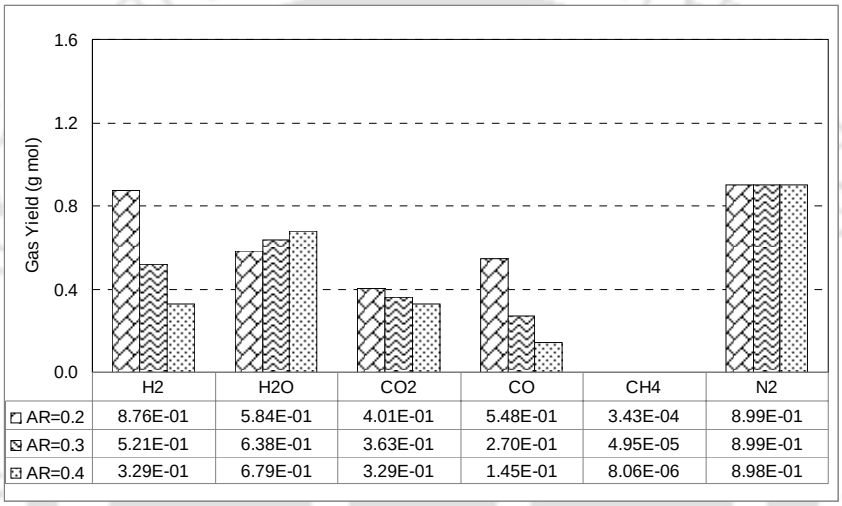


| | H2 | H2O | CO2 | CO | CH4 | N2 |
|---|---|---|---|---|---|---|
| AR=0.2 | 8.76E-01 | 5.84E-01 | 4.01E-01 | 5.48E-01 | 3.43E-04 | 8.99E-01 |
| AR=0.3 | 5.21E-01 | 6.38E-01 | 3.63E-01 | 2.70E-01 | 4.95E-05 | 8.99E-01 |
| AR=0.4 | 3.29E-01 | 6.79E-01 | 3.29E-01 | 1.45E-01 | 8.06E-06 | 8.98E-01 |

(B)

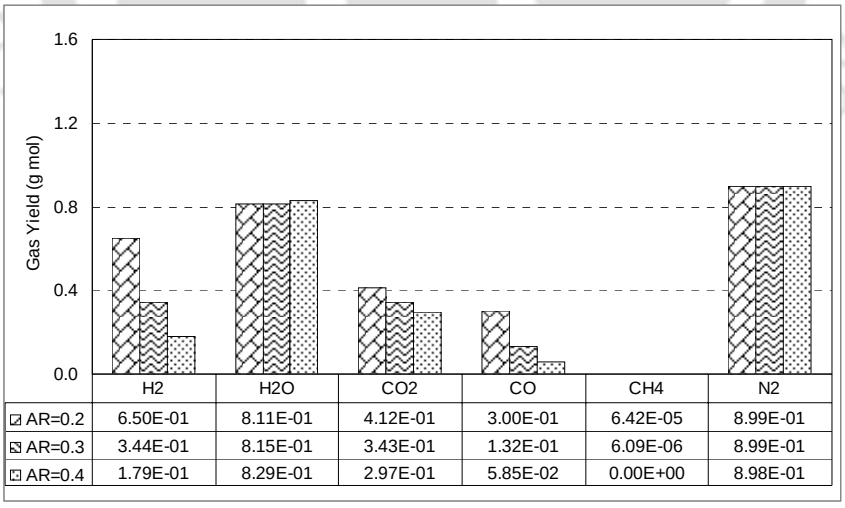


| | H2 | H2O | CO2 | CO | CH4 | N2 |
|---|---|---|---|---|---|---|
| AR=0.2 | 6.50E-01 | 8.11E-01 | 4.12E-01 | 3.00E-01 | 6.42E-05 | 8.99E-01 |
| AR=0.3 | 3.44E-01 | 8.15E-01 | 3.43E-01 | 1.32E-01 | 6.09E-06 | 8.99E-01 |
| AR=0.4 | 1.79E-01 | 8.29E-01 | 2.97E-01 | 5.85E-02 | 0.00E+00 | 8.98E-01 |

(C)

**Figure 7.12:** Results of simulations of biomass gasification with equilibrium and semi-equilibrium models for wood particles under different gasifying conditions. (A) Temperature = 1073 K, Carbon conversion = 100%. (B) Temperature = 1073 K, Carbon conversion = 80%. (C) Temperature = 1073 K, Carbon conversion = 60%.

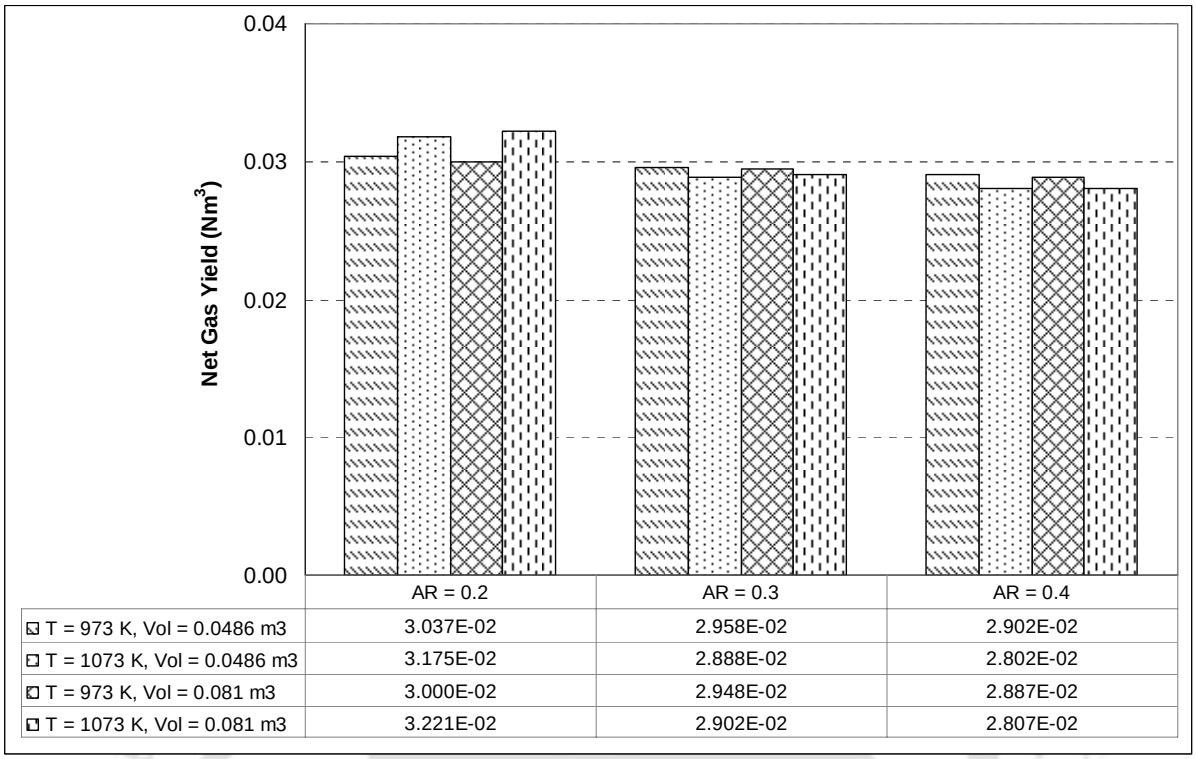


| | AR = 0.2 | AR = 0.3 | AR = 0.4 |
|---|---|---|---|
| T = 973 K, Vol = 0.0486 m3 | 3.037E-02 | 2.958E-02 | 2.902E-02 |
| T = 1073 K, Vol = 0.0486 m3 | 3.175E-02 | 2.888E-02 | 2.802E-02 |
| T = 973 K, Vol = 0.081 m3 | 3.000E-02 | 2.948E-02 | 2.887E-02 |
| T = 1073 K, Vol = 0.081 m3 | 3.221E-02 | 2.902E-02 | 2.807E-02 |

(A)

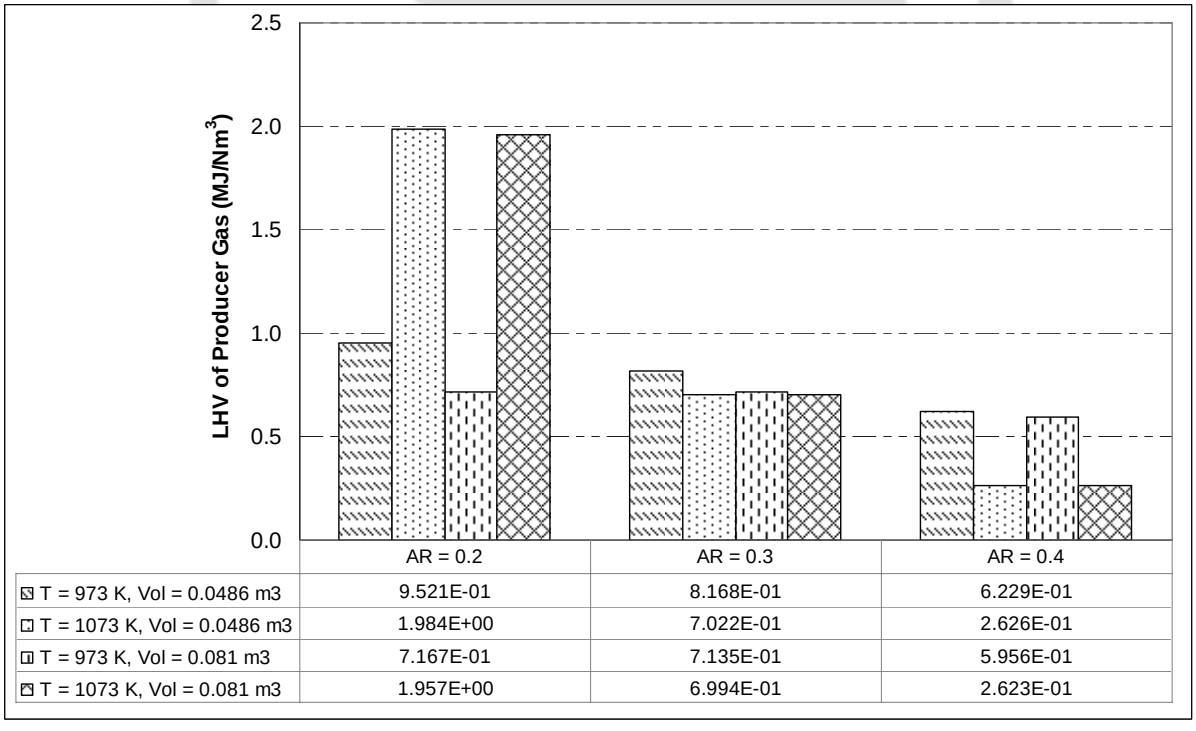


| | AR = 0.2 | AR = 0.3 | AR = 0.4 |
|---|---|---|---|
| T = 973 K, Vol = 0.0486 m3 | 9.521E-01 | 8.168E-01 | 6.229E-01 |
| T = 1073 K, Vol = 0.0486 m3 | 1.984E+00 | 7.022E-01 | 2.626E-01 |
| T = 973 K, Vol = 0.081 m3 | 7.167E-01 | 7.135E-01 | 5.956E-01 |
| T = 1073 K, Vol = 0.081 m3 | 1.957E+00 | 6.994E-01 | 2.623E-01 |

(B)

**Figure 7.13:** Results of simulations of biomass gasification with kinetic models: Net gas yield and LHV of the producer gas for different gasification conditions (temperature and carbon conversion) with wood particles as biomass under different gasifying conditions.

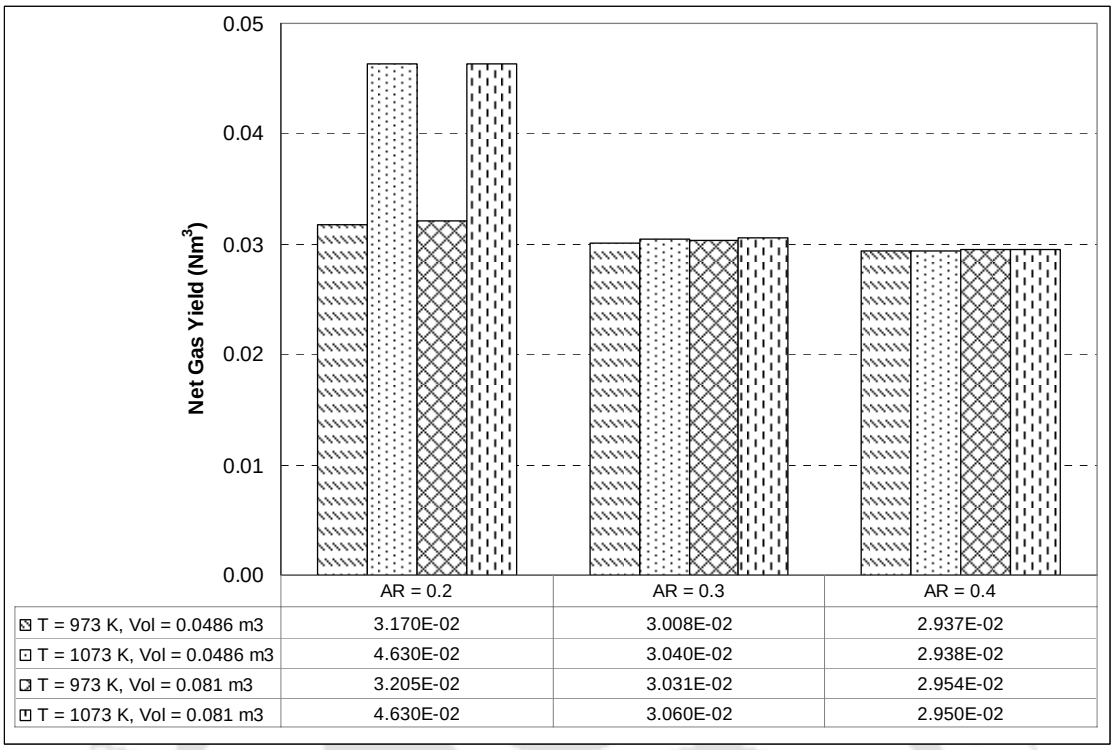


| | AR = 0.2 | AR = 0.3 | AR = 0.4 |
|---|---|---|---|
| T = 973 K, Vol = 0.0486 m3 | 3.170E-02 | 3.008E-02 | 2.937E-02 |
| T = 1073 K, Vol = 0.0486 m3 | 4.630E-02 | 3.040E-02 | 2.938E-02 |
| T = 973 K, Vol = 0.081 m3 | 3.205E-02 | 3.031E-02 | 2.954E-02 |
| T = 1073 K, Vol = 0.081 m3 | 4.630E-02 | 3.060E-02 | 2.950E-02 |

(A)

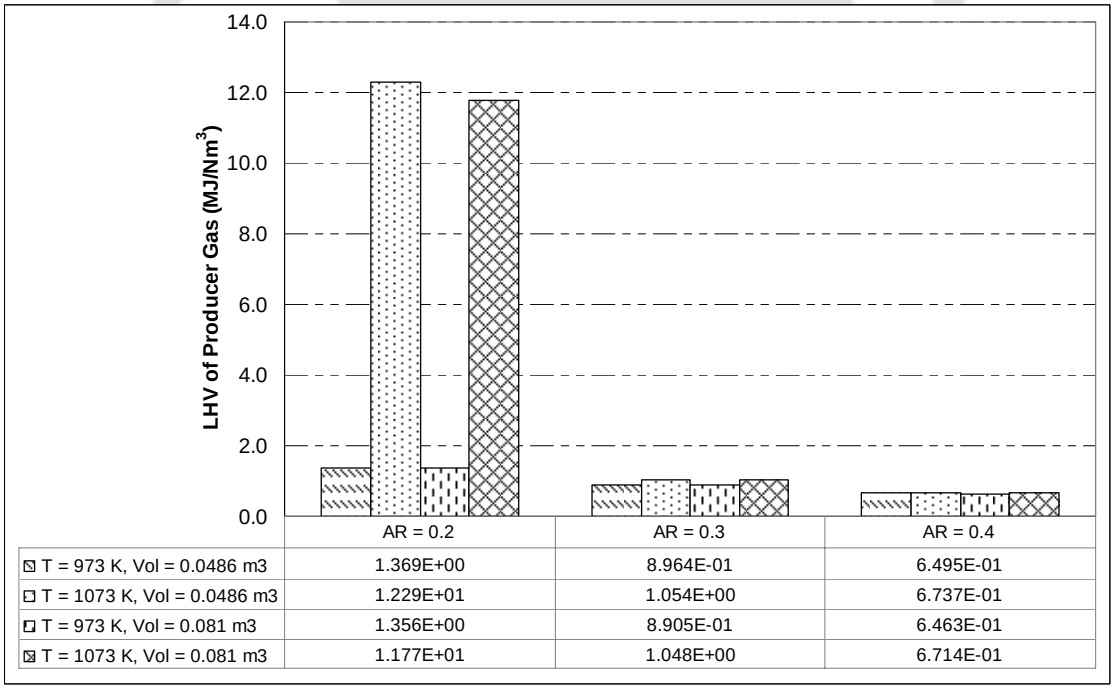


| | AR = 0.2 | AR = 0.3 | AR = 0.4 |
|---|---|---|---|
| T = 973 K, Vol = 0.0486 m3 | 1.369E+00 | 8.964E-01 | 6.495E-01 |
| T = 1073 K, Vol = 0.0486 m3 | 1.229E+01 | 1.054E+00 | 6.737E-01 |
| T = 973 K, Vol = 0.081 m3 | 1.356E+00 | 8.905E-01 | 6.463E-01 |
| T = 1073 K, Vol = 0.081 m3 | 1.177E+01 | 1.048E+00 | 6.714E-01 |

(B)

**Figure 7.14:** Results of simulations of biomass gasification with kinetic models: (A) Net gas yield, and (B) LHV of the producer gas for different gasification conditions (temperature and carbon conversion) with rice husk as biomass under different gasifying conditions.

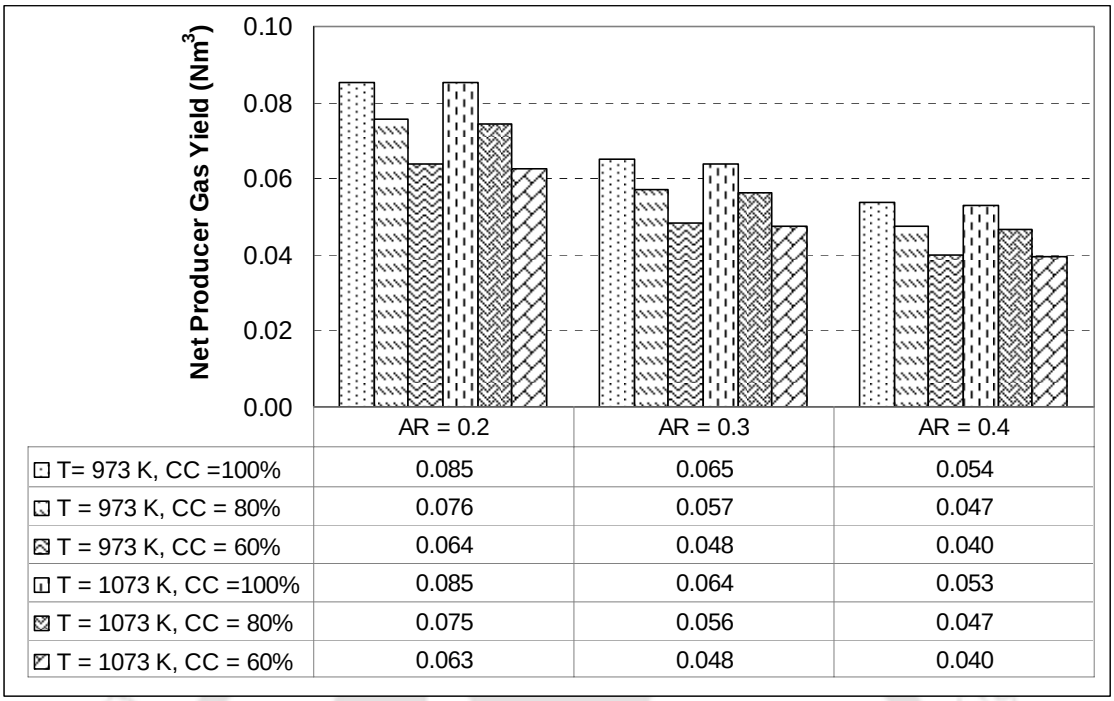


| | AR = 0.2 | AR = 0.3 | AR = 0.4 |
|---|---|---|---|
| T= 973 K, CC =100% | 0.085 | 0.065 | 0.054 |
| T = 973 K, CC = 80% | 0.076 | 0.057 | 0.047 |
| T = 973 K, CC = 60% | 0.064 | 0.048 | 0.040 |
| T = 1073 K, CC =100% | 0.085 | 0.064 | 0.053 |
| T = 1073 K, CC = 80% | 0.075 | 0.056 | 0.047 |
| T = 1073 K, CC = 60% | 0.063 | 0.048 | 0.040 |

(A)

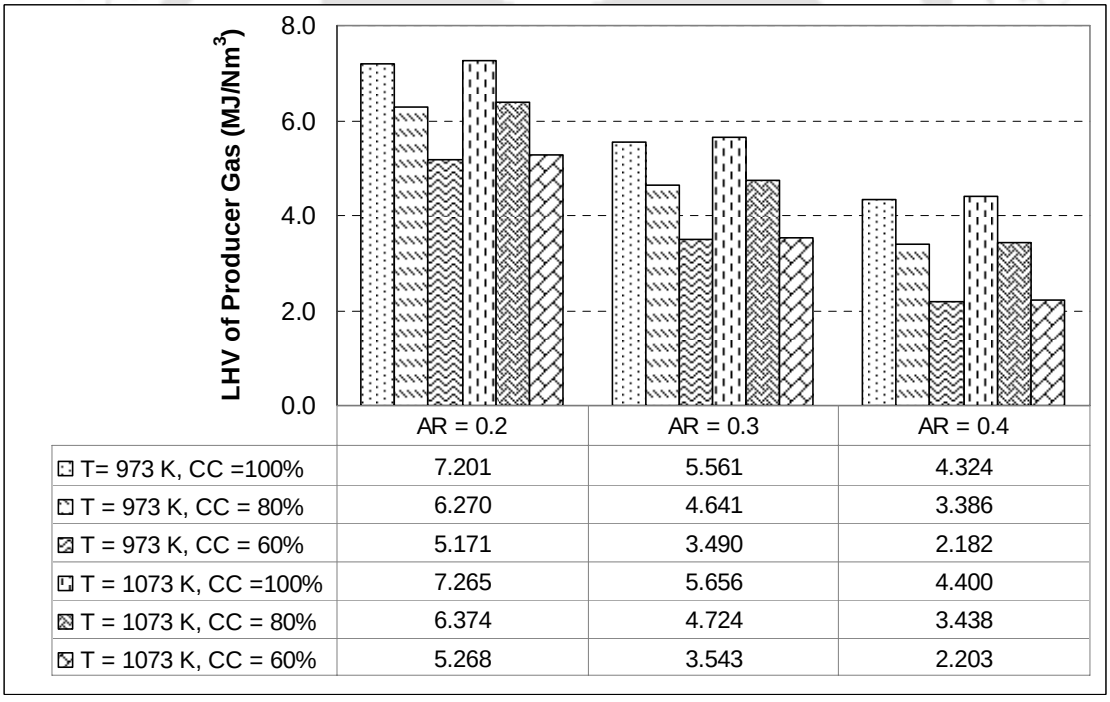


| | AR = 0.2 | AR = 0.3 | AR = 0.4 |
|---|---|---|---|
| T= 973 K, CC =100% | 7.201 | 5.561 | 4.324 |
| T = 973 K, CC = 80% | 6.270 | 4.641 | 3.386 |
| T = 973 K, CC = 60% | 5.171 | 3.490 | 2.182 |
| T = 1073 K, CC =100% | 7.265 | 5.656 | 4.400 |
| T = 1073 K, CC = 80% | 6.374 | 4.724 | 3.438 |
| T = 1073 K, CC = 60% | 5.268 | 3.543 | 2.203 |

(B)

**Figure 7.15:** Results of simulations of biomass gasification with equilibrium and semi-equilibrium models: (A) Net gas yield, and (B) LHV of the producer gas for different gasification conditions (temperature and carbon conversion) with wood particles as biomass under different gasifying conditions.

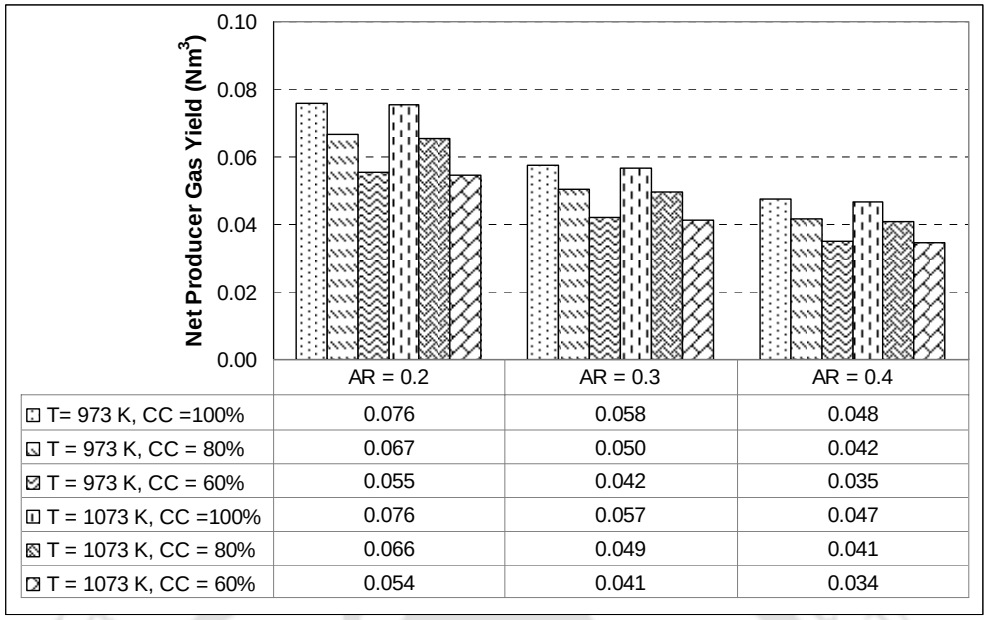


| | AR = 0.2 | AR = 0.3 | AR = 0.4 |
|---|---|---|---|
| T= 973 K, CC =100% | 0.076 | 0.058 | 0.048 |
| T = 973 K, CC = 80% | 0.067 | 0.050 | 0.042 |
| T = 973 K, CC = 60% | 0.055 | 0.042 | 0.035 |
| T = 1073 K, CC =100% | 0.076 | 0.057 | 0.047 |
| T = 1073 K, CC = 80% | 0.066 | 0.049 | 0.041 |
| T = 1073 K, CC = 60% | 0.054 | 0.041 | 0.034 |

(A)

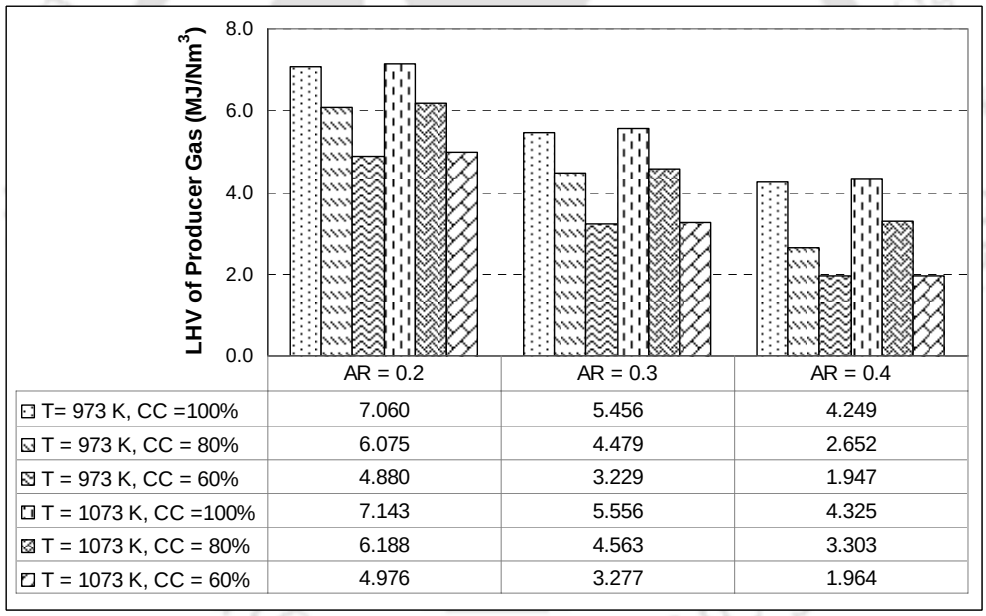


| | AR = 0.2 | AR = 0.3 | AR = 0.4 |
|---|---|---|---|
| T= 973 K, CC =100% | 7.060 | 5.456 | 4.249 |
| T = 973 K, CC = 80% | 6.075 | 4.479 | 2.652 |
| T = 973 K, CC = 60% | 4.880 | 3.229 | 1.947 |
| T = 1073 K, CC =100% | 7.143 | 5.556 | 4.325 |
| T = 1073 K, CC = 80% | 6.188 | 4.563 | 3.303 |
| T = 1073 K, CC = 60% | 4.976 | 3.277 | 1.964 |

(B)

**Figure 7.16:** Results of simulations of biomass gasification with equilibrium and semi-equilibrium models: (A) Net gas yield, and (B) LHV of the producer gas for different gasification conditions (temperature and carbon conversion) with rice husk as biomass under different gasifying conditions.

Table 7.6 and 7.7 for different operating conditions. Fraction of two key components of the producer gas, viz. CO and $H_2$ generated in pyrolysis shows drastic reduction with increasing air ratio. However, the fraction of these gases shows marginal increase with temperature of pyrolysis. As the gasification mixture emerges out of pyrolysis zone and travels upward in the riser, an interesting observation is seen for carbon monoxide in that it shows a maxima with volume of riser. Fraction of CO in the producer gas for riser of 10 m height is less than that for 6 m height. As in pyrolysis, the fraction of CO and $H_2$ in the final producer gas resulting from gasifier also shows reduction with air ratio, and marginal rise with temperature. Extent of $CO_2$ generation in pyrolysis is rather insensitive to temperature. As the gasification proceeds the fraction of $CO_2$ in the producer gas increases. The extent of this rise, obviously, varies directly with the air ratio and inversely with the temperature of gasification. Volume of the riser, however, has no effect on the fraction of $CO_2$ in the producer gas. Tar content of the gas generated from pyrolysis shows reduction with temperature. Thereafter, however, the reduction in tar content is rather low, due to slow kinetics of tar oxidation. The tar content of the gas (in terms of moles) remains almost constant from pyrolysis zone till exit from the gasifier. Composition of methane, ethane and ethylene in the gas is quite small, and shows marginal reduction from pyrolysis zone till exit from gasifier. In the pyrolysis zone, the extent of generation of these three gases shows increase with temperature. Once again, the volume of the gasifier has no effect on the composition of these species in the final gas. Char generation and subsequent gasification also shows interesting trends. As seen from Figure 7.7, a significant mass fraction of biomass ends up in the form of char. This fraction (with respect to moisture free biomass) is practically independent of the air ratio. However, it shows reduction with temperature of pyrolysis. Comparing among the two biomass used in this study, we see that reduction in weight fraction of char is more marked for wood particles than rice husk. Some interesting

trends in the gasification (or oxidation) of the char are seen in Figure 7.8. These are (1) extent of char gasification increases with air ratio, (2) fractional gasification of char reduces with temperature (for a particular air ratio and gasification volume), and (3) fractional gasification of char is independent of the volume of the gasifier.

*Trends in Net Gas Yield and LHV:* The yield of producer gas shows small reduction with increasing air ratio (for given gasifier volume and temperature), marginal rise with temperature of gasification (for a given air ratio and gasification volume) and rather insensitivity to volume of gasifier. The LHV of the producer gas shows following trends: (1) rise with gasification temperature for given air ratio and reactor volume, (2) reduction with air ratio for a given gasification temperature and reactor volume, and (3) reduction with increasing reactor volume for a given air ratio and gasification temperature. Comparing among the two biomass, we observe that fluctuations in LHV are more marked for wood chops than rice husk. In fact, for air ratios of 0.3 and 0.4, the LHV of producer gas from rice husk becomes almost independent of gasification temperature and reactor volume. For air ratio 0.2 and temperature 800$^{o}$C (1073 K), the LHV of producer gas shows a drastic 10 fold rise, as compared to the LHV at 700$^{o}$C at same air ratio. This trend demonstrates critical sensitivity of LHV towards gasification temperature at low air ratios.

### 7.6.2 Analysis of Equilibrium and Semi–Equilibrium Model

*Trends in molar composition*: From the results presented in Figures 7.7–7.10, we can identify following trends in the content of the producer gas with operating parameters: (1) Fraction of both $H_2$ and CO shows inverse variation with air ratio. However , CO content of gas shows direct variation with temperature of gasification, while $H_2$ content reduces with increasing temperature for a particular air ratio and level of carbon conversion.(2) Obviously, the number of moles of both $H_2$ and CO reduce with extent of carbon conversion. (3) Amount of $CO_2$ in the producer gas shows relative insensitivity towards air ratio for high carbon

conversion. However, for low carbon conversion (60%), the $CO_2$ content of producer gas shows significant reduction with air ratio. (4) Amount of $H_2O$ in the producer gas shows increase with both air ratio and temperature of gasification. (5) Methane content of the gas is quite small, and for high air ratio of 0.4, methane content practically reduces to zero, (6) No formation of any other hydrocarbon such as ethane, ethylene or even higher hydrocarbon is seen under equilibrium conditions (i.e. 100% carbon conversion). However, for the semi–equilibrium conditions, the unconverted carbon can appear in the form of char, tar and other hydrocarbons, (7) Comparing among the two biomass, slightly lesser CO and $H_2$ is seen in the producer gas resulting from gasification of wood particles than rice husk under similar operating conditions. Amount of $CO_2$ in the producer gas, however, is higher for wood particles than rice husk.

*Trends in LHV and Gas Yield:* (1) For a given air ratio and gasification temperature, the gas yield obviously reduces with carbon conversion, (2) Gas yield reduces with increasing air ratio at a given gasification temperature and level of carbon conversion, (3) Temperature, however, is not a significant parameter affecting gas yield. At any air ratio and level of carbon conversion, the net gas yield at both 700 and 800$^oC$ is essentially the same. (4) Comparing among rice husk and wood particles, we find higher gas yield for wood particles, and this is obviously attributed to higher ash content of rice husk. Trends in LHV are as follows: (1) For a given gasification temperature and air ratio, the LHV of the producer gas obviously falls with carbon conversion, (2) LHV also shows inverse trend with air ratio for a particular gasification temperature and carbon conversion, (3) Like the net gas yield, temperature does not seem to influence the LHV significantly for same gasification temperature and air ratio, (4) Higher LHV of producer gas is seen for wood particles than rice husk under similar gasifying conditions. This is attributed to higher carbon content of wood particles that results in higher CO content of the producer gas.

### 7.6.3 Comparative Analysis of Three Models

The trends in the net yield and characteristics of the producer gas resulting from gasification of wood particles and rice husk predicted by the three models are in concurrence. Nonetheless, the results of simulations (molar composition of gas, net gas yield and LHV of producer gas) from the three models show significant quantitative difference. The quantitative comparison of the results of three models clearly indicates that the gasification mixture is far from equilibrium (even with as height of riser as 10 m), and the overall carbon conversion in single pass is very small (~ 30–40%). Major differences are: (1) extent carbon monoxide and hydrogen content of the producer gas as predicted by kinetic model is much smaller than that calculated using equilibrium and semi–equilibrium models. Equilibrium and semi–equilibrium models do not predict formation of any other hydrocarbon than $CH_4$, while kinetic model gives smaller quantities of ethane and ethylene. Significant fraction of carbon in the biomass remains unconverted in the form char. The tar produced in the pyrolysis zone also remains unconverted (or unoxidized). Thus, both LHV and net gas yield predicted by kinetic model are lesser than equilibrium and semi–equilibrium model, even with least carbon conversion of 60%.

The results of equilibrium and semi–equilibrium model indicate that air ratio is more critical factor influencing biomass conversion to producer gas than temperature. This conclusion is endorsed by kinetic model as well. However, results of kinetic model show that at low air ratios, temperature could have significant influence on net gas yield as well as LHV of the gas. This is evident from results depicted in Figures 7.13 and 7.14, where we see sharp rise in gas yield and LHV with temperature rising from 700 to 800$^{o}$C. Increasing air ratio at a particular temperature helps enhancement of char gasification; however, it also enhances conversion of $H_2$ and CO to $H_2O$ and $CO_2$, respectively, reducing the quality of the producer gas. Increasing temperature of gasification has adverse effect on char gasification as revealed

by Figure 7.8. This is attributed to factor consumption of $O_2$ in other parallel reactions in the gasification. Nonetheless, higher temperature prevents conversion of CO and $CO_2$ and increases the LHV of gas.

The kinetic model also reveals the role of volume of the gasifier (i.e. the height of the riser section of the CFB gasifier) in the gasification process. Relative insensitivity of the gas yield and LHV to the volume of gasifier indicates need for optimization of this parameter. Merely raising the height of the riser section does not help increasing the quality of the gas. This is clearly attributed to slow kinetics of char gasification and tar oxidation. On the other hand, maintenance of proper air ratio and temperature is critical to achieving efficient conversion of biomass to producer gas. The results of the simulation give important clues for enhancing performance of the gasifier. Efficient capture and recycle of the char is crucial to increasing overall carbon conversion in the process. Enhancing oxidation of tar by using a suitable catalyst (sintered–olivine or calcined dolomite) can also augment the gas yield and LHV of the gas. The most critical factor, however, seems to be the pyrolysis of biomass occurring at the bottom of the riser itself. An optimization of the pyrolysis in terms of temperature, biomass particle size and use of suitable catalyst, so as to reduce the formation of char and tar, with concurrent enhancement in view of gaseous species, will help increase conversion of biomass to desired species of CO, $H_2$ and $CH_4$.

## 7.7 CONCLUSIONS

In this chapter, we have attempted to present a comparison of equilibrium, semi–equilibrium and kinetic models for biomass gasification. A circulating fluidized bed biomass gasifier has been taken as basis for comparison. Two common biomass, viz. rice husk and wood particles have been used as model biomass. The input for equilibrium and semi–equilibrium model is in terms of an elemental vector, while a stream of 9 species resulting

from pyrolysis of biomass forms the input for kinetic models. In semi–equilibrium model, the extent of carbon conversion has been considered as manipulation parameter. Although the trends in molar composition, net yield and LHV of producer gas predicted by the three models under similar conditions of gasification match, there is significant quantitative difference. Carbon conversion achieved in single pass of biomass through the riser of the CFB gasifier is found to be less than the least carbon conversion considered in semi–equilibrium model. Analysis of the kinetic model reveals that formation of significant quantities of char and tar in the biomass pyrolysis, and slow kinetics of gasification /oxidation of these species leads to low per pass carbon conversion, which in turn renders total gas yield and LHV of the gas significantly low. Comparative analysis of the three models has given an insight into the relative influence of two major operational parameters, viz. temperature and air ratio, on the gasification process. The equilibrium and semi–equilibrium models predict that characteristics of producer gas are relatively insensitive to temperature, while the kinetic model reveals greater sensitivity of producer gas characteristics towards temperature at low air ratios. Another important outcome of the kinetic model analysis is the revelation of effect of gasifier volume. The producer gas composition, yield and LHV have been found to be insensitive to this parameter, i.e. a riser of 6 m height essentially yields producer gas with same characteristics as that from riser of 10 m height. This result gives a strong indication towards optimization of this parameter. Moreover, this result emphasizes on alternative means of enhancing overall carbon conversion through char recycle and catalytic tar oxidation. However, we must also mention that scheme of 13 reactions used in the kinetic model may not include all reactions that could occur in gasification process. Due to this limitation, the actual outcome of the gasification process could differ from predictions of the kinetic model.

On a whole, comparative analysis of the equilibrium and kinetic models has

highlighted the potential of the equilibrium, semi–equilibrium and models to represent gasification process. Our analysis asserts that equilibrium and semi–equilibrium models could be a useful tool for qualitative assessment / prediction of gasifier performance under different combinations of operating parameters. However, kinetic models provide physically more realistic insight into the various facets of the gasification process and reveal relative influence of various operating and design parameters on the gasification. We believe that results and analysis presented in this chapter could be useful for further research in modeling of gasification, and will also give useful guidelines for design engineers for optimization of biomass gasifiers.

## REFERENCES

[1] Eriksson G.Thermodynamic studies of high temperature equilibria – XII: SOLGASMIX, A computer program for calculation of equilibrium composition in multiphase systems. Chemica Scripta 1975;8:100–103.

[2] Rhinehart RR, Felder RM, Ferrel JK. Dynamic modeling of a pilot scale fluidized bed coal gasification reactor. Industrial and Engineering Chemistry Research 1987;26:738– 745.

[3] Ciesielzyk E, Gawdzik A. Non–isothermal fluidzed bed reactor model for char gasification taking into account bubble growth. Fuel 1994;73:105–112.

[4] Sotudeh–Gharebaagh R, Legros R, Chaouki J, Paris J. Simulations of circulating fluidized bed reactor using ASPEN PLUS. Fuel 1998;77:327–337.

[5] Srinivasan RA, Sriramulu S, Kulasekaran S, Agarwal PK. Mathematical modeling of fluidized bed combustion. 2. Combustion of gases. Fuel 1998;77:1033–1049.

[6] Yan HM, Heidenreich C, Zhang DK. Mathematical modeling of bubbling fluidized bed coal gasifier and the significance of "net flow". Fuel 1998;77:1067–1079.

[7] Wang Q, Huo Z, Li X, Fang M, Ni M, Cen K. A mathematical model for a circulating fluidized bed (CFB) boiler. Energy 1999;24:633–653.

[8] Huilin L, Rushan B, Wenti L, Binxi L, Lidan Y. Computations of a circulating fluidized bed boiler with wide particle size distributions. Industrial and Engineering Chemistry Research 2000;39:3212–3220.

[9] Kim YJ, Lee JM, Kim SD. Modeling of coal gasification in an internally circulating fluidized bed reactor with draught tube. Fuel 2000;79:69–77.

[10] Chen C, Horio M, Kojima T. Numerical simulations of entrained flow coal gasifiers: Part I. Modeling of coal gasifiers in an entrained flow gasifier. Chemical Engineering Science 2000;55:3861–3874.

[11] Chen C, Horio M, Kojima T. Numerical simulations of entrained flow coal gasifiers: Part II. Effects of operating conditions on gasifier performance. Chemical Engineering Science 2000;55:3875–3883.

[12] Chejne F, Hernandez JP. Modeling and simulation of coal gasification process in fluidized bed. Fuel 2002;81:1687–1702.

[13] Belleville P, Capart R. A model for predicting outlet gas concentration from a wood gasifier. In: Thermochemical Processing of Biomass (Bridgwater AV, editor), Butterworths: London, 1983. pp. 217–228.

[14] Chang CC, Fan LT, Walawender WP. Dynamic modeling of biomass gasification in a fluidized bed. AIChE Symposium Series 1984;80(234):80–90.

[15] van den Aarsen FG. Fluidized Bed Wood Gasifier Performance and Modeling. Ph.D. Dissertation, University of Twente, Enschede (Netherlands), 1985.

[16] Corella J, Alday FJ, Herguido J. A model for non–stationary states of a commercial fluidized bed air gasifier of biomass. In: Biomass for Energy and Industry (Grassi G, editor), Vol. 2, Elsevier: London, 1990. pp. 2804–2809.

[17] Jiang H, Morey RV. A numerical model of fluidized bed biomass gasifier. Biomass and Bioenergy 1992;3:431–447.

[18] Jiang H, Morey RV. Pyrolysis of corn cobs at fluidization. Biomass and Bioenergy 1992;3:81–85.

[19] Wang Y, Kinoshita CM. Kinetic model of biomass gasification. Solar Energy 1993;51(1):19–25.

[20] Mansaray KG, Al–Taweel AM, Ghaly AE, Hamdullahpur F, Ugursal VI. Mathematical modeling of a fluidized bed rice husk gasifier: part I – model development. Energy Sources 2000;22(1):83–98.

[21] Mansaray KG, Ghaly AE, Al–Taweel AM, Ugursal VI, Hamdullahpur F. Mathematical modeling of a fluidized bed rice husk gasifier: part II – model verification. Energy Sources 2000;22(3):281–296.

[22] Sadaka SS, Ghaly AE, Sabbah MA. Two phase biomass air–steam gasification model for fluidized bed reactors: part I – model development. Biomass and Bioenergy 2002;22:439–462.

[23] Sadaka SS, Ghaly AE, Sabbah MA. Two phase biomass air–steam gasification model for fluidized bed reactors: part II – model sensitivity. Biomass and Bioenergy 2002;22:463–477.

[24] Sadaka SS, Ghaly AE, Sabbah MA. Two phase biomass air–steam gasification model for fluidized bed reactors: part III – model validation. Biomass and Bioenergy 2002;22:479–487.

[25] Hammel S, Krumm W. Mathematical modeling and simulation of bubbling fluidized bed gasifiers. Powder Technology 2001;120:105–112.

[26] Jennen T, Hiller R, Koneke D, Weinspach P–M. Modeling of gasification of wood in a circulating fluidized bed. Chemical Engineering and Technology 1999;22(10):822–

826.

[27] Kersten SRA, Prins W, van der Drift A, van Swaaij WPM. Experimental fact finding in CFB biomass gasification for ECN's 500 kWth pilot plant. Industrial and Engineering Chemistry Research 2003;42:6755–6764.

[28] Corella J, Sanz A. Modeling circulating fluidized bed biomass gasifiers. A pseudo–rigorous model for stationary state. Fuel Processing Technology 2005;86(9):1021–1053.

[29] Liu H, Gibbs BM. Modelling of NO and $N_2O$ emissions from biomass–fired circulating fluidized bed combustores. Fuel 2002;81:271–280.

[30] Liu H, Gibbs BM. Modeling $NH_3$ and HCN emissions from biomass circulating fluidized bed gasifiers. Fuel 2003;82:1591–1604.

[31] Dupont C, Boissonnet G, Seiler J–M, Gauthier P, Schweich D. Study about the kinetic processes of biomass steam gasification. Fuel 2007;86(1–2):32–40.

[32] Radmanesh R, Chaouki J, Guy C. Biomass gasification in a bubbling fluidized bed reactor: experiments and modeling. AIChE Journal 2006;52(12):4258–4272.

[33] Nikoo MB, Mahinpey N. Simulation of biomass gasification in fluidized bed reactor using ASPEN PLUS. Biomass and Bioenergy 2008;32(12):1245–1254.

[34] Rodrigues R, Secchi AR, Marcilio NR, Godinho M. Modeling of biomass gasification applied to a combined gasifier–combustor unit: equilibrium and kinetic approaches. Computer–Aided Chemical Engineering 2009;27A ($10^{th}$ Int. Symp. Process Syst. Eng.): 657–662.

[35] Roy PC, Datta A, Chakraborty N. Modelling of a downdraft biomass gasifier with finite rate kinetics in the reduction zone. International Journal of Energy Research 2009;33(9):833–851.

[36] Kaushal P, Abedi J, Mahinpey N. A comprehensive mathematical model for biomass

gasification in a bubbling fluidized bed reactor. Fuel 2010;89(12):3650–3661.

[37] Evans P, Paskach T, Reardon J. Detailed kinetic modeling to predict syngas composition from biomass gasification in a PBFB reactor. Environmental Progress & Sustainable Energy 2010;29(2):184–192.

[38] Cousins WJ. A theoretical study of wood gasification processes. New Zealand Journal of Science 1978;21(2):175–183.

[39] Denn MM, Yu W–C, Wei J. Parameter sensitivity and kinetics–free modeling of moving bed coal gasifiers. Industrial and Engineering Chemistry Fundamentals 1979;18(3):286–288.

[40] Kosky PG, Floess JK. Global model of countercurrent coal gasifiers. Industrial and Engineering Chemistry Process Design and Development 1980;19(4):586–592.

[41] Kovacik G, Oguztoreli M, Chambers A, Ozum B. Equilibrium calculations in coal gasification. International Journal of Hydrogen Energy 1990;15(2):125–131.

[42] Shesh KK, Sunawala PD. Thermodynamics of pressurized air–steam gasification of biomass. Indian Journal of Technology 1990;28(4):133–138.

[43] Watkinson AP, Lucas JP, Lim CJ. A prediction of performance of commercial coal gasifiers. Fuel 1991;70:519–527.

[44] Garcia EY, Laborde MA. Hydrogen production by steam reforming of ethanol: thermodynamic analysis. International Journal of Hydrogen Energy 1991;16(5):307–312.

[45] Schuster G, Loffler G, Weigl K, Hofbauer H. Biomass steam gasification – an extensive parametric modeling study. Bioresource Technology 2001;77(1):71–79.

[46] Zainal, ZA, Ali R, Lean CH, Seetharamu KN. Prediction of performance of a downdraft gasifier using equilibrium modeling for different biomass materials. Energy Conversion and Management 2001;42(12):1499–1515.

[47] Alderucci V. Thermodynamic analysis of SOFC fueled by biomass derived gas. International Journal of Hydrogen Energy 1994;19(4):369–376.

[48] Ruggiero M, Manfrida G. An equilibrium model for biomass gasification process. Renewable Energy 1999;16:1106–1109.

[49] Altafini CR, Wander PR, Barreto RM. Prediction of working parameters of a wood waste gasifier through an equilibrium model. Energy Conversion and Management 2003;44:2763–2777.

[50] Melgar A, Perez JF, Laget H, Horillo A. Thermochemical equilibrium modelling of a gasifying process. Energy Conversion and Management 2007;48(1):59–67.

[51] Brown DWM, Fuchino T, Marechal FMA. Stoichiometric equilibrium modeling of biomass gasification: Validation of artificial neural network temperature difference parameter regression. Journal of Chemical Engineering Japan 2007;40(3):244–254.

[52] Vera D, Jurado F, Panopoulos KD, Grammelis P. Modelling of biomass gasifier and microturbine for the olive oil industry. International Journal of Energy Research in press. DOI: 10.1002/er.1802.

[53] Saxena SC, Thomas LA. An equilibrium model for predicting flue–gas composition of an incinerator. International Journal of Energy Research 1995;19(4):317–327.

[54] Reynolds WC. The element potential method for chemical equilibrium analysis: Implementation in the interactive program STANJAN. Technical Report, Stanford University, Stanford, 1986. 48 pp.

[55] Smith WR, Missen RW. Chemical Reaction Equilibrium Analysis: Theory and Algorithms. Wiley: New York, 1982.

[56] Bharadwaj A. Gasification and Combustion Technologies of Agro–Residues and Their Application to Rural Electric Power Systems in India. Ph.D. Dissertation, Carnegie Mellon University, Pittsburgh, PA (USA); 2002.

[57] Mahishi MR, Goswami DY. Thermodynamic optimization of biomass gasifier for hydrogen production. International Journal of Hydrogen Energy 2007;32(16):3831–3840.

[58] Li X, Grace JR, Watkinson AP, Lim CJ, Ergudenler A. Equilibrium modeling of gasification: a free energy minimization approach and its application to a circulating fluidized bed coal gasifier. Fuel 2001;80:195–207.

[59] Kersten SRA. Biomass Gasification in Circulating Fluidized Beds. Ph.D. Dissertation, University of Twente, Twente University Press: Enschede, 2002.

[60] Shand RN, Bridgwater AV. Fuel gas from biomass: status and new modeling approaches. In: Thermochemical Processing of Biomass (Bridgwater AV, editor), Butterworths: London; 1984, pp. 229–254.

[61] Nemtsov DA, Zabaniotou. Mathematical modeling and simulation approaches of agricultural residues air gasification in a bubbling fluidized bed reactor. Chemical Engineering Journal 2008;143:10–31.

[62] Puig–Arnavat M, Bruno JC, Coronas, A. Review and analysis of biomass gasification models. Renewable and Sustainable Energy Reviews 2010;14(9):2841–2851.

[63] Prakash N, Karunanithi T. Advances in modeling and simulation of biomass pyrolysis. Asian Journal of Scientific Research 2009;2(1):1–27.

[64] Luo CH, Aoki K, Uemiya S, Kojima T. Numerical modeling of a jetting fluidized bed gasifier and the comparison with the experimental data. Fuel Processing Technology 1998;55(3):193–218.

[65] Saito M, Sadakata M, Sakai T. Measurements of surface combustion rate of single coal particles in laminar–flow furnace. Combustion Science and Technology 1987;51:109–128.

[67] Biba V, Macak J, Klose E, Malecha J. Mathematical model for the gasification of coal

under pressure. Industrial and Engineering Chemistry Process Design and Development 1978;17:92–98.

[68] Gururajan VS, Agarwal PK, Agnew JB. Mathematical–model of fluidized–bed coal gasifiers. Chemical Engineering Research and Design 1992;70:211–238.

[69] Jensen A, Johnsson JE, Andreies J, Laughli K, Read G, Mayer M, Baaumann H, Bonn B. Formation and reduction of $NO_X$ in pressurized fluidized bed combustion of coal. Fuel 1995;74(11):1555–1569.

[70] Jones WP, Lindstedt RP. Global reaction schemes for hydrocarbon combustion. Combustion and Flame 1988;73:233–249.

[71] Fletcher DF, Haynes BS, Christo FC, Joseph SD. A CFD based combustion model of an entrained flow biomass gasifier . Applied Mathematical Modeling 2000;24:165–182.

[72] Zimont VL, Trushin YM. Total combustion kinetics of hydrocarbon fuels. Combustion, Explosion and Shockwaves 1969;5(4) 391–394.

[73] FactWeb. Homepage: http://www.factsage.com (accessed November 2009).

[74] Bale CW, Chartrand P, Degterov SA, Eriksson G, Hack K, Mahfoud RB, Melancon J, Pelton AD, Petersen S. FACTSAGE thermochemical software and databases. Calphad 2002;26(2): 189–228.

[75] Narvaez I, Orio A, Aznar MP, Corella J. Biomass gasification with air in an atmospheric bubbling fluidized bed. Effect of six operational variables on the quality of the produced raw gas. Industrial and Engineering Chemistry Research 1996;35:2110–2120.

[76] Mansaray KG, Ghaly AE, Al–Taweel AM, Hamdullahpur F, Ugursal VI. Air gasification of rice husk in a dual distributor type fluidized bed reactor. Biomass and Bioenergy 1999;17:315–332.

[77] Kunii D, Levenspiel O. Fluidization Engineering (2nd Ed.), Butterworth–Heinemann: Boston, 1992.

[78] Lv PM, Xiong ZH, Chang J, Wu CZ, Chen Y, Zhu JX. An experimental study on biomass air–steam gasification in a fluidized bed. Bioresource Technology 2004;95:95–101.

[79] Cao Y, Wang Y, Riley JT, Pan W–P. A novel biomass air gasification process for producing tar–free higher heating value fuel gas. Fuel Processing Technology 2006;87:343–353.

[80] Zhao Y, Sun S, Tian H–M, Qian J, Su F–M, Ling F. Characteristics of rice husk gasification in an entrained flow reactor. Bioresource Technology 2009;100:6040–6044.

[81] Scott DS, Piskorz J. The flash pyrolysis of aspen–poplar wood. Canadian Journal of Chemical Engineering 1982;60:666–674.

[82] Scott DS, Piskorz J. The continuous flash pyrolysis of biomass. Canadian Journal of Chemical Engineering 1984;62:404–412.

[83] Scott DS, Piskorz J, Bergougnou MA, Graham R, Overend RP. The role of temperature in the fast pyrolysis of cellulose and wood. Industrial and Engineering Chemistry Research 1988;27:8–15.

[84] Beaumont O, Schwob Y. Influence of physical or chemical parameters on wood pyrolysis. Industrial and Engineering Chemistry Process Design and Development 1984;23(4):637–641.

[85] Gray MR, Corcoran WH, Gavalas GR. Pyrolysis of a wood derived material: Effect of moisture content and ash content. Industrial and Engineering Chemistry Process Design and Development 1985;24:646–651.

[86] Nunn TR, Howard JB, Longwell JP, Peters WA. Product compositions and kinetics in

the rapid pyrolysis of sweet gum hardwood. Industrial and Engineering Chemistry Process Design and Development 1985;24(3):836–844.

[87] Kashiwaji T, Ohlemiller T, Werner K. Effects of external radiant flux and ambient oxygen concentration on non–flaming gasification rates and evolved products of white pine. Combustion and Flame 1987;69(3):331–345.

[88] Chan WR, Kelbon M, Krieger–Brockett B. Single particle pyrolysis: correlations of reaction products and process conditions. Industrial and Engineering Chemistry Research 1988;27(12):2261–2275.

[89] Bilbao R, Millera A, Murillo MB. Temperature profiles and weight loss in the thermal decomposition of large spherical wood particles. Industrial and Engineering Chemistry Research 1993;32:1811–1817

[90] Figueiredo JL, Valenzuela C, Bernalte A, Encinar JM. Pyrolysis of holm–oak wood: influence of temperature and particle size. Fuel 1989;68(8):1012–1016

[91] Scott DS, Piskorz J, Radlein D. Liquid products from the continuous flash pyrolysis of biomass. Industrial and Engineering Chemistry Process Design and Development 1985;24(3):581–588.

[92] Williams PT, Besler S. The pyrolysis of rice husk in a thermogravimetric analyzer and static batch reactor. Fuel 1993;72(2):151–159.

[93] Janse AMC, de Jonge HG, Prins W, van Swaaij WPM. Combustion kinetics of char obtained by flash pyrolysis of pine wood. Industrial and Engineering Chemistry Research 1998;37(10):3909–3918.

[94] Di Blasi C, Signorelli G, Di Russo C, Rea G. Product distribution from pyrolysis of wood and agricultural residues. Industrial and Engineering Chemistry Research 1999;38:2216–2224.

CHAPTER 8

# Overview and Suggestion for Further Research

## 8.1 OVERVIEW

Biomass gasification has emerged as a viable technology for decentralized power generation in rural and remote areas in developing countries like India. Given its potential for large scale implementation which could help meeting power needs of rural population, there is an urgent need to study the intricacies of the gasification process from fundamental viewpoint. The results of such a study would form crucial input efficient design, scale-up and optimization of biomass gasifiers. It is in this spirit that this thesis work was undertaken.

As noted in Chapter 1, the principal objective of this thesis was to present a unified frame work that puts together different approaches of modeling and optimization of biomass gasifiers, and also to give a comprehensive assessment of the gasification process under diverse range of operating conditions, using different feedstocks. In accordance with this

objective, we have presented the results of our investigations in previous chapters. These results, when put together, give an interesting overview of characteristics of the gasification process. We summarize the major findings and conclusions of this thesis below and try to give suggestions for further research in this area.

- In Chapter 4, we analyzed gasification characteristics of three common biomass, viz. rice husk, bamboo dust and saw dust under a wide range of temperature and air ratios, using air or air-steam mixture (with different mole % of steam) as gasification medium. This analysis was done using the non-stoichiometric SOLGASMIX thermodynamic equilibrium model. The quality of the producer gas was assessed with two measures; viz. the $H_2$/CO molar ratio and LHV of the producer gas. We also assessed the trends in efficiency of the gasifier under wide range of operating conditions. Results of these simulations revealed influence of different parameters on gasification process. For very low air ratios, significant fraction of carbon in biomass remained unconverted, even under total equilibrium conditions. On the other hand, at high air ratios, most of the carbon and hydrogen in biomass got converted to $CO_2$ and $H_2O$, respectively. Use of air-steam mixture as gasification medium did not yield significant change in the molar composition of producer gas, so as to justify additional costs associated with use of steam. At low temperature of gasification, the $H_2$/CO molar ratio in the gas was high, yet the net molar content of $H_2$ and CO was low. The LHV of the gas and also the efficiency of the gasifier stayed constant above 700 $^oC$ for any given air ratio. However, both LHV and efficiency showed marked reduction with air ratio at a particular gasification temperature. This was a consequence of two causes: (1) complete conversion of carbon and hydrogen in biomass, and (2) greater partition of carbon and hydrogen in biomass to $CO_2$ and $H_2O$ at high air ratios. All of these results pointed that most

optimum range of operating conditions for any biomass was air ratio of 0.2-0.4, temperature range of 700-1000 $^{o}$C and gasification medium as air.

- With results of Chapter 4 on gasification of individual biomass, we proceeded to assess the characteristics of gasification of mixtures of the biomass in Chapter 5. Justification of this study was on the basis of possible non-availability of single biomass in large quantities through out year for plants with capacities exceeding 1 MWe. We considered same three biomass again; however, in the form of 9 binary mixtures of different proportions. In addition, we also considered gasification of these mixtures with semi-equilibrium models, in which a restriction was imposed on the extent of carbon conversion in biomass. The level of carbon conversion was chosen on the basis of experimental studies on gasification of the biomass considered. We assessed several characteristics of the gasification of biomass mixtures such as net yield, hydrogen and carbon monoxide content of the producer gas, LHV and net thermal energy content of the gas and net enthalpy change in gasification for different gasification conditions. However, based on the conclusions of the previous chapter, we used a smaller range of air ratio and temperature in this analysis, which was essentially the optimum range (AR = 0.2-0.4, Temperature = 700-1000 $^{o}$C). For all biomass mixtures, the most optimum air ratio was found to be 0.3, with gasification temperature being 800$^{o}$C. Although the trends in these characteristics with operating conditions (temperature and air ratio) are similar to these observed for single biomass, these was significant quantitative difference. For mixtures with higher proportions of saw dust, the LHV and gas yield was higher than the mixtures rich in rice husk. Similarly, relative large temperature and/or air ratio was required for complete carbon conversion in saw dust rich mixtures. This was essentially attributed to higher carbon content of saw dust and higher ash content of rice husk. We compared our results with those reported in literature and found good agreement .We also analyzed the

specific consumption biomass mixtures per unit electricity (per kWh) under equilibrium (total carbon conversion) and semi-equilibrium (partial carbon conversion) conditions. It was further revealed that, for typical engine-generator efficiency of 30%, the least specific fuel (biomass mixture) consumption (under equilibrium condition) was 0.8 kg/kWh, which could double to 1.5 kg/kWh for carbon conversion of ~ 60% observed in most commercial gasifiers. On a whole, this study ascertained that performance of gasifier for decentralized power generation stays same after replacement of single biomass by mixture of biomass.

- In Chapter 6, we attempted to devise correlations for 4 principal parameters that benchmark the performance of the gasifier, either for decentralized power generation or as a precursor for the Fischer-Tropsch Synthesis. These parameters are LHV and net yield of producer gas and mole (or volume) fraction of CO and $CO_2$ in the gas. The data for constituting these correlations was generated through simulations of gasification of 3 common biomass feedstock, viz. rice husk, saw dust and corn cob, under 4 different gasification temperatures, 3 air ratios and 4 levels of carbon conversion (totally yielding 144 sets of simulations with permutation-combination). The choice of temperatures and air ratios was based on results of Chapter 4 on optimization of biomass gasification conditions. The independent variables used in the correlation were parameters mentioned above, in addition to the 3 elemental ratios in the gasification mixture, H/C, O/C and O/H. The simulation data was fitted against 8 correlation of linear and non-linear type, and the compatibility of each correlation for best fit of the data was assessed on the basis of three statistical indicators, viz. regression co-efficient, root mean square deviation and average absolute error. The correlations were also evaluated against experimental data on gasification of the model biomass. This analysis resulted in the following correlation for each performance parameter.

$$\mathrm{LHV} = 0.936(\mathrm{Temp})^{0.114}(\mathrm{AR})^{-0.796}(\mathrm{H/C})^{-0.142}$$

$$Y = -8.585\times10^{-10}\left(\text{Temp}\right)^{2.413} - 0.263\left(\text{H/C}\right)^{0.753} + 0.571\left(\text{O/C}\right)^{0.306}$$

$$X_{CO} = 1.56\times10^{-3}\left(\text{Temp}\right)^{0.636}\left(\text{AR}\right)^{-0.768}\left(\text{H/C}\right)^{-0.611}$$

$$X_{CO2} = -1.917\times10^{-6}\left(\text{Temp}\right) + 0.316\left(\text{AR}\right) + 0.0137\left(\text{H/C}\right)$$

The best correlation for each parameter was on the basis of least average absolute error than highest regression coefficient, so as to have best prediction than fit. These correlations were able to predict the values of performance parameters within engineering accuracy of ±10-20%. Moreover, the coefficient and exponents of various independent variables in each correlation gave the relative impact of the variable on performance parameters. LHV and yield of gas and the mole fraction $CO_2$ were rather insensitive to temperature. Air ratio was the principal variable affecting all parameters, and the H/C elemental ratio in the fuel also had marginal effect. These correlations are independent of the design of the gasifier and were equally applicable for both moving bed and fluidized bed designs.

- In the last study of this thesis (Chapter 7), we made a comparative assessment of the three kinds of models that have been used for biomass gasification. These are thermodynamic equilibrium model, semi-equilibrium model and kinetic model. The approach in this study was similar to previous ones, in that we considered a variety of operating conditions (air ratios and temperatures) for simulations with wood particles and rice husk was as model biomass. A circulating fluidized bed biomass gasifier was taken as basis for the analysis, in which a sand bed acts as inert material. The thermodynamic model used same algorithm, SOLGASMIX, as in previous chapters. For the semi-equilibrium model, a restriction was put on the level carbon conversion in biomass. Two levels of carbon conversion, viz. 60% and 80% were chosen for this analysis . The kinetic model comprised of a scheme of 13 reactions (4 heterogeneous and 9 homogeneous ) among various species resulting from the pyrolysis of

biomass.

The gasification medium was hot air at temperature ~ 700-800Oc . The velocity of air was decided on the basis of the fluidization characteristic of biomass and sand particle . The sand bed was designed to be in turbulent fluidization mode , while pneumatic conveyance regime was assumed for the biomass particles. the biomass feed rate was varied in order to achieve a particular air ratio at the bottom of the riser section (zone near the distributor plate). the biomass entering the gasifier gets mixed with hot and turbulent sand bed and undergoes pyrolysis yielding 9 species , viz , char, tar, CO, $CO_2$, $CH_4$,$H_2$,$C_2H_4$,$C_2H_6$ and $H_2O$.

The simulation with kinetic model indicated following optimization techniques for enhancement of carbon conversion in gasification , and hence the performance of the gasifier. these are : (1) reduction of the size of biomass , so as to have char particle also of smaller size . This would enhance the gasification kinetics of char , (2) Addition of a in-bed catalyst that would enhance oxidation of the tar (3) efficient capture and recycle of char particles in the gasifier.

## 8.2 SCOPE AND RECOMMENDATION FOR FUTURE WORK

Research presented in this thesis could be advanced in two ways, i.e. experimental and modeling. Simulations of biomass gasification with different models, for different biomass and numerous combinations of operating conditions yielded interesting trends in performance of gasification in terms of quality and quantity of producer gas obtained from it. However, these trends need to be rigorously assessed and validated with experiments on lab / pilot scale. The simulations with equilibrium and semi-equilibrium models (which constitute major part of this thesis) are independent of the type of gasifier, and are equally applicable for moving bed and fluidized bed designs. From viewpoint of efficient scale-up of gasifier,

experiments using mixtures of biomass are crucial. Our results have indicated that replacement of single biomass with mixtures of biomass does not make significant changes in the performance of gasifier. However, this result is based on several assumptions made in the model such as spatial uniformity of temperature, air ratio, biomass mixture composition, heat and mass transfer coefficients in the reactor etc. There is a need to assess these results with experiments, which would reveal practical limitations and operational problems / difficulties in the gasification process employing biomass mixture as feedstock. These practical issues are bound to deviate performance of the gasifier from the predictions of the model.

Another dimension of extending the research work in this thesis is to develop more rigorous semi-equilibrium models that are physically more realistic and at the same time, versatile in terms of application under wide range of operational and design parameters. As we saw in the previous chapter, although kinetic model was physically more realistic, it was system specific (developed for gasifier of particular type and capacity), and thus, its adaptability to other gasifier systems was very limited. This limitation was overcome by the semi-equilibrium models, which were independent of the gasifier type and capacity. Nonetheless, the approach taken by us in the semi-equilibrium model was also approximate, in that we put limitation only on the carbon conversion. Another approach adapted by researchers, employing semi-equilibrium models of stoichiometric type, was to determine the equilibrium constants of various reactions using a quasi-temperature. These two approaches could be combined to develop semi-equilibrium models that depict the physical picture more closely. The semi-equilibrium models could also be coupled to the experimental data, by determining carbon conversion in semi-empirical manner using correlations developed on analysis of experimental results.

We believe that the results of this thesis would provide useful inputs for further research along the lines mentioned above.

भारतीय प्रौद्योगिकी संस्थान गुवाहाटी
Indian Institute of Technology Guwahati

# Acknowledgments

It is my pleasure to thank those who made this thesis possible. I recollect numerous occasions and moments which make me proud to be a part of this world class Center of Excellence. It is my privilege to be amidst some intellectual genius, who guided in my pursuit of knowledge. I owe my deepest gratitude to all of them.

The first and foremost appreciation goes to my supervisors Dr. V. S. Moholkar and Professor P. Mahanta for their valuable guidance throughout the research work. I thank them for their encouragement, guidance and support from the initial to the final level, which enabled me to develop a better understanding of the subject and leads to a successful completion. I would like to acknowledge my sincere gratitude to my doctoral committee members, Dr. U. K. Saha, Dr. A. Singh and Dr. K Mohanty and, for their insightful advices and suggestions throughout the research. I also acknowledge the kind advice and suggestion of former doctoral committee members Professor M.K. Chaudhuri (currently Vice Chancellor, Tezpur University) and Professor Anupam Dewan (Indian Institute of Technology Delhi) during my research work.

My sincere thanks go to the Center for Energy and also to the faculty members associated with Center for their constant inspiration and valuable suggestions. The kind and constant help of the staff member of the Center is also duly acknowledged. I am also thankful to the Indian Institute of Technology Guwahati for providing me with the infrastructure and facilities for advanced research.

I extend my sincerest thanks to staff members of Center for Energy for extending helping hands in various part of the research work. My special thanks go to Pankaj Kalita, Lepakshi Borbora, Archana Rajbanshi, Dhiren Huzuri for their constant encouragement and help during the course of the research.

I am also thankful to my colleague and friends Sushovan, Gouri Sankar, Monikankana , Biraj, Gunin, Dhruba, Debajit, Amrita, Swati, Hanif and Peeush for their constant help, motivation, and enthusiastic company and all the wonderful time we spent in various events.

I am also thankful to Late Prof. D. Konwer, Sadhan Mahapatra, Dr. Dhanapati Deka, Dr. Rupam Kataki, Dr Anil Sarma, Anol Chandra Sarmah, Tribeni, Hiranya, Raj kumar, Ratul.

I am also thankful to all the members of “Bohagor Duwardolit”, “XOBDO (The one and only online multi-lingual dictionary of the languages of the North-East India)”, FASS (Friends of Assam and Seven Sisters), Xomidhan, Enajori.

I acknowledge Ministry of New and Renewable Energy for providing financial assistance through a project between November 2009 – February 2011.

At last but not least, I am highly indebted to my sisters, Dhanakshi Buragohain Phukan (Juri) and Chuni Buragohain (Minti), brother-in-law Bhaskar J Phukan, nephew Chow Neywin Phukan (Jishnu) their endless love and inspiration. Finally, my Ph. D. endeavor could not be completed without the endless love, unending support, and blessings from my parents (Nomal Buragohain and Late Saruj Dihingia Buragohain).

Date:26.08.2011

Buljit Buragohain
August, 2011
Guwahati – 781 039

# RESEARCH OUTPUT OF THE THESIS

## BOOK CHAPTERS

- B. Buragohain, P. Mahanta and V.S. Moholkar. First Principles Design of a Circulating Fluidized Bed (CFB) Biomass Gasifier. In: *New Technologies for Rural Development Having Potential for Commercialization* (Editor, J.P. Shukla), Allied Publishers Pvt. Ltd., New Delhi (2009) pp. 210 – 223.
- B. Buragohain, P. Mahanta, V.S. Moholkar. Thermodynamic Approach to Design and Optimization of Biomass Gasifiers Utilizing Agro-Residues. In: Waste-to-Energy in Developing Countries and Transitional Economies (Editor, A. Karagiannidis), Springer – Verlag (*in press*).

## JOURNAL PAPERS

- B. Buragohain, P. Mahanta and V.S. Moholkar. Biomass Gasification for Decentralized Power Generation: The Indian Perspective. *Renewable and Sustainable Energy Reviews* **Vol. 14**, pp. 73 – 92 (2010).
- B. Buragohain, P. Mahanta and V.S. Moholkar. Thermodynamic Optimization of Biomass Gasification for Decentralized Power Generation and Fischer-Tropsch Synthesis. *Energy* **Vol. 35**, pp. 2557 – 2579 (2010).
- B. Buragohain, P. Mahanta and V.S. Moholkar. Investigations in Gasification of Biomass Mixtures Using Thermodynamic Equilibrium and Semi-equilibrium Models. *International Journal of Energy and Environment* **Vol. 2(3)**, pp. 551 – 578 (2011).
- B. Buragohain, P. Mahanta and V.S. Moholkar. Performance Correlations for Biomass Gasifiers Using Semi-equilibrium Non-stoichiometric Thermodynamic

Models. *International Journal of Energy Research* accepted for publication (doi:10.1002/er.1818, volume 35, issue 6, May 2011).

## CONFERENCE PRESENTATIONS

- B. Buragohain, P. Mahanta, V.S. Moholkar. Biomass Gasification: A Viable Alternative to Coal Gasification. International Seminar on Coal Gasification: Challenges and Opportunities for India, I. I. T. Bombay, Mumbai, October 2007 (poster presentation).
- B. Buragohain, P. Mahanta, V.S. Moholkar. First Principles Design of a Circulating Fluidized Bed (CFB) Biomass Gasifier. National Workshop on New Technology for Rural Development Having Potential for Commercialization, Advanced Materials for Process Research Institute (CSIR), Bhopal, May 2009 (oral presentation).
- B. Buragohain, P. Mahanta, V.S. Moholkar. Material and Energy Balance Calculations (MEBC) for Circulating Fluidized Bed Biomass Gasifier. CHEMCON 2009, Andhra University, Visakhapatnam, December 2009 (oral presentation).
- B. Buragohain, P. Mahanta, V.S. Moholkar. Performance Correlations for Biomass Gasifiers. CHEMCON 2010, Annamalai University, Chidambaram, December 2010 (oral presentation).